



# Elucidation of the Cation-π Interaction in Small-Molecule Asymmetric Catalysis

## Citation

Lin, Song. 2013. Elucidation of the Cation-π Interaction in Small-Molecule Asymmetric Catalysis. Doctoral dissertation, Harvard University.

## Permanent link

<http://nrs.harvard.edu/urn-3:HUL.InstRepos:11169771>

## Terms of Use

This article was downloaded from Harvard University's DASH repository, and is made available under the terms and conditions applicable to Other Posted Material, as set forth at <http://nrs.harvard.edu/urn-3:HUL.InstRepos:dash.current.terms-of-use#LAA>

## Share Your Story

The Harvard community has made this article openly available.  
Please share how this access benefits you. [Submit a story](#).

[Accessibility](#)

**Elucidation of the Cation– $\pi$  Interaction in Small-Molecule Asymmetric Catalysis**

A thesis presented

by

Song Lin

to

The Department of Chemistry and Chemical Biology

in partial fulfillment of the requirements

for the degree of

Doctor of Philosophy

in the subject of

Chemistry

Harvard University

Cambridge, Massachusetts

August 2013



## Elucidation of the Cation– $\pi$ Interaction in Small-Molecule Asymmetric Catalysis

### Abstract

The cation– $\pi$  interaction has been long-established to play an important role in molecular recognition, supramolecular chemistry, and molecular biology. In contrast, its potential application in small-molecule catalysis, especially as a selectivity-determining factor in asymmetric synthesis has been overlooked until very recently. This dissertation begins with an extensive literature review on the state-of-the-art research on the application of cation– $\pi$  interactions in non-enzymatic catalysis of organic and organometallic transformations. The research in this field has been largely inspired and guided by the related biosynthetic systems incorporating the same type of interactions.

Squalene cyclases, for instance, exploit cation– $\pi$  interactions elegantly in the catalysis of cationic polycyclizations *en route* to terpene synthesis. Their remarkable rate acceleration effect and precise stereoinduction are governed by a network of aromatic amino acid residues lining the active site. Mindful of this mode of enzymatic catalysis, we have identified multifunctional thiourea compounds bearing specifically oriented aromatic substituents as potent catalysts for a cationic bicyclization proceeding through an *N*-acyliminium ion intermediate. Experimental physical organic studies indicate that the mechanism of thiourea-catalyzed polycyclization resembles that of the squalene cyclases. The prominent role of a cation– $\pi$  interaction provided by

the thiourea catalyst in the selective stabilization of the reaction transition state is particularly intriguing.

We then established that this family of thiourea catalysts could also enable a highly enantioselective indole alkylation by episulfonium ions. Experimental mechanistic studies in combination with computational modeling have allowed us to identify a cation- $\pi$  interaction between the catalyst aromatic group and the episulfonium ion. This interaction, in concert with a series of hydrogen bonding interactions, serves to organize the reaction transition state in a specific geometry, imparting enantioselectivity. Studies on the episulfonium ion ring-opening system inspired the development of enantioselective selenoetherification reactions catalyzed by structurally related squaramide catalysts in the context of flavonoid synthesis.

The elucidation of noncovalent interactions in the context of small molecule asymmetric catalysis has changed the way we think about the mechanism of stereinduction in other systems. In the last chapter, we present a computational analysis of a previously reported carbonyl-ene reaction catalyzed by Lewis acidic chromium complexes. We have obtained evidence that attractive interactions exist between the aromatic motif of the ligand and the developing positive charge on the reaction transition state. These cation- $\pi$  interactions serve to preferentially stabilize one of the two competing diastereomeric pathways, resulting in high enantioselectivity.

## Table of Contents

<b>Abstract</b>	iii
<b>Table of Contents</b>	v
<b>Acknowledgments</b>	x
<b>List of Abbreviations</b>	xv
<b>Chapter 1. Cation–<math>\pi</math> Interactions in Small-Molecule Catalysis</b>	1
1.1 Introduction	1
1.2 Cyclophane-Catalyzed S <sub>N</sub> 2 Alkyl Transfer Reactions	4
1.3 Supramolecular Assemblies in Organic and Organometallic Catalysis	8
1.4 Pyridinium/Amidinium-Mediated Acyl Transfer Reactions	14
1.5 Copper(II) Supported by Aromatic Amino Acids in Lewis Acid Catalysis	19
1.6 Multifunctional H-Bond Donors in Synergistic Ion-Pair Binding Catalysis	22
1.7 Miscellaneous	31
1.8 Summary and Outlook	34
<b>Chapter 2. Enantioselective Thiourea-Catalyzed Polycyclizations</b>	35
2.1 Introduction	35
2.2 A Case Study – Squalene–Hopene Cyclase	37
2.2.1 Crystallographic Studies	38
2.2.2 Stepwise Nature of the Cyclization Cascade	40
2.2.3 Catalysis of Polycyclization	41
2.2.4 Conclusion	48
2.3 Polycyclization in Complex Target Synthesis	50
2.3.1 Substrate-Controlled Polycyclization	50

2.3.2	Catalyst/Reagent-Controlled Asymmetric Polycyclizations	53
2.3.3	Catalytic Asymmetric Polycyclizations	55
2.4	Enantioselective Thiourea-Catalyzed Cationic Polycyclizations	58
2.4.1	Introduction	58
2.4.2	Method Development	59
2.4.3	Substrate Scope	61
	2.4.3.1 Development of a Modular Substrate Synthesis via <i>B</i> -Alkyl Suzuki Coupling	61
	2.4.3.2 Substrate Scope of Thiourea-Catalyzed Polycyclization	64
2.5	Mechanistic Studies: Implication for a Biomimetic Catalytic System	66
2.5.1	Stepwise Cyclization with Selectivity-Determining First Ring- Closure	66
2.5.2	Cation- $\pi$ Stabilization of the Cyclization Transition State	68
2.5.3	Cation- $\pi$ Stabilization of the C–Cl Bond Ionization	71
2.6	Outlook	73
2.6.1	Substrate Scope	73
2.6.2	Cyclization of Unfunctionalized Polyenes – a Traceless Leaving Group Approach	75
2.6.3	Enantioselective Hydroarylation of Dienes	76
2.7	Conclusion	78
2.8	Experiment section	79
<b>Chapter 3. Development of Enantioselective Thiourea-Catalyzed Ring-Opening of Episulfonium Ions and Seleniranium Ions</b>		97
3.1	Enantioselective Ring-Opening of Episulfonium Ions by Indoles	97
3.1.1	Introduction	97
3.1.2	Method development	98

3.1.3	Substrate Synthesis	101
3.1.4	Substrate Scope	101
3.2	Enantioselective Squaramide-Catalyzed Selenoetherifications	104
3.2.1	Introduction	101
3.2.2	Method Development	106
3.2.3	Substrate Synthesis	109
3.2.4	Substrate Scope	110
3.3	Derivatization of Episulfonium Ion and Seleniranium Ion Ring-Opening Products	112
3.4	Outlook	114
3.5	Experimental Section	116
<b>Chapter 4. Mechanistic Analyses of Thiourea-Catalyzed Episulfonium Ion Ring-Opening with Indoles: Evidence for an Enantioselectivity-Determining Cation-<math>\pi</math> Interaction</b>		143
4.1	Introduction	143
4.2	Kinetic Studies	148
4.2.1	Kinetic Profile of the Uncatalyzed Reaction	148
4.2.2	Kinetic Profile of the Thiourea-Catalyzed Reaction	150
4.2.3	Rate Acceleration Effect by Thiourea	153
4.3	Elemental Steps and Catalytic Cycle of the Reaction	154
4.3.1	Irreversible Protonolysis of Precursor <b>3a</b>	154
4.3.2	Resting State of the Episulfonium Ion and the Catalyst	154
4.3.3	Identification of the Rate-Determining Step	157
4.4	Mechanism of Rate-Acceleration by Thiourea	160
4.4.1	Promotion of the Ionization Step	161

4.4.2	Facilitation of the Nucleophilic Addition Step	165
4.5	Mechanism of Enantioinduction by Thiourea	172
4.6	Computational Analyses	175
4.6.1	Ground State Structures of the Episulfonium Ion and Catalyst	176
4.6.2	Energy Diagram	177
4.6.3	Enantio-Determining Transition States	180
4.6.4	Enantioselectivity Dependence on the Aromatic Group of the Catalyst	185
4.7	Conclusion	189
4.8	Experimental section	191
<b>Chapter 5. Mechanistic Analysis of Chromium-Catalyzed Intermolecular Carbonyl-Ene Reaction</b>		<b>259</b>
5.1	Background – Recapitulation of the Chromium-Catalyzed Carbonyl-Ene Reaction	259
5.2	Kinetic Analysis and Non-Linear Effect Studies	265
5.3	Computational Analyses of the Intermolecular Carbonyl-Ene Reaction	267
5.3.1	Determination of the Catalyst Spin State	267
5.3.2	Asynchronicity of the Rearrangement	268
5.3.3	Origin of Enantioselectivity	274
5.3.4	Effect of the <i>ortho</i> -Substituents on Arylaldehyde Substrate	278
5.4	Outlook	280
5.5	Experimental Section	281
<b>Appendix I. Syntheses of Arylpyrrolidine-Derived Thiourea Catalysts</b>		<b>311</b>
A1.1	Conventional Methods for Arylpyrrolidine Preparation	311

A1.2	A New <i>trans</i> -1,2-Cyclohexanediamine-Based Ligand for Asymmetric Deprotonation	312
A1.3	Proposed Total Synthesis of Sparteine and “Sparteine surrogate” Using Hydrolytic Kinetic Resolution of Terminal Epoxide and Stereoselective Aza-Sakurai Cyclization	313
<b>Appendix II. Crystal Structure of Arylpyrrolidine-Derived Thiourea and Squaramide Binding to Tetramethylammonium Chloride</b>		316
A2.1	Arylpyrrolidine-Derived Thiourea Binding to Tetramethylammonium Chloride	316
A2.2	Arylpyrrolidine-Derived Squaramide Binding to Tetramethylammonium Chloride	318

## Acknowledgments

I express sincere gratitude to Professor Eric N. Jacobsen for his tremendous support of my graduate work at Harvard. My research has benefited from his remarkable wisdom and extraordinary insights, and to match these characters of his has been an ultimate career goal of mine. In addition to being a devoted chemist, he is also an exceptional educator. His eagerness to pass on his knowledge as well as research philosophy is priceless to the students and will always be much appreciated; his advice for my future career path has also been invaluable to me. My graduate life has been supported by the talent-studded group he gathers and manages.

I thank Professor Tobias Ritter and Professor Emily Balskus for the valuable advice they have provided during our meetings in the past five years. Tobias' enthusiasm for organic chemistry has been a true inspiration to me and encouraged me to pursue a career in this field. Emily has been a role model to me as both a graduate student and a postdoctoral researcher, and will keep influencing my future career with her infinite energy and amazing success as a young professor. I was also lucky to have had an opportunity to interact with Professor David Evans, a legendary figure in the field of organic synthesis, in my junior years.

I am grateful to Professor Zhang-Jie Shi of Peking University, who was my first mentor in chemistry when I was an undergraduate student. My passion in scientific research started at the moment when I became immersed in his wisdom and enthusiasm. I also built a good personal relationship with Professor Zhi-Xiang Yu while he visited Harvard, and his advice on research as well as on career choices was instrumental.

My graduate life has gained immeasurable benefits from Dr. Robert Knowles. He took me under his wing when I was a young graduate student to collaborate on the polycyclization

project, and remained my mentor in the rest of his tenure in the Jacobsen group. During our interactions, Rob used his unrivaled knowledge and intelligence to influence my understanding of chemistry, and his tremendous kindness and patience to nurture me from a nobody to a qualified graduate student.

I gratefully acknowledge Nicole Minotti for her tireless work and happy spirit. Her support in my graduate life, especially during my visa application, was truly instrumental.

Naomi Rajapaksa, David Ford, Mike Witten, Adam Brown, Cheyenne Brindle, Charles Yeung, Andrew Bjonnes, Amanda Turek and Steven Banik all read and corrected parts of this thesis. My writing would not have been readable without their kind help.

During my time in the Jacobsen group I have had the privilege of working with many talented scientists. Among them, Hu Zhang collaborated with me on the squaramide-catalyzed selenocyclization reaction. His persistence at the hardest time of the project was very impressive and eventually paid off. My mentorship skills were forged during our constant debate on chemistry and lab etiquette.

In my early days at Harvard, senior members of the group, including Stephan Zuend, Naomi Rajapaksa, Adam Brown, Rebecca Loy, Kristine Nolin, Rebekka Klausen, Christopher Uyeda, Ye Tao and Hao Xu, not only recruited me into the group, but also introduced me to the American culture. The growth of both my tolerance to alcohols and caffeine, and my interest in fat- and sugar-rich dietary is inevitably linked to their “help”. I would not have been able to enjoy my life in this totally different country as much as I do now without the interactions with them.

My interest in understanding reaction mechanisms was initially inspired by Stephan’s outstanding Ph.D. work as well as his dedication to teaching Chem 205. In addition, Chris and

Bekka also set great examples that have encouraged me to pursue a graduate career in physical organic chemistry.

Most of my time here in the Jacobsen group was shared with Naomi Rajapaksa, Adam Brown, David Ford, James Birrell and Andreas Rötheli. I was fortunate to be taken care of by Naomi and Adam in all the five years of graduate school. The two of them have not only played irreplaceable roles as leaders of the group, but have also served as exceptional friends. Naomi has the ability of imparting positive spirit on people surrounding her with her virtue, kindness, and optimistic attitude of life, the latter of which has been a great inspiration to me in both research and life. In addition, I cannot thank her enough for the support and the help she has offered to me throughout graduate school. I look forward to continuing our friendship on the west coast. I have always viewed Adam as a big brother of mine. Despite being casual and occasionally ditzy in life, his meticulousness and intelligence in research made him one who I constantly try to match myself to during graduate school.

I could not ask for a combination of classmates better than Dave and Jim. Their talents in chemistry and hard work have always driven me to strive for success. Outside of the lab, we remain close friends and have supported each other over all these years. Dave's wisdom and passion are unmatched, while his willingness to spare no efforts to help his friends is even more treasured. I will miss the days when Jim would slow down the speed of talking in order for me to understand him. His encouragements both in the lab and during sports activities will also be remembered. Andy has been a role model of mine when it comes to cultural transition. I'm always impressed by his masterful language and communication skills despite his Swiss accent. I hope the next time when Andy, Naomi and I sit down for a classy, enjoyable date won't be too far.

Mike Witten and Amanda Turek are in the class one year my junior. Sharing an office/bay with them has been an important part of my graduate school experience. In addition to their support, I will always miss Mike's hair and Amanda's face. Steven has also been a good friend of mine, spending time together and providing shelter to me. I am thankful to the advice I gained from Yongho Park on synthetic issues and Rose Kennedy on computations. It has been enjoyable to work with a group of younger graduate students during my time in the group, and I look forward to seeing their future successes.

I am fortunate enough to have shared time with talented postdocs such as Eric Fang, Noah Burns, Jean-Nicolas Desrosiers, Elizabeth Beck, Cheyenne Brindle, Corinna Schindler, Katrien Brak, Sean Kedrowski, David Hardee, Charles Yeung, and Roland Appel. These people have all been great scientific role models, excellent resources, and supportive friends.

Yang Yang and Nick Colcernian have constituted the most important piece of my life in the past four years. Spending time outside of the lab with them is an indispensable fuel to graduate school.

Although my career pursuit has taken me far, far from home, my mom and dad have always supported me fully in my endeavors. I love you and cannot thank you enough for what I have gained from you.

谨以此论文献给我的父母：林云金，杜振英  
*to Mom and Dad*

## List of Abbreviations

4-NBSA	4-nitrobenzenesulfonic acid
$[\alpha]_{25}^D$	specific rotation at 25 °C and 589 nm
Å	Angstrom
Ac	acetyl
Ach	acetylcholine
AIBN	2,2'-azobis(2-methylpropionitrile)
<i>anti</i>	<i>L.</i> , against, opposite
Ar	aryl
Arg	arginine
B3LYP	Becke-3-Lee-Yang-Parr
BAr <sub>F</sub>	tetrakis[(3,5-trifluoromethyl)phenyl]borate
BINOL	1,1'-bi-2-naphthol
Bn	benzyl
Boc	<i>tert</i> -butyloxycarbonyl
Bu	butyl
<i>c</i>	concentration
°C	degree Celsius
cal	calorie
cat	catalyzed
CD	circular dichroism
cinnamyl	3-phenyl-2-propenyl
<i>cis</i>	<i>L.</i> , on the same side
conv.	conversion

CM	chorismate mutase
CPMC	conductor-like polarizable continuum model
Cys	cysteine
$\delta$	chemical shift in parts per million
<i>d</i>	deuterium
DA	Diels–Alder
DBAD	di- <i>tert</i> -butyl azodicarboxylate
DBU	1,8-diazabicycloundec-7-ene
DCM	dichloromethane
DFT	density functional theory
DKR	dynamic kinetic resolution
DMAP	4-( <i>N,N</i> -dimethylamino)pyridine
DMF	<i>N,N</i> -dimethylformamide
DMSO	dimethylsulfoxide
DNA	deoxyribonucleic acid
dppf	1,1'-bis(diphenylphosphino)ferrocene
dr	diastereomeric ratio
<i>E</i>	energy
<i>E</i>	<i>Ger.</i> , entegen
EDC	<i>N</i> -(3-dimethylaminopropyl)- <i>N'</i> -ethylcarbodiimide hydrochloride
ee	enantiomeric excess
EIE	equilibrium isotope effect
<i>ent</i>	enantiomeric
eq.	equation
equiv	equivalent

ESI	electrospray ionization
Et	ethyl
g	gram
<i>G</i>	Gibbs free energy
GC	gas chromatography
Glu	glutamic acid
h	hour
HOBt	1-hydroxybenzotriazole hydrate
HOTf	triflic acid, trifluoromethanesulfonic acid
HPLC	high-performance liquid chromatography
Hz	Hertz
<i>i</i>	iso
i	initial
IR	infrared
<i>k</i>	rate constant
<i>K</i>	equilibrium constant
K	Kelvin
KIE	kinetic isotope effect
L	ligand
<i>m</i>	<i>meta</i>
M	molar
M05-2X	Minnesota 2005 hybrid meta density functional theory
M06-2X	Minnesota 2006 hybrid meta density functional theory
mCPBA	<i>m</i> -chloroperbenzoic acid
Me	methyl

mol	mole
Ms	mesyl, methanesulfonyl
naph	naphthyl
NMR	nuclear magnetic resonance
nOe	nuclear Overhauser effect
Nu, Nuc	nucleophile
<i>o</i>	<i>ortho</i>
obs	observed
OTf	triflate, trifluoromethanesulfonate
<i>p</i>	<i>para</i>
PCM	polarizable continuum model
Ph	phenyl
Phe	phenylalanine
phen	phenanthryl
Pr	propyl
Py	pyridine
pyr	pyrenyl
rr	regiomer ratio
<i>R</i>	rectus
rt	room temperature
<i>S</i>	sinister
<i>s-trans</i>	antiperiplanar
S <sub>N</sub> 1	unimolecular nucleophilic substitution
S <sub>N</sub> 2	bimolecular nucleophilic substitution
SAM	<i>S</i> -adenosylmethionine

SMD	solvation model using solute electron density
<i>t</i>	tertiary
TBDPS	<i>tert</i> -butyldiphenylsilyl
TBS	<i>tert</i> -butyldimethylsilyl
TBME	<i>tert</i> -butyl methyl ether
TCA	trichloroacetamide
THF	tetrahydrofuran
TLC	thin-layer chromatography
THMPA	thiohexamethylphosphoramidate
<i>trans</i>	<i>L.</i> , on the opposite side
Ts	tosyl, <i>p</i> -toluenesulfonyl
TS	transition state
Tyr	tyrosine
uncat	uncatalyzed
UV	ultraviolet
<i>Z</i>	<i>Ger.</i> zusammen
ZPE	zero-point energy

# Chapter One

## Cation– $\pi$ Interactions in Small-Molecule Catalysis

### 1.1 Introduction

Noncovalent interactions play a central role in many forefront areas of modern chemistry, including molecular recognition, supramolecular chemistry, materials design and molecular biology.<sup>1</sup> The chemical community has devoted extensive efforts to elucidating the physical origin and scope of these interactions. In contrast to other more “conventional” noncovalent interactions, such as hydrogen bonding, hydrophobic interactions, and  $\pi$ – $\pi$  stacking, the cation– $\pi$  interaction has been relatively underappreciated.<sup>2</sup>

---

<sup>1</sup> (a) Mahadevi, A. S.; Sastry, G. N. *Chem. Rev.* **2013**, *113*, 2100–2138; (b) Bissantz, C.; Kuhn, B.; Stahl, M. *J. Med. Chem.* **2010**, *53*, 5061–5084; (c) Bohm, H.-J.; Schneider, G. *Protein-Ligand Interactions—From Molecular Recognition to Drug Design*. Wiley-VCH, Weinheim, 2003; (d) Lehn, J.-M. *Supramolecular Chemistry. Concepts and Perspectives*. Wiley VCH, Weinheim, 1995; (e) Schneider, H. *J. Angew. Chem. Int. Ed.* **2009**, *48*, 3924–3977; (f) Moulton, B.; Zaworotko, M. J. *Chem. Rev.* **2001**, *101*, 1629–1658; (g) Aakeroy, C. B.; Seddon, K. R. *Chem. Soc. Rev.* **1993**, *22*, 397–407.

<sup>2</sup> Dougherty, D. A. *Science* **1996**, *271*, 163–168.

Since the cation– $\pi$  interaction was uncovered in the 1980s,<sup>3</sup> experimental and computational methods have been applied to elucidate and quantify this molecular phenomenon.<sup>4</sup> Early research revealed that in the gas phase, the association enthalpy between  $K^+$  and benzene is 19 kcal/mol. This finding is remarkable, giving that the binding between  $K^+$  and water is only 18 kcal/mol.<sup>5</sup> The fundamentals of the cation– $\pi$  interaction in the solution phase have also been well documented, and indicated that this force is strong enough to drive aggregation of molecules, even in the presence of polar solvents.<sup>6,7</sup> These and subsequent studies shed light on the thermodynamics of this weak noncovalent interaction in the context of molecular binding and recognition events.<sup>8</sup>

As with other attractive noncovalent interactions, the cation– $\pi$  interaction also plays a key role in catalysis by lowering the kinetic barriers to reactions through transition state stabilization.<sup>9</sup>

---

<sup>3</sup> (a) Sunner, J.; Nishizawa, K.; Kebarle, P. *J. Phys. Chem.* **1981**, *85*, 1814–1820; (b) Deakyne, C. A.; Meot-Ner, M. *J. Am. Chem. Soc.* **1985**, *107*, 474–479.

<sup>4</sup> For a review on studies of cation– $\pi$  interactions with computational methods, see: (a) Raju, R. K.; Bloom, J. W. G.; An, Y.; Wheeler, S. E. *ChemPhysChem* **2011**, *12*, 3116–3130; for a review on studies of cation– $\pi$  interactions in structural biology, see: (b) Gallivan, J. P.; Dougherty, D. A. *Proc. Natl Acad. Sci. USA* **1999**, *17*, 9459–9464. For a review on dissecting noncovalent interactions, including cation– $\pi$  interaction with double-mutant cycle, see: Cockroft, S.L.; Hunter, C.A. *Chem. Soc. Rev.* **2007**, *36*, 172–188. For studies of cation– $\pi$  interactions in other contexts, see references below.

<sup>5</sup> Cabarcos, O. M.; Weinheimer, C. J.; Lisy, J. M. *J. Chem. Phys.* **1998**, *108*, 5151–5154.

<sup>6</sup> For early studies of cation– $\pi$  interactions in aqueous media, see: (a) Shepodd, T. J.; Petti, M. A.; Dougherty, D. A. *J. Am. Chem. Soc.* **1988**, *110*, 1983–1985; (b) Schneider, H.-J. *Angew. Chem. Int. Ed.* **1991**, *30*, 1417–1436; (c) Dhaenens, M.; Lacombe, L.; Lehn, J.-M.; Vigneron, J.-P. *J. Chem. Soc., Chem. Commun.* **1984**, 1097–1099; (d) Araki, K.; Shimizu, H.; Shinkai, S. *Chem. Lett.* **1993**, 205–208; (e) Schwabacher, A. W.; Zhang, S.; Davy, W. *J. Am. Chem. Soc.* **1993**, *115*, 6995–6996; (f) Harrowfield, J. M.; Ogden, M. I.; Richmond, W. R.; Skelton, B. W.; White, A. H. *J. Chem. Soc., Perkin Trans. 2* **1993**, 2183–2190.

<sup>7</sup> For early studies of cation– $\pi$  interactions in organic solvents, see: (a) Stauffer, D. A.; Dougherty, D. A. *Tetrahedron Lett.* **1988**, *29*, 6039–6042; (b) Cattani, A.; Dalla Cort, A.; Mandolini, L. *J. Org. Chem.* **1995**, *60*, 8313–8314; (c) MERIC, R.; Lehn, J.-M.; Vigneron, J.-P. *Bull. Soc. Chim. Fr.* **1994**, *131*, 579–583; (d) Canceill, J.; Lacombe, L.; Collet, A. *J. Chem. Soc., Chem. Commun.* **1987**, 219–221; (e) Odell, B.; V., R. M.; Slawin, A. M. Z.; Spencer, N.; Stoddart, J. F.; Williams, D. J. *Angew. Chem. Int. Ed.* **1988**, *27*, 1547–1550.

<sup>8</sup> Ma, J.; Dougherty, D. A. *Chem. Rev.* **1997**, *97*, 1303–1324.

<sup>9</sup> (a) Pauling, L. *Chem. Eng. News* **1946**, *24*, 1377; (b) Jencks, W. P. *Catalysis in Chemistry and Enzymology*. McGraw Hill, New York, 1989.

In fact, it is responsible for many of the remarkable rate accelerations and stereoselectivities characteristic of enzymatic catalysis, wherein specific aromatic residues in the active site can stabilize the electrostatic character of a bound transition structure complex.<sup>10</sup> For instance, the crystal structure of a cytosine-DNA methyltransferase reveals a van der Waals contact between the S<sup>+</sup>-CH<sub>3</sub> unit of *S*-adenosylmethionine (SAM, methylating cofactor) and the  $\pi$ -face of a tryptophan residue, which orients the residue in a favorable alignment for catalysis assisted by cation- $\pi$  interactions.<sup>11</sup> The squalene cyclases showcase elegant use of cation- $\pi$  interactions in its catalysis of cationic polyene cyclization to form steroids.<sup>12</sup> As revealed in the crystal structure of enzymes of this family, the active pocket is lined with an array of aromatic amino acid side chains, which would provide sufficient stabilization to the developing positive charges in the cyclization transition state, leading to extraordinary rate acceleration and exquisite selectivity.

Inspired by enzymatic catalysis, the importance of cation- $\pi$  interactions in the control of reaction kinetics and selectivity has recently started to captivate the attention of synthetic organic chemists. In this chapter, we highlight recent advances on cation- $\pi$  interactions in small molecule catalysis, with particular emphasis on mechanistic elucidation of the role of these weak interactions in promoting the reactivity and/or governing the selectivity of reactions.

---

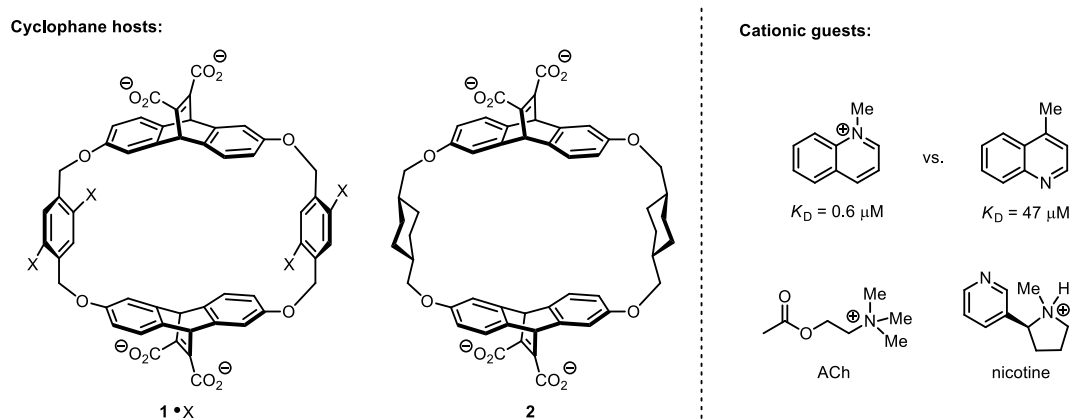
<sup>10</sup> (a) Warshel, A.; Sharma, P. K.; Kato, M.; Xiang, Y.; Liu, H.; Olsson, M. H. M. *Chem. Rev.* **2006**, *106*, 3210–3235; (b) Zacharias, N.; Dougherty, D. A. *Trends Pharmacol. Sci.* **2002**, *23*, 281–287.

<sup>11</sup> For the crystal structure elucidation of SAM-bound methyltransferase, see: (a) Cheng, X.; Kumar, S.; Posfai, J.; Pflugrath, J. W.; Roberts, R. J. *Cell* **1993**, *74*, 299–307; for the invoke of a cation- $\pi$  interaction in the enzymatic catalysis of SAM-mediated methyl transfer, see: (b) Kagan, R. M.; Clarke, S. *Arch. Biochem. Biophys.* **1994**, *310*, 417–427. Also see ref. 2.

<sup>12</sup> (a) Johnson, W. S.; Lindell, S. D.; Steele, J. J. *Am. Chem. Soc.* **1987**, *109*, 5882–5883; (b) Wendt, K. U.; Poralla, K.; Schulz, G. E. *Science* **1997**, *277*, 1811–1815; (c) Hoshino, T.; Sato, T. *Chem. Commun.* **2002**, 291–301.

## 1.2 Cyclophane-Catalyzed S<sub>N</sub>2 Alkyl Transfer Reactions

As part of their program on investigating the cation- $\pi$  interaction in solution phase, Dougherty and coworkers devised a class of molecular flasks grounded on cyclophane scaffold with the central cavity surrounded by an array of aromatic groups (such as **1**, Scheme 1-1).<sup>13</sup> This family of small molecules were found to be capable of recognizing cationic species such as quaternary ammonium ions and desolvate them from the aqueous solution.<sup>14</sup> The preference of these cyclophane hosts for positively charged guests over the isostructural neutral analogs led to the proposal that the cation- $\pi$  interaction play a central role in the recognition event. A neurotransmitter – acetylcholine (ACh) was also found to be a potent guest binder to **1**. This finding drove Dougherty to overturn the longstanding notion that ACh is accommodated by its host enzyme through a salt bridge, and postulate instead that it is a cation- $\pi$  interaction that empowers this enzyme-substrate binding phenomenon.<sup>15</sup> This hypothesis was later confirmed by the elucidation of a crystal structure of the acetylcholine esterase.<sup>16</sup>



**Scheme 1-1.** Representative cyclophane hosts and their small molecule guests.

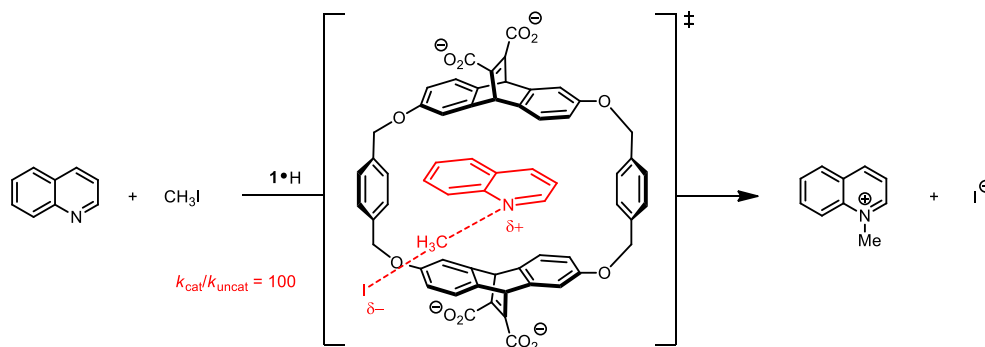
<sup>13</sup> (a) Dougherty, D. A. *Acc. Chem. Res.* **2013**, *46*, 885–893; (b) Petti, M. A.; Shepodd, T. J.; Dougherty, D. A. *Tetrahedron Lett.* **1986**, *27*, 807–810; (c) Diederich, F.; Dick, K. A. *J. Am. Chem. Soc.* **1984**, *106*, 8024–8036.

<sup>14</sup> Shepodd, T. J.; Petti, M. A.; Dougherty, D. A. *J. Am. Chem. Soc.* **1986**, *108*, 6085–6087.

<sup>15</sup> Dougherty, D. A.; Stauffer, D. A. *Science* **1990**, *250*, 1558–1560.

<sup>16</sup> Sussman, J. L.; Harel, M.; Frolow, F.; Oefner, C.; Goldman, A.; Toker, L.; Silman, I. *Science* **1991**, *253*, 872–879.

Having established the thermodynamics of the host-guest complexation events with these molecular flasks, Dougherty further examined their abilities in binding cationic transition states and altering the kinetics of chemical reactions. Indeed, these cyclophane molecules (such as **1**•H) imparted notable rate acceleration in the *N*-alkylation of quinoline with methyl iodide, namely the Menshutkin reaction, in aqueous buffer (Scheme 1-2).<sup>17</sup> Given that the Menshutkin reaction favors polar solvents over non-polar media, the catalysis cannot be simply explained by the hydrophobic effect provided by the host molecule. The cation- $\pi$  interaction between the aromatic groups of cyclophane and the developing positive charge in the reaction transition state was therefore invoked to account for the improved reactivity. In support of this hypothesis, a structurally analogous host **2** with two benzene linkers replaced by cyclohexane motifs exhibited lower catalytic activity ( $k_{\text{cat}}/k_{\text{uncat}} = 20$ ), presumably due to its diminished  $\pi$ -donating ability.



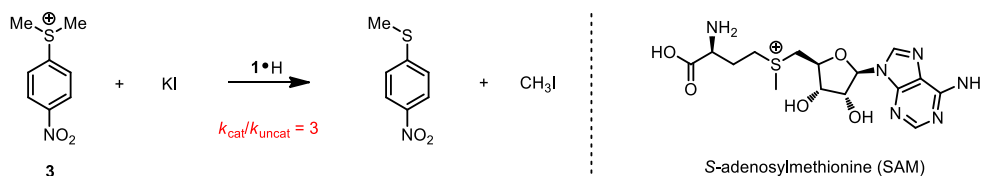
**Scheme 1-2.** Cyclophane **1**-catalyzed Menshutkin reaction.

The cation- $\pi$  interaction has been inferred to play crucial roles in biosynthetic alkylation reactions (ref. 11). Encouraged by the enzyme-like behavior of these cyclophane hosts, Dougherty group further investigated their catalytic effect in the methylation reactions mediated by sulfonium ions,<sup>18</sup> analogs of *S*-adenosylmethionine (SAM), nature's overwhelmingly versatile methyl

<sup>17</sup> Stauffer, D. A.; Barrans, R. E., Jr.; Dougherty, D. A. *Angew. Chem. Int. Ed.* **1990**, *29*, 915–918.

<sup>18</sup> McCurdy, A.; Jimenez, L.; Stauffer, D. A.; Dougherty, D. A. *J. Am. Chem. Soc.* **1992**, *114*, 10314–10321.

transfer agent.<sup>19</sup> Interestingly, although the positive charge is formally destroyed in the demethylation of sulfonium **3** by iodide anion, the overall reaction is still accelerated by **1**•H by a factor of 3.



**Scheme 1-3.** Demethylation of sulfonium by cyclophane **1**.

Both an alkylation reaction involving formal creation of positive charge in the transition state and a dealkylation reaction wherein positive charge is reduced are promoted by the host. These findings established that a transition state with only a partial positive charge can be stabilized more effectively than either fully charged or neutral substrates. To rationalize this counterintuitive observation, Dougherty advanced the notion that in addition to the electrostatic component,<sup>20</sup> polarizability (dispersion forces) also contributes to the overall strength of the cation– $\pi$  interaction, and it plays a prominent role in catalysis.<sup>21</sup> Since transition states have longer, weaker bonds and more spread charge distribution, they are expected to be more polarizable than the substrates and products. The host therefore associates with transition states more tightly through the cation– $\pi$  interaction than the corresponding ground states, leading to lowering of the energy of activation, which is manifested as the observed rate acceleration.

To test this hypothesis, a series of substituted cyclophanes (**1**•X) with distinct polarizability were subjected to the dealkylation of **3** (Table 1-1). The substitution effect was shown to be

<sup>19</sup> Chiang, P.K.; Gordon, R. K.; Tal, J.; Zeng, G. C.; Doctor, B. P.; Pardhasaradhi, K.; McCann, P. P. *FASEB J.* **1996**, *10*, 471–480.

<sup>20</sup> For a discussion on the electrostatic component of the cation– $\pi$  interaction, see: Mecozzi, S.; West, A.P.; Dougherty, D. A. *J. Am. Chem. Soc.* **1996**, *118*, 2307–2308.

<sup>21</sup> For other reports that documented the importance of polarizability component in the cation– $\pi$  interaction, see: (a) Cubero, E.; Luque, F. J.; Orozco, M. *Proc. Natl. Acad. Sci. USA* **1998**, *95*, 5976–5980; (b) Vijay, D.; Sastry, G. N. *Phys. Chem. Chem. Phys.* **2008**, *10*, 582–590.

unimportant to the ground state binding of the cationic substrate, as the free energy of association ( $\Delta G_{\text{binding}}$ ) is essentially the same across the series of catalysts studied. However, a pronounced correlation was displayed between the dispersion property of the cyclophane and the level of catalysis, with more polarizable host facilitating the alkyl transfer to a greater degree. These data provide compelling evidence that cation- $\pi$  interaction is indeed responsible for the binding of the cationic transition state in these alkylation reactions, and that in addition to the electrostatic component of this interaction, the polarizability of the  $\pi$ -donor plays a pivotal role in the differential stabilization of the transition state over the ground state, enabling catalysis.

**Table 1-1.** Correlation between polarizability, binding and catalysis of demethylation by **1**.

host	polarizability	$-\Delta G_{\text{binding}}$ (kcal/mol)	$k_{\text{cat}}/k_{\text{uncat}}$	$-\Delta\Delta G$ (kcal/mol)
1•H	10.3 (benzene)	5.7	4.9	1.0
1•Me	12.3 (toluene)	5.2	6.4	1.2
1•MeO	13.1 (anisole)	4.6	9.7	1.4
1•Cl	14.1 (chlorobenzene)	5.8	9.8	1.4
1•Br	14.7 (bromobenzene)	5.6	12.0	1.6

Spectroscopic data provided detailed depiction for the guest-host association event (Figure 1-1).<sup>22</sup> CD spectrum revealed that the positively charged sulfur atom in **3** is positioned for maximal interaction with one of the aromatic rings of host **1•H**, while proton NMR analysis indicated that the methyl groups of **3** are also in close proximity to the  $\pi$ -faces of the host cavity.

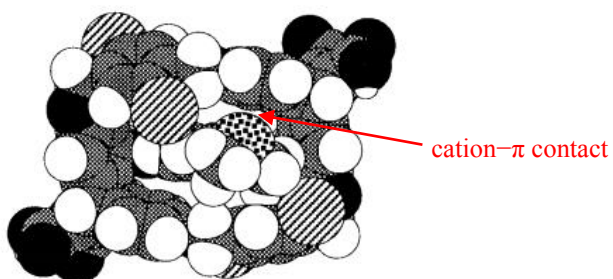


**Figure 1-1.** Binding model of **1•Cl** and **3** (grey: C, white: H, black: O, striped: Cl, and dotted: S)

<sup>22</sup> Ngola, S. M.; Dougherty, D. A. *J. Org. Chem.* **1996**, *61*, 4355–4360.

### 1.3 Supramolecular Assemblies in Organic and Organometallic Catalysis

As part of their program in developing supramolecular assemblies for exploring host-guest chemistry, Raymond group designed a series pyramidal molecular containers that bear thermodynamic stability and structural rigidity, in a general form of  $M_4L_6$  ( $M = Ga^{3+}$ ,  $Al^{3+}$ ,  $In^{3+}$  or  $Fe^{3+}$ , and  $L =$  bis-bidentate catchol ligand with naphthalene linker).<sup>23</sup> While these supramolecular scaffolds are negatively charged and soluble in water, they contain a hydrophobic cavity of between  $0.35 - 0.5 \text{ nm}^3$ , which renders them highly potent in guest-binding of organic molecules, especially those bearing cationic characters. The intrinsic chirality of the host molecule also makes stereoselective recognition possible. Solution phase binding studies show that species such as ammonium ions and iminium ions with a suitable size can be pulled out of the aqueous solution and encapsulated in the host molecule, with an association constant of up to  $10^6$ .<sup>24</sup> Crystallographic analysis of the host-guest complex containing encapsulated  $BnNMe_3^+$  reveals a close contact of the cation to the naphthalene rings of the host interior by a distance of  $3.63 \text{ \AA}$ , indicating the presence of a cation- $\pi$  interaction between the two that likely contributes to the overall binding strength.<sup>25</sup>

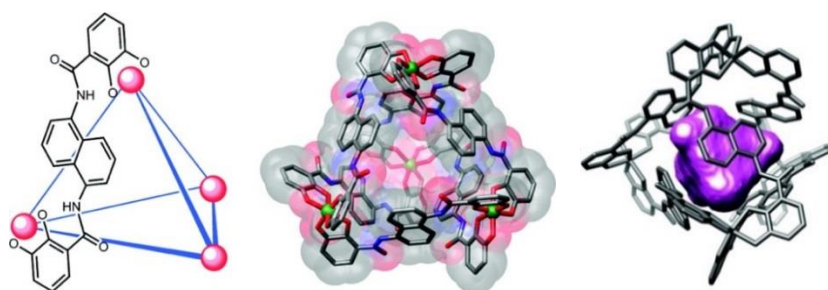


**Figure 1-2.** (Left) Schematic representation of the  $M_4L_6$  assembly, with one molecule of ligand  $L$  shown explicitly in chemical structure. (Middle) A space-filling model of the assembly. (Right) Diagram showing a  $NEt_4^+$  molecule encapsulated in  $Ga_4L_6$  (**4**).

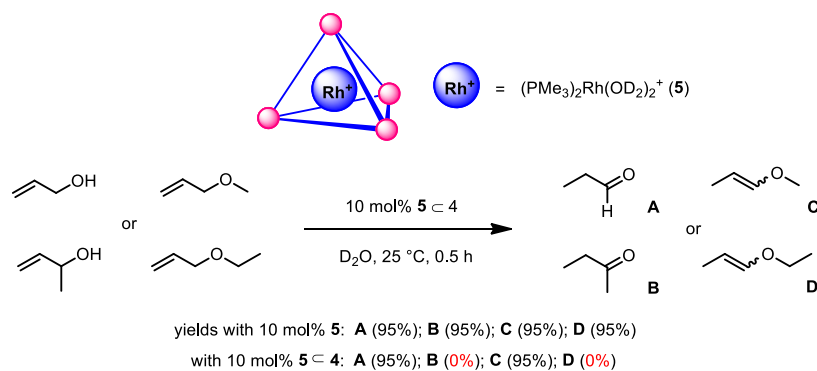
<sup>23</sup> Pluth, M. D.; Raymond, K. N. *Chem. Soc. Rev.* **2007**, *36*, 161–171.

<sup>24</sup> Dong, V. M.; Fiedler, D.; Carl, B.; Bergman, R.G.; Raymond, K. N. *J. Am. Chem. Soc.* **2006**, *128*, 14464-14465.

<sup>25</sup> Pluth, M. D.; Johnson, D. W.; Szigethy, G.; Davis, A. V.; Teat, S. J.; Oliver, A. G.; Bergman, R. G.; Raymond, K. N. *Inorg. Chem.* **2009**, *48*, 111–120.

In a collaborative effort, the Bergman and the Raymond groups explored the potential of these supramolecular assemblies in the catalysis of organic and organometallic transformations. Results showed that molecules encapsulated within a supramolecular host are subject to a unique chemical environment in which reactions take place with enhanced rates and/or selectivity. The rate acceleration and selectivity in these reactions are inevitably linked to the constrained space inside the binding cavity, which provides prominent entropic benefit and strict size-sifting.<sup>26</sup> In addition, it seems reasonable that cation- $\pi$  interactions imparted by the aromatic groups lining the host cavity play a crucial role in the strength, directionality and selectivity of guest-binding event.

Tetrahedral  $[\text{Ga}_4\text{L}_6]^{12-}$  host was shown to encapsulate a variety of cationic organometallic compounds in aqueous solution, including iridium, rhodium and gold complexes with proper ligands. These supramolecular assemblies have been used to promote organometallic reaction. For instance, an encapsulated bisphosphine-Rh(I) complex catalyzes the isomerization of allylic alcohols and ethers to aldehydes and enol ethers, respectively. In this process, the catalyst exhibits strict size and shape selectivity, which is not seen in the absence of the host (Scheme 1-4).<sup>27</sup>

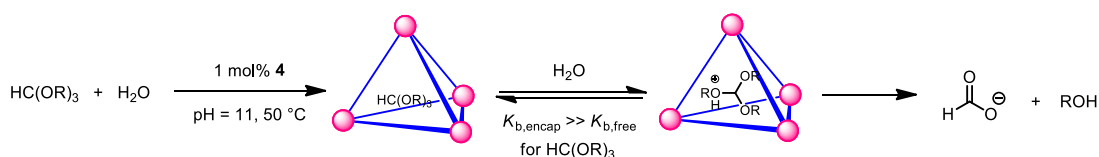


**Scheme 1-4.** Rh-catalyzed isomerization of allylic alcohols and ethers.

<sup>26</sup> Fiedler, D.; Leung, D. H.; Bergman, R. G.; Raymond, K. N. *Acc. Chem. Res.* **2005**, 38, 351–360.

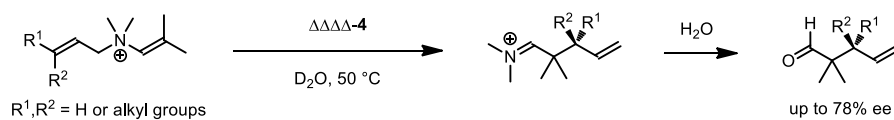
<sup>27</sup> Leung, D. H.; Bergman, R. G.; Raymond, K. N. *J. Am. Chem. Soc.* **2007**, 129, 2746–2747.

Due to the strong preference for binding cationic guests over their neutral counterparts,  $[M_4L_6]^{12-}$  assembly is capable of enhancing the basicity of molecules captured inside the cavity. For example, encapsulated amines can be basified by up to 4  $pK_a$  units.<sup>28</sup> This property was exploited to turn on the reactivity of strong acid-catalyzed transformations in neutral or basic aqueous solutions. For instance, the hydrolysis of orthoformates or acetals can be carried out inside of the assembly with rate accelerations of up to  $10^3$  compared to the background reaction (Scheme 1-5).<sup>29</sup>



**Scheme 1-5.** Proton-catalyzed hydrolysis of orthoformate under basic condition.

The supramolecular metal-ligand assembly can also be employed as a catalytic host for the unimolecular sigmatropic rearrangement of enammonium cations, achieving up to 1000-fold rate acceleration (Scheme 1-6).<sup>30</sup> Release and hydrolysis of the product allow for catalytic turnover. When enantiomerically pure supramolecular host (such as  $\Delta\Delta\Delta\Delta$ -**4** was used as the catalyst, the product can be isolated in enantioenriched form with up to 78% ee.<sup>31</sup>



**Scheme 1-6.** Asymmetric Aza-Claisen rearrangement catalyzed by supramolecular host **4**.

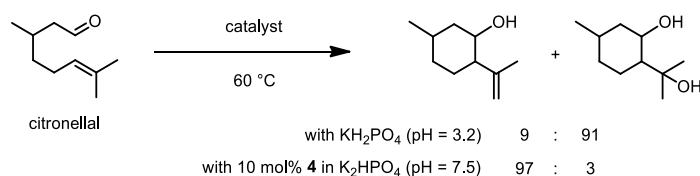
<sup>28</sup> Pluth, M. D.; Bergman, R. G.; Raymond, K. N. *J. Am. Chem. Soc.* **2007**, *129*, 11459-11467.

<sup>29</sup> Pluth, M. D.; Bergman, R. G.; Raymond, K. N. *Science* **2007**, *316*, 85-88.

<sup>30</sup> (a) Fiedler, D.; Bergman, R. G.; Raymond, K. N. *Angew. Chem. Int. Ed.* **2004**, *43*, 6748-6751; (b) Fiedler, D.; van Halbeek, H.; Bergman, R. G.; Raymond, K. N. *J. Am. Chem. Soc.* **2006**, *128*, 10240-10252.

<sup>31</sup> Brown, C. J.; Bergman, R. G.; Raymond, K. N. *J. Am. Chem. Soc.* **2009**, *131*, 17530-17531.

In collaboration with Toste, Bergman and Raymond also showed that supramolecular assembly **4** can catalytically cyclize monoterpene citronellal via protonation of the carbonyl group (Scheme 1-7).<sup>32</sup> In contrast to the uncatalyzed pathway, the hydrophobic interior of **4** stabilizes the cyclized carbonocation intermediate and prevents the capture of it by water, altering the product distribution. This system bears analogy to the biosynthetic terpene cyclization, in which the mechanistic control over the selective catalysis is achieved through transition state stabilization by the hydrophobic pocket enriched with aromatic functionalities.



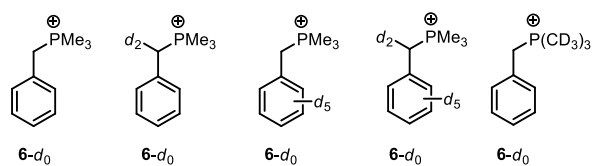
**Scheme 1-7.** Selective terpene cyclization catalyzed by supramolecular assembly **4**.

The prominent role of the cation– $\pi$  interaction plays in associating with cationic species and enabling catalysis was demonstrated by Bergman and Raymond with equilibrium isotope effect (EIE) studies.<sup>33</sup> Isotopologues of benzyl trimethylphosphonium ion (**6-d<sub>n</sub>**) were used in the binding studies as analogs to the cationic substrates and transition states of reaction, and the relative binding affinities ( $K_{d0}/K_{dn}$ ) of these molecules to the interior of host **4** were measured using NMR competition titrations (Scheme 1-8). All EIE values obtained through these experiments are greater than or equal to 1, indicating that the protiated isotopologues are more strongly bound to the interior of **4** than their deuterated counterparts (Table 1-2). Such type of EIE values can be explained by changes in bond vibrational frequencies, which can be further attributed to attractive interactions associated with these C–H/D bonds. Specifically, upon complexation, cation– $\pi$  or  $\pi$ –

<sup>32</sup> (a) Hart-Cooper, W. M.; Clary, K. N.; Toste, F. D.; Bergman, R. G.; Raymond, K. N. *J. Am. Chem. Soc.* **2012**, *134*, 17873–17876; for an Au-catalyzed hydroalkoxylation of allenes that bears mechanistic analogy to the terpene cyclization, see: (b) Wang, J. Z.; Brown, C. J.; Bergman, R. G.; Raymond, K. N.; F. Dean Toste. *J. Am. Chem. Soc.* **2011**, *133*, 7358–7360.

<sup>33</sup> Mugridge, J. S.; Bergman, R. G.; Raymond, K. N. *J. Am. Chem. Soc.* **2012**, *134*, 2057–2066.

$\pi$  interactions with the aromatic lining of the cavity will lower the vibrational force constant for these C–H/D bonds, illustrated in Figure 1-3 by a shallower vibrational potential energy well. This will lead to more closely spaced C–H and C–D zero-point energy (ZPE) levels in the bound state. Therefore, given the exothermic nature of the encapsulation, the protiated guests will have a larger association energy ( $\Delta E_H > \Delta E_D$ ), and therefore a greater binding constant than the deuterated guests.



**Scheme 1-8.** Isotopologues of benzyltrimethylphosphonium ion used in the EIE studies.

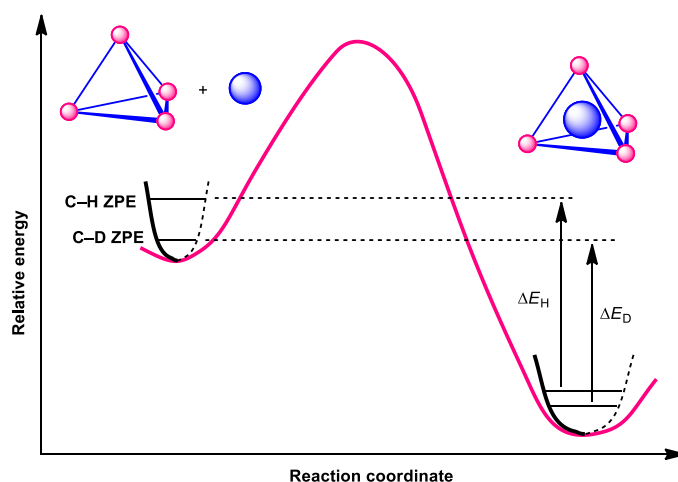


**Figure 1-3.** Diagram showing the qualitative changes in guest  $6-d_n$  C–H and C–D ZPEs upon binding to the interior of host **4**. Encapsulation weakens the guest vibrational force constants, illustrated above by shallower vibrational potential energy wells; this results in closer spacing of the ZPE levels for the encapsulated  $2-d_n$  and a larger association constant for protiated guests ( $K_{d0}/K_{dn} > 1$ ).

The EIE values are consistent with that the methyl/benzyl C–H/D bonds are weakened due to attractive cation– $\pi$  interactions with the host molecule (Table 1-2, entries 1,3-4), while the aromatic C–H/D bonds were not engaged in specific interactions (Table 1-2, entry 2). These conclusions were further consolidated by DFT calculations using the same guest molecules in combination with naphthalene as the model for the supramolecular assembly **4**. The calculated

$\Delta$ ZPE numbers as a result of cation– $\pi$  interactions are consistent with the experimental data, whereas the theoretical prediction based on simple desolvation model is far off.

**Table 1-2.** EIE values on interior guesting binding of **6-d<sub>n</sub>** to host **4** in D<sub>2</sub>O at 298 K.

entry	ratio	EIE	EIE per D = $(K_{d0}/K_{dn})^{1/n}$
1	$K_{d0}/K_{d2}$	1.07(1)	1.034(6)
2	$K_{d0}/K_{d5}$	1.00(2)	1.000(3)
3	$K_{d0}/K_{d7}$	1.103(7)	1.014(1)
4	$K_{d0}/K_{d9}$	1.14(1)	1.015(1)

Taken together, these studies provide strong evidence that the cation– $\pi$  interaction plays an important role in the encapsulation of cationic small molecules by these supramolecular containers. It is therefore reasonable to postulate that, in the reactions catalyzed by **4**, an analogous stabilization effect to the cationic transition state is strengthened as well by the attractive  $\pi$ -donation from the aromatic walls of the host. Drawing analogy from Dougherty’s cyclophane system, the increased polarizability of reaction transition states compared to ground states allows for stronger association of them to the host via dispersion forces, leading to rate acceleration. Furthermore, the exquisite sensitivity of molecular recognition to even the smallest, isotopic perturbation of the guest structure implies that the cation– $\pi$  interaction also contributes to the control over substrate sifting and product distribution in the catalytic reactions.

## 1.4 Pyridinium/Amidinium-Mediated Acyl Transfer Reactions

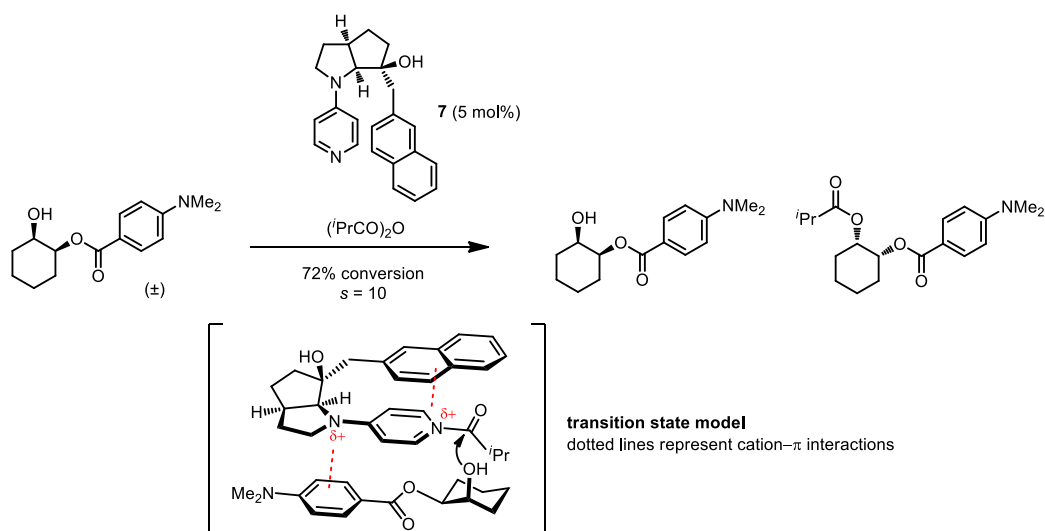
As described in Section 1.2, Dougherty discovered a strong cation– $\pi$  interaction between *N*-methylquinolinium ion and cyclophane hosts they developed. One would anticipate that structurally analogous pyridinium ions can also interact attractively with an electron-rich aromatic species through either face-to-face ( $\pi$ – $\pi$  stacking) or edge-to-face (C–H– $\pi$ ) manner. Given that pyridinium ions mediate an important class of catalytic processes, acyl transfer reactions, a notion arises that  $\pi$ -donating elements can be integrated to the catalytic system to facilitate catalysis and/or induce selectivity.

In 1997, Fuji disclosed an acylative kinetic resolution of secondary alcohols with DMAP derivative **7** bearing a naphthalene substituent (Scheme 1-9).<sup>34</sup> Based on nuclear Overhauser effect (nOe) experiments, Fuji concluded that upon acylation of the DMAP core, the emerging positive charge induces a conformation change of the catalyst to accomplish an intramolecular cation– $\pi$  interaction between the aromatic group on the catalyst and the pyridinium ion. As such, a well-defined chiral environment is constructed to accommodate the alcohol substrate. The differential recognition of one of the two enantiomeric substrates is proposed to be assisted by an additional cation– $\pi$  interaction occurring intermolecularly between the aromatic group on the substrate and the pyridinium ion. This hypothesis was later supported by a computational analysis by Zipse.<sup>35</sup> Although the selectivity factor of kinetic resolution is only moderate, the concept of using cation– $\pi$  interactions to control the stereochemical outcome of nucleophilic acyl transfer reaction has proved promising.

---

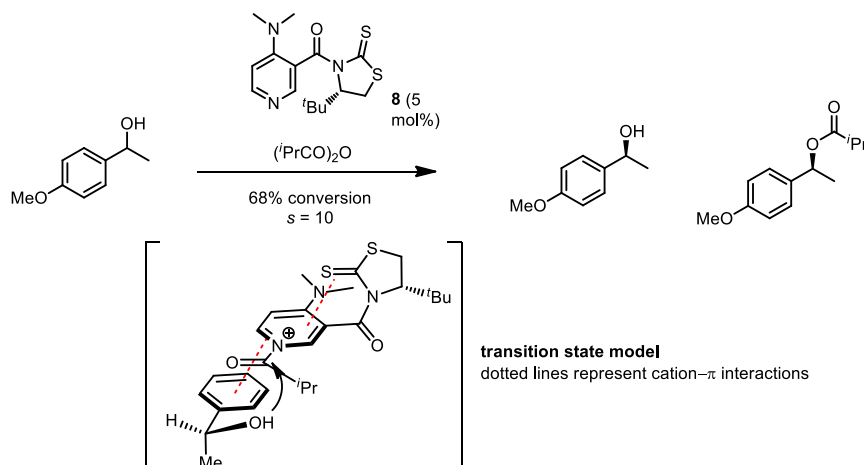
<sup>34</sup> Kawabata, T.; Nagato, M.; Takasu, K.; Fuji, K. *J. Am. Chem. Soc.* **1997**, 119, 3169–3170.

<sup>35</sup> Wei, Y.; Held, I.; Zipse, H. *Org. Biomol. Chem.* **2006**, 4, 4223–4230.



**Scheme 1-9.** Fuji's acylative kinetic resolution of secondary alcohols.

Since the seminal report by Fuji, this strategy has captivated a few other groups. Following their work on diastereoselective allylation of pyridinium ions using a chiral auxiliary containing a  $\pi$ -donating functionality,<sup>36</sup> Yamada et. al. further extended this strategy to achieve kinetic resolution of 1-arylethanol using acylation chemistry catalyzed by a DMAP derivative (**8**) similar to Fuji's original catalyst (Scheme 1-10).<sup>37</sup> An array of two cation- $\pi$  interactions centered around the pyridinium ion organizes the transition state, resulting in moderate selectivity.

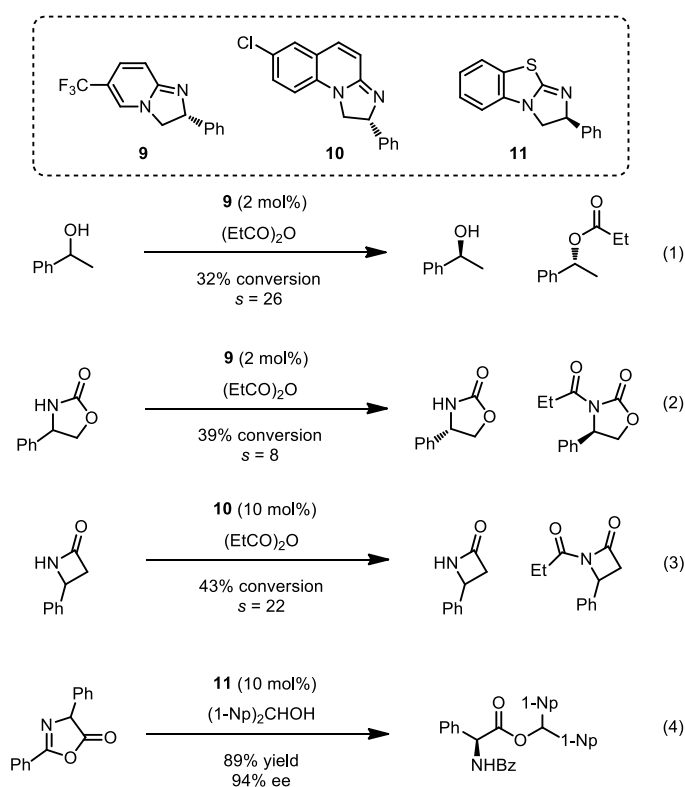


**Scheme 1-10.** Yamada's acylative kinetic resolution of secondary alcohols.

<sup>36</sup> Yamada, S.; Inoue, M. *Org. Lett.* **2007**, *9*, 1477–1480.

<sup>37</sup> Yamada, S.; Misono, T.; Iwai, Y.; Masumizu, A.; Akiyama, Y. *J. Org. Chem.* **2006**, *71*, 6872–6880.

Recently, Birman et. al. devised a new family of enantioselective acyl transfer catalysts on the basis of amidine/tetramisole frameworks (Scheme 1-11).<sup>38</sup> Having been demonstrated their superior efficacy in kinetic resolution of secondary alcohol (eq. 1), these small organic molecules also constitute the first class of catalysts that can resolve chiral racemic lactams/oxazolidinones (eqs. 2 & 3).<sup>39</sup> In addition, these catalysts have been engaged in the dynamic kinetic resolution (DKR) of azlactones with benzhydryl alcohols *en route* to natural and unnatural amino acids (eq. 4)<sup>40</sup>



**Scheme 1-11.** Birman's acylative kinetic resolutions.

<sup>38</sup> Birman, V. B.; Uffman, E. W.; Jiang, H.; Li, X.; Kilbane, C. J. *J. Am. Chem. Soc.* **2004**, *126*, 12226–12227.

<sup>39</sup> (a) Birman, V. B.; Jiang, H.; Li, X.; Guo, L.; Uffman, E. W. *J. Am. Chem. Soc.* **2006**, *128*, 6536–6537; (b) Yang, X.; Bumbu, V. D.; Liu, P.; Li, X.; Jiang, H.; Uffman, E. W.; Guo, L.; Zhang, W.; Jiang, X.; Houk, K. N.; Birman, V. B. *J. Am. Chem. Soc.* **2012**, *134*, 17605–17612.

<sup>40</sup> Yang, X.; Lu, G.; Birman, V. B. *Org. Lett.* **2010**, *12*, 892–895.

In these reactions, Birman found that in the absence of a  $\pi$ -donating group on the substrate, little reactivity and no resolution were achieved by the catalysts. This observation points to the possibility that these groups participate in attractive interactions with the cationic acylated catalyst, and these interactions are important to catalysis. In collaboration with Houk, they carried out computational analyses to ascertain this hypothesis.

In the dynamic kinetic resolution of azlactones, the predicted lowest energy conformations of both the major and the minor diastereomeric transition states possess a strong cation- $\pi$  interaction between the benzhydryl group and the cationic acylating agent, as indicated by an interacting distance close to van der Waals' contact (Figure 1-4).<sup>41</sup> In the resulted, orderly-arranged catalyst-substrate assembly, secondary attractive interactions exist that differentiate the two diastereomeric pathways. Specifically, an electrostatic interaction between the counteranion acetate and the benzamide on the substrate (Figure 1-4A) and a  $\pi$ - $\pi$  stacking between the two phenyl groups on the *N*-acyltetramisolum ion (Figure 1-4B) are responsible for the highly selective kinetic resolution of  $\alpha$ -methyl and  $\alpha$ -phenyl azlactones, respectively.

In the case with acylative resolution of secondary alcohols and oxazolidinones, DFT-computational models suggest that the cation- $\pi$  interaction is the selectivity-determining factor, which is present only in the lowest energy conformer of the major transition state between the amidinium ion and the aryl group on the substrate, but absent in the minor pathway (Scheme 1-12).<sup>39b,42</sup>

---

<sup>41</sup> Liu, P.; Yang, X.; Birman, V. B.; Houk, K. N. *Org. Lett.* **2012**, *14*, 3288–3291.

<sup>42</sup> Li, X.; Liu, P.; Houk, K. N.; Birman, V. B. *J. Am. Chem. Soc.* **2008**, *130*, 13836–13837.

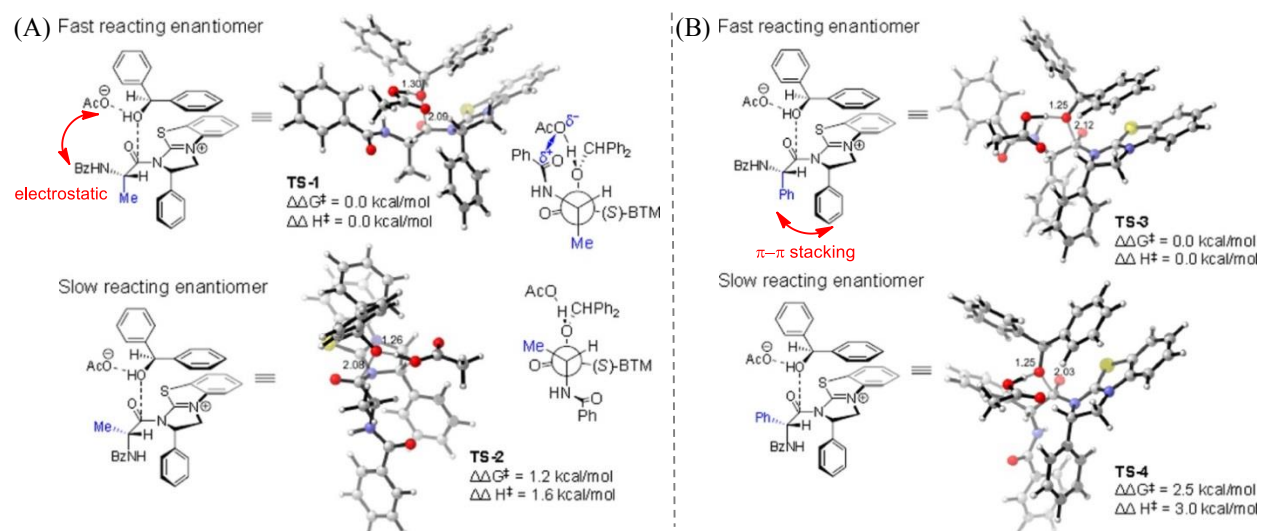
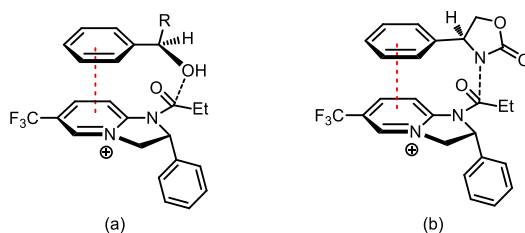


**Figure 1-4.** Computational stereochemical models for the azlactone DKR. (A) major and minor transition states in the resolution of methyl azlactone; (B) major and minor transition states in the resolution of  $\alpha$ -phenyl azlactone. This figure is reproduced from ref. 42. Structures were optimized using M06-2X/6-31G(d) with the SMD solvation model in chloroform, and single point energies were calculated with M06-2X/6-311+G(d,p).



**Scheme 1-12.** Computational models represented in chemdraw structures for the major transition state of: (a) kinetic resolution of a secondary alcohol, and (b) kinetic resolution of an oxazolidinone. Structures were optimized using (a) B3LYP/6-31G(d) with the CPMC solvation model in chloroform, and (b) M06-2X/6-31G(d) with the SMD solvation model in chloroform.

## 1.5 Copper(II) Supported by Aromatic Amino Acids in Lewis Acid Catalysis

Recently, Ishihara started a program on designing Lewis acid-based small molecule catalysts for Diels–Alder reactions using cation– $\pi$  interaction as selectivity-controlling element.<sup>43</sup> Such catalysts encompasses a cationic copper(II) center and a bidentate ligand derived from tyrosine (Scheme 1-13). The authors noted in their report that this design principle was inspired by Yamamoto’s acyloxyborane catalyst and Corey’s oxazaborolidinone catalyst, which provide  $\pi$ – $\pi$  stacking and charge-transfer interactions, respectively, to the coordinated substrate to control the stereochemical outcome of reaction.<sup>44</sup>

Prior to Ishihara’s initial report, the Engberts group disclosed that the Diels–Alder (DA) reaction of cyclopentadiene with 3-phenyl-1-(2-pyridinyl)-2-propen-1-one can be catalyzed by the combination of  $\text{Cu}(\text{NO}_3)_2$  and the sodium salt of *L*-abrine (**12**) (Scheme 13, eq. 5).<sup>45</sup> During the screening of reaction conditions, they found that aqueous medium is superior to a wide range of organic solvents, generating products in substantially enhanced enantiomeric excess (ee) (74% vs. 17–44% ee in MeCN, THF,  $\text{CHCl}_3$ , etc.).

The crystallographic data of bis(*L*-tyrosinato)copper(II) complex, a structural analogue of Engberts’ catalyst reveals a weak attractive interaction between the  $\pi$ -electrons of the phenol group and the cationic metal center (Figure 1-5).<sup>46</sup> This type of interactions have also been found in between metal cations and aromatic side chains of proteins, which is known to play an important

---

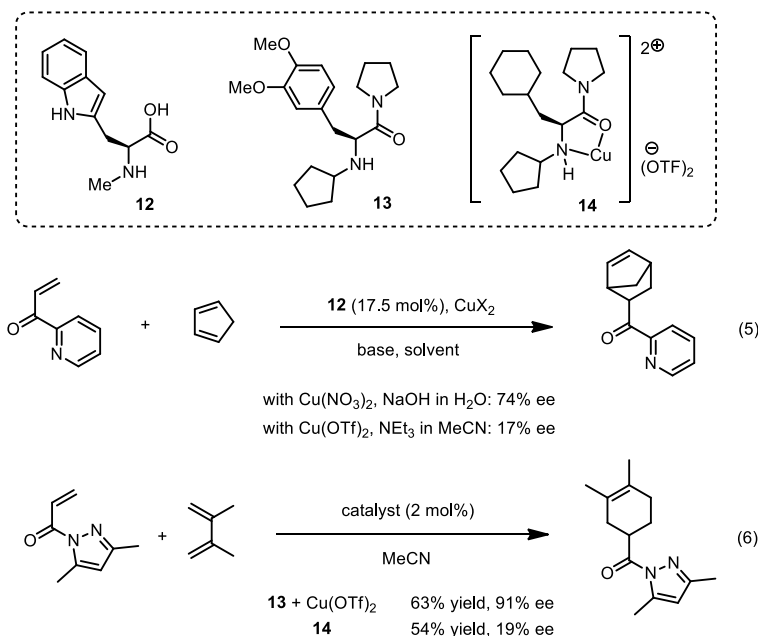
<sup>43</sup> Ishihara, K.; Fushimi, M.; Akakura, M. *Acc. Chem. Res.* **2007**, *40*, 1049–1055.

<sup>44</sup> (a) Furuta, K.; Miwa, Y.; Iwanaga, K.; Yamamoto, H. *J. Am. Chem. Soc.* **1988**, *110*, 6254–6255; (b) Corey, E. J.; Loh, T.-P. *J. Am. Chem. Soc.* **1991**, *113*, 8966–8967.

<sup>45</sup> (a) Otto, S.; Boccaletti, G.; Engberts, J. B. F. N. *J. Am. Chem. Soc.* **1998**, *120*, 4238–4239; (b) Otto, S.; Engberts, J. B. F. N. *J. Am. Chem. Soc.* **1999**, *121*, 6798–6806.

<sup>46</sup> van der Helm, D.; Lawson, M. B.; Enwall, E. L. *Acta Crystallogr., Sect. B: Struct. Sci.* **1972**, *28*, 2307–2312.

role in biological systems.<sup>47</sup> Taken together, Ishihara postulated that an intramolecular cation– $\pi$  interaction exists in a similar manner in Engberts' catalyst, which may play a critical role in the enantioinduction mechanism of the DA reaction it promotes. This hypothesis provides a rational for Engberts' experimental findings, as water may enhance the cation– $\pi$  interaction with hydrophobic effects.



**Scheme 1-13.** Cu-catalyzed enantioselective Diels–Alder reaction.

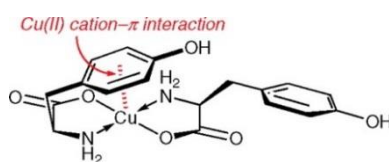


**Figure 1-5.** Chemdraw representation of the crystal structure of a copper complex analogous to **12**• $\text{Cu}(\text{OTf})_2$ .

This proposal was employed by Ishihara as a design principle in the development of Lewis acid catalysts for enantioselective DA reaction. A neutral ligand **13** derived from tyrosine was prepared based on the notion that its copper complex would possess larger cationic character at the metal center and serve as a stronger cation– $\pi$  acceptor compared to Engberts' catalyst with an

<sup>47</sup> Meyer, E. A.; Castellano, R. K.; Diederich, F. *Angew. Chem. Int. Ed.* **2003**, *42*, 1210–1250. See also ref. 2.

anionic ligand. The new catalyst proved effective in the Diels-Alder reaction involving a diene and pyridine-substituted propenone or pyrazole-coupled acrylamide (Scheme 1-14, eq. 6).<sup>48</sup> The transformation can now be conducted in MeCN with the product generated in high ee. A control experiment with a structurally similar catalyst **14** derived from *L*-cyclohexylalanine resulted in significantly compromised enantioselectivity. This result suggests that the cation- $\pi$  interaction linking the metal and the ligand side chain play a critical role in the enantioinduction mechanism.

Based on this hypothesis, a stereochemical model was advanced to explain the selectivity observed in the DA reactions (Figure 1-6). The steric environment created by the pyrrolidine on the catalyst and the pyrazole on the substrate enforces the substrate to coordinate *trans* to the ligand and the olefin to adopt an *s-cis* geometry. The catalyst was predicted by DFT calculations to remain in a folded conformation upon complexation with the dienophile, with an energy 6.9 kcal/mol lower than the most favorable unfolded structure. Such conformation is presumably retained during the approach of the diene, and the facial-selectivity of the cycloaddition process is governed by the steric effect that the tyrosine residue introduces on the top face of the electrophile.

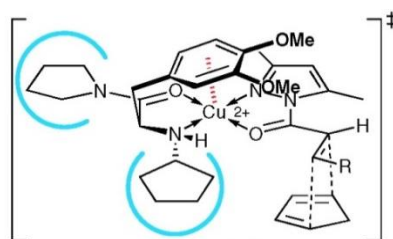


**Figure 1-6.** Postulated stereochemical model. Blue curves represent the steric interaction that define the conformation of the substrate coordination. Dotted line in red indicates a cation- $\pi$  interaction.

The scope of this class of catalysts was also extended to highly enantioselective Mukaiyama-Michael reaction involving the same type of electrophiles and silyl ketene acetals or silyl enol ethers with excellent enantioselectivity (see ref. 48).

<sup>48</sup> Ishihara, K.; Fushimi, M. *Org. Lett.* **2006**, 8, 1921–1924.

## 1.6 Multifunctional H-Bond Donors in Synergistic Ion-Pair Binding Catalysis<sup>49</sup>

Catalysis by chiral dual hydrogen-bond donors has emerged as an important approach in organic asymmetric synthesis.<sup>50</sup> In reactions promoted by this family of small molecules, the H-bond donating group, such as thiourea, urea and guanidinium, has been shown to be critical for catalytic activity by engaging in an attractive H-bonding interaction to an electronegative motif in the reaction transition structure. Mechanistic studies have also indicated that in addition to the dual hydrogen-bond donor, other functionalities on the catalyst scaffold can also play crucial roles in the mechanisms of catalysis and stereoselection. Complementary to the role of the hydrogen-bonding unit, these electron-rich groups usually provide electrostatic stabilization to the positively-charged portion of the transition structure. Chiral information on the catalyst directs the relative spatial relationship of these interactions, which is ultimately translated into the reaction enantioselectivity. This mode of catalysis by transition state stabilization highly resembles the manner through which nature accomplishes biosynthesis with enzymes.<sup>51</sup>

Chroismate mutase catalyzes the Claisen rearrangement with overwhelming rate acceleration (up to  $10^6$ ) and exquisite enantioselectivity. The crystal structure of this enzyme with an analogue of the rearrangement transition state bound in the active site was elucidated, showing that the transition state stabilization of the sigmatropic rearrangement is likely achieved through a network of attractive noncovalent interactions provided by the amino acid side chains lining the catalyst pocket (Figure 1-7). In addition to hydrogen bonding interactions with a few arginine,

---

<sup>49</sup> Much of the work summarized in this section will also be discussed in-depth in subsequent chapters. It is included in this chapter for the purpose of presenting a complete review on the state of the art in this field.

<sup>50</sup> (a) Doyle, A. G.; Jacobsen, E. N. *Chem. Rev.* **2007**, *107*, 5713–5743 (b) Brak, K.; Jacobsen, E. J. *Angew. Chem. Int. Ed.* **2013**, *52*, 534–561.

<sup>51</sup> Knowles, R. R.; Jacobsen, E. N. *Proc. Natl. Acad. Sci. USA* **2010**, *107*, 20678–20685.

tyrosine and cysteine residues, a cation– $\pi$  interaction delivered by a phenylalanine residue to the partial positive charge on the allyl fragment of the transition structure has also been inferred.<sup>52</sup>

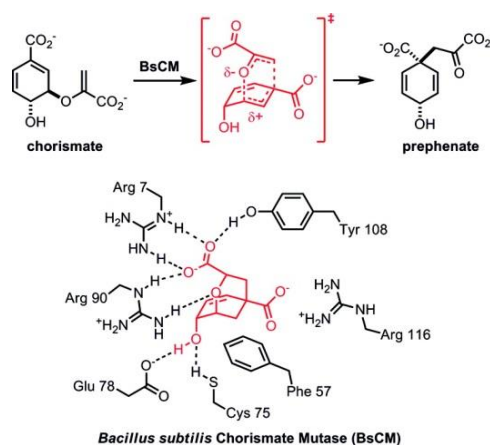


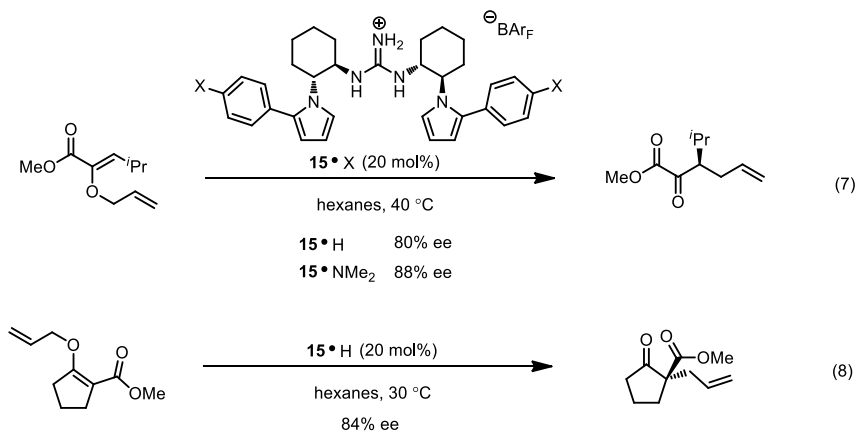
**Figure 1-7.** Depiction of the crystal structure of chorismate mutase binding to a structural analogue of the Claisen rearrangement transition state.

Inspired by this biosynthetic hypothesis, Jacobsen group developed a class of chiral guanidinium ion catalysts that facilitates the enantioselective rearrangements of  $\alpha$ -ketoester and  $\beta$ -ketoester substrates (Scheme 1-14).<sup>53</sup> Structural and computational investigations revealed that, in the lowest-energy conformation of the catalyst, both pyrrole rings of **15**•H are engaged in cation– $\pi$  interactions with the positively charged  $\text{NH}_2$  group of the guanidinium ion, splaying the pendant phenyl substituents of the pyrrole into an orientation that creates a well-defined box-like space surrounding the H-bond donor functionality (Figure 1-8). In this conformation, the catalyst is found to bind to the  $\alpha$ -ketoester substrate through a dual hydrogen bonding interaction to both the ether and ester oxygens, which defines the geometry of the complexation. Such interaction is strengthened in the rearrangement transition state due to the negative character of the enol

<sup>52</sup> a) Chook, Y.-M.; Ke, H.; Lipscomb, W. H. *Proc. Natl. Acad. Sci. U.S.A.* **1993**, *90*, 8600–8603; (b) Chook, Y.-M.; Gray, J. V.; Lipscomb, W. N. *J. Mol. Biol.* **1994**, *240*, 476–500; (c) Lee, A. Y.; Karplus, A.; Ganem, B.; Clardy, J. *J. Am. Chem. Soc.* **1995**, *117*, 3627–3628.

<sup>53</sup> (a) Uyeda, C.; Jacobsen, E. N. *J. Am. Chem. Soc.* **2008**, *130*, 9228–9229; (b) Uyeda, C.; Roetheli, A. R.; Jacobsen, E. J. *Angew. Chem. Int. Ed.* **2010**, *50*, 9753–9756.

fragment. Computational modeling indicates that the allyl fragment of the transition state bears a significant partial positive charge, and that this cationic character is stabilized by the catalyst phenyl rings through a cation- $\pi$  interaction in only one of the two competing diastereomeric pathways (Figure 1-8A vs. Figure 1-8B).<sup>54</sup> This intriguing rationale for stereoinduction was evaluated by examining catalysts of type **15** bearing different aryl substituents, showing the reaction enantioselectivity improves as the electron density of the aryl group increases (Scheme 1-14, eq. 7). This experimental trend was also reproduced by DFT calculations. These data come together to consolidate the hypothesis that a stabilizing cation- $\pi$  interaction plays an indispensable role in the mechanism of enantioinduction, echoing the biosynthetic pathway associated with chroismate mutase.



**Scheme 1-14.** Guanidinium-catalyzed asymmetric Claisen rearrangements.

<sup>54</sup> Uyeda, C.; Jacobsen, E. N. *J. Am. Chem. Soc.* **2011**, *133*, 5062–5075.

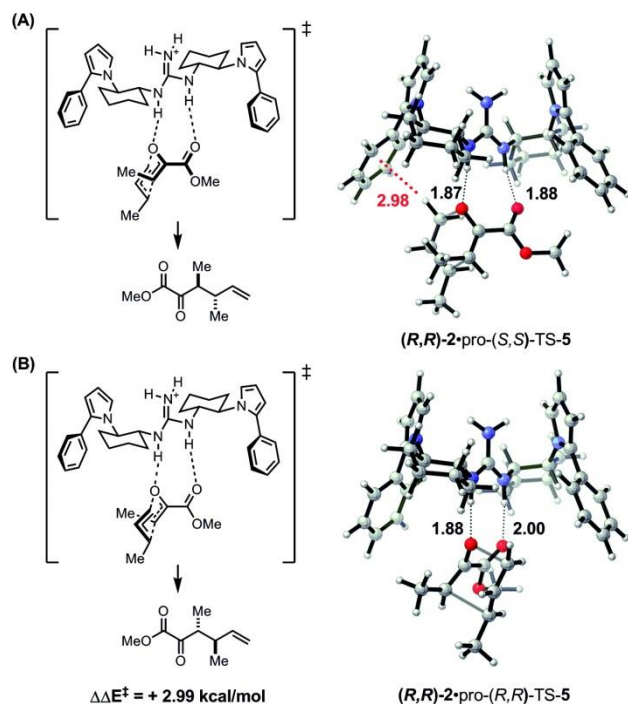


**Figure 1-8.** Calculated major (A) and minor (B) transition states of guanidinium 14•H-catalyzed Claisen rearrangement. Calculations were performed using the B3LYP/6-31G(d) level of theory. Dotted lines in black represent hydrogen bonding interactions, while the one in red indicates the cation– $\pi$  interaction between the allyl fragment of the transition state and the catalyst phenyl group. Numbers represent the distances of key noncovalent interactions in Å, with the number in red corresponding to the cation– $\pi$  interaction.

The catalysis of the Claisen rearrangement relies on the selective catalyst stabilization of transition state bearing a relatively small degree of charge separation. In principle, cooperative catalysis with cation– $\pi$  and H-bonding interactions can be accentuated in reactions involving ion pair intermediates bearing full formal charges. Centered around this hypothesis, Jacobsen and coworkers developed a family of thiourea catalysts (**16**) bearing precisely positioned aromatic substituents. In the crystal structures of these catalysts binding to tetramethylammonium chloride, the aryl group and the H-bond donor motif are held by the amido acid linker in positions favorable for binding an ion pair species, and the ammonium and chloride ions are accommodated into the catalyst pocket nicely by associating with the  $\pi$ -face of the aromatic group and the thiourea, respectively (Figure 1-9).

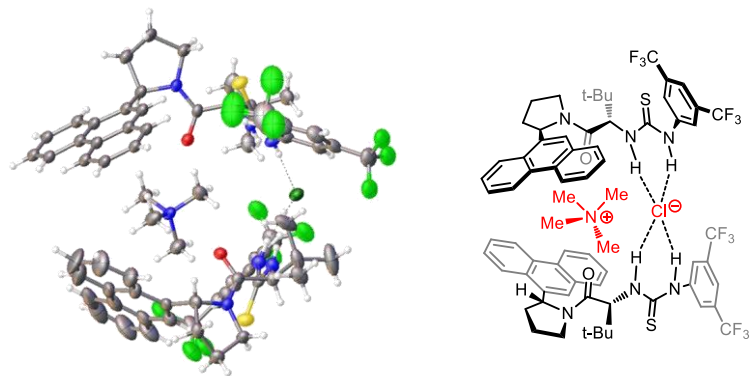


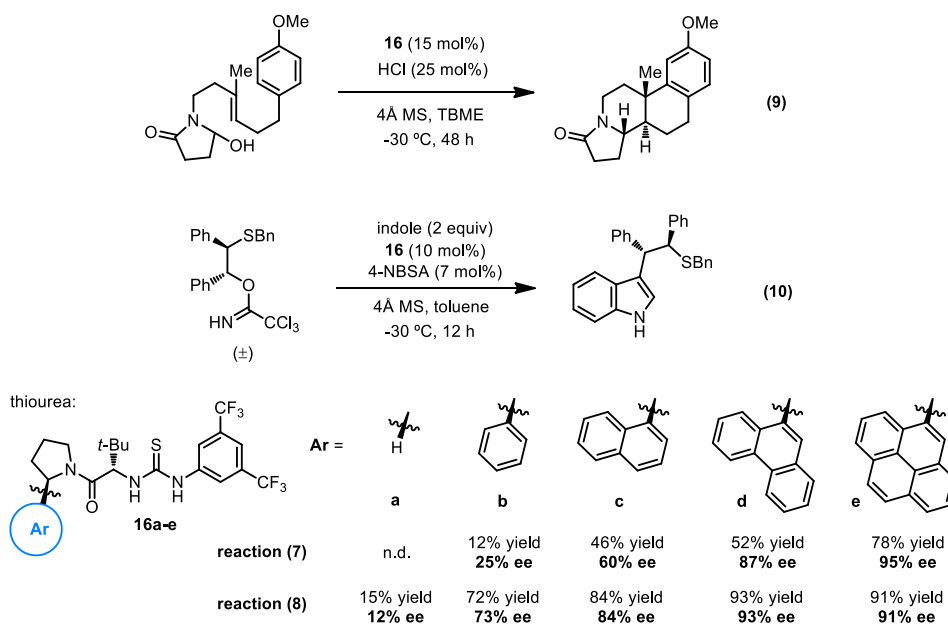
**Figure 1-9.** Crystal structure of thiourea **16d** binding to tetramethylammonium chloride in the solid phase with a 2:1 stoichiometry. Chemdraw representation is shown on the right.

The binding between tetramethylammonium chloride and thiourea implies that transition states comprising ion pairs can in principle be recognized by the catalyst, with selectivity imparted through the chiral environment created by the binding site. This concept was first proved in a cationic polycyclization of hydroxylactam derivatives (Scheme 1-15, eq. 9).<sup>55</sup> Through catalyst structure investigation, Jacobsen et al. observed an intriguing correlation between the size of the aromatic group on the thiourea and the enantioselectivity of reaction, with more expansive catalyst providing the product in higher ee. Given the cationic nature of the reaction and fact that larger polycyclic aromatic hydrocarbons bind cations more strongly than their smaller analogs, this trend suggested that stabilizing cation– $\pi$  interactions profoundly influence the degree of asymmetric induction.

Several experimental results and observations offer support for this hypothesis. Eyring analysis reveals that the enantioselectivity of reaction is controlled by enthalpy, and linear free-energy relationships were established between  $\ln(er)$  and the polarizability or the quadrupole moment of the aromatic substituents. Both results are evident of an attractive cation– $\pi$  interaction

<sup>55</sup> Knowles, R. R.; Lin, S.; Jacobsen, E. N. *J. Am. Chem. Soc.* **2010**, *132*, 5030–5032.

between the transition state and the catalyst dictating the stereochemical outcome of the cyclization cascade.



**Scheme 1-15.** Thiourea-catalyzed enantioselective polycyclization (eq. 9) and ring-opening of episulfonium ions (eq. 10).

To extend the scope of this synergistic noncovalent catalysis, the Jacobsen group subsequently developed a desymmetrization of *meso*-episulfonium ions with indole derivatives (Scheme 15, eq. 10).<sup>56</sup> The enantioselectivity of the reaction was again shown to correlate with the expanse of the aryl residue on the catalyst. The fact that both the rate-limiting and the enantio-determining steps are the indole addition to the episulfonium ion allows elucidation of the role of the catalyst aromatic group in the reaction mechanism by absolute rate comparisons of different catalysts. As shown in Figure 1-10, the reaction rate and enantioselectivity data exhibit a significant positive correlation in the pathway leading to the major enantiomeric product. This provides unambiguous evidence that enantioselectivity increases because variations of the aryl component of the catalyst **16** are, indeed, tied to stabilization of the major transition structure.

<sup>56</sup> Lin, S.; Jacobsen, E. N. *Nat. Chem.* **2012**, *4*, 817–824.

To further understand the mechanism of stereoselection guided by the catalyst aromatic group, DFT calculations were conducted with a simplified system involving catalyst **17** (Figure 1-11).<sup>57</sup> The sense of stereoselection was correctly predicted with a differential energy of activation of 3.1 kcal/mol. The noncovalent interactions present between the catalyst and the reactant assembly were visualized in the two diastereomeric transition structures using NCIPLLOT, a program specifically developed for such purpose.<sup>58</sup> In this analysis, an attractive interaction was revealed in the major transition state in between the  $\pi$ -face of the phenanthryl group on **17** and the episulfonium motif, which is almost completely absent in the minor pathway. Taken together, the data constitute compelling evidence that the difference in the strength of the cation– $\pi$  interaction in the two diastereomeric pathways lies at the center of the high enantioselectivity observed.

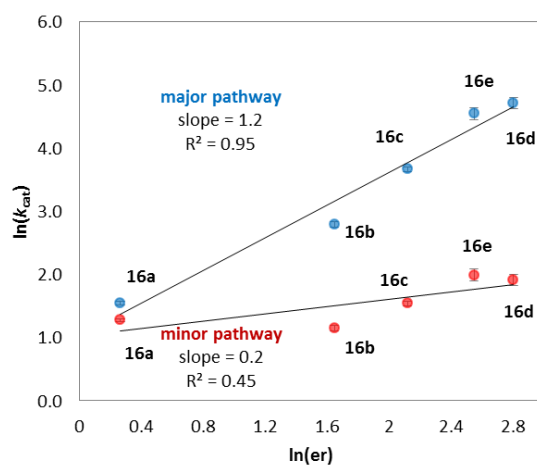


**Figure 1-10.** Correlation between rate and selectivity data in the episulfonium ion ring-opening reaction.

<sup>57</sup> Lin, S.; Jacobsen, E. N. *Manuscript in preparation*.

<sup>58</sup> (a) Johnson, E. R.; Keinan, S.; Mori-Sánchez, P.; Contreras-García, J.; Cohen, A. J.; Yang, W. *J. Am. Chem. Soc.* **2010**, *132*, 6498–6506; (b) Contreras-García, J.; Johnson, E. R.; Keinan, S.; Chaudret, R.; Piquemal, J.-P.; Beratan, D. N.; Yang, W. *J. Chem. Theory. Comput.* **2011**, *7*, 625–632.

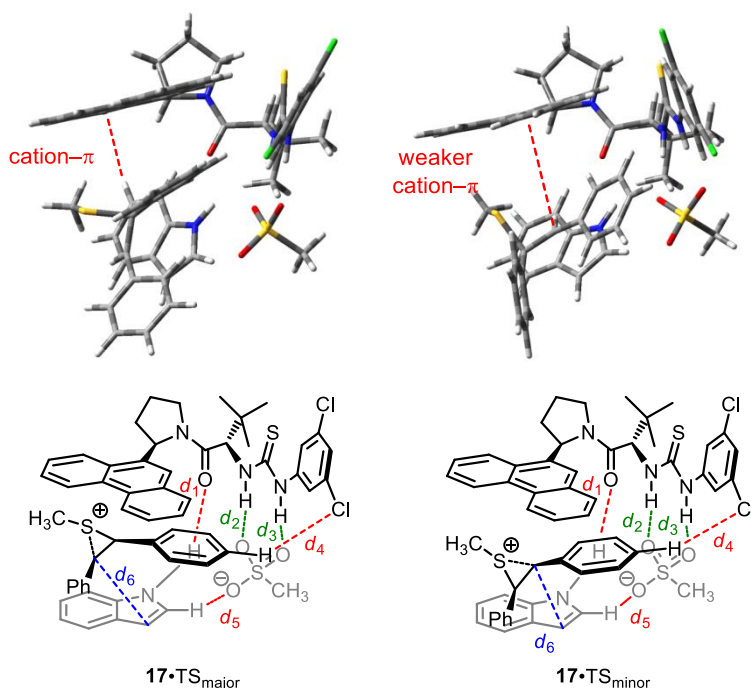


**Figure 1-11.** Calculated structures of the major (left) and minor (right) transition states involving catalyst **17**. Calculations were performed using Gaussian 09 with the M05-2X/6-31G(d) level of theory. Distances in the calculated structures: major TS –  $d_1 = 2.03 \text{ \AA}$ ,  $d_2 = 1.89 \text{ \AA}$ ,  $d_3 = 1.85 \text{ \AA}$ ,  $d_4 = 3.20 \text{ \AA}$ ,  $d_5 = 2.14 \text{ \AA}$ ,  $d_6 = 2.60 \text{ \AA}$ ; minor TS –  $d_1 = 2.11 \text{ \AA}$ ,  $d_2 = 1.82 \text{ \AA}$ ,  $d_3 = 1.86 \text{ \AA}$ ,  $d_4 = 3.25 \text{ \AA}$ ,  $d_5 = 2.15 \text{ \AA}$ ,  $d_6 = 2.68 \text{ \AA}$ .

After the initial disclosure of this family of arylpyrroline-derived thiourea catalysts, chemistry developed under its umbrella has been flourishing in the Jacobsen group. Highly enantioselective reactions catalyzed by these small molecules and their close analogues include acylation of silyl ketene acetals via *N*-acylpyridinium ions<sup>59</sup>, alkylation of oxocarbenium ions<sup>60</sup>, aza-Sakurai cyclization via *N*-acylimminium ions, photoredox alkylation of isoquinolines<sup>61</sup>, selenocyclization reactions and Cope-type hydroamination<sup>62</sup>.

To bring the story full cycle, the pyrenylpyrrolidine-derived thiourea catalyst **15e** has recently been discovered to catalyze the enantioselective alkylation of  $\beta$ -ketoesters with

<sup>59</sup> Birrell, J. A.; Desrosiers, J-N; Jacobsen, E. N. *J. Am. Chem. Soc.* **2011**, *133*, 13872–13875.

<sup>60</sup> Reisman, S. E.; Doyle, A. G; Jacobsen, E. N. *J. Am. Chem. Soc.* **2008**, *130*, 7198–7199.

<sup>61</sup> Bergonzini, G.; Schindler, C. S.; Wallentin, C.-J.; Jacobsen, E. N.; Stephenson, C. R. *J. Chem. Sci.* **2013**, *Accepted Manuscript*.

<sup>62</sup> Brown, A. R.; Uyeda, C.; Brotherton, C. A. Jacobsen, E. N. *J. Am. Chem. Soc.* **2013**, *30*, 6747–6749.

alkyldiarylsulfonium ions as the alkylating agent.<sup>63</sup> This advance has clearly drawn inspiration from both the biosynthetic mechanism of SAM and the demethylation of sulfonium salts by Dougherty et al., and is anticipated to encourage the application of this biomimetic approach in the catalysis of other organic transformations involving cationic intermediates.

---

<sup>63</sup> Kedrowski, S. M. A.; Jacobsen, E. N. *Unpublished results*.

## 1.7 Miscellaneous

In addition to the extensively explored programs outlined in the preceding sections, a few other reports have invoked the importance of cation- $\pi$  interactions in tuning the reactivity and selectivity of small molecules catalysts. This section summarizes two systems in which experimental and/or theoretical evidence were provided to support such a notion.<sup>64</sup>

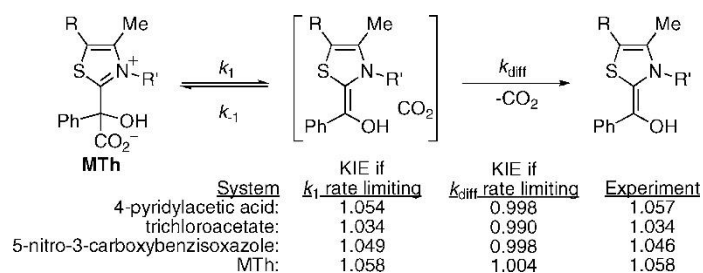
Singleton studied the decarboxylation of mandelinthiamine catalyzed by pyridinium ion in water through textbook-like classical KIE analysis (Scheme 1-16).<sup>65</sup> In an earlier report, Kruger proposed that the reaction undergoes a pre-equilibrium between the substrate and the decarboxylation product followed by rate-limiting diffusion of CO<sub>2</sub>, and that the role of pyridinium ion is to protonate the enolate product and prevent CO<sub>2</sub> rebound.<sup>66</sup> Skeptical of this original mechanistic proposal, Singleton compared the experimental KIE with the predicted values using DFT functional, finding that in fact, the decarboxylation possesses the highest energy barrier. Through DFT modeling, the role of pyridinium ion in the promotion of the decarboxylation process was identified as binding to the enolate oxygen via H-bonding as well as stabilizing negative charge built up on the phenyl group or the thiazole via cation- $\pi$  interaction (Figure 1-12). The two-point chelation mode of binding is stated to be critical to catalysis.

---

<sup>64</sup> For other systems in which cation- $\pi$  interactions were proposed to account for the reactivity and/or the selectivity observed in small molecule catalysis, although with insufficient experimental or theoretical support, see: (a) Rueping, M.; Uria, U.; Lin, M.-Y.; Atodiresei, I. *J. Am. Chem. Soc.* **2011**, *133*, 3732–3735; (b) Frisch, K.; Landa, A.; Saaby, S.; Jørgensen, K. A. *Angew. Chem. Int. Ed.* **2005**, *44*, 6058–6063; for studies of cation- $\pi$  interactions in the context of non-catalytic reactions, see: (c) Lakshminarasimhan, P.; Sunoj, R. B.; Chandrasekhar, J.; Ramamurthy, V. *J. Am. Chem. Soc.* **2000**, *122*, 4815–4816; (d) Neda, I.; Sakhaii, P.; Waßmann, A.; Niemeyer, U.; Günther, E.; Engel, J. *Synthesis* **1999**, 1625–1632; (e) Comins, D. L.; Joseph, S. P.; Goehring, R. R. *J. Am. Chem. Soc.* **1994**, *116*, 4719–4728; (f) Krenske, E. H. *Org. Lett.* **2011**, *13*, 6572–6575; Yao, L.; Aubé, J. *J. Am. Chem. Soc.* **2007**, *129*, 2766–2767; (g) Gutierrez, O.; Aubé, J.; Tantillo, D. J. *J. Org. Chem.* **2012**, *77*, 640–647; (h) Yamada, S.; Uematsu, N.; Yamashita, K. *J. Am. Chem. Soc.* **2007**, *129*, 12100–12101;

<sup>65</sup> Gonzalez-James, O. M.; Singleton, D. A. *J. Am. Chem. Soc.* **2010**, *132*, 6896–6897.

<sup>66</sup> Kluger, R.; Ikeda, G.; Hu, Q.; Cao, P., and Drewry, J. *J. Am. Chem. Soc.* **2006**, *128*, 15856–15864.



**Scheme 1-16.** Reaction pathway of mandelinthiamine decarboxylation.

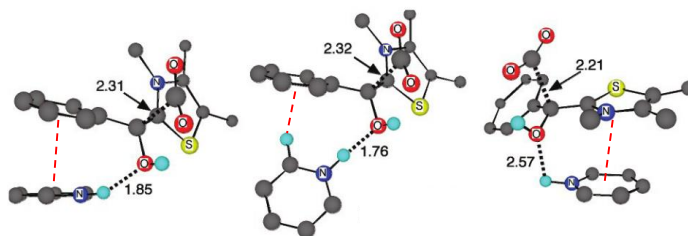


**Figure 1-12.** Three lowest energy transition structures of the decarboxylation with M06-2X/6-31G\*\*/PCM(water), showing cation- $\pi$  interactions between the phenyl group and the pyridinium (left: face-to-face, and middle: face-to-edge), or between the thiazole and the pyridinium (right: face-to-face). Red dotted lines represent the cation- $\pi$  interactions.

The last example presented in this chapter is another biomimetic system wherein an iron complex was developed as a mimic of nitrogenase and shown to be adept at weakening the N–N bond in dinitrogen (Figure 1-13).<sup>67</sup> The iron species is supported by a bidentate anionic ligand L, and bind to dinitrogen in the crystal structure as a side-on  $\eta^1$ -complex with 2:1 stoichiometry. The bond distance in nitrogen is lengthened by almost 0.1 Å. Perhaps more intriguingly in the context of this assay, the N–N bond is further stretched by up to 0.06 Å upon treating this compound with potassium metal. In the resulting complex, the  $[\text{FeNNFe}]^{2+}$  core of  $\text{LFeNNFeL}$  is reduced by two electrons to  $[\text{FeNNFe}]^0$ , and the alkali metal cations coordinate to the  $\text{N}_2$  fragment and the aryl rings of the ligand. The distance and vibrational frequencies of the N–N bond indicates a double bond character, showing substantial weakening effect by the reduction and the cation- $\pi$  interaction with  $\text{K}^+$ . Later, Holland and coworkers showed that iron complexes supported by L can break the

<sup>67</sup> Smith, J. M.; Lachicotte, R. J.; Pittard, K. A.; Cundari, T. R.; Lukat-Rodgers, G.; Rodgers, K. R.; Holland, P. L. *J. Am. Chem. Soc.* **2001**, 123, 9222–9223.

N–N triple bond in  $N_2$  and reduce it to ammonia in the presence of  $H_2$ .<sup>68</sup> Although this example doesn't fall into the category of catalytic reactions involving cation– $\pi$  interactions, it reminds one that the Haber-Bosch catalyst typically contains potassium “promoter” that is known to contribute to  $N_2$  binding.

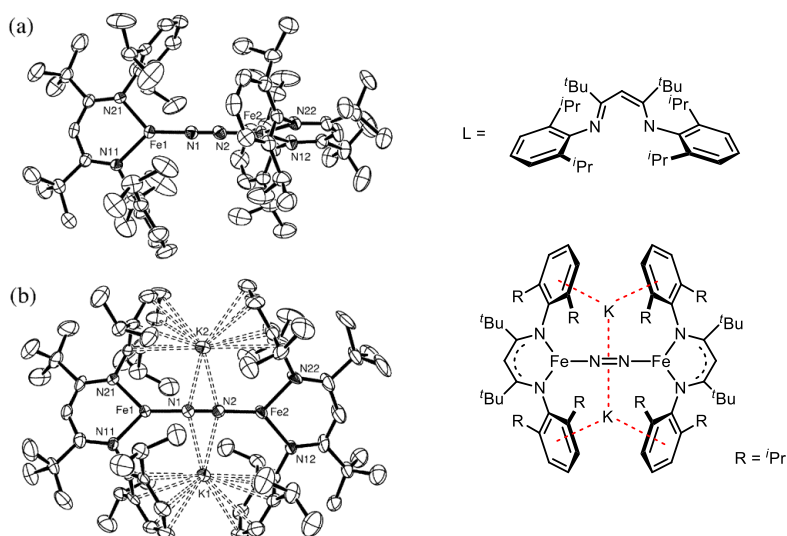


**Figure 1-13.** Crystal structures of complexes  $[LFeN=NFeL]$  (a) and  $K_2[LFeN=NFeL]$  (b). In (a), N–N distance is 1.182(5) Å, and in (b) N–N distance is 1.233(6) Å. Chemdraw depictions of ligand L and complex  $K_2[LFeN=NFeL]$  are shown on the right. Red dotted lines represent the cation– $\pi$  interactions.

<sup>68</sup> Rodriguez, M. M.; Bill, E.; Brennessel, W. W.; Holland, P. L. *Science* **2011**, 334, 780–783.

## 1.8 Summary and Outlook

Since its discovery in 1980s, the cation- $\pi$  interaction has become increasingly important in many fields of chemical sciences. Grounded on extensive elucidation of the thermodynamic characters of the cation- $\pi$  interaction, chemists have recently become captivated in exploring the potential of such interaction in stabilizing high energy transition structures and controlling the kinetics and selectivity of chemical reactions. In this chapter, we presented a few case studies on relatively well-understood systems regarding small-molecule catalysis in which the nature of the cation- $\pi$  interaction has been carefully examined and comprehensively elucidated. In addition to classical experimental physical organic methods that can precisely quantify the properties of the cation- $\pi$  interaction, modern computational methods have empowered chemists to vividly discern the nature and the role of this interaction in binding and catalysis. Despite of the substantial efforts we have devoted to understanding this noncovalent interaction in the context of small-molecule catalysis and applying it in rational catalyst design, the field still remains largely underdeveloped. The relatively weak nature of the cation- $\pi$  interaction still obscures the dissection of it from a complicated binding event. We anticipate that the work summarized in this chapter will raise the attention of chemical community on the potential power of the cation- $\pi$  interaction in the design of catalytic systems for selective organic transformations. In addition, we hope that the development of new reaction based on this strategy will in turn lay ground for further understanding of this intriguing noncovalent interaction.

# *Chapter Two*

## **Enantioselective Thiourea-Catalyzed Polycyclizations**

### **2.1 Introduction**

The polyene cyclization arguably constitutes the most efficient method for the increase of structural complexity in organic synthesis. This reaction constructs polycyclic hydrocarbon architectures from linear precursors in one operation, setting up an array of stereogenic centers. Precise control over the selectivity of this process with respect to both the structure and the stereochemistry would greatly increase the synthetic value of this reaction. Nature's terpene synthases set a transcendent standard in this regard, catalyzing polycyclization cascades with remarkable rate acceleration and exquisite selectivity. The field of terpene synthesis has been largely influenced by the biosynthetic mechanism of these enzymes, with major emphasis on tuning the steric and electronic properties of the polyene scaffolds to yield the desired constitutional and stereochemical outcome via substrate-control of the reaction pathway.

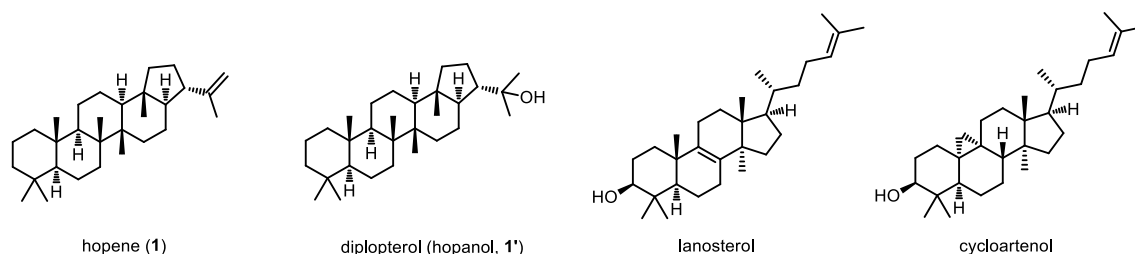
As suggested by the biosynthetic pathway, catalyst-control of the polycyclization reactions represents an attractive alternative approach to achieving non-enzymatic cyclic terpene synthesis.

This strategy not only allows the use of less contrived, more generic polyene precursors, but also provides the opportunity of inducing enantioselectivity. Although seminal progress on catalytic asymmetric polycyclization has been made in the past few years, this field remains largely underdeveloped.

In this chapter, we present the development and mechanistic study of an enantioselective polycyclization catalyzed by multifunctional thioureas. The logic behind the catalyst design has drawn important inspiration from squalene cyclases, a family of enzymes that promotes cationic terpene synthesis.

## 2.2 A Case Study – Squalene–Hopene Cyclase

The enzyme-catalyzed cyclization of terpenes via carbocationic transition states gives rise to numerous natural products, more than 25,000 of which have been discovered to date. In particular, the cyclization of the triterpenes squalene and 2,3-oxidosqualene into various polycarbocyclic compounds has intrigued chemists for half a century.<sup>1</sup> These enzymatic polycyclization reactions proceed with precise stereo- and regio-selectivity to construct multiple C–C bonds leading to a variety of triterpenoid carbocyclic skeletons, including hopene (bacteria), lanosterol (vertebrates and fungi), and cycloartenol (plants) (Scheme 2-1).



**Scheme 2-1.** Steroids produced in nature by squalene and oxidosqualene cyclases.

The importance of understanding the catalytic mechanism of these terpene cyclases is twofold. First, it provides information for the development of small molecule inhibitors that are capable of blocking the synthesis of steroids detrimental to human health, such as cholesterol. Second, it may guide the discovery of both engineered artificial enzymes and biomimetic small molecules that are capable of generating unnatural polycyclic hydrocarbons for drug discovery.

Although special attention has long been paid to the functional mechanism of squalene hopene cyclase (SHC) and 2,3-oxidosqualene cyclase (OSC), rapid progress in this field has occurred only in the last two decades as a result of advances in molecular-biological technologies.<sup>2</sup>

<sup>1</sup> (a) Abe, I.; Rohmer, M.; Prestwich, G. D. *Chem. Rev.* **1993**, 93, 2189–2206; (b) Seckler, B.; Poralla, K. *Biochem. Biophys. Acta.* **1986**, 881, 356–363.

<sup>2</sup> Hoshino, T.; Sato, T. *Chem. Commun.* **2002**, 291–301.

X-ray crystallography data of SHC and OSC were first obtained in 1997 and 2005, respectively, and structural determination of these enzymes has prompted extensive research on their function using methods such as site-selective mutagenesis.<sup>3</sup> The black box surrounding these fascinating enzymatic polycyclizations has been gradually uncovered since then. Studies have shown that these two enzymes have related peptide sequences, similar spatial structures, as well as analogous functions in the cyclization reactions. In this section, we conducted a case study on the mechanism of SHC-catalyzed polycyclization cascade through literature reviewing.<sup>4</sup>

### 2.2.1 Crystallographic Studies

SHC from *Alicyclobacillus acidocaldarius* has been crystalized and its structure determined at 2.9 Å resolution (Figure 2-1).<sup>5</sup> The crystal structure reveals the presence of a dimeric enzyme (Figure 2-1A), with each subunit consisting of 631 amino acid residues. The active site is located in the large 1200 Å central cavity, as indicated by the bound competitive inhibitor *N,N*-di-methyldodecylamine-*N*-oxide (LDAO) (inhibition constant  $K_i = 50.14$  mM) (Figures 1B, 2A). The central cavity can be accessed through a nonpolar channel between the helices of domain 2. A large and rather mobile nonpolar plateau on the protein surface surrounds the channel entrance (Figure 2-2B). This plateau has a solvent-accessible surface of about 1600 Å<sup>2</sup> and is encircled by a ring of positively charged residues, which suggests that the plateau plunges into the nonpolar center of a membrane, whereas the ring forms salt bridges with the displaced phospholipid and sulfolipid head groups. Such a model explains how the substrate squalene diffuses from the membrane interior, where it is dissolved into the central cavity.

---

<sup>3</sup> Feil, C.; Sussmuth, R.; Jung, G.; Poralla, K. *Eur. J. Biochem.* **1996**, *242*, 51–55.

<sup>4</sup> (a) Reinert, D. J.; Balliano, G.; Schulz, G. E. *Chem. Biol.* **2004**, *11*, 121–126; (b) Siedenburg, G.; Jendrossek, D. *Appl. Environ. Microbiol.* **2011**, *77*, 3905–3915.

<sup>5</sup> Wendt, K. U.; Poralla, K.; Schulz, G. E. *Science* **1997**, *277*, 1811–1815.

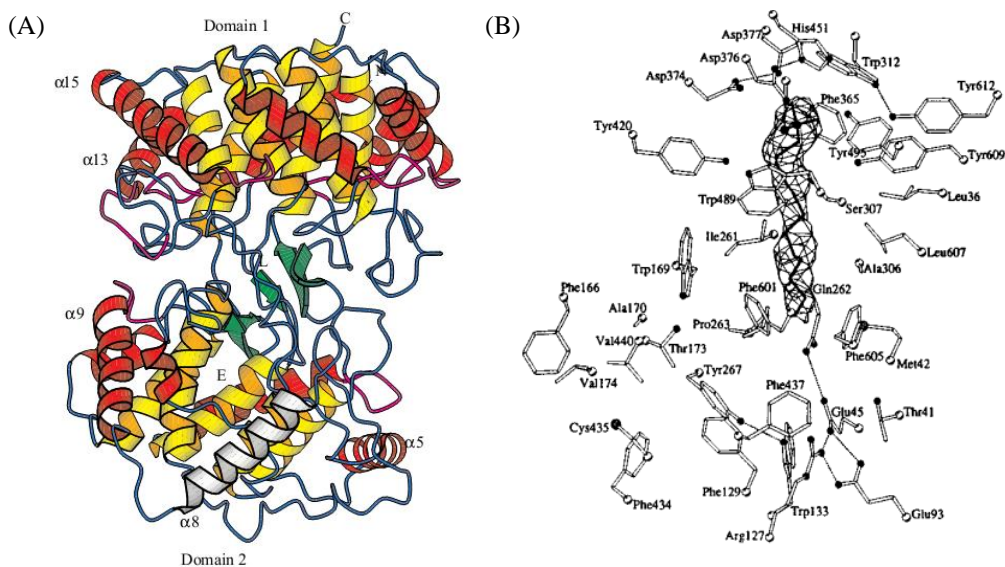


**Figure 2-1.** (A) Stereoview of squalene-hopene cyclase chain fold with labeled NH<sub>2</sub>- and CO<sub>2</sub>H-termini (N and C), inhibitor position (L), and channel entrance (E); (B) Stereoview of the active site cavity with the inhibitor LDAO with amino acid residues drawn out.

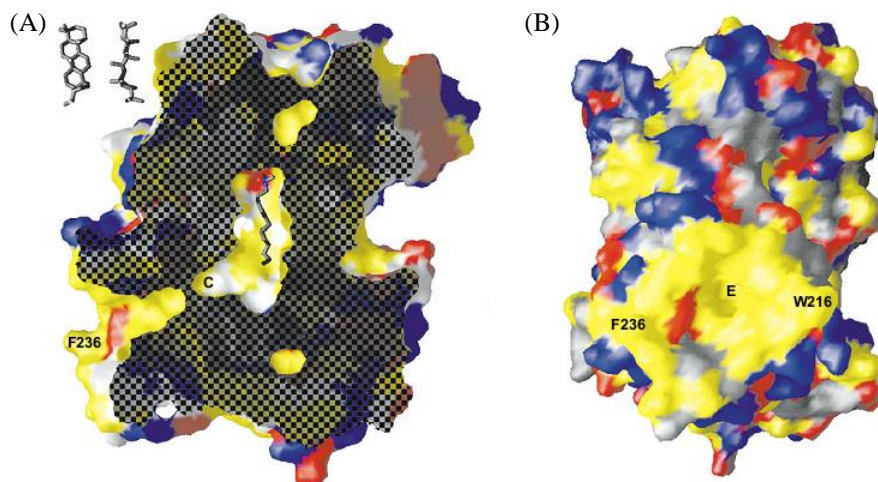


**Figure 2-2.** Squalene-hopene cyclase. The color-coded surface representations nonpolar (yellow), positive (blue), and negative (red) areas. (A) Showing the large internal cavity with the bound inhibitor LDAO and the nonpolar channel with the channel constriction C. At the upper left, hopane (two views) is shown at scale. (B) Showing the only large nonpolar plateau and the channel entrance E at its center.

In SHC, the channel between the nonpolar plateau and active site contains a constriction formed by four amino acid residues, which appears to block the entrance of substrate (Figure 2-2A). However, the high mobility of these residues allows the constriction to behave as a gate that permits substrate passage.

The central active site cavity is mainly nonpolar, but it has a highly polar patch at the top, with sequence motif DXDD (D = aspartic acid; X = any amino acid). The rest of the pocket is lined by numerous aromatic residues that could stabilize the carbocationic intermediates of the cyclization reaction by their  $\pi$ -electrons (*vide infra*). The residues lining the cavity are well conserved but show a gradient with highest conservation at the top and lowest at the bottom. This gradient indicates that the first reaction step common to SHC and OSC occurs at the polar top of the cavity and that the variable features are at the bottom. Accordingly, the initially protonating acid (B1:H) should be at the top (*vide infra*), base B2 of SHC should accept a proton at the bottom end of the cavity, and base B2 of the OSC should be near to the center of the substrate where proton uptake from the lanosteryl cation is expected.

### 2.2.2 Stepwise Nature of the Cyclization Cascade

The mechanism of the cyclization cascade has been the subject of lively discussion. The majority of early suggestions favored a concerted process, whereas current hypotheses implicate a series of carbocationic intermediates.<sup>6</sup> Although the concomitant cyclization pathway provides the simplest explanation to account for the exquisite diastereoselectivity of the reaction, energetically disfavored anti-Markovnikov additions are involved in such a process. In his early work on carbenium-induced cyclizations, Stork acknowledged the possibility of “mixed single-transition-state polycyclizations separated by discrete carbenium ion intermediates”.<sup>7</sup> An analogous hypothesis was also advanced by Eschenmoser *et. al.* involving formation of non-classical carbocations.<sup>8</sup> Recent studies have uncovered that polycyclization reactions by SHC and

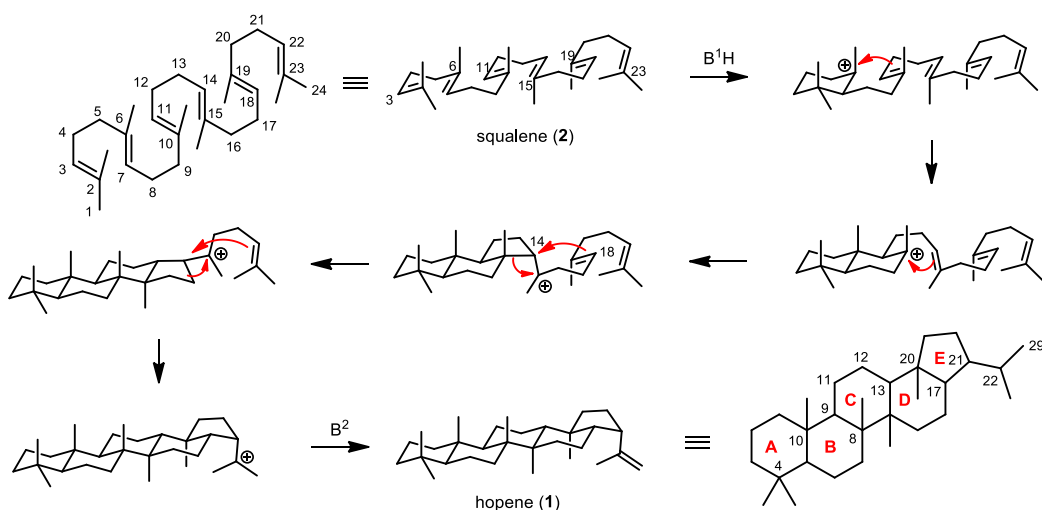
---

<sup>6</sup> Pale-Grosdemange, C.; Feil, C.; Rohmer, M.; Poralla, K. *Angew. Chem. Int. Ed.* **1998**, *37*, 2237–2240.

<sup>7</sup> Stork, G.; Burgstahler, A. W. *J. Am. Chem. Soc.* **1955**, *77*, 5068–5077.

<sup>8</sup> Stadler, P. A.; Nechvatal, A.; Frey, A. J.; Eschenmoser, A. *Helv. Chim. Acta* **1957**, *40*, 1373–1409.

OSC proceed most likely via discrete and rigidly held carbocation intermediates and ring enlargement reactions. Hoshino *et. al.* postulated that the 5-membered C- and/or D-rings are formed according to the Markovnikov rule prior to the ring expansion into the corresponding *anti*-Markovnikov 6-membered C-and/or D rings of **1**, which is shown in Scheme 2-2 in an arrow pushing formalism.<sup>9</sup> A different mechanistic proposal was put forward by Schultz and coworkers, which includes a concerted (6,6,6,5)-tetracycle formation, followed by D-ring expansion (ref. 4a). More details regarding the asynchronous mechanism including evidence obtained through site-selective mutagenesis are presented in Section 2.1.3.3.



**Scheme 2-2.** Proposed stepwise cyclization cascade. The standard numbering systems of **1** and **2** are shown, which are different from each other. The discussion in the following sections will use that for squalene.

### 2.2.3 Catalysis of Polycyclization

In this section, single-letter codes for amino acid residues are frequently used while describing their functions in the catalysis. The translation table is presented below to aid reading. In addition, the numbering of the carbon framework of all the substrates, intermediates and products follows the standard numbering system for squalene show in Scheme 2-2.

<sup>9</sup> C/D-ring expansion was shown as a separate step in ref. 2 with formation of a discrete secondary carbocation at C14/C18. In Scheme 2-2, the ring expansion processes were drawn in concomitant with the formation of the subsequent ring to avoid the intermediacy of high energy secondary carbocations.

**Table 2-1.** Natural amino acids.

name	code	name	code	name	code	name	code
Arginine	R	Threonine	T	Glycine	G	Phenylalanine	F
Histidine	H	Asparagine	N	Alanine	A	Tyrosine	Y
Lysine	K	Glutamine	Q	Valine	V	Tryptophan	W
Aspartic acid	D	Cysteine	C	Isoleucine	I		
Glutamic acid	E	Selenocysteine	U	Leucine	L		
Serine	S	Proline	P	Methionine	M		

### 2.2.3.1 Substrate Recognition

Following intake of squalene from the entrance of the active site, the substrate recognition and optimal folding are primarily achieved through hydrophobic interactions,  $\pi$ - $\pi$  stacking and steric constriction.

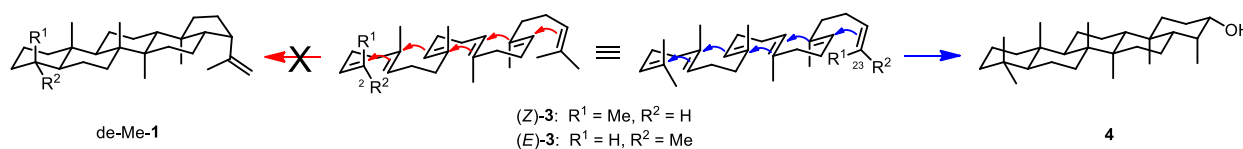
**Hydrophobic interactions.** Modifications – demethylation at a few specific sites on the substrate squalene led to diminished substrate binding and/or altered product distribution. These results led Hoshino et. al. to propose that methyl-binding sites of the enzyme have specific sizes to allow precise accommodation of each of these methyl groups through hydrophobic interactions.<sup>10</sup>

For instance, the two terminal methyl groups (at C2) are indispensable for the initiation of the cyclization cascade, as C2-demethylation resulted in no observation of the C2-demethyl steroids (Scheme 2-3). Instead, in the incubation mixture, (6,6,6,6,6)-fused pentacycle tetrahymanol **4** was observed as the major product. The E-ring formation of **4** is presumably favored by stereoelectronic control of the substrate. A weakened hydrophobic interaction in the absence of the methyl group was proposed to be responsible for the alteration of the reaction mechanism. Interestingly, C23-demethylhopene was generated as a minor product with (*Z*)-**3** as

---

<sup>10</sup> This hydrophobic binding argument was suggested by Hoshino in ref. 2. However, change of reaction pathway as a result of demethylation can also be due to decrease in electronic stabilization of the carbocation intermediates by the methyl groups.

the substrate, but not with (*E*)-**3**, showing the C23 *Z*-methyl group interacts more strongly with the binding site compared to the *E*-methyl group.



**Scheme 2-3.** SHC-catalyzed cyclization with demethylsqualenes.

**$\pi$ - $\pi$  interactions.** A few aromatic side chains in the active site were shown to be important to the binding of the polyene substrate. Mutants W169V and W312L exhibit no cyclase activity, while W169F enabled the recovery of enzyme activity, but with decreased activities (Table 2-2). This is due to the loss in substrate-binding affinity ( $K_m$  of W169F and W312F substantially increased), instead of decrease of the reaction rate. These data are consistent with the hypothesis that W312 and W169 residues function in the binding of squalene. In addition to hydrophobic attraction,  $\pi$ - $\pi$  stacking interactions between these aromatic amino acids and the alkene units in close proximity to them can also contribute to the substrate binding.

**Table 2-2.** Substrate binding and reactivity of SHC mutants (incubated at 30°C, pH 6.0, for 60 min).

entry	mutation pattern	$K_m/\mu\text{M}$	$k_{\text{cat}}/\text{min}^{-1}$
1	Wild-type	16.7	6.43
2	W169V	-	-
3	W169F	276	5.43
4	W312L	-	-
5	W312F	55.1	5.86

**Steric constrictions.** Evidence has been obtained that the steric bulk of the amino acid residue I261 controls the stereochemical outcome. The replacement of I261 by less bulky Ala or Gly resulted in the accumulation of products with an unusual  $\alpha$ -configuration for 13H and 17H.

### 2.2.3.2 Initiation of the Cyclization

Squalene-hopene cyclase was also co-crystallized with a substrate analogue, 2-azasqualene, and analyzed by X-ray diffraction to 2.13 Å resolution. The tertiary amine of the analog forms a salt bridge to D376 at the top of the active center cavity, indicating this aspartic acid residue may serve to initiate the cyclization by protonation of the double bond.

Indeed, the mutation of D376N resulted in a complete loss of activity (Table 2-3). H451 was confirmed to function as a proton donor to enhance the acidity of D376 upon protonation by the adjacent D374: the cyclase activity of the H451F mutant was completely lost, while H451R retained the activity to some extent. It was also suggested that the residues of D313 and D447 may facilitate initiation of the cyclization reaction.

**Table 2-3.** Substrate binding and reactivity of SHC mutants (incubated at 60 °C (entries 1-2), 30 °C (entries 3-5) or 45 °C (entries 6-7), pH 6.0).

entry	mutation pattern	$K_m/\mu\text{M}$	$k_{\text{cat}}/\text{min}^{-1}$
1	Wild-type	16.7	289
2	D376N	-	-
3	Wild-type	16.7	6.43
4	H451F	-	-
5	H451R	16.9	1.22
6	Wild-type	16.2	51.8
7	Y495A	17.2	28.7

The mutant Y495A displayed degraded reactivity with little change in  $K_m$  value and no abortive cyclization product. It has been pointed out that the phenolic hydroxy group of Y495 may further enhance the D376 acidity for initial protonation through a hydrogen-bond with a water molecule. Re-protonation of D376 is suggested to occur also through this H-bond network which is ultimately connected to the cytosol.

### 2.2.3.3 Stabilization of Various Cationic Intermediates and Transition States

During his work in steroid total synthesis, in 1987 Johnson advanced the notion of point charge stabilization for the enzymatic polycyclization, predicting an electronic role of the active site in alleviating the positive charges built up at different positions of the substrate.<sup>11</sup> This hypothesis was later corroborated by mutagenesis studies by Hoshino, Poralla and others (refs. 2 & 3).

Site-specific mutants of D377N or D377C gave abortive cyclization product **5** (Scheme 2-4), indicating that this motif is arranged in proximity to the initiation site in the active cavity and that D377 is likely to stabilize first cyclized carbocation intermediate at C6.

The incubation of **2** with the cell-free homogenates of the mutant F365A afforded bicyclic compounds **6** and **7** in large quantity without completion of the polycyclization reaction, indicating that the F365 is placed on bicyclic carbocation at C10, which is stabilized via the interaction between the intermediary cation and the  $\pi$ -electrons of F365. Based upon this presumption, the mutant F365Y was examined and it completed the polycyclization reaction leading to final product **2** without any abortive cyclization product while exhibiting a remarkable increase in the reaction rate (Table 2-4). F365Y produced **1** even at a temperature as low as 10 °C, where the wild-type SHC has no activity. The significantly increased reaction rate through electronic tuning of the phenyl side chain strongly suggests that the cation- $\pi$  interaction is operative for the polycyclization reaction. The occurrence of a looser binding ( $K_m$ ) might be due to the introduction of steric bulk (-OH) at *para*-position of the phenyl ring.

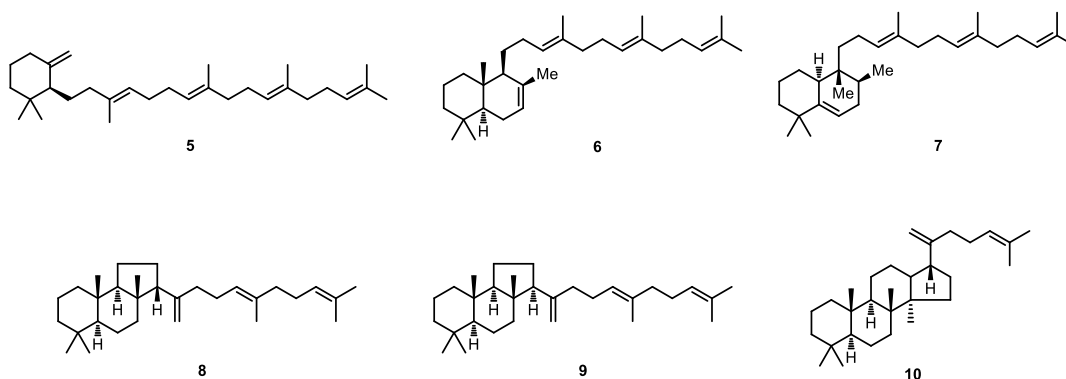
---

<sup>11</sup> Johnson, W. S.; Telfer, S. J.; Cheng, S.; Schubert, U. *J. Am. Chem. Soc.* **1987**, *109*, 2517–2518.

**Table 2-4.** Substrate binding and reactivity of SHC mutants (incubated at 30 °C and pH 6.0).

entry	mutation pattern	$K_m/\mu\text{M}$	$k_{\text{cat}}/\text{min}^{-1}$
1	Wild-type	16.7	6.43
2	F365A	-	-
3	F365Y	502	266
4	F605A	-	-
5	F605Y	22.6	14.4
6	F605W	23.2	22.9

The mutant F601A gave one (6,6,6,5)-tetracycle **10** and two (6,6,5)-tricycles **8** and **9** along with final products **1** and **1'**. Isolation of these intercepted cyclization products led to the proposition that the ring expansion process from 5-membered to 6-membered ring occurs with respect to the C- and D-ring formation in **1**. The computational studies suggest that the most favorable placement of the aromatic ring on the secondary cation at C14 and C18 may facilitate the ring expansion reaction from the thermodynamically favorable tertiary cation, which is presumably the pivotal role of F601.



**Scheme 2-4.** Abortive cyclization products generated with SHC mutants lacking certain aromatic side chains.

The F605A mutant afforded a number of triterpenes consisting of (6,6,5)-tricyclic, (6,6,6,5)-tetracyclic, and (6,6,6,6,5)-pentacyclic skeletons, while the quantities of these abortive cyclization products produced by the mutants F605Y and F605W were negligible. The enhanced cyclization rate by the Y and W mutants, compared to the wild-type, indicated that the F605 residue

may facilitate the ring expansion as a result of the stabilization of the secondary cation at C18 as well as the hopanyl cation at C23, possibly via the cation– $\pi$  interaction (Table 2-3).

Studies also show that Y609 and Y612 may intensify the stabilizing function of D377 and F365, possibly by placing D377 and F365 at positions sufficiently favorable for stabilizing the carbocation intermediates.

#### **2.2.3.4 Termination of the Cascade and Product Release**

Terminating base B2 of SHC should be located at C24 of the hopanyl cation, which is near to the last carbon of inhibitor LDAO, where the protein offers no suitable residue. Because the reported SHC shows a side reaction resulting in about 10% diplopterol (hopanol) **1'**, it was suggested that B2 is a water molecule X1 incorporated in the enzymatic pocket.

Water X1 has never been observed in any SHC structure, indicating that it has no defined binding site. However, after the hopanyl cation has been formed, there is enough space in the cavity to accommodate water X1 with a hydrogen bond to another water molecule X2, which is in turn fixed by Glu45 and Gln262. Water X2 is visible in several SHC structures and connected via a chain of four water molecules to the cytosol. Therefore, the proton accepted by X1 is easily transferred to the cytosol, completing the reaction.

The final deprotonation reaction to form **1** has been verified to be from the *Z*-methyl group at C23 instead of the *E*-methyl group via deuterium-labeling experiments.

Release of hopene into membrane is also proposed to occur through the substrate-uptake channel. The increased size of the product compared to the substrate may introduce steric encumbrance during its ejection. However, such problem can be overcome by the considerable energy (ca. 48 kcal/mol) dissipated from the cyclization cascade.

### **2.2.3.5 Reinforcement of the Protein Structure**

The SHC contains eight QW-sequence motifs that connect the outer barrel helices. These units are responsible for reinforcement of the protein structure against thermal denaturation by the unusually high energy liberated during the cyclization process.

The mutations targeted at several QW motifs afforded significantly lower optimal temperature for the enzyme catalysis.

### **2.2.4 Conclusion**

The terpene synthesis via cationic cyclization cascades of linear polyenes had once been considered one of the most complicated transformations in nature, not only constructing polycyclic hydrocarbon framework in one operation with high efficiency, but also setting up multiple stereogenic centers with precise selectivity. Recently, the mechanism of such enzymatic processes has been uncovered, which is strikingly simple, yet exquisitely organized (Figure 2-3). The most fascinating part of this biosynthetic pathway is perhaps the integral role of the  $\pi$ -electrons expansively distributed inside the wall of the enzyme cavity. With the remarkable reactivity and the superb selectivity, squalene cyclases certainly have demonstrated the most delicate use of the cation- $\pi$  interaction in catalysis.

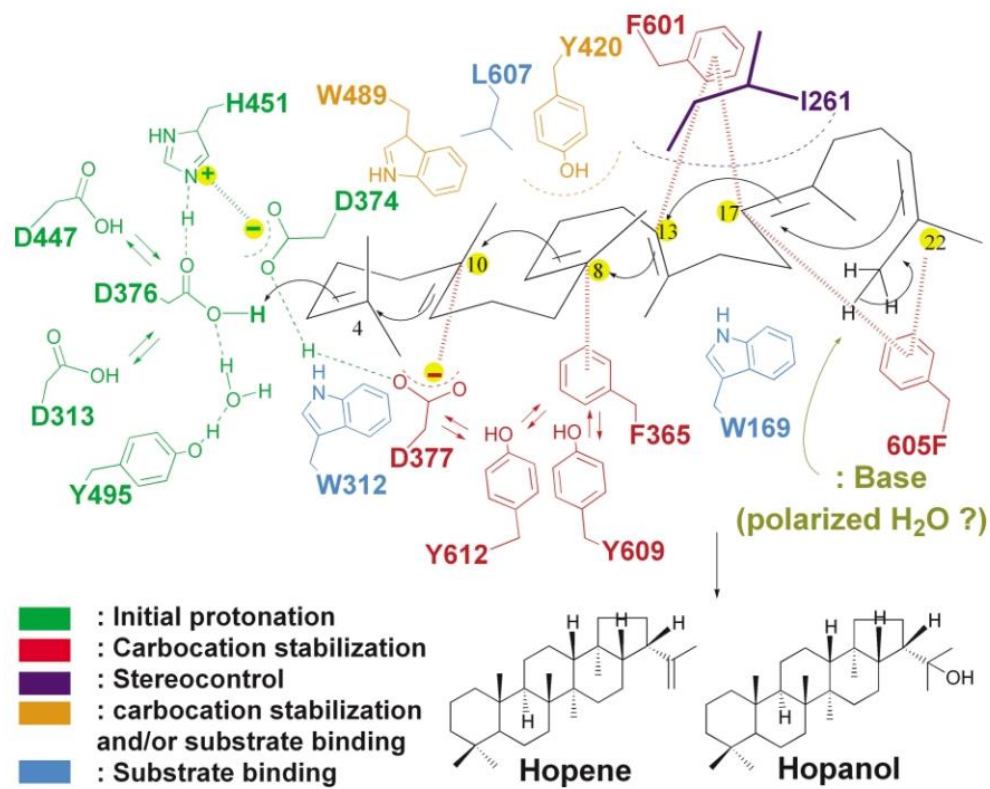


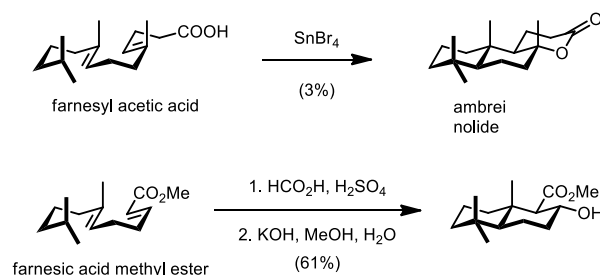
**Figure 2-3.** Cartoon representation of catalysis of polycyclization by SHC. The numbering system in this figure follows the standard numbering of hopene, and is different from that used in this chapter. The interconversion between the two numbering systems is shown in Scheme 2-2.

## 2.3 Polycyclization in Complex Target Synthesis

Development of synthetic organic approaches for biomimetic polycyclizations has captivated chemists for more than half a century. Inspirations have been drawn from the enzymatic polycyclization that imparts exquisite selectivity in a multiple carbon-carbon bond forming cascade.<sup>12</sup>

### 2.3.1 Substrate-Controlled Polycyclization

**Strategies based on Squalene-Hopene Cyclase.** The earliest work in the area of terpene biomimetic synthesis dates back to the 1950s (refs. 7 & 8). As part of their efforts toward understanding the stereochemical outcome of the SHC polycyclizations, Stork, Eschenmoser and a few others explored synthetic models such as farnesic acid, farnesyl acetic acid and their derivatives under Brønsted/Lewis acid-catalysis (Scheme 2-5).<sup>13</sup> Bicyclic and tricyclic scaffolds can be produced with high diastereoselectivity, albeit with low to moderate efficiency.



**Scheme 2-5.** Stork's and Eschenmoser's polycyclizations.

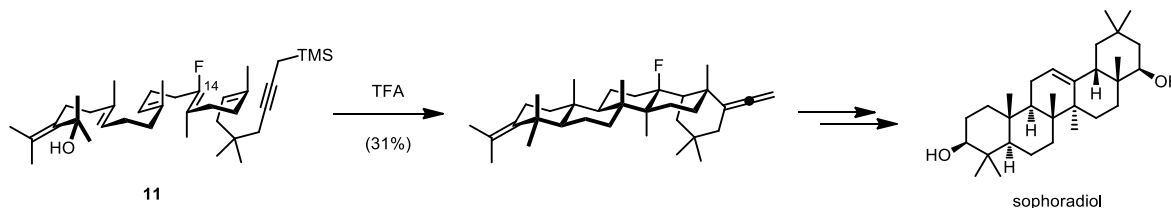
A remarkable pentacarbocyclization was developed by Johnson, which enabled a delicate biomimetic synthesis of ( $\pm$ )-sophoradiol (Scheme 2-6).<sup>14</sup> A linear polyene precursor **11** was subjected to acidic condition to form an allyl cation, which is sequentially trapped by an array of

<sup>12</sup> Yoder, R. A.; Johnston, J. N. *Chem. Rev.* **2005**, *105*, 4730–4756.

<sup>13</sup> Stadler, P.A.; Nechvatal, A.; Frey, A.J.; Eschenmoser, A. *Helv. Chim. Acta* **1957**, *40*, 1373–1409.

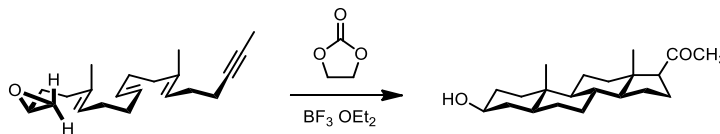
<sup>14</sup> Fish, P. V.; Johnson, W. S. *J. Org. Chem.* **1994**, *59*, 2324–2335.

olefins until terminated via desilylation. A fluorine atom was introduced to stabilize the charge buildup at C14 during the cyclization – a Markovnikov-type ring-closure to form a five member C-ring would otherwise be dominant. The product was advanced in three simple operations to the highly complex target molecule. He then applied such strategy in the synthesis of a few other polycyclic natural products.



**Scheme 2-6.** Johnson's polycyclization *en route* to sophoradiol.

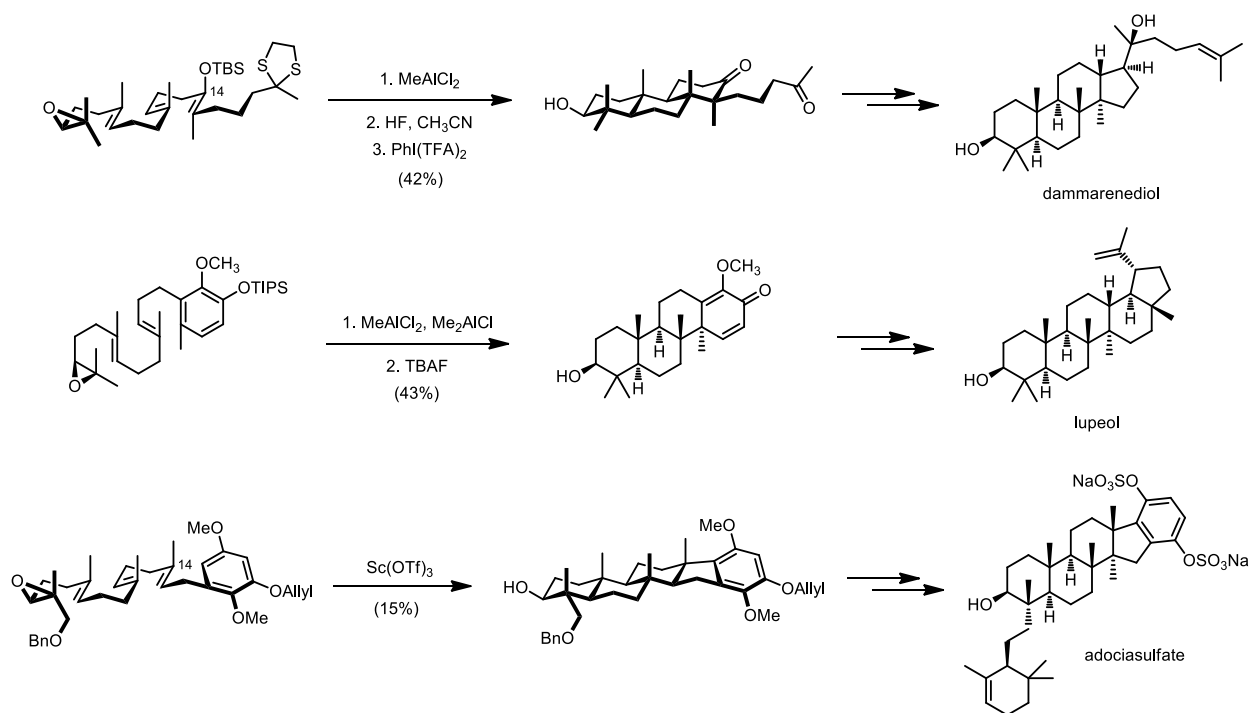
**Strategies based on Oxidosqualene Cyclase.** In van Tamelen's tetracyclization towards formation of (6,6,6,5)-fused scaffold, a terminal epoxide was used as the initiating electrophile, drawing inspiration from OSC-type enzymes (Scheme 2-7).<sup>15</sup> Stork, Corey and Overman also utilized analogous strategies to facily build the polycyclic framework of the hydroxyhopene-type natural products (Scheme 2-8).<sup>16</sup> A common feature of their cyclization reactions is the tactical substitution of the C14 proton with an electron-releasing group, which allows a desired chair-chair-chair cyclization conformation, thus avoiding the cyclopentane formation-methyl migration sequence typically present in the biosynthetic pathways.



**Scheme 2-7.** van Tamelen's tetracyclization.

<sup>15</sup> van Tamelen, E. E.; Leiden, T. M. *J. Am. Chem. Soc.* **1982**, *104*, 2061–2062.

<sup>16</sup> (a) Corey, E. J.; Lin, S. *J. Am. Chem. Soc.* **1996**, *118*, 8765–8766; (b) Surendra, K.; Corey, E. J. *J. Am. Chem. Soc.* **2009**, *131*, 13928–13929; (c) Bogenstätter, M.; Limberg, A.; Overman, L. E.; Tomasi, A. L. *J. Am. Chem. Soc.* **1999**, *121*, 12206–12207.

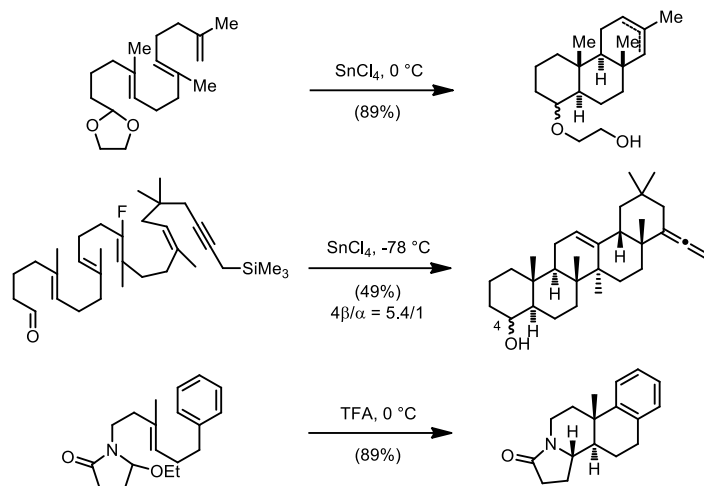


**Scheme 2-8.** Corey's and Overman's polycyclizations *en route* to complex natural products.

**Other types of polycyclizations.** Various cationic polycyclization cascades using other initiating electrophiles have been reported from different laboratories (Scheme 2-9). Among these, Johnson developed Prins-type cyclizations through formation of an oxocarbenium ion or an activated aldehyde,<sup>17</sup> while Speckamp contributed to an *N*-acyliminium ion-triggered tandem bicyclization.<sup>18</sup>

<sup>17</sup> (a) Johnson, W. S.; Kinnel, R. B. *J. Am. Chem. Soc.* **1966**, *88*, 3861–3862; (b) Fish, P. V.; Johnson, W. S. *J. Org. Chem.*, **1994**, *59*, 2324–2335.

<sup>18</sup> Dijkink, J.; Speckamp, W.N. *Tetrahedron* **1978**, *34*, 173–178.



**Scheme 2-9.** Johnson's and Speckamp's "unnatural" polycyclizations.

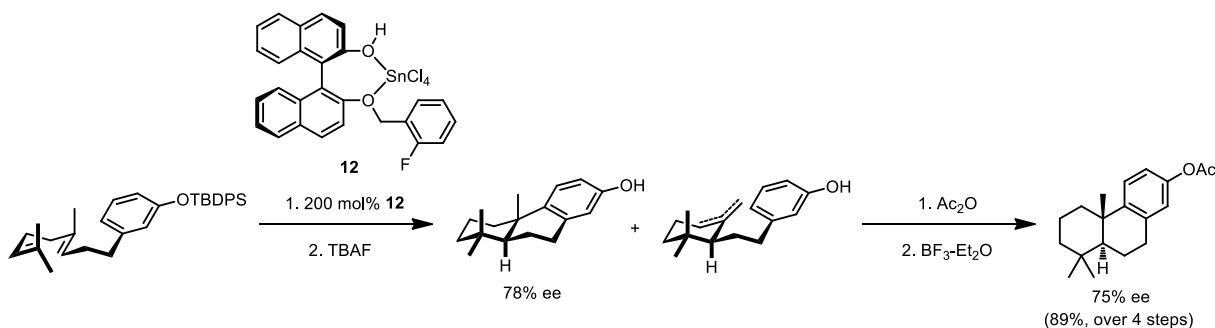
### 2.3.2 Catalyst/Reagent-Controlled Asymmetric Polycyclizations

When a chiral Brønsted acid is used to promote the cascade reaction, high enantioselectivity might be achieved if one of the following scenarios applies:

- A) Concerted protonation-cyclization dominates the reaction pathway;
- B) C6,C7-olefin assists the protonation by electrostatic interaction or non-classical carbenium ion formation;
- C) The counteranion of the acid tightly associates with the carbocation during the cyclization event.

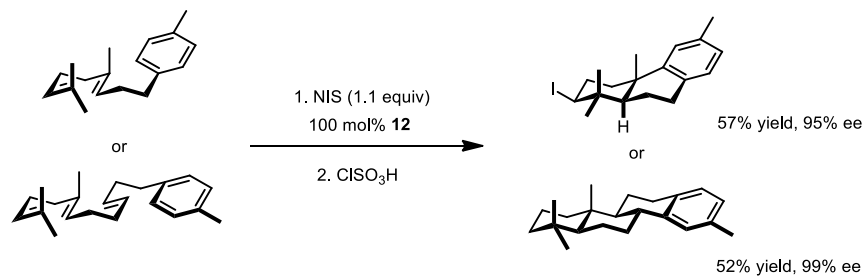
In 1999, Yamamoto advanced the first enantioselective polycyclization with reagent-control (Scheme 2-10).<sup>19</sup> A chiral BINOL coordinated to a Lewis acid – SnCl<sub>4</sub> imparts moderate to high selectivity in several bicyclization systems. The reaction undergoes an enantioselective closure of the A ring, followed by a diastereoselective trapping of the tertiary carbocation to complete the cascade.

<sup>19</sup> Ishihara, K.; Nakamura, S.; Yamamoto, H. *J. Am. Chem. Soc.* **1999**, *121*, 4906–4907.



**Scheme 2-10.** Yamamoto's enantioselective polycyclization.

Inspired by haloperoxidases that can initiate polycyclizations with electrophilic halogen species, Ishihara disclosed a novel approach to a formal bicyclization promoted by a nucleophilic phosphoramidate additive and *N*-iodosuccinamide (Scheme 2-11).<sup>20</sup> Bicyclic scaffolds were constructed through first iodocyclization followed by an achiral Brønsted acid-catalyzed second- (and third-) ring formation, in high enantioselectivities.

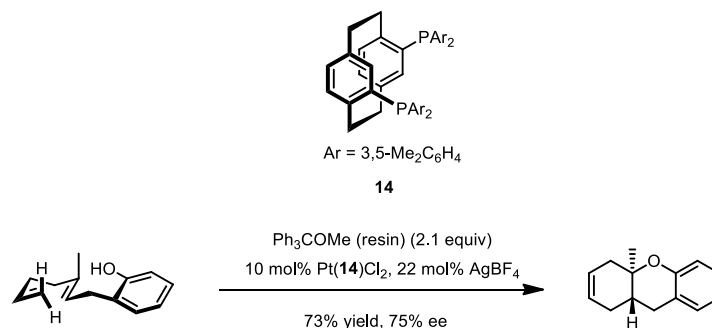


**Scheme 2-11.** Ishihara's enantioselective iodopolycyclizations.

In 2008, Gagné took advantage of the olefin-binding and activation ability of late transition metals and realized platinum-catalyzed asymmetric bi- and tri-cyclizations with good to excellent enantioselectivities (Scheme 2-12).<sup>21</sup> An axial chiral bidentate phosphine ligand was used to support the metal and render a chiral environment. This example constitutes the first asymmetric catalytic polycyclization cascade.

<sup>20</sup> Sakakura, A.; Ukai, A.; Ishihara, K. *Nature* **2007**, *445*, 900–903.

<sup>21</sup> Mullen, C. A.; Campbell, A. N.; Gagné, M. R. *Angew. Chem. Int. Ed.* **2008**, *47*, 6011–6014.



**Scheme 2-12.** Gagné's catalytic asymmetric polycyclization.

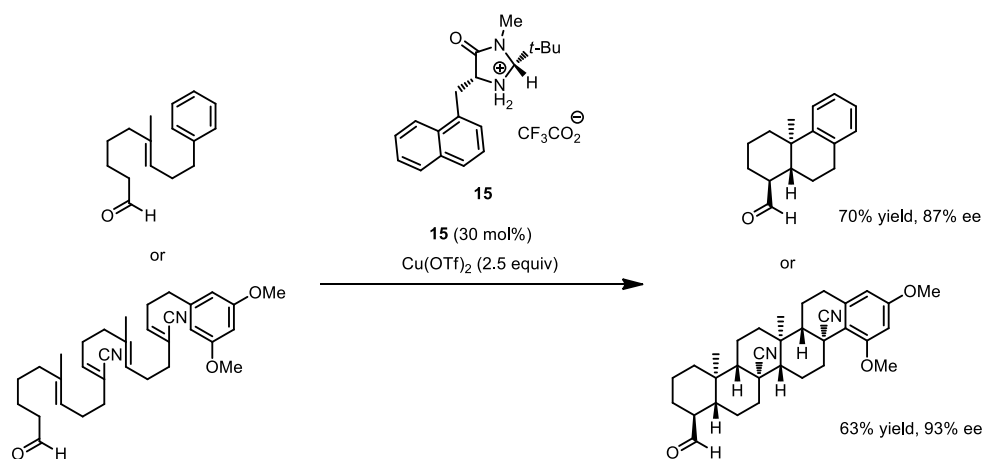
### 2.3.3 Catalytic Asymmetric Polycyclizations<sup>22</sup>

In 2010, as a back-to-back publication with our initial report on thiourea-catalyzed cationic polycyclizations,<sup>23</sup> MacMillan applied organo-SOMO catalysis to develop an organocatalytic enantioselective cyclization strategy for accessing steroidal and terpenoidal skeletons.<sup>24</sup> In this work, they used the imidazolidinone salt **15**, with the aid of cupric triflate as the stoichiometric oxidant, to catalyze the bi-, tri-, tetra-, penta- and hexacyclization of  $\omega$ -aryl-substituted polyunsaturated aldehydes (Scheme 2-13). The reaction presumably undergoes a radical mechanism, and the alternating electron-rich/electron-deficient olefin connection is important for the propagation of the cyclization cascade.

<sup>22</sup> The work summarized in this section were all reported subsequent to our initial publication of the thiourea-catalyzed cationic polycyclization (see ref. 23), with the exception of MacMillan's work, which was concomitant with our research.

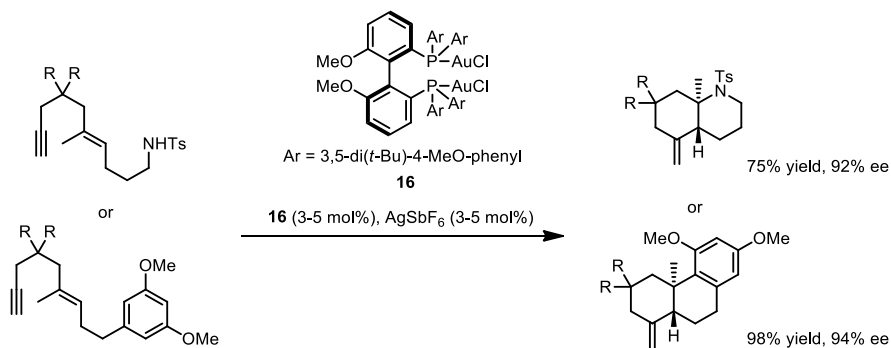
<sup>23</sup> Knowles, R. R.; Lin, S.; Jacobsen, E. N. *J. Am. Chem. Soc.* **2010**, *132*, 5030–5032.

<sup>24</sup> Rendler, S.; MacMillan, D. W. C. *J. Am. Chem. Soc.* **2010**, *132*, 5027–5029.



**Scheme 2-13.** MacMillan's SOMO-catalyzed polycyclizations.

Later, the Toste group realized a series of enantioselective polycyclization reactions catalyzed by a cationic bisphosphine gold complex **16** (Scheme 2-14).<sup>25</sup> These reactions, which employ an alkyne as an initiating group, begin with a gold-promoted 6-*exo*-dig cyclization and can be terminated with a variety of nucleophiles including carboxylic acids, phenols, sulfonamides, and electron-rich aryl groups. Polycyclic products are generated in excellent diastereo- and enantioselectivity.



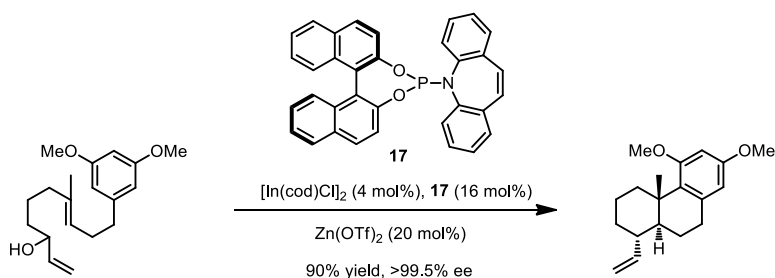
**Scheme 2-14.** Toste's Au-catalyzed polycyclizations.

In 2012, Carreira disclosed a highly enantioselective polycyclization method using the combination of Lewis acid activation with iridium-catalyzed allylic substitution (Scheme 2-15).<sup>26</sup>

<sup>25</sup> Sethofer, S. G.; Mayer, T.; Toste, F. D. *J. Am. Chem. Soc.* **2010**, *132*, 8276–8277.

<sup>26</sup> Schafroth, M. A.; Sarlah, D.; Krautwald, S.; Carreira, E. K. *J. Am. Chem. Soc.* **2012**, *134*, 20276–20278.

This strategy relies on direct use of branched, racemic allylic alcohols and furnishes a diverse and unique set of carbo- and heteropolycyclic ring systems in good yields and  $\geq 99\%$  ee.



**Scheme 2-15.** Carreira's In and Zn co-catalyzed polycyclization.

In addition, Ishihara, Corey, Loh and Gagné individually reported cationic polycyclization cascades using Lewis-acid assisted Brønsted acid, Lewis acid and late transition metals as catalysts.<sup>27</sup>

<sup>27</sup> (a) Sakakura, A.; Sakuma, M.; Ishihara, K. *Org. Lett.* **2011**, *13*, 3130–3133; (b) Surendra, K.; Corey, E. J. *J. Am. Chem. Soc.*, **2012**, *134*, 11992–11994; (c) Zhao, Y.-J.; Li, B.; Tan, L.-J. S.; Shen, Z.-L.; Loh, T.-P. *J. Am. Chem. Soc.* **2010**, *132*, 10242–10244; (d) Cochrane, N. A.; Nguyen, H.; Gagne, M. R. *J. Am. Chem. Soc.* **2013**, *135*, 628–631.

## 2.4 Enantioselective Thiourea-Catalyzed Cationic Polycyclizations<sup>28</sup>

### 2.4.1 Introduction

As discussed in previous sections, recent advances in (oxido)squalene cyclase enzymology have provided strong evidence that the cation– $\pi$  interaction plays an essential catalytic role in biosynthetic polyene cyclizations. Structural, kinetic, and site-directed mutagenesis studies all suggest that the cationic intermediates and transition states accessed in these transformations are stabilized through a series of attractive interactions with aromatic residues that line the cyclase active site. This mechanistic insight suggests the intriguing possibility that analogous stabilizing cation– $\pi$  interactions might also be engineered into selective small-molecule catalysts.<sup>29</sup>

We became interested in developing an asymmetric polycyclization jointly predicated on this biosynthetic model and our recent work in anion-binding thiourea catalysis.<sup>30</sup> The ability of arenes to stabilize cations offers a logical complement to the anion-binding properties of thioureas.<sup>31</sup> As such, an appropriate bifunctional catalyst would be capable of electrostatically stabilizing both poles of a reactive ion pair in a spatially resolved manner, increasing the probability of strong binding to the enantioselectivity-determining transition state structure (Scheme 2-16).

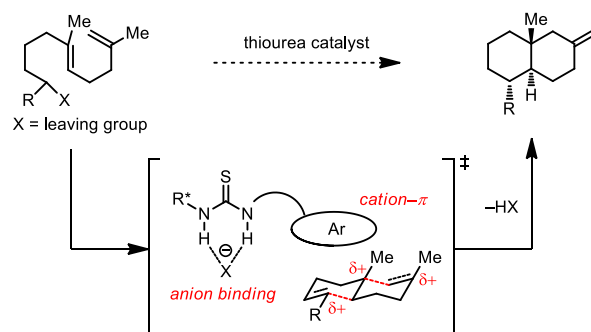
---

<sup>28</sup> The work summarized in this section has been done in collaboration with Dr. Robert R. Knowles. Much of it has been published in ref. 23.

<sup>29</sup> Paschall, C. M.; Hasserodt, J.; Jones, T.; Lerner, R. A.; Janda, K. D.; Christianson, D. W. *Angew. Chem. Int. Ed.* **1999**, *38*, 1743–1747.

<sup>30</sup> Reisman, S. E.; Doyle, A. G.; Jacobsen, E. N. *J. Am. Chem. Soc.* **2008**, *130*, 7198–7199.

<sup>31</sup> Ma, J.; Dougherty, D. A. *Chem. Rev.* **1997**, *97*, 1303–1324.



**Scheme 2-16.** Proposal for enantioselective polycyclization by thiourea.

## 2.4.2 Method Development

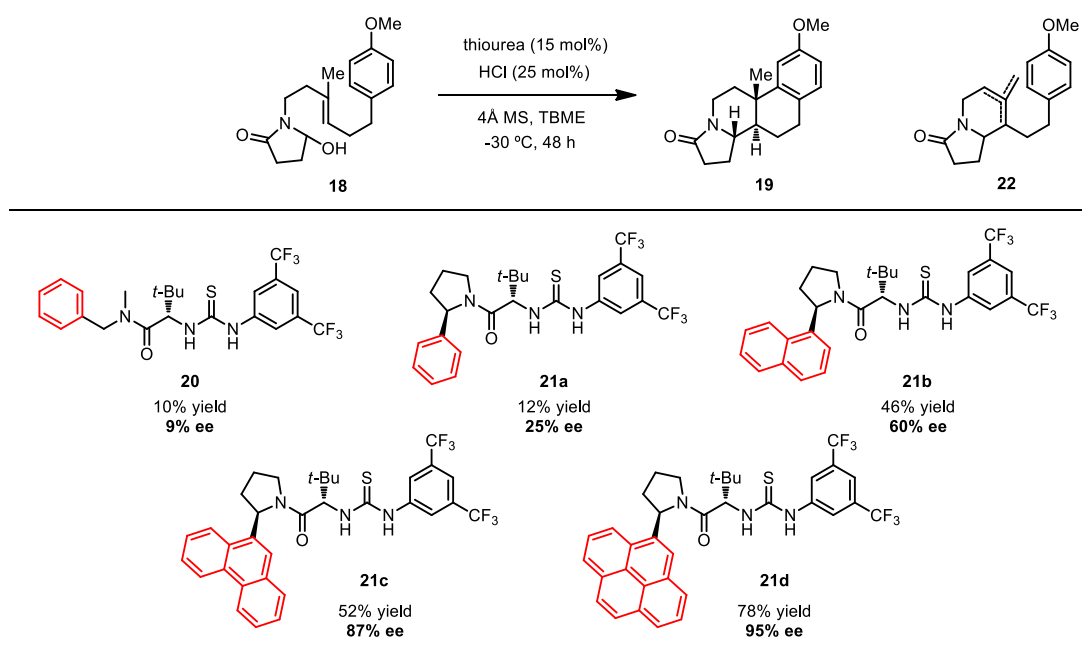
Our efforts focused on developing an enantioselective variant of a polycyclization originally reported by Speckamp that proceeds through an *N*-acyliminium ion intermediate (ref. 18). In accord with our previous reports on asymmetric transformations utilizing this type of electrophiles, we envisioned that treatment of a hydroxylactam substrate with hydrochloric acid would result in dehydrative formation of a chlorolactam intermediate.<sup>32</sup> Hydrogen bond-mediated ionization of this chlorolactam by the thiourea would generate a catalyst-bound iminium•chloride ion pair that would in turn undergo cyclization enantioselectively.

In evaluating the bicyclization of hydroxylactam **18**, a preliminary survey of thioureas and solvents produced a lead result with thiourea **20**, with tetracycle **19** generated in 10% yield and 9% ee upon treatment with 25 mol% of HCl in TBME containing 4 Å molecular sieves at  $-30\text{ }^{\circ}\text{C}$  (Table 2-4). Catalyst **21a**, a conformationally constrained analogue of **20** containing a 2-phenylpyrrolidine ring, afforded a modest increase in enantioselectivity. Modification of the electronic properties of the aromatic group of **21a** by introduction of simple substituents had little effect on catalyst performance (Table 2-5). In contrast, 2-arylpyrrolidine catalysts with larger aromatic groups proved substantially more reactive and enantioselective. The naphthyl-

<sup>32</sup> Raheem, I. T., Thiara, P. S., Peterson, E. A., and Jacobsen, E. N. *J. Am. Chem. Soc.* **2007**, 129, 13404–13405.

substituted catalyst **21b** provided **19** in greater than 60% ee, while 9-phenanthryl-derived catalyst **21c** furnished product **19** in 52% yield and 87% ee. Spurred by the apparent correlation between the expanse of the pyrrolidine arene and catalytic performance, we prepared and evaluated 4-pyrenyl-substituted thiourea derivative **21d**. This proved to be the optimal catalyst, providing **19** in 78% yield and 95% ee. The urea analogue of **21d** catalyzed the reaction with marginally lower 85% ee, showing that the sulfur atom in thiourea **21** doesn't participate in a key function in the enantio-induction mechanism.

**Table 2-5.** Catalyst structure investigation.<sup>a</sup>



<sup>a</sup> Reactions performed 0.033 mol scale, with yields determined by GC analysis and ee determined by SFC analysis.

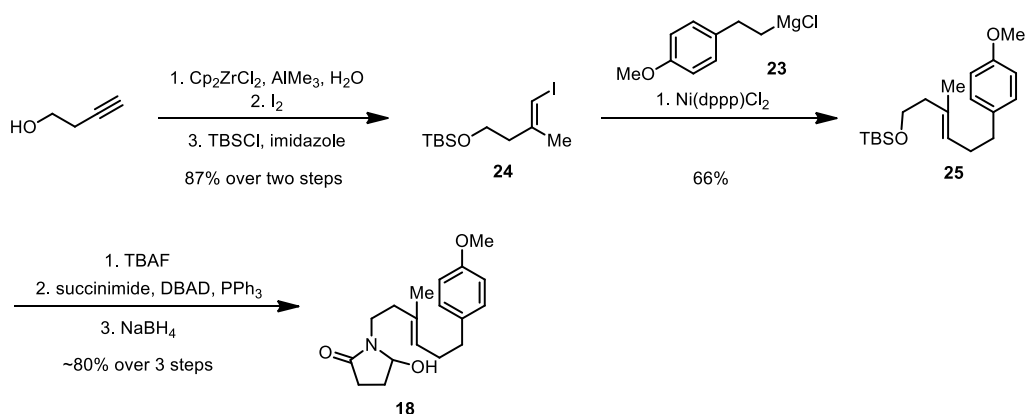
Under the action of all the catalysts described in Table 2-4, tetracycle **19** was formed as a single detectable diastereomer, the relative stereochemistry of which was secured by X-ray crystallography. Notably, reactions performed in the absence of a thiourea catalyst provided none of the desired bicyclization product. Instead, HCl alone promotes a monocyclization pathway that

yields a mixture of bicyclic structures **22** as olefin regioisomers. These byproducts were also observed under thiourea-catalyzed conditions in very small quantities and in nearly racemic form.

## 2.4.3 Substrate Scope

### 2.4.3.1 Development of a Modular Substrate Synthesis via *B*-Alkyl Suzuki Coupling

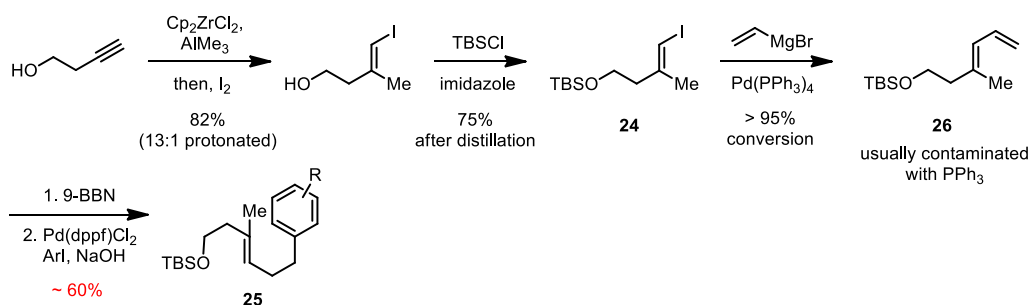
The synthesis of the parent *para*-methoxy substrate (**18**) was initially achieved through a sequence of six reaction steps (Scheme 2-17), including hydrozirconation of a terminal alkyne followed by electrophilic quenching with iodine, nickel-catalyzed Kumada coupling with commercially available Grignard reagent **23**, and installation of the hydroxylactam via Mitsunobu reaction followed by reduction. Although this route proved efficient for the synthesis of **18**, the accessibility of other homobenzylic Grignard reagents of type **23** and the relatively poor productivity of the cross-coupling step reduced the modularity of the method and impeded its application in streamlined synthesis of a large variety of substrates.



**Scheme 2-17.** First generation substrate synthesis.

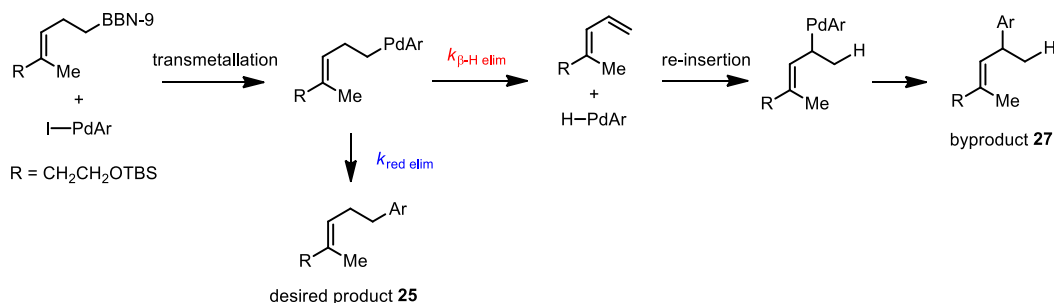
An analogous strategy was proposed to improve the practicality of the substrate synthesis (Scheme 2-18). Upon obtaining the same vinyl iodide intermediate **24**, Kumada coupling with vinylmagnesium bromide cleanly yields diene **26**, which is then converted to a common intermediate **25** before the final incorporation of the hydroxylactam. The robustness of most

reactions in this sequence and commercial availability of all reagents made it more attractive than the previous approach. However, the *B*-alkyl Suzuki coupling of diene **26** with aryl iodide baffled us with its low yield and low selectivity. The byproduct of this reaction was identified to be regioisomer **27** from Markovnikov-type addition. This observation can potentially be due to a non-selective hydroboration. However, quenching the 9-BBN addition product of **26** with H<sub>2</sub>O<sub>2</sub> under basic condition furnished the terminal alcohol exclusively, in accord with the characteristic high regioselectivity associated with this type of hydroboration processes.



**Scheme 2-18.** Second generation substrate synthesis.

We proposed that the regioselectivity issue arises from the tendency of the terminal alkyl palladium species generated via transmetalation to undergo  $\beta$ -hydride elimination and re-insertion in a Markovnikov manner (Scheme 2-19). The reversal of regioselectivity in the hydroboration event is driven by the high stability of the  $\pi$ -allyl palladium intermediate, and is thus predicted to be almost complete. Reductive elimination would finally provide the unwanted byproduct **27**. The regioisomeric distribution of the coupling products (**25** & **27**) should reflect the relative rate of the direct reductive elimination to the  $\beta$ -hydride elimination ( $k_{\text{red elim}}/k_{\beta\text{-H elim}}$ ).



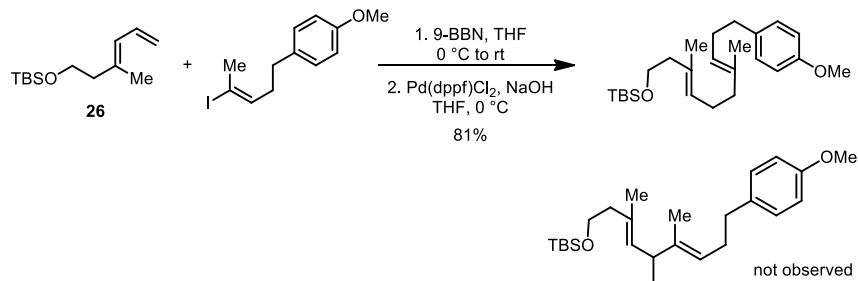
**Scheme 2-19.** Hypothesis for the byproduct generation.

Based on this hypothesis, we applied a few classical approaches that have been developed for facilitating reductive elimination and/or suppressing  $\beta$ -hydride elimination in Pd-catalysis, such as using bulky phosphine ligands to enhance the orbital overlap of the two eliminating substituents, and introducing exogenous Lewis bases to block open coordination sites on the metal center for  $\beta$ -hydride acceptance. However, the optimal selectivity we observed was no better than 2:1. Considering the difficulty in separating the two regioisomeric products through chromatographical methods, this product distribution ratio is not acceptable for large scale synthesis of multiple targets.

In principle, if the electrophilic component of the Suzuki coupling is vinyl iodide instead of aryl iodide, the selectivity of the reaction should be improved due to the more facile reductive elimination from the corresponding vinylalkylpalladium species than the arylalkylpalladium species. Observations made by us as well as a few other groups showed that the terminal cross-coupling product of dienes of type **26** was generated exclusively under analogous Suzuki coupling conditions, in agreement with this hypothesis (Scheme 2-20).<sup>33</sup> We therefore proposed an alternative approach in which vinyl iodide **24** and *B*-styrenyl-9-BBN **28** are cross-coupled via Pd-catalysis. Although the terminal-alkylvinylpalladium species derived from transmetalation

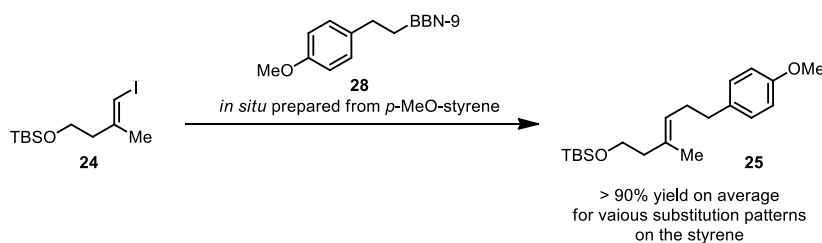
<sup>33</sup> For another example besides in Scheme 2-19, see: Surendra, K.; Corey, E. J. *J. Am. Chem. Soc.* **2008**, *130*, 8865–8869.

between **24** and **28** can also isomerize into a more stable vinylbenzylpalladium species through the same mechanism discussed above, the regioselectivity of the reaction should still be enhanced due to the high reactivity of alkylvinylpalladium in reduction elimination events.



**Scheme 2-20.** Synthesis of tricyclization precursor via *B*-alkyl Suzuki coupling with diene **26**.

Results showed that the desired product **25** was formed in high yield and perfect selectivity. Taken together with its modularity, this method was then incorporated in the synthesis of a series of substrates.



**Scheme 2-21.** Key *B*-alkyl Suzuki coupling in the third generation substrate synthesis.

### 2.4.3.2 Substrate Scope of Thiourea-Catalyzed Polycyclization

With the substrates in hand, we evaluated the scope of this bicyclization protocol under the optimal reaction conditions. A variety of aromatic groups were found to be efficient and selective as terminating nucleophiles (Table 2-6). In addition to the model substrate **18**, the unsubstituted phenyl substrate **29** (entry 1), a number of *para*-substituted phenyl derivatives (entries 2–5), an extended naphthyl-containing substrate **37** (entry 6), and a chlorinated thiophene **39** (entry 7) all underwent cyclization with high enantioselectivity under catalysis with **21d**. Furthermore, in each

case the bicyclization products were formed as single diastereomers, as determined by NMR analysis. The use of more electron-rich arene nucleophiles led to significant losses in either reactivity or enantioselectivity (see Section 2.5).

**Table 2-6.** Substrate scope.<sup>a</sup>

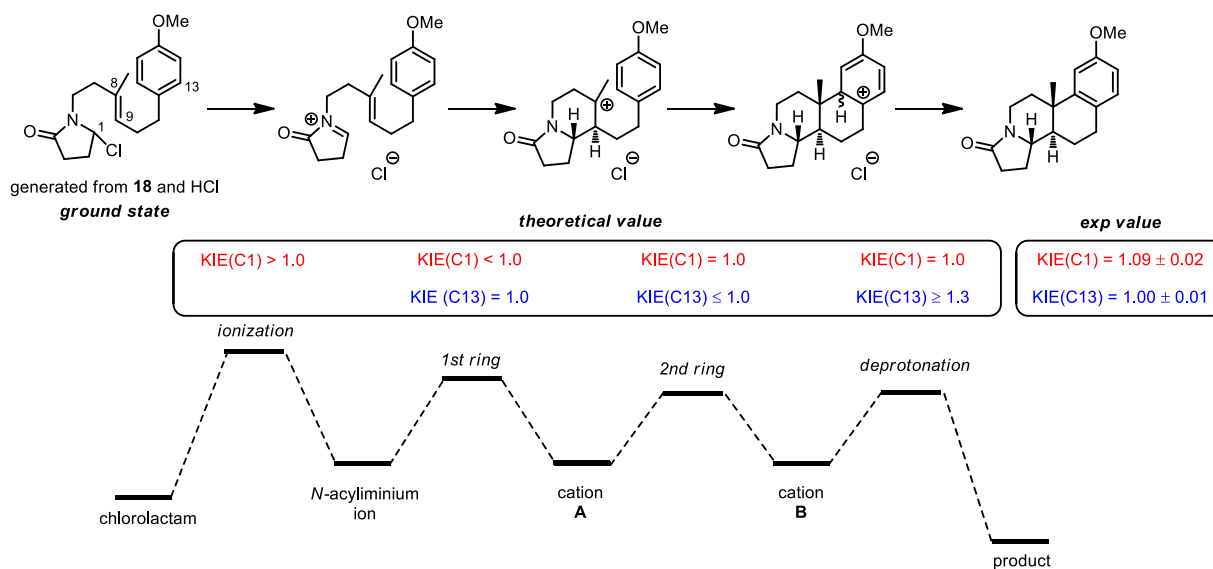
entry	substrate	product	time (h)	yield%	ee%	entry	substrate	product	time (h)	yield%	ee%
1			96	51	89	5 <sup>c</sup>			96	71	91
2			72	72	94	6			72	75	92
3			96	62	91	7 <sup>d</sup>			72	77	91
4 <sup>b</sup>			120	54	91						

<sup>a</sup> Reactions performed 0.25 mol scale, with isolated yields by column chromatography and ee determined by SFC/HPLC analysis reported. <sup>b</sup> Reaction run with 2 equiv of TMSCl instead of HCl. <sup>c</sup> Reaction run with 50 mol% HCl. <sup>d</sup> Reaction run at  $-10$  °C.

## 2.5 Mechanistic Studies: Implication for a Biomimetic Catalytic System

### 2.5.1 Stepwise Cyclization with Selectivity-Determining First Ring-Closure

Kinetic isotope effect (KIE) was determined at C1 and C13/13' positions using deuterated substrates. Under homogeneous conditions at room temperature, the **21d**/HCl-catalyzed pathway displays a normal secondary KIE of  $1.09 \pm 0.02$ . This value is consistent with C–Cl bond ionization being the rate-limiting step (Scheme 2-22). The enantio-determining cyclization cascade is therefore post-rate-limiting and unfortunately cannot be probed through kinetic analysis directly.



**Scheme 2-22.** Analysis of possible KIE values with different rate-limiting steps. In the box on the left, the numbers in the top row (red) are the predicted values if the corresponding step is rate-limiting in the overall reaction, and the numbers in the bottom row (blue) are the predicted values if the corresponding step is the slowest step post-rate-limiting. The numbers in the box on the right are experimental results, with error bars reflecting the range of three independent measurements.

An energy surface of the cyclization cascade under uncatalyzed condition was generated using DFT calculations, and results are in favor of a stepwise mechanism (Figure 2-4). No concerted pathway was located on the energy surface. Although thiourea **21d** would likely alter the energy landscape of the reaction, based on the calculated high activation energy associated with the concerted pathway in the uncatalyzed reaction (over 15 kcal/mol higher than the stepwise

pathway), we reasoned that the asynchronicity of the cyclization cascade would not be perturbed by the catalyst.

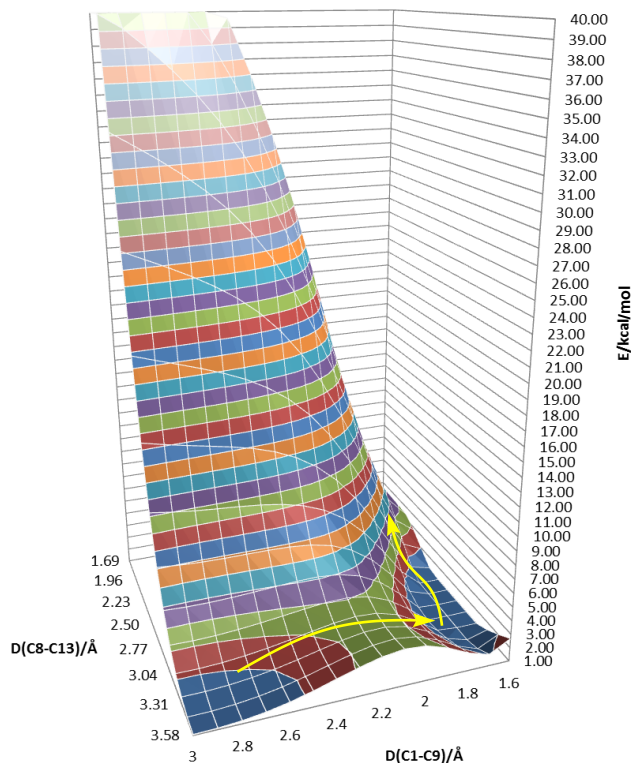


**Figure 2-4.** Energy surface of the racemic pathway (C1–C9 and C8–C13 bond-formation) by DFT calculation (Gaussian 09, B3LYP/6-31g(d)). Yellow arrows represent the lowest energy pathway. Chloride anion was omitted during the calculation.

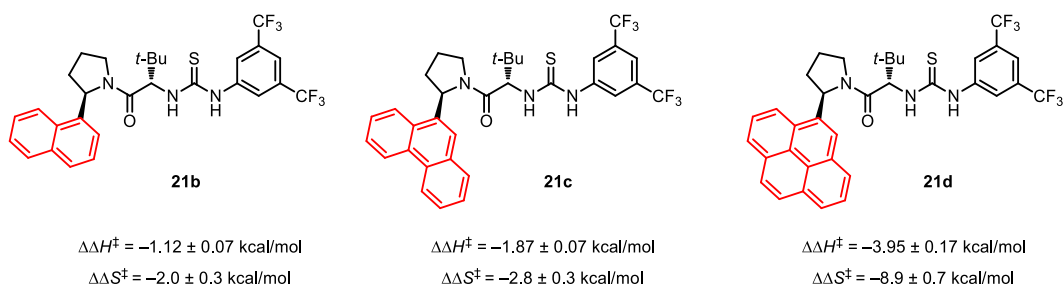
To elucidate the rate-limiting step after the ionization, which would also be the selectivity-determining step, an intramolecular isotope competition experiment with substrate deuterated at C13 was conducted. Upon generation of the *N*-acyliminium ion, if the first ring closure bears the highest barrier, no KIE would be observed because C13 is not involved in this step; if the second ring formation possess the largest activation energy, an inverse secondary KIE should be exhibited, as C13 undergoes a hybridization change from  $sp^2$  to  $sp^3$ ; and if the re-aromatization is rate-limiting, a large primary KIE is expected due to the cleavage of C13–H/D bond during this step. In addition, if the two cyclization events are in concert, an inverse secondary KIE should also be

anticipated again due to the hybridization change at C13 in this scenario. Experimental measurements revealed the absence of a secondary KIE, indicating the C1–C9 bond formation being the highest energy barrier among all the post-rate-limiting steps (Scheme 2-22). This also rules out the cyclization being a concerted process.

Taken together, these data provided compelling evidence for a two-step cyclization sequence, in which the first ring-closure is the enantio-determining step. The diastereoselectivity in the subsequent cyclization event is governed by the stereogenic centers set in this step. This mechanism resembles the biosynthesis of hopene wherein the complex polycyclic framework of the product is completed in a series of ring-closing events intermediated by discrete carbocations.

### 2.5.2 Cation- $\pi$ Stabilization of the Cyclization Transition State

The fact that the enantioselectivity observed in these polycyclizations is highly dependent upon the expanse of the catalyst arene, taken together with the cationic nature of the reaction, raises the possibility that stabilizing cation- $\pi$  interactions may play a key role in asymmetric induction. To evaluate this hypothesis, an Eyring analysis of enantioselectivity was conducted for catalysts **21b**, **21c**, and **21d** in the bicyclization of substrate **18**. All three catalysts displayed linear correlations between  $\ln(er)$  and reciprocal temperature over a 70 °C range (Scheme 2-23). Evaluation of the differential activation parameters derived from these plots revealed that enantioselectivity was enthalpically controlled in all cases and that the magnitude of the differential enthalpy increased markedly as the catalyst arene increased in size. In fact, this term roughly doubles in magnitude with the addition of each new aromatic ring, reaching nearly 4 kcal/mol for the optimal catalyst **21d**. The effect of this increase was attenuated slightly by a compensating increase in the differential entropy terms across the series.



**Scheme 2-23.** Differential activation parameters of the polycyclization catalyzed by **21b-d**.

The energetic benefits of increasing the strength of a noncovalent binding interaction are typically manifested enthalpically.<sup>34</sup> As such, the increasing magnitude of the differential enthalpy in catalysts with more extended arenes is consistent in principle with a progressively more stabilizing cation- $\pi$  interaction in the dominant transition state structure and with the fact polycyclic aromatic hydrocarbons are known to bind cations more strongly as they increase in size.<sup>35</sup> However, these data do not rule out the possibility that increasing the size of the arene energetically destabilizes the minor transition state assembly, presumably through steric interactions. The fact that the ee-determining cyclization steps are all post-rate-limiting makes it impossible to distinguish between these two possibilities by absolute rate comparisons of the different catalysts. To ascertain whether the extended aromatic system is stabilizing the transition state leading to the major enantiomer or destabilizing the minor pathway, we investigated whether correlations existed between the degree of observed enantioinduction and the physical properties that underlie cation- $\pi$  interactions. The strength with which a given arene interacts with a positive charge in a transition state is primarily a function of electrostatic and dispersion forces.<sup>36</sup> As such, if the strength of a cation- $\pi$  interaction is a determinant in enantioselectivity, there may be a

<sup>34</sup> Williams, D. H.; Calderone, C. T. *J. Am. Chem. Soc.* **2001**, 123, 6262–6267.

<sup>35</sup> Gal, J.-F.; Maria, P.-C.; Decouzon, M.; Mo, O.; Yanez, M.; Abboud, J. L. M. *J. Am. Chem. Soc.* **2003**, 125, 10394–10401.

<sup>36</sup> (a) Mecozzi, S.; West, A. P.; Dougherty, D. A. *J. Am. Chem. Soc.* **1996**, 118, 2307–2308; (b) McCurdy, A.; Jimenez, L.; Stauffer, D. A.; Dougherty, D. A. *J. Am. Chem. Soc.* **1992**, 114, 10314–10321.

correlation between the degree of asymmetric induction observed and the quadrupole moment and polarizability of the arene involved. Conversely, if the effect was largely steric and repulsive in origin, no significant correlation with these physical properties would be expected. The enantioselectivity observed with catalysts **21a-d** under standard conditions was found to correlate strongly with both the polarizability and the quadrupole moment of the arenes found in each catalyst ( $R^2 = 0.99, 0.97$  respectively, see Figure 2-5). Taken altogether, these data provide compelling evidence for a mechanism incorporating a selectivity-determining cation- $\pi$  interaction.

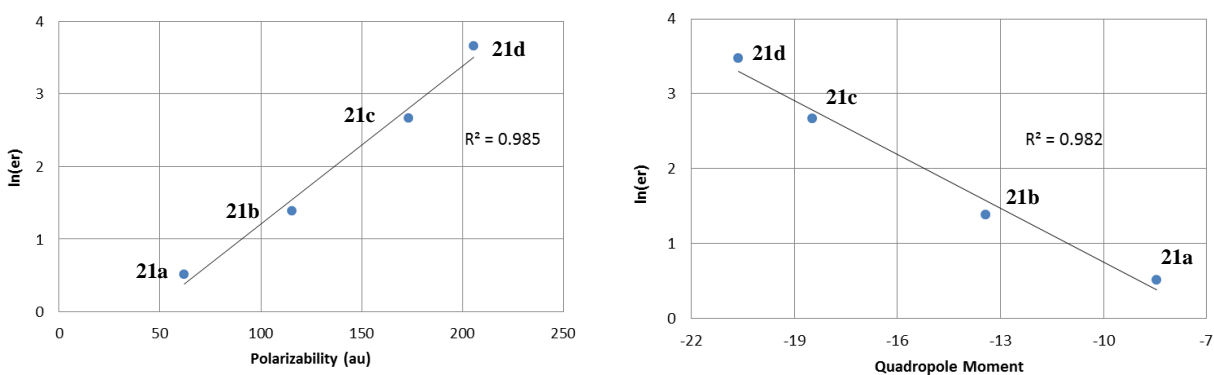


**Figure 2-5.** Linear free-energy relationships between selectivity and cation- $\pi$  donating ability of the catalyst.

In this respect, these findings emulate the particularly striking role cation- $\pi$  interactions play in the catalysis of biosynthetic polyene cyclizations and provide clear support for the notion that these interactions can dictate stereocontrol in small-molecule catalysis contexts as well.

As a side note, we reasoned that the observation of the monocyclization product **22** in the absence of the thiourea catalyst is due to the lack of cation- $\pi$  stabilization of the tertiary carbocation intermediate (charge at C8), which allowed undesirable deprotonation to outcompete the second ring-closure. This observation also echoes the biosynthetic mechanism of squalene polycyclization, in which enzyme mutant lacking certain aromatic amino acid residues fails to complete the entire cyclization cascade and furnishes abortive products instead.

### 2.5.3 Cation- $\pi$ Stabilization of the C–Cl Bond Ionization

Although the formation of the *N*-acyliminium ion does not exist in the enzymatic polycyclization pathways, the possibility that the aromatic group on the catalyst might act in concert with the dual hydrogen bond donor to stabilize both poles of the transition state of the ionization event and facilitate the ion pair formation is quite intriguing. To probe this hypothesis, we conducted kinetic analysis as well as KIE study on the series of arylpyrrodine-derived catalysts **21b-d**, taking advantage that the C–Cl bond cleavage is involved in the rate-limiting step. A correlation between the rate of the reaction and the secondary KIE value emerged, with more sizable catalyst providing both higher reactivity and less C–Cl breaking character in the transition state. Therefore, according to the Hammond postulate, the rate acceleration by thiourea **21b-d** arises from stabilization of the high energy intermediate – *N*-acyliminium chloride (Figure 2-6). Based on previous studies on thiourea anion-binding catalysis, the primary cause for such a stabilization effect is presumably through the dual H-bond donation of thiourea to the chloride anion. In addition, the more pronounced stabilization effect with more sizable catalyst is inevitably linked to the cation- $\pi$  donating ability of the aryl substituent.

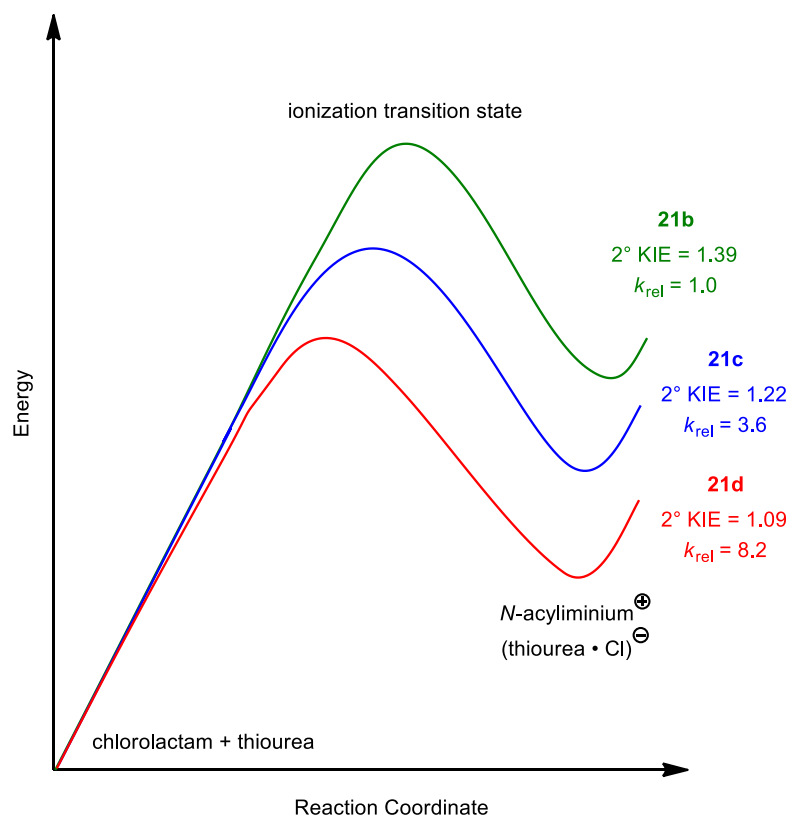
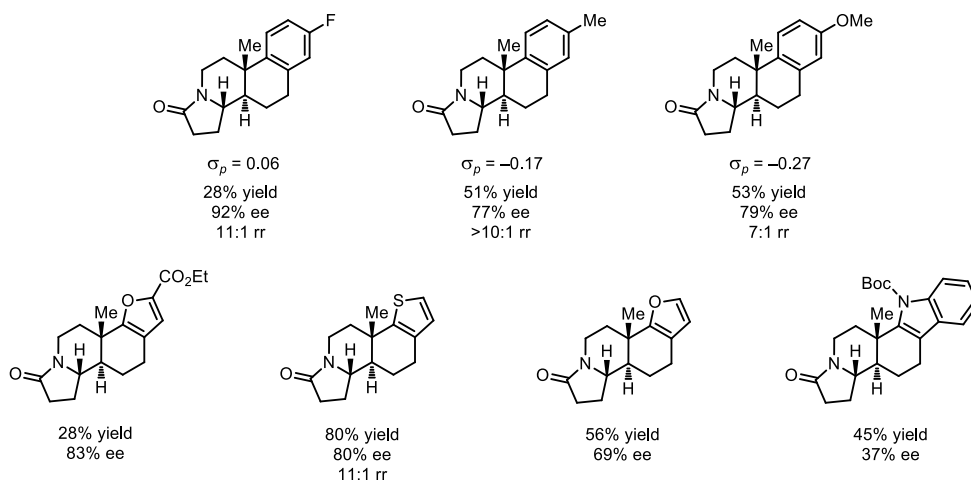


**Figure 2-6.** Rate and KIE data of polycyclization catalyzed by **21b-d** and application of the Hammond postulate.

## 2.6 Outlook

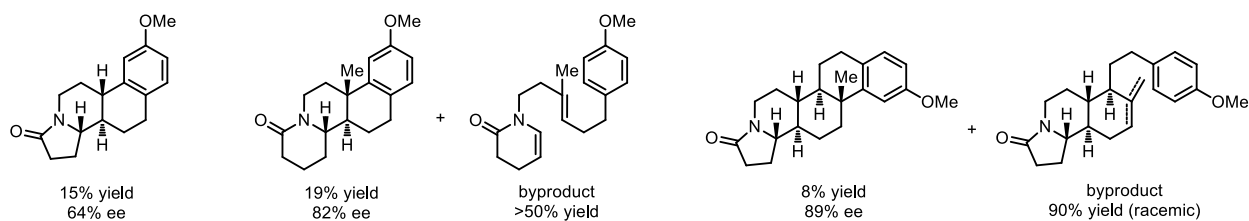
### 2.6.1 Substrate Scope

A subset of the systems providing sub-optimal, yet promising results is shown in this section. We found that the reaction enantioselectivity is dependent on the electronic properties of the terminating aromatic nucleophile on the substrate, with electron-rich groups being detrimental to the ee (Scheme 2-24). The direct participation of the aryl group in the enantio-determining event has been ruled out by the KIE studies. An alternative explanation is that the aromatic substituent competes with the thiourea catalyst in stabilization of the cationic transition state of the first ring-closure through cation- $\pi$  interactions, disrupting the catalyst-substrate association.



**Scheme 2-24.** Suboptimal substrate scope.

Variations on the structure of the *N*-acyliminium ion and the olefin nucleophile led to promising results (Scheme 2-25). Moderate to high enantioselectivity was observed with a glutarimide-derived substrate and a disubstituted olefin containing substrate. However, in both cases the yield of the desired product was not satisfactory. In the case with the glutarimide-derived substrate, a large amount of byproduct resulting from elimination of H<sub>2</sub>O was isolated. We presumed that the low reactivity with both substrates was caused by the instability of the cationic intermediates.



**Scheme 2-25.** Suboptimal substrates.

A tricyclization precursor with an addition olefin component inserted into substrate **18** was also synthesized and subjected to the optimal conditions with thiourea **21d** (Scheme 2-25). An encouraging 89% ee was observed with the desired pentacyclic product. The similarity between the enantioselectivity of this substrate and that of the model substrate **18** provides evidence for the stepwise cyclization mechanism with first ring-closure being selectivity-determining. Nevertheless, the majority of the mass balance resides in the abortive bicyclization product, which is produced in racemic form.

The low reactivity and/or low enantioselectivity of all the above examples are likely linked to the insufficient cation- $\pi$  stabilizing ability of the catalyst. In order to expand the substrate diversity in these directions, a stronger cation- $\pi$  donor on the catalyst needs to be incorporated to tame the highly reactive cationic intermediates from participating in undesired pathways.

A more challenging but also more fascinating approach would be to design a different type of catalyst framework with higher functionality density, drawing inspiration from SHC. Synthetically accessible structures such as aromatic short peptides and cyclophanes can be appended to thiourea motif to provide additional cation- $\pi$  stabilization in the selectivity-determining transition state. Such a catalyst needs to have a relatively rigid scaffold to position the aromatic group(s) favorable for synergistic stabilization of the cyclization event, avoiding undesired pathways. Computational analysis would be a good approach to examine the feasibility of this strategy and devise new catalysts. Successful design principles can be further utilized in

the development of a more generic cyclization of unfunctionalized polyenes that involves carbocationic intermediates of even higher energies.

### 2.6.2 Cyclization of Unfunctionalized Polyenes – a Traceless Leaving Group Approach

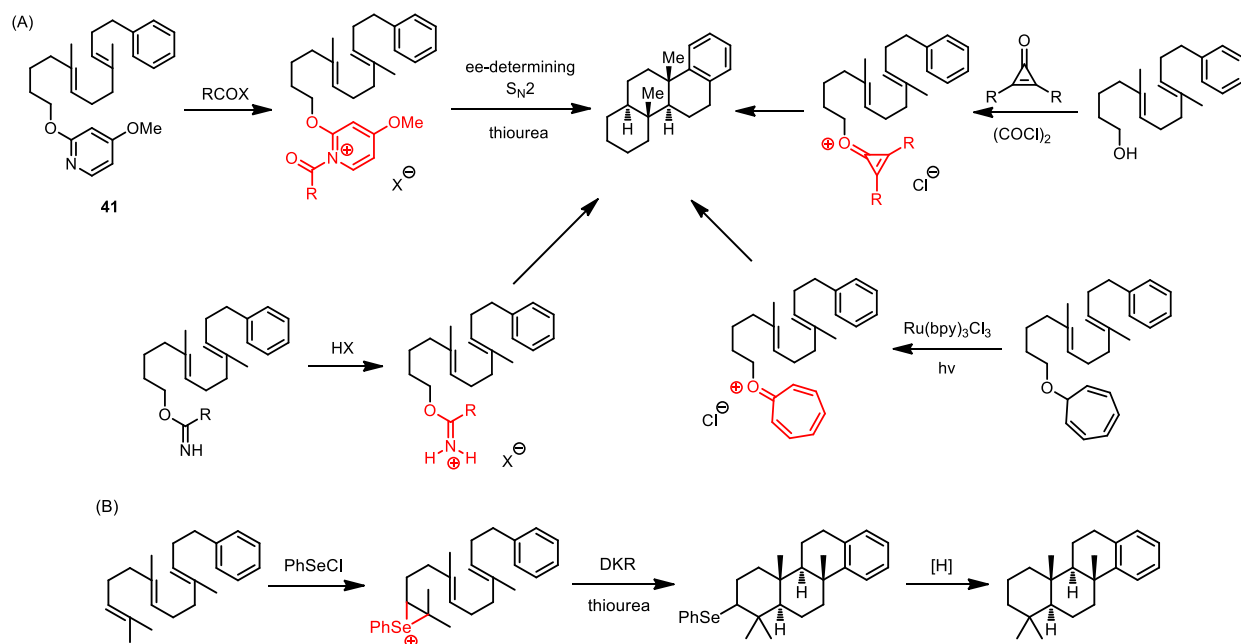
Considering the energy profile and the non-coordinating nature of an all-alkyl substituted carbocation, efficient binding and stabilization of such type of intermediates are extremely difficult. To get around the direct association of carbocations with catalyst, one can rely on the introduction of a traceless cationic leaving group that is more stable and known to bind thiourea of type **21** through anion-binding and cation- $\pi$  interactions.

Promising candidates include *N*-protio-imidinium, *N*-protio-pyrridinium, *N*-acyl-pyrridinium and structures of related types. These cationic intermediates or their analogs have been studied extensively in anion-binding catalysis. For instance, *N*-acylpyridinium ions have been integrated in the acylation of silyl ketene acetals and in the Mannich-type alkylation of pyridines.<sup>37</sup> We envisioned that upon protonation/acylation of the pyridinyl substrate **41**, thiourea would associate with the ion pair and direct the S<sub>N</sub>2-type cyclization event to occur in a selective manner. Other cationic leaving group candidates are also summarized in Scheme 2-26A. As will be discussed in the subsequent chapter, seleniranium ions, which can participate in nucleophilic addition reactions in highly enantioselective fashion, can also be used to initiate the cyclization process (Scheme 2-26B). Such reactive intermediates can be formed through addition of high valence selenium reagent to prochiral olefins. Due to the ability of seleniranium ions to scramble between two olefin molecules at a rate close to diffusion control, a dynamic kinetic resolution is possible in the nucleophilic cyclization step to render the product chiral. The selenium group, if

---

<sup>37</sup> (a) Birrell, J. A.; Desrosiers, J.-N.; Jacobsen, E. N. *J. Am. Chem. Soc.* **2011**, *133*, 13872–13875; (b) Martin, C. L.; Rötheli, A. R.; Jacobsen, E. N. *Manuscript in preparation*.

not desired in the ultimate product, can be removed under very mild conditions using a suitable reductant.



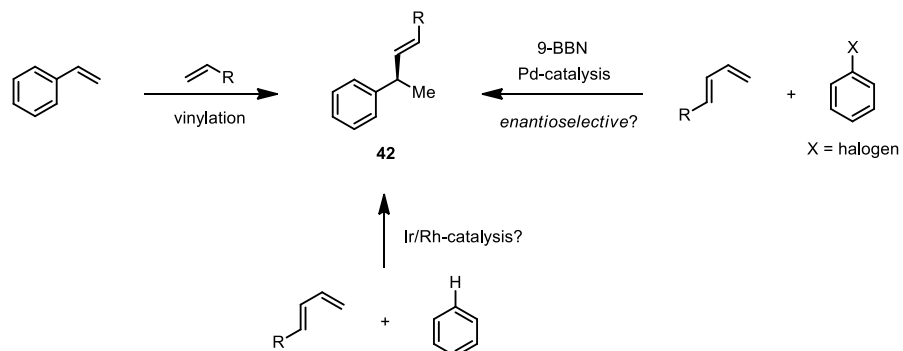
**Scheme 2-26.** Proposed traceless cationic leaving group strategy for polycyclization of unfunctionalized olefin precursors.

### 2.6.3 Enantioselective Hydroarylation of Dienes

In Section 2.3.3.1, we discussed that in the substrate synthesis via *B*-alkyl Suzuki coupling involving a diene substrate (Scheme 2-18), the undesired  $\beta$ -H elimination pathway leads to the formation of a branched cross-coupling product **27** in about 30% yield (Scheme 2-19). Compound **42** (analogous to **27**) is a formal styrene vinylation product, which can potentially be used as a building block in material synthesis.<sup>38</sup> Conditions that favor this “undesired pathway” and induce high enantioselectivity in the C–C bond formation process are of great interest (Scheme 2-27). Perhaps a more interesting scenario would be that this hydroarylation process is achieved through Ir/Rh-catalyzed C–H activation and Markovnikov-type addition to the diene, forming a  $\pi$ -allyl-metal species, which then reductively eliminate the desired product. Recently, Hartwig reported

<sup>38</sup> Direct vinylation of styrene might encounter chemoselectivity problem, as homodimerization could occur.

an Ir-catalyzed hydroheteroarylation of norbornene, supporting that such process can be realized in principle.<sup>39</sup> Due to the irrelevance of this research proposal to the central topic of this chapter, it will not be elaborated here.



**Scheme 2-27.** Proposed hydroarylation approach to enantioenriched vinylstyrene.

<sup>39</sup> Sevov, C. S.; Hartwig, J. F. *J. Am. Chem. Soc.* **2013**, *135*, 2116–2119.

## 2.7 Conclusion

The enantioselective cationic polycyclization reactions catalyzed by **21d** appear to engage a stabilizing cation– $\pi$  interaction as a principal element of enantioselectivity. In this respect, these findings emulate the particularly striking role cation– $\pi$  interactions play in the catalysis of biosynthetic polyene cyclizations and provide clear support for the notion that these interactions can dictate stereocontrol in small-molecule catalysis contexts as well. Moreover, this work further advances the view that stabilization of the dominant transition state structure through noncovalent interactions is a viable means of achieving high levels of enantioselectivity in counterion catalysis. Such strategy will be applied to the development of polycyclization reactions involving more challenging substrate classes as well as other synthetically useful asymmetric transformations.

## Experimental Section

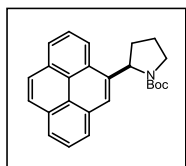
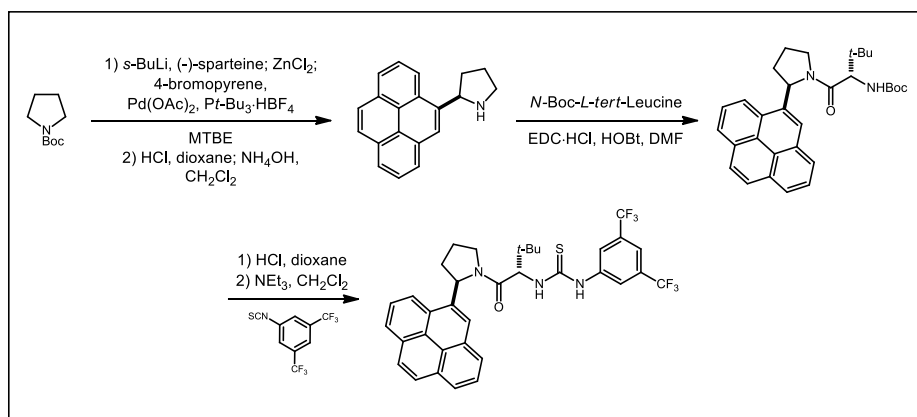
### Table of Content

1. General Information	79
2. General procedures for the preparation of thiourea catalysts	80
3. General procedures for thiourea-catalyzed polycyclization	83
4. General procedure for the synthesis of hydroxylactam substrates	88
5. Eyring Analysis of Enantioselectivity for catalysts <b>21b-d</b>	92
6. Correlation of arene properties with enantioselectivity for catalysts <b>21a-d</b>	94
7. Sub-optimal Substrates	95

### 1. General Information

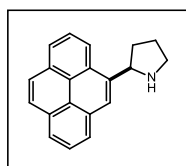
Optimization reactions were performed in oven-dried 2-dram vials; all other reactions were performed in oven-dried round bottom flasks unless otherwise noted. The vials and flasks were fitted with rubber septa and reactions were conducted under air. Stainless steel syringes were used to transfer air- and moisture-sensitive liquids. Flash chromatography was performed using silica gel 60 (230-400 mesh) from EM Science. Commercial reagents were purchased from Sigma Aldrich, Alfa Aesar, Strem, Lancaster or TCI, and used as received with the following exceptions: dichloromethane, tetrahydrofuran, diethyl ether, *t*-butyl methyl ether and methanol were dried by passing through columns of activated alumina; dimethylformamide was dried by passing through columns of activated molecular sieves. Triethylamine and chlorotrimethylsilane were distilled from CaH<sub>2</sub> at 760 torr. *s*-Butyllithium was titrated using diphenylacetic acid as an indicator. Proton nuclear magnetic resonance (<sup>1</sup>H NMR) spectra and carbon nuclear magnetic resonance (<sup>13</sup>C NMR) spectra were recorded on Varian-Mercury-400 (400 MHz) and Inova-500 (500 MHz) spectrometers. Chemical shifts for protons are reported in parts per million downfield from tetramethylsilane and are referenced to residual protium in the NMR solvent (CHCl<sub>3</sub> = δ 7.27). Chemical shifts for carbon are reported in parts per million downfield from tetramethylsilane and are referenced to the carbon resonances of the solvent (CDCl<sub>3</sub> = δ 77.0). Data are represented as follows: chemical shift, multiplicity (br. s = broad, s = singlet, d = doublet, t = triplet, q = quartet, m = multiplet), coupling constants in Hertz (Hz), integration. Infrared (IR) spectra were obtained using a Bruker Optics Tensor 27 FTIR spectrometer. Optical rotations were measured using a 1 mL cell with a 0.5 dm path length on a Jasco DIP 370 digital polarimeter. The mass spectral data were obtained on an Agilent Technologies 6120 quadrupole LC/MS spectrometer. Chiral SFC analysis was performed using a Berger analytical supercritical fluid chromatograph with commercial Chiralpak columns.

## 2. General procedures for the preparation of thiourea catalysts



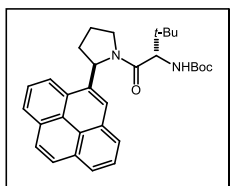
***N*-Boc-(*R*)-2-(4-pyrenyl)pyrrolidine** According to the procedure of Campos, *N*-Boc-pyrrolidine (0.77 mL, 4.4 mmol) and (-)-sparteine (1.01 mL, 4.4 mmol) were dissolved in MTBE (10 mL) and the resulting solution was cooled to  $-78\text{ }^{\circ}\text{C}$ .<sup>1</sup> To this solution *s*-BuLi (1.1 M in cyclohexane, 4 mL, 4.4 mmol) was added dropwise via syringe pump over 40 min and

the resulting solution was stirred for 3 h at  $-78\text{ }^{\circ}\text{C}$ . A solution of ZnCl<sub>2</sub> (1 M in Et<sub>2</sub>O, 4.4 mL, 4.4 mmol) was then added via syringe pump over 30 min with rapid stirring. The resulting suspension was aged at  $-78\text{ }^{\circ}\text{C}$  for 30 min, and then warmed to room temperature. After 30 min, 4-bromopyrene was added, followed by Pd(OAc)<sub>2</sub> (49.4 mg, 0.22 mmol) and Pt-Bu<sub>3</sub>·HBF<sub>4</sub> (69.6 mg, 0.24 mmol) in one portion. The reaction was stirred for 16 hours at room temperature. To facilitate the filtration, ~0.3 mL NH<sub>4</sub>OH was added, and the mixture was stirred for 1 h. The resulting slurry was filtered over Celite and rinsed with MTBE. The filtrate was washed with 1 M HCl and then twice with water. The organic layer was dried over Na<sub>2</sub>SO<sub>4</sub>, filtered and concentrated. The crude product was purified on the silica gel flash chromatography to obtain the desired coupling product as a pale orange gel (1.12 g, 77%), which was applied to the next step directly.

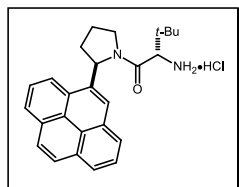


**(*R*)-2-(4-pyrenyl)pyrrolidine** To a solution of *N*-Boc-(*R*)-2-(4-pyrenyl)pyrrolidine (743 mg, 2 mmol) in dioxane (10 mL) was added HCl (4 M in dioxane, 7.5 mL, 30 mmol). The reaction mixture was stirred at room temperature for 6 h, then diluted with CH<sub>2</sub>Cl<sub>2</sub> (30 mL), and quenched with a mixture of water (20 mL) and 33% aqueous NH<sub>4</sub>OH (9 mL). The resulting biphasic liquid was stirred for 1 h. The organic layer was separated, dried over Na<sub>2</sub>SO<sub>4</sub>, and concentrated under vacuum. The crude product was purified by silica gel flash chromatography to obtain the desired amine product as pale orange crystals

(0.41 g, 76%). IR (Film) 3043, 2962, 1589, 1433, 1302, 1175, 1097, 907, 824 (s), 718 (s)  $\text{cm}^{-1}$ ;  $^1\text{H}$  NMR (400 MHz,  $\text{CDCl}_3$ )  $\delta$  = 8.40 (d,  $J$  = 8.1 Hz, 1 H), 8.32 (s, 1 H), 8.18 (dd,  $J$  = 2.9, 7.7 Hz, 2 H), 8.14 (dd,  $J$  = 1.1, 7.7 Hz, 1 H), 8.06 (s, 2 H), 7.99 (td,  $J$  = 7.7, 15.4 Hz, 2 H), 5.08 (t,  $J$  = 7.1 Hz, 1 H), 3.41 (td,  $J$  = 5.9, 10.2 Hz, 1 H), 3.25 (td,  $J$  = 7.5, 9.9 Hz, 1 H), 2.91 (br. s., 1 H), 2.57 (dt,  $J$  = 7.1, 13.5 Hz, 1 H), 2.10 - 1.96 (m, 2 H), 1.96 - 1.85 (m, 1 H);  $^{13}\text{C}$  NMR (100 MHz,  $\text{CDCl}_3$ )  $\delta$  = 139.4, 131.5, 130.8, 129.9, 127.5, 127.2, 125.9, 125.5, 125.2, 125.1, 124.9, 124.6, 123.8, 122.8, 121.2, 58.8, 46.8, 33.3, 25.4; MS (ESI-APCI) exact mass calculated for  $[\text{M}+\text{H}]$  ( $\text{C}_{20}\text{H}_{18}\text{N}$ ) requires  $m/z$  272.1, found  $m/z$  272.1;  $[\alpha]_{\text{D}}^{23}$  = +113.5 ( $c$  = 1.0,  $\text{CHCl}_3$ ).

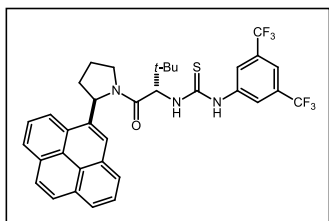


**tert-butyl ((S)-3,3-dimethyl-1-oxo-1-((R)-2-(pyren-4-yl)pyrrolidin-1-yl)butan-2-yl)carbamate** A 100 mL round bottom flask was charged with (*R*)-2-(4-pyrenyl)pyrrolidine (0.81 g, 3.0 mmol), *N*-Boc-*L*-*tert*-Leucine (762 mg, 3.3 mmol), EDC·HCl (630 mg, 3.3 mmol), HOBt (446 mg, 3.3 mmol) and DMF (15 mL). The solution was stirred at room temperature for 6 h, and quenched with water. The aqueous layer was separated and extracted three times with EtOAc. The combined organic layers were washed with  $\text{NH}_4\text{Cl}$  and brine, dried over  $\text{Na}_2\text{SO}_4$ , and concentrated to obtain the crude product, which purified by silica gel flash chromatography to give the desired amide product as pale yellow crystals (1.21 g, 83%). IR (Film) 2966 (s), 1779 (s), 1708 (s), 1647 (s), 1497, 1423, 1366, 1242, 1170 (s)  $\text{cm}^{-1}$ ;  $^1\text{H}$  NMR (500 MHz,  $\text{CDCl}_3$ )  $\delta$  = 8.33 (d,  $J$  = 7.8 Hz, 1 H), 8.19 (d,  $J$  = 7.8 Hz, 1 H), 8.16 - 7.89 (m, 6 H), 7.66 (s, 1 H), 6.17 (d,  $J$  = 8.3 Hz, 1 H), 5.23 (d,  $J$  = 9.8 Hz, 1 H), 4.58 (d,  $J$  = 9.8 Hz, 1 H), 4.50 - 4.41 (m, 1 H), 3.95 - 3.89 (m, 1 H), 2.54 - 2.44 (m, 1 H), 2.18 - 2.06 (m, 3 H), 1.54 (s, 9 H), 1.11 (s, 9 H);  $^{13}\text{C}$  NMR (125 MHz,  $\text{CDCl}_3$ )  $\delta$  = 170.8, 156.3, 136.0, 131.6, 130.8, 130.4, 128.8, 127.4, 127.2, 126.1, 125.8, 125.6, 125.4, 125.0, 124.8, 124.0, 122.4, 120.9, 79.6, 58.8, 58.3, 48.5, 34.8, 32.3, 28.5, 26.5, 23.6; MS (ESI-APCI) exact mass calculated for  $[\text{M}+\text{Na}]$  ( $\text{C}_{31}\text{H}_{36}\text{N}_2\text{NaO}_3$ ) requires  $m/z$  507.3, found  $m/z$  507.2;  $[\alpha]_{\text{D}}^{23}$  = +139.5 ( $c$  = 0.84,  $\text{CHCl}_3$ ).



**(S)-3,3-dimethyl-1-oxo-1-((R)-2-(pyren-4-yl)pyrrolidin-1-yl)butan-2-ylamine hydrochloride** To a solution of *tert*-butyl ((*S*)-3,3-dimethyl-1-oxo-1-((*R*)-2-(pyren-4-yl)pyrrolidin-1-yl)butan-2-yl) carbamate (1.2 g, 2.5 mmol) in dioxane (10 mL) at 0 °C was

added HCl (4 M in dioxane, 35 mL, 140 mmol) slowly. The reaction was warmed to room temperature and stirred until the starting material was consumed, as judged by TLC analysis. The reaction mixture was then concentrated under vacuum, yielding a yellow/brown solid that was used directly without further purification.



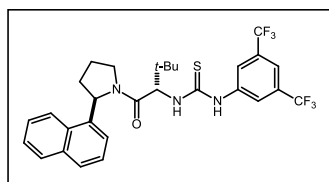
**1-(3,5-bis(trifluoromethyl)phenyl)-3-((S)-3,3-dimethyl-1-oxo-1-((R)-2-**

**(pyren-4-yl)pyrrolidin-1-yl)butan-2-yl)thiourea (21d)** To a solution of crude

(S)-3,3-dimethyl-1-oxo-1-((R)-2-(pyren-4-yl)pyrrolidin-1-yl)butan-2-aminium chloride (obtained from the previous step, ~2.5 mmol) in CH<sub>2</sub>Cl<sub>2</sub> was added NEt<sub>3</sub>

(1.0 mL, 7.5 mmol) dropwise. The mixture was stirred for 15 min, and 3,5-bis(trifluoromethyl)phenyl isothiocyanate (0.50 mL, 2.75 mmol) was added dropwise. The reaction was stirred overnight, concentrated under vacuum, and purified by silica gel flash chromatography to obtain the desired thiourea as yellow crystals (1.16 g, 71% over two steps). IR (Film) 3319, 2970, 1610 (s), 1523, 1473, 1443, 1382 (s), 1274 (s), 1173 (s), 1130 (s), 961, 883, 826, 754 (s), 722 cm<sup>-1</sup>; <sup>1</sup>H NMR (500 MHz, CDCl<sub>3</sub>) δ = 8.67 (br. s., 1 H), 8.19 (d, *J* = 7.8 Hz, 1 H), 8.14 (d, *J* = 7.8 Hz, 1 H), 8.12 - 8.08 (m, 2 H), 8.02 (s, 2 H), 8.00 - 7.92 (m, 1 H), 7.89 - 7.80 (m, 2 H), 7.70 (br. s., 2 H), 7.49 (br. s., 1 H), 6.99 (br. s., 1 H), 6.10 (d, *J* = 7.3 Hz, 1 H), 5.60 (d, *J* = 9.8 Hz, 1 H), 4.86 (t, *J* = 9.0 Hz, 1 H), 3.95 (dd, *J* = 9.8, 17.1 Hz, 1 H), 2.52 (td, *J* = 10.0, 19.5 Hz, 1 H), 2.16 (d, *J* = 10.7 Hz, 1 H), 2.14 - 2.06 (m, 2 H), 1.18 (s, 9 H); <sup>13</sup>C NMR (125 MHz, CDCl<sub>3</sub>) δ = 180.9, 170.3, 139.3, 134.4, 131.9, 131.6, 131.4, 130.6, 130.3, 128.4, 127.7, 127.4, 127.2, 125.8, 125.5, 125.3, 125.0, 124.9, 124.8, 124.1, 123.8, 123.6, 122.9, 122.7, 121.6, 120.5, 118.1, 63.2, 60.4, 58.8, 48.8, 47.5, 35.9, 35.3, 32.2, 27.1, 26.8, 23.4, 21.0, 14.1; MS (ESI-APCI) exact mass calculated for [M+H] (C<sub>35</sub>H<sub>32</sub>F<sub>6</sub>N<sub>3</sub>OS) requires *m/z* 656.2, found *m/z* 656.3; [α]<sub>D</sub><sup>23</sup> = +66.0 (c = 1.1, CHCl<sub>3</sub>).

**Characterization data for all novel catalysts in Table 1**



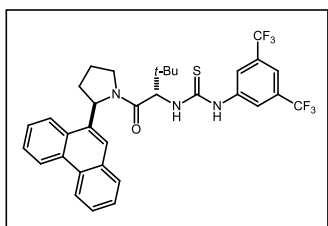
**1-(3,5-bis(trifluoromethyl)phenyl)-3-((S)-3,3-dimethyl-1-oxo-1-((R)-2-(naphthalen-**

**1-yl)pyrrolidin-1-yl)-1-oxobutan-2-yl)thiourea (21b).** IR (Film) 3335 (br),

2963, 1699, 1609, 1525, 1474, 1445, 1384, 1275 (s), 1175, 1131 (s), 961, 884,

777 cm<sup>-1</sup>; <sup>1</sup>H NMR (400 MHz, CDCl<sub>3</sub>) δ = 7.86 - 7.67 (m, 3 H), 7.55 - 7.35 (m, 4 H), 7.18 - 7.01 (m, 2 H), 5.83 (d, *J* = 8.1 Hz, 1 H), 5.55 (d, *J* = 9.5 Hz, 1 H), 4.63 (t, *J* = 9.0 Hz, 1 H), 3.88 (dd, *J* = 10.2, 17.6 Hz, 1 H), 2.45 - 2.26 (m,

1 H), 2.02 - 1.87 (m, 3 H), 1.16 (s, 9 H);  $^{13}\text{C}$  NMR (100 MHz,  $\text{CDCl}_3$ )  $\delta$  = 181.3, 170.3, 139.4, 137.4, 136.0, 133.7, 132.1, 131.8, 129.7, 128.8, 127.3, 126.6, 125.8, 125.3, 124.8, 123.7, 122.8, 121.7, 118.5, 63.1, 58.7, 48.7, 35.6, 32.8, 27.1, 26.9, 23.3; MS (ESI-APCI) exact mass calculated for  $[\text{M}-\text{H}]$  ( $\text{C}_{29}\text{H}_{28}\text{F}_6\text{N}_3\text{OS}$ ) requires  $m/z$  580.2, found  $m/z$  580.2;  $[\alpha]_{\text{D}}^{24}$  = -61.5 ( $c$  = 1.0,  $\text{CHCl}_3$ ).



**1-(3,5-bis(trifluoromethyl)phenyl)-3-((S)-3,3-dimethyl-1-oxo-1-((R)-2-**

**(phenanthren-9-yl)pyrrolidin-1-yl)butan-2-yl)thiourea (21c).** IR (Film) 3328

(br), 2963, 1611, 1529, 1474, 1447, 1383, 1276 (s), 1177, 1134 (s), 962, 885, 749

$\text{cm}^{-1}$ ;  $^1\text{H}$  NMR (400MHz,  $\text{CDCl}_3$ )  $\delta$  = 9.66 (br. s., 1 H), 8.56 (d,  $J$  = 8.1 Hz, 1 H),

8.47 (d,  $J$  = 8.4 Hz, 1 H), 7.74 (br. s., 10 H), 5.82 (d,  $J$  = 8.1 Hz, 1 H), 5.60 (d,  $J$  = 9.1 Hz, 1 H), 4.84 (t,  $J$  = 9.1 Hz, 1 H), 3.88 (dd,  $J$  = 9.9, 17.6 Hz, 1 H), 2.48 - 2.31 (m, 1 H), 2.10 - 1.92 (m, 3 H), 1.16 (s, 9 H);  $^{13}\text{C}$  NMR (100 MHz,  $\text{CDCl}_3$ )  $\delta$  = 181.1, 170.6, 139.6, 133.4, 131.8, 131.5, 131.2, 130.7, 129.5, 129.1, 128.6, 126.6, 126.4, 126.4, 126.0, 123.5, 123.3, 122.7, 122.1, 118.0, 63.1, 58.7, 48.8, 35.3, 32.2, 26.7, 23.3; MS (ESI-APCI) exact mass calculated for  $[\text{M}-\text{H}]$  ( $\text{C}_{33}\text{H}_{30}\text{F}_6\text{N}_3\text{OS}$ ) requires  $m/z$  630.2, found  $m/z$  630.2;  $[\alpha]_{\text{D}}^{24}$  = +20.7 ( $c$  = 1.0,  $\text{CHCl}_3$ ).

### 3. General procedures for thiourea-catalyzed polycyclization

#### Method A (reaction optimization):

An oven-dried vial was charged with starting material (0.033 mmol, 1.0 equiv), thiourea catalyst (0.00495 mmol, 0.15 equiv), 4Å molecular sieves (20 mg) and MTBE (1.3 mL). The flask was cooled to  $-78$  °C and HCl (2 M in diethyl ether, 0.00825 to 0.0165 mmol, 0.25 to 0.50 equiv) was added dropwise. The reaction was placed in a  $-30$  °C cryocool, stirred for 48 h, and then quenched at that temperature by addition of pre-cooled  $\text{NEt}_3$  (~0.1 mL of 20% v/v solution in EtOAc). The reaction was diluted with acetone, filtered through a pipette containing  $\frac{3}{4}$  inch of silica gel, and rinsed with acetone. The solvent was removed by rotary evaporation under reduced pressure to give the crude residue, which was purified by preparative silica gel thin layer chromatography.

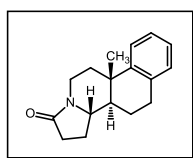
#### Method B (hydroxylactam substrate scope):

An oven-dried round bottom flask (25 mL) was charged with starting material (0.25 mmol, 1.0 equiv), thiourea catalyst (0.375 mmol, 0.15 equiv), 4Å molecular sieves (160 mg) and MTBE (10 mL). The flask was cooled to –

78 °C and HCl (2 M in diethyl ether, 0.0625 to 0.125 mmol, 0.25 to 0.50 equiv) was added dropwise. The reaction was placed in a -30 °C cryocool, stirred for 72-96 h, and then quenched at that temperature by addition of pre-cooled NEt<sub>3</sub> (~1 mL of 20% v/v solution in EtOAc). The reaction was filtered through a pipette containing 1 inch of silica gel, and rinsed with acetone. The solvent was removed by rotary evaporation under reduced pressure to give the crude residue, which was purified by silica gel chromatography.

#### Method C (for acyloxylactam 13):

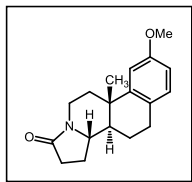
An oven-dried round bottom flask (25 mL) was charged with starting material (0.25 mmol, 1.0 equiv), CH<sub>2</sub>Cl<sub>2</sub> (2.5 mL) and NEt<sub>3</sub> (0.78 mmol, 3.1 equiv). The solution was cooled to 0 °C, and acetyl chloride (0.73 mmol, 2.9 equiv) was added dropwise with stirring. The reaction was aged at room temperature for 1.5 h. The resulting light yellow suspension was filtered through a short neutral alumina plug, rinsed with acetone, and then subjected to vacuum to remove the remaining reagents and solvent. To the oily residue was added thiourea catalyst (0.375 mmol, 0.15 equiv), 4Å molecular sieves (160 mg) and MTBE (10 mL). The flask was cooled to -78 °C and TMSCl (0.50 mmol, 2.0 equiv) was added dropwise. The reaction was placed in a -30 °C cryocool, stirred for 117 h, and then quenched at that temperature by addition of pre-cooled NEt<sub>3</sub> (~1 mL of 20% v/v solution in EtOAc). The reaction was filtered through a pipette containing 1 inch of silica gel, and rinsed with acetone. The solvent was removed by rotary evaporation under reduced pressure to give the crude residue, which was purified by silica gel chromatography.



**(4bS,10aS,10bR)-4b-methyl-5,6,9,10,10a,10b,11,12-octahydrobenzo[f]pyrrolo[2,1-a]isoquinolin-8(4bH)-one (30)**

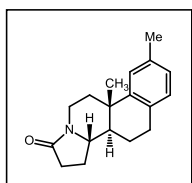
Followed method B from **9** (68.3 mg, 0.25 mmol), with 0.25 equiv HCl (31.3 μL, 0.0625 mmol), for 96 h, and purified using silica gel chromatography to give 32.5 mg (51% yield) of **10** as a colorless gel. This material was determined to be 89% ee by chiral SFC analysis (ChiralPak AS, 30% MeOH, 3 mL/min, 225 nm, *t*<sub>r</sub>(major) = 3.6 min, *t*<sub>r</sub>(minor) = 5.6 min). IR (Film): 2931, 1685 (s), 1420, 1275, 762, 668 cm<sup>-1</sup>; <sup>1</sup>H NMR (500 MHz, CDCl<sub>3</sub>) δ = 7.31 - 7.26 (m, 1 H), 7.22 - 7.13 (m, 2 H), 7.10 (d, *J* = 7.3 Hz, 1 H), 4.18 (ddd, *J* = 1.5, 5.4, 13.7 Hz, 1 H), 3.49 (ddd, *J* = 7.3, 8.3, 10.7 Hz, 1 H), 3.08 (dt, *J* = 3.9, 13.4 Hz, 1 H), 2.98 - 2.91 (m, 2 H), 2.45 - 2.38 (m, 2 H), 2.34 - 2.24 (m, 2 H), 1.84 - 1.76 (m, 1 H), 1.72 - 1.54 (m, 3 H), 1.42 (ddd, *J* = 2.9, 10.7, 13.2 Hz, 1 H), 1.23 (s, 3 H); <sup>13</sup>C NMR (125 MHz, CDCl<sub>3</sub>) δ = 173.5, 145.5, 134.7, 129.4, 126.0, 126.0, 124.6, 56.7, 48.7, 36.4, 36.2, 35.8, 30.7,

28.7, 24.9, 21.4, 19.6; MS (APCI) exact mass calculated for [M+H] (C<sub>17</sub>H<sub>22</sub>NO) requires *m/z* 256.2, found *m/z* 256.2; [α]<sub>D</sub><sup>23</sup> = +6.5 (c = 1.2, CHCl<sub>3</sub>).



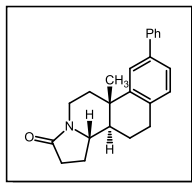
**(4bS,10aS,10bR)-3-methoxy-4b-methyl-5,6,9,10,10a,10b,11,12-octahydrobenzo[f]pyrrolo[2,1-a]isoquinolin-8(4bH)-one (19)**

Followed method B from **1** (76 mg, 0.25 mmol), with 0.25 equiv HCl (31.3 μL, 0.0625 mmol), for 72 h, and purified by silica gel chromatography to give 51 mg (72% yield) of **2** as a white solid. This material was determined to be 94% ee by chiral SFC analysis (ChiralPak AD-H, 25% MeOH, 3 mL/min, 210 nm, *t*<sub>r</sub>(major) = 3.8 min, *t*<sub>r</sub>(minor) = 4.8 min). IR (Film): 2932, 2870, 1686 (s), 1610, 1502, 1285, 1245, 1214, 1067, 1041, 911, 853, 807, 735 cm<sup>-1</sup>; <sup>1</sup>H NMR: (500 MHz, CDCl<sub>3</sub>) δ 7.02 (d, 1H, *J* = 8.5 Hz), 6.81 (d, 1H, *J* = 2.5 Hz), 6.81 (dd, 1H, *J* = 2.5, 8.5 Hz), 4.16 (dd, 1H, 5.0, 13.5 Hz), 3.80 (s, 3H), 3.48 (dt, 1H, *J* = 10.5, 7.6 Hz), 3.06 (td, 1H, 13.5, 3.0 Hz), 2.88 (m, 2H), 2.41 (m, 1H), 2.40 (d, 1H, *J* = 10 Hz), 2.29 (m, 1H), 2.23 (dd, 1H, *J* = 2.5, 13.5 Hz), 1.77 (m, 1H), 1.62 (m, 3H), 1.39 (m, 1H), 1.22 (s, 3H); <sup>13</sup>C NMR: (125 MHz, CDCl<sub>3</sub>) δ 173.8, 158.1, 147.0, 130.5, 127.1, 11.4, 110.7, 57.0, 55.5, 49.0, 36.9, 36.5, 36.1, 31.0, 28.2, 25.1, 21.6, 20.0; MS (APCI) exact mass calculated for [M+H] (C<sub>18</sub>H<sub>24</sub>NO<sub>2</sub>) requires *m/z* 286.2, found *m/z* 286.2; [α]<sub>D</sub><sup>23</sup> = +30.2 (c = 0.86, CHCl<sub>3</sub>).



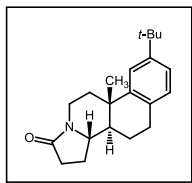
**(4bS,10aS,10bR)-3,4b-dimethyl-5,6,9,10,10a,10b,11,12-octahydrobenzo[f]pyrrolo[2,1-a]isoquinolin-8(4bH)-one (32)**

Followed method B from **11** (72 mg, 0.25 mmol), with 0.25 equiv HCl (31.3 μL, 0.0625 mmol), for 96 h, and purified using silica gel chromatography to give 42.0 mg (62% yield) of **12** as a colorless gel. This material was determined to be 91% ee by chiral SFC analysis (ChiralPak AD-H, 10% MeOH, 3 mL/min, 210 nm, *t*<sub>r</sub>(major) = 6.9 min, *t*<sub>r</sub>(minor) = 8.8 min). IR (Film): 2931, 2870, 1686 (s), 1419, 1299 (s), 1184 (s), 1104, 973, 852, 808, 731, 666 cm<sup>-1</sup>; <sup>1</sup>H NMR: (500 MHz, CDCl<sub>3</sub>) δ 7.06 (s, 1H), 6.96 (app. q, 2H, *J* = 8.0 Hz), 4.15 (ddd, 1H *J* = 1.5, 5.5, 14.0 Hz), 3.46 (m, 1H), 3.05 (td, 1H, *J* = 4.0, 14.0), 2.88 (m, 2H), 2.38 (m, 2H), 2.31 (s, 3H), 2.27 (dd, 2H, *J* = 4.0, 12.0 Hz), 1.75 (m, 1H), 1.60 (m, 3H), 1.38 (m, 1H), 1.20 (s, 3H); <sup>13</sup>C NMR: (125 MHz, CDCl<sub>3</sub>) δ 173.8, 145.5, 135.6, 131.9, 129.5, 127.1, 125.5, 57.0, 49.1, 36.6, 36.5, 36.1, 31.0, 28.6, 25.2, 21.6, 21.5, 19.9; MS (APCI) exact mass calculated for [M+H] (C<sub>18</sub>H<sub>24</sub>NO) requires *m/z* 270.2, found *m/z* 270.2; [α]<sub>D</sub><sup>23</sup> = +18.2 (c = 2.28, CHCl<sub>3</sub>).



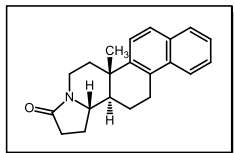
**(4bS,10aS,10bR)-4b-methyl-3-phenyl-5,6,9,10,10a,10b,11,12-octahydrobenzo[f]pyrrolo[2,1-a]isoquinolin-8(4bH)-one (34)**

Followed method C from **13** (87.9 mg, 0.25 mmol), with 2.0 equiv TMSCl (63.5  $\mu$ L, 0.50 mmol), for 117 h, and purified using silica gel chromatography to give 44.9 mg (54% yield) of **14** as a white foam. This material was determined to be 91% ee by chiral SFC analysis (ChiralPak AS-H, 20% MeOH, 3 mL/min, 210 nm,  $t_r$ (major) = 4.9 min,  $t_r$ (minor) = 6.0 min). IR (Film): 2930 (s), 1676 (s), 1482, 1420, 1274, 1184, 909, 760, 727 (s), 698  $\text{cm}^{-1}$ ;  $^1\text{H}$  NMR (500 MHz,  $\text{CDCl}_3$ )  $\delta$  = 7.58 - 7.54 (m, 2 H), 7.47 (d,  $J$  = 2.0 Hz, 1 H), 7.43 (t,  $J$  = 7.8 Hz, 2 H), 7.39 - 7.31 (m, 2 H), 7.16 (d,  $J$  = 7.8 Hz, 1 H), 4.18 (ddd,  $J$  = 1.7, 5.6, 13.7 Hz, 1 H), 3.50 (ddd,  $J$  = 6.8, 8.8, 10.7 Hz, 1 H), 3.08 (dt,  $J$  = 3.9, 13.4 Hz, 1 H), 3.00 - 2.93 (m, 2 H), 2.44 - 2.34 (m, 3 H), 2.30 (dtd,  $J$  = 4.4, 6.8, 11.2 Hz, 1 H), 1.84 - 1.78 (m, 1 H), 1.73 - 1.60 (m, 3 H), 1.44 (ddd,  $J$  = 2.9, 10.5, 12.9 Hz, 1 H), 1.26 (s, 3 H);  $^{13}\text{C}$  NMR (125 MHz,  $\text{CDCl}_3$ )  $\delta$  = 173.6, 145.8, 141.3, 139.1, 133.9, 129.9, 128.7, 127.1, 127.0, 124.9, 123.5, 56.7, 48.7, 36.7, 36.3, 35.8, 30.7, 28.5, 24.9, 21.5, 19.6; MS (ESI-APCI) exact mass calculated for  $[\text{M}+\text{H}]$  ( $\text{C}_{23}\text{H}_{25}\text{NO}$ ) requires  $m/z$  332.2, found  $m/z$  332.2;  $[\alpha]_{\text{D}}^{23}$  = +85.5 (c = 0.6  $\text{CHCl}_3$ ).



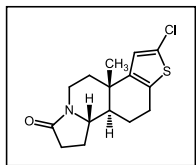
**(4bS,10aS,10bR)-3-(tert-butyl)-4b-methyl-5,6,9,10,10a,10b,11,12-octahydrobenzo[f]pyrrolo[2,1-a]isoquinolin-8(4bH)-one (36)**

Followed method B from **15** (82.4 mg, 0.25 mmol), with 0.25 equiv HCl (31.3  $\mu$ L, 0.0625 mmol), for 96 h, and purified using silica gel chromatography to give 55.3 mg (71% yield) of **16** as a colorless gel. This material was determined to be 91% ee by chiral SFC analysis (ChiralPak OD-H, 10% MeOH, 3 mL/min, 225 nm,  $t_r$ (minor) = 5.5 min,  $t_r$ (major) = 6.0 min). IR (Film) 2961 (s), 2868, 1685 (s), 1499, 1419, 1313, 1270, 1185, 909, 819, 729 (s)  $\text{cm}^{-1}$ ;  $^1\text{H}$  NMR (500 MHz,  $\text{CDCl}_3$ )  $\delta$  = 7.29 (d,  $J$  = 2.0 Hz, 1 H), 7.26 (s, 1 H), 7.18 (dd,  $J$  = 2.2, 8.1 Hz, 1 H), 7.03 (d,  $J$  = 8.3 Hz, 1 H), 4.16 (ddd,  $J$  = 1.5, 5.4, 13.7 Hz, 1 H), 3.47 (ddd,  $J$  = 6.8, 8.3, 10.7 Hz, 1 H), 3.07 (dt,  $J$  = 3.7, 13.6 Hz, 1 H), 2.91 - 2.86 (m, 2 H), 2.43 - 2.36 (m, 2 H), 2.33 - 2.23 (m, 2 H), 1.79 - 1.72 (m, 1 H), 1.68 - 1.53 (m, 3 H), 1.44 - 1.36 (m, 1 H), 1.31 (s, 9 H), 1.22 (s, 3 H);  $^{13}\text{C}$  NMR (125 MHz,  $\text{CDCl}_3$ )  $\delta$  = 173.6, 148.8, 144.9, 131.8, 129.0, 123.2, 121.3, 56.7, 48.9, 36.7, 36.3, 35.8, 34.5, 31.4, 30.7, 28.3, 25.0, 21.4, 19.6; MS (ESI-APCI) exact mass calculated for  $[\text{M}+\text{H}]$  ( $\text{C}_{21}\text{H}_{29}\text{NO}$ ) requires  $m/z$  312.2, found  $m/z$  312.1;  $[\alpha]_{\text{D}}^{23}$  = +34.7 (c = 1.0,  $\text{CHCl}_3$ ).



**(6a*S*,14a*R*,14b*S*)-6a-methyl-1,5,6,6a,13,14,14a,14b-octahydronaphtho[2,1-  
f]pyrrolo[2,1-a]isoquinolin-3(2*H*)-one (38)**

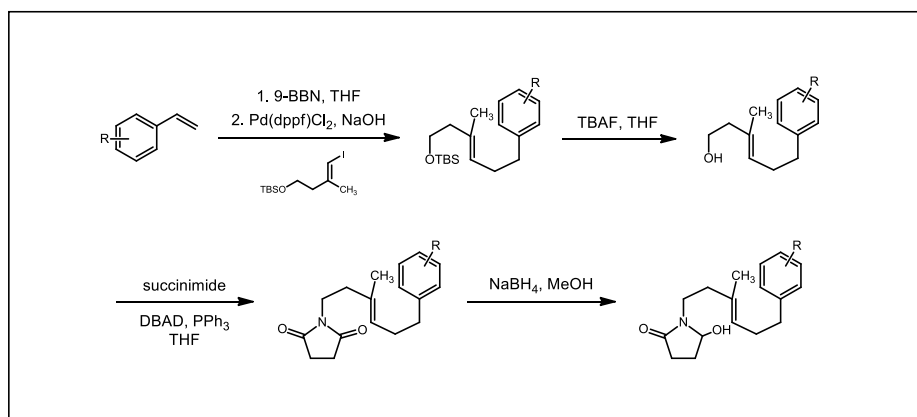
Followed method B from **17** (80.9 mg, 0.25 mmol), with 0.50 equiv HCl (62.5  $\mu$ L, 0.125 mmol), for 72 h, and purified using silica gel chromatography to give 57.2 mg (75% yield) of **18** as a white solid. This material was determined to be 92% ee by chiral SFC analysis (ChiralPak AD-H, 30% MeOH, 3 mL/min, 225 nm,  $t_r$ (minor) = 10.4 min,  $t_r$ (major) = 12.5 min). IR (Film) 2931, 1675 (s), 1508, 1421, 1380, 1285, 1264, 1162, 813, 732 (s)  $\text{cm}^{-1}$ ;  $^1\text{H}$  NMR (500 MHz,  $\text{CDCl}_3$ )  $\delta$  = 7.97 (d,  $J$  = 8.3 Hz, 1 H), 7.80 (d,  $J$  = 8.3 Hz, 1 H), 7.71 (d,  $J$  = 8.8 Hz, 1 H), 7.51 (ddd,  $J$  = 1.5, 6.8, 8.3 Hz, 1 H), 7.49 - 7.42 (m, 2 H), 4.19 (ddd,  $J$  = 1.7, 5.5, 13.8 Hz, 1 H), 3.55 (ddd,  $J$  = 6.5, 8.4, 10.5 Hz, 1 H), 3.38 (dd,  $J$  = 6.3, 17.6 Hz, 1 H), 3.23 - 3.16 (m, 1 H), 3.12 (dt,  $J$  = 3.9, 13.7 Hz, 1 H), 2.46 - 2.37 (m, 3 H), 2.37 - 2.29 (m, 1 H), 1.99 (dd,  $J$  = 7.8, 13.2 Hz, 1 H), 1.78 (ddd,  $J$  = 6.8, 11.7, 13.2 Hz, 1 H), 1.69 (dtd,  $J$  = 8.3, 10.3, 12.2 Hz, 1 H), 1.58 (dt,  $J$  = 5.4, 13.2 Hz, 1 H), 1.51 (ddd,  $J$  = 2.4, 10.7, 13.2 Hz, 1 H), 1.31 (s, 3 H);  $^{13}\text{C}$  NMR (125 MHz,  $\text{CDCl}_3$ )  $\delta$  = 173.5, 142.3, 132.2, 131.8, 129.5, 128.3, 126.6, 126.1, 125.3, 123.1, 123.1, 56.6, 48.7, 36.8, 36.2, 36.1, 30.7, 25.8, 24.8, 20.9, 19.4; MS (ESI-APCI) exact mass calculated for  $[\text{M}+\text{H}]$  ( $\text{C}_{21}\text{H}_{24}\text{NO}$ ) requires  $m/z$  306.2, found  $m/z$  306.2;  $[\alpha]_{\text{D}}^{23}$  = -16.1 ( $c$  = 1.0,  $\text{CHCl}_3$ ).



**(3b*S*,9a*S*,9b*R*)-2-chloro-3b-methyl-4,5,8,9,9a,9b,10,11-octahydropyrrolo[2,1-  
a]thieno[3,2-f]isoquinolin-7(3b*H*)-one (40)**

Followed method B from **19** (78.5 mg, 0.25 mmol), with 0.25 equiv HCl (31.3  $\mu$ L, 0.0625 mmol), at -10  $^{\circ}\text{C}$  for 72 h, and purified using silica gel chromatography to give 57.3 mg (77% yield) of **20** as a white solid. This material was determined to be 91% ee by chiral SFC analysis (ChiralPak OD-H, 15% MeOH, 3 mL/min, 254 nm,  $t_r$ (minor) = 7.8 min,  $t_r$ (major) = 8.5 min). IR (Film) 2936, 1666 (s), 1455, 1283, 1183, 967  $\text{cm}^{-1}$ ;  $^1\text{H}$  NMR (500 MHz,  $\text{CDCl}_3$ )  $\delta$  = 6.64 (s, 1 H), 4.11 (ddd,  $J$  = 1.5, 5.6, 13.9 Hz, 1 H), 3.45 (ddd,  $J$  = 6.8, 8.3, 10.7 Hz, 1 H), 3.01 (dt,  $J$  = 3.9, 13.4 Hz, 1 H), 2.82 (ddd,  $J$  = 1.5, 6.3, 16.6 Hz, 1 H), 2.78 - 2.69 (m, 1 H), 2.43 - 2.35 (m, 2 H), 2.30 - 2.20 (m, 1 H), 1.95 (ddd,  $J$  = 1.5, 3.9, 13.2 Hz, 1 H), 1.79 (tdd,  $J$  = 2.0, 6.8, 13.2 Hz, 1 H), 1.73 - 1.49 (m, 4 H), 1.38 (ddd,  $J$  = 2.4, 10.7, 12.7 Hz, 1 H), 1.17 (s, 3 H);  $^{13}\text{C}$  NMR (125 MHz,  $\text{CDCl}_3$ )  $\delta$  = 173.6, 143.9, 133.1, 127.1, 123.0, 56.0, 49.0, 35.9, 35.7, 30.6, 24.8, 24.5, 20.1, 19.8; MS (ESI-APCI) exact mass calculated for  $[\text{M}+\text{H}]$  ( $\text{C}_{15}\text{H}_{18}\text{ClNOS}$ ) requires  $m/z$  296.1, found  $m/z$  296.0;  $[\alpha]_{\text{D}}^{23}$  = +34.7 ( $c$  = 1.0,  $\text{CHCl}_3$ ).

#### 4. General procedure for the synthesis of hydroxylactam substrates



#### **B-Alkyl Suzuki-Miyaura coupling of vinyl iodide and styrenes**

A round bottom flask was charged with a solution of vinylarene (6.1 mmol, 2.0 equiv) in THF (3 mL), flushed with N<sub>2</sub>, and cooled to 0 °C. A solution of 9-BBN (0.5 M in THF, 13.5 mL, 6.75 mmol, 2.2 equiv) was added slowly. The homogeneous solution was warmed to room temperature and stirred for 6 hours. (White precipitates occasionally formed upon addition of 9-BBN, but disappeared during as the reaction warmed). When the hydroboration was complete, the reaction was cooled to 0 °C, and aqueous NaOH (3 M, 6 mL, 18.4 mmol, 6 equiv), Pd(dppf)Cl<sub>2</sub>·2CH<sub>2</sub>Cl<sub>2</sub> (253 mg, 0.31 mmol, 0.10 equiv), and (*E*)-(4-iodo-3-methylbut-3-en-1-yl) *tert*-butyldimethylsilylether (1.0 g, 3.07 mmol, 1.0 equiv) were added sequentially.<sup>2</sup> The reaction mixture was moved to a 4 °C refrigerated reactor and stirred overnight. Saturated aqueous NH<sub>4</sub>Cl solution was added to neutralize NaOH, and separated from the organic layer. The aqueous layer was extracted with ethyl acetate. The combined organic layers were washed with brine, dried over NaSO<sub>4</sub>, concentrated, and the crude extracts were purified by silica gel column chromatography (gradient from 100% hexane to 10% EtOAc/hexane) to obtain the coupling product.

#### **Deprotection of *tert*-butyl dimethylsilyl group**

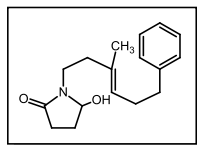
To a solution of (*E*)-*tert*-butyldimethyl((3-methyl-6-arylhex-3-en-1-yl)oxy)silane (3.5 mmol, 1.0 equiv) in THF (6 mL) was added TBAF (1 M in THF, 4.6 mmol, 1.2 equiv) at room temperature. After the reaction was complete, the reaction was diluted with a saturated aqueous NH<sub>4</sub>Cl solution. The biphasic mixture was separated and the aqueous layer was extracted with EtOAc once. The combined organic layers were washed with brine, dried over Na<sub>2</sub>SO<sub>4</sub> and concentrated. The crude extracts were purified by silica gel column chromatography to obtain the alcohol product.

### Mitsunobu reaction between homoallylic alcohols and succinimide

A solution of (*E*)-3-methyl-6-arylhex-3-en-1-ol (3.4 mmol, 1.0 equiv), succinimide (3.7 mmol, 1.1 equiv) and PPh<sub>3</sub> (3.7 mmol, 1.1 equiv) in THF (20 mL) was cooled to 0 °C. To this solution was added a solution of DBAD (3.7 mmol, 1.1 equiv) in THF (5 mL) dropwise by syringe. The resulting yellow solution was warmed to room temperature and aged for 6 h. Saturated aqueous NH<sub>4</sub>Cl solution was added to quench the reaction. The aqueous layer was separated, extracted with EtOAc. The combined organic layers were washed with brine, dried over Na<sub>2</sub>SO<sub>4</sub> and concentrated. The crude product was purified by silica gel column chromatography to obtain the desired succinimide product.

### Reduction of *N*-alkyl succinimides

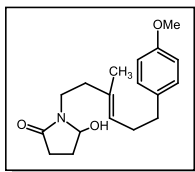
To a solution of (*E*)-1-(3-methyl-6-arylhex-3-en-1-yl)pyrrolidine-2,5-dione (3.1 mmol, 1.0 equiv) in MeOH (31 mL) at 0 °C was added NaBH<sub>4</sub> (9.3 mmol, 3 equiv) over 2 min. The reaction was sealed with a needle-pierced rubber septa and stirred vigorously at the same temperature. After 30 min, a second portion of NaBH<sub>4</sub> (9.3 mmol, 3 equiv) was added over 2 min. The reaction solution was further stirred for 1 h, and then poured into a mixture of CH<sub>2</sub>Cl<sub>2</sub> (~50 mL) and saturated NaHCO<sub>3</sub> (~50 mL). The resulting white biphasic liquid was stirred vigorously for 15 min and separated, and the aqueous layer was extracted with EtOAc. The combined organic layers were washed with brine, dried over Na<sub>2</sub>SO<sub>4</sub> and concentrated. The crude extracts were purified by silica gel column chromatography to obtain the hydroxylactam product.



#### **(*E*)-5-hydroxy-1-(3-methyl-6-phenylhex-3-en-1-yl)pyrrolidin-2-one (29)**

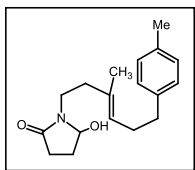
Followed general procedure on 3.49 mmol scale and purified using silica gel chromatography to give 720 mg (76% yield) of (*E*)-5-hydroxy-1-(3-methyl-6-phenylhex-3-en-1-yl)pyrrolidin-

2-one. IR (Film): 3306 (br), 2929, 1658 (s), 1453, 1421, 1329, 1283, 1162, 1069, 984, 909, 748, 698, 669 cm<sup>-1</sup>; <sup>1</sup>H NMR: (500 MHz, CDCl<sub>3</sub>) δ 7.27 (m, 2H), 7.18 (m, 3H), 5.21 (t, 1H, *J* = 6.5 Hz), 5.11 (t, 1H, *J* = 6.5 Hz), 3.57 (dt, 1H, *J* = 7.0, 7.0 Hz), 3.21 (dt, 1H, *J* = 7.0, 6.5 Hz), 2.62 (t, 2H, *J* = 9.0 Hz), 2.49 (m, 1H), 2.30 (m, 2H), 2.21 (m, 4H), 1.83 (m, 1H), 1.61 (s, 3H); <sup>13</sup>C NMR: (125 MHz, CDCl<sub>3</sub>) δ 175.0, 142.2, 133.2, 128.6, 128.5, 126.3, 126.0, 88.5, 38.5, 37.8, 36.0, 30.0, 29.1, 28.5, 16.0; MS (APCI) exact mass calculated for [M+Na] (C<sub>17</sub>H<sub>23</sub>NNaO<sub>2</sub>) requires *m/z* 296.2, found *m/z* 296.2.



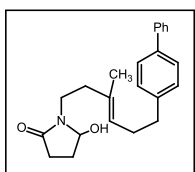
**(E)-5-hydroxy-1-(6-(4-methoxyphenyl)-3-methylhex-3-en-1-yl)pyrrolidin-2-one (18)**

Followed general procedure on 2.33 mmol scale and purified using silica gel chromatography to give 550 mg (78% yield) of (*E*)-5-hydroxy-1-(6-(4-methoxyphenyl)-3-methylhex-3-en-1-yl)pyrrolidin-2-one as a white solid. IR (Film): 3306 (br), 2933, 1660 (s), 1612, 1511, 1463, 1298, 1244, 1177, 1069, 1036, 984, 827, 669  $\text{cm}^{-1}$ ;  $^1\text{H}$  NMR: (500 MHz,  $\text{CDCl}_3$ )  $\delta$  7.09 (d, 2H,  $J = 8.5$  Hz), 6.82 (d, 2H,  $J = 8.5$  Hz), 5.20 (t, 1H,  $J = 7.0$  Hz), 5.11 (t, 1H,  $J = 6.0$  Hz), 3.78 (s, 3H), 3.57 (dt, 1H,  $J = 7.5, 7.5$  Hz), 3.23 (dt,  $J = 7.5, 7.0$  Hz), 2.88 (d, 1H,  $J = 8.5$  Hz), 2.57 (t, 2H,  $J = 7.5$  Hz), 2.50 (m, 1H), 2.25 (m, 5H), 1.82 (m, 1H), 1.61 (s, 3H);  $^{13}\text{C}$  NMR: (125 MHz,  $\text{CDCl}_3$ )  $\delta$  174.8, 158.0, 143.3, 133.3, 129.5, 126.4, 113.9, 83.6, 55.5, 38.7, 37.9, 35.1, 30.2, 29.0, 28.7, 16.1; MS (APCI) exact mass calculated for  $[\text{M}+\text{Na}]$  ( $\text{C}_{18}\text{H}_{25}\text{NNaO}_3$ ) requires  $m/z$  326.2, found  $m/z$  326.1.



**(E)-5-hydroxy-1-(3-methyl-6-(p-tolyl)hex-3-en-1-yl)pyrrolidin-2-one (31)**

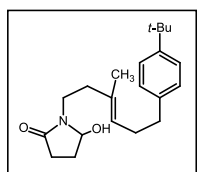
Followed general procedure on 2.0 mmol scale and purified using silica gel chromatography to give 388 mg (68% yield) of (*E*)-5-hydroxy-1-(3-methyl-6-(p-tolyl)hex-3-en-1-yl)pyrrolidin-2-one as a white solid. IR (Film) 3308 (br), 2924, 1663 (s), 1456, 1284, 1163, 1069, 985, 807  $\text{cm}^{-1}$ ;  $^1\text{H}$  NMR (500 MHz,  $\text{CDCl}_3$ )  $\delta$  = 7.08 (dd,  $J = 8.2, 11.9$  Hz, 4 H), 5.22 (dt,  $J = 1.4, 6.9$  Hz, 1 H), 5.12 (ddd,  $J = 1.8, 6.0, 7.8$  Hz, 1 H), 3.58 (td,  $J = 7.3, 14.2$  Hz, 1 H), 3.25 (td,  $J = 6.7, 13.6$  Hz, 1 H), 2.91 (br. s., 1 H), 2.60 (t,  $J = 7.8$  Hz, 2 H), 2.55 - 2.46 (m, 1 H), 2.32 (s, 3 H), 2.30 (dd,  $J = 6.0, 13.7$  Hz, 2 H), 2.27 - 2.18 (m, 4 H), 1.87 - 1.79 (m, 1 H), 1.63 (s, 3 H);  $^{13}\text{C}$  NMR (125 MHz,  $\text{CDCl}_3$ )  $\delta$  = 174.5, 138.9, 135.2, 133.0, 128.9, 128.2, 126.2, 83.3, 38.4, 37.6, 35.3, 29.8, 28.8, 28.4, 21.0, 15.8; MS (ESI-APCI) exact mass calculated for  $[\text{M}-\text{H}_2\text{O}+\text{H}]$  ( $\text{C}_{18}\text{H}_{24}\text{NO}$ ) requires  $m/z$  270.2, found  $m/z$  270.2.



**(E)-1-(6-([1,1'-biphenyl]-4-yl)-3-methylhex-3-en-1-yl)-5-hydroxy-2-pyrrolidinone (33)**

Followed general procedure on 3.2 mmol scale and purified using silica gel chromatography to give 500 mg (45% yield) of (*E*)-1-(6-([1,1'-biphenyl]-4-yl)-3-methylhex-3-en-1-yl)-5-hydroxy-2-pyrrolidinone as a white solid (the starting material wasn't completely soluble in MeOH, and ~50% of it was recovered). IR (Film) 3307 (br), 2930, 1663 (s), 1486, 1450, 1283, 1163, 1070, 985,

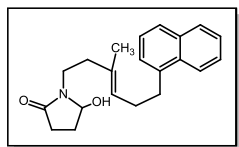
833, 762  $\text{cm}^{-1}$ ;  $^1\text{H}$  NMR (500 MHz,  $\text{CDCl}_3$ )  $\delta$  = 7.58 (d,  $J$  = 6.8 Hz, 2 H), 7.52 (d,  $J$  = 8.3 Hz, 2 H), 7.43 (t,  $J$  = 7.1 Hz, 2 H), 7.33 (t,  $J$  = 6.8 Hz, 1 H), 7.25 (d,  $J$  = 6.3 Hz, 2 H), 5.25 (dt,  $J$  = 1.2, 7.0 Hz, 1 H), 5.12 (ddd,  $J$  = 2.2, 6.0, 7.9 Hz, 1 H), 3.57 (td,  $J$  = 7.8, 14.6 Hz, 1 H), 3.28 (td,  $J$  = 6.7, 13.9 Hz, 1 H), 2.68 (t,  $J$  = 7.8 Hz, 2 H), 2.55 - 2.46 (m, 1 H), 2.36 (dd,  $J$  = 7.3, 15.1 Hz, 2 H), 2.30 - 2.18 (m, 4 H), 2.10 (br. s., 1 H), 1.84 - 1.75 (m, 1 H), 1.65 (s, 3 H);  $^{13}\text{C}$  NMR (125 MHz,  $\text{CDCl}_3$ )  $\delta$  = 174.5, 141.1, 141.0, 138.8, 133.2, 128.8, 128.7, 127.0, 127.0, 126.9, 126.0, 83.3, 38.4, 37.6, 35.4, 29.6, 28.8, 28.4, 15.9; MS (ESI-APCI) exact mass calculated for  $[\text{M}-\text{H}_2\text{O}+\text{H}]$  ( $\text{C}_{23}\text{H}_{26}\text{NO}$ ) requires  $m/z$  332.2, found  $m/z$  332.2.



**(E)-1-(6-(4-(tert-butyl)phenyl)-3-methylhex-3-en-1-yl)-5-hydroxypyrrolidin-2-one (35)**

Followed general procedure on 2.5 mmol scale and purified using silica gel chromatography to give 745 mg (90% yield) of (E)-1-(6-([1,1'-biphenyl]-4-yl)-3-methylhex-3-en-1-yl)-5-hydroxypyrrolidin-2-one as a white solid. IR (Film) 3325 (br), 2960, 1666 (s), 1459, 1270,

1164, 1070, 829  $\text{cm}^{-1}$ ;  $^1\text{H}$  NMR (500 MHz,  $\text{CDCl}_3$ )  $\delta$  = 7.36 - 7.29 (m, 2 H), 7.13 (d,  $J$  = 8.3 Hz, 2 H), 5.24 (dt,  $J$  = 1.2, 7.0 Hz, 1 H), 5.12 (ddd,  $J$  = 2.0, 5.9, 7.8 Hz, 1 H), 3.58 (td,  $J$  = 7.3, 14.2 Hz, 1 H), 3.27 (td,  $J$  = 6.8, 13.7 Hz, 1 H), 2.61 (t,  $J$  = 7.8 Hz, 2 H), 2.56 - 2.46 (m, 1 H), 2.40 - 2.19 (m, 7 H), 1.86 - 1.77 (m, 1 H), 1.64 (s, 3 H), 1.32 (s, 9 H);  $^{13}\text{C}$  NMR (125 MHz,  $\text{CDCl}_3$ )  $\delta$  = 174.4, 162.1, 148.6, 138.9, 128.0, 126.3, 125.2, 83.4, 38.5, 37.6, 35.2, 34.3, 31.4, 29.6, 28.7, 28.5, 15.8; MS (ESI-APCI) exact mass calculated for  $[\text{M}-\text{H}_2\text{O}+\text{H}]$  ( $\text{C}_{21}\text{H}_{30}\text{NO}$ ) requires  $m/z$  312.2, found  $m/z$  312.2.

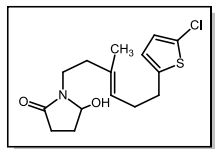


**(E)-5-hydroxy-1-(3-methyl-6-(naphthalen-1-yl)hex-3-en-1-yl)pyrrolidin-2-one (37)**

Followed general procedure on 3.1 mmol scale and purified using silica gel chromatography to give 880 mg (86% yield) of (E)-5-hydroxy-1-(3-methyl-6-(naphthalen-

1-yl)hex-3-en-1-yl)pyrrolidin-2-one as a colorless gel, which turned into a white solid slowly after stored at room temperature for weeks. IR (Film) 3306 (br), 2934, 1660 (s), 1458, 1282, 1163, 1068, 984, 778 (s)  $\text{cm}^{-1}$ ;  $^1\text{H}$  NMR (500 MHz,  $\text{CDCl}_3$ )  $\delta$  = 8.06 (d,  $J$  = 8.2 Hz, 1 H), 7.87 (d,  $J$  = 7.8 Hz, 1 H), 7.73 (d,  $J$  = 8.2 Hz, 1 H), 7.51 (td,  $J$  = 7.3, 22.0 Hz, 2 H), 7.41 (t,  $J$  = 7.3 Hz, 1 H), 7.33 (d,  $J$  = 6.9 Hz, 1 H), 5.34 (t,  $J$  = 6.9 Hz, 1 H), 5.14 (t,  $J$  = 6.4 Hz, 1 H), 3.59 (td,  $J$  = 7.8, 14.7 Hz, 1 H), 3.24 (td,  $J$  = 6.9, 13.7 Hz, 1 H), 3.10 (t,  $J$  = 7.8 Hz, 2 H), 3.06 (br. s., 1 H), 2.56 - 2.41 (m, 3 H), 2.33 - 2.16 (m, 4 H), 1.89 - 1.78 (m, 1 H), 1.62 (s, 3 H);  $^{13}\text{C}$  NMR (125 MHz,  $\text{CDCl}_3$ )  $\delta$  = 174.5,

138.0, 133.8, 133.2, 131.8, 128.7, 126.6, 126.1, 125.9, 125.7, 125.5, 125.4, 123.6, 83.3, 38.5, 37.6, 32.8, 29.1, 28.8, 28.4, 15.8; MS (ESI-APCI) exact mass calculated for [M-H<sub>2</sub>O+H] (C<sub>21</sub>H<sub>24</sub>NO) requires *m/z* 306.2, found *m/z* 306.2.



**(E)-1-(6-(5-chlorothiophen-2-yl)-3-methylhex-3-en-1-yl)-5-hydroxypyrrolidin-2-one (39)**

Followed general procedure on 2.5 mmol scale and purified using silica gel chromatography to give 760 mg (98% yield) of (E)-1-(6-(5-chlorothiophen-2-yl)-3-methylhex-3-en-1-yl)-5-

hydroxypyrrolidin-2-one as a pale brown solid. IR (Film) 3306 (br.), 2930, 1660 (s), 1454 (s), 1283, 1163, 1062, 984, 791 cm<sup>-1</sup>; <sup>1</sup>H NMR (500 MHz, CDCl<sub>3</sub>) δ = 6.70 (d, *J* = 3.7 Hz, 1 H), 6.54 (d, *J* = 3.7 Hz, 1 H), 5.18 (t, *J* = 6.9 Hz, 1 H), 5.13 (br. s., 1 H), 3.58 (td, *J* = 7.8, 14.7 Hz, 1 H), 3.24 (td, *J* = 6.7, 13.6 Hz, 1 H), 3.04 (br. s., 1 H), 2.74 (t, *J* = 7.3 Hz, 2 H), 2.55 - 2.46 (m, 1 H), 2.31 (dd, *J* = 7.3, 14.7 Hz, 2 H), 2.28 - 2.18 (m, 4 H), 1.90 - 1.80 (m, 1 H), 1.64 (s, 3 H); <sup>13</sup>C NMR (125 MHz, CDCl<sub>3</sub>) δ = 174.5, 143.7, 134.1, 126.8, 125.6, 125.0, 123.5, 83.3, 38.3, 37.6, 30.2, 29.6, 28.8, 28.4, 15.9; MS (ESI-APCI) exact mass calculated for [M-H<sub>2</sub>O+H] (C<sub>15</sub>H<sub>19</sub>ClNOS) requires *m/z* 296.1, found *m/z* 296.1.

**References:**

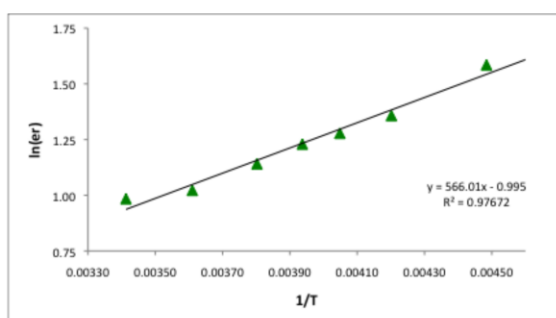
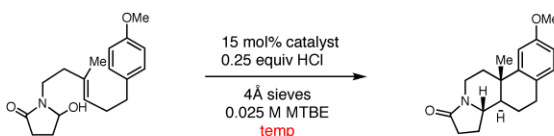
1. For the enantioselective synthesis of 2-aryl pyrrolidines, see: Campos, K. R.; Klapars, A.; Waldman, J. H.; Dormer, P. G.; Chen, C.-Y. *J. Am. Chem. Soc.* **2006**, *128*, 3538.
2. For the synthesis of (E)-(4-iodo-3-methylbut-3-en-1-yl) *tert*-butyldimethylsilylether, see: Wipf, P.; Lim, S. *Angew. Chem. Int. Ed.* **1993**, *32*, 1068.

**5. Eyring Analysis of Enantioselectivity for catalysts 21b-d**

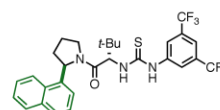
**Procedure:** An oven-dried vial was charged with starting material (0.033 mmol, 1.0 equiv), thiourea catalyst (0.00495 mmol, 0.15 equiv), 4Å molecular sieves (20 mg) and MTBE (1.3 mL). The flask was cooled to the indicated temperature in cryogenic bath and HCl (2 M in diethyl ether, 0.00825 mmol, 0.25 equiv) was added in one portion. The reaction was stirred for 24-48 h, and then quenched at that temperature by addition of pre-cooled NEt<sub>3</sub> (~0.1 mL of 20% v/v solution in EtOAc). The reaction was diluted with acetone, filtered through a pipette containing ¾ inch of silica gel, and rinsed with acetone. The solvent was removed by rotary evaporation under

reduced pressure and the crude residue was purified by preparative silica gel thin layer chromatography (100% EtOAc). The enantiomeric excess was determined by chiral SFC analysis (ChiralPak AD-H, 25% MeOH, 3ml/min,  $t_1 = 3.80$  min,  $t_2 = 4.81$  min). The differential activation parameters were calculated using the following relationship:

$$\ln(er) = -\Delta\Delta H^\ddagger/RT + \Delta\Delta S^\ddagger/RT \text{ (where } R = 1.986 \text{ cal/mol}\cdot\text{K)}$$

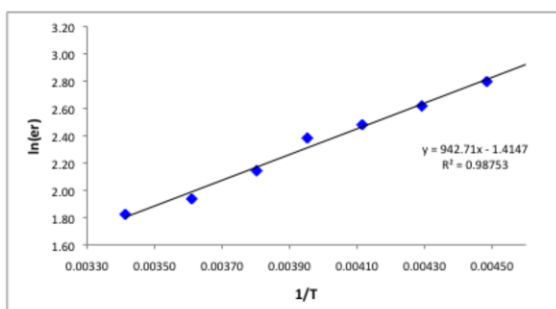


Temp °C	ee
+20	45.6
+4	47.1
-10	51.6
-19	54.8
-26	56.4
-35	59.1
-50	66.0

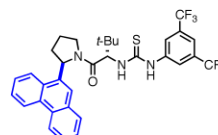


$$\Delta\Delta H^\ddagger = -1.12 \pm 0.07 \text{ kcal/mol}$$

$$\Delta\Delta S^\ddagger = -2.0 \pm 0.3 \text{ cal/mol}\cdot\text{K}$$

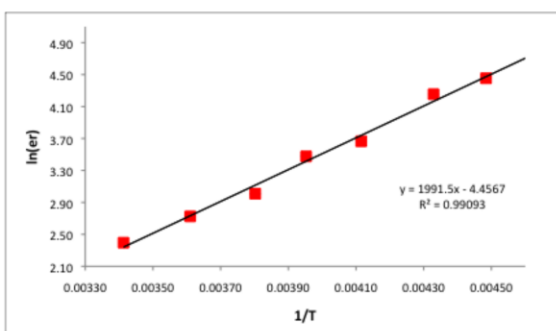


Temp °C	ee
+20	72.2
+4	74.8
-10	79.0
-20	83.1
-30	84.6
-40	86.4
-50	88.5

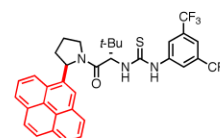


$$\Delta\Delta H^\ddagger = -1.87 \pm 0.08 \text{ kcal/mol}$$

$$\Delta\Delta S^\ddagger = -2.8 \pm 0.3 \text{ cal/mol}\cdot\text{K}$$



Temp °C	ee
+20	83.3
+4	87.7
-10	90.6
-20	94.0
-30	95.0
-42	97.2
-50	97.7

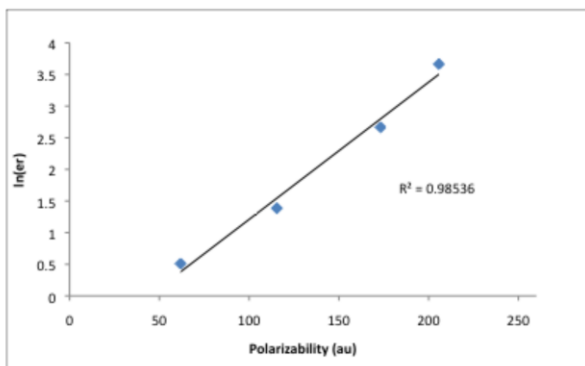
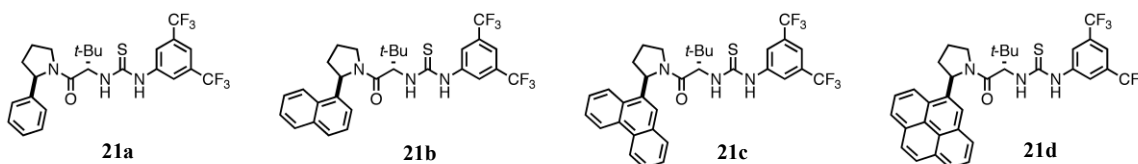


$$\Delta\Delta H^\ddagger = -3.95 \pm 0.17 \text{ kcal/mol}$$

$$\Delta\Delta S^\ddagger = -8.9 \pm 0.7 \text{ cal/mol}\cdot\text{K}$$

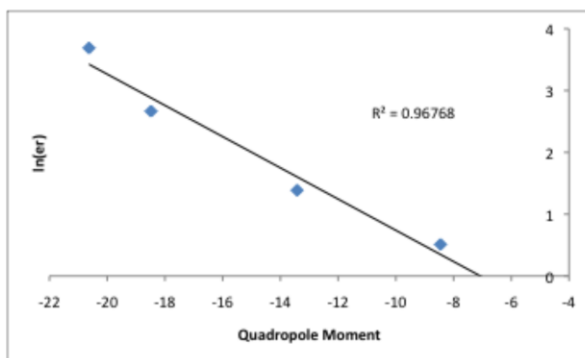
## 6. Correlation of arene properties with enantioselectivity for catalysts 21a-d

**Procedure:** An oven-dried vial was charged with starting material (0.033 mmol, 1.0 equiv), thiourea catalyst (0.00495 mmol, 0.15 equiv), 4Å molecular sieves (20 mg) and MTBE (1.3 mL). The flask was cooled to  $-78\text{ }^{\circ}\text{C}$  and HCl (2 M in diethyl ether, 0.00825 mmol, 0.25 equiv) was added in one portion. The reaction was then moved to a  $-30\text{ }^{\circ}\text{C}$  cryogenic bath and stirred for 24-48 h, and then quenched at that temperature by addition of pre-cooled  $\text{NEt}_3$  ( $\sim 0.1\text{ mL}$  of 20% v/v solution in EtOAc). The reaction was diluted with acetone, filtered through a pipette containing  $\frac{3}{4}$  inch of silica gel, and rinsed with acetone. The solvent was removed by rotary evaporation under reduced pressure and the crude residue was purified by preparative silica gel thin layer chromatography (100% EtOAc). The enantiomeric excess was determined by chiral SFC analysis (ChiralPak AD-H, 25% MeOH, 3ml/min,  $t_1 = 3.80\text{ min}$ ,  $t_2 = 4.81\text{ min}$ ).



Arene	Polarizability	catalyst	ee
Benzene	61.9	21a	25
Napthalene	115.5	21b	60
Phenanthrene	173.2	21c	87
Pyrene	205.7	21d	95

Polarizabilities: Waite et al. *J. Chem. Phys.* **1982**, *77*, 2536

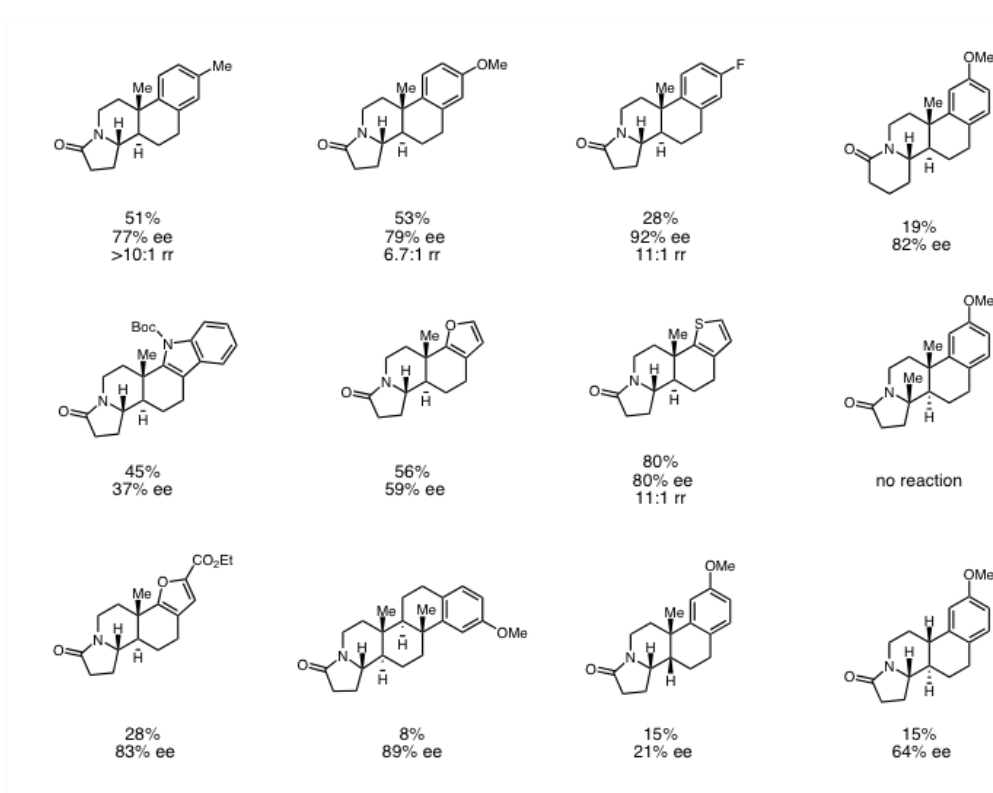


Arene	quad. mom.	catalyst	ee
Benzene	-8.45	21a	25
Napthalene	-13.42	21b	60
Phenanthrene	-18.48	21c	87
Pyrene	-20.63	21d	95

Quadropole moments: Boyd et al. *J. Phys. Chem. A* **1997**, *101*, 5374

## 7. Sub-optimal Substrates

**General Procedure:** An oven-dried vial was charged with hydroxylactam (0.033 mmol, 1.0 equiv), thiourea catalyst **21d** (0.00495 mmol, 0.15 equiv), 4Å molecular sieves (20 mg) and MTBE (1.3 mL). The flask was cooled to  $-78\text{ }^{\circ}\text{C}$  and HCl (2 M in diethyl ether, 0.00825 mmol, 0.25 equiv) was added in one portion. The reaction was then moved to a cryogenic bath and stirred for 24-48 h, and then quenched by the addition of pre-cooled  $\text{NEt}_3$  ( $\sim 0.1$  mL of 20% v/v solution in EtOAc). The reaction was diluted with acetone, filtered through a pipette containing  $\frac{3}{4}$  inch of silica gel, and rinsed with acetone. The solvent was removed by rotary evaporation under reduced pressure and the crude residue was purified by preparative silica gel thin layer chromatography (100% EtOAc). Yields were obtained by GC analysis relative to an internal dodecane standard. The enantiomeric excess was determined by chiral SFC analysis on commercial chiral columns.



Page intentionally left blank

# Chapter Three

## Development of Enantioselective Thiourea-Catalyzed Ring-Opening of Episulfonium Ions and Seleniranium Ions

### 3.1 Enantioselective Ring-Opening of Episulfonium Ions by Indole Derivatives<sup>1</sup>

#### 3.1.1 Introduction

Despite the long-established importance of cation– $\pi$  interactions in molecular biology, molecular recognition and supramolecular chemistry,<sup>2</sup> its potential application in small molecule catalysis, especially as a selectivity-determining factor in asymmetric synthesis has been overlooked until very recently.<sup>3</sup> Mechanistic studies directed at understanding the role of cation–

---

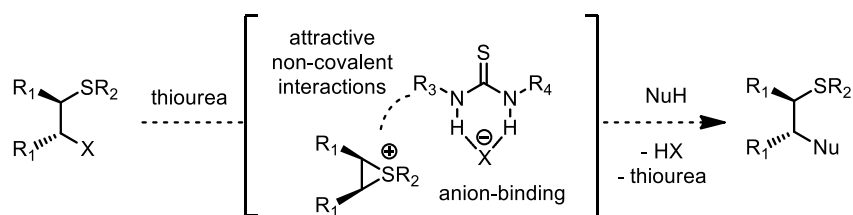
<sup>1</sup> Much of the content of this section has been published: Lin, S.; Jacobsen, E. N. *Nat. Chem.* **2012**, *4*, 817–824.

<sup>2</sup> (a) Ma, J.; Dougherty, D. A. *Chem. Rev.* **1997**, *97*, 1303–1324; (b) Mahadevi, A. S.; Sastry, G. N. *Chem. Rev.* **2013**, *113*, 2100–2138.

<sup>3</sup> For examples invoking cation– $\pi$  interactions as important factors in small molecule catalysis, see: (a) McCurdy, A.; Jimenez, L.; Stauffer, D. A.; Dougherty, D. A. *J. Am. Chem. Soc.* **1992**, *114*, 10314–10321; (b) Mugridge, J. S.; Bergman, R. G.; Raymond, K. N. *J. Am. Chem. Soc.* **2012**, *134*, 2057–2066; (c) Guo, L.; Zhang, W.; Jiang, X.; Houk, K. N.; Birman, V. B. *J. Am. Chem. Soc.* **2012**, *134*, 17605–17612; (d) Ishihara, K.; Fushimi, M.; Akakura, M. *Acc. Chem. Res.* **2007**, *40*, 1049–1055; (e) Uyeda, C.; Jacobsen, E. N. *J. Am. Chem. Soc.*, **2011**, *133*, 5062–5075; (f) Gonzalez-James, O. M.; Singleton, D. A. *J. Am. Chem. Soc.* **2010**, *132*, 6896–6897.

$\pi$  interactions in selective catalysis of reactions are even less prevalent. The successful development of the thiourea-catalyzed enantioselective polycyclization described in Chapter 1 as well as earlier research in this field provide clear support for the notion that these interactions can dictate stereocontrol in the context of small-molecule catalysis.

We sought to extend the concept of synergistic cation- $\pi$ /anion-binding catalysis to episulfonium ions, which are highly reactive electrophilic species that readily undergo diastereospecific bond-forming reactions with nucleophiles.<sup>4</sup> Recently, Toste and co-workers demonstrated enantioselectivity in the addition of alcohols to episulfonium ions using a chiral phosphoric acid catalyst.<sup>5</sup> On the basis of our previous work in anion-binding catalysis, we envisioned that a urea or thiourea could serve as a suitable host for an episulfonium ion formed *in situ* through interactions with the counteranion (Scheme 3-1). High enantioselectivity might be achieved if additional interactions between the catalyst and episulfonium intermediate could be incorporated to differentially stabilize the diastereomeric pathways. This hypothesis was investigated in the context of a Friedel-Crafts indole alkylation reaction.



**Scheme 3-1.** Proposed thiourea-catalyzed ring-opening of episulfonium ions via anion binding.

### 3.1.2 Method development

Preliminary efforts to identify a suitable episulfonium-ion precursor revealed that a relatively non-nucleophilic leaving group was required to achieve the desired reactivity. Anionic

<sup>4</sup> (a) Fox, D. J.; House, D.; Warren, S. *Angew. Chem. Int. Ed.* **2002**, *41*, 2462–2482; (b) Smit, W. A.; Caple, R.; Smoliakova, I. P. *Chem. Rev.* **1994**, *94*, 2359–2382.

<sup>5</sup> Hamilton, G. L.; Kanai, T.; Toste, F. D. *J. Am. Chem. Soc.* **2008**, *130*, 14984–14986.



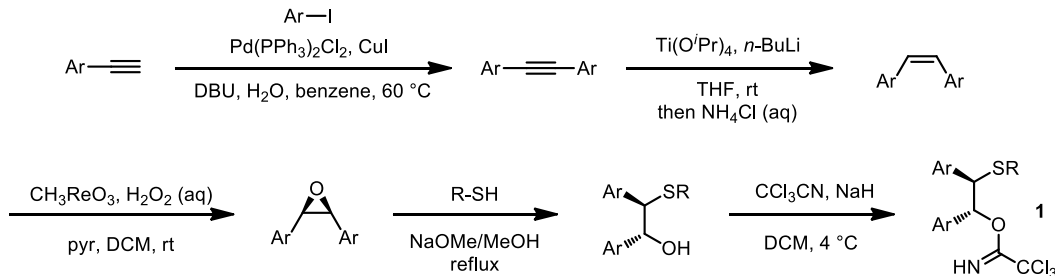
A wide variety of chiral urea and thiourea derivatives was evaluated in the model reaction between substrate **1a** and indole (Table 3-1). Only arylpyrrolidine-derived thioureas of type **3** were found to induce reactivity above the background rate of **1a** and acid alone. A broad screen of Brønsted acids revealed a pronounced counterion effect. In conjunction with thiourea **3b**, mineral acids with a nucleophilic counteranion, such as HCl, produced only trace amounts of the desired indole addition product **2a** (entry 1); instead the corresponding chloride addition product predominated. In contrast, sulfonic acid co-catalysts afforded **2a** in useful yields and varying levels of enantioselectivity, with the most promising result obtained by using 4-nitrobenzenesulfonic acid (4-NBSA) (entry 5). The identity of the aromatic substituent on the pyrrolidino amide portion of the catalyst also exerted a profound effect on reaction enantioselectivity (entries 5, 7–12, Table 3-1). Catalyst **3a**, which lacks an aryl group, induced little rate acceleration above that of the background reaction (entry 6) and afforded a nearly racemic product. In contrast, catalysts **3c–3g**, which bear more-extended aromatic substituents, proved more enantioselective than catalyst **3b**. Correlation between enantiomeric excess (ee) and either the electronic properties of the aryl substituents or the polarizability of the aromatic ring occurs in other reactions using this family of catalysts.<sup>6</sup> However, in the present case no such straightforward relationship was observed. Instead, ee improved on expanding the aryl group from phenyl to phenanthryl (entries 5, 8–10), and then decreased slightly with more expansive aryl substituents (entries 11–12). Urea catalyst **4e** induced only a marginally lower ee than its thiourea counterpart (entries 10 vs. 13), which indicates that any mechanism wherein the thiourea sulfur is engaged productively as a Lewis base catalyst is unlikely to be operative.<sup>7</sup>

---

<sup>6</sup> (a) Reisman, S. E.; Doyle, A. G.; Jacobsen, E. N. *J. Am. Chem. Soc.* **2008**, *130*, 7198–7199. (b) Knowles, R. R.; Lin, S.; Jacobsen, E. N. *J. Am. Chem. Soc.* **2010**, *132*, 5030–5032.

<sup>7</sup> Denmark, S. E.; Kornfilt, D. J. P.; Vogler, T. *J. Am. Chem. Soc.* **2011**, *133*, 15308–15311.

### 3.1.3 Substrate Synthesis



**Scheme 3-2.** Synthesis of episulfonium ion precursors.

Various stilbene-derived substrates were synthesized in five steps from simple chemical commodities (Scheme 3-2). Sonogashira coupling followed by titanium-mediated hydrogenation of the alkyne via an  $\eta^2$ -alkene-Ti(II) complex furnishes the stilbene derivative, which is then epoxidized using  $\text{CH}_3\text{ReO}_3/\text{H}_2\text{O}_2$  or *m*CPBA to form *cis*-stilbene oxide. Nucleophilic ring-opening of the epoxide intermediate with various thiols under basic condition yields the  $\beta$ -hydroxysulfide, which adds across the C–N triple bond of trichloroacetonitrile upon deprotonation, producing the final  $\beta$ -trichloroacetimidoylsulfide substrates **1**.

### 3.1.4 Substrate Scope

A variety of substrate combinations were evaluated to define the scope as well as gain insight into the mechanism of the reaction (equation 2, Table 3-2). Substrates bearing electronically and sterically diverse sulfur substituents ( $\text{R}^2$ ) underwent enantioselective reactions (entries 1–8), with *S*-benzyl-substituted derivatives affording the highest ee values (entries 1 and 6). Electron-potential maps calculated using density functional theory showed that the benzylic protons in the *S*-benzyl episulfonium ions bear a substantial amount of partial positive charge, which may serve to enhance attractive interactions between the cationic intermediate and an electronegative functionality on the catalyst. Various indole derivatives with electron-donating and -withdrawing substituents at the 2-, 4-, 5- or 6-positions all underwent the addition reaction

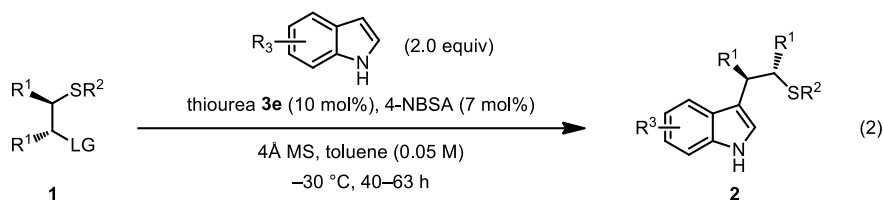
with high levels of enantioselectivity (entries 9–15). In sharp contrast, *N*-methylindole provided the desired product **2p** with a moderate yield and in almost racemic form (entry 16). This suggested that the indole N–H motif may be involved in a key interaction during the ee-determining transition state. Benzotriazole also underwent an addition reaction to form a C–N bond with synthetically useful ee (entry 17). Less nucleophilic heterocycles (for example,  $\pi$ -nucleophiles with Mayr nucleophilicity parameters  $N < 4$ )<sup>8</sup> proved unreactive.<sup>9</sup> Variation of the substituents on the carbon backbone of the electrophile revealed that aryl groups with *meta*- and *ortho*-functionalities were compatible (entries 18–21); substrates that carry a *para*-substituent, regardless of its steric and electronic properties, afforded products in substantially lower enantioselectivity (entries 22–25). *c*-Hexane-derived episulfonium precursor proved barely reactive and non-selective under the conditions developed for stilbene-type substrates (entry 26). Finally, three different acetimidate leaving groups displayed essentially the same reactivity and enantioselectivity, which suggests that the leaving group is not directly involved in the ee-determining step (entries 27–29).

---

<sup>8</sup> Mayr, H.; Kempf, B; Ofial, A. R. *Acc. Chem. Res.* **2003**, *36*, 66–77.

<sup>9</sup> The unreactive nucleophiles include benzothiophene, benzofuran, 4-cyanoindole, 5-formylindole, etc.

**Table 3-2.** Substrate scope of episulfonium ion ring-opening with indole derivatives.<sup>a</sup>



entry	R <sup>2</sup>	product	yield%	ee%
Variations on 1:				
1	Bn	<b>2a</b>	99	93
2	Ph	<b>2b</b>	83	85
3	4-F-C <sub>6</sub> H <sub>4</sub>	<b>2c</b>	73	81
4	4-Me-C <sub>6</sub> H <sub>4</sub>	<b>2d</b>	76	87
5	2-naph	<b>2e</b>	90	88
6	PMB	<b>2f</b>	>99	94
7	Me	<b>2g</b>	72	84
8	<i>t</i> -Bu	<b>2h</b>	89	87

entry	R <sup>3</sup>	product	yield%	ee%
Variations on indole:				
9	5-Me	<b>2i</b>	97	91
10	5-MeO	<b>2j</b>	93	93
11	5-Br	<b>2k</b>	83	92
12	5-F	<b>2l</b>	88	95
13	6-F	<b>2m</b>	92	85
14	4-MeO	<b>2n</b>	83	91
15	2-Me	<b>2o</b>	95	79
16	1-Me	<b>2p</b>	54	3
17 <sup>e</sup>	benzotriazole	<b>2q</b>	92	80

entry	R <sup>1</sup>	product	yield%	ee%
Variations on LG:				
18 <sup>b</sup>	3-MeO-C <sub>6</sub> H <sub>4</sub>	<b>2r</b>	85	93
19	3-F-C <sub>6</sub> H <sub>4</sub>	<b>2s</b>	97	95
20	3-Me-C <sub>6</sub> H <sub>4</sub>	<b>2t</b>	95	93
21	2-Me-C <sub>6</sub> H <sub>4</sub>	<b>2u</b>	>99	79
22	4-F-C <sub>6</sub> H <sub>4</sub>	<b>2v</b>	91	45
23	4-Me-C <sub>6</sub> H <sub>4</sub>	<b>2w</b>	89	60
24 <sup>b</sup>	4-MeO-C <sub>6</sub> H <sub>4</sub>	<b>2x</b>	67	6
25	4-CF <sub>3</sub> -C <sub>6</sub> H <sub>4</sub>	<b>2y</b>	18	5
26 <sup>c</sup>	-(CH <sub>2</sub> ) <sub>4</sub> -	<b>2z</b>	16	9

entry	R <sup>3</sup>	product	yield%	ee%
Variations on LG:				
27 <sup>d</sup>		<b>2b</b>	87	87
28 <sup>d</sup>		<b>2b</b>	91	85
29 <sup>d</sup>		<b>2b</b>	85	85

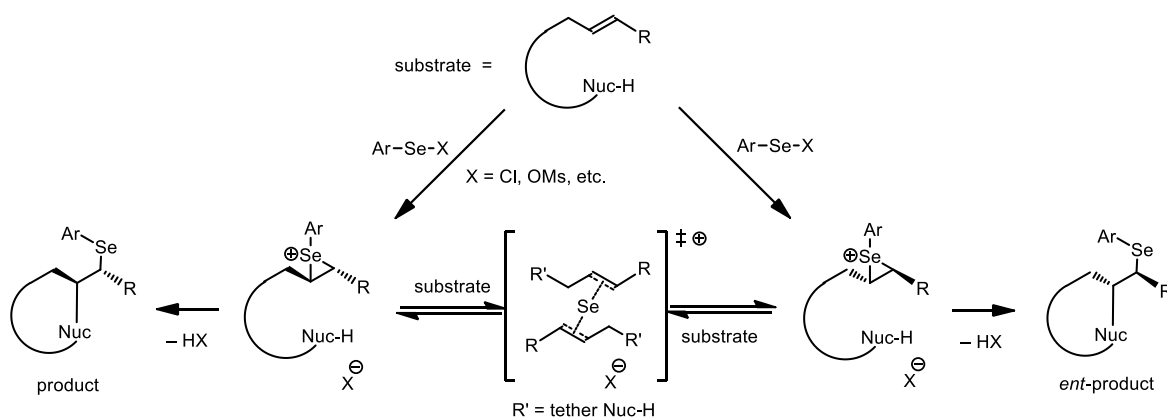
<sup>a</sup> Isolated yields of material purified chromatographically are reported. <sup>b</sup> Yields determined by <sup>1</sup>H NMR are reported. Product isolated via flash column chromatography usually contains a small amount of **3e**. <sup>c</sup> R<sup>2</sup> = Ph, with HOTf. <sup>d</sup> With 20 mol% **3e** and 10 mol% 4-NBSA. <sup>e</sup> Benzotriazole as nucleophile instead of indole.

## 3.2 Enantioselective Squaramide-Catalyzed Selenoetherifications

### 3.2.1 Introduction

The successful development of an asymmetric catalytic method for the ring-opening of episulfonium ions showcases the potential power of thiourea catalysts of type **3** bearing both anion- and cation-stabilizing elements in the selective catalysis of reactions comprising ion-pair intermediates and transition states. We were encouraged to apply this strategy in a more synthetically relevant context involving seleniranium ions.<sup>10</sup>

Selenofunctionalization reactions, in which electrophilic seleniranium ions are generated from carbon–carbon double bonds and opened by nucleophiles, provide a powerful approach to rapid construction of vicinal functional groups and heterocycles (Scheme 3-3). Due to the chemical versatility of selenides in oxidation, reduction, and radical reactions, the products of the selenofunctionalization reactions can be further derivatized to generate various multifunctional structures. In combination with the ease of preparation of electrophilic selenium reagents, this method has been widely used in complex target synthesis to increase the functional complexity of intermediate molecules.



**Scheme 3-3.** Electrophilic selenocyclization reaction.

<sup>10</sup> (a) Nicolaou, K. C.; Petasis, N. A. *Selenium in Natural Product Synthesis*; CIS: Philadelphia, 1984; (b) Back, T. G., Ed.; *Organoselenium Chemistry—A Practical Approach*; Oxford University Press: Oxford, 1999.

Configurational scrambling of seleniranium cations has been long considered as an undesirable feature for developing an enantioselective variant of selenocyclization, as the rapid equilibrium between the two seleniranium enantiomers would diminish or eliminate any enantioenrichment from the facial selectivity of seleniranium formation (Scheme 3-3).<sup>11</sup> Hence, the currently used strategy for developing enantioselective selenofunctionalization reactions relies on finding a selenenylating reagent that could suppress the racemization pathway. For instance, this scheme has been exploited by Denmark and coworkers in the development of a chiral Lewis base-catalyzed asymmetric selenoetherification reaction with moderate enantioselectivity (Scheme 3-4, Route II).<sup>12</sup>

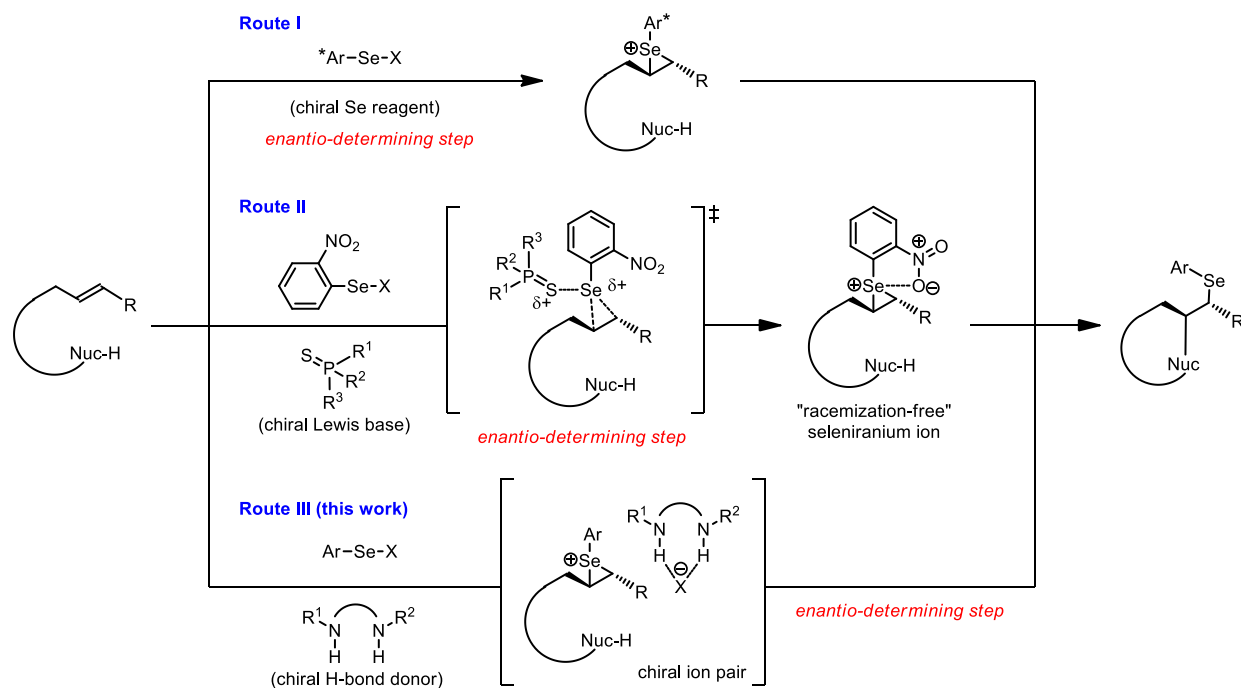
This restriction could be lifted if the enantioselectivity is imparted by the catalyst in the cyclization step upon formation of the seleniranium ion, rather than by facial discrimination of the prochiral olefin in the electrophilic addition step. To realize this strategy, one could take advantage of the ability of arylpyrrolidine-derived thiourea catalysts in engaging in ion-pair binding catalysis (Scheme 3-4, Route III). We envisaged that if the chiral thiourea/urea catalyst binds to the counteranion ( $X^-$ ) of the *in situ* generated seleniranium ion and remains tightly associated with the reactive intermediate during the cyclization event, high enantioselectivity could be relayed from the catalyst to the product during this step. In order for the cyclization to be truly selectivity-determining, a dynamic kinetic resolution has to be achieved, in which the intermolecular transfer of the selenium atom between the two olefins is significantly faster than the intramolecular cyclization event (see Scheme 3-3). Based on Denmark's mechanistic analysis, upon formation of the seleniranium ion, the selenium group-transfer between olefins happens at a rate near the

---

<sup>11</sup> Denmark, S. E.; Collins, W. R.; Cullen, M. D. *J. Am. Chem. Soc.* **2009**, *131*, 3490–3492.

<sup>12</sup> Denmark, S. E.; Kalyani, D.; Collins, W. R. *J. Am. Chem. Soc.* **2010**, *132*, 15752–15765.

diffusion limit. This constitutes the final piece of the mechanistic basis for the proposed asymmetric selenocyclization reaction.



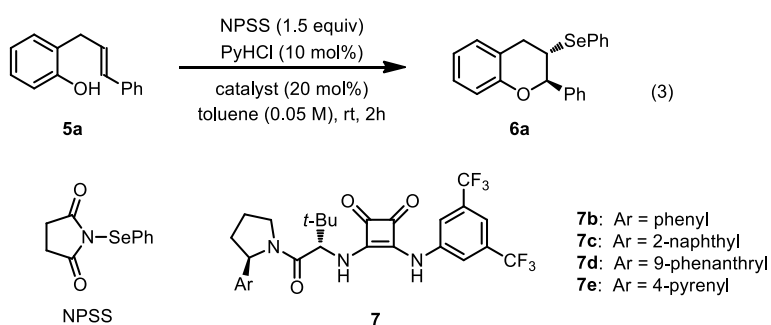
**Scheme 3-4.** Strategies for enantioselective selenocyclizations. Route I: facial-selective addition of selenium to the olefin by using a chiral selenium reagent; Route II: Chiral Lewis base-catalyzed facial-selective formation of a seleniranium ion that cannot participate in group transfer to another olefin; Route III: proposed enantioselective cyclization strategy relying on a dynamic kinetic resolution scenario.

### 3.2.2 Method Development

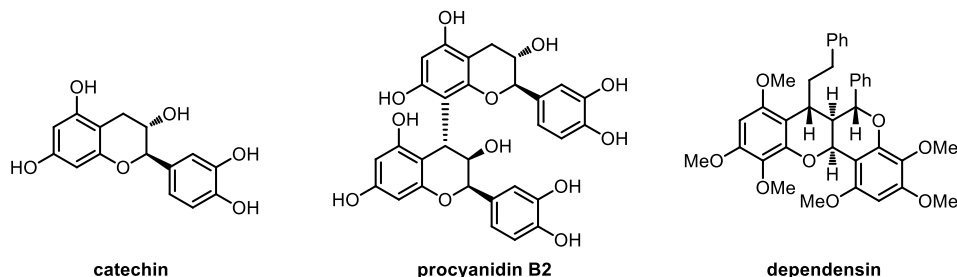
*Ortho*-cinnamyl phenol **5a** was selected as a model substrate (Equation 3, Table 3-3), as the cyclization product **6a** resembles the core structure of flavonoids, a family of natural products that has shown a broad spectrum of biological activities (Scheme 3-5). After a preliminary survey of H-bond donor catalysts, acids, and other conditions, we found that 20 mol% urea **4b** catalyzed the formation of **6a** with 92% yield and in 33% ee in the presence of HCl and *N*-phenylselenosuccinimide (NPSS) (Table 3-3, entry 1). Erosion of the product ee was observed during the course of the reaction, which was attributed to the racemization of cycloadduct **6a** presumably through protonation at the ether oxygen, ring-opening, then re-cyclization in a non-

selective fashion. This problem was solved by replacing HCl with a weaker proton donor – pyridinium chloride (PyHCl). With the new acid, the product was generated in improved enantioselectivity (36% ee), which remained constant over the course of the reaction (entry 2). The reaction outcome was further upgraded by using the more potent H-bond donor, squaramide **7b** as the catalyst (entry 3). In addition, expanding the size of the aromatic group in the arylpyrrolidino portion of the catalyst resulted in a notable improvement of the enantioselectivity, with the 4-pyrenyl derivative proving optimal (entries 3-6).

**Table 3-3.** Catalyst investigation.



entry	catalyst	yield%	ee%
1	<b>3b</b> (with HCl)	92	33
2	<b>3b</b>	85	36
3	<b>7b</b>	82	46
4	<b>7c</b>	82	60
5	<b>7d</b>	88	64
6	<b>3e</b>	84	67



**Scheme 3-5.** Representative flavonoid natural products.

Attempts to increase the enantioselectivity by lowering the reaction temperature were initially unsuccessful due to dramatically decreased reactivity at temperatures below  $-30\text{ }^{\circ}\text{C}$  (Table 3-4, entries 1-3). In clear contrast, high conversion was observed in the cyclization even at  $-78\text{ }^{\circ}\text{C}$  when PhSeCl was added directly to the reaction mixture.<sup>13</sup> This reactivity difference between the two selenium reagents led us to reason that the generation of seleniranium ion from NPSS becomes rate-limiting at low temperature. It has been reported that a strong Lewis base can facilitate the selenium group transfer from NPSS to an olefin.<sup>14</sup> Through a brief survey of different Lewis bases, we found that the reactivity was significantly improved by using a catalytic amount of thiohexamethylphosphoramide (THMPA) at  $-45\text{ }^{\circ}\text{C}$ , and the enantioselectivity was elevated as well, as expected from lowering the temperature (entry 4). Substitution on the aryl group of the selenium reagent also proved to be influential to the selectivity, with the more electron-rich *N*-(*p*-anisylselenyl)succinimide (NASS) providing the optimal result with up to 88% ee (entry 5).

**Table 3-4.** Reaction condition optimization.<sup>a</sup>

entry	selenium	T ( $^{\circ}\text{C}$ )	additive	time (h)	yield%	ee%
1	NPSS	rt	none	2	84	67
2	NPSS	$-30$	none	48	67	72
3	NPSS	$-45$	none	48	< 5	nd
4	NPSS	$-45$	THMPA	48	89	84
5	NASS	$-45$	THMPA	48	85	88

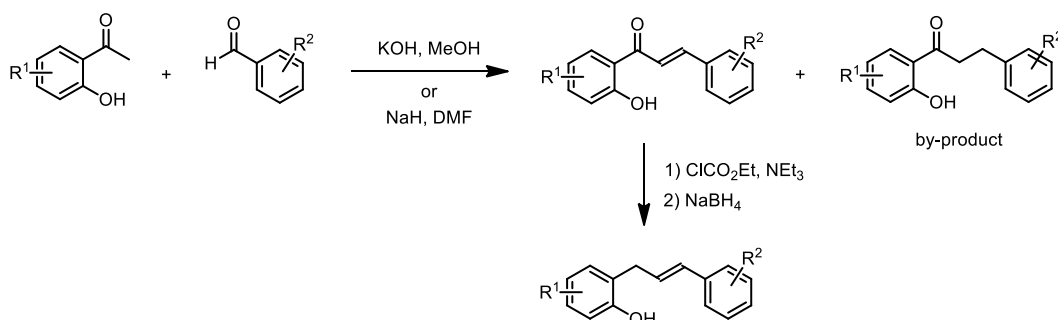
<sup>a</sup> Isolated yields by chromatography and ee determined by HPLC analysis are reported.

<sup>13</sup> The enantioselectivity of reactions with PhSeCl are substantially lower than those with NPSS as a result of the enhanced rate of the background reaction induced by excessive PhSeCl. In case with NPSS, the reactive seleniranium ion is generated catalytically under the action of the acid cocatalyst.

<sup>14</sup> Denmark, S. E.; Collins, W. R. *Org. Lett.* **2007**, *9*, 3801–3804.

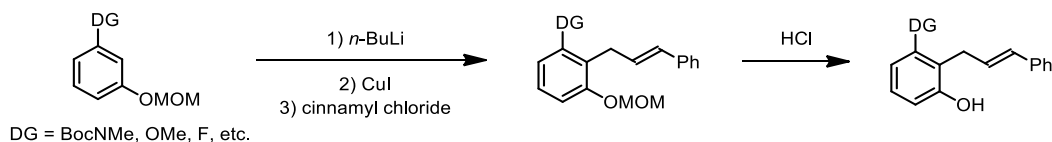
### 3.2.3 Substrate Synthesis

A few different routes were initially proposed for the synthesis of a variety of substrates. Aldol condensation between 2-hydroxyacetophenone and benzaldehyde derivatives followed by a selective Clemmensen-type reduction of the chalcone furnishes the desired substrates in high yields (Scheme 3-5). Over-reduction of the enone to the saturated alkane is avoided by conducting the reaction at low temperature ( $< 0\text{ }^{\circ}\text{C}$ ).



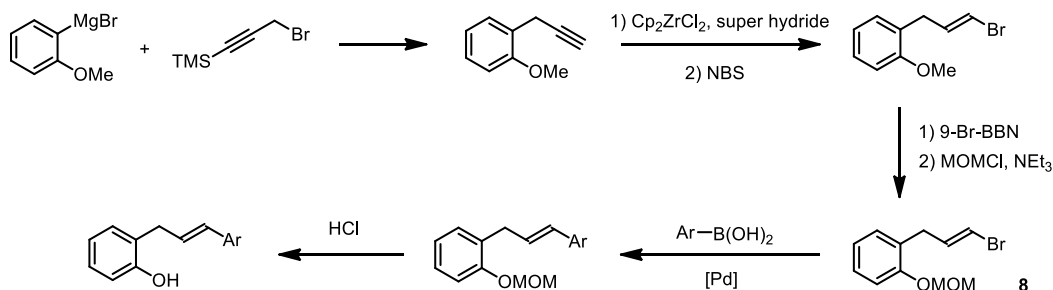
**Scheme 3-6.** Substrate synthesis via aldol condensation and reduction.

*ortho*-Lithiation of *O*-MOM phenyl derivatives followed by cinnamylation represents a complementary method to the aldol/reduction route for the synthesis of substrates possessing an additional directing group at the *meta*-position. The availability of the *meta*-substituted phenol derivatives makes this method more appealing for this particular type of substrate.



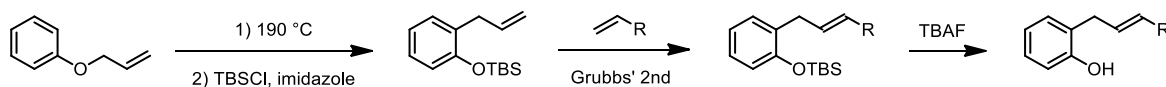
**Scheme 3-7.** Substrate synthesis via directed-lithiation/cinnamylation.

Substrates varying only the styryl portion can be synthesized more efficiently using Suzuki coupling from common intermediate **8**. Vinyl bromide **8** can be obtained in four steps from 2-anisylmagnesium bromide and TMS-protected propargyl bromide on large scale.



**Scheme 3-8.** Substrate synthesis via Suzuki coupling.

Another alternative approach to substrate preparation utilizes a Claisen rearrangement of *O*-allylphenol, followed by cross metathesis. The minor olefin stereoisomer (*cis*-configuration) resulting from the cross metathesis process can usually be removed by column chromatography and/or recrystallization.



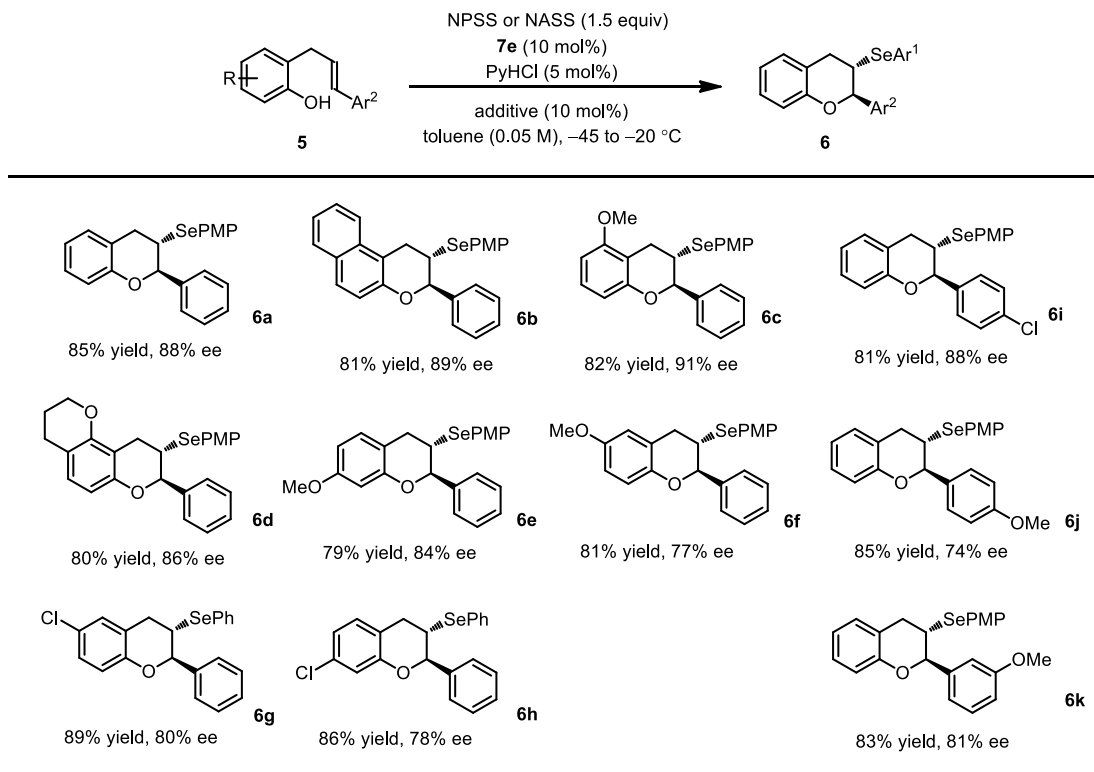
**Scheme 3-9.** Substrate synthesis employing a Claisen rearrangement.

### 3.2.4 Substrate Scope

The optimal conditions of the selenocyclization reaction of **5a** were applicable to a variety of other substrates with different substitution patterns on both the phenol and the styryl moiety (Table 3-5). Electron-donating groups, halogen atoms, and extended aromatic groups can be incorporated in the substrate scaffold without significant perturbation to the reaction outcome. Generally, substitution at the 3-position of the phenol (**6b-d**) provides higher enantioselectivity than at other positions (**6e-h**). With *meta*- and *para*-substituted styryl substrates, the reaction also proceeds with high enantioselectivity (**6i,k**). *p*-Anisylstyrene-derived substrates have been a historically problematic class of precursors for asymmetric halocyclizations, likely due to their

strong cation-stabilizing ability.<sup>15</sup> Notably, substrate **5j** bearing this electron-rich structural unit participated in the selenocyclization with remarkable enantioselectivity (**6j**, 74% ee). The substrate scope for the selenocyclization reaction is still under exploration.<sup>16</sup>

**Table 3-5.** Substrate scope of selenoetherifications.



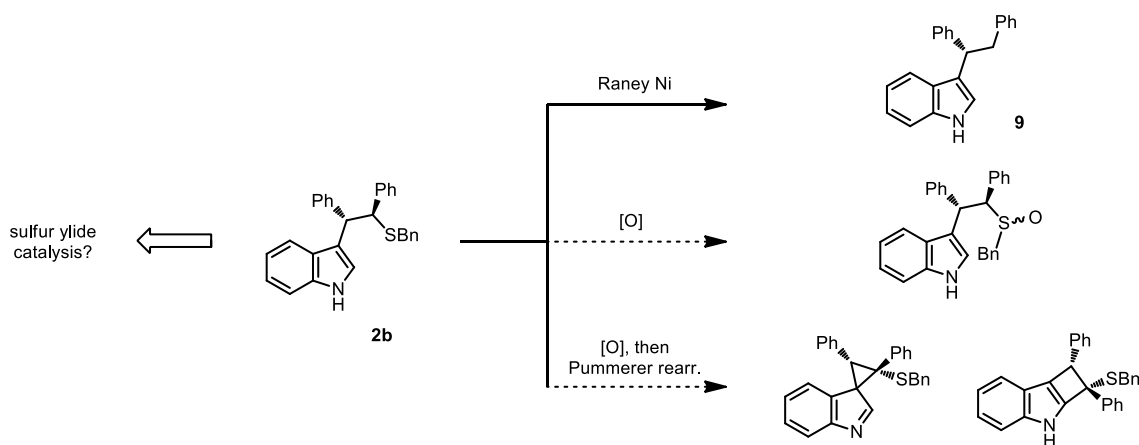
<sup>a</sup> Isolated yields by chromatography and ee determined by HPLC analysis are reported. PMP = *p*-methoxyphenyl.

<sup>15</sup> For examples, see: (a) Whitehead, D. C.; Yousefi, R.; Jaganathan, A.; Borhan, B. *J. Am. Chem. Soc.* **2010**, *132*, 3298–3300; (b) Veitch, G. E.; Jacobsen, E. N. *Angew. Chem. Int. Ed.* **2010**, *49*, 7332–7335; (c) Zhou, L.; Tan, C.-K.; Jiang, X.; Chen, F.; Yeung, Y.-Y. *J. Am. Chem. Soc.* **2010**, *132*, 15474–15476; (d) Brindle, C. S.; Yeung, C. S. *Chem. Sci.* **2013**, *4*, 2100–2104.

<sup>16</sup> Research directed at expanding the substrate scope is currently undertaken by Gary Hu Zhang.

### 3.3 Derivatization of Episulfonium Ion and Seleniranium Ion Ring-Opening Products

The episulfonium ion ring-opening product 2,3-diphenyl thiotryptophol (**2b**) has been reduced with Raney Ni to form (1'-phenyl)phenylethylindole (**9**) (Scheme 3-10). Future synthetic operations to be explored include oxidation to the sulfoxide or sulfone, and Pummerer rearrangement from the sulfoxide product to spiro-/fused tricyclic scaffolds. The products might also be examined as chiral catalyst for sulfur ylide chemistry, such as the Corey-Chaykovsky reaction.



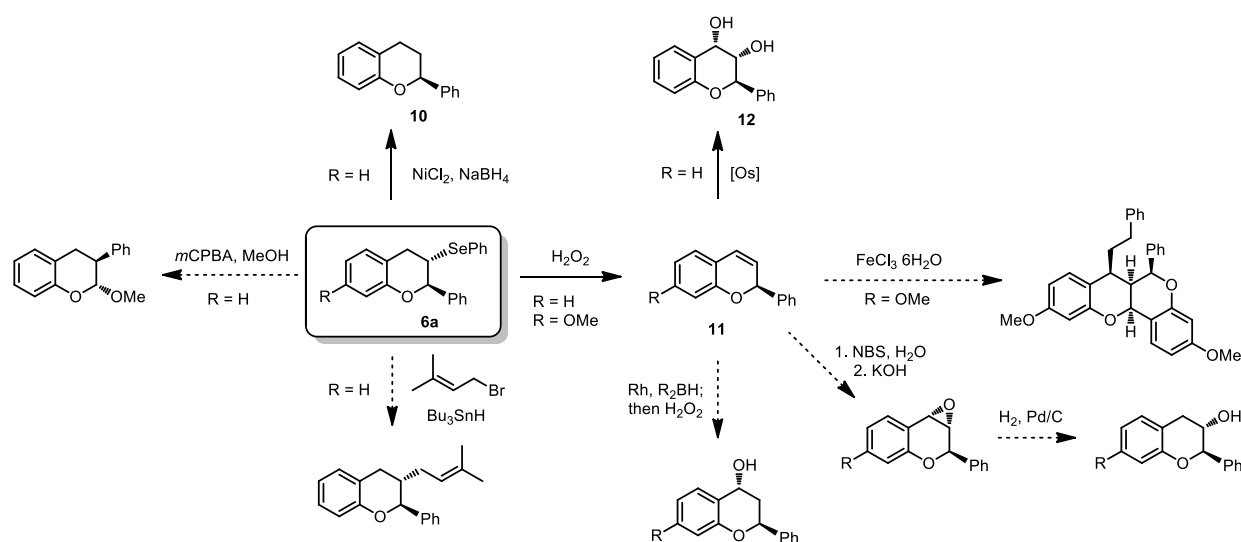
**Scheme 3-10.** Proposed applications of the product of episulfonium ion ring-opening.

The selenofunctionalization product core, 2-phenylchromane (**6a**), has been found in a large variety of natural products, most of which belong to the flavonoid family.<sup>17</sup> The biological activity of these products is highly dependent on the oxidation state and substitution pattern of the molecules.<sup>18</sup> The chemical versatility of selenide compounds provides us with the opportunity to access these structurally diverse flavonoid molecules efficiently from a common precursor. For instance, we have so far been able to both reduce and oxidatively eliminate the arylselenium group in product *rac*-**6a** to form 2-phenylchromane (**10**) and 2-phenylchrom-3-ene (**11**), respectively.

<sup>17</sup> Veitch, N. C.; Grayer, R. J. *Nat. Prod. Rep.* **2011**, *28*, 1626–1695.

<sup>18</sup> Pietta, P.-G. *J. Nat. Prod.* **2000**, *63*, 1035–1042.

The formation of **11** is completely regioselective, and the resultant olefin functionality constitutes another multifaceted handle for further synthetic elaboration. For instance, osmium-catalyzed dihydroxylation provides **12** in good diastereoselectivity,<sup>19</sup> and the highly functionalized ring system maps nicely onto a few different natural products. Another synthetically attractive reaction is radical prenylation of the arylseleno group, which, although yet to be tested, promises to be highly useful.<sup>20</sup> Precedent examples of the proposed reactions in Scheme 3-11 on similar substrate structures are listed in ref. 20 as well.



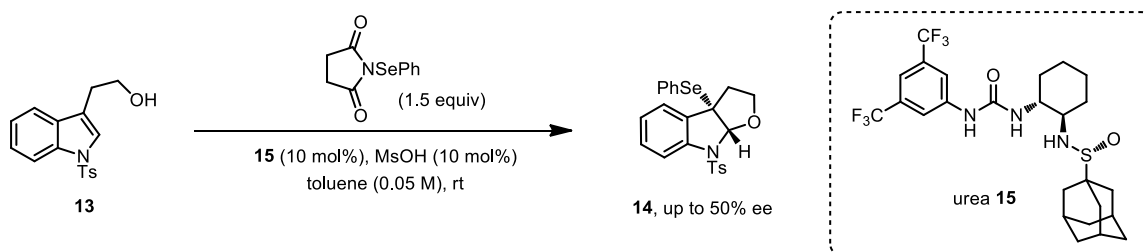
**Scheme 3-11.** Selenoetherification product derivatization. Conditions and results for reactions: **6a** to **10** – NiCl<sub>2</sub>•6H<sub>2</sub>O, NaBH<sub>4</sub>, THF/MeOH, rt – 100% conversion; from **6a** to **11** – H<sub>2</sub>O<sub>2</sub>, pyridine, THF, rt – 80% yield, >20:1 olefin-regioselectivity; from **11** to **12** – OsO<sub>4</sub>, NMO, THF, rt – 70% yield of the *syn/anti* product.

<sup>19</sup> The determination of *dr* value was inconclusive due to the poor resolution of the crude <sup>1</sup>H NMR spectrum. However, the olefin facial-selectivity in the dihydroxylation of a structurally very similar substrate is reportedly excellent. See: Nay, B.; Arnaudinaud, V.; Vercauteren, J. *Eur. J. Org. Chem.* **2001**, 2379–2384.

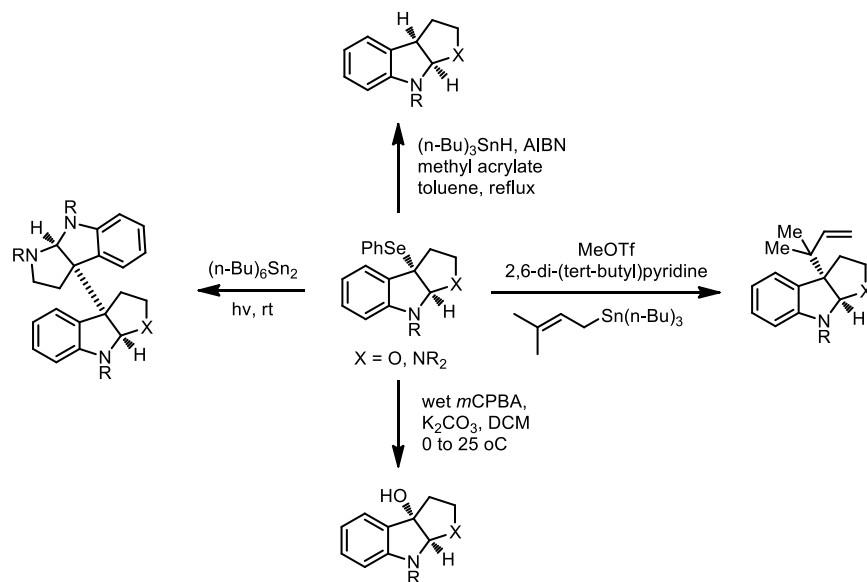
<sup>20</sup> Radical allylation: (a) Wipf, P.; Spencer, S. *J. Am. Chem. Soc.* **2005**, *127*, 225–235; *m*CPBA-mediated phenyl migration: (b) Uemura, S.; Fukuzawa, S. *J. Chem. Soc., Perkin Trans. 1*, **1985**, 471–480; Fe-catalyzed dimerization: (c) Luan, Y.; Sun, H.; Schaus, S. E. *Org. Lett.* **2011**, *13*, 6480–6483; Rh-catalyzed hydroboration: (d) Evans, D. A.; Fu, G. C. *J. Org. Chem.* **1990**, *55*, 2280–2282.

### 3.4 Outlook

Future work includes the expansion of the substrate scope of the selenocyclization reaction to tryptophol derivatives (Scheme 3-12). Following the addition of an electrophilic selenium reagent to the C<sup>2</sup>–C<sup>3</sup> double bond of indole, an intramolecular nucleophilic attack of the alcohol to the seleniranium ion occurs at C<sup>2</sup> position, producing a bicyclic furoindoline core structure with two contiguous stereogenic centers. The arylselenenyl group can be reduced, oxidized, or alkylated using radical chemistry to form molecules that closely resemble a variety of indole alkaloid natural products (Scheme 3-13). Through preliminary condition optimization, we have obtained promising results. Tosyl-protected tryptophol **13** can be selenocyclized under the action of urea **15** to provide the (5,5)-fused polycyclic product **14** in 67% yield and 50% ee.

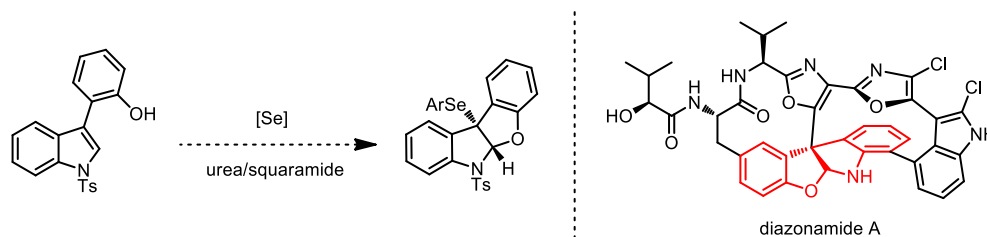


**Scheme 3-12.** Selenoetherification *en route* to furoindoline natural products.



**Scheme 3-13.** Elaboration of tryptophol/tryptamine cyclization products into core structures of natural products.

Re-examination of this system is encouraged by the possibility that the catalyst/substrate-structure-selectivity relationships observed in the chromane-cyclization reaction can be translated into this system. Particularly, a phenol nucleophile can be introduced to replace the alcohol, which would not only change the nucleophilicity of the group, but also introduce a more acidic proton that can potentially interact with a Lewis basic functionality on the catalyst (Scheme 3-14). The corresponding product also bears resemblance to the core structure of a few natural products, such as diazonamide A. In addition, the electron-density of the indole can be tuned by changing the nitrogen protecting group to match that of styrene in order to facilitate the selenium group transfer process, enabling the necessary dynamic kinetic resolution to proceed. Finally, the incorporation of extended aromatic substituents in the catalyst framework might be fruitful in inducing higher levels of enantioselectivity through cation- $\pi$  stabilization of the putative cyclization transition state.



**Scheme 3-14.** Modified selenoetherification of tryptophol derivative for further study.

In conclusion, the development of highly enantioselective methods for both the episulfonium ion ring-opening and the selenocyclization reactions showcase the potential power of using cation- $\pi$  interactions in addition to thiourea-anion-binding to dictate the stereochemical outcome of reactions involving ion-pair intermediates. We anticipate that these systems will encourage the future design and application of similar ion-pair binding strategies in organic asymmetric synthesis.

## Experimental Section

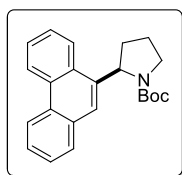
### Table of Content

1. General Information	116
2. Preparation and characterization of thiourea catalysts <b>3e</b> , <b>3f</b> and <b>3g</b>	117
3. General procedures for thiourea-catalyzed ring opening of episulfonium ions	120
4. Catalyst structure investigations	120
5. Preparation and characterization of substrates <b>1a-1z</b>	122
6. Characterization of products <b>2a-2z</b>	130
7. Nucleophiles that didn't produce desired products	142

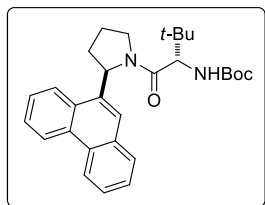
### 1. General information

All reactions were performed in oven-dried 1.5-dram vials unless otherwise noted. The vials were fitted with rubber septa and reactions were conducted under air. Stainless steel syringes were used to transfer air- and moisture-sensitive liquids. Flash chromatography was performed using silica gel 60 (230-400 mesh) from EM Science. Commercial reagents were purchased from Sigma Aldrich, Alfa Aesar, Strem, Lancaster or TCI, and used as received with the following exceptions: toluene, dichloromethane, tetrahydrofuran, diethyl ether, *t*-butyl methyl ether and methanol were dried by passing through columns of activated alumina; dimethylformamide was dried by passing through columns of activated molecular sieves. Triethylamine were distilled from CaH<sub>2</sub> at 760 torr. *s*-Butyllithium was titrated using diphenylacetic acid as an indicator. Proton nuclear magnetic resonance (<sup>1</sup>H NMR) spectra and carbon nuclear magnetic resonance (<sup>13</sup>C NMR) spectra were recorded on Inova-500 (500 MHz) and Inova-600 (600 MHz) spectrometers. Chemical shifts for protons are reported in parts per million downfield from tetramethylsilane and are referenced to residual protium in the NMR solvent (CHCl<sub>3</sub> = δ 7.27, toluene -CH<sub>3</sub> = δ 2.09). Chemical shifts for carbon are reported in parts per million downfield from tetramethylsilane and are referenced to the carbon resonances of the solvent (CDCl<sub>3</sub> = δ 77.0). Data are represented as follows: chemical shift, multiplicity (br. s = broad, s = singlet, d = doublet, t = triplet, q = quartet, m = multiplet), coupling constants in Hertz (Hz), integration. Infrared (IR) spectra were obtained using a Bruker Optics Tensor 27 FTIR spectrometer. Optical rotations were measured using a 1 mL cell with a 0.5 dm path length on a Jasco DIP 370 digital polarimeter. The mass spectral data were obtained on an Agilent Technologies 6120 quadrupole LC/MS spectrometer. Chiral HPLC analysis was performed using a Shimadzu VP series instrument or an Agilent Technologies 1200 series instrument with commercial Chiralpak columns.

## 2. Preparation and characterization of thiourea catalysts 3e, 3f and 3g

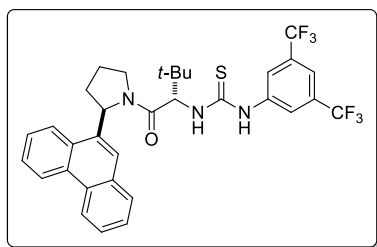


***N*-Boc-(*R*)-2-(9-phenanthryl)pyrrolidine** *N*-Boc-pyrrolidine (0.75 mL, 4.3 mmol) and (–)-sparteine (0.98 mL, 4.3 mmol) were dissolved in MTBE (10 mL) and the resulting solution was cooled to –78 °C. To this solution *s*-BuLi (1.4 M in cyclohexane, 3.1 mL, 4.3 mmol) was added dropwise via syringe pump over 40 min and the resulting solution was stirred for 3 h at –78 °C. A solution of ZnCl<sub>2</sub> (1 M in Et<sub>2</sub>O, 4.3 mL, 4.3 mmol) was then added via syringe pump over 30 min with rapid stirring. The resulting suspension was aged at –78 °C for 30 min, and warmed to room temperature. After 30 min, 9-bromophenanthrene (1.00 g, 3.9 mmol) was added, followed by Pd(OAc)<sub>2</sub> (47.0 mg, 0.21 mmol) and *Pt*-Bu<sub>3</sub>·HBF<sub>4</sub> (69.6 mg, 0.24 mmol) in one portion. The reaction was stirred for 28 hours at room temperature. To facilitate the filtration, ~0.3 mL NH<sub>4</sub>OH was added, and the mixture was stirred for 1 h. The resulting slurry was filtered over Celite and rinsed with MTBE. The filtrate was washed with 1 M HCl and then twice with water. The organic layer was dried over Na<sub>2</sub>SO<sub>4</sub>, filtered and concentrated. The crude product was purified on the silica gel flash chromatography to obtain the desired coupling product as a pale yellow solid (0.70 g, 52%). IR (Film) 2974, 1689 (s), 1390 (s)1248, 1162 (s), 1121, 907 cm<sup>-1</sup>; <sup>1</sup>H NMR (500 MHz, CDCl<sub>3</sub>, exists as rotamers, resonances of the minor rotamer are shown with \*) δ = 8.80 - 8.74 (m, 1H), 8.69 (d, *J*=7.8 Hz, 1H), 8.08 (d, *J*=7.3 Hz, 1H), 7.87 (d, *J*=7.8 Hz, 1H), 7.72 - 7.59 (m, 4H), 7.52 - 7.47 (m, 1H), 5.81\* (d, *J*=7.8 Hz, 0.3H), 5.67 (d, *J*=7.8 Hz, 0.7H), 3.93 - 3.88 (m, 0.7H), 3.85\* (m, 0.3H), 3.75 - 3.71 (m, 0.7H), 2.63 - 2.69\* (m, 0.3H), 2.55 - 2.49 (m, 1H), 2.04 - 1.91 (m, 3H), 1.55\* (s, 3H), 1.17 (s, 6H); <sup>13</sup>C NMR (100 MHz, CDCl<sub>3</sub>) δ = 154.7, 137.4, 131.4, 130.8, 129.7, 128.4, 126.7, 126.4, 126.2, 126.0, 124.0, 123.6, 123.3, 122.3, 122.2, 79.2, 58.3, 47.3, 46.9, 33.7, 32.8, 28.5, 28.1, 23.4, 22.8; MS (ESI-APCI) exact mass calculated for [M+Na] (C<sub>23</sub>H<sub>25</sub>NNaO<sub>2</sub>) requires *m/z* 370.2, found *m/z* 370.1; [α]<sub>D</sub><sup>24</sup> = +141.8 (c = 1.0, CH<sub>2</sub>Cl<sub>2</sub>).



***tert*-butyl ((*S*)-3,3-dimethyl-1-oxo-1-((*R*)-2-(phenanthren-9-yl)pyrrolidin-1-yl)butan-2-yl)carbamate** To *N*-Boc-(*R*)-2-(9-phenanthryl) pyrrolidine (0.70 g, 2.0 mmol) was added HCl (4 M in dioxane, 6 mL). The reaction mixture was stirred at room temperature for 2 h, then diluted with EtOAc (ca. 10 mL), and quenched with a mixture of water (10 mL) and 33% aqueous NH<sub>4</sub>OH (5 mL). The resulting biphasic liquid was stirred for 10 min. The aqueous layer was separated and extracted with EtOAc twice. The combined organic layers were then dried over Na<sub>2</sub>SO<sub>4</sub>, and concentrated under vacuum in a 100 mL round bottom flask to afford (*R*)-2-(4-pyrenyl)pyrrolidine as a

pale yellow gel. A 100 mL round bottom flask was charged with (*R*)-2-(phenanthren-9-yl)pyrrolidine (494 mg, 2.0 mmol), *N*-Boc-*L*-tert-Leucine (508 mg, 2.2 mmol), EDC·HCl (420 mg, 2.2 mmol), HOBT (297 mg, 2.2 mmol) and DMF (10 mL). The solution was stirred at room temperature overnight, and quenched with water. The aqueous layer was separated and extracted three times with EtOAc. The combined organic layers were washed with NH<sub>4</sub>Cl and brine, dried over Na<sub>2</sub>SO<sub>4</sub>, and concentrated to obtain the crude product, which was purified by silica gel flash chromatography to give the desired amide product as pale yellow crystals (750 mg, 83% over two steps). IR (Film) 3444, 2971, 1706 (s), 1645 (s), 1495, 1421 (s), 1365, 1245, 1164 (s), 1061, 1004, 906, 748 (s) cm<sup>-1</sup>; <sup>1</sup>H NMR (500 MHz, CDCl<sub>3</sub>, exists as rotamers, resonances of the minor rotamer are shown with \*) δ = 8.86 - 8.54 (m, 2H), 8.09 (d, *J*=7.8 Hz, 1H), 7.80 (d, *J*=7.8 Hz, 1H), 7.94 - 7.49 (m, 4H), 7.33 (s, 1H), 6.43\* (d, *J*=8.3 Hz, 0.2H), 6.02 (d, *J*=8.3 Hz, 0.8H), 5.25 (d, *J*=10.3 Hz, 0.8H), 5.11\* (d, *J*=10.3 Hz, 0.2H), 4.56 (d, *J*=9.8 Hz, 1H), 4.39 (m, 1H), 3.95 - 3.77 (m, 1H), 2.41 (m, 1H), 2.20 - 1.95 (m, 3H), 1.68 - 1.52 (m, 9H), 1.21 - 1.05 (m, 9H); <sup>13</sup>C NMR (125 MHz, CDCl<sub>3</sub>) δ = 170.43, 156.09, 134.90, 131.29, 131.03, 129.89, 129.49, 128.76, 128.44, 126.57, 126.35, 126.27, 126.15, 126.08, 124.62, 124.18, 123.95, 123.22, 122.43, 122.24, 122.12, 79.54, 58.56, 57.94, 48.29, 47.00, 34.78, 34.42, 33.68, 32.17, 28.45, 28.30, 26.41, 23.43, 21.55; MS (ESI-APCI) exact mass calculated for [M+Na] (C<sub>29</sub>H<sub>36</sub>N<sub>2</sub>NaO<sub>3</sub>) requires *m/z* 483.3, found *m/z* 483.3; [α]<sub>D</sub><sup>24</sup> = +93.4 (*c* = 1.0, CH<sub>2</sub>Cl<sub>2</sub>).

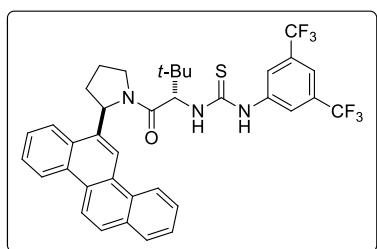


**1-(3,5-bis(trifluoromethyl)phenyl)-3-((*S*)-3,3-dimethyl-1-oxo-1-((*R*)-2-(phenanthren-9-yl)pyrrolidin-1-yl)butan-2-yl)thiourea (3e)**

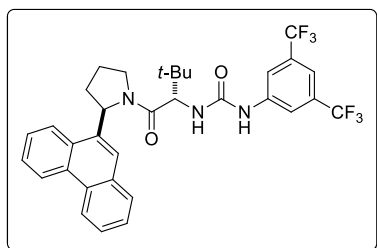
To a solution of *tert*-butyl ((*S*)-3,3-dimethyl-1-oxo-1-((*R*)-2-(phenanthren-9-yl)pyrrolidin-1-yl)butan-2-yl) carbamate (950 mg, 2.1 mmol) at 0 °C was added HCl (4 M in dioxane, 10 mL) slowly. The reaction was warmed to room temperature and stirred until the starting material was consumed, as judged by TLC analysis (ca. 4 h). The reaction mixture was then concentrated under vacuum, yielding a yellow oil, (*S*)-3,3-dimethyl-1-oxo-1-((*R*)-2-(phenanthren-9-yl)pyrrolidin-1-yl)butan-2-aminium chloride. This crude material was dissolved in CH<sub>2</sub>Cl<sub>2</sub> (14 mL), and NEt<sub>3</sub> (860 μL, 6.2 mmol) was added dropwise. The mixture was stirred for 15 min, and 3,5-bis(trifluoromethyl)phenyl isothiocyanate (414 μL, 2.3 mmol) was added dropwise. The reaction was stirred overnight, concentrated *in vacuo*, and purified by silica gel flash chromatography to obtain the desired thiourea as pale yellow crystals (940 mg, 72% over two steps). IR (Film) 3328 (br), 2963, 1611, 1529,

1474, 1447, 1383, 1276 (s), 1177, 1134 (s), 962, 885  $\text{cm}^{-1}$ ;  $^1\text{H}$  NMR (400MHz,  $\text{CDCl}_3$ )  $\delta$  = 9.66 (br. s., 1 H), 8.56 (d,  $J$  = 8.1 Hz, 1 H), 8.47 (d,  $J$  = 8.4 Hz, 1 H), 7.74 (br. s., 10 H), 5.82 (d,  $J$  = 8.1 Hz, 1 H), 5.60 (d,  $J$  = 9.1 Hz, 1 H), 4.84 (t,  $J$  = 9.1 Hz, 1 H), 3.88 (dd,  $J$  = 9.9, 17.6 Hz, 1 H), 2.48 - 2.31 (m, 1 H), 2.10 - 1.92 (m, 3 H), 1.16 (s, 9 H);  $^{13}\text{C}$  NMR (100 MHz,  $\text{CDCl}_3$ )  $\delta$  = 181.1, 170.6, 139.6, 133.4, 131.8, 131.5, 131.2, 130.7, 129.5, 129.1, 128.6, 126.6, 126.4, 126.0, 123.5, 123.3, 122.7, 122.1, 118.0, 63.1, 58.7, 48.8, 35.3, 32.2, 26.7, 23.3; MS (ESI-APCI) exact mass calculated for  $[\text{M}+\text{H}]$  ( $\text{C}_{33}\text{H}_{30}\text{F}_6\text{N}_3\text{OS}$ ) requires  $m/z$  630.2, found  $m/z$  630.2;  $[\alpha]_{\text{D}}^{24}$  = +20.7 (c = 1.0,  $\text{CHCl}_3$ ).

#### Characterization data for all novel catalysts.



**1-(3,5-bis(trifluoromethyl)phenyl)-3-((S)-1-((R)-2-(chrysen-6-yl)pyrrolidin-1-yl)-3,3-dimethyl-1-oxobutan-2-yl)thiourea (3f).** IR (Film) 3327 (br), 2980, 1607 (s), 1525 (s), 1473, 1443, 1383 (s), 1275 (s), 1175 (s), 1133 (s), 961, 885, 758  $\text{cm}^{-1}$ ;  $^1\text{H}$  NMR (500 MHz,  $\text{CDCl}_3$ )  $\delta$  = 9.32 (br. s., 1H), 8.83 - 8.76 (m, 1H), 8.70 (d,  $J$ =8.3 Hz, 1H), 8.54 (d,  $J$ =9.3 Hz, 1H), 8.21 - 8.13 (m, 1H), 8.02 - 7.83 (m, 3H), 7.77 - 7.22 (m, 8H), 6.00 (d,  $J$ =8.3 Hz, 1H), 5.95 (d,  $J$ =10.2 Hz, 1H), 4.86 (t,  $J$ =6.6 Hz, 1H), 4.12 - 4.00 (m, 1H), 2.53 - 2.46 (m, 1H), 2.14 - 2.01 (m, 3H), 1.18 (s, 9H);  $^{13}\text{C}$  NMR (125 MHz,  $\text{CDCl}_3$ )  $\delta$  = 181.08, 170.71, 140.56, 139.88, 135.79, 134.36, 132.30, 132.11, 131.84, 131.58, 131.31, 130.44, 129.15, 128.98, 128.49, 127.71, 127.44, 127.04, 126.52, 124.63, 124.14, 123.66, 122.63, 122.04, 121.19, 120.91, 118.12, 116.61, 62.84, 58.98, 49.41, 47.45, 36.31, 33.60, 32.88, 27.28, 27.00, 23.59, 21.30; MS (ESI-APCI) exact mass calculated for  $[\text{M}+\text{Na}]$  ( $\text{C}_{37}\text{H}_{33}\text{F}_6\text{N}_3\text{NaOS}$ ) requires  $m/z$  704.2, found  $m/z$  704.2;  $[\alpha]_{\text{D}}^{24}$  = +107.4 (c = 1.0,  $\text{CH}_2\text{Cl}_2$ ).



**1-(3,5-bis(trifluoromethyl)phenyl)-3-((S)-3,3-dimethyl-1-oxo-1-((R)-2-(phenanthren-9-yl)pyrrolidin-1-yl)butan-2-yl)urea (3g).** IR (Film) 3348 (br), 2979, 1701, 1610, 1568, 1474, 1443, 1387, 1275 (s), 1174 (s), 1128 (s), 949, 879, 747  $\text{cm}^{-1}$ ;  $^1\text{H}$  NMR (500 MHz,  $\text{CDCl}_3$ )  $\delta$  = 8.69 - 8.26 (m, 3H), 8.04 - 6.95 (m, 10H), 5.94 (d,  $J$ =7.8 Hz, 1H), 4.92 (d,  $J$ =9.3 Hz, 1H), 4.50 (t,  $J$ =8.5 Hz, 1H), 3.91 (q,  $J$ =8.3 Hz, 1H), 2.46 (d,  $J$ =6.8 Hz, 1H), 2.17 - 1.93 (m, 3H), 1.17 (s, 9H);  $^{13}\text{C}$  NMR (125 MHz,  $\text{CDCl}_3$ )  $\delta$  = 172.06, 155.68, 154.97, 141.02, 135.46, 133.96, 132.19, 131.92, 131.14, 130.82, 130.34, 129.73, 129.32, 128.57, 127.24, 126.72, 126.59, 126.44, 125.02, 124.55, 123.59, 123.42, 122.77, 122.38, 119.98, 118.33,

115.48, 58.63, 57.57, 49.04, 47.42, 35.29, 34.84, 33.38, 32.35, 26.85, 23.60, 21.50; MS (ESI-APCI) exact mass calculated for [M+H] (C<sub>33</sub>H<sub>32</sub>F<sub>6</sub>N<sub>3</sub>O<sub>2</sub>) requires *m/z* 616.2, found *m/z* 616.2; [α]<sub>D</sub><sup>23</sup> = +146.3 (c = 1.0, CH<sub>2</sub>Cl<sub>2</sub>).

### 3. General procedures for thiourea-catalyzed ring opening of episulfonium ions

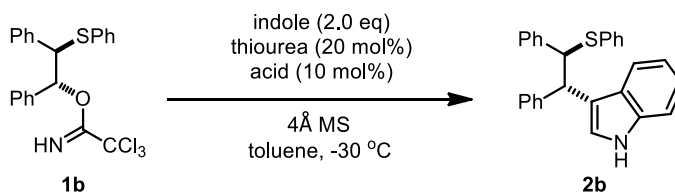
#### Method A (for condition optimization):

An oven-dried vial was charged with starting material (0.050 mmol, 1.0 equiv), thiourea catalyst (0.010 mmol, 0.20 equiv), nucleophile (0.10 mmol, 2.0 equiv) and 4Å molecular sieves (25 mg, powder, activated). The vial was cooled to -78 °C, and toluene (1 mL) was added with stirring. The vial was then placed in a -30 °C cryocool until all the reactants and catalyst were fully dissolved. The acid (5.0 μmol, 0.10 equiv) was added via a 10 μL syringe (for liquid acid), or directly into the solution (for solid acid). The reaction mixture was stirred at -30 °C for 12 h, and then quenched at the same temperature by addition of NEt<sub>3</sub> (~10 μL). The reaction was directly applied to flash column chromatography with a pipette containing 4-5 cm of silica gel using hexanes/EtOAc (20:1 to 10:1) as eluent.

#### Method B (for substrate scope):

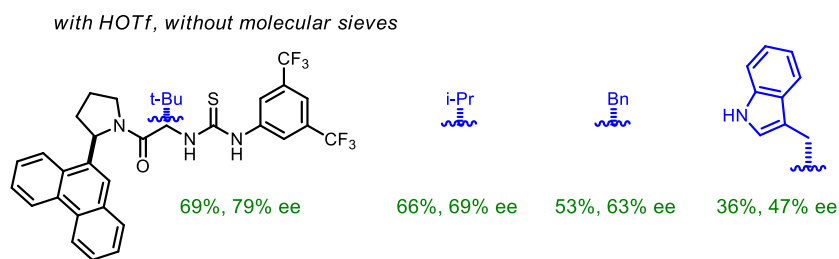
An oven-dried vial was charged with starting material (0.05 mmol, 1.0 equiv), thiourea catalyst (0.0050 mmol, 0.10 equiv), nucleophile (0.10 mmol, 2.0 equiv) and 4Å molecular sieves (25 mg, powder, activated). The vial was cooled to -78 °C, and toluene (1 mL) was added with stirring. The vial was then placed in a -30 °C cryocool until all the reactants and catalyst were fully dissolved, and was cooled to -78 °C again. 4-NBSA (0.6-0.8 mg, ca. 0.0035 mmol, ca. 0.07 equiv) was added directly into the solution. The reaction mixture was stirred at -30 °C until full conversion of the starting material, and then quenched at the same temperature by addition of NEt<sub>3</sub> (~10 μL). The reaction was directly applied to flash column chromatography with a pipette containing 4-5 cm of silica gel using hexanes/EtOAc (20:1 to 10:1) as eluent.

### 4. Catalyst structure investigations

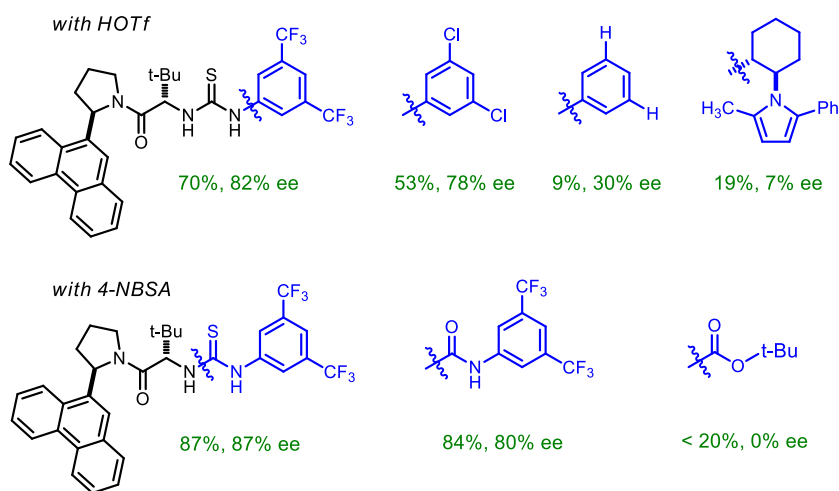


Investigation of the arylpyrrolidine moiety has been presented in the main text.

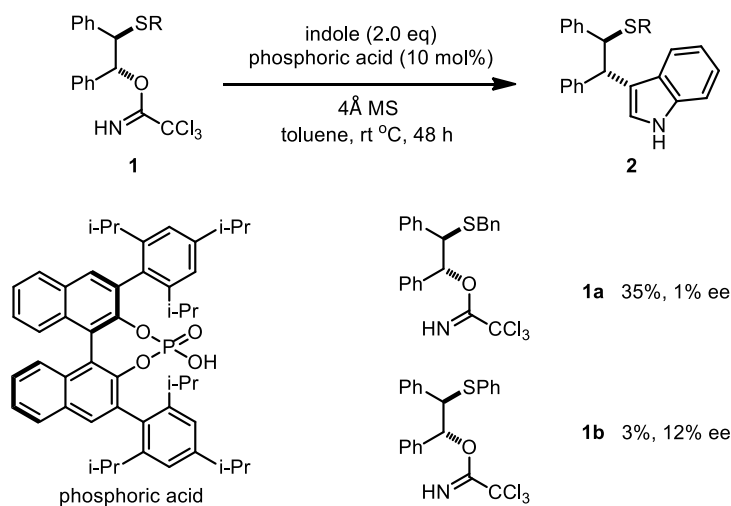
Investigation of the amino acid linker:



Investigation of the thiourea unit:

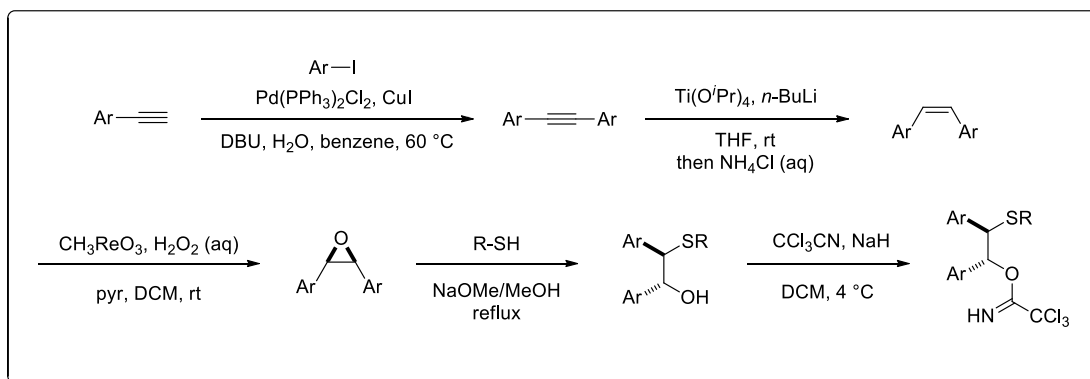


The chiral phosphoric acid that Toste and coworkers used in their episulfonium ion ring opening with alcohols does not work well in this indole alkylation reaction:



Note: at -30 °C, no desired product was observed (by TLC) after 48 h.

## 5. Preparation and characterization of substrates 1a-1z



**Sonogashira coupling.** An oven-dried round bottom flask was charged with CuI (10 mol%), Pd(PPh<sub>3</sub>)<sub>2</sub>Cl<sub>2</sub> (2 mol%) and flushed with N<sub>2</sub>. Aryl iodide (1.1 equiv) in anhydrous benzene (0.2 M) was added, followed by water (0.4 equiv) and DBU (6.0 equiv) sequentially. Arylacetylene (1.0 equiv) was added at last. The flask was packaged with aluminum foil and heated to 60 °C. After TLC showed complete conversion of arylacetylene, the reaction was cooled down to room temperature, and quenched by saturate NH<sub>4</sub>Cl (aq). After diluted with EtOAc, the mixture was stirred for 5 min before partition of the aqueous and organic layers. The aqueous layer was extracted with EtOAc. The combined organic layers were washed with brine, dried over NaSO<sub>4</sub>, concentrated, and the crude extracts were purified by silica gel column chromatography to obtain the coupling product.

**Ti-mediated reduction of diarylacetylene.** An oven-dried flask was charged with diarylacetylene (1.0 equiv) and flushed with N<sub>2</sub>. THF (0.23 M) was added and the solution was cooled down to -78 °C. Freshly distilled titanium tetraisopropoxide (2.0 equiv) was added, followed by *n*-butyllithium (2.5 M in hexanes, 4 equiv) via syringe pump over 10 min. The resulting yellow/orange solution was warmed to room temperature and stirred for 2–4 h until the starting material was consumed. Saturated NH<sub>4</sub>Cl (aq) was added slowly and carefully to quench the reaction (ice bath may be necessary). The mixture was diluted with EtOAc and stirred for 10 min. The aqueous layer was separated and extracted with EtOAc. The combined organic layers were washed with brine, dried over NaSO<sub>4</sub>, concentrated, and the crude extracts were purified by silica gel column chromatography to obtain the reduction product.

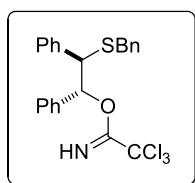
**Epoxidation of *cis*-diarylethene.** A round bottom flask was charged with *cis*-diarylethene (1.0 equiv) and DCM (0.4 M). The mixture was cooled to 0 °C, and methylrhenium trioxide (2.5-10%, electron-deficient substrate required more rhenium catalyst) was added. Pyridine (13 mol%) and hydrogen peroxide (30% wt. aqueous solution, 1.5-5.0

equiv, electron-deficient substrate required more oxidant). The resulting yellow biphasic mixture was warmed to room temperature and stirred vigorously until TLC showed complete conversion of the alkene (usually 24-120 h). Manganese dioxide (~10 mg) was added carefully to decompose remaining hydrogen peroxide and the mixture was allowed to age for 20 min. Peroxides test sticks were used to evaluate the amount of remaining peroxide. The aqueous layer was separated and extracted with DCM. In case there was a detectable amount of peroxide residue, the combined organic layers after extraction were washed with aqueous sodium thiosulfate solution until no peroxide was detected. Otherwise, the combined organic layers were washed with brine, dried over NaSO<sub>4</sub>, concentrated, and the crude extracts were purified by silica gel column chromatography to obtain the epoxidation product.

**Epoxide opening with thiol.** An oven-dried flask was charged with benzyl mercaptan (1.6 equiv), sodium methoxide (0.5 M in methanol, 1.5 equiv) and a refluxing condenser. The solution was heated to reflux and stirred for 10 min. After cooling down to room temperature, *cis*-diarylepoxyde (1.0 equiv) was added to the resulting sodium benzylthiolate solution neat or as a stock solution in methanol (~2 M). The mixture was again brought to 60 °C and stirred for ca. 4 h until all starting material was consumed. The reaction was cooled down to room temperature, diluted with EtOAc, and quenched by addition of water. The aqueous layer was separated and extracted with EtOAc. The combined organic layers were washed with brine, dried over NaSO<sub>4</sub>, concentrated, and the crude extracts were purified by silica gel column chromatography to obtain the sulfanyl alcohol product.

**Trichloroacetimidate synthesis.** To a solution of 1,2-diaryl-2-sulfanylethanol (1.0 equiv) in DCM (0.5 M) at 0 °C was added trichloroacetonitrile (2.0 equiv) followed by sodium hydride (20 mol%). The reaction was stirred at that temperature overnight before quenched by addition of water. The resulting mixture was separated, and the aqueous layer was extracted with EtOAc. The combined organic layers were washed with brine, dried over Na<sub>2</sub>SO<sub>4</sub> and concentrated. The crude extracts were purified by silica gel column chromatography (hexanes/EtOAc with 1% NEt<sub>3</sub>) to obtain the trichloroacetimidate product.

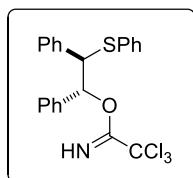
#### Characterization data for substrates 1a-1z



#### 2-(benzylthio)-1,2-diphenylethyl 2,2,2-trichloroacetimidate (1a)

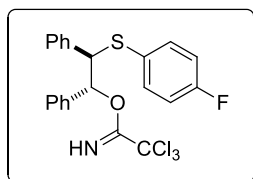
IR (Film): 3337, 3029, 1663 (s), 1583, 1493, 1453, 1322, 1287 (s), 1071 (s), 991, 793 (s), 696 (s) cm<sup>-1</sup>; <sup>1</sup>H NMR: (500 MHz, CDCl<sub>3</sub>) δ 8.34 (s, 1H), 7.41 - 7.17 (m, 11H), 7.17 - 7.01 (m,

4H), 6.14 (d,  $J=7.3$  Hz, 1H), 4.18 (d,  $J=7.3$  Hz, 1H), 3.72 (d,  $J=13.2$  Hz, 1H), 3.57 (d,  $J=13.2$  Hz, 1H);  $^{13}\text{C}$  NMR: (125 MHz,  $\text{CDCl}_3$ )  $\delta$  161.06, 137.97, 137.67, 137.21, 129.16, 129.05, 128.34, 128.11, 128.04, 127.76, 127.48, 127.04, 126.96, 83.32, 54.64, 36.16; MS (ESI-APCI) exact mass calculated for  $[\text{M}-(\text{CCl}_3\text{C}=\text{NHO})]$  ( $\text{C}_{21}\text{H}_{19}\text{S}$ ) requires  $m/z$  303.1, found  $m/z$  303.1.



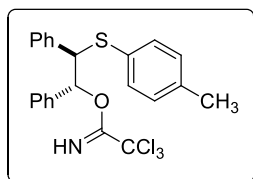
**1,2-diphenyl-2-(phenylthio)ethyl 2,2,2-trichloroacetimidate (1b)**

IR (Film): 3338, 3031, 1663 (s), 1583, 1479, 1453, 1322, 1288 (s), 1071 (s), 992, 835, 794 (s), 696 (s)  $\text{cm}^{-1}$ ;  $^1\text{H}$  NMR: (500 MHz,  $\text{CDCl}_3$ )  $\delta$  8.37 (br. s., 1H), 7.28 (d,  $J=7.3$  Hz, 4H), 7.23 (m, 5H), 7.20 - 6.96 (m, 6H), 6.23 (d,  $J=6.8$  Hz, 1H), 4.74 (d,  $J=7.3$  Hz, 1H);  $^{13}\text{C}$  NMR: (125 MHz,  $\text{CDCl}_3$ )  $\delta$  161.07, 137.89, 136.78, 134.81, 131.69, 129.13, 128.69, 128.20, 127.90, 127.79, 127.43, 127.27, 126.90, 82.48, 58.82; MS (ESI-APCI) exact mass calculated for  $[\text{M}-(\text{CCl}_3\text{C}=\text{NHO})]$  ( $\text{C}_{20}\text{H}_{17}\text{S}$ ) requires  $m/z$  289.1, found  $m/z$  289.0.



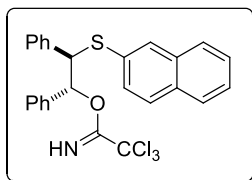
**1,2-diphenyl-2-(p-tolylthio)ethyl 2,2,2-trichloroacetimidate (1c)**

IR (Film): 3339, 3032, 1663 (s), 1588, 1489 (s), 1453, 1322, 1289 (s), 1226 (s), 1156, 1071 (s), 991, 829, 793 (s), 696 (s)  $\text{cm}^{-1}$ ;  $^1\text{H}$  NMR: (500 MHz,  $\text{CDCl}_3$ )  $\delta$  8.38 (s, 1H), 7.43 - 7.19 (m, 7H), 7.19 - 7.12 (m, 3H), 7.12 - 7.02 (m, 2H), 6.95 - 6.76 (m, 2H), 6.22 (d,  $J=7.8$  Hz, 1H), 4.62 (d,  $J=7.3$  Hz, 1H);  $^{13}\text{C}$  NMR: (125 MHz,  $\text{CDCl}_3$ )  $\delta$  163.34, 161.37, 161.08, 137.78, 136.87, 135.10, 135.04, 129.11, 128.25, 127.96, 127.88, 127.50, 127.25, 115.87, 115.69, 82.31, 60.05; MS (ESI-APCI) exact mass calculated for  $[\text{M}-(\text{CCl}_3\text{C}=\text{NHO})]$  ( $\text{C}_{20}\text{H}_{16}\text{FS}$ ) requires  $m/z$  307.1, found  $m/z$  307.0.



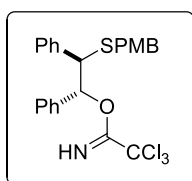
**2-((4-fluorophenyl)thio)-1,2-diphenylethyl 2,2,2-trichloroacetimidate (1d)**

IR (Film): 3338, 3031, 1663 (s), 1492, 1453, 1322, 1288 (s), 1073 (s), 991, 794 (s), 697 (s)  $\text{cm}^{-1}$ ;  $^1\text{H}$  NMR: (500 MHz,  $\text{CDCl}_3$ )  $\delta$  8.36 (s, 1H), 7.33 - 7.09 (m, 12H), 6.99 (d,  $J=8.3$  Hz, 2H), 6.22 (d,  $J=6.8$  Hz, 1H), 4.66 (d,  $J=7.3$  Hz, 1H), 2.27 (s, 3H);  $^{13}\text{C}$  NMR: (125 MHz,  $\text{CDCl}_3$ )  $\delta$  161.09, 138.11, 137.18, 136.85, 132.44, 130.97, 129.51, 129.19, 128.15, 127.85, 127.77, 127.33, 82.39, 59.35, 21.04; MS (ESI-APCI) exact mass calculated for  $[\text{M}-(\text{CCl}_3\text{C}=\text{NHO})]$  ( $\text{C}_{21}\text{H}_{19}\text{S}$ ) requires  $m/z$  303.1, found  $m/z$  303.1.



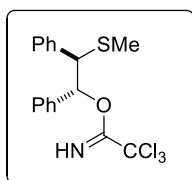
**2-(naphthalen-2-ylthio)-1,2-diphenylethyl 2,2,2-trichloroacetimidate (1e)**

IR (Film): 3336, 3056, 1664 (s), 1586, 1497, 1453, 1322, 1290(s), 1072 (s), 992, 794 (s), 697 (s)  $\text{cm}^{-1}$ ;  $^1\text{H}$  NMR: (500 MHz,  $\text{CDCl}_3$ )  $\delta$  8.40 (s, 1H), 7.76 (s, 2H), 7.71 - 7.59 (m, 2H), 7.52 - 7.38 (m, 2H), 7.35 (dd,  $J=1.7, 8.5$  Hz, 1H), 7.31 - 7.22 (m, 5H), 7.22 - 7.09 (m, 5H), 6.29 (d,  $J=7.3$  Hz, 1H), 4.86 (d,  $J=6.8$  Hz, 1H);  $^{13}\text{C}$  NMR: (125 MHz,  $\text{CDCl}_3$ )  $\delta$  161.12, 137.91, 136.83, 133.53, 132.31, 132.10, 130.26, 129.13, 129.06, 128.24, 128.20, 127.98, 127.84, 127.56, 127.52, 127.31, 126.31, 125.95, 82.55, 58.78; MS (ESI-APCI) exact mass calculated for  $[\text{M}-(\text{CCl}_3\text{C}=\text{NHO})]$  ( $\text{C}_{24}\text{H}_{19}\text{S}$ ) requires  $m/z$  339.1, found  $m/z$  339.1.



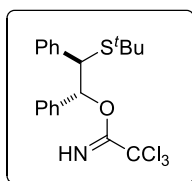
**2-((4-methoxybenzyl)thio)-1,2-diphenylethyl 2,2,2-trichloroacetimidate (1f)**

IR (Film): 3338, 2980 (s), 2889, 1663 (s), 1609, 1510, 1453, 1382, 1299, 1249 (s), 1174, 1073 (s), 991, 825, 794 (s), 697 (s)  $\text{cm}^{-1}$ ;  $^1\text{H}$  NMR: (500 MHz,  $\text{CDCl}_3$ )  $\delta$  8.33 (s, 1H), 7.35 - 7.17 (m, 6H), 7.17 - 7.05 (m, 6H), 6.80 (d,  $J=8.8$  Hz, 2H), 6.12 (d,  $J=7.3$  Hz, 1H), 4.17 (d,  $J=7.3$  Hz, 1H), 3.80 (s, 3H), 3.67 (d,  $J=13.2$  Hz, 1H), 3.52 (d,  $J=13.2$  Hz, 1H);  $^{13}\text{C}$  NMR: (125 MHz,  $\text{CDCl}_3$ )  $\delta$  161.34, 158.85, 138.34, 137.52, 130.41, 129.45, 128.36, 128.31, 128.02, 127.72, 127.33, 114.02, 83.62, 55.53, 54.80, 35.84; MS (ESI-APCI) exact mass calculated for  $[\text{M}-(\text{CCl}_3\text{C}=\text{NHO})]$  ( $\text{C}_{22}\text{H}_{21}\text{OS}$ ) requires  $m/z$  333.1, found  $m/z$  333.1.



**2-(methylthio)-1,2-diphenylethyl 2,2,2-trichloroacetimidate (1g)**

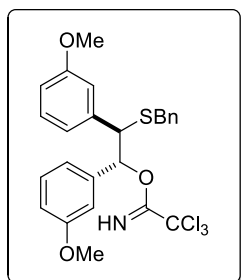
IR (Film): 3338, 3031, 2916, 1663 (s), 1492, 1453, 1288 (s), 1072 (s), 793 (s), 696 (s)  $\text{cm}^{-1}$ ;  $^1\text{H}$  NMR: (500 MHz,  $\text{CDCl}_3$ )  $\delta$  8.35 (s, 1H), 7.37 - 7.15 (m, 10H), 6.14 (d,  $J=7.8$  Hz, 1H), 4.29 (d,  $J=7.8$  Hz, 1H), 1.98 (s, 3H);  $^{13}\text{C}$  NMR: (125 MHz,  $\text{CDCl}_3$ )  $\delta$  161.09, 137.67, 137.29, 129.08, 128.14, 128.11, 127.82, 127.49, 127.05, 83.25, 57.31, 15.22; MS (ESI-APCI) exact mass calculated for  $[\text{M}-(\text{CCl}_3\text{C}=\text{NHO})]$  ( $\text{C}_{15}\text{H}_{15}\text{S}$ ) requires  $m/z$  227.1, found  $m/z$  227.1.



**2-(tert-butylthio)-1,2-diphenylethyl 2,2,2-trichloroacetimidate (1h)**

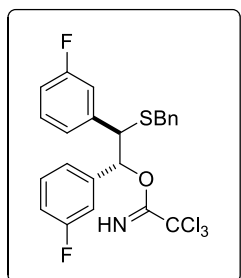
IR (Film): 3340, 3030, 2960, 1663 (s), 1493, 1453, 1322, 1290 (s), 1159, 1074 (s), 988, 853, 795 (s), 698 (s)  $\text{cm}^{-1}$ ;  $^1\text{H}$  NMR: (500 MHz,  $\text{CDCl}_3$ )  $\delta$  8.31 (s, 1H), 7.29 - 7.07 (m, 10H), 6.12

(d,  $J=5.4$  Hz, 1H), 4.31 (d,  $J=5.4$  Hz, 1H), 1.20 (s, 9H);  $^{13}\text{C}$  NMR: (125 MHz,  $\text{CDCl}_3$ )  $\delta$  161.49, 141.04, 137.26, 129.79, 128.28, 128.23, 128.04, 127.90, 127.80, 127.60, 127.22, 127.11, 83.80, 52.68, 44.48, 31.46; MS (ESI-APCI) exact mass calculated for  $[\text{M}-(\text{CCl}_3\text{C}=\text{NHO})]$  ( $\text{C}_{20}\text{H}_{17}\text{S}$ ) requires  $m/z$  289.1, found  $m/z$  289.0.



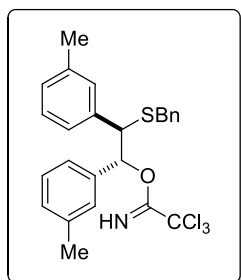
**2-(benzylthio)-1,2-bis(3-methoxyphenyl)ethyl 2,2,2-trichloroacetimidate (1r)**

IR (Film): 3337, 2980, 2835, 1664 (s), 1600 (s), 1491 (s), 1285, 1262 (s), 1153, 1071 (s), 994, 832, 794 (s), 695 (s)  $\text{cm}^{-1}$ ;  $^1\text{H}$  NMR: (500 MHz,  $\text{CDCl}_3$ )  $\delta$  8.35 (s, 1H), 7.40 - 7.19 (m, 5H), 7.19 - 7.02 (m, 2H), 6.86 - 6.71 (m, 4H), 6.71 - 6.55 (m, 2H), 6.09 (d,  $J=6.8$  Hz, 1H), 4.12 (d,  $J=6.8$  Hz, 1H), 3.70 (s, 3H), 3.71 (d,  $J=12.7$  Hz, 5H), 3.66 (s, 3H), 3.58 (d,  $J=13.2$  Hz, 1H);  $^{13}\text{C}$  NMR: (125 MHz,  $\text{CDCl}_3$ )  $\delta$  161.00, 159.36, 159.03, 139.53, 138.73, 137.69, 129.08, 128.78, 128.33, 126.97, 121.64, 119.39, 114.40, 114.05, 113.47, 112.07, 91.45, 83.05, 55.18, 55.07, 54.67, 36.23; MS (ESI-APCI) exact mass calculated for  $[\text{M}-(\text{CCl}_3\text{C}=\text{NHO})]$  ( $\text{C}_{23}\text{H}_{23}\text{O}_2\text{S}$ ) requires  $m/z$  363.1, found  $m/z$  363.1.



**2-(benzylthio)-1,2-bis(3-fluorophenyl)ethyl 2,2,2-trichloroacetimidate (1s)**

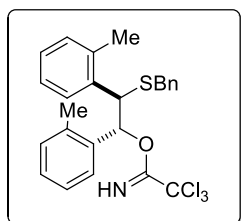
IR (Film): 3340, 3029, 1665 (s), 1614, 1591 (s), 1488 (s), 1449 (s), 1300, 1282, 1253, 1140, 1069 (s), 1000, 912, 879, 833, 794 (s), 739, 691 (s), 648  $\text{cm}^{-1}$ ;  $^1\text{H}$  NMR: (500 MHz,  $\text{CDCl}_3$ )  $\delta$  8.38 (s, 1H), 7.38 - 7.15 (m, 7H), 7.09 - 6.85 (m, 6H), 6.08 (d,  $J=6.8$  Hz, 1H), 4.10 (d,  $J=6.8$  Hz, 1H), 3.72 (d,  $J=13.2$  Hz, 1H), 3.56 (d,  $J=13.2$  Hz, 1H);  $^{13}\text{C}$  NMR: (125 MHz,  $\text{CDCl}_3$ )  $\delta$  163.55, 163.32, 161.59, 160.90, 140.45, 139.43, 137.20, 129.67, 129.61, 129.44, 129.00, 128.45, 127.18, 124.78, 122.71, 116.14, 115.96, 115.29, 115.12, 114.79, 114.62, 114.00, 113.82, 91.13, 82.12, 53.89, 36.16; MS (ESI-APCI) exact mass calculated for  $[\text{M}-(\text{CCl}_3\text{C}=\text{NHO})]$  ( $\text{C}_{21}\text{H}_{17}\text{F}_2\text{S}$ ) requires  $m/z$  339.1, found  $m/z$  339.1.



**2-(benzylthio)-1,2-di-*m*-tolyethyl 2,2,2-trichloroacetimidate (1t)**

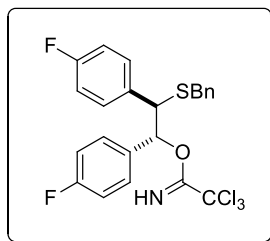
IR (Film): 3338, 3027, 2919, 1663 (s), 1606, 1491, 1453, 1287 (s), 1071 (s), 988, 832, 794 (s), 697 (s)  $\text{cm}^{-1}$ ;  $^1\text{H}$  NMR: (500 MHz,  $\text{CDCl}_3$ )  $\delta$  8.32 (s, 1H), 7.38 - 7.16 (m, 5H), 7.16 - 7.05 (m, 2H), 7.05 - 6.85 (m, 6H), 6.08 (d,  $J=6.8$  Hz, 1H), 4.11 (d,  $J=6.8$  Hz, 1H), 3.68 (d,  $J=13.7$  Hz, 1H), 3.55 (d,  $J=13.2$  Hz, 1H), 2.24 (s, 3H), 2.27 (s, 3H);  $^{13}\text{C}$  NMR: (125 MHz,  $\text{CDCl}_3$ )  $\delta$  161.36, 138.33, 137.52, 130.11, 129.32, 129.02, 128.55, 128.45, 128.13, 127.91, 127.86, 127.15, 126.52,

124.26, 83.62, 54.99, 36.46, 21.62, 21.56; MS (ESI-APCI) exact mass calculated for [M-(CCl<sub>3</sub>C=NHO)] (C<sub>23</sub>H<sub>23</sub>S) requires *m/z* 331.2, found *m/z* 331.2.



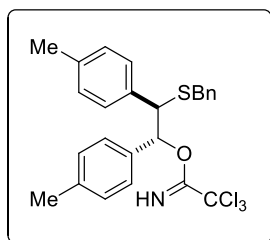
**2-(benzylthio)-1,2-di-*o*-tolylethyl 2,2,2-trichloroacetimidate (1u)**

IR (Film): 2980 (s), 2888, 3031, 1662 (s), 1491, 1461, 1382 (s), 1251, 1152 (s), 1073 (s), 954 (s), 829, 795, 739 cm<sup>-1</sup>; <sup>1</sup>H NMR: (500 MHz, CDCl<sub>3</sub>) δ 8.33 (s, 1H), 7.61 (d, *J*=7.3 Hz, 1H), 7.52 (d, *J*=7.3 Hz, 1H), 7.40 - 7.20 (m, 5H), 7.20 - 7.07 (m, 3H), 7.05 (t, *J*=7.6 Hz, 1H), 6.89 (d, *J*=7.3 Hz, 1H), 6.84 (d, *J*=7.8 Hz, 1H), 6.28 (d, *J*=9.3 Hz, 1H), 4.47 (d, *J*=9.8 Hz, 1H), 3.98 (d, *J*=13.2 Hz, 1H), 3.65 (d, *J*=13.7 Hz, 1H), 2.00 (s, 3H), 1.43 (s, 3H); <sup>13</sup>C NMR: (125 MHz, CDCl<sub>3</sub>) δ 160.90, 138.33, 136.59, 136.36, 135.92, 130.08, 129.81, 129.31, 129.18, 128.42, 128.04, 127.24, 126.97, 126.78, 126.03, 125.55, 81.33, 48.59, 36.99, 19.06, 18.68; MS (ESI-APCI) exact mass calculated for [M-(CCl<sub>3</sub>C=NHO)] (C<sub>23</sub>H<sub>23</sub>S) requires *m/z* 331.2, found *m/z* 331.2.



**2-(benzylthio)-1,2-bis(4-fluorophenyl)ethyl 2,2,2-trichloroacetimidate (1v)**

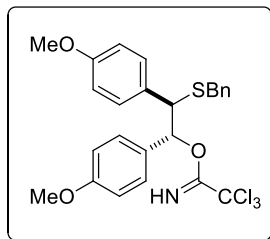
IR (Film): 3339, 1727 (s), 1665 (s), 1603 (s), 1508 (s), 1453, 1295, 1225 (s), 1158, 1071 (s), 994, 832 (s), 796 (s) cm<sup>-1</sup>; <sup>1</sup>H NMR: (500 MHz, CDCl<sub>3</sub>) δ 8.35 (s, 1H), 7.36 - 7.12 (m, 5H), 7.12 - 6.95 (m, 4H), 6.95 - 6.72 (m, 4H), 6.06 (d, *J*=6.8 Hz, 1H), 4.13 (d, *J*=6.8 Hz, 1H), 3.71 (d, *J*=13.7 Hz, 1H), 3.55 (d, *J*=13.7 Hz, 1H); <sup>13</sup>C NMR: (125 MHz, CDCl<sub>3</sub>) δ 165.24, 163.06, 160.91, 137.37, 133.32, 132.57, 130.87, 130.80, 130.22, 128.99, 128.87, 128.81, 128.43, 127.13, 115.13, 114.96, 114.91, 114.73, 82.31, 53.54, 36.08; MS (ESI-APCI) exact mass calculated for [M-(CCl<sub>3</sub>C=NHO)] (C<sub>21</sub>H<sub>17</sub>F<sub>2</sub>S) requires *m/z* 339.1, found *m/z* 339.1.



**2-(benzylthio)-1,2-di-*p*-tolylethyl 2,2,2-trichloroacetimidate (1w)**

IR (Film): 3338, 3027, 2920, 1664 (s), 1513, 1453, 1320, 1288 (s), 1073 (s), 985, 832, 794 (s), 741, 701, 646 (s) cm<sup>-1</sup>; <sup>1</sup>H NMR: (500 MHz, CDCl<sub>3</sub>) δ 8.31 (s, 1H), 7.39 - 7.16 (m, 5H), 7.16 - 6.92 (m, 8H), 6.08 (d, *J*=7.3 Hz, 1H), 4.14 (d, *J*=7.3 Hz, 1H), 3.69 (d, *J*=13.2 Hz, 1H), 3.55 (d, *J*=13.2 Hz, 1H), 2.27 (s, 3H), 2.30 (s, 3H); <sup>13</sup>C NMR: (125 MHz, CDCl<sub>3</sub>) δ 161.10, 137.85, 137.69, 137.03, 134.95, 134.30, 129.08, 129.04, 128.82, 128.49, 128.31, 127.03,

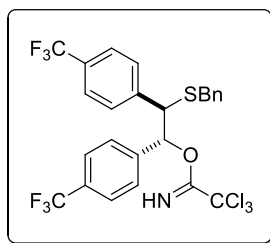
126.89, 91.53, 83.32, 54.33, 36.13, 21.20, 21.12; MS (ESI-APCI) exact mass calculated for [M-(CCl<sub>3</sub>C=NHO)] (C<sub>23</sub>H<sub>23</sub>S) requires *m/z* 331.1, found *m/z* 331.2.



**2-(benzylthio)-1,2-bis(4-methoxyphenyl)ethyl 2,2,2-trichloroacetimidate (1x)**

IR (Film): 3336, 2980 (s), 1662 (s), 1633, 1610 (s), 1511 (s), 1454, 1381, 1302, 1248 (s), 1175 (s), 1072 (s), 1032 (s), 970, 829, 793 (s), cm<sup>-1</sup>; <sup>1</sup>H NMR: (500 MHz, CDCl<sub>3</sub>) δ 8.32 (s, 1H), 7.37 - 7.17 (m, 5H), 7.04 (d, *J*=8.8 Hz, 2H), 7.02 (d, *J*=8.8 Hz, 2H), 6.74 (d, *J*=8.8 Hz, 2H), 6.72 (d, *J*=8.8 Hz, 2H), 6.05 (d, *J*=7.3 Hz, 1H), 4.16 (d, *J*=7.3 Hz,

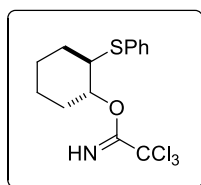
1H), 3.85 - 3.76 (m, 5H), 3.76 - 3.72 (m, 3H), 3.70 (d, *J*=13.2 Hz, 1H), 3.56 (d, *J*=13.2 Hz, 1H); <sup>13</sup>C NMR: (125 MHz, CDCl<sub>3</sub>) δ 161.04, 159.20, 158.75, 137.84, 130.32, 129.81, 129.24, 129.04, 128.44, 128.31, 126.89, 113.42, 113.11, 91.53, 83.06, 55.14, 55.06, 53.91, 36.02; MS (ESI-APCI) exact mass calculated for [M-(CCl<sub>3</sub>C=NHO)] (C<sub>23</sub>H<sub>23</sub>O<sub>2</sub>S) requires *m/z* 363.1, found *m/z* 363.1.



**2-(benzylthio)-1,2-bis(4-(trifluoromethyl)phenyl)ethyl 2,2,2-trichloroacetimidate (1y)**

IR (Film): 3342, 2980, 1667 (s), 1619, 1419, 1323 (s), 1165 (s), 1124 (s), 1067 (s), 1001, 992, 834, 796 (s) cm<sup>-1</sup>; <sup>1</sup>H NMR: (500 MHz, CDCl<sub>3</sub>) δ 8.39 (s, 1H), 7.48 (dd, *J*=4.4, 8.3 Hz, 4H), 7.40 - 7.19 (m, 7H), 7.14 (dd, *J*=1.7, 7.6 Hz, 2H), 6.16 (d, *J*=5.9 Hz,

1H), 4.15 (d, *J*=5.9 Hz, 1H), 3.72 (d, *J*=13.7 Hz, 1H), 3.53 (d, *J*=13.7 Hz, 1H); <sup>13</sup>C NMR: (125 MHz, CDCl<sub>3</sub>) δ 160.77, 141.83, 140.57, 136.91, 129.57, 128.94, 128.49, 127.26, 125.17, 124.92, 122.78, 90.97, 81.86, 53.65, 36.16; MS (ESI-APCI) exact mass calculated for [M-(CCl<sub>3</sub>C=NHO)] (C<sub>23</sub>H<sub>17</sub>F<sub>6</sub>S) requires *m/z* 439.1, found *m/z* 439.0.

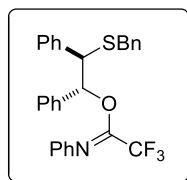


**2-(benzylthio)cyclohexyl 2,2,2-trichloroacetimidate (1z)**

IR (Film): 3343, 2938, 2860, 1660 (s), 1584, 1480, 1439, 1322, 1298 (s), 1073 (s), 1015, 975, 829, 794 (s), 645 cm<sup>-1</sup>; <sup>1</sup>H NMR: (500 MHz, CDCl<sub>3</sub>) δ 8.33 (s, 1H), 7.62 - 7.40 (m, 2H), 7.40 - 7.20 (m, 3H), 4.99 (dt, *J*=3.9, 7.8 Hz, 1H), 3.42 (dt, *J*=4.4, 8.1 Hz, 1H), 2.43 - 2.19 (m, 2H),

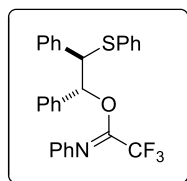
2.19 - 2.00 (m, 1H), 1.93 - 1.71 (m, 3H), 1.71 - 1.53 (m, 3H), 1.53 - 1.32 (m, 3H); <sup>13</sup>C NMR: (125 MHz, CDCl<sub>3</sub>) δ 162.10, 134.70, 132.44, 129.04, 127.20, 78.72, 49.16, 30.94, 28.84, 24.06, 22.80; MS (ESI-APCI) exact mass

calculated for [M-(CCl<sub>3</sub>C=NHO)] (C<sub>13</sub>H<sub>17</sub>S) requires *m/z* 191.1, found *m/z* 191.1.



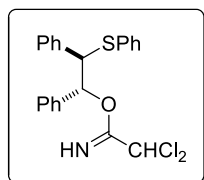
**2-(benzylthio)-1,2-diphenylethyl 2,2,2-trifluoro-N-phenylacetimidate (1a')**

IR (Film): 3031, 1707 (s), 1598, 1490, 1453, 1310, 1207 (s), 1137 (s), 1073, 1028, 968, 913, 695 (s) cm<sup>-1</sup>; <sup>1</sup>H NMR: (500 MHz, CDCl<sub>3</sub>) δ 7.44 - 7.20 (m, 13H), 7.20 - 6.97 (m, 5H), 6.61 (d, *J*=7.8 Hz, 2H), 6.25 (br. s., 1H), 4.21 (d, *J*=7.8 Hz, 1H), 3.76 (d, *J*=13.3 Hz, 1H), 3.62 (d, *J*=13.3 Hz, 1H); <sup>13</sup>C NMR: (125 MHz, CDCl<sub>3</sub>) δ 143.93, 137.82, 137.59, 136.97, 129.09, 129.00, 128.54, 128.41, 128.23, 128.11, 127.86, 127.55, 127.25, 127.05, 123.78, 119.33, 81.90, 54.17, 36.36; MS (ESI-APCI) exact mass calculated for [M-(CCl<sub>3</sub>C=NHO)] (C<sub>21</sub>H<sub>19</sub>S) requires *m/z* 303.1, found *m/z* 303.1.



**1,2-diphenyl-2-(phenylthio)ethyl 2,2,2-trifluoro-N-phenylacetimidate (1b')**

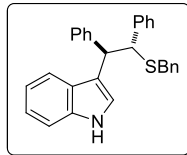
IR (Film): 3032, 1706 (s), 1597, 1489, 1453, 1308, 1205 (s), 1135 (s), 1073, 1026, 964, 912, 794, 692 (s) cm<sup>-1</sup>; <sup>1</sup>H NMR: (500 MHz, CDCl<sub>3</sub>) δ 7.55 - 7.31 (m, 5H), 7.31 - 7.12 (m, 12H), 7.11 - 7.07 (m, 1H), 6.88 - 6.65 (m, 2H), 6.37 (br. s., 1H), 4.76 (d, *J*=7.8 Hz, 1H); <sup>13</sup>C NMR: (125 MHz, CDCl<sub>3</sub>) δ 144.20, 138.17, 136.91, 135.03, 132.34, 129.22, 129.06, 128.86, 128.53, 128.37, 128.19, 127.80, 127.77, 127.45, 124.10, 119.62, 81.36, 59.28; MS (ESI-APCI) exact mass calculated for [M-(CCl<sub>3</sub>C=NHO)] (C<sub>20</sub>H<sub>17</sub>S) requires *m/z* 289.1, found *m/z* 289.1.



**1,2-diphenyl-2-(phenylthio)ethyl 2,2-dichloroacetimidate (1b'')**

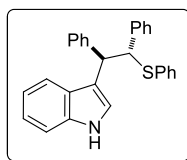
IR (Film): 3323, 3031, 2980, 1667 (s), 1583, 1479, 1453, 1337, 1216, 1072 (s), 987, 798, 746, 695 (s) cm<sup>-1</sup>; <sup>1</sup>H NMR: (500 MHz, CDCl<sub>3</sub>) δ 8.23 (s, 1H), 7.33 (dd, *J*=1.2, 8.1 Hz, 2H), 7.29 - 7.06 (m, 13H), 6.27 (d, *J*=7.8 Hz, 1H), 5.74 (s, 1H), 4.71 (d, *J*=8.3 Hz, 1H); <sup>13</sup>C NMR: (125 MHz, CDCl<sub>3</sub>) δ 163.64, 137.70, 137.22, 135.26, 131.72, 128.96, 128.72, 128.53, 128.07, 127.85, 127.51, 127.23, 126.94, 81.76, 65.60, 58.66; MS (ESI-APCI) exact mass calculated for [M-(CCl<sub>3</sub>C=NHO)] (C<sub>20</sub>H<sub>17</sub>S) requires *m/z* 289.1, found *m/z* 289.1.

## 6. Characterization of products 2a-2z



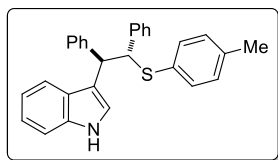
### 3-((1*R*,2*R*)-2-(benzylthio)-1,2-diphenylethyl)-1*H*-indole (**2a**)

Followed method B from **1a** (23.2 mg, 0.05 mmol), for 45 h, and purified using silica gel chromatography to give 20.8 mg (99% yield) of **10** as a white solid. This material was determined to be 93% ee by chiral HPLC analysis (ChiralPak AD-H, 10% *i*-PrOH, 1 mL/min, 240 nm,  $t_r(\text{major}) = 24$  min,  $t_r(\text{minor}) = 33$  min). IR (Film): 3419 (s), 3026, 1599, 1491, 1453 (s), 1417, 1336, 1264, 1071, 736 (s), 694 (s)  $\text{cm}^{-1}$ ;  $^1\text{H}$  NMR (500 MHz,  $\text{CDCl}_3$ )  $\delta = 8.02$  (br. s., 1H), 7.44 (d,  $J=7.8$  Hz, 1H), 7.37 - 6.90 (m, 19H), 4.66 (d,  $J=10.5$  Hz, 1H), 4.46 (d,  $J=10.5$  Hz, 1H), 3.45 (d,  $J=13.7$  Hz, 1H), 3.28 (d,  $J=13.7$  Hz, 1H);  $^{13}\text{C}$  NMR (125 MHz,  $\text{CDCl}_3$ )  $\delta = 142.64$ , 140.94, 138.40, 136.00, 129.19, 129.09, 128.45, 128.41, 128.23, 127.91, 127.72, 127.25, 126.80, 126.76, 125.88, 122.38, 121.90, 119.44, 119.36, 117.11, 111.00, 54.07, 49.59, 35.77; MS (ESI-APCI) exact mass calculated for [M-SBn] ( $\text{C}_{22}\text{H}_{18}\text{N}$ ) requires  $m/z$  296.1, found  $m/z$  296.1;  $[\alpha]_{\text{D}}^{23} = +130.6$  ( $c = 0.5$ ,  $\text{CH}_2\text{Cl}_2$ ).



### 3-((1*R*,2*R*)-1,2-diphenyl-2-(phenylthio)ethyl)-1*H*-indole (**2b**)

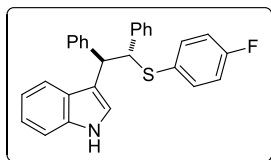
Followed method B from **1b** (22.6 mg, 0.05 mmol), for 63 h, and purified using silica gel chromatography to give 16.8 mg (83% yield) of **2b** as a white solid. This material was determined to be 85% ee by chiral HPLC analysis (ChiralPak AD-H, 10% *i*-PrOH, 1 mL/min, 220 nm,  $t_r(\text{major}) = 29$  min,  $t_r(\text{minor}) = 18$  min). IR (Film): 3412 (s), 3058, 3027, 1582, 1490, 1454 (s), 1418, 1337, 1098, 1026, 740 (s), 695 (s)  $\text{cm}^{-1}$ ;  $^1\text{H}$  NMR: (500 MHz,  $\text{CDCl}_3$ )  $\delta$  8.04 (br. s., 1H), 7.57 (d,  $J=8.3$  Hz, 1H), 7.46 - 7.30 (m, 2H), 7.23 - 7.01 (m, 17H), 5.02 (d,  $J=9.3$  Hz, 1H), 4.83 (d,  $J=9.8$  Hz, 1H);  $^{13}\text{C}$  NMR: (125 MHz,  $\text{CDCl}_3$ )  $\delta$  142.32, 140.98, 136.02, 135.54, 132.10, 128.84, 128.61, 128.42, 127.83, 127.66, 127.26, 126.63, 126.06, 122.46, 122.01, 119.46, 119.29, 117.19, 111.11, 58.93, 49.23; MS (ESI-APCI) exact mass calculated for [M-SPh] ( $\text{C}_{22}\text{H}_{18}\text{N}$ ) requires  $m/z$  296.1, found  $m/z$  296.2;  $[\alpha]_{\text{D}}^{25} = +38.6$  ( $c = 1.0$ ,  $\text{CH}_2\text{Cl}_2$ ).



### 3-((1*R*,2*R*)-1,2-diphenyl-2-(*p*-tolylthio)ethyl)-1*H*-indole (**2d**)

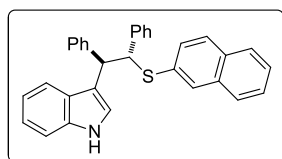
Followed method B from **1d** (23.2 mg, 0.05 mmol), for 63 h, and purified using silica gel chromatography to give 16.0 mg (76% yield) of **2d** as a colorless gel. This material was determined to be 87% ee by chiral HPLC analysis (ChiralPak AD-H, 10% *i*-PrOH, 1 mL/min, 220 nm,  $t_r(\text{major}) = 33$  min,  $t_r(\text{minor}) = 16$  min). IR (Film): 3421 (br, s), 3026, 1491, 1454 (s), 1418, 1337, 1098, 1030, 909, 808, 739

(s), 696 (s)  $\text{cm}^{-1}$ ;  $^1\text{H NMR}$ : (500 MHz,  $\text{CDCl}_3$ )  $\delta$  8.05 (br. s., 1H), 7.55 (d,  $J=8.2$  Hz, 1H), 7.42 - 7.33 (m, 2H), 7.21 - 6.98 (m, 14H), 6.92 (d,  $J=7.8$  Hz, 2H), 4.94 (d,  $J=9.6$  Hz, 1H), 4.81 (d,  $J=9.6$  Hz, 1H), 2.24 (s, 3H);  $^{13}\text{C NMR}$ : (125 MHz,  $\text{CDCl}_3$ )  $\delta$  142.42, 141.20, 136.83, 136.04, 132.75, 131.66, 129.23, 128.87, 128.63, 127.80, 127.61, 127.29, 126.55, 126.00, 122.44, 121.98, 119.44, 119.33, 117.35, 111.10, 59.33, 49.08, 21.03; MS (ESI-APCI) exact mass calculated for [M-SAr] ( $\text{C}_{22}\text{H}_{18}\text{N}$ ) requires  $m/z$  296.1, found  $m/z$  296.1;  $[\alpha]_{\text{D}}^{24} = +56.2$  ( $c = 1.0$ ,  $\text{CH}_2\text{Cl}_2$ ).



### 3-((1*R*,2*R*)-2-((4-fluorophenyl)thio)-1,2-diphenylethyl)-1*H*-indole (**2c**)

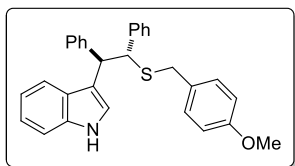
Followed method B from **1c** (23.4 mg, 0.05 mmol), for 63 h, and purified using silica gel chromatography to give 15.4 mg (73% yield) of **2c** as a colorless gel. This material was determined to be 81% ee by chiral SFC analysis (ChiralPak AD-H, 10% *i*-PrOH, 1 mL/min, 220 nm,  $t_{\text{r}}$ (major) = 16 min,  $t_{\text{r}}$ (minor) = 30 min). IR (Film): 3422 (s), 3059, 1588, 1488 (s), 1454, 1337, 1223, 1155, 1096, 1012, 829, 740 (s), 698 (s)  $\text{cm}^{-1}$ ;  $^1\text{H NMR}$ : (500 MHz,  $\text{CDCl}_3$ )  $\delta$  8.08 (br. s., 1H), 7.61 (d,  $J=7.8$  Hz, 1H), 7.41 - 7.31 (m, 2H), 7.24 - 6.93 (m, 14H), 6.85 - 6.72 (m, 2H), 4.93 (d,  $J=10.1$  Hz, 1H), 4.82 (d,  $J=10.5$  Hz, 1H);  $^{13}\text{C NMR}$ : (125 MHz,  $\text{CDCl}_3$ )  $\delta$  162.46 (d,  $J=246.3$  Hz, 1C), 142.65, 141.06, 136.35, 135.65, 135.58, 130.44, 129.06, 128.75, 128.16, 128.01, 127.48, 126.99, 126.32, 122.63, 122.36, 119.80, 119.57, 117.56, 115.79, 115.63, 111.45, 60.24, 49.30; MS (ESI-APCI) exact mass calculated for [M-SAr] ( $\text{C}_{22}\text{H}_{18}\text{N}$ ) requires  $m/z$  296.1, found  $m/z$  296.1;  $[\alpha]_{\text{D}}^{24} = +58.0$  ( $c = 1.0$ ,  $\text{CH}_2\text{Cl}_2$ ).



### 3-((1*R*,2*R*)-2-(naphthalen-2-ylthio)-1,2-diphenylethyl)-1*H*-indole (**2e**)

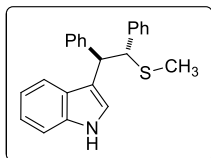
Followed method B from **1e** (25.0 mg, 0.05 mmol), for 63 h, and purified using silica gel chromatography to give 20.5 mg (90% yield) of **2e** as a white solid. This material was determined to be 88% ee by chiral HPLC analysis (ChiralPak AS-H, 10% *i*-PrOH, 1 mL/min, 220 nm,  $t_{\text{r}}$ (major) = 16 min,  $t_{\text{r}}$ (minor) = 31 min). IR (Film): 3422 (s), 3055, 1585, 1491, 1454 (s), 1337, 1098, 1073, 907 (s), 813, 738 (s), 697 (s)  $\text{cm}^{-1}$ ;  $^1\text{H NMR}$ : (500 MHz,  $\text{CDCl}_3$ )  $\delta$  8.02 (br. s., 1H), 7.88 - 7.68 (m, 1H), 7.68 - 7.52 (m, 3H), 7.52 - 7.39 (m, 2H), 7.39 - 7.31 (m, 2H), 7.31 - 7.17 (m, 5H), 7.17 - 6.93 (m, 6H), 5.14 (d,  $J=9.8$  Hz, 1H), 4.90 (d,  $J=9.8$  Hz, 1H);  $^{13}\text{C NMR}$ : (125 MHz,  $\text{CDCl}_3$ )  $\delta$  142.33, 140.99, 136.01, 133.43, 133.06, 131.94, 130.50, 129.49, 128.79, 128.60, 127.87, 127.80, 127.76, 127.50, 127.30, 127.26, 126.72, 126.10, 126.08, 125.75, 122.47, 122.04, 119.49, 119.31, 117.23, 111.12, 58.88, 49.27; MS (ESI-APCI) exact mass calculated for [M-SAr] ( $\text{C}_{22}\text{H}_{18}\text{N}$ ) requires  $m/z$

296.1, found  $m/z$  296.1;  $[\alpha]_D^{24} = +40.9$  ( $c = 1.0$ ,  $\text{CH}_2\text{Cl}_2$ ).



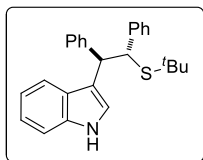
### 3-((1*R*,2*R*)-((4-methoxybenzyl)thio)-1,2-diphenylethyl)-1*H*-indole (**2f**)

Followed method B from **1f** (24.7 mg, 0.05 mmol), for 45 h, purified using silica gel chromatography to give 22.7 mg (>99% yield) of **2f** as a colorless gel. This material was determined to be 94% ee by chiral HPLC analysis (ChiralPak AD-H, 10% *i*-PrOH, 1 mL/min, 240 nm,  $t_r(\text{major}) = 30$  min,  $t_r(\text{minor}) = 45$  min). IR (Film): 3420 (s), 3027, 2910, 1609, 1510 (s), 1454, 1249 (s), 1175, 1032, 741 (s)  $\text{cm}^{-1}$ ;  $^1\text{H}$  NMR: (500 MHz,  $\text{CDCl}_3$ )  $\delta$  8.02 (br. s., 1H), 7.43 (d,  $J=8.2$  Hz, 1H), 7.33 (d,  $J=8.2$  Hz, 1H), 7.25 - 7.10 (m, 7H), 7.09 - 6.92 (m, 8H), 6.89 - 6.77 (m, 2H), 4.65 (d,  $J=10.5$  Hz, 1H), 4.45 (d,  $J=10.1$  Hz, 1H), 3.84 (s, 3H), 3.40 (d,  $J=13.7$  Hz, 1H), 3.23 (d,  $J=13.3$  Hz, 1H);  $^{13}\text{C}$  NMR: (125 MHz,  $\text{CDCl}_3$ )  $\delta$  158.43, 142.67, 141.02, 136.02, 130.34, 130.13, 129.19, 128.43, 127.88, 127.72, 127.26, 126.75, 125.87, 122.41, 121.89, 119.47, 119.34, 117.18, 113.60, 110.99, 55.28, 53.96, 49.59, 35.12; MS (ESI-APCI) exact mass calculated for  $[\text{M}+\text{H}]$  ( $\text{C}_{30}\text{H}_{28}\text{NOS}$ ) requires  $m/z$  450.2, found  $m/z$  450.2;  $[\alpha]_D^{23} = +134.5$  ( $c = 0.4$ ,  $\text{CH}_2\text{Cl}_2$ ).



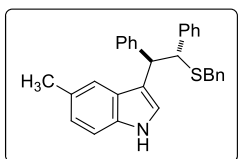
### 3-((1*R*,2*R*)-2-(methylthio)-1,2-diphenylethyl)-1*H*-indole (**2g**)

Followed method B from **1g** (19.4 mg, 0.25 mmol), for 45 h, and purified using silica gel chromatography to give 12.3 mg (72% yield) of **2g** as a colorless gel. This material was determined to be 84% ee by chiral HPLC analysis (ChiralPak AS-H, 10% *i*-PrOH, 1 mL/min, 220 nm,  $t_r(\text{major}) = 14$  min,  $t_r(\text{minor}) = 17$  min). IR (Film): 3419 (s), 3027, 2913, 1714, 1600, 1490, 1454 (s), 1420, 1337, 1276, 1098, 1012, 740 (s), 697 (s)  $\text{cm}^{-1}$ ;  $^1\text{H}$  NMR: (500 MHz,  $\text{CDCl}_3$ )  $\delta$  8.08 (br. s., 1H), 7.62 (d,  $J=8.2$  Hz, 1H), 7.39 (d,  $J=2.7$  Hz, 1H), 7.36 (d,  $J=7.8$  Hz, 1H), 7.33 - 7.25 (m, 2H), 7.25 - 7.05 (m, 9H), 7.04 - 6.94 (m, 1H), 4.72 (d,  $J=10.5$  Hz, 1H), 4.61 (d,  $J=10.1$  Hz, 1H);  $^{13}\text{C}$  NMR: (125 MHz,  $\text{CDCl}_3$ )  $\delta$  142.79, 140.89, 136.00, 128.85, 128.39, 127.97, 127.84, 127.33, 126.73, 125.92, 122.25, 122.00, 119.44, 119.30, 117.43, 111.11, 56.99, 49.50, 15.09; MS (ESI-APCI) exact mass calculated for  $[\text{M}-\text{SMe}]$  ( $\text{C}_{22}\text{H}_{18}\text{N}$ ) requires  $m/z$  296.1, found  $m/z$  296.1;  $[\alpha]_D^{24} = +39.7$  ( $c = 0.62$ ,  $\text{CH}_2\text{Cl}_2$ ).



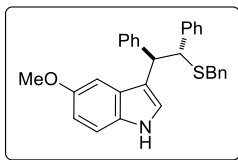
### 3-((1*R*,2*R*)-2-(tert-butylthio)-1,2-diphenylethyl)-1*H*-indole (**2h**)

Followed method B from **1h** (21.5 mg, 0.05 mmol), for 45 h, and purified using silica gel chromatography to give 17.2 mg (89% yield) of **2h** as a colorless gel. This material was determined to be 87% ee by chiral HPLC analysis (ChiralPak AD-H, 5% *i*-PrOH, 1 mL/min, 300 nm,  $t_r(\text{major}) = 9$  min,  $t_r(\text{minor}) = 10$  min). IR (Film): 3419 (s), 3026, 2960, 1600, 1491, 1455 (s), 1363, 1161, 1098, 909 (s), 738 (s), 697 (s)  $\text{cm}^{-1}$ ;  $^1\text{H}$  NMR: (500 MHz,  $\text{CDCl}_3$ )  $\delta$  8.03 (br. s., 1H), 7.44 (d,  $J=7.8$  Hz, 1H), 7.34 (d,  $J=8.2$  Hz, 1H), 7.31 (d,  $J=2.3$  Hz, 1H), 7.29 - 7.23 (m, 2H), 7.21 - 6.99 (m, 10H), 4.71 (d,  $J=7.8$  Hz, 1H), 4.66 (d,  $J=7.8$  Hz, 1H), 1.12 (s, 9H);  $^{13}\text{C}$  NMR: (125 MHz,  $\text{CDCl}_3$ )  $\delta$  143.68, 142.46, 135.91, 129.19, 129.05, 127.61, 127.50, 126.29, 125.97, 122.61, 121.81, 119.35, 119.25, 117.00, 110.92, 53.28, 50.49, 43.82, 31.32; MS (ESI-APCI) exact mass calculated for  $[\text{M}-\text{S}^t\text{Bu}]$  ( $\text{C}_{22}\text{H}_{18}\text{N}$ ) requires  $m/z$  296.1, found  $m/z$  296.1;  $[\alpha]_{\text{D}}^{25} = +2.9$  ( $c = 0.1$ ,  $\text{CH}_2\text{Cl}_2$ ).



### 3-((1*R*,2*R*)-2-(benzylthio)-1,2-diphenylethyl)-5-methyl-1*H*-indole (**2i**)

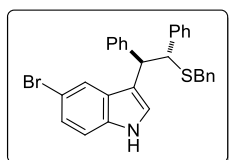
Followed method B from **1i** (23.2 mg, 0.05 mmol), for 40 h, and purified using silica gel chromatography to give 20.3 mg (97% yield) of **2i** as a colorless gel. This material was determined to be 91% ee by chiral HPLC analysis (ChiralPak AD-H, 10% *i*-PrOH, 1 mL/min, 230 nm,  $t_r(\text{major}) = 15$  min,  $t_r(\text{minor}) = 30$  min). IR (Film): 3422 (s), 3026, 2914, 1492, 1452, 1098, 1072, 1029, 909, 696 (s)  $\text{cm}^{-1}$ ;  $^1\text{H}$  NMR: (500 MHz,  $\text{CDCl}_3$ )  $\delta$  7.90 (br. s., 1H), 7.31 - 7.08 (m, 12H), 7.05 (d,  $J=2.3$  Hz, 1H), 7.02 - 6.86 (m, 5H), 4.61 (d,  $J=10.5$  Hz, 1H), 4.42 (d,  $J=10.1$  Hz, 1H), 3.42 (d,  $J=13.7$  Hz, 1H), 3.24 (d,  $J=13.7$  Hz, 1H), 2.38 (s, 3H);  $^{13}\text{C}$  NMR: (125 MHz,  $\text{CDCl}_3$ )  $\delta$  153.80, 142.61, 140.96, 138.43, 131.16, 129.19, 129.05, 128.40, 128.23, 127.93, 127.74, 126.81, 126.77, 125.90, 123.24, 116.80, 111.91, 111.61, 101.48, 55.80, 54.03, 49.47, 35.80; MS (ESI-APCI) exact mass calculated for  $[\text{M}-\text{SBn}]$  ( $\text{C}_{23}\text{H}_{20}\text{N}$ ) requires  $m/z$  310.2, found  $m/z$  310.1;  $[\alpha]_{\text{D}}^{23} = +137.7$  ( $c = 1.0$ ,  $\text{CH}_2\text{Cl}_2$ ).



### 3-((1*R*,2*R*)-2-(benzylthio)-1,2-diphenylethyl)-5-methoxy-1*H*-indole (**2j**)

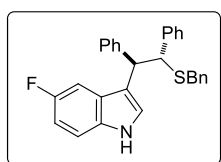
Followed method B from **1j** (23.2 mg, 0.05 mmol), for 40 h, and purified using silica gel chromatography to give 21.0 mg (93% yield) of **2j** as a colorless gel. This material was determined to be 93% ee by chiral HPLC analysis (ChiralPak AD-H, 15% *i*-PrOH, 1 mL/min, 230 nm,  $t_r(\text{major}) = 19$  min,  $t_r(\text{minor}) = 27$  min). IR (Film): 3421 (br), 3026, 2916, 1624, 1583, 1483, 1452 (s), 1208 (s), 1169, 1060,

1028, 929, 696 (s)  $\text{cm}^{-1}$ ;  $^1\text{H}$  NMR: (500 MHz,  $\text{CDCl}_3$ )  $\delta$  7.92 (br. s., 1H), 7.35 - 7.12 (m, 11H), 7.09 (d,  $J=2.4$  Hz, 1H), 7.06 - 7.00 (m, 4H), 6.98 (dd,  $J=3.9, 4.9$  Hz, 1H), 6.85 (d,  $J=2.4$  Hz, 1H), 6.81 (dd,  $J=2.4, 8.8$  Hz, 1H), 4.61 (d,  $J=10.3$  Hz, 1H), 4.44 (d,  $J=9.8$  Hz, 1H), 3.76 (s, 3H), 3.46 (d,  $J=13.7$  Hz, 1H), 3.28 (d,  $J=13.7$  Hz, 1H);  $^{13}\text{C}$  NMR: (125 MHz,  $\text{CDCl}_3$ )  $\delta$  153.80, 142.61, 140.96, 138.43, 131.16, 129.19, 129.05, 128.40, 128.23, 127.93, 127.74, 126.81, 126.77, 125.90, 123.24, 116.80, 111.91, 111.61, 101.48, 55.80, 54.03, 49.47, 35.80; MS (ESI-APCI) exact mass calculated for [M-SBn] ( $\text{C}_{23}\text{H}_{20}\text{NO}$ ) requires  $m/z$  326.2, found  $m/z$  326.1;  $[\alpha]_{\text{D}}^{24} = +155.4$  (c = 1.0,  $\text{CH}_2\text{Cl}_2$ ).



### 3-((1*R*,2*R*)-2-(benzylthio)-1,2-diphenylethyl)-5-bromo-1*H*-indole (**2k**)

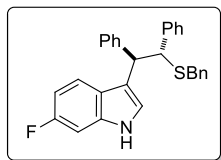
Followed method B from **1k** (22.3 mg, 0.05 mmol), for 45 h, and purified using silica gel chromatography to give 20.8 mg (83% yield) of **2k** as a colorless gel. This material was determined to be 92% ee by chiral HPLC analysis (ChiralPak AD-H, 10% *i*-PrOH, 1 mL/min, 230 nm,  $t_{\text{r}}$ (major) = 14 min,  $t_{\text{r}}$ (minor) = 19 min). IR (Film): 3426 (s) 3027, 1492, 1453 (s), 1100, 909 (s) 727 (s), 696 (s)  $\text{cm}^{-1}$ ;  $^1\text{H}$  NMR: (500 MHz,  $\text{CDCl}_3$ )  $\delta$  7.97 (br. s., 1H), 7.47 (d,  $J=1.8$  Hz, 1H), 7.24 - 7.00 (m, 14H), 6.98 - 6.83 (m, 4H), 4.48 (d,  $J=10.1$  Hz, 1H), 4.30 (d,  $J=10.1$  Hz, 1H), 3.36 (d,  $J=13.7$  Hz, 1H), 3.18 (d,  $J=13.7$  Hz, 1H);  $^{13}\text{C}$  NMR: (125 MHz,  $\text{CDCl}_3$ )  $\delta$  142.47, 140.94, 138.51, 134.84, 129.38, 129.27, 128.57, 128.53, 128.25, 128.12, 127.18, 127.13, 126.35, 125.12, 123.86, 122.16, 117.18, 113.06, 112.72, 111.33, 54.24, 49.66, 36.00; MS (ESI-APCI) exact mass calculated for [M-SBn] ( $\text{C}_{27}\text{H}_{17}\text{BrN}$ ) requires  $m/z$  374.1 and 376.1, found  $m/z$  374.0 and 376.1;  $[\alpha]_{\text{D}}^{25} = +96.4$  (c = 1.0,  $\text{CH}_2\text{Cl}_2$ ).



### 3-((1*R*,2*R*)-2-(benzylthio)-1,2-diphenylethyl)-5-fluoro-1*H*-indole (**2l**)

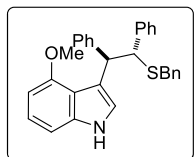
Followed method B from **1l** (23.2 mg, 0.05 mmol), for 45 h, and purified using silica gel chromatography to give 19.3 mg (88% yield) of **2l** as a colorless gel. This material was determined to be 95% ee by chiral SFC analysis (ChiralPak AD-H, 10% *i*-PrOH, 1 mL/min, 205 nm,  $t_{\text{r}}$ (major) = 21 min,  $t_{\text{r}}$ (minor) = 33 min). IR (Film): 3425 (br), 3027, 2919, 1628, 1581, 1484 (s), 1452 (s), 1242, 1162 (s), 1029, 939, 848, 796, 695 (s)  $\text{cm}^{-1}$ ;  $^1\text{H}$  NMR: (500 MHz,  $\text{CDCl}_3$ )  $\delta$  8.00 (br. s., 1H), 7.35 - 7.11 (m, 12H), 7.09 - 6.93 (m, 6H), 6.93 - 6.76 (m, 1H), 4.54 (d,  $J=10.1$  Hz, 1H), 4.40 (d,  $J=10.1$  Hz, 1H), 3.44 (d,  $J=13.7$  Hz, 1H), 3.26 (d,  $J=13.7$  Hz, 1H);  $^{13}\text{C}$  NMR: (125 MHz,  $\text{CDCl}_3$ )  $\delta$  157.54 (d,  $J=236.2$  Hz, 1C), 142.35, 140.77, 138.28, 132.51, 130.24, 129.13, 129.05, 128.28, 127.97, 127.82, 127.62, 126.89, 126.86, 126.03, 124.19, 117.27, 111.63, 111.55, 110.41,

110.20, 104.48, 104.30, 53.87, 49.61, 35.73; MS (ESI-APCI) exact mass calculated for [M-SBn] (C<sub>22</sub>H<sub>17</sub>FN) requires  $m/z$  314.1, found  $m/z$  314.1;  $[\alpha]_D^{23} = +103$  (c = 1.0, CH<sub>2</sub>Cl<sub>2</sub>).



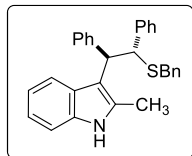
### 3-((1*R*,2*R*)-2-(benzylthio)-1,2-diphenylethyl)-6-fluoro-1*H*-indole (**2c**)

Followed method B from **11** (23.2 mg, 0.25 mmol), for 43 h, and purified using silica gel chromatography to give 20.2 mg (92% yield) of **12** as a colorless gel. This material was determined to be 85% ee by chiral HPLC analysis (ChiralPak AD-H, 10% *i*-PrOH, 1 mL/min, 230 nm,  $t_r$ (major) = 19 min,  $t_r$ (minor) = 36 min). IR (Film): 3425 (s), 3027, 2916, 1627, 1600, 1548, 1494 (s), 1453 (s), 1343, 1255, 1138, 909, 801, 697 (s) cm<sup>-1</sup>; <sup>1</sup>H NMR: (500 MHz, CDCl<sub>3</sub>)  $\delta$  7.98 (br. s., 1H), 7.39 - 7.24 (m, 4H), 7.24 - 7.11 (m, 7H), 7.11 - 6.93 (m, 7H), 6.84 - 6.71 (m, 1H), 4.60 (d,  $J=10.5$  Hz, 1H), 4.42 (d,  $J=10.1$  Hz, 1H), 3.46 (d,  $J=13.3$  Hz, 1H), 3.27 (d,  $J=13.3$  Hz, 1H); <sup>13</sup>C NMR: (125 MHz, CDCl<sub>3</sub>)  $\delta$  160.13 (d,  $J=236.2$  Hz, 1C), 142.70, 141.05, 138.60, 136.21, 136.12, 129.41, 129.35, 128.57, 128.53, 128.22, 128.06, 127.14, 127.09, 126.28, 124.08, 122.93, 122.90, 120.45, 120.37, 117.49, 108.51, 108.32, 97.65, 97.44, 54.21, 49.84, 36.01; MS (ESI-APCI) exact mass calculated for [M-SBn] (C<sub>22</sub>H<sub>17</sub>FN) requires  $m/z$  314.1, found  $m/z$  314.1;  $[\alpha]_D^{25} = +115$  (c = 1.0, CH<sub>2</sub>Cl<sub>2</sub>).



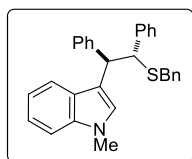
### 3-((1*R*,2*R*)-2-(benzylthio)-1,2-diphenylethyl)-4-methoxy-1*H*-indole (**2n**)

Followed method B from **1n** (23.2 mg, 0.05 mmol), for 43 h, and purified using silica gel chromatography to give 18.6 mg (83% yield) of **2n** as a colorless gel. This material was determined to be 91% ee by chiral HPLC analysis (ChiralPak AD-H, 10% *i*-PrOH, 1 mL/min, 230 nm,  $t_r$ (major) = 15 min,  $t_r$ (minor) = 19 min). IR (Film): 3422 (s), 3027, 2929, 1584, 1507, 1452, 1361, 1261 (s), 1091 (s) 1029, 732, 697 (s) cm<sup>-1</sup>; <sup>1</sup>H NMR: (500 MHz, CDCl<sub>3</sub>)  $\delta$  7.97 (br. s., 1H), 7.32 - 7.20 (m, 6H), 7.20 - 7.08 (m, 8H), 7.01 (s, 1H), 6.96 (s, 2H), 6.94 - 6.85 (m, 2H), 6.40 (d,  $J=7.9$  Hz, 1H), 3.77 (s, 2H), 3.44 (d,  $J=13.8$  Hz, 1H), 3.26 (d,  $J=13.8$  Hz, 1H); <sup>13</sup>C NMR: (125 MHz, CDCl<sub>3</sub>)  $\delta$  142.79, 140.89, 136.00, 128.85, 128.39, 127.97, 127.84, 127.33, 126.73, 125.92, 122.25, 122.01, 119.44, 119.30, 117.43, 111.11, 56.99, 49.50, 15.09; MS (ESI-APCI) exact mass calculated for [M-SBn] (C<sub>23</sub>H<sub>20</sub>NO) requires  $m/z$  326.2, found  $m/z$  326.1;  $[\alpha]_D^{25} = +162.8$  (c = 1.0, CH<sub>2</sub>Cl<sub>2</sub>).



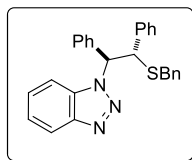
### 3-((1*R*,2*R*)-2-(benzylthio)-1,2-diphenylethyl)-2-methyl-1*H*-indole (**2c**)

Followed method B from **1o** (22.3 mg, 0.05 mmol), for 63 h, and purified using silica gel chromatography to give 20.5 mg (95% yield) of **2o** as a colorless gel. This material was determined to be 78% ee by chiral HPLC analysis (ChiralPak AD-H, 10% *i*-PrOH, 1 mL/min, 230 nm,  $t_r(\text{major}) = 12$  min,  $t_r(\text{minor}) = 17$  min). IR (Film): 3407 (br), 3026, 2972, 2921, 1492, 1453 (s), 1379, 1303, 1163, 950, 740, 697 (s)  $\text{cm}^{-1}$ ;  $^1\text{H}$  NMR: (500 MHz,  $\text{CDCl}_3$ )  $\delta$  7.74 (br. s., 1H), 7.44 (d,  $J=8.3$  Hz, 1H), 7.37 - 7.14 (m, 9H), 7.14 - 6.90 (m, 9H), 4.73 (d,  $J=10.7$  Hz, 1H), 4.54 (d,  $J=10.7$  Hz, 1H), 3.37 (d,  $J=13.7$  Hz, 1H), 3.18 (d,  $J=13.7$  Hz, 1H), 2.33 (s, 3H);  $^{13}\text{C}$  NMR: (125 MHz,  $\text{CDCl}_3$ )  $\delta$  142.94, 141.60, 138.12, 135.14, 132.05, 129.19, 129.12, 128.12, 128.11, 128.07, 127.91, 127.75, 126.84, 126.67, 125.65, 120.75, 119.86, 119.27, 112.23, 110.29, 53.06, 49.86, 35.41, 12.44; MS (ESI-APCI) exact mass calculated for [M-SBn] ( $\text{C}_{23}\text{H}_{20}\text{N}$ ) requires  $m/z$  310.2, found  $m/z$  310.1;  $[\alpha]_D^{25} = +57.5$  ( $c = 0.65$ ,  $\text{CH}_2\text{Cl}_2$ ).



### 3-((1*R*,2*R*)-2-(benzylthio)-1,2-diphenylethyl)-1-methyl-1*H*-indole (**2p**)

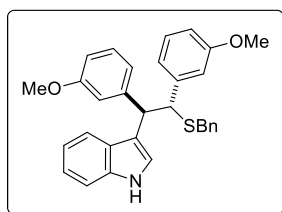
Followed method B from **1p** (23.2 mg, 0.05 mmol), for 45 h, and purified using silica gel chromatography to give 11.8 mg (54% yield) of **2p** as a colorless gel. This material was determined to be 3% ee by chiral HPLC analysis (ChiralPak OD-H, 5% *i*-PrOH, 1 mL/min, 220 nm,  $t_r(\text{major}) = 9$  min,  $t_r(\text{minor}) = 10$  min). IR (Film): 3062, 2915, 1599, 1491, 1452, 1373, 1329, 1154, 1071, 1029, 735 (s), 697 (s)  $\text{cm}^{-1}$ ;  $^1\text{H}$  NMR: (500 MHz,  $\text{CDCl}_3$ )  $\delta$  7.42 (d,  $J=7.8$  Hz, 1H), 7.36 - 7.12 (m, 12H), 7.06 - 6.92 (m, 6H), 6.87 (s, 1H), 4.62 (d,  $J=10.5$  Hz, 1H), 4.43 (d,  $J=10.5$  Hz, 1H), 3.74 (s, 3H), 3.45 (d,  $J=13.7$  Hz, 1H), 3.27 (d,  $J=13.7$  Hz, 1H);  $^{13}\text{C}$  NMR: (125 MHz,  $\text{CDCl}_3$ )  $\delta$  142.95, 141.12, 138.47, 136.77, 129.16, 128.33, 128.21, 127.88, 127.72, 127.68, 127.09, 126.75, 125.79, 121.36, 119.50, 118.77, 115.52, 109.08, 54.08, 49.54, 35.73, 32.78; MS (ESI-APCI) exact mass calculated for [M-SBn] ( $\text{C}_{23}\text{H}_{20}\text{N}$ ) requires  $m/z$  310.2, found  $m/z$  310.2.



### 1-((1*S*,2*S*)-2-(benzylthio)-1,2-diphenylethyl)-1*H*-benzo[*d*][1,2,3]triazole (**2q**)

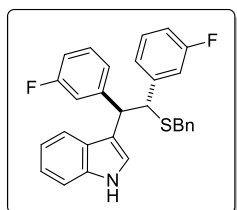
Followed method B from **1q** (22.3 mg, 0.05 mmol), for 63 h, and purified using silica gel chromatography to give 19.3 mg (92% yield) of **2q** as a colorless gel. This material was determined to be 80% ee by chiral HPLC analysis (ChiralPak AD-H, 15% *i*-PrOH, 1 mL/min, 230 nm,  $t_r(\text{major}) = 33$  min,  $t_r(\text{minor}) = 21$  min). IR (Film): 3029, 2923, 1492, 1452 (s), 1241, 1070, 910, 743, 723, 695 (s)  $\text{cm}^{-1}$ ;  $^1\text{H}$

NMR: (500 MHz, CDCl<sub>3</sub>)  $\delta$  8.11 (d,  $J=8.2$  Hz, 1H), 7.56 (d,  $J=8.2$  Hz, 1H), 7.49 (d,  $J=7.3$  Hz, 1H), 7.43 - 7.34 (m, 1H), 7.34 - 7.14 (m, 10H), 7.14 - 6.97 (m, 5H), 6.00 (d,  $J=11.4$  Hz, 1H), 5.21 (d,  $J=11.4$  Hz, 1H), 3.44 (d,  $J=13.3$  Hz, 1H), 3.36 (d,  $J=13.3$  Hz, 1H); <sup>13</sup>C NMR: (125 MHz, CDCl<sub>3</sub>)  $\delta$  145.78, 138.64, 137.04, 136.66, 133.50, 129.01, 128.76, 128.47, 128.33, 128.22, 127.99, 127.55, 127.33, 127.04, 123.91, 120.07, 109.50, 68.20, 54.06, 35.99; MS (ESI-APCI) exact mass calculated for [M+H] (C<sub>27</sub>H<sub>24</sub>N<sub>3</sub>S) requires  $m/z$  422.1, found  $m/z$  422.1;  $[\alpha]_D^{25} = +74.2$  (c = 0.6, CH<sub>2</sub>Cl<sub>2</sub>).



### 3-((1R,2R)-2-(benzylthio)-1,2-bis(3-methoxyphenyl)ethyl)-1H-indole (2r)

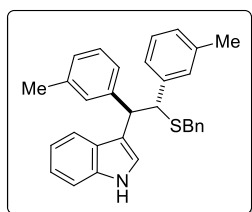
Followed method B from **1r** (26.2 mg, 0.05 mmol), for 40 h, and the yield of **2r** was determined by <sup>1</sup>H NMR to be 85%. This material was determined to be 93% ee by chiral HPLC analysis (ChiralPak AD-H, 15% *i*-PrOH, 1 mL/min, 230 nm,  $t_r$ (major) = 14 min,  $t_r$ (minor) = 33 min). IR (Film): 3374, 1724, 1693 (s), 1599 (s), 1489, 1455, 1264 (s), 1048, 910 (s), 738 (s) cm<sup>-1</sup>; <sup>1</sup>H NMR: (500 MHz, CDCl<sub>3</sub>)  $\delta$  8.03 (br. s., 1H), 7.43 (d,  $J=8.2$  Hz, 1H), 7.37 - 7.22 (m, 4H), 7.20 - 7.08 (m, 5H), 7.03 (t,  $J=7.3$  Hz, 1H), 6.95 (t,  $J=8.0$  Hz, 1H), 6.82 (d,  $J=7.3$  Hz, 1H), 6.79 - 6.74 (m, 1H), 6.74 - 6.68 (m, 1H), 6.65 (d,  $J=7.8$  Hz, 1H), 6.59 (d,  $J=1.8$  Hz, 1H), 6.56 - 6.50 (m, 1H), 4.62 (d,  $J=10.1$  Hz, 1H), 4.42 (d,  $J=10.1$  Hz, 1H), 3.71 (s, 2H), 3.61 (s, 2H), 3.46 (d,  $J=13.7$  Hz, 1H), 3.30 (d,  $J=13.7$  Hz, 1H); <sup>13</sup>C NMR: (125 MHz, CDCl<sub>3</sub>)  $\delta$  159.28, 144.23, 142.56, 138.39, 136.00, 129.09, 128.81, 128.64, 128.21, 127.26, 126.77, 122.47, 121.91, 121.77, 121.00, 119.44, 119.38, 116.94, 114.45, 114.42, 112.78, 111.24, 110.99, 55.16, 55.00, 54.03, 49.46, 35.82; MS (ESI-APCI) exact mass calculated for [M-SBn] (C<sub>24</sub>H<sub>22</sub>NO<sub>2</sub>) requires  $m/z$  356.2, found  $m/z$  356.2;  $[\alpha]_D^{24} = -6.7$  (c = 0.06, CH<sub>2</sub>Cl<sub>2</sub>).



### 3-((1R,2R)-2-(benzylthio)-1,2-bis(3-fluorophenyl)ethyl)-1H-indole (2s)

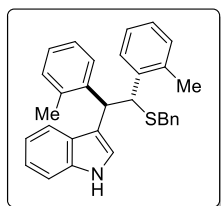
Followed method B from **1s** (25.0 mg, 0.05 mmol), for 45 h, and purified using silica gel chromatography to give 22.2 mg (97% yield) of **2s** as a colorless gel. This material was determined to be 95% ee by chiral HPLC analysis (ChiralPak AD-H, 10% *i*-PrOH, 1 mL/min, 230 nm,  $t_r$ (major) = 27 min,  $t_r$ (minor) = 45 min). IR (Film): 3419 (s), 3059, 2917, 1613, 1588 (s), 1487 (s), 1449 (s), 1249 (s), 1134, 909, 739 (s) cm<sup>-1</sup>; <sup>1</sup>H NMR: (500 MHz, CDCl<sub>3</sub>)  $\delta$  8.06 (br. s., 1H), 7.47 - 7.23 (m, 6H), 7.23 - 7.11 (m, 4H), 7.11 - 6.95 (m, 4H), 6.95 - 6.83 (m, 2H), 6.83 - 6.60 (m, 2H), 4.60 (d,  $J=10.3$  Hz, 1H), 4.37 (d,

$J=10.3$  Hz, 1H), 3.50 (d,  $J=13.7$  Hz, 1H), 3.28 (d,  $J=13.7$  Hz, 1H);  $^{13}\text{C}$  NMR: (125 MHz,  $\text{CDCl}_3$ )  $\delta$  162.70 (d,  $J=246.3$  Hz, 1C), 162.44 (d,  $J=245.3$  Hz, 1C), 144.98, 143.59, 143.53, 137.95, 135.99, 129.44, 129.37, 129.25, 129.19, 129.03, 128.36, 127.00, 124.89, 124.09, 122.39, 122.14, 119.57, 119.16, 116.12, 115.79, 115.61, 115.10, 114.94, 114.09, 113.92, 113.14, 112.98, 111.12, 106.77, 53.36, 49.27, 35.78; MS (ESI-APCI) exact mass calculated for [M-SBn] ( $\text{C}_{22}\text{H}_{16}\text{F}_2\text{N}$ ) requires  $m/z$  332.1, found  $m/z$  332.1;  $[\alpha]_{\text{D}}^{22} = +83.9$  ( $c = 1.0$ ,  $\text{CH}_2\text{Cl}_2$ ).



### 3-((1R,2R)-2-(benzylthio)-1,2-di-*m*-tolylethyl)-1H-indole (**2t**)

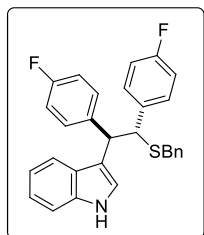
Followed method B from **1t** (24.6 mg, 0.05 mmol), for 45 h, and purified using silica gel chromatography to give 21.3 mg (95% yield) of **2t** as a colorless gel. This material was determined to be 93% ee by chiral HPLC analysis (ChiralPak AD-H, 10% *i*-PrOH, 1 mL/min, 230 nm,  $t_r(\text{major}) = 16$  min,  $t_r(\text{minor}) = 23$  min). IR (Film): 3420 (s), 3027, 2918, 1604, 1489, 1455, 1418, 1096, 909 (s), 738 (s)  $\text{cm}^{-1}$ ;  $^1\text{H}$  NMR: (500 MHz,  $\text{CDCl}_3$ )  $\delta$  7.98 (br. s., 1H), 7.42 (d,  $J=8.2$  Hz, 1H), 7.31 (d,  $J=7.8$  Hz, 1H), 7.30 - 7.21 (m, 3H), 7.16 - 7.10 (m, 3H), 7.09 - 6.98 (m, 4H), 6.94 (d,  $J=7.3$  Hz, 2H), 6.90 (t,  $J=7.3$  Hz, 1H), 6.84 (d,  $J=7.8$  Hz, 1H), 6.80 (s, 1H), 6.77 (d,  $J=7.3$  Hz, 1H), 4.61 (d,  $J=9.6$  Hz, 1H), 4.41 (d,  $J=9.6$  Hz, 1H), 3.42 (d,  $J=13.3$  Hz, 1H), 3.26 (d,  $J=13.7$  Hz, 1H), 2.26 (s, 3H), 2.12 (s, 2H);  $^{13}\text{C}$  NMR: (125 MHz,  $\text{CDCl}_3$ )  $\delta$  142.54, 140.86, 138.52, 137.32, 137.02, 135.98, 129.87, 129.33, 129.09, 128.19, 127.63, 127.50, 127.37, 126.70, 126.63, 126.35, 125.44, 122.47, 121.85, 119.52, 119.31, 117.29, 110.94, 54.07, 49.26, 35.83, 21.36, 21.32; MS (APCI) exact mass calculated for [M-SBn] ( $\text{C}_{24}\text{H}_{22}\text{N}$ ) requires  $m/z$  324.2, found  $m/z$  324.1;  $[\alpha]_{\text{D}}^{24} = +13.0$  ( $c = 0.1$ ,  $\text{CH}_2\text{Cl}_2$ ).



### 3-((1R,2R)-2-(benzylthio)-1,2-di-*o*-tolylethyl)-1H-indole (**2u**)

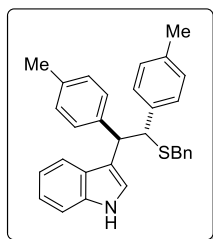
Followed method B from **1u** (24.6 mg, 0.05 mmol), for 40 h, and purified using silica gel chromatography to give 22.5 mg (>99% yield) of **2u** as a colorless gel. This material was determined to be 79% ee by chiral HPLC analysis (ChiralPak AD-H, 10% *i*-PrOH, 1 mL/min, 230 nm,  $t_r(\text{major}) = 8$  min,  $t_r(\text{minor}) = 12$  min). IR (Film): 3148 (s), 3059, 1600, 1489, 1455 (s), 1419, 1380, 1277, 1176, 1133, 1097, 1011, 737 (s)  $\text{cm}^{-1}$ ;  $^1\text{H}$  NMR: (500 MHz,  $\text{CDCl}_3$ )  $\delta$  8.04 (br. s., 1H), 7.75 - 7.56 (m, 2H), 7.44 (d,  $J=7.8$  Hz, 1H), 7.33 (d,  $J=8.3$  Hz, 1H), 7.26 - 7.03 (m, 9H), 7.02 - 6.97 (m, 3H), 6.95 - 6.78 (m, 2H), 5.07 (d,  $J=9.8$  Hz, 1H), 4.85 (d,  $J=9.8$  Hz, 1H), 3.22 (d,  $J=13.7$  Hz, 1H), 3.11 (d,  $J=13.2$  Hz, 1H), 2.17 (s, 3H), 1.92 (s, 3H);  $^{13}\text{C}$  NMR: (125 MHz,  $\text{CDCl}_3$ )  $\delta$  141.90, 139.52, 138.43, 136.13, 135.84, 135.43, 130.11, 128.99, 128.19,

127.83, 127.62, 127.13, 126.68, 126.52, 126.01, 125.76, 125.47, 123.44, 121.92, 119.71, 119.38, 117.51, 111.06, 49.74, 44.22, 36.29, 19.85, 19.27; MS (ESI-APCI) exact mass calculated for [M-SBn] (C<sub>23</sub>H<sub>23</sub>S) requires *m/z* 324.2, found *m/z* 324.2; [α]<sub>D</sub><sup>23</sup> = +129 (c = 1.0, CH<sub>2</sub>Cl<sub>2</sub>).



### 3-((1*R*,2*R*)-2-(benzylthio)-1,2-bis(4-fluorophenyl)ethyl)-1*H*-indole (**2v**)

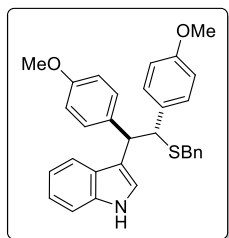
Followed method B from **1v** (25.0 mg, 0.05 mmol), for 47 h, and purified using silica gel chromatography to give 20.8 mg (91% yield) of **2v** as a colorless gel. This material was determined to be 45% ee by chiral HPLC analysis (ChiralPak AD-H, 10% *i*-PrOH, 1 mL/min, 230 nm, *t<sub>r</sub>*(major) = 18 min, *t<sub>r</sub>*(minor) = 26 min). IR (Film): 3418 (s), 3060, 2915, 1602, 1505 (s), 1455, 1417, 1218 (s), 1157, 1095, 908, 736 (s) cm<sup>-1</sup>; <sup>1</sup>H NMR: (500 MHz, CDCl<sub>3</sub>) δ 8.03 (br. s., 1H), 7.43 - 7.24 (m, 5H), 7.23 - 7.00 (m, 7H), 6.99 - 6.83 (m, 4H), 6.79 - 6.64 (m, 2H), 4.58 (d, *J*=10.1 Hz, 1H), 4.36 (d, *J*=10.1 Hz, 1H), 3.49 (d, *J*=13.7 Hz, 1H), 3.26 (d, *J*=13.7 Hz, 1H); <sup>13</sup>C NMR: (125 MHz, CDCl<sub>3</sub>) δ 161.59 (d, *J*=246.3 Hz, 1C), 161.09 (d, *J*=245.3 Hz, 1C), 138.15, 138.11, 136.44, 136.42, 136.03, 130.64, 130.58, 129.80, 129.74, 129.65, 129.01, 128.31, 126.99, 126.91, 122.35, 122.09, 119.50, 119.25, 116.63, 114.95, 114.78, 114.69, 114.53, 111.10, 53.24, 49.05, 35.75; MS (ESI-APCI) exact mass calculated for [M+H] (C<sub>29</sub>H<sub>23</sub>F<sub>2</sub>NS) requires *m/z* 456.2, found *m/z* 456.1; [α]<sub>D</sub><sup>25</sup> = +42.8 (c = 1.0, CH<sub>2</sub>Cl<sub>2</sub>).



### 3-((1*R*,2*R*)-2-(benzylthio)-1,2-di-*p*-tolylethyl)-1*H*-indole (**2w**)

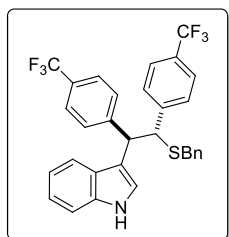
Followed method B from **1w** (24.6 mg, 0.05 mmol), for 47 h, and purified using silica gel chromatography to give 20.0 mg (89% yield) of **2w** as a colorless gel. This material was determined to be 60% ee by chiral HPLC analysis (ChiralPak AD-H, 10% *i*-PrOH, 1 mL/min, 230 nm, *t<sub>r</sub>*(major) = 12 min, *t<sub>r</sub>*(minor) = 26 min). IR (Film): 3420 (br), 3025, 2929, 1510, 1454, 1417, 1337, 1096, 907 (s), 731 (s) cm<sup>-1</sup>; <sup>1</sup>H NMR: (500 MHz, CDCl<sub>3</sub>) δ 7.94 (br. s., 1H), 7.45 (d, *J*=8.1 Hz, 1H), 7.37 - 7.22 (m, 4H), 7.20 - 7.08 (m, 5H), 7.08 - 6.99 (m, 4H), 6.93 (d, *J*=8.1 Hz, 2H), 6.84 (d, *J*=8.1 Hz, 2H), 4.64 (d, *J*=10.0 Hz, 1H), 4.45 (d, *J*=10.0 Hz, 1H), 3.42 (d, *J*=13.4 Hz, 1H), 3.25 (d, *J*=13.7 Hz, 1H), 2.31 (s, 3H), 2.16 (s, 3H); <sup>13</sup>C NMR: (125 MHz, CDCl<sub>3</sub>) δ 139.66, 138.51, 137.87, 136.20, 135.99, 135.18, 129.09, 129.06, 128.60, 128.43, 128.29, 128.18, 127.21, 126.67, 122.35, 121.79, 119.48, 119.27, 117.48, 110.96, 53.71, 48.99, 35.73, 21.10, 20.91; MS (ESI-APCI) exact mass calculated for [M-SBn] (C<sub>24</sub>H<sub>22</sub>N) requires *m/z* 324.2, found *m/z*

324.2;  $[\alpha]_D^{25} = +91.2$  ( $c = 1.0$ ,  $\text{CH}_2\text{Cl}_2$ ).



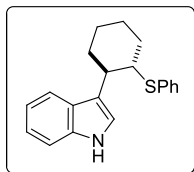
### 3-((1*R*,2*R*)-2-(benzylthio)-1,2-bis(4-methoxyphenyl)ethyl)-1*H*-indole (**2x**)

Followed method B from **1x** (26.2 mg, 0.05 mmol), for 40 h, and yield of **2x** was determined by  $^1\text{H}$  NMR to be 67%. This material was determined to be 6% ee by chiral HPLC analysis (ChiralPak AD-H, 15% *i*-PrOH, 1 mL/min, 230 nm,  $t_r(\text{major}) = 36$  min,  $t_r(\text{minor}) = 31$  min). IR (Film): 3373, 3030, 2836, 1723, 1694, 1609, 1583, 1509 (s), 1455, 1247 (s), 1175, 1107, 1032, 908, 833, 734 (s)  $\text{cm}^{-1}$ ;  $^1\text{H}$  NMR: (500 MHz,  $\text{CDCl}_3$ )  $\delta$  7.84 (br. s., 1H), 7.38 - 7.14 (m, 10H), 7.12 - 7.01 (m, 1H), 7.01 - 6.86 (m, 3H), 6.80 (d,  $J=8.8$  Hz, 2H), 6.76 (d,  $J=8.3$  Hz, 2H), 4.62 (d,  $J=9.3$  Hz, 1H), 4.45 (d,  $J=8.8$  Hz, 1H), 3.78 (s, 3H), 3.76 (s, 3H), 3.37 (d,  $J=13.2$  Hz, 1H), 3.27 (d,  $J=13.2$  Hz, 1H);  $^{13}\text{C}$  NMR: (125 MHz,  $\text{CDCl}_3$ )  $\delta$  158.24, 158.13, 138.30, 135.76, 134.17, 133.86, 129.95, 129.62, 129.40, 129.07, 128.21, 126.82, 126.73, 121.85, 121.71, 119.18, 119.09, 118.20, 113.43, 113.24, 110.80, 55.12, 53.30, 48.54, 35.65; MS (ESI-APCI) exact mass calculated for  $[\text{M}-\text{SBn}]$  ( $\text{C}_{24}\text{H}_{23}\text{NO}_2$ ) requires  $m/z$  356.2, found  $m/z$  356.1.



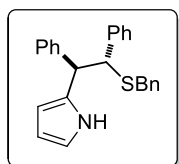
### 3-((1*R*,2*R*)-2-(benzylthio)-1,2-bis(4-(trifluoromethyl)phenyl)ethyl)-1*H*-indole (**2y**)

Followed method B from **1y** (30.0, 0.05 mmol), for 42 h, and purified using silica gel chromatography to give 5.1 mg (18% yield) of **2y** as a colorless gel. This material was determined to be 5% ee by chiral HPLC analysis (ChiralPak AD-H, 10% *i*-PrOH, 1 mL/min, 230 nm,  $t_r(\text{major}) = 12$  min,  $t_r(\text{minor}) = 14$  min). IR (Film): 3417, 2923, 1617, 1456, 1417, 1324 (s), 1164, 1120 (s), 1068, 1017, 742  $\text{cm}^{-1}$ ;  $^1\text{H}$  NMR: (500 MHz,  $\text{CDCl}_3$ )  $\delta$  8.08 (br. s., 1H), 7.45 (d,  $J=8.3$  Hz, 1H), 7.37 - 7.20 (m, 10H), 7.17 (ddd,  $J=1.0, 7.0, 8.2$  Hz, 1H), 7.13 - 7.05 (m, 5H), 7.02 (ddd,  $J=1.0, 6.8, 7.8$  Hz, 1H), 4.68 (d,  $J=9.8$  Hz, 1H), 4.44 (d,  $J=9.8$  Hz, 1H), 3.48 (d,  $J=13.7$  Hz, 1H), 3.23 (d,  $J=13.7$  Hz, 1H);  $^{13}\text{C}$  NMR: (125 MHz,  $\text{CDCl}_3$ )  $\delta$  146.16, 144.90, 137.67, 136.04, 129.38, 129.01, 128.58, 128.42, 127.12, 126.82, 125.35, 125.10, 124.96, 122.60, 122.33, 119.72, 119.07, 115.64, 111.23, 53.18, 49.29, 35.81 (the two  $\text{CF}_3$  groups not observed); MS (ESI-APCI) exact mass calculated for  $[\text{M}+\text{H}]$  ( $\text{C}_{31}\text{H}_{23}\text{F}_6\text{NS}$ ) requires  $m/z$  432.1, found  $m/z$  432.1.



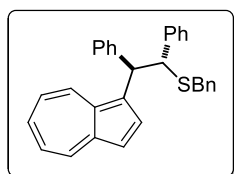
### 3-((1*R*,2*S*)-2-(benzylthio)cyclohexyl)-1*H*-indole (**2z**)

Followed method B from **1z** (17.6 mg, 0.05 mmol), for 26 h, and purified using silica gel chromatography to give 2.5 mg (16% yield) of **2z** as a white solid/gel. This material was determined to be 9% ee by chiral HPLC analysis (ChiralPak AS-H, 10% *i*-PrOH, 1 mL/min, 220 nm,  $t_r(\text{major}) = 10$  min,  $t_r(\text{minor}) = 11$  min). IR (Film): 3420 (br., s), 3056, 2928 (s), 2852, 1581, 1477, 1455, 1336, 1095, 910, 739 (s), 694  $\text{cm}^{-1}$ ;  $^1\text{H NMR}$ : (500 MHz,  $\text{CDCl}_3$ )  $\delta$  7.92 (br. s., 1H), 7.69 (d,  $J=7.8$  Hz, 1H), 7.34 (d,  $J=7.8$  Hz, 1H), 7.25 - 7.09 (m, 6H), 7.04 (d,  $J=2.4$  Hz, 2H), 3.50 (dt,  $J=3.4, 11.0$  Hz, 1H), 2.94 (dt,  $J=3.9, 11.2$  Hz, 1H), 2.38 - 2.16 (m, 1H), 2.16 - 2.02 (m, 1H), 1.92 - 1.68 (m, 3H), 1.60 - 1.36 (m, 3H);  $^{13}\text{C NMR}$ : (125 MHz,  $\text{CDCl}_3$ )  $\delta$  136.29, 135.17, 132.53, 128.38, 126.75, 126.43, 121.74, 121.14, 119.80, 119.37, 119.06, 111.25, 52.45, 41.30, 35.33, 34.66, 26.52, 26.27; MS (ESI-APCI) exact mass calculated for  $[\text{M}+\text{H}]$  ( $\text{C}_{20}\text{H}_{22}\text{NS}$ ) requires  $m/z$  308.2, found  $m/z$  308.1.



### 2-(benzylthio)-1,2-diphenylethyl)-1*H*-pyrrole

Followed method B from **1a** (22.3 mg, 0.05 mmol), for 46 h, and purified using silica gel chromatography to give 13.6 mg (67% yield) of the desired product and bis-alkylation products (7.6:1 favoring the desired product) as a colorless gel. The desired product was determined to be 9% ee by chiral HPLC analysis (ChiralPak AD-H, 5% *i*-PrOH, 1 mL/min, 230 nm,  $t_r(\text{major}) = 19$  min,  $t_r(\text{minor}) = 30$  min). The products resulting from bis-alkylation of pyrrole were a mixture of diastereomers and were not separable by HPLC. IR (Film): 3428 (br.), 3027, 2914, 1600, 1492, 1452 (s), 1174, 1095, 1072, 1029, 911, 696 (s)  $\text{cm}^{-1}$ ;  $^1\text{H NMR}$ : (500 MHz,  $\text{CDCl}_3$ )  $\delta$  8.25 (br. s., 1H), 7.38 - 7.21 (m, 4H), 7.20 - 6.97 (m, 11H), 6.69 (dd,  $J=2.9, 4.4$  Hz, 1H), 6.14 (dd,  $J=2.9, 5.9$  Hz, 1H), 6.00 (dd,  $J=2.9, 4.4$  Hz, 1H), 4.38 (d,  $J=9.3$  Hz, 1H), 4.24 (d,  $J=9.3$  Hz, 1H), 3.42 - 3.35 (m, 1H), 3.33 - 3.25 (m, 1H);  $^{13}\text{C NMR}$ : (125 MHz,  $\text{CDCl}_3$ )  $\delta$  141.33, 140.78, 137.91, 131.94, 129.06, 128.71, 128.34, 128.30, 128.03, 127.96, 126.93, 126.86, 126.36, 116.87, 108.16, 107.66, 54.24, 51.15, 36.04; MS (ESI-APCI) exact mass calculated for  $[\text{M}+\text{H}]$  ( $\text{C}_{25}\text{H}_{24}\text{NS}$ ) requires  $m/z$  370.2, found  $m/z$  370.2.



### 2-(azulen-1-yl)-1,2-diphenylethyl(benzyl)sulfane

Followed method B from **1a** (23.2 mg, 0.05 mmol), for 72 h, and purified using silica gel



# *Chapter Four*

## **Mechanistic Analyses of Thiourea-Catalyzed Episulfonium Ion Ring-Opening with Indoles: Evidence for an Enantioselectivity-Determining Cation– $\pi$ Interaction**

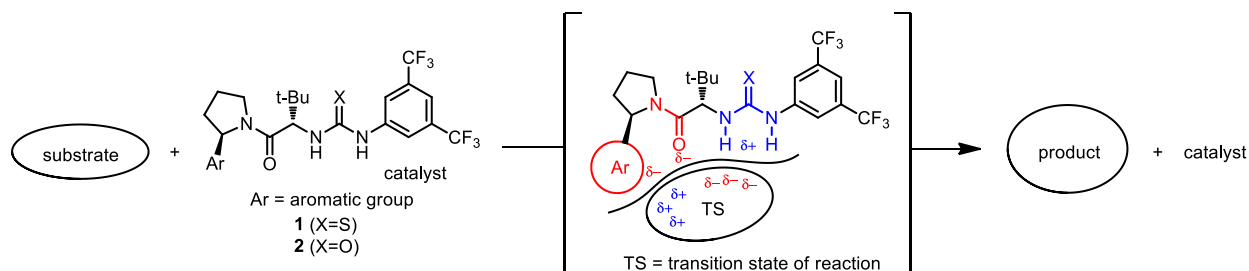
### **4.1 Introduction**

Catalysis by neutral, organic small molecules capable of binding and activating substrates solely via noncovalent interactions has emerged as an important approach in asymmetric organic synthesis.<sup>1</sup> Among catalysts adept at this type of activation, urea and thiourea derivatives bearing an arylpyrrolidino-amido group have recently been discovered as a “privileged catalyst” framework for asymmetric organic transformation involving polar intermediates and transition states (Schemes 4-1 & 4-2). Reactions promoted by this family of catalysts include nucleophilic

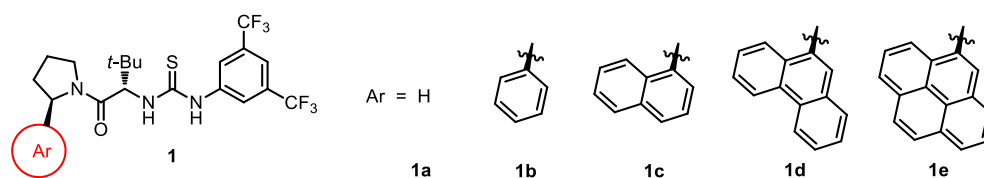
---

<sup>1</sup> For reviews, see: (a) Zhang, Z. G.; Schreiner, P. R. *Chem. Soc. Rev.* **2009**, 38, 1187–1198; (b) Knowles, R. R.; Jacobsen, E. N. *Proc. Natl. Acad. Sci. USA* **2010**, 107, 20678–20685. For an example, see: (c) Zuend, S. J.; Jacobsen, E. N. *J. Am. Chem. Soc.* **2009**, 131, 15358–15374.

additions to cationic electrophiles, such as oxocarbenium-based  $\alpha$ -chloroether alkylation,<sup>2</sup> *N*-acyliminium-initiated polycyclization<sup>3</sup> and *N*-acylpyridinium-mediated acyl transfer<sup>4</sup>, as well as pericyclic rearrangements, such as Cope-type hydroaminations<sup>5</sup>.



**Scheme 4-1.** Transition state stabilization in reaction catalyzed by thiourea **1**/urea **2**.



**Scheme 4-2.** A subset of arylpyrrolidine-derived thiourea **1** that will be discussed in this chapter.

In these reactions, the identity of the aromatic substituent on the arylpyrrolidine portion of the catalyst (Ar) was shown to have a pronounced effect on enantioselectivity, with larger Ar groups generally producing higher levels of enantioinduction. Given the polar nature of the selectivity-determining transition structures in these reactions, we advanced the notion that the  $\pi$ -electrons of the Ar group can interact with and stabilize the positive charge built up in the transition state. This hypothesis would explain the size effect of the catalyst on the reaction selectivity that we usually observe in these systems, as the physical properties predict that larger arenes are better  $\pi$ -donors through both electrostatic effects and dispersion forces. However, one cannot rule out

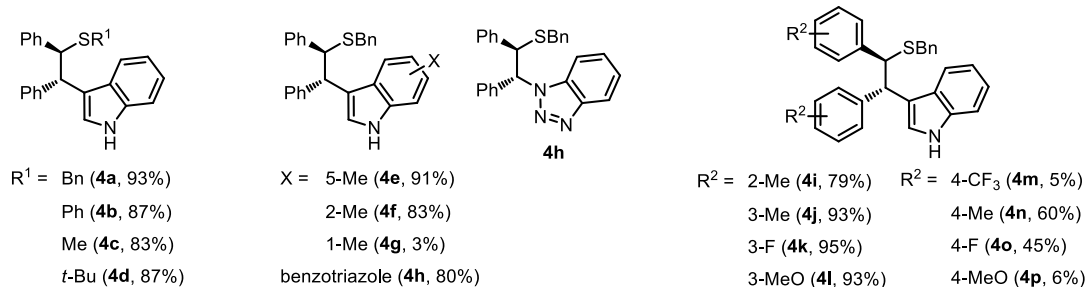
<sup>2</sup> Reisman, S. E.; Doyle, A. G.; Jacobsen, E. N. *J. Am. Chem. Soc.* **2008**, *130*, 7198–7199.

<sup>3</sup> Knowles, R. R.; Lin, S.; Jacobsen, E. N. *J. Am. Chem. Soc.* **2010**, *132*, 5030–5032.

<sup>4</sup> Birrell, J. A.; Desrosiers, J.-N.; Jacobsen, E. N. *J. Am. Chem. Soc.* **2011**, *133*, 13872–13875.

<sup>5</sup> Brown, A. R.; Uyeda, C.; Brotherton, C. A. *J. Am. Chem. Soc.* **2013**, *135*, 6747–6749.





**Scheme 4-4.** Representative substrate scope (compound numbers and ee values are in parentheses).

From a synthetic point of view, both of the reaction components: the episulfonium ion and the indole derivatives are very important classes of nucleophiles and electrophiles, respectively, in organic chemistry. Nucleophilic ring-opening of episulfonium ions has been a longstanding and efficient method for setting adjacent chirality in organic synthesis.<sup>7</sup> The intermediacy of a highly electrophilic episulfonium ion leads not only to good reactivity in the functionalization process, but also imparts stereospecificity, resulting in an overall retention of the relative stereochemistry. On the other hand, the indole framework has become widely identified as a “privileged” pharmacophore, being represented in over 3000 natural isolates and ca. 100 medicinal agents of diverse therapeutic actions.<sup>8</sup> Friedel–Crafts type alkylations of indole derivatives have been extensively utilized in the synthesis of these heterocyclic structures.<sup>9</sup>

We consider the enantioselective reaction between episulfonium ions and indoles as an appropriate platform to conduct a detailed mechanistic analysis primarily for the following reasons:

1) it will help elucidate how thiourea catalysts interact and activate episulfonium ions and indole

<sup>7</sup> For reviews, see: (a) Fox, D. J.; House, D.; Warren, S. *Angew. Chem. Int. Ed.* **2002**, *41*, 2462–2482; (b) Smit, W. A.; Caple, R.; Smoliakova, I. P. *Chem. Rev.* **1994**, *94*, 2359–2382.

<sup>8</sup> (a) Wu, Y. J. in *Heterocyclic Scaffolds II: Topics in Heterocyclic Chemistry* Vol. 26 (ed. Gribble, G. W.) 1–29 (Springer, 2011); (b) Kleeman, A. E. J.; Kutscher, B.; Reichert, D. *Fourth ed. Pharmaceutical Substances*; 2001.

<sup>9</sup> For a review, see: (a) Rueping, M.; Nachtsheim, B. J. *Beilstein J. Org. Chem.* **2010**, *6*, No. 6; For examples on asymmetric Friedel–Crafts indole alkylations, see: (b) Jensen, K. B.; Thorhauge, J.; Hazell, R. G.; Jørgensen, K. A. *Angew. Chem. Int. Ed.* **2001**, *40*, 160–163; (c) Evans, D. A.; Scheidt, K. A.; Fandrick, K.R.; Lam, H. W.; Wu, J. *J. Am. Chem. Soc.* **2003**, *125*, 10780–10781; (d) Jones, S. B.; Simmons, B.; Mastracchio, A.; MacMillan, D. W. C. *Nature* **2011**, *475*, 183–188.

nucleophiles in a synthetic context, stimulating new strategies for solving synthetically challenging problem involving these types of reactants;<sup>10</sup> 2) it may provide insights to the mechanism of previously developed reactions with the same family of catalysts; 3) it will aid in the understanding of fundamental mechanisms of activation and stereinduction by means of noncovalent interactions.

Here in this chapter, we provide an in-depth characterization of the enantioselective thiourea-catalyzed ring-opening of episulfonium ions with indole derivatives relying on experimental and computational methods. Through kinetic analyses, we found that thiourea **1** serves to catalyze multiple elemental steps along the reaction pathway with networks of noncovalent interactions. In addition, a series of catalyst structure-selectivity relationship studies in combination with computational transition-state modeling provide compelling evidence for a mechanism incorporating a cation- $\pi$  interaction as an integral feature of the origin of the enantioselectivity.

---

<sup>10</sup> Since the discovery and mechanistic analysis of the episulfonium ion ring-opening reaction, a few other reactions involving structurally analogous sulfonium ions and seleniranium ions, as well as tetrahydrocarbolines and tryptophols have been developed by other members of the Jacobsen group. Some of these systems will be reported shortly.

## 4.2 Kinetic Studies

In order to elucidate the role the thiourea plays in the mechanism of catalysis and stereoinduction, we initiated detailed kinetic studies to gain insights into the energy landscape of the episulfonium ring-opening reaction under conditions both in the presence and in the absence of the thiourea catalyst (referred to below as catalyzed and uncatalyzed reactions, respectively). To establish the stoichiometry of the rate-limiting transition structure, reaction progress kinetic analysis was carried out (Figures 4-1 and 4-2).<sup>11</sup> Rate studies were executed with representative substrate **3a** at synthetically relevant concentrations using in situ infrared (IR) spectroscopy. The kinetic experiments were conducted under homogeneous conditions at 0 °C, and under the catalyzed conditions, the product was typically generated with 80-85% enantiomeric excess.<sup>12</sup>

### 4.2.1 Kinetic Profile of the Uncatalyzed Reaction

The uncatalyzed reaction exhibits apparent zero-order kinetics in the first 60% conversion, followed by a positive order rate-decrease between 60% and full conversion (Figure 4-1A, filled circles). This uncommon kinetic scenario can be explained by the concentration variation of a reaction byproduct, trichloroacetamide (TCA) during the reaction course. By following the concentration of TCA as a function of time, we found that this compound accumulates and reaches super-saturation after ca. 55% conversion of **3a**, and suddenly decreases to its saturation concentration (0.030 M) also at ca. 60% conversion, and remains constant thereafter (Figure 4-1B, diamonds). The zero-order consumption of **3a** ends as soon as TCA precipitates from the solution, indicating TCA has an influence on the rate of the reaction. Indeed, by conducting the reaction in a medium that was pre-saturated with this byproduct ( $[TCA] = 0.03 \text{ M}$ ), we found that the initial

---

<sup>11</sup> Blackmond, D. G. *Angew. Chem. Int. Ed.* **2005**, *44*, 4302–4320.

<sup>12</sup> When the catalyst loading is smaller than 2 mol%, ee deterioration due to competing background reaction becomes significant.

rate at 10% conversion of **3a** is improved by a factor of 1.5; the reaction displays an overall first order kinetics (Figure 4-1A, diamonds). Under conditions when no initial concentration of TCA is present, the magnitude of the 1<sup>st</sup> order rate decay and that of the rate amplification arising from solution-phase TCA accumulation are coincidentally similar in the first 60% of the reaction, resulting in the apparent rate constant. In contrast to TCA, dimethylformamide (DMF), a structurally analogous molecule lacking the two acidic amide protons does not provide an appreciable rate acceleration effect under the same conditions. Taken together, it shows that H-bond donor molecules are capable of facilitating this transformation.<sup>13</sup>

Detailed reaction progress kinetic analysis (see ref. 11) yielded an empirical rate equation:

$$r_{\text{uncat,obs}} = k_{\text{uncat,obs}} [4\text{-NBSA}]_{\text{T}} [\text{indole}] \quad (1)$$

Here,  $r_{\text{uncat,obs}}$  is the observed rate of the uncatalyzed reaction,  $k_{\text{uncat,obs}}$  is the observed second order rate constant, and  $[4\text{-NBSA}]_{\text{T}}$  is the initial concentration of 4-NBSA.

The independence of reaction rate on substrate **3a** concentration (eq. 1) implies a quantitative reaction between **3a** and 4-nitrobenzenesulfonic acid (4-NBSA) through protonation prior to the rate-limiting step. This hypothesis is consistent with the large  $pK_{\text{a}}$  discrepancy between the two species ( $pK_{\text{a}}(4\text{-NBSA}) = -7$  vs.  $pK_{\text{a}}(\mathbf{3a}) = 2$ ).<sup>14</sup> The rate law also indicates the involvement of indole in the rate-determining step.

---

<sup>13</sup> As will be discussed later, this rate acceleration effect is likely due to facilitation of the ionization of the covalent resting state **9** (see Scheme 4-7) by stabilizing the developing negative charge on the sulfonate through H-bonding interactions.

<sup>14</sup> For  $pK_{\text{a}}$  of 4-NBSA, see: French, D. C.; Crumrine, D. S. *J. Org. Chem.* **1990**, *55*, 5494–5496. The  $pK_{\text{a}}$  of **3a** was calculated using ACD/labs: ACD/ $pK_{\text{a}}$ , version 12.01, Advanced Chemistry Development, Inc., Toronto, ON, Canada, www.acdlabs.com, 2013.

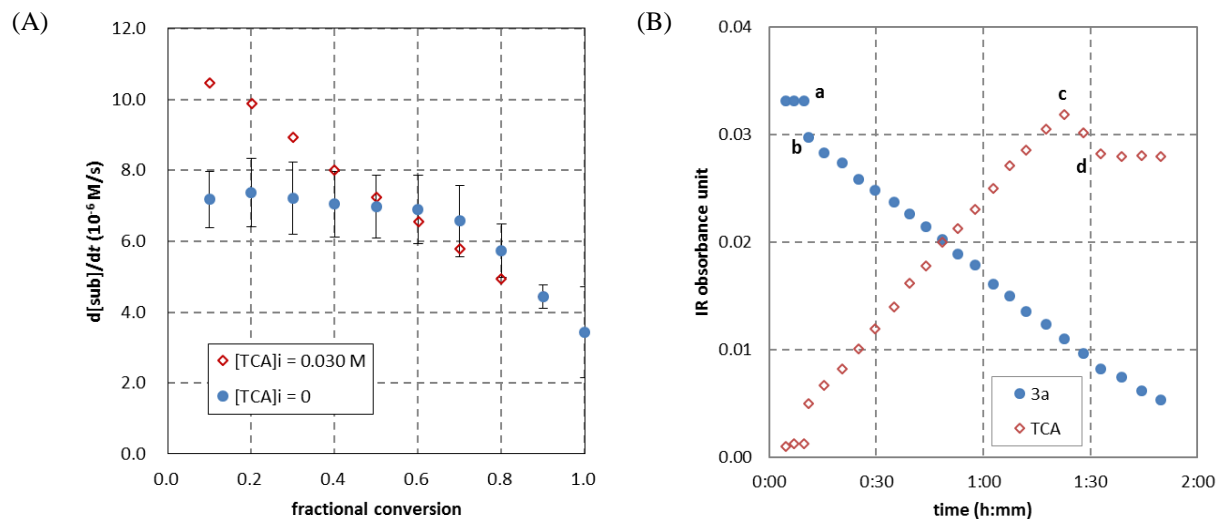
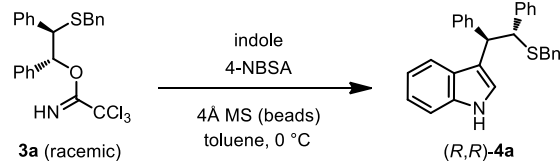


**Figure 4-1.** Representative kinetic data with *in situ* IR spectroscopy. Reaction conditions: **3a** (0.050 M), indole (0.10 M), 4-NBSA (0.0050 M), 4 Å molecular sieves (MS) (beads), TCA (0 or 0.030 M), toluene, at 0 °C. (A) Rate of the reaction as a function of conversion of **3a**. Error bars represent the standard deviation of data from four experimental run under identical conditions. (B) Reaction progress monitored by IR spectroscopy as the consumption of **3a** and the accumulation of TCA over reaction time. Data point (a) represents the initiation of the reaction by addition of 4-NBSA; (b) represents the instantaneous, quantitative protonolysis of **3a** by 4-NBSA; (c) represents the precipitation of TCA after reaching supersaturation in the reaction medium; and (d) represents the beginning of the regime when [TCA] remains constant.

#### 4.2.2 Kinetic Profile of the Thiourea-Catalyzed Reaction

Under conditions catalyzed by thiourea **1d**, the reaction displays first order dependence on **1d**, 4-NBSA and indole. TCA does not exhibit a beneficial effect on the kinetics of the catalyzed reaction; in contrast, this byproduct strongly dampens the reaction rate (Table 4-1). A number of other Lewis basic compounds were also found to be detrimental to the catalysis, including substrate **3a** and product **4a**. We reasoned that this rate deceleration presumably arises from binding and inhibition of thiourea by these Lewis basic molecules, since they do not deteriorate the rate of the uncatalyzed pathway.

**Table 4-1.** Catalyst deactivation by various reaction components and products.<sup>a</sup>

additive (concentration)	$r_{\text{rel}}$
none	1.00
<b>3a</b> (25 mM) <sup>b</sup>	0.78
<b>3a</b> (50 mM) <sup>c</sup>	0.52
<b>4a</b> (17 mM)	0.80
TCA (30 mM)	0.32

<sup>a</sup> Based on initial rates at 10% conversion of **3a**.  $r_{\text{rel}}$  is the initial rate of reaction relative to that under the standard reaction conditions. Standard reaction conditions: [**3a**]<sub>i</sub> = 0.050 M, [indole]<sub>i</sub> = 0.10 M, [4-NBSA] = 1.0 mM (2 mol%), [**1d**]<sub>T</sub> = 5.0 M (10 mol%), 4Å MS (beads), toluene, 0 ° C. <sup>b</sup> [**3a**]<sub>i</sub> = 0.075 M. <sup>c</sup> [**3a**]<sub>i</sub> = 0.10 M.

Although the initial rate is negatively correlated with the initial substrate concentration due to its catalyst-inhibition effect, we presume that, same as the uncatalyzed reaction, 4-NBSA also quantitatively reacts with **3a** under the thiourea-catalyzed conditions prior to the rate-determining step. Therefore, the concentration of **3a** does not show up as part of the numerator of the rate equation. All the information led to the following one-plus rate equation:

$$r_{\text{cat,obs}} = r_{\text{cat}} + r_{\text{uncat}} = \frac{a [\mathbf{1d}]_{\text{T}} [4\text{-NBSA}]_{\text{T}} [\text{indole}]}{1 + b [\mathbf{3a}] + c [\mathbf{4a}] + d [\text{TCA}]} + r_{\text{uncat}} \quad (2)$$

Here,  $r_{\text{cat,obs}}$  is the overall observed rate of the reaction involving **1d**,  $r_{\text{cat}}$  is the rate of the pathway catalyzed by **1d**, and  $r_{\text{uncat}}$  is the rate of the uncatalyzed background reaction. [**1d**]<sub>T</sub> and [4-NBSA]<sub>T</sub> are the initial concentrations of catalyst **1d** and 4-NBSA, respectively. Coefficient  $a$  represents the rate constant of the overall reaction, and  $b$ - $d$  represent the catalyst-binding affinity of **3a**, **4a**, and TCA, respectively.

Because of the kinetic complication introduced by substrate and product inhibition and byproduct (TCA) catalysis, we were not able to fit kinetic data to a single rate equation over the full course of the reaction. For the purpose of determining the stoichiometry of the rate-limiting transition structure, analysis using initial rates (at 10% conversion of **3a**) proved practical and informative. The rate of the uncatalyzed reaction is negligible compared to that of the catalyzed

reaction ( $r_{\text{uncat}} \ll r_{\text{cat}}$ , see the following discussion in this section). Therefore, the rate equation is simplified as (assuming  $[\mathbf{3a}] = [\mathbf{3a}]_i$ , which is the initial concentration of  $\mathbf{3a}$ ,  $[\mathbf{4a}] = [\text{TCA}] = 0$ ):

$$r_{\text{cat,obs}} = r_{\text{cat}} = k_{\text{cat,obs}} [\mathbf{1d}]_{\text{T}} [4\text{-NBSA}]_{\text{T}} [\text{indole}] \quad (3)$$

Here,  $k_{\text{cat,obs}}$  is the observed third order rate constant of reaction, and:

$$k_{\text{cat,obs}} = a/(1+b [\mathbf{3a}]_i) \quad (4)$$

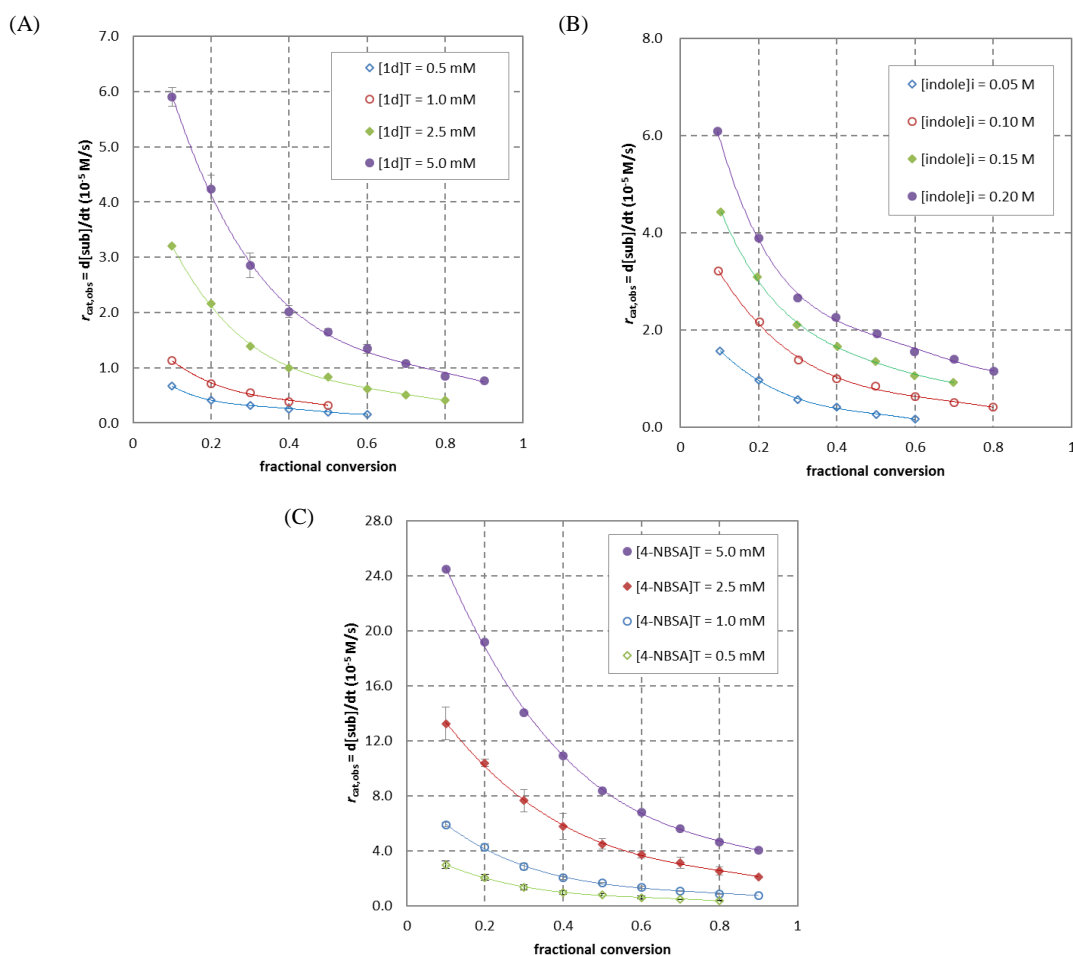
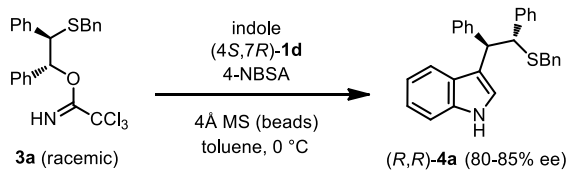


**Figure 4-2.** Reaction rate dependence on the concentration of **1d** (A), indole (B) and 4-NBSA (C). Error bars reflect the standard deviation of data from multiple parallel measurements. Solid lines represent polynomial fit of the data points. Conditions used for the kinetic studies:  $4\text{ \AA}$  MS (beads), toluene,  $0^\circ\text{C}$ , and (A)  $[\mathbf{3a}]_i = 0.050 \text{ M}$ ,  $[\text{indole}]_i = 0.10 \text{ M}$ ,  $[4\text{-NBSA}] = 1.0 \text{ mM}$  (2 mol%); (B)  $[\mathbf{3a}]_i = 0.050 \text{ M}$ ,  $[\mathbf{1d}]_{\text{T}} = 2.5 \text{ mM}$  (5 mol%),  $[4\text{-NBSA}] = 2.5 \text{ mM}$  (2 mol%); (C)  $[\mathbf{3a}]_i = 0.050 \text{ M}$ ,  $[\text{indole}]_i = 0.10 \text{ M}$ ,  $[\mathbf{1d}]_{\text{T}} = 5.0 \text{ mM}$  (10 mol%).

Based on these results (eqs. 1 and 3), we concluded that both the uncatalyzed and the thiourea-catalyzed pathways bear the same stoichiometry of reactants in the rate-limiting step. These transition states encompass one molecule of the episulfonium ion equivalent and one molecule of indole. In the catalyzed reaction, one molecule of thiourea **1d** is also involved. These conclusions are advanced assuming that the resting state of all the reaction components is monomeric, which is supported by evidence presented in Section 4.3.2.

### 4.2.3 Rate Acceleration Effect by Thiourea

In the presence of thiourea **1d**, the reaction rate is substantially increased. For instance, at 10 mol% catalyst loading, the  $r_{\text{cat,obs}}/r_{\text{uncat,obs}}$  at 10% conversion of **3a** is  $43.4 \pm 5.0$ . By application of the Eyring equation, this rate acceleration effect corresponds to a lowering of the free energy of activation of the reaction by **1d** of  $2.0 \pm 0.1$  kcal/mol.<sup>15</sup> The rate profile for catalyst **1d** was also compared to that of a simple, achiral thiourea, *N,N'*-bis[3,5-bis(trifluoromethyl)phenyl] thiourea (**5**). Although **5** is substantially more acidic than **1d**, making it a better H-bond donor, the rate acceleration effect it provided over the background is remarkably smaller ( $r_{\text{cat,obs}}/r_{\text{uncat,obs}} = 1.2$ ), suggesting that the functionalities on the arylpyrrolidino-amido moiety of **1d** may also play significant roles in lowering the activation barrier of the overall reaction.

---

<sup>15</sup> Based on the Eyring equation, the difference in free energy of activation between catalyzed and uncatalyzed reactions:  $\Delta(\Delta G^\ddagger) = -RT \ln(r_{\text{cat,obs}}/r_{\text{uncat,obs}})$ . Here,  $R$  is the gas constant and  $T$  is the reaction temperature (273 K).

### 4.3 Elemental Steps and Catalytic Cycle of the Reaction

#### 4.3.1 Quantitative and Irreversible Protonolysis of Precursor **3a**

As discussed previously, the initiation of the reaction includes a quantitative proton transfer from 4-NBSA to substrate **3a**. This hypothesis was further ascertained by *in situ* monitoring of the reaction between 4-NBSA and **3a** using IR spectroscopy. We observed an instantaneous, complete disappearance of **3a** signals upon addition of 1 equiv of 4-NBSA, with a concomitant, quantitative formation of TCA. This suggests that the formation of the episulfonium ion is both kinetically and thermodynamically favorable. To assess the reversibility of the episulfonium ion formation process, we conducted a racemization experiment using enantioenriched substrate. When **3a** in 51% enantiomeric excess was subjected to the conditions shown in Scheme 4-3, the remaining starting material isolated after ca. 20% conversion exhibited no erosion of enantiomeric excess both in the presence and the absence of thiourea **1d**.<sup>16</sup> This result is consistent with the extrusion of TCA leaving group being an irreversible process.

#### 4.3.2 Resting State of the Episulfonium Ion and the Catalyst

In the ground state, the product of protonolysis generated from **3a** can exist as either an ion pair or a covalent adduct with the sulfonate anion added back onto the episulfonium ion. To distinguish between these two possibilities, we synthesized an analog **7/8** (Scheme 4-5) by treating the corresponding  $\beta$ -chlorosulfide **6** with silver *p*-toluenesulfonate in CD<sub>2</sub>Cl<sub>2</sub>.<sup>17,18</sup> Through comparison with known compounds **3b**, **6** and **8'**, this experiment allowed us to obtain direct NMR

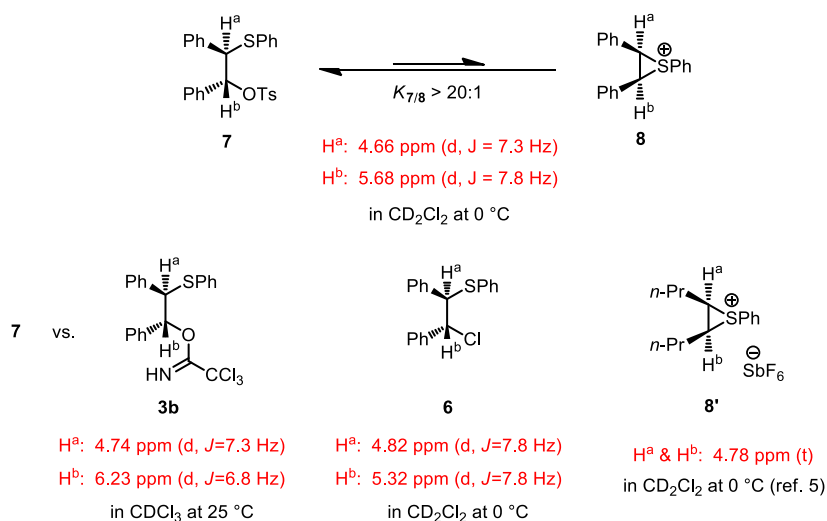
---

<sup>16</sup> Without thiourea, **3a** was isolated in 51% ee, with 10 mol% **1d**, **3a** was isolated in 50% ee.

<sup>17</sup> Denmark, S. E.; Collins, W. R.; Cullen, M. D. *J. Am. Chem. Soc.* **2009**, *131*, 3490–3492.

<sup>18</sup> Under the conditions in Scheme 4-3, TsOH instead of 4-NBSA furnishes **4a** in 94% yield and 89% ee.

evidence that the episulfonium *p*-toluenesulfonate exists predominantly as a covalent adduct **7**.<sup>19,20</sup> The ion pair species **8** remained undetectable by <sup>1</sup>H NMR upon the addition of 1 equiv of thiourea **1d**. We assume that the *p*-nitrobenzenesulfonate analog also exists as a covalent adduct under the reaction conditions, since the nucleofugality of the leaving groups are predicted to be very similar based on the *pK*<sub>a</sub> values of the conjugate acids (*pK*<sub>a,4-NBSA</sub> = -7.2, *pK*<sub>a,TsOH</sub> = -6.6).<sup>21</sup> This is also consistent with the observation that the reaction does not exhibit saturation kinetics even in the presence of a large excess of thiourea **1d** relative to 4-NBSA in the reaction mixture (Figure 4-2A, also see Figure 4-3A).



**Scheme 4-5.** NMR study of the ground state of the episulfonium *p*-toluenesulfonate.

In non-polar solvents such as toluene, thioureas of type **1** exists as mixtures of monomeric and self-aggregated dimeric complexes, a finding which is supported by NMR and calorimetry

<sup>19</sup> **8** was not observed by <sup>1</sup>H NMR.

<sup>20</sup> The reaction between **6** and AgOTs in *d*<sub>8</sub>-toluene instead of CH<sub>2</sub>Cl<sub>2</sub> only produces trace amount of **7** at room temperature after prolonged stirring. Since toluene has an even smaller dielectric constant (2.38 vs. 8.93 with CH<sub>2</sub>Cl<sub>2</sub>), it is reasonable to assume that in toluene, the ionization equilibrium is even more skewed to the side of **7**.

<sup>21</sup> Broeckaert, L.; Moens, J.; Roos, G.; De Proft, F.; Geerlings, F. *J. Phys. Chem. A* **2008**, *112*, 12164–12171.

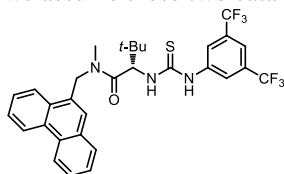
titration experiments.<sup>22, 23</sup> Despite the aggregated state of the catalyst, no evidence for diastereomeric interactions between multiple thiourea molecules was found in either the ground state or the transition state of the episulfonium ion ring-opening reaction, as the reactions conducted with scalemic mixtures of catalyst **1d'**, a structurally analogous thiourea to **1d** displayed a strictly linear dependence of product ee on catalyst ee and nearly identical conversions over the same reaction time (see experimental section).<sup>24,25</sup> The effect of catalyst inhibition by substrate **3a** in the kinetic studies suggests that the discrepancy between the resting states of the thiourea catalyst in the presence and absence of other reaction components can be simply explained by off-cycle thiourea-substrate association. From the kinetic data regarding the reaction rate dependence on the initial concentration of substrate **3a**, the binding constant between thiourea **1d** and **3a** was determined using eq. 4 to be  $2.0 \times 10^3 \text{ M}^{-1}$ . Based on this result, thiourea **1** is predicted to exist predominantly as a substrate-bound monomer (>95%) under the reaction conditions in the presence of a large excess of **3a** ( $[\mathbf{3a}]_i : [\mathbf{1}]_T = 10:1$ ).

The mode of catalyst-substrate association in the resting state was probed using NMR spectroscopy. Thiourea **1a** and **1b** were used because their <sup>1</sup>H NMR spectra are cleanly resolved in the  $\delta = 7\text{--}9$  ppm region where the thiourea N–H resonances reside. When **3a** and **1a/1b** were

<sup>22</sup> Ford, D. D.; Lehnher, D.; Jacobsen, E. N. *Manuscript in preparation*.

<sup>23</sup> Roetheli, A. R.; Appel, R.; Jacobsen, E. N. *Unpublished results*.

<sup>24</sup> **1d'** – an analog of **1d** was used due to easy access to both enantiomeric forms of the molecule. Under the same conditions in Scheme 4-3, enantiomerically pure **1d'** catalyzes the reaction with 85% ee (vs. 93% ee by **1d**). Therefore, we assume these two catalysts bear the same mechanism of stereoinduction. Structure of **1d'**:



<sup>25</sup> For reviews on non-linear effect studies, see: (a) Girard, C.; Kagan, H. B. *Angew. Chem. Int. Ed.* **1998**, *37*, 2922–2955; (b) Kagan, H. B. *Synlett* **2011**, 888–899; (c) Satyanarayana, T.; Abraham, S.; Kagan, H. B. *Angew. Chem. Int. Ed.* **2009**, *48*, 456–494.

mixed in a 3:1 ratio in  $d_8$ -toluene, a subtle but nevertheless significant spectroscopic response was identified: the chemical shifts of thiourea N–H protons and an aromatic proton on the 3,5-bis(trifluoromethyl)phenyl group moved downfield by about 0.01–0.10 ppm. This pattern of chemical shift change has been observed in the binding of structurally similar thioureas to neutral Lewis basic molecules.<sup>26</sup> Thus, the catalyst-substrate binding is presumably due to a dual hydrogen bonding donation of thiourea to an electron-rich functionality on **3a**, such as the imidate or the thioether.<sup>27</sup>

### 4.3.3 Identification of the Rate-Determining Step

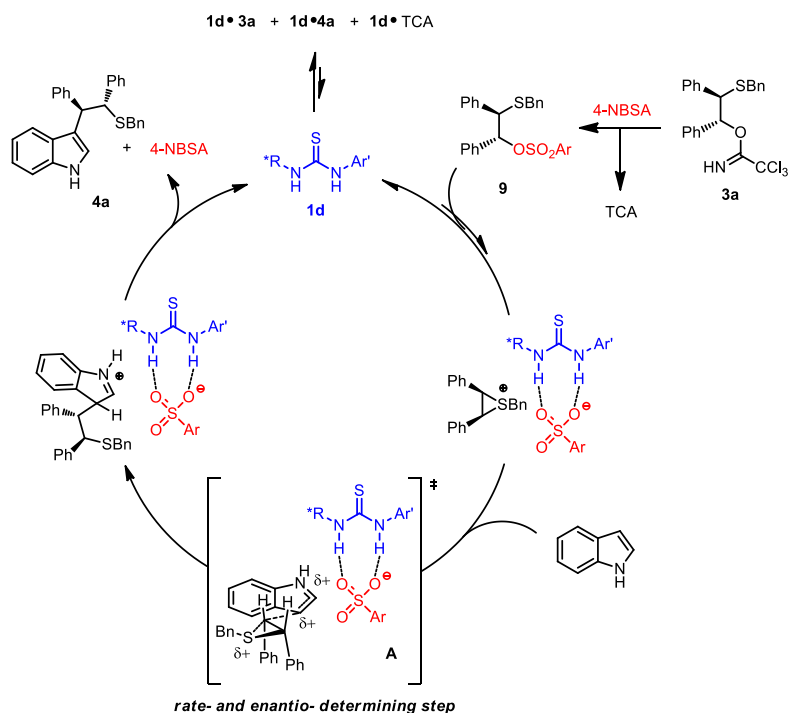
On the basis of the kinetic analyses detailed in the preceding sections as well as previous studies that involved thiourea-anion binding pathways, a detailed catalytic cycle for the reaction between indole and **3a** catalyzed by **1d** and 4-NBSA can be advanced (Scheme 4-6). The reaction is triggered by quantitative protonation of substrate **3a** with 4-NBSA to form covalent adduct **9** as the resting state of the electrophile. This species then undergoes ionization to generate episulfonium 4-nitrobenzenesulfonate prior to being captured by the indole nucleophile. Upon dissociation, **1d** participates in the recognition of the episulfonium ion pair through anion-binding, and remains associated with the reactive intermediate throughout the course of the nucleophilic ring-opening process. The resultant indolium species proceeds through C3 deprotonation to furnish the product and regenerate the catalyst. The resting state of the thiourea catalyst includes complexes with a few Lewis basic substances in the reaction medium. The first order reaction rate

---

<sup>26</sup> Lippert, K. M.; Hof, K.; Gerbig, D.; Ley, D.; Hausmann, D.; Guenther, S.; Schreiner, P. R. *Eur. J. Org. Chem.* **2012**, 5919–5927.

<sup>27</sup> For a reference describing thiourea-imine binding, see: (a) Vachal, P.; Jacobsen, E. N. *J. Am. Chem. Soc.* **2002**, *124*, 10012–10014; for studies on H-bond accepting ability of thioethers, see: (b) Spencer, J. N.; Harner, R. S.; Freed, L. I.; Penturelli, C. D. *J. Phys. Chem.* **1975**, *79*, 332–335; (c) Jolley, K. W.; Hughes, L. M.; Watson, I. D. *Aust. J. Chem.* **1974**, *27*, 287–290.

dependence on indole concentration is consistent with a reaction with indole that involves either slow addition or reversible addition followed by slow re-aromatization as the rate-determining step.



**Scheme 4-6.** Proposed catalytic cycle.

To distinguish between these two possibilities, studies of linear free-energy relationships and kinetic isotope effects were carried out. In the reaction catalyzed by 4-NBSA alone, a linear correlation was observed between the reaction rate and Mayr's nucleophilicity parameter  $N$  for five different 5-substituted indoles ( $\log(k_{\text{uncat,obs}})$  vs.  $s_N N$ ,  $R^2 = 0.997$ , where  $N$  is the Mayr nucleophilicity parameter,  $s_N$  is the nucleophile-specific parameter, and  $R^2$  is the correlation coefficient), consistent with an indole addition step that results in nucleophilic ring opening of the episulfonium ion being rate-limiting (see experimental section).<sup>28</sup> A correlation between indole nucleophilicity and rate was also obtained in the thiourea-catalyzed reaction ( $\log(k_{\text{cat,obs}})$  vs.  $s_N N$ ,  $R^2 = 0.757$ ). As discussed in Section 4.4.2, a strict linear correlation is not observed in this

<sup>28</sup> Phan, T. B.; Breugst, M.; Mayr, H. *Angew. Chem. Int. Ed.* **2006**, *45*, 3869–3874.

case because the Brønsted acidity of the indole N–H group also influences the reaction rate in the thiourea-catalyzed reaction. Evaluation of 3-deuterioindole in the thiourea-catalyzed addition reaction revealed a very small effect of isotopic substitution ( $k_H/k_D = 0.93 \pm 0.12$ ).<sup>29</sup> This rules out re-aromatization as the rate-determining step, which would be expected to display a significant primary isotope effect ( $k_H/k_D > 2.5$ ),<sup>30</sup> and is fully consistent with a rate-determining indole addition. It can also be concluded that indole addition is enantio-determining, because the stereogenic centers in the product are generated in this rate-determining step.<sup>31</sup>

---

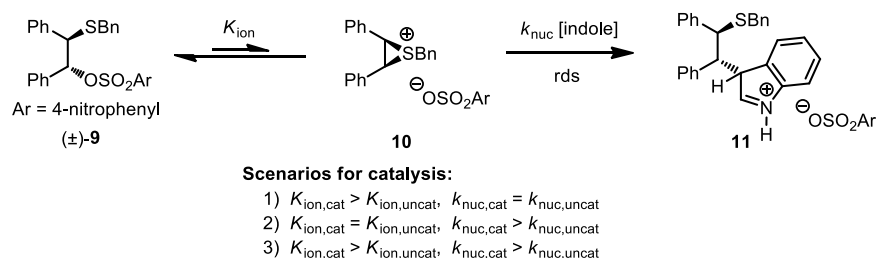
<sup>29</sup> This value represents the intermolecular KIE. The competition KIE cannot be obtained, because the indole C3 proton/deuteron can scramble under 4-NBSA catalysis.

<sup>30</sup> (a) Maresh, J. J.; Giddings, L. A.; Friedrich, A.; Loris, E. A.; Panjekar, S.; Trout, B. L.; Stöckigt, J.; Peters, B.; O'Connor, S. E. *J. Am. Chem. Soc.* **2008**, *130*, 710–723; (b) Klausen, R. S. Ph. D. dissertation, Harvard University, 2010.

<sup>31</sup> Bosnich, B. *Asymmetric Catalysis 14* (Marinus Nijhoff, 1986).

#### 4.4 Mechanism of Rate-Acceleration by Thiourea

Based on the catalytic cycle, a reaction scheme dissected into elementary steps was generated including only the processes that are relevant to catalysis (i.e. the formation and the nucleophilic ring-opening of the episulfonium intermediate) (Scheme 4-7). All the previous data are consistent with an endothermic pre-equilibrating ionization followed by a rate-limiting, irreversible nucleophilic trapping of the ion pair by indole. The irreversible conversion of **3a** to **9** and the post-rate-limiting deprotonation of **11** are therefore not investigated in our studies presented in this section.



**Scheme 4-7.** Elemental steps relevant to catalysis by thiourea **1d**.

Using a pre-equilibrium approximation, the rate equation of the reaction can be deduced as follows:

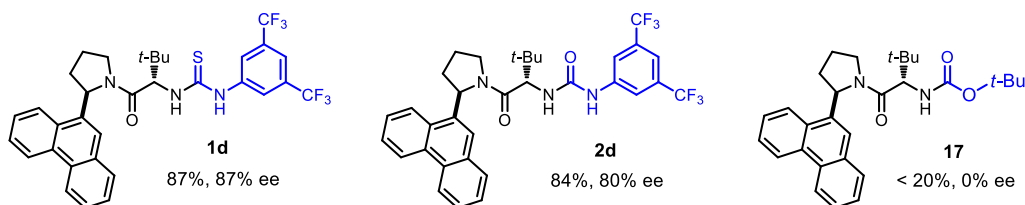
$$r = k_{\text{nuc}} K_{\text{ion}} [\mathbf{9}] [\text{indole}], \text{ in which } [\mathbf{9}] = [4\text{-NBSA}]_{\text{T}} \quad (4)$$

Here,  $k_{\text{nuc}}$  is the rate constant of the nucleophilic addition step, and  $K_{\text{ion}}$  is the equilibrium constant of the ionization process from **9** to **10**.

Given that the ground state association between the covalent  $\beta$ -sulfonylsulfide **9** and the thiourea is negligible (*vide supra*), the substantial rate acceleration effect suggested that thiourea **1d** must decrease the overall activation energy of the rate-determining transition state ( $\Delta G^\ddagger$ ). This rate acceleration effect can presumably be due to catalysis of only the ionization step (Scheme 4-7, scenario 1), or only the nucleophilic addition step (scenario 2), or both (scenario 3).

#### 4.4.1 Promotion of the Ionization Step

Anion-binding is recognized as the primary mode of substrate activation in a variety of asymmetric reactions that involve hydrogen-bond donors. In studies relevant to the system described here, sulfonate-ion associations with urea or thiourea derivatives via dual hydrogen-bond donation interactions were identified in both binding and reactivity studies.<sup>32</sup> The ability of thiourea and urea derivatives to bind sulfonate ions makes it possible that these catalysts can also facilitate the ionization of covalent adduct **9** through stabilizing the developing negative charge on the anionic leaving group. To probe the role of such an interaction in the mechanism of catalysis, we synthesized analogs of thiourea **1d** whose H-bonding ability is attenuated either by reduction of its acidity (**2d**) or by excision of one of the donor N–H groups (**17**) (Scheme 4-8).<sup>33</sup> In both cases, measurable or complete decreases in reactivity and enantioselectivity in the indole addition reaction were observed.<sup>34</sup> These data support that the thiourea–sulfonate H-bonding interaction is a key element in the mechanism of catalysis.



**Scheme 4-8.** Reactivity and selectivity dependence on the structure of the H-bond donor. Yields and ee's are shown for the generation of product **4b** under reaction conditions described in Scheme 4-3.

The structure of the arylpyrrolidine motif of thiourea **1** also exhibits a substantial effect on the reactivity of the episulfonium ring-opening (Table 4-2). Generally, catalysts with a more

<sup>32</sup> (a) Xu, H.; Zuend, S. J.; Woll, M. G.; Tao, Y.; Jacobsen, E. N. *Science* **2010**, 327, 986–990; (b) Kelly, T. R.; Kim, M. H. *J. Am. Chem. Soc.* **1994**, 116, 7072–7080.

<sup>33</sup>  $pK_a(\text{thiourea}) = 20$ ,  $pK_a(\text{urea}) = 27$  in DMSO. Data from: F. G. Bordwell, *Acc. Chem. Res.* **1988**, 21, 456–463.

<sup>34</sup> Although the urea derivative appears to be less selective, the difference from that of thiourea **1d** is relatively small, suggesting that the thiourea sulfur atom does not participate directly in the activation of reaction substrates/intermediates.

extended aromatic residue display higher levels of catalysis. Previous studies on catalysts with analogous structures have revealed that substituents rich in  $\pi$ -electrons can act in concert with H-bond donors to stabilize both poles of polar reaction transition states, leading to rate acceleration.<sup>3,35</sup> We reason that in the ionization of intermediate **9** *en route* to episulfonium sulfonate formation, as the anionic leaving group is being abstracted by thiourea, the accumulation of positive charge on the episulfonium unit can be alleviated by a cation- $\pi$  interaction<sup>36</sup> provided by a specifically positioned aryl group on the catalyst. The synergistic stabilization of the reactive intermediate through anion-binding and cation-binding by thiourea **1** increases the efficiency of catalysis, while also organizing the guest substrate to participate in the selective nucleophilic addition step.

**Table 4-2.** Reactivity and selectivity dependence on the structure of the arylpyrrolidine portion of the catalyst. Yields and ee's are shown for the generation of product **4a** under reaction conditions described in Scheme 4-3.

entry	catalyst <b>1</b>	yield (%)	ee (%)
1	<b>1a</b>	16	12
2	<b>1b</b>	72	73
3	<b>1c</b>	84	84
4	<b>1d</b>	93	93
5	<b>1e</b>	91	91

This hypothetical dual-activation mode of catalysis was evaluated in NMR model binding studies. Since episulfonium sulfonate **10** cannot be detected spectroscopically, we utilized dibenzylmethylsulfonium triflate **12**, a stable analog of **10** (Scheme 4-9) in these experiments together with thiourea of type **1**. This trialkylsulfonium ion bears similarity to the episulfonium ion in both structure and charge distribution. Salt **12** is nearly insoluble in *d*<sub>8</sub>-toluene, but it can be solubilized by thiourea **1d** via the formation of a 1:1 complex. Upon complexation, the

<sup>35</sup> Uyeda, C.; Jacobsen, E. N. *J. Am. Chem. Soc.* **2011**, *133*, 5062–5075.

<sup>36</sup> Ma, J.; Dougherty, D. A. *Chem. Rev.* **1997**, *97*, 1303–1324.

resonances of the benzylic and methyl protons underwent a significant upfield shift (0.6-0.8 ppm), and those of the thiourea N–H protons are sharpened and also shifted downfield (0.4 & 1.0 ppm). These types of variation patterns of chemical shift have been observed to associate with attractive interactions between aromatic groups and cationic complexes,<sup>37</sup> and between thiourea and anionic species,<sup>38</sup> respectively. The binding constant ( $K_{\text{assoc}}$ ) was determined by NMR titration experiments to be  $7.0 \times 10^5 \text{ M}^{-1}$ , indicating a strong association between the two species in a non-polar medium.<sup>39</sup> Interestingly, when the series of arylpyrrolidine-derived thiourea catalysts (**1a–d**) were subjected to the same binding assay, we observed an incremental change in the chemical shift of the benzylic and methyl protons (labeled in blue and green, respectively) as the aromatic residue on the catalyst increases in size. The binding constant also appears to improve accordingly. Because NMR dilution experiments are not suitable for accurate measurements of association constant ( $K_{\text{assoc}}$ ) greater than  $10^5$ , the quantitative comparison of the binding strength of **12** to different arylpyrrolidino thiourea catalysts were made using  $\text{CDCl}_3$  as the solvent. The  $K_{\text{assoc}}$  values were determined for **1b**:  $(1.16 \pm 0.16) \times 10^2 \text{ M}^{-1}$ , **1c**:  $(7.02 \pm 0.37) \times 10^2 \text{ M}^{-1}$ , and **1d**:  $(1.00 \pm 0.03) \times 10^3 \text{ M}^{-1}$ .<sup>40</sup> The cation– $\pi$  interaction is expected to increase in magnitude with more extended aromatic substituents.<sup>41</sup> Taken together, these data are consistent with the hypothesis

---

<sup>37</sup> Ngola, S. M.; Dougherty, D. A. *J. Org. Chem.* **1996**, *61*, 4355–4360.

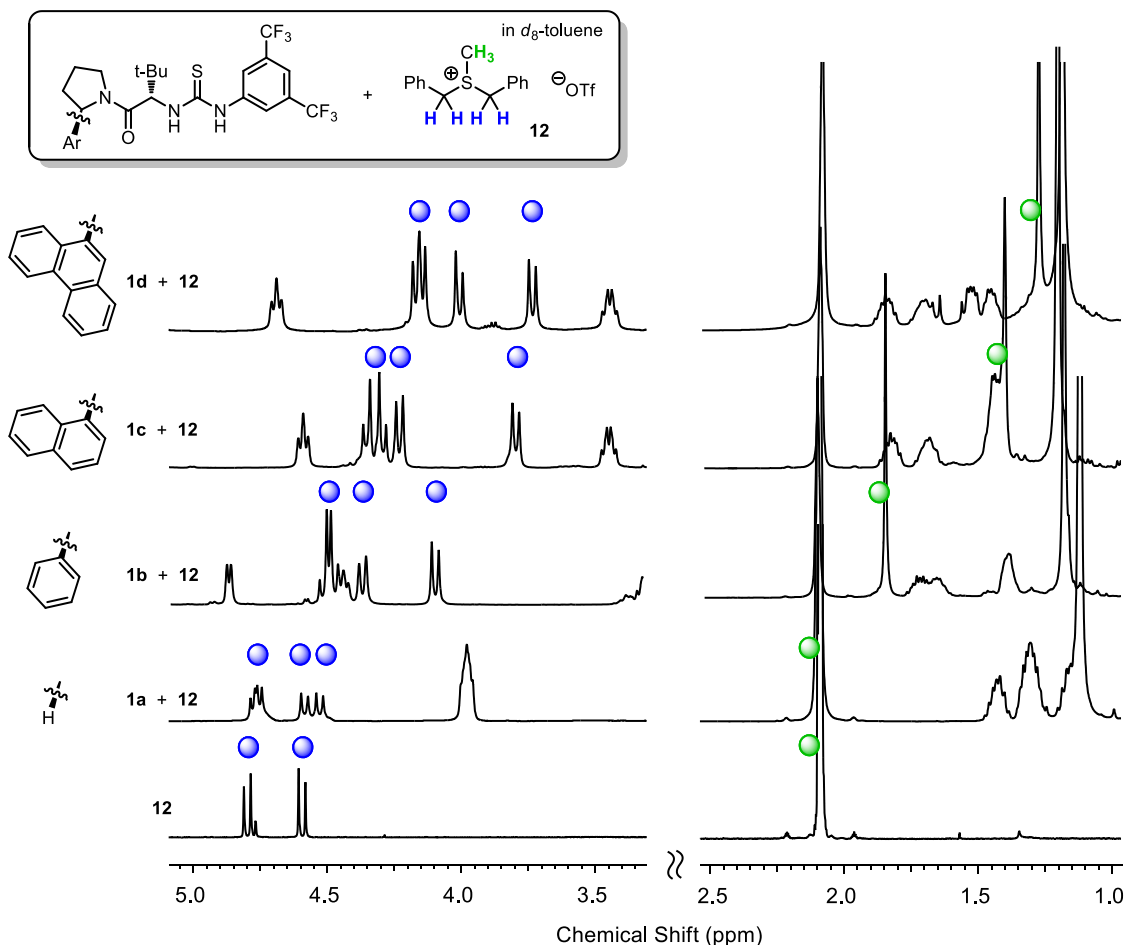
<sup>38</sup> (a) Lee, K. H.; Hong, J.-I. *Tetrahedron Lett.* **2000**, *41*, 6083–6087; (b) Ali, H. D. P.; Quinn, S. J.; McCabe, T.; Kruger, P. E.; Gunnlaugsson, T. *New J. Chem.* **2009**, *33*, 793–800.

<sup>39</sup> For an example of using NMR titration to determine binding strength via hydrogen bonding interactions in the context of molecular recognition, see: (a) Tresca, B. W.; Zakharov, L. N.; Carroll, C. N.; Johnson, D. W.; Haley, M. M. *Chem. Commun.* **2013**, *Advance Article*, DOI: 10.1039/C3CC44574G; for the method for data analysis, see: (b) the Sanderson group webpage: <http://www.dur.ac.uk/j.m.sanderson/science/downloads.html>.

<sup>40</sup> These binding constants are consistent with previously reported data on the association between thioureas and sulfonates. See: Wilcox, C. S.; Kim, E.; Romano, D.; Kuo, L. H.; Burt, A. L.; Curran, D. P. *Tetrahedron* **1995**, *51*, 621–634.

<sup>41</sup> (a) Vijay, D.; Sastry, G. N. *Phys. Chem. Chem. Phys.* **2008**, *10*, 582–590. (b) Gal, J.-F.; Maria, P.-C.; Decouzon, M.; M6, O.; Y6ñez, M.; Abboud, J. L. M. *J. Am. Chem. Soc.* **2003**, *125*, 10394–10401.

that thiourea is capable of binding to the sulfonium triflate through a cation– $\pi$  interaction in addition to anion-binding. We speculated that this type of ion-pair binding also exists in between thiourea **1** and the episulfonium sulfonate intermediate (**10**) of the episulfonium ring-opening reaction. According to the Hammond postulate, due to the endothermic nature of the sulfonate ionization process, the structure and charge distribution of the transition state of this step is similar to the ion pair intermediate **10**, and should also be bound to and stabilized by the thiourea catalyst presumably through the same combination of attractive interactions. Such a stabilization effect should lead to favorable perturbation of the equilibrium of the ionization step ( $K_{\text{ion,cat}} > K_{\text{ion,uncat}}$ ).



**Scheme 4-9.** Model binding studies between thiourea **1** and **12**. The complex between **1d** and **12** has a stoichiometry of 1:1.02. The resonances of the benzylic protons and the methyl protons in **12** are labelled with blue and green dots, respectively. In the bottom two spectra, the methyl resonance overlaps with the solvent peak, but can be identified in expanded displays.

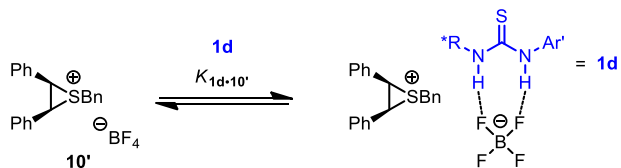
#### 4.4.2 Facilitation of the Nucleophilic Addition Step

To probe the effect thiourea **1** has in the nucleophilic addition of indole to the episulfonium ion, we designed a set of control experiments. We envisioned that if we could devise an episulfonium intermediate that exist as an ion pair (structure analogous to **10**) in the resting state, the ionization would not be relevant to catalysis, and the observed overall rate of reaction would reflect only the rate of the nucleophilic addition step. By varying the Brønsted acid co-catalyst, we found that under the same conditions used in previous kinetic studies (see Figure 4-2), tetrafluoroboric acid (HBF<sub>4</sub>) instead of 4-NBSA can also promote the reaction together with **1d**, with product **4a** formed in 74% ee (vs. 85% ee with 4-NBSA and **1d**). It is therefore reasonable to assume that the reactions promoted by these two acids possess the same general mechanism in the enantio-determining nucleophilic addition step. In contrast to the neutral, covalent ground state of episulfonium 4-nitrobenzenesulfonate, the resting state of the corresponding tetrafluoroborate complex **10'** is presumably an ion pair due to the non-coordinating nature of the anion.<sup>42</sup> In agreement with this statement, the rate of the HBF<sub>4</sub>-catalyzed reaction shows saturation kinetics when a large excess of thiourea is used relative to the acid, opposing to the strict first-order rate dependence on thiourea concentration in the case with 4-NBSA (Figure 4-3B vs. Figure 4-3A). The Michalis-Menten type kinetic behavior of the HBF<sub>4</sub>-promoted reaction indicates that there is a substantial binding phenomenon in the ground state between episulfonium tetrafluoroborate **10'** and thiourea **1d** (Scheme 4-10); when the ratio between **1d** and HBF<sub>4</sub> is equal to or larger than 10:1, the rate of the reaction becomes essentially independent of the thiourea loading, revealing that the ion pair electrophile is saturated by **1d** in the ground state under these

---

<sup>42</sup> The ion pair ground state is also supported by DFT calculations, which shows that a covalent adduct between BF<sub>4</sub><sup>-</sup> and the episulfonium ion does not exist.

conditions. The binding constant between **1d** and **10'** ( $K_{1d\cdot 10'}$ ) can be deduced from the rate data to be  $(7.9 \pm 4.6) \times 10^2 \text{ M}^{-1}$ ,<sup>43</sup> in agreement with calorimetry measurements.<sup>44</sup> The kinetic analysis with  $\text{HBF}_4$  under thiourea-catalysis was conducted with 10 mol% of **1d** when the regime of saturation kinetics was reached, in which the resting state of the episulfonium ion is a  $\text{BF}_4^-$  ion pair bound to thiourea.



**Scheme 4-10.** Binding between the episulfonium tetrafluoroborate **10'** and thiourea **1d**.

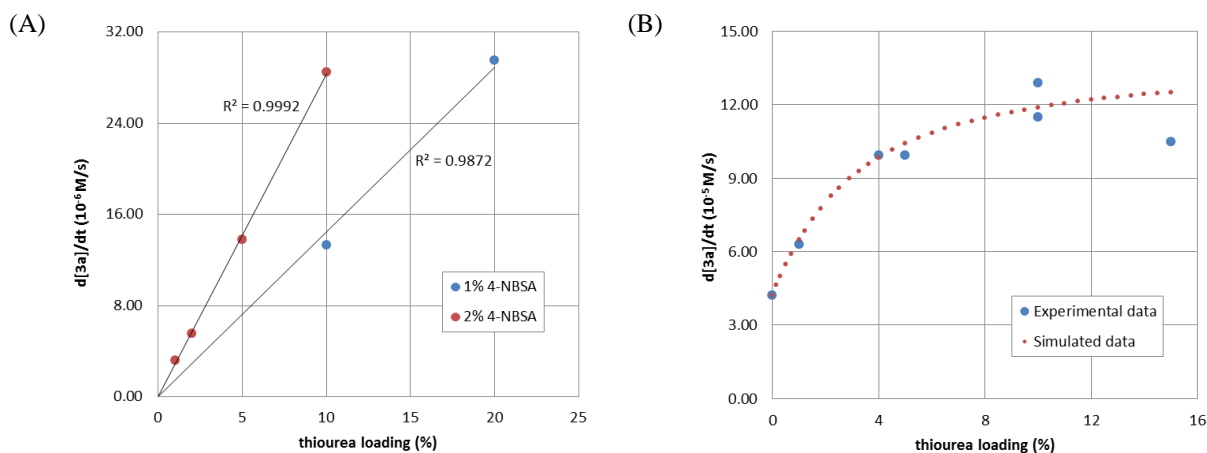


**Figure 4-3.** Reaction rate dependence on the loading of **1d** with (A) 1 or 2 mol% 4-NBSA (initial rates at 10% conversion) or (B) 1 mol%  $\text{HBF}_4$  (initial rates at 30% conversion). In (A) the solid black lines represent linear fit; with 1% 4-NBSA, the line is forced to go through point (0,0) due to the small size of the sample set. In (B), the dotted line in red represents the simulated data using the calculated binding constant ( $K_{1d\cdot 10'}$ ) and maximum reaction rate at saturation kinetics ( $r_{\text{cat,max}}$ ).

As previously discussed, the ion-pair resting state of episulfonium tetrafluoroborate made it possible for us to evaluate the catalytic effect of the thiourea on the nucleophilic addition step

<sup>43</sup> The deduction of the binding constant  $K_{1d\cdot 10'}$  is relied on the following equations: (1)  $r_{\text{asym}} = r_{\text{rac}} + r_{\text{cat}} = r_{\text{rac,max}} \times [\mathbf{10}'] / [\mathbf{10}']_{\text{T}} + r_{\text{cat,max}} \times [\mathbf{1d}\cdot\mathbf{10}'] / [\mathbf{10}']_{\text{T}}$ ;  $K_{1d\cdot 10'} = [\mathbf{1d}\cdot\mathbf{10}'] / ([\mathbf{10}'] [\mathbf{1d}])$ ;  $[\mathbf{10}']_{\text{T}} = [\mathbf{1d}\cdot\mathbf{10}'] + [\mathbf{10}']$ ; and  $[\mathbf{1d}]_{\text{T}} = [\mathbf{1d}\cdot\mathbf{10}'] + [\mathbf{1d}]$ . Here,  $r_{\text{rac,max}}$  is the rate of the reaction in the absence of **1d** ( $4.22 \times 10^{-5} \text{ M/s}$ ), and  $r_{\text{cat,max}}$  is the rate of the reaction under saturation kinetics regime, which is also deduced from the above equations to be  $1.4 \times 10^{-5} \text{ M/s}$ .

<sup>44</sup> Binding constant of thiourea **5** and  $(\text{NBu}_4)^+(\text{BF}_4)^-$  is  $7.4 \times 10^2 \text{ M}^{-1}$  in DCM at 23 °C by calorimetry titration.

directly. From rate data obtained in these experiments, we found that the reaction with  $\text{HBF}_4$  is also promoted by thiourea **1d**, albeit to a substantially lesser extent ( $r_{\text{cat,obs}}/r_{\text{uncat,obs}} = 4.9$ , vs. 43.5 with 4-NBSA) (Figure 4-4).<sup>45</sup> This result is clearly in agreement with thiourea **1d** being capable of catalyzing the nucleophilic addition of indole to the ionized episulfonium electrophile ( $k_{\text{nuc,cat}} > k_{\text{nuc,uncat}}$ ). Although the mechanism of the reactions with 4-NBSA and  $\text{HBF}_4$  may be slightly different due to the different thiourea-affinity of the counteranions, the pronounced rate acceleration effect by thiourea with 4-NBSA with respect to  $\text{HBF}_4$  suggests that the thiourea also catalyzes the ionization step in the case with 4-NBSA, presumably by means of sulfonate-abstraction. This finding is in agreement with our discussion in the preceding section.

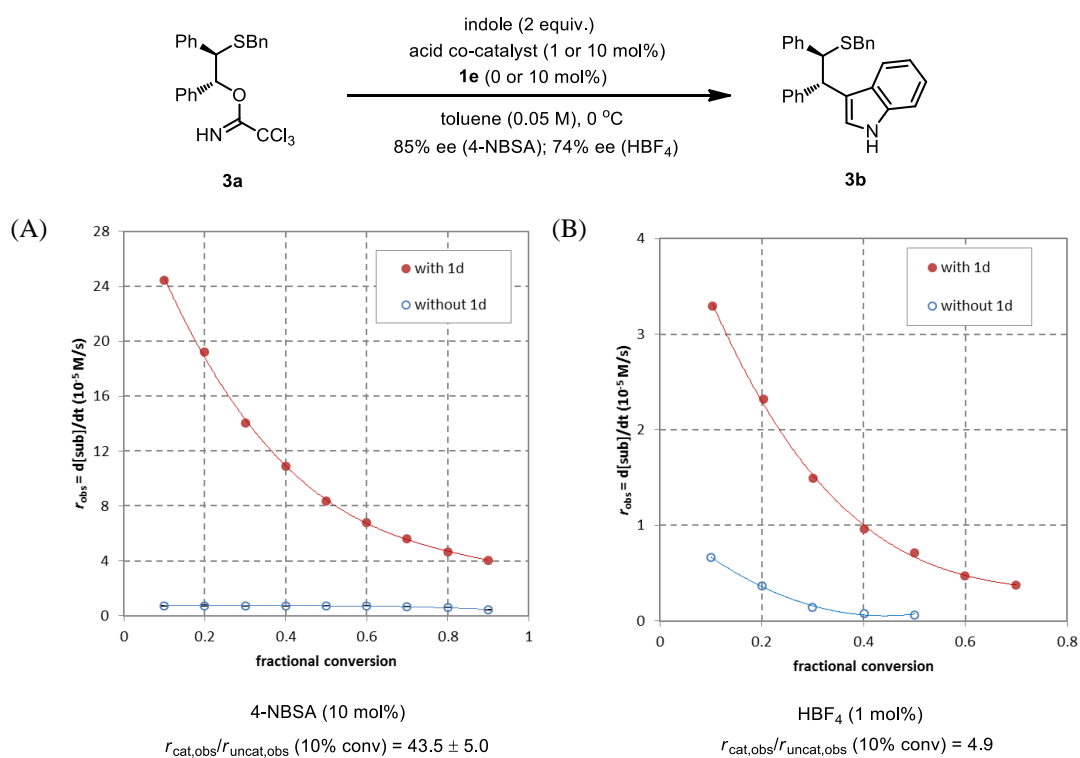


**Figure 4-4.** Control experiment I: 4-NBSA (A) vs.  $\text{HBF}_4$  (B). Solid trendlines represent polynomial fit of the data points. Conditions: 4 Å MS, toluene, 0 ° C, and (A)  $[\mathbf{3a}]_i = 0.050 \text{ M}$ ,  $[\text{indole}]_i = 0.10 \text{ M}$ ,  $[\mathbf{1d}] = 5.0 \text{ mM}$ ,  $[\text{4-NBSA}] = 5.0 \text{ mM}$  (10 mol%); (B)  $[\mathbf{3a}]_i = 0.050 \text{ M}$ ,  $[\text{indole}]_i = 0.10 \text{ M}$ ,  $[\mathbf{1d}] = 5.0 \text{ mM}$ ,  $[\text{HBF}_4] = 0.50 \text{ mM}$  (1 mol%).

<sup>45</sup> Initial rate data were measured at 10% conversion of **3a**.

The mechanism through which thiourea **1d** induces rate acceleration in the nucleophilic addition step was defined by comparing the kinetic behavior of indole with its structural analogs. When *N*-methylindole was used as the nucleophile, the rate of the **1d**-catalyzed reaction is substantially decreased compared to that with indole, regardless of the identity of the acid co-catalyst (Figure 4-5).<sup>46</sup> More generally, among a series  $\pi$ -nucleophiles we examined, the absence of an N–H motif in a (1,3)-relationship with the reactive nucleophilic site led to very low levels of rate acceleration and enantioselectivity (Figure 4-6A, entries 1 and 2 vs. entries 3–5). These data revealed an eminent role of the acidic indole N–H unit in the catalysis of the rate- and ee-determining nucleophilic addition, presumably achieved through hydrogen-bonding with a Lewis basic functionality on the catalyst.

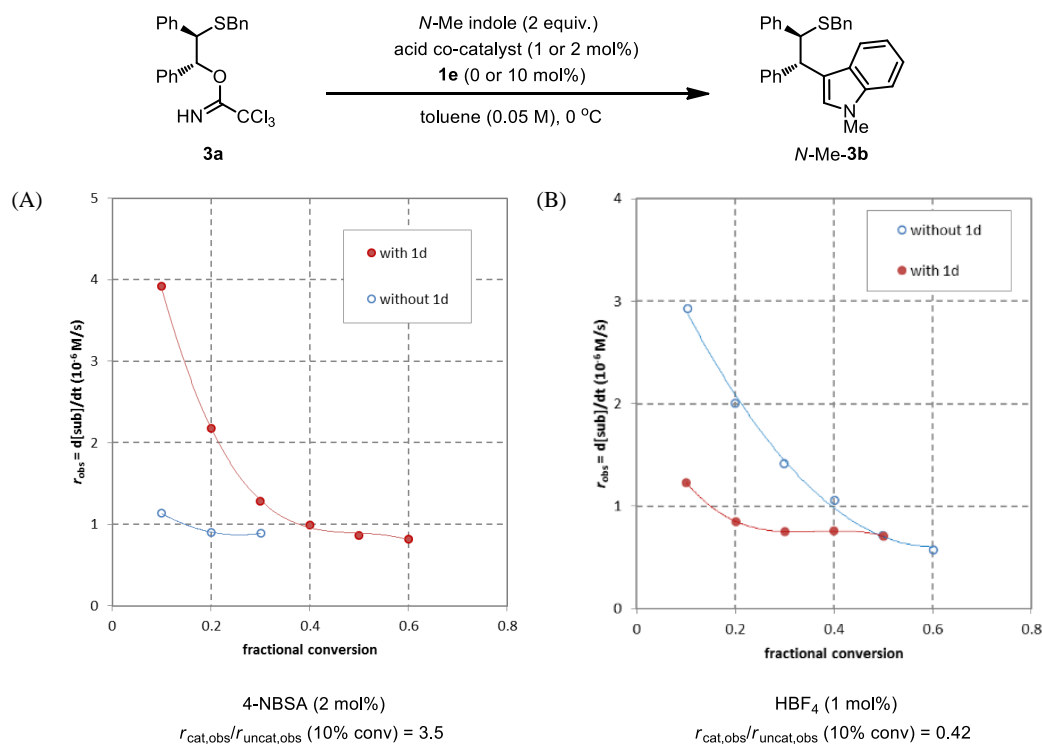


**Figure 4-5.** Control experiment II (with *N*-methylindole): 4-NBSA (A) vs. HBF<sub>4</sub> (B). Solid trendlines represent polynomial fit of the data points. Conditions see Figure 4-4.

<sup>46</sup> With 4-NBSA,  $k_{\text{cat,obs}}(\text{indole})/k_{\text{cat,obs}}(\text{methylindole}) = 12$ , and with HBF<sub>4</sub>,  $k_{\text{cat,obs}}(\text{indole})/k_{\text{cat,obs}}(\text{methylindole}) = 24$ .

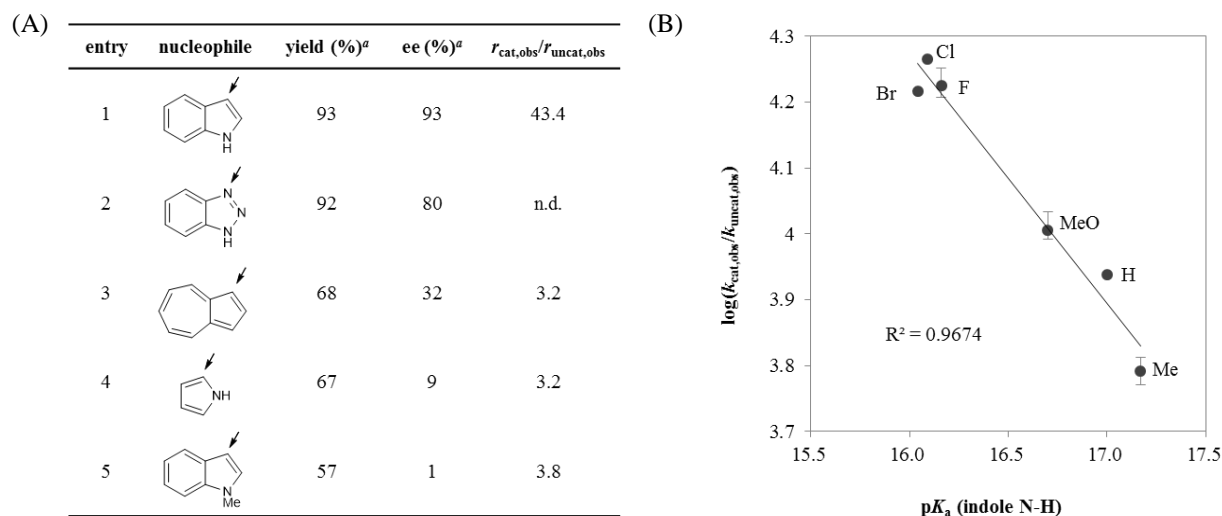


**Figure 4-6.** Reactivity- and enantioselectivity- dependence on the presence and the acidity of an N–H group in the nucleophile. (A) Structure-reactivity and -enantioselectivity relationship of  $\pi$ -nucleophiles. <sup>a</sup> Yields and enantiomeric excesses were obtained under reaction conditions described in Scheme 3. <sup>b</sup> The initial reaction rates with 4-NBSA alone ( $r_{\text{uncat,obs}}$ ) and with 4-NBSA/**1d** ( $r_{\text{cat,obs}}$ ) were determined directly by in situ IR spectroscopy. The ( $r_{\text{cat}}/r_{\text{uncat}}$ ) value was not determined for benzotriazole (entry 2) because the kinetic analysis was complicated by the poor solubility of the nucleophile in the reaction medium. (B) Correlation between the degree of rate acceleration by **1d** over the background racemic reaction ( $k_{\text{cat,obs}}/k_{\text{uncat,obs}}$ ) and the acidity of the N–H motif of 5-substituted indole derivatives ( $\text{p}K_{\text{a}}$ ). The rate data were obtained by in situ IR and <sup>1</sup>H NMR spectroscopy (see experimental section for detailed experimental procedure and data analysis). Error bars reflect the range of experimental data from 2-3 individual measurements, and the line represents the least-squares fit.

The importance of this H-bonding interaction in the mechanism of catalysis was further ascertained through a comprehensive examination of the reactivity of a series of 5-substituted indole derivatives in the presence and the absence of **1d**. We uncovered an intriguing linear correlation between the degree of rate acceleration [ $\log(k_{\text{cat,obs}}/k_{\text{uncat,obs}})$ ] by thiourea **1d** and the acidity of the indole nucleophile ( $\text{p}K_{\text{a}}$ ) (Figure 4-6B). This result led to the conclusion that in the presence of thiourea, the rate of the reaction is linked not only to the intrinsic nucleophilicity of the indole, but also to its hydrogen-bond donor ability.

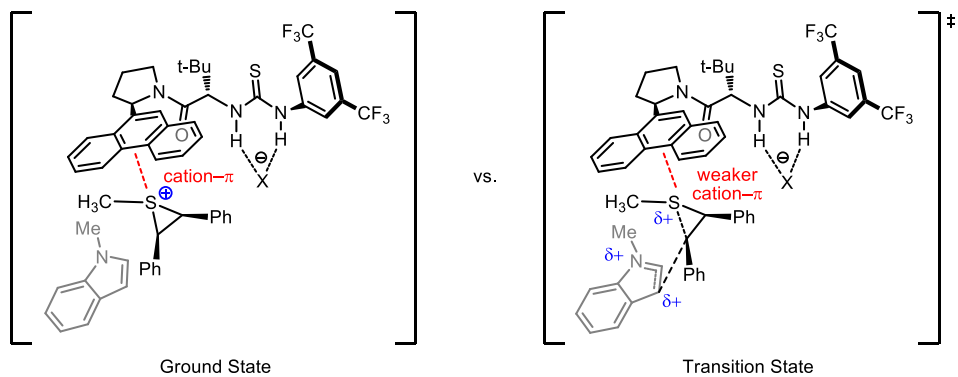
The functional groups on the catalyst that can potentially participate in such H-bonding interaction with indole include the amide, the thiourea and the extended aromatic substituent on the catalyst, as well as the sulfonate anion bound to thiourea. The similar reactivity and enantioselectivity displayed with thiourea **1d** and its urea analogue **2d** appear to rule out a direct

role for the thiourea sulfur atom (see Scheme 4-8). As discussed below, the extended aromatic group plays a key role that can be tied to interactions with the episulfonium ion. Therefore, we propose that the amide oxygen and the sulfonate anion are the most likely hydrogen-bond acceptor sites for the activation of indole. Computational analysis presented in Section 4.6 will provide more insights into this topic.

The function of thiourea **1d** as a general base in the reaction mechanism can be used to explain an unusual negative catalysis effect we observed in the addition of *N*-methylindole to the episulfonium ion promoted by HBF<sub>4</sub> (Figure 4-5B). Under these conditions, the **1d**-catalyzed pathway is slower than the uncatalyzed reaction by a factor of 2.4. An analogous situation has been observed previously in a urea and HOTf co-catalyzed Povarov reaction.<sup>32a</sup> This phenomenon can be rationalized by the differences in charge buildup between resting state and transition state.<sup>47</sup> As we discussed in the previous section, in both the ground state and the transition state of the episulfonium ion ring-opening reaction, the catalyst is associated with the episulfonium ion through an attractive cation- $\pi$  interaction with the extended aromatic substituent. In the nucleophilic addition, as *N*-Me indole approaches, the full positive charge on the electrophile disperses onto the nucleophile as well, resulting in a slightly less charged cation and therefore diminished catalyst-episulfonium interaction (Scheme 4-11). On the other hand with indole, the positive charge redistributed from the electrophile onto the nucleophile can also be stabilized by a catalyst-indole H-bonding interaction, which compensates for the reduced catalyst-episulfonium ion attraction.

---

<sup>47</sup> Zuend, S. J. Ph.D. dissertation, Harvard University, 2009.



**Scheme 4-11.** Model for explaining the rate deceleration effect by **1d** in the reaction between **3a** and *N*-methylindole in the presence of  $\text{HBF}_4$ .

## 4.5 Mechanism of Enantioinduction

Previous experimental data have suggested that catalyst **1d** associates with the rate- and enantio-determining transition state of indole addition to the episulfonium ion primarily through a network of three attractive noncovalent interactions. These include dual H-bond donation from thiourea N–H protons to the sulfonate anion, general base activation of indole by the catalyst amide, and cation– $\pi$  interaction between the catalyst aromatic group and the episulfonium ion. All these interactions play critical organizing roles in the mechanism of stereoinduction, as excision of any one leads to essentially complete erosion of reaction enantioselectivity.

Through a series of structure-enantioselectivity relationship studies, we found that the reaction ee has a rather marginal dependence on the strength of the dual H-bond (Table 4-3, entries 1-5) or that of the indole–amide interaction (entries 6-8). Therefore, these two interactions presumably exist in both the transition state leading to the major enantiomeric product (TS<sub>major</sub>) and the one leading to the opposite minor product (TS<sub>minor</sub>).

**Table 4-3.** Relationship between the strength of the dual H-bond or indole–catalyst interaction with reaction ee.

entry	thiourea (p <i>K</i> <sub>a</sub> )	acid (p <i>K</i> <sub>a</sub> )	indole (p <i>K</i> <sub>a</sub> )	ee (%)
1	<b>1d</b> (20) <sup>a</sup>	4-NBSA	indole	93
2	<b>2d</b> (26) <sup>b</sup>			92
3		4-NBSA (–4.0) <sup>c</sup>		93
4	<b>1d</b>	TsOH (–3.0) <sup>c</sup>	indole	89
5		MsOH (–1.9) <sup>c</sup>		89
6			5-Me indole (3.8) <sup>b</sup>	91
7	<b>1d</b>	4-NBSA	indole (3.9) <sup>b</sup>	93
8			5-Br indole (4.2) <sup>b</sup>	92

<sup>a</sup> p*K*<sub>a</sub> of thiourea. <sup>b</sup> p*K*<sub>a</sub> of urea. <sup>c</sup> See ref. 48. <sup>d</sup> Calculated with ACD/labs. See Scheme 4-3 for reaction conditions. TsOH = toluenesulfonic acid. MsOH = methanesulfonic acid.

<sup>48</sup> Guthrie, J. P. *Can. J. Chem.* **1978**, *56*, 2342–2354.

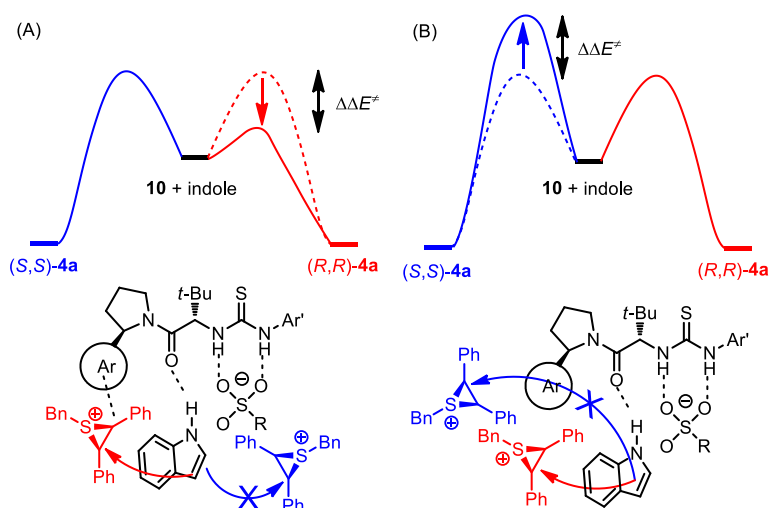
In contrast, the strong correlation between reaction enantioselectivity and the identity of the arene on the catalyst (Table 4-2) suggests a direct role of the extended  $\pi$ -system in the mechanism of stereo-differentiation. In principle, this arene effect may be caused primarily either by an acceleration of the major pathway through transition-state *stabilization* (Scheme 4-12A) or by inhibition of pathways that lead to the minor enantiomer through *destabilizing* interactions (Scheme 4-12B). Previous data are all consistent with the former scenario in which an attractive cation– $\pi$  interaction selectively promotes the major pathway. Definitive evidence is presented in this section through a kinetic analysis of the reaction, taking advantage of the fact that the indole addition step is both rate- and ee-determining. The rate constant that corresponds to the major pathway ( $k_{\text{cat,major}}$ ) could be deduced for catalysts **1a–1e** from *in situ* infrared spectroscopy-based kinetic measurements combined with enantiomeric ratio (er) determinations.<sup>49</sup> A strong correlation between this rate and reaction enantioselectivity was observed: a good linear fit was obtained in plots of  $\ln(k_{\text{cat,major}})$  vs.  $\ln(\text{er})$  ( $R^2 = 0.95$ ) (Figure 4-7).<sup>50</sup> This provides unambiguous evidence that enantioselectivity improvement due to variations of the aryl component of the catalyst **1** are, indeed, tied to stabilization of the major transition structure. The rate of the pathway that leads to the minor enantiomer also displays a weak, positive correlation with the reaction er ( $R^2 = 0.45$ ), which indicates that the minor transition structure is also stabilized selectively by the more enantioselective catalysts, albeit to a substantially lesser extent. Based on the kinetic and enantioselectivity data, as well as conclusions drawn from the model binding studies in the previous section, we propose that the difference in the strength of the cation– $\pi$  interaction between

---

<sup>49</sup> The rate constant for the thiourea-catalyzed pathway ( $k_{\text{cat}}$ ) was calculated with the following equation from experimental rate data ( $k_{\text{cat,obs}}$ ):  $k_{\text{cat,obs}} = k_{\text{cat}} + k_{\text{uncat}}$ . And the rate constants of the major and the minor diastereomeric pathways were derived from the following calculations:  $k_{\text{cat,major}} + k_{\text{cat,minor}} = k_{\text{cat}}$  and  $k_{\text{cat,major}}/k_{\text{cat,minor}} = \text{er}$ .

<sup>50</sup> For a previously reported reaction that also displays a positive correlation between reaction rate and selectivity, see: Uyeda, C.; Jacobsen, E. N. *J. Am. Chem. Soc.* **2011**, *133*, 5062–5075.

the major and minor pathways is the mechanistic basis for the high reaction enantioselectivity observed.



**Scheme 4-12.** Qualitative energy diagram of the nucleophilic addition step showing possible mechanisms of stereinduction by thiourea **1**. In the energy diagrams, dashed lines represent the original reaction pathways in the absence of thiourea **1**; solid lines represent the reaction pathway under the influence of thiourea **1**. The pathway leading to the minor enantiomeric product is designated as blue, while the one leading to the major enantiomeric product is designated as red. The color code also applies to the arrow pushing formalism, and the minor pathway is also labeled with an “X” symbol. Black dotted lines represent the noncovalent interactions between the catalyst and the reaction components. R = 4-nitrophenyl, and Ar’ = 3,5-bis(trifluoromethyl)phenyl.

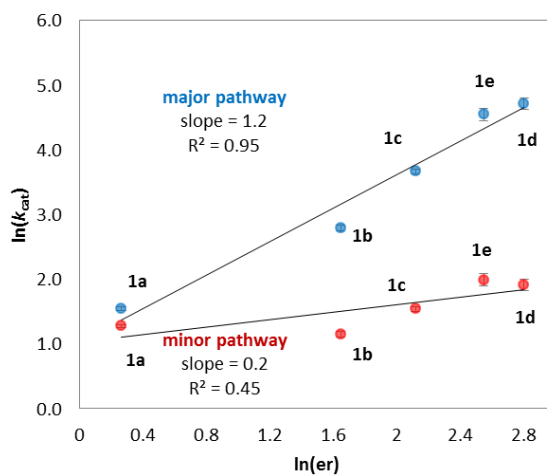


**Figure 4-7.** Correlation between rate and enantioselectivity data in the reaction between **1a** and indole. Each data point represents the average rate determined from two individual kinetic experiments, and the error bar shows the range of the measurements. The lines represent least-square fits.

## 4.6 Computational Analysis

Finally, we conducted theoretical calculations to evaluate the hypotheses that we had advanced based on analyses of experimental results. We chose to study our reaction at the M05-2X/6-31G(d) level of density functional theory (DFT),<sup>51</sup> because it has been specifically parametrized to accurately describe weak noncovalent interactions such H-bonding and cation- $\pi$  interactions and has been extensively used for such purposes.<sup>52</sup> The remarkable similarity of reaction enantioselectivity across a range of non-polar organic solvents suggested a common mechanism of catalysis and asymmetric induction that is unlikely to involve the explicit participation of solvent molecules in the nucleophilic addition transition state.<sup>53</sup> A combination of simplified substrate and catalyst was utilized in our studies to reduce computational expenses. The use of these abbreviated structures for representing the original compounds employed in the experimental analyses was validated by the comparable reactivity and enantioselectivity they exhibit to the parent system (Scheme 4-13). These simplifications include: 1) the methylthioether substrate **3c** was utilized instead of the parent benzylthioether substrate **3a** to eliminate the possibility of multiple conformations via rotation of the benzylic C-S bond; 2) the 4-nitrobenzenesulfonate anion was replaced with methanesulfonate to reduce the size of the system; and 3) the 3,5-bis(trifluoromethyl)phenyl group on catalyst **1d** was substituted with 3,5-

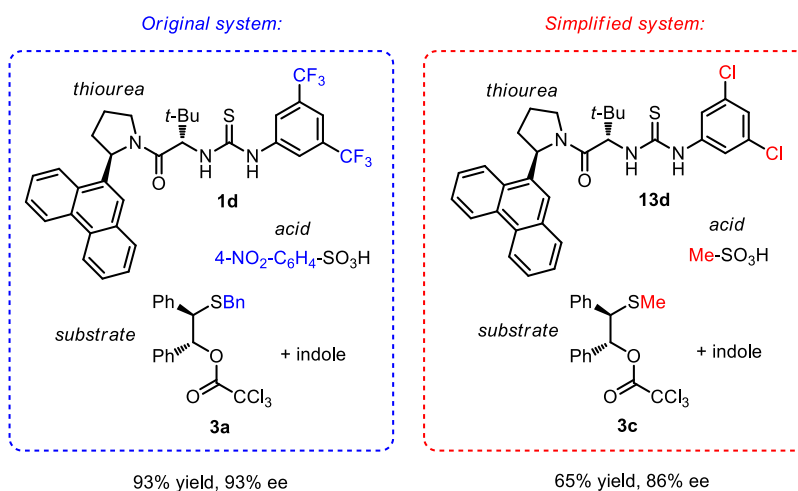
---

<sup>51</sup> Zhao, Y.; Schultz, N. E.; Truhlar, D. G. *J. Chem. Theory Comput.* **2006**, *2*, 364–382.

<sup>52</sup> For comparisons of functionals for systems involving weak noncovalent interactions, see ref. 35 and: (a) Zhao, Y.; Truhlar, D. G. *J. Chem. Theory Comput.* **2007**, *3*, 289–300; (b) Zhao, Y.; Truhlar, D. G. *Acc. Chem. Res.* **2008**, *41*, 157–167; (c) Burns, L. A.; Vázquez-Mayagoitia, A.; Sumpter, B. G.; Sherrill, C. D. *J. Chem. Phys.* **2011**, *134*, 084107.

<sup>53</sup> For example, under conditions outlined in Scheme 4-3, *tert*-butylbenzene gives **4a** in 92% yield and 90% ee, while *tert*-butylmethylether (TBME) gives **4a** in 59% yield and 90% ee.

dichlorophenyl (**13d**) to avoid the potential problems caused by inaccurate prediction of the electronegativity of fluorine by DFT methods.<sup>54</sup>



**Scheme 4-13.** Simplification of the structure of the reaction components for DFT computational studies. The yield and ee of the product are obtained using conditions shown in Scheme 4-3.

#### 4.6.1 Ground State Structures of the Episulfonium Ion and Catalyst

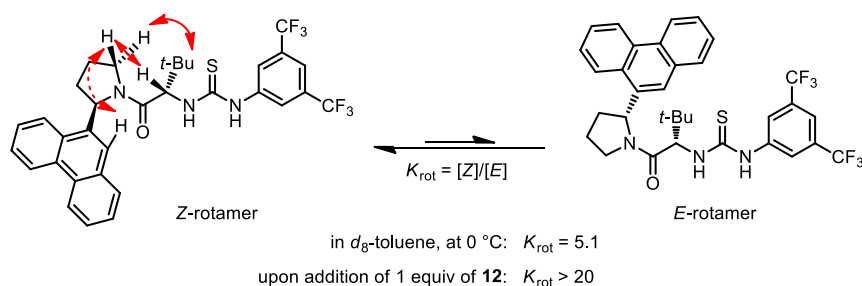
The episulfonium ion can exist as two different diastereomers differing in the *cis/trans*-relationship between the *S*-substituent and the two phenyl groups in the three-membered ring. The energy difference between the two isomers ranges from roughly 1-2 kcal/mol with methyl, phenyl and benzyl substitution on sulfur to 9 kcal/mol with the *tert*-butyl derivative, all favoring the *trans*-isomer. Because all the corresponding substrates react to furnish products with similar ee's, and with the same sense of enantioinduction (see Scheme 4-4), we inferred that the episulfonium ion adopts a *trans*-substitution pattern while participating in the reaction.

Catalyst **1d** exists as two rotamers due to the rotation barrier around the amide bond.<sup>55</sup> The *Z*-rotamer is energetically more favorable, as it is the predominant form of the catalyst in toluene (*Z:E* = 5.1:1 by <sup>1</sup>H NMR, 5 mM total concentration, 0 °C). Upon complexation with sulfonium

<sup>54</sup> (a) Chan, J. C. C.; Eckert, H. J. *Mol. Struct. (Theochem)* **2001**, 535, 1–8; (b) Lee, J. M.; Helquist, P.; Wiest, O. J. *Am. Chem. Soc.* **2012**, 134, 14973–14981.

<sup>55</sup> Lehnerr, D.; Ford, D. D.; Jacobsen, E. N. *Manuscript in preparation*.

salt **12**, the isomeric distribution is altered, and the *Z*-rotamer is exclusively observed, an assignment that was made based on nuclear Overhauser effect analysis (Scheme 4-14). We reasoned that the change of rotameric distribution arose from the presence of an attractive cation– $\pi$  interaction between the sulfonium ion and the suitably positioned phenanthryl group in the *Z*-rotamer, which is not possible in the case with the *E*-rotamer. Given the ion-pair nature of the intermediates and transition states of the episulfonium ion ring-opening reaction, it is very likely that the *Z*-rotamer is also the active species that catalyzes the reaction by effectively providing the cation– $\pi$  stabilization.



**Scheme 4-14.** Rotameric isomers of catalyst **1d**. Solid arrows in red indicate the nOe observed both in the presence and in the absence of **12**; dashed arrow in red indicates the nOe also observed in complex **1d**•**12**.

## 4.6.2 Energy Diagram

The energy diagram of the reaction catalyzed solely by 4-NBSA and by both thiourea **13d** and 4-NBSA was examined at the M05-2X level of theory using the 6-31G(d) basis set. Stationary points were located for the covalent resting state of the substrate, the episulfonium sulfonate, the nucleophilic addition product (prior to re-aromatization), and the transition states that lie between these energy minima.<sup>56</sup>

In the racemic pathway, the relative energies of all the ion-pair intermediates and transition states relative to the neutral ground state **14** are enormously exaggerated by DFT calculations

<sup>56</sup> Stationary points were verified by frequency analyses, as energy minima bear no imaginary frequencies and energy maxima bear one imaginary frequency.

(Scheme 4-15, top path). This is likely due to the following reasons: 1) charge separation in the gas-phase calculation is extremely unfavorable; and 2) the nucleofugality of methanesulfonate ( $\text{MsO}^-$ ) is smaller than that of 4-nitrobenzenesulfonate, making the ionization process more difficult. To address these issues, we analyzed the C–O bond ionization step of the uncatalyzed reaction with 4-NBSA as the acid co-catalyst instead of  $\text{MsOH}$  and by using a polarizable continuum model (PCM) of solvation with toluene. The resultant energy profile has a more realistic energy barrier, but there were still substantial discrepancies between this computational model and the experimental rate measurements.<sup>57</sup> We reasoned that in the absence of a catalyst, the highly polarized, high energy transition states are likely solvated to a substantial extent. Therefore, explicit solvent molecules may need to be incorporated in order to predict the reaction energy accurately.

Qualitatively, the computational results are consistent with the reaction being initiated by an exothermic extrusion of trichloroacetamide and an addition of the sulfonate anion, which results in the covalent ground state adduct **14**. This is followed by an endothermic formation of the episulfonium ion via ionization of the C–O bond. Indole addition to the electrophile was predicted to possess the highest kinetic barrier, in accord with experimental data. The deprotonation of intermediate **16** was not modeled, but is likely facile based on the strong acidity of the indoleninium ion ( $\text{p}K_{\text{b}}(\text{indole}) = -3.5$ ).

When thiourea **13d** was introduced to the system, indole addition was still predicted to be the rate-limiting step, with an overall electronic energy of activation ( $\Delta E^{\ddagger}$ ) of 19.0 kcal/mol, consistent with the observed rate of reaction in the kinetic analysis.<sup>58</sup>

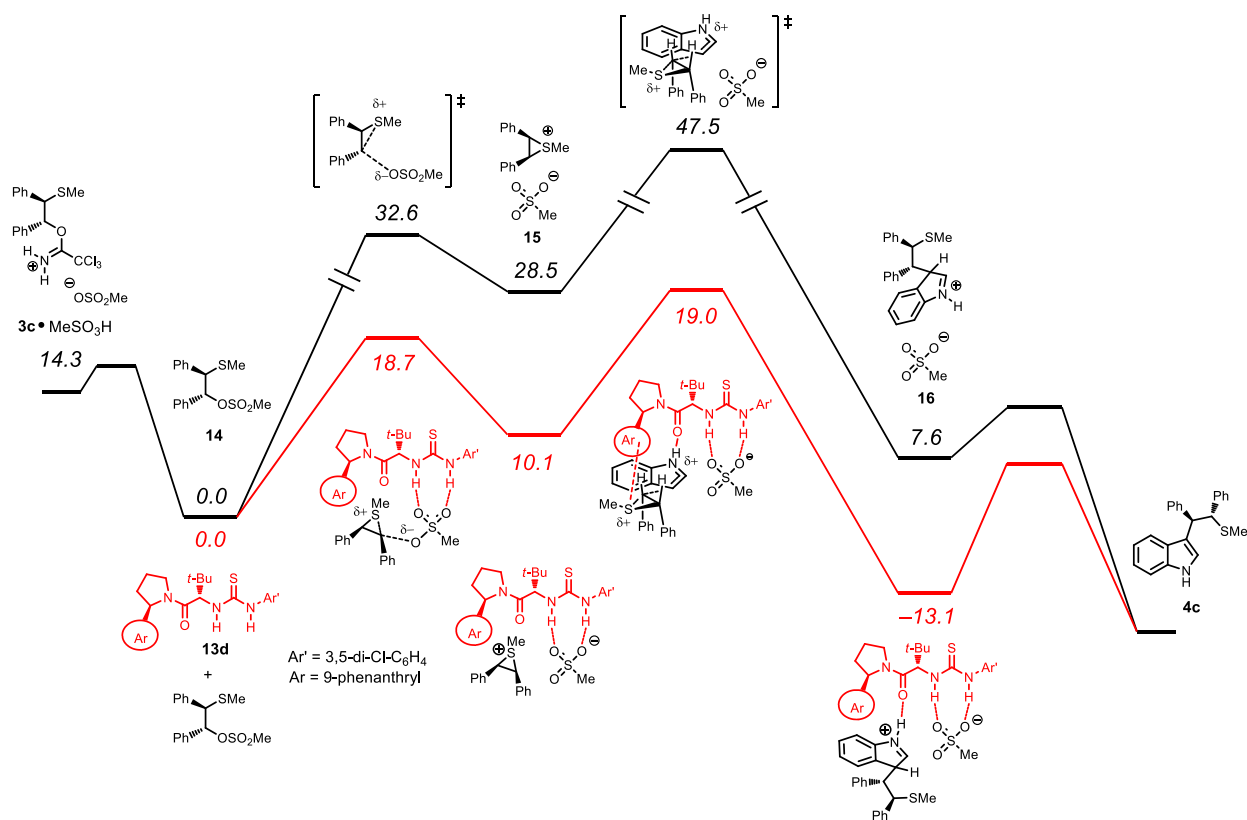
---

<sup>57</sup> The ionization step with 4-NBSA using PCM model has an energy of activation of 26.8 kcal/mol and an overall reaction energy of 20.1 kcal/mol, ca. 8 kcal/mol lower than the  $\text{MsOH}$ -involving conditions in the gas phase.

<sup>58</sup> Using Eyring equation and the rate constant of reaction catalyzed by **1d** ( $k_{\text{cat}} = k_{\text{cat,obs}} [\mathbf{1d}]_{\text{T}} = 0.605 \text{ M}^{-1}\cdot\text{s}^{-1}$ ), the free energy of activation ( $\Delta E^{\ddagger}$ ) is calculated to be 16.3 kcal/mol.

In the ionization step, we observed a tremendous decrease in the energy of activation upon introduction of catalyst **13d**. This data is again likely overestimated by the gas phase calculation. In order to accurately assess the role of the cation- $\pi$  interaction in the episulfonium ion formation step, we compared catalyst **13b** with **13d** in the DFT calculations and found that with **13b** bearing a smaller aromatic substituent, the energy barrier for the ionization of **14** is higher ( $\Delta E^\ddagger = 19.4$  kcal/mol, vs. 18.7 kcal/mol with **13d**). This result is in agreement with the hypothesis that the cation- $\pi$  interaction contributes to the facilitation of the sulfonate ionization process in concert with the anion-binding interaction.

To verify the catalytic effect of the thiourea catalyst in the indole addition step, we compared the computational data between the catalyzed and the uncatalyzed pathways directly. We reasoned that such a comparison is qualitatively meaningful, because the intermediate and the transition state in this step are both ion pairs, and the errors introduced by gas phase calculation should be mostly canceled out in the deduction of the energy of activation. The thiourea-promoted ring-opening of episulfonium ion **15** has a barrier worth 8.9 kcal/mol, 9.5 kcal/mol lower than its uncatalyzed counterpart. This result validates the conclusion advanced through experimental studies that thioureas of type **1/13** are capable of activating the indole addition to the electrophile.



**Scheme 4-15.** Energy diagram of the uncatalyzed reaction (in black) and the thiourea **13d**-catalyzed reaction (in red) involving **3c**, indole and methanesulfonic acid. All stationary points are fully optimized at the M05-2X/6-31G(d) level of theory and verified by frequency analysis. Uncorrected electronic energies in kcal/mol are relative to the lowest energy structure of the substrate or catalyst-substrate complex.

#### 4.6.3 Enantio-Determining Transition States

When the rate- and selectivity- determining transition states of the indole addition were analyzed more closely, a series of noncovalent interactions were discerned besides the primary sulfonate-binding by thiourea ( $d_1$ – $d_5$ , Figure 4-8). This includes an indole N–H – amide O interaction ( $d_1$ ) that we predicted through experimental mechanistic studies and indole N–H/C2–H – sulfonate interactions ( $d_5$ ) that further aid in the arrangement and activation of the nucleophile in the addition step. This observation explains why products **4f** and **4h** generated from nucleophiles lacking the C2 proton display reduced enantiomeric excess (see Scheme 4-4). The *para*-proton of a phenyl group on the substrate is spatially proximate to a chlorine atom on the thiourea catalyst **13d** ( $d_4 = 3.2 \text{ \AA}$ ); when catalyst **1d** was modeled instead, such observation was

also made between the same proton and the CF<sub>3</sub> group with a H...F distance of 2.5 Å. Therefore, a subtle electrostatic attraction might exist between this partial positive proton on the episulfonium ion and the electronegative halogen atom on the catalyst in the transition states. This finding provides an explanation for the pronounced detrimental effect of the *para*-substitution on the substrate to the reaction enantioselectivity, as the presence of *para*-substituent would either interrupt such an electrostatic attraction or introduce an unfavorable steric repulsion, leading to disorganization of the transition states. Finally, the methyl group at sulfur is shown to point to an empty space away from the substrate-catalyst assembly, explaining the good enantioselectivity observed for substrates with a range of structurally distinct *S*-substituents. This finding raises the possibility that a chiral *S*-substituent can be incorporated in the product with the diastereoselectivity of the nucleophilic addition imparted primarily by the catalyst. Accordingly, a diastereoselective indole alkylation reaction was developed with high levels of catalyst-control (Scheme 4-16).

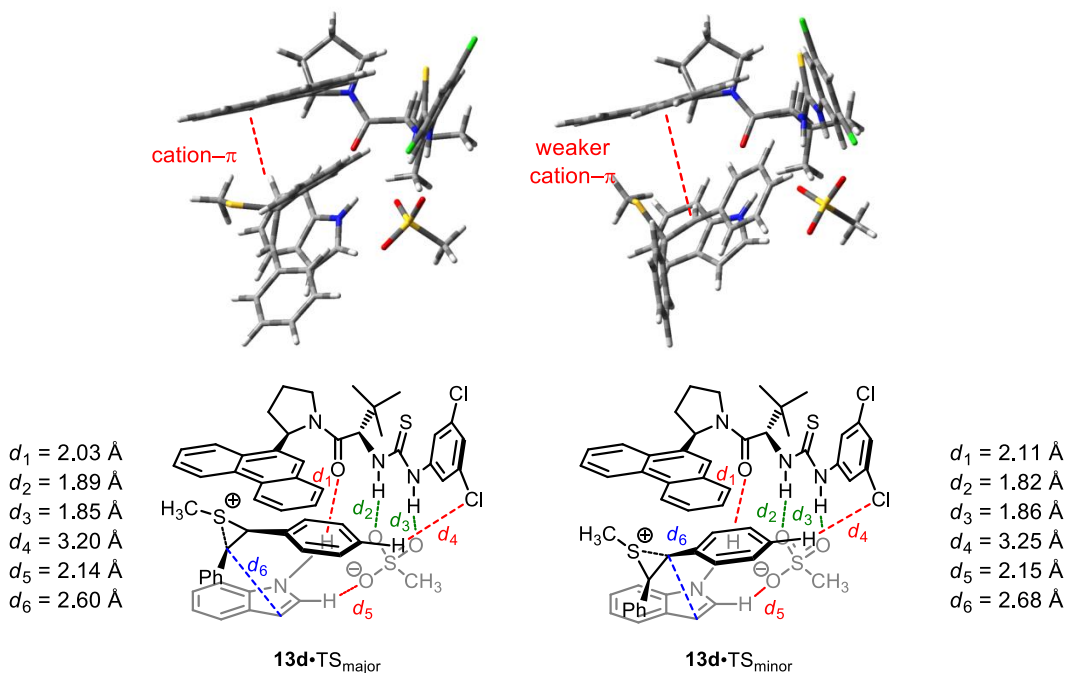
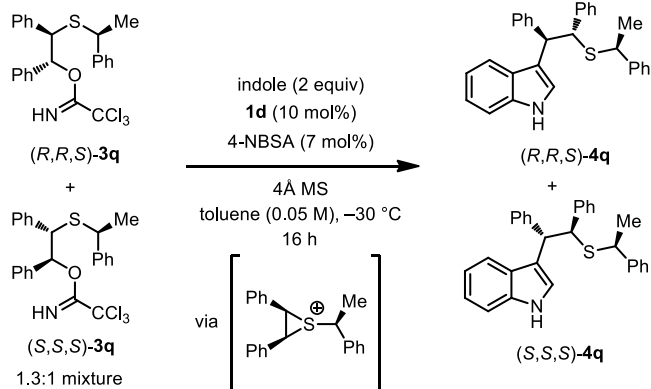


**Figure 4-8.** Calculated structures of the major (left) and minor (right) transition states with the chemdraw depiction and key bond distances.



catalyst	conversion <sup>a</sup>	[( <i>R,R,S</i> )- <b>4q</b> : ( <i>S,S,S</i> )- <b>4q</b> ] <sup>a</sup>
none	>99% <sup>b</sup>	1.3 : 1 <sup>b</sup>
( <i>4S,7R</i> )- <b>1d</b>	>99%	<b>27.7</b> : 1
( <i>4R,7S</i> )- <b>1d</b>	>99%	1 : <b>11.4</b>

<sup>a</sup> Conversion and diastereomeric ratio determined by <sup>1</sup>H NMR analysis of the crude reaction mixture. <sup>b</sup> At 0 °C.

**Scheme 4-16.** Catalyst-controlled diastereoselective indole alkylation with an enantioenriched episulfonium ion. The relative stereochemistry of the substrates **3q** was not assigned, while that of the products **4q** was assigned by comparison with product **3a**.

The minor diastereomeric transition state of the nucleophilic addition step is 3.04 kcal/mol higher in energy than the major one. Single point energies for the two diastereomeric transition structures were also calculated using larger basis sets as well as  $\omega$ B97X-D, a functional containing dispersion corrections in order to establish that the model for selectivity is robust across different levels of theory (Table 4-4).<sup>59</sup> The transition structures were also fully optimized using  $\omega$ B97X-D. All computational methods presented above are in agreement with respect to the sense of enantioinduction and accurately predict the observed absolute configuration of the product. In contrast, when B3LYP was used for a single-point energy calculation on structures optimized by M05-2X, the minor diastereomeric pathway was calculated to be favored over the major one by 1.31 kcal/mol. When the transition models initially predicted by M05-2X were subjected to optimization with B3LYP, the structures appear to relax in a way to avoid the steric repulsion

<sup>59</sup> For a reference describing the  $\omega$ B97X-D level of theory, see: Chai, J. D.; Head-Gordon, M. *Phys. Chem. Chem. Phys.* **2008**, *10*, 6615–6620.

between the extended aryl group on **13d** and the episulfonium ion, eventually leading to two diastereomeric complexes with essentially no energy difference (0.21 kcal/mol favoring the major pathway). The failure of the B3LYP functional to accurately predict dispersion-involving interactions, such as the cation- $\pi$  interaction has been documented in other systems.<sup>60</sup> Therefore, this level of theory is not suitable for the computational evaluation of the episulfonium ion ring-opening reaction.

**Table 4-4.** Comparison between different theories and basis sets in prediction of enantioselectivity.

optimization method	single-point energy method	$\Delta\Delta E^\ddagger$ (kcal/mol)
M05-2X/6-31G(d)	M05-2X/6-31G(d)	3.04 (2.47)
M05-2X/6-31G(d)	M05-2X/6-311+G(d,p)	2.93
M05-2X/6-31G(d)	M05-2X/6-311+G(2df,2p)	2.38
M05-2X/6-31G(d)	M06-2X/6-31G(d)	4.78
M05-2X/6-31G(d)	B3LYP/6-31G(d)	-1.31
$\omega$ B97X-D/6-31G(d)	$\omega$ B97X-D/6-31G(d)	4.83 (5.14)
B3LYP/6-31G(d)	B3LYP/6-31G(d)	0.21 (0.75)
B3LYP/6-31G(d)	M05-2X/6-31G(d)	3.34

<sup>a</sup> Uncorrected differences in transition-state energies. Values in parentheses include an unscaled correction for zero-point vibrational energy.

In the models obtained with the M05-2X/6-31G(d) level of theory (Figure 4-8), both transition structures possess the hydrogen-bonding interactions ( $d_1$ - $d_5$ ) discussed previously. The most significant disparity between the two assemblies is the distance between the episulfonium motif and the phenanthryl group on the catalyst. In the major transition state, a phenyl group and the  $\text{CH}_3\text{-S}^+\text{-CH}$  moiety on the episulfonium ion are both within 4.3 Å to the  $\pi$ -face of the extended aromatic residue, implying the presence of attractive interactions between the two.<sup>61</sup> This distance

<sup>60</sup> Liu, P.; Yang, X.; Birman, V. B.; Houk, K. N. *Org. Lett.* **2012**, *14*, 3288–3291. Also see ref. 35.

<sup>61</sup> For a paper that describes the cation- $\pi$  interaction between a sulfonium ion and an aromatic group, in which the  $\text{CH}_3\text{S}^+$  group is in close proximity to the  $\pi$ -face of the aromatic group, see ref. 37.

is significantly larger in the minor transition state (by ca. 1 Å). To further elucidate the interaction provided by the phenanthryl group that differentiates the two transition structures, we relied on NCIPLOT, a program developed by Johnson et al. specifically for visualizing noncovalent interactions on the basis of electron density calculations.<sup>62,63</sup> Diagrams generated using NCIPLOT clearly reveal the difference between the two transition states in terms of the interactions between the cation and the aromatic group on the catalyst (Figure 4-9). This interaction was visualized as an expansive, continuous surface in between these two interacting partners in the major transition state, which is mostly absent in the minor transition state. The nature of this interaction is determined to be attractive by analysis of the Laplacian eigenvalues of the electron density, which is consistent with a cation- $\pi$  interaction.<sup>64</sup> An attractive  $\pi$ - $\pi$  stacking can also be extracted from the major transition state between the proximal phenyl group on the substrate and the phenanthryl group of the catalyst, which is likely strengthened by the cationic character of the episulfonium.<sup>65</sup> The cation- $\pi$  interaction also exists in the minor transition state, although to a substantially lesser extent. Therefore, this pathway is also loosely stabilized by the catalyst, explaining why the rate vs. enantioselectivity plot also exhibits a small positive correlation in the minor pathway (Figure 4-7).

---

<sup>62</sup> (a) Johnson, E. R.; Keinan, S.; Mori-Sánchez, P.; Contreras-García, J.; Cohen, A. J.; Yang, W. *J. Am. Chem. Soc.* **2010**, *132*, 6498–6506; (b) Contreras-García, J.; Johnson, E. R.; Keinan, S.; Chaudret, R.; Piquemal, J.-P.; Beratan, D. N.; Yang, W. *J. Chem. Theory. Comput.* **2011**, *7*, 625–632.

<sup>63</sup> This program has been used for the analyses of multiple types of noncovalent interaction, including H-bonding and cation- $\pi$  interactions. For examples using NCIPLOT to elucidate cation- $\pi$  interactions, see: (a) Hong, Y. J.; Tantillo, D. J. *Chem. Sci.* **2013**, *4*, 2512–2518; (b) Mandal, T. K.; Samanta, S.; Chakraborty, S.; Datta, A. *ChemPhysChem* **2013**, *14*, 1149–1154. For examples using NCIPLOT to visualize hydrogen bonding, see ref. 62, as well as: (a) Contreras-García, J.; Yang, W.; Johnson, E. R. *J. Phys. Chem. A* **2011**, *115*, 12983–12990; (b) Otero-de-la-Roza, A.; Johnson, E. R.; Contreras-García, J. *Phys. Chem. Chem. Phys.* **2012**, *14*, 12165–12172; (c) Saleh, G.; Gatti, C.; Lo Presti, L.; Contreras-García, J. *Chem. Euro. J.* **2012**, *18*, 15523–15536.

<sup>64</sup> Dougherty, D. A. *Acc. Chem. Res.* **2013**, *46*, 885–893.

<sup>65</sup> Calculated charge distribution shows that the phenyl ring on the episulfonium ion bears an overall partial positive charge of ca. +0.2, more than that of a neutral phenyl group in toluene (ca. +0.1).

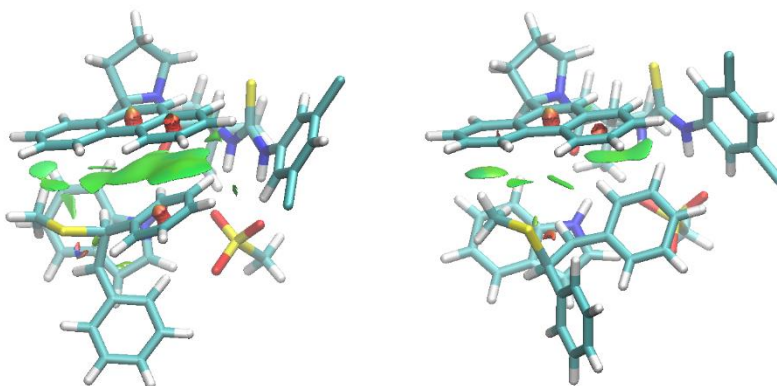


**Figure 4-9.** Cation– $\pi$  in the major (left) and minor (right) transition states visualized by NCIPLOT program (green areas). Only interactions in between the aromatic group of **13d** and the cationic assembly of reacting components are visualized for clarity. Full visualization of all the noncovalent interactions present in the two structures is shown in experimental section.

#### 4.6.4 Enantioselectivity Dependence on the Aromatic Group of the Catalyst

In order to test the proposed stabilizing role of the extended aryl substituent on the catalyst in the lowest energy diastereomeric transition state, we evaluated a series of arylpyrrolidino amido thiourea catalysts **13b-e**. The difference in the cation– $\pi$  donating abilities of these catalysts was manifested by the different levels of catalysis and enantioinduction observed experimentally, with catalysts containing a more expansive aryl group generally providing higher reactivity and higher enantioselectivity (see Figure 4-7). The overall trend in enantioselectivity was reproduced by the computation, with a good correlation observed between the experimental  $\Delta\Delta G^\ddagger$  and the calculated  $\Delta\Delta E^\ddagger$  ( $R^2 = 0.98$ ) (Table 4-5 and Figure 4-10A).<sup>66</sup>

The length of the forming C–C bond ( $d_6$ , labeled in Figure 4-8) in the major transition state correlates with the calculated  $\Delta\Delta E^\ddagger$  and the size of the aromatic substituents on **13**, with the more stabilizing group providing the shorter C–C distance (Table 4-5). This correlation can be rationalized using a simple energy diagram analysis of the addition step in combination with the

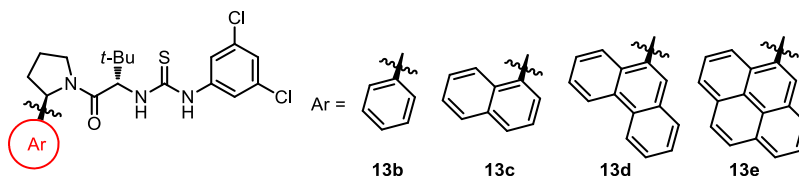
<sup>66</sup> Because of the large size of the systems being modeled and the presence of multiple small vibrational frequencies, zero-point vibrational energy corrections and free energies, derived from frequency calculations using the rigid-rotor/harmonic oscillator approximation, were not used to estimate enantioselectivities.

Hammond postulate (Figure 4-10B).<sup>67</sup> A shorter forming C–C bond distance corresponds to a later transition state, which is a result of either stabilization of the substrate or destabilization of the product in an exothermic reaction. According to the calculated structure of adduct **13d**•**16**, no repulsive interaction is observed between the catalyst and the ion pair **16** that is likely to depend on the size of the aromatic group. On the other hand, the strength of a cation– $\pi$  stabilization of the episulfonium ion intermediate **15** should improve as the catalyst aryl group increases in size. Therefore, this data is most consistent with the attractive nature of the interaction between the extended aryl substituent and the episulfonium unit in the major transition state, consolidating our proposed model for stereoinduction.

**Table 4-5.** Calculated energy and structure profiles of transition states involving catalysts **13b–e** with comparisons to the experimental data

catalyst	ee	exp. $\Delta\Delta G^\ddagger$ (kcal/mol) <sup>a</sup>	calc. $\Delta\Delta E^\ddagger$ (kcal/mol) <sup>b</sup>	$d_{6,\text{major}}$ (Å)	$d_{6,\text{minor}}$ (Å)
<b>13e</b>	85.7	1.24	3.25	2.588	2.650
<b>13d</b>	86.3	1.27	3.07	2.600	2.676
<b>13c</b>	76.6	0.98	2.42	2.613	2.666
<b>13b</b>	55.3	0.61	1.63	2.621	2.732

<sup>a</sup> Differential free energy of activation determined by experiments under conditions described in Scheme 4-3 with substrate **3c**, MsOH and catalyst of type **13**. <sup>b</sup> Predicted energy difference between the calculated diastereomeric transition structures encompassing substrate **3c**, MsOH and catalyst of type **13**. The distances referred to as  $d_6$  are labeled in the major/minor transition states in Figure 4-8. Structures of **13b–e**:



<sup>67</sup> For examples using the Hammond postulate to analyze selectivity trend observed in catalysis, see: (a) Palucki, M.; Finney, N.S.; Pospisil, P.J.; Güler, M.L.; Ishida, T.; Jacobsen, E.N. *J. Am. Chem. Soc.* **1998**, *120*, 948–954; (b) Wilcock, B. C.; Uno, B. E.; Bromann, G. L.; Clark, M. J.; Anderson, T. M.; Burke, M. D. *Nat. Chem.* **2012**, *4*, 996–1003.

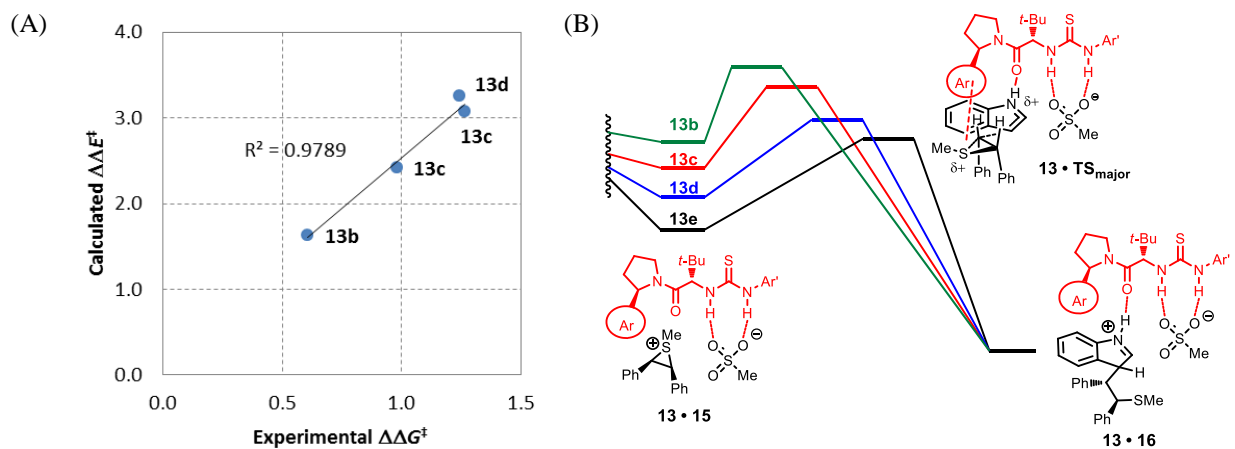


**Figure 4-10.** (A) Experimental vs. calculated enantioselectivity. The black line represents a linear least-square fit. (B) Qualitative energy diagram depicting the position change of the major transition state on the reaction coordinate as a function of the size of the aromatic group.

Based on their cation– $\pi$  donating abilities (quadrupole moments and polarizabilities), pyrenyl catalyst **1e** (or **13e**) is predicted to be more enantioselective than phenanthryl catalyst **1d** (or **13d**). However, the experimental ee's of the reaction products imparted by these two catalysts are very similar. From the DFT calculation, the additive effect of the fourth benzene ring of catalyst **13e** on the differential energy of activation ( $\Delta\Delta E^\ddagger$ ) is also significantly smaller ( $\Delta(\Delta\Delta E^\ddagger) = 0.18$  kcal/mol) than that of the third ring (from **13c** to **13d**,  $\Delta(\Delta\Delta E^\ddagger) = 0.65$  kcal/mol), and that of the second ring (from **13b** to **13c**,  $\Delta(\Delta\Delta E^\ddagger) = 0.79$  kcal/mol). The discrepancy between the cation– $\pi$  donation ability of pyrene and the enantiodifferentiation ability of the corresponding thiourea can be explained by the computational model of reaction transition states. The distance of the forming C–C bond ( $d_6$ ) in the minor transition state of the **13e**-catalyzed pathway is significantly shorter than those with catalysts **13b-d**. This implies that the cation– $\pi$  stabilization of the minor transition state by **13e** is stronger compared to other thioureas of type **13**. By examining the computed minor transition structures, the additional benzene ring on the pyrenyl group relative to phenanthryl group appears to be in position to pick up an additional attractive interaction with the sulfur atom on the episulfonium ion, which bears a partial positive charge of

+0.2, with a distance of 3.4 Å (Figure 4-11).<sup>68</sup> This computational observation is reflected in the experimental results in Figure 4-8, which shows that the rate of the minor pathway with catalyst **13e** is the fastest among the series. Taken together, we postulate that the lower reaction ee with catalyst **13e** than its smaller analog **13d** is a result of additional stabilization effect of the minor transition state provided by the pyrenyl substituent, leading to reduced energy differentiation between the two diastereomeric pathways.

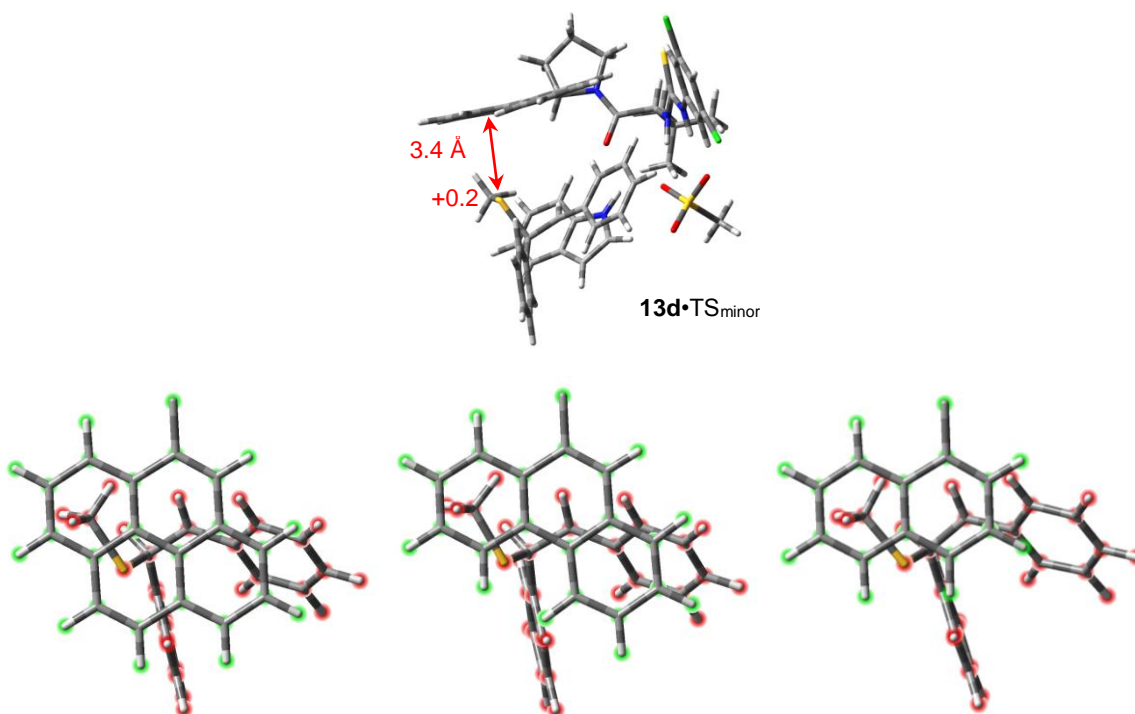


**Figure 4-11.** Interaction between the aromatic group on catalysts **13c-e** and the episulfonium ion. Top structure: side view of the minor transition state with catalyst **13d**, showing close distance between the sulfur atom and the phenanthryl group. Bottom structures: top view of the minor transition state with catalysts **13e** (left), **13d** (middle), **13b** (right). The view is from the top of the aromatic group in a direction perpendicular to its  $\pi$ -face. The aromatic group is labeled in green, and the episulfonium ion in red. The sulfur atom is yellow. These are part of the calculated structures at the M05-2X/6-31G(d) level of theory, corresponding to the results shown in Table 4-5. The rest of the molecules is omitted for clarity.

<sup>68</sup> This number reflects the shortest distance between the sulfur atom and the  $\pi$ -face of the aromatic group.

## 4.7 Conclusion

Kinetic studies showed that the phenanthrylpyrrolidine-derived thiourea **1d** lowers the energy of activation by 2.0 kcal/mol in the nucleophilic addition of indole to **3a**, as compared to the background reaction catalyzed by 4-NBSA alone. This corresponds to a rate acceleration effect of ca. 40-fold. Based on experimental and theoretical mechanistic analyses, the catalytic effect of **1d** is shown to be realized by selective stabilization of the intermediates and transition states of the reaction through a network of attractive, noncovalent interactions. This includes a series of hydrogen bonding interactions between the thiourea and the sulfonate counteranion, the amide group on the catalyst and the indole N–H, the sulfonate and the indole C2–H, as well as the *para*-C–H on the phenyl ring of episulfonium ion and the CF<sub>3</sub> group on the catalyst. In addition, the presence of a cation– $\pi$  interaction between the phenanthryl group on **1d** and the episulfonium portion of the transition state assembly has been supported by DFT computations. This mode of catalysis is reminiscent of the mechanism of biosynthetic pathways facilitated by enzymes.

In his analysis on the mechanism of triosephosphate isomerase (TIM), Knowles advanced the notion that this enzyme achieves remarkable catalytic activity primarily through the following actions: stabilization of all the internal states (intermediates) with respect to the external states (substrate and product) through “uniform binding”; further optimization of the internal thermodynamics by “differential binding” of specific intermediates; and catalysis of elemental steps by lowering the free energies of kinetically significant transition states with respect to their preceding intermediates.<sup>69</sup> Despite inferior rate acceleration, the mechanistic model proposed for the episulfonium ion ring-opening promoted by a synthetic small-molecule catalyst bears intriguing resemblance to the enzymatic catalysis with TIM. First, the thiourea uniformly binds

---

<sup>69</sup> Albery, W. J.; Knowles, J. R. *Angew. Chem. Int. Ed.* **1977**, *16*, 285–293.

to all the internal states of the reaction (ion-pair intermediates **10** and **11**) and lowers their energies relative to the neutral substrate and product. Second, the catalyst binds more tightly to the indoleninium intermediate **11** than to the episulfonium ion **10**, driving the nucleophilic addition. Finally, the thiourea catalyzes the elemental step of nucleophilic addition by lowering the energy of the transition structure with respect to intermediate **10** via general base catalysis.

Through close analysis of the selectivity-determining transition structures, we found out that the difference in the strength of the cation- $\pi$  interaction between the catalyst and the episulfonium ion lies at the origin of the high enantioselectivity observed. Despite the relatively extensive studies on the computational modeling of the cation- $\pi$  interaction in ground state structures of various systems,<sup>70</sup> only few reports have systematically characterized these effects in transition states of chemical reactions.<sup>71</sup> This study constitutes the first example of using DFT methods to elucidate the cation- $\pi$  interaction in the transition state wherein the fully charged cationic component associates with the catalyst only through weak, noncovalent interactions.

On the basis of the computational analyses, models for catalysis and stereochemical induction were advanced for the ring-opening of episulfonium ions with indole, demonstrating excellent correlations with the experimental observations. We anticipate that the use of the cation- $\pi$  interaction in cooperation with other attractive noncovalent interactions will emerge as a general principle in small-molecule catalysis involving polarized transition structures.

---

<sup>70</sup> For a review, see: Mahadevi, A. S.; Sastry, G. N. *Chem. Rev.* **2013**, *113*, 2100–2138.

<sup>71</sup> For representative precedent studies on the cation- $\pi$  interaction in catalysis related contexts, see: (a) Mugridge, J. S.; Bergman, R. G.; Raymond, K. N. *J. Am. Chem. Soc.* **2012**, *134*, 2057–2066; (b) Yang, X.; Bumbu, V. D.; Liu, P.; Li, X.; Jiang, H.; Uffman, E. W.; Guo, L.; Zhang, W.; Jiang, X.; Houk, K. N.; Birman, V. B. *J. Am. Chem. Soc.* **2012**, *134*, 17605–17612; (c) Liu, P.; Yang, X.; Birman, V. B.; Houk, K. N. *Org. Lett.* **2012**, *14*, 3288–3291; (d) Li, X.; Liu, P.; Houk, K. N.; Birman, V. B. *J. Am. Chem. Soc.* **2008**, *130*, 13836–13837; (e) Ishihara, K.; Fushimi, M.; Akakura, M. *Acc. Chem. Res.* **2007**, *40*, 1049–1055. See also refs. 3 and 35.

## Experimental Section

### Table of Content

1. General Information	191
2. Synthetic procedure for the enantioselective episulfonium ion ring-opening with indoles	192
3. Data for kinetic analysis with in situ IR spectroscopy and derivation of the rate laws	192
4. Data for linear free energy relationship study – Mayr analysis	198
5. Data for kinetic isotope effect study	200
6. Data sets for non-linear effect study	203
7. Data kinetic analysis of reactions catalyzed by thiourea <b>1a-1e</b>	204
8. Correlations of arene properties with rate and enantioselectivity for catalysts <b>1b-1e</b>	205
9. NMR binding study of thiourea <b>1</b> and dibenzylmethylsulfonium triflate <b>12</b>	206
10. Structure-reactivity and structure-selectivity relationships of indoles and other $\pi$ -nucleophiles	213
11. Reaction kinetics with tetrafluoroboric acid (HBF <sub>4</sub> )	215
12. Thiourea <b>1a/1b</b> – substrate <b>3a</b> association	217
13. NMR spectrum of covalent adduct <b>7</b>	218
14. Nuclear Overhauser effect studies on thiourea <b>1d</b> and complex <b>1d•12</b>	219
15. Catalyst-controlled diastereoselective episulfonium ion ring-opening	222
16. Crystallographic data of compounds <b>4b</b> , <b>4c</b> and <b>4h</b>	226
17. NCIPLOT visualization of noncovalent interactions	228
18. Computational data	234
19. Data sets for Eyring analysis	257

### 1. General information

Synthetic reactions were performed in oven-dried 1.5-dram vials, and in situ monitored reactions were conducted in oven-dried 5 mL glass reactors (two-necked, pictures see below). The vessels were fitted with rubber septa and reactions were conducted under air. Flash chromatography was performed using silica gel 60 (230-400 mesh) from EM Science. Commercial reagents were purchased from Sigma Aldrich, Alfa Aesar, Lancaster, Oakwood, Strem or TCI, and used as received with the following exceptions: toluene, *t*-butyl methyl ether and benzene were dried by passing through columns of activated alumina; dimethylformamide was dried by passing through columns of activated molecular sieves. Proton nuclear magnetic resonance (<sup>1</sup>H NMR) spectra and carbon nuclear magnetic resonance (<sup>13</sup>C NMR) spectra were recorded on Inova-500 (500 MHz) and Inova-600 (600 MHz) spectrometers. Chemical shifts for protons are reported in parts per million downfield from tetramethylsilane and are referenced to residual protium in the NMR solvent (CHCl<sub>3</sub> =  $\delta$  7.27, toluene –CH<sub>3</sub> =  $\delta$  2.09). Chemical shifts for carbon are reported in parts per million downfield from tetramethylsilane and are referenced to the carbon resonances of the solvent (CDCl<sub>3</sub> =  $\delta$  77.0). Chiral HPLC analysis was performed using an Agilent Technologies 1200 series instrument with commercial Chiralpak columns. In situ infrared spectroscopy was performed using Mettler Toledo Reactor IR IC10, and data analyzed using iC IR 4.2 software.



## 2. Synthetic procedure for the enantioselective episulfonium ion ring-opening with indoles

### Method A: substrate scope study

An oven-dried 1.5 dram vial was charged with substrate **1** (0.05 mmol, 1.0 equiv), thiourea catalyst (0.0050 mmol, 0.10 equiv), nucleophile (0.10 mmol, 2.0 equiv) and 4Å molecular sieves (25 mg, powder, activated). The vial was cooled to  $-30\text{ }^{\circ}\text{C}$ , and toluene (1 mL) was added with stirring. Once the reactants and catalyst were fully dissolved, the mixture was cooled to  $-78\text{ }^{\circ}\text{C}$ , and solid 4-NBSA (0.7 mg, 0.0035 mmol, 0.07 equiv) was added at once. The resulting solution was stirred at  $-30\text{ }^{\circ}\text{C}$  and the progress of the reaction was monitored by TLC.<sup>a</sup> When the progress of the reaction was determined to be complete,  $\text{NEt}_3$  ( $\sim 10\text{ }\mu\text{L}$ ) was added at  $-30\text{ }^{\circ}\text{C}$ . The resulting mixture was applied directly to a pipette column containing 4-5 cm of silica gel, and product was isolated by eluting hexanes/EtOAc (20:1 to 10:1) and solvent removal.

### Method B: structure-selectivity relationship studies and catalyst-controlled diastereoselective reactions

An oven-dried 1.5 dram vial was charged with substrate **1** (0.025 mmol, 1.0 equiv), thiourea catalyst (0.0025 mmol, 0.10 equiv), nucleophile (0.05 mmol, 2.0 equiv) and 4Å molecular sieves (15 mg, powder, activated). The vial was cooled to  $-30\text{ }^{\circ}\text{C}$ , and toluene (0.5 mL) was added with stirring. Once the reactants and catalyst were fully dissolved, 4-NBSA solution (0.5 M in THF;  $3.5\text{ }\mu\text{L}$ , 0.0035 mmol, 0.07 equiv) was added at once to the reaction mixture. The resulting solution was stirred at  $-30\text{ }^{\circ}\text{C}$  and the progress of the reaction was monitored by TLC.<sup>a</sup> When the progress of the reaction was determined to be complete, 20%  $\text{NEt}_3$  in EtOAc ( $\sim 10\text{ }\mu\text{L}$ ) was added at  $-30\text{ }^{\circ}\text{C}$ . The resulting mixture was applied directly to a pipette column containing 4-5 cm of silica gel, and product was isolated by eluting hexanes/EtOAc (20:1 to 10:1) and solvent removal.

<sup>a</sup> Retired GC column was cut into pieces and used as the capillary tubes. A properly sized needle containing a piece of GC column inside was used to pierce the septa of the reaction vial, and an aliquot for TLC analysis was taken using the GC column and applied directly on the silica gel TLC plate.

## 3. Data for kinetic analysis with in situ IR spectroscopy and derivation of the rate laws

### Kinetic analysis by in situ infrared spectroscopy

Representative procedure: An oven-dried two-necked reaction vessel equipped with a 1/8" long stir bar was charged with indole (23.4 mg, 0.20 mmol), thiourea **1d** (6.3 mg, 10.0  $\mu\text{mol}$ ) and molecular sieves (4Å, beads, 50 mg). It was capped with a rubber septum, and anhydrous toluene (1.5 mL) was added to dissolve the reactants. The vessel was then attached to an in situ infrared (IR) spectroscopy probe that had been dried with a heat gun. An ice bath was applied to cool the reaction mixture down to  $0\text{ }^{\circ}\text{C}$  with stirring, and a background IR spectrum was collected (256 scans) after 5 min. Continuous data collection was started (4 spectra/min, 50 scans/spectrum) at  $0\text{ }^{\circ}\text{C}$ . A freshly prepared stock solution of **3a** (44.6 mg, 0.10 mmol) in toluene (0.5 mL) was added by syringe to the vessel. When the IR absorbance of the trichloroacetimidate C=N bond (height to two-point baseline,  $1670\text{ cm}^{-1}$  to  $1698/1648\text{ cm}^{-1}$ ) had become level (ca. 3 min). A freshly prepared stock solution of 4-NBSA (4  $\mu\text{L}$  of a solution of 101.6 mg 4-NBSA in 1 mL THF, 2.0  $\mu\text{mol}$ ) was added to start the reaction. The reaction was monitored until the absorbance of **3a** at

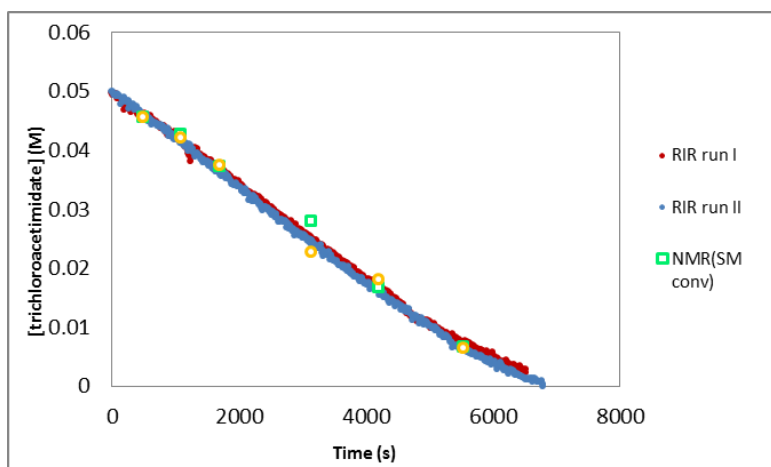
1670  $\text{cm}^{-1}$  had become level or, in several cases when the reaction was slow ( $t_{1/2} > 10$  hours), until the absorbance of **3a** had reached  $< 30\%$  of its initial value.

The trichloroacetamide (a by-product of the reaction) C=O bond appeared as a doublet peak (1745 and 1733  $\text{cm}^{-1}$ ) close to the monitored **3a** absorbance on all the spectrums collected after the reaction was started. Due to the partial solubility of trichloroacetamide in toluene at 0 °C, it usually reached saturation point (at ca. 50% conversion), went supersaturated, and finally precipitated from the solution and became leveled at the saturation point (usually at ca. 60-80% conversion, depending on the rate of the reaction). The resulted IR spectrum after this by-product precipitation could be relatively messy and the absorbance of the **3a** trichloroacetimidate peak could be influenced in some cases. In order to obtain accurate data information, the reaction progress after precipitation of the amide by-product was disposed during data analysis.

After 4-NBSA was added to the reaction mixture, an immediate decrease of the monitored acetimidate absorbance and a concurrent increase of the amide by-product peak were observed, and the amount of decrease/increase, after converted to the concentration change by the beers law plot, is equivalent to the amount of acid added. This shows that after acid addition, **3a** is immediately quantitatively protonated and forms the epi-sulfonium ion and trichloroacetamide. If this step is prior to the rate limiting process (this is proved later by different access experiments, see data analysis below), at the point when  $x\%$  **3a** was consumed ( $x\%$  = the amount of 4-NBSA added), the product formation is about zero. Therefore, when data was analyzed, the first  $x\%$  conversion of **3a** was not considered as part of the reaction progress, and the “0% conversion point” and “zero time point” was placed at  $[\mathbf{3a}] = (1-x\%) \cdot [\mathbf{3a}]_{\text{initial}}$ .

Data under steady state conditions (5–60% conversion) were used in the kinetic analysis. Acid-catalyzed addition reaction (i.e., racemic background reaction) does not contribute substantially to the overall reaction rate under thiourea-catalyzed conditions; the initial rate of the racemic background reaction is  $\sim 2\%$  of the initial rate of the asymmetric reaction. The enantiomeric excess of the reaction under the standard in situ IR condition was 80-85%.

The figure below depicts a representative plot of [trichloroacetimidate (**3a**)] versus time. The red and blue data points are two independent ReactIR (RIR) reaction progresses monitored at the same condition (except that RIR run II also had added dibromomethane as NMR internal standard). The green and orange data points are  $^1\text{H}$  NMR analysis of RIR run II by taking aliquots at certain time points to validate that the RIR data represents both consumption of starting material (SM) and accumulation of product **4a** (pdt) (the orange data points were applied to equation:  $\text{conversion}(M) = [\mathbf{3a}]_{\text{initial}} - \text{yield}(M)$ , so that it could overlay with the RIR data). Concentration versus time data were converted to rate versus concentration data by analytical differentiation of a seventh-order polynomial fit to the concentration versus time data using methods described in the following reference: Zuend, S. J.; Jacobsen E. N. *J. Am. Chem. Soc.* **2007**, *129*, 15872–15883.



Rates of epi-sulfonium ring opening with indole catalyzed by 4-NBSA at different  $[3a]$ ,  $[indole]$  and  $[4-NBSA]$ . Rates are provided in  $M s^{-1}$  ( $\times 10^{-6}$ ).

Reaction condition:  $[3a]_i = 0.050 M$ ,  $[indole]_i = 0.10 M$ .

conversion of $3a$ (%)	$[3a]$ (M)	$[indole]$ (M)	$[4-NBSA]_T = 2.5 \text{ mM}$	$[4-NBSA]_T = 5.0 \text{ mM}$	$[4-NBSA]_T = 7.5 \text{ mM}$	$[4-NBSA]_T = 10 \text{ mM}$
10	0.045	0.095	4.84	7.24	9.32	12.6
20	0.040	0.090	4.53	7.93	9.29	13.4
30	0.035	0.085	4.27	8.11	9.30	13.6
40	0.030	0.080	4.04	7.98	9.26	13.4
50	0.025	0.075	3.82	7.96	9.05	13.2
60	0.020	0.070	3.54	8.08	8.67	12.8
70	0.015	0.065	3.15	7.86	8.31	12.5

Reaction condition:  $[3a]_i = 0.050 M$ ,  $[4-NBSA]_T = 0.0050 M$ .

conversion of $3a$ (%)	$[3a]$ (M)	$[indole]_i = 0.050 M$	$[indole]_i = 0.10 M$	$[indole]_i = 0.20 M$	$[indole]_i = 0.30 M$
10	0.045	3.48	6.65	16.1	26.1
20	0.040	3.19	6.55	17.8	30.7
30	0.035	2.94	6.30	18.5	33.7
40	0.030	2.70	6.18	18.7	35.1
50	0.025	2.45	6.13	19.1	36.1
60	0.020	2.18	5.94	19.9	37.6
70	0.015	1.84	5.49	20.3	39.5

Reaction condition:  $[indole]_i = 0.10 M$ ,  $[4-NBSA]_T = 0.0050 M$ .

conversion of indole (%)	$[indole]$ (M)	$[3a]_i = 0.050 M$	$[3a]_i = 0.025 M$
5	0.095	6.65	5.19
10	0.090	6.55	5.20
15	0.085	6.30	4.95
20	0.080	6.18	
25	0.075	6.13	
30	0.070	5.94	
35	0.065	5.49	

Reaction condition:  $[3a]_i = 0.050$  M,  $[\text{indole}]_i = 0.10$  M,  $[4\text{-NBSA}]_T = 0.0050$  M.

conversion of <b>3a</b> (%)	$[\text{indole}]$ (M)	$[\text{TCAA}]_i = 0^a$	$[\text{TCAA}]_i = 0.010$ M	$[\text{TCAA}]_i = \text{ca. } 0.025$ M <sup>b</sup>
10	0.045	6.68	8.67	10.5
20	0.040	7.21	8.91	9.87
30	0.035	7.36	9.04	8.94
40	0.030	7.14	8.76	8.01
50	0.025	6.82	8.09	7.23
60	0.020	6.66	7.09	6.55
70	0.015	6.58	6.01	5.79

<sup>a</sup> TCAA = trichloroacetamide.

<sup>b</sup> Pre-saturated with TCAA. The saturation concentration of TCAA in toluene at 0 °C is ca. 0.025 M.

Rates of epi-sulfonium opening with indole catalyzed by 4-NBSA and chiral thiourea **1a** at different  $[\text{indole}]$ ,  $[4\text{-NBSA}]$  and  $[1d]$ . Rates are provided in  $\text{M s}^{-1}$  ( $\times 10^{-5}$ ).

Reaction condition:  $[3a]_i = 0.050$  M,  $[\text{indole}]_i = 0.10$  M,  $[1d]_T = 0.0050$  M.

conversion of <b>3a</b> (%)	$[3a]$ (M)	$[\text{indole}]$ (M)	$[4\text{-NBSA}]_T = 0.5$ mM	$[4\text{-NBSA}]_T = 1.0$ mM	$[4\text{-NBSA}]_T = 2.5$ mM	$[4\text{-NBSA}]_T = 5.0$ mM
10	0.045	0.095	2.79	6.06		
20	0.040	0.090	1.90	4.50	10.4	19.4
30	0.035	0.085	1.20	3.10	8.20	14.7
40	0.030	0.080	0.86	2.13	6.42	10.8
50	0.025	0.075	0.72	1.68	4.76	8.23
60	0.020	0.070	0.54	1.42	3.87	6.72
70	0.015	0.065	0.45	1.10	3.40	5.59

Reaction condition:  $[3a]_i = 0.050$  M,  $[\text{indole}]_i = 0.10$  M,  $[4\text{-NBSA}]_T = 0.0010$  M.

conversion of <b>3a</b> (%)	$[3a]$ (M)	$[\text{indole}]$ (M)	$[1d]_T = 0.5$ mM	$[1d]_T = 1.0$ mM	$[1d]_T = 2.5$ mM	$[1d]_T = 5.0$ mM
10	0.045	0.095	0.67	1.13	3.18	6.06
20	0.040	0.090	0.41	0.71	2.16	4.50
30	0.035	0.085	0.32	0.55	1.38	3.10
40	0.030	0.080	0.26	0.39	1.00	2.13
50	0.025	0.075	0.20	0.32	0.84	1.68
60	0.020	0.070			0.62	1.42
70	0.015	0.065			0.50	1.10

Reaction condition:  $[3a]_i = 0.050$  M,  $[4\text{-NBSA}]_T = 0.0010$  M,  $[1d]_T = 0.0025$  M.

conversion of <b>3a</b> (%)	$[3a]$ (M)	$[\text{indole}]_i = 0.050$ M	$[\text{indole}]_i = 0.10$ M	$[\text{indole}]_i = 0.15$ M	$[\text{indole}]_i = 0.20$ M
10	0.045	1.57	3.18	4.48	5.96
20	0.040	0.97	2.16	3.03	3.89
30	0.035	0.56	1.38	2.08	2.66
40	0.030	0.41	1.00	1.66	2.25
50	0.025	0.26	0.84	1.35	1.91
60	0.020	0.16	0.62	1.06	1.55
70	0.015		0.50	9.23	1.40

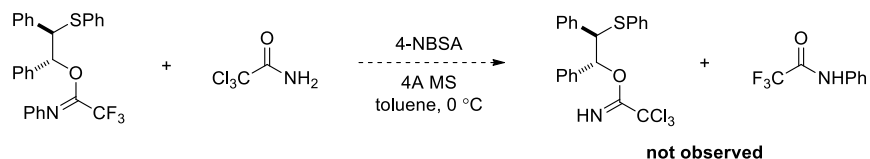
Reaction condition: [indole]<sub>i</sub> = 0.10 M, [1d]<sub>T</sub> = 0.0050 M.

conversion of indole (%)	[indole] (M)	[4-NBSA] <sub>T</sub> = 0.0010 M		[4-NBSA] <sub>T</sub> = 0.0025 M	
		[3a] <sub>i</sub> = 0.050 M	[3a] <sub>i</sub> = 0.075 M	[3a] <sub>i</sub> = 0.050 M	[3a] <sub>i</sub> = 0.075 M
5	0.095	5.85	5.23		
10	0.090	4.29	3.50		
15	0.085	2.94	2.18		
20	0.080	2.05	1.63	6.81	6.15
25	0.075	1.65	1.42	5.05	4.88
30	0.070	1.40	1.08	3.95	3.76
35	0.065	1.09	0.92	3.43	3.02

### Derivation of empirical rate law

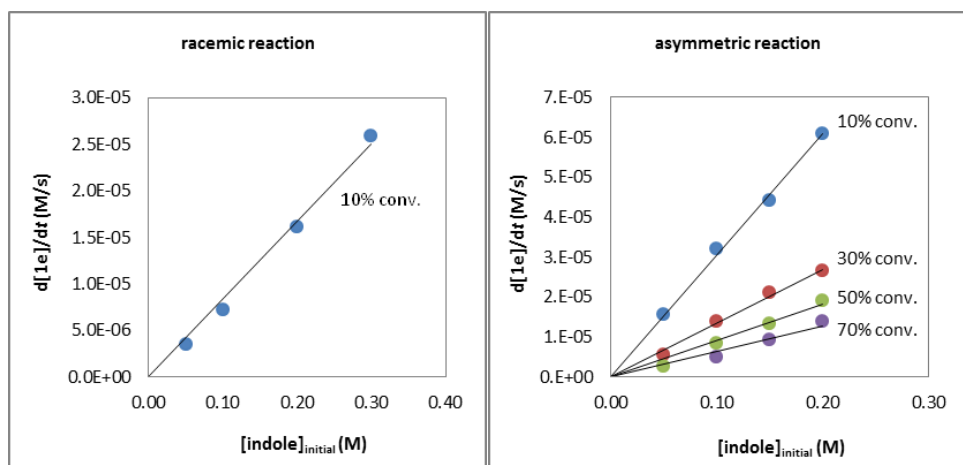
Rate dependence on starting material **3a**: 0<sup>th</sup> order – formation of epi-sulfonium ion from **3a** is quantitative. This is based on:

- 1) Kinetic data by in situ IR study showed that the rate of the reaction is independent on the concentration of **3a** in both racemic and asymmetric conditions.
- 2) An inverse rate dependence on trichloroacetamide – a by-product generated during the decomposition of **3a** to form epi-sulfonium ion, was NOT observed.
- 3) Treatment of **3a'** with trichloroacetamide under acid-catalyzed condition did not furnish anion-metathesis product **3a** (see equation below).

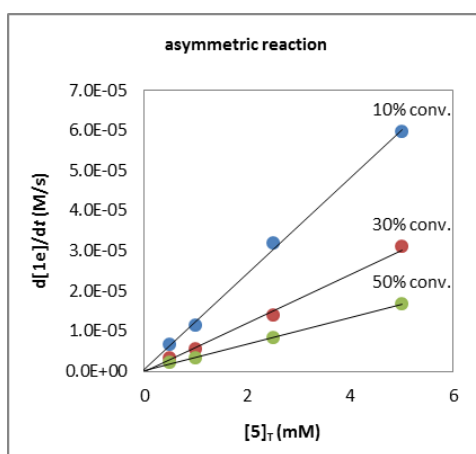
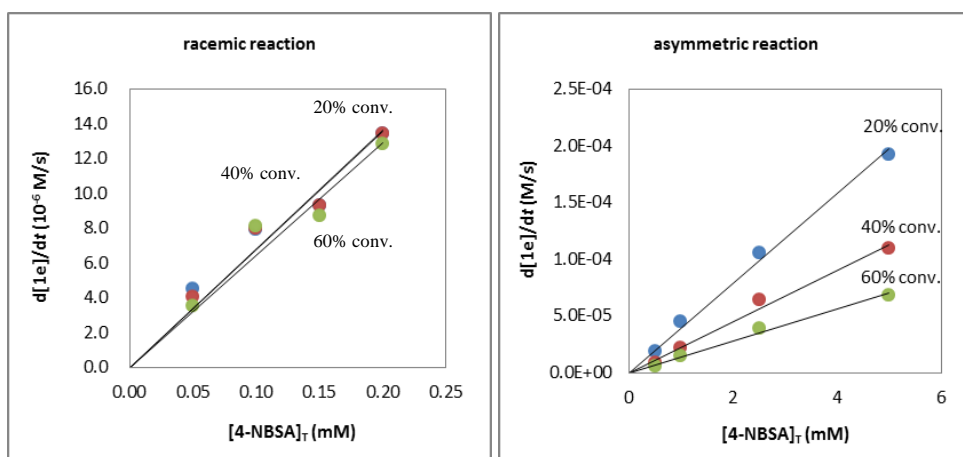


- 4) During in situ IR study, an immediate decrease of the monitored acetimidate absorbance and a concurrent increase of the amide by-product peak were observed after 4-NBSA was added to the reaction mixture. The amount of decrease/increase of absorbance, after converted to the concentration change by the beers law plot, is equivalent to the amount of acid added.

Rate dependence on indole: 1<sup>st</sup> order.



Rate dependence on acid and catalyst: 1<sup>st</sup> order.



Empirical rate laws:

For racemic reaction (catalyzed by 4-NBSA only):

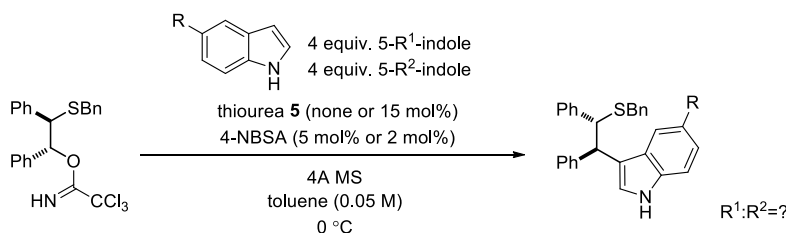
$$d[\mathbf{3a}]/dt = k_{\text{rac}} [4\text{-NBSA}]_{\text{T}} [\text{indole}].$$

For asymmetric reaction (catalyzed by thiourea and 4-NBSA):

$$d[\mathbf{3a}]/dt = k_{\text{asym,observed}} [4\text{-NBSA}]_{\text{T}} [\mathbf{1d}]_{\text{T}} [\text{indole}].$$

#### 4. Data for linear free energy relationship study – Mayr analysis

General procedure for competition experiments:



An oven-dried vial was charged with **3a** (11.6 mg, 0.025 mmol), thiourea catalyst (none for a racemic reaction or, 2.4 mg, 3.75  $\mu$ mol for an asymmetric reaction), nucleophile I (0.10 mmol, 4.0 equiv), nucleophile II (0.10 mmol, 4.0 equiv) and 4Å molecular sieves (15 mg, powder, activated). The vial was cooled to  $-78$  °C, and toluene was added with stirring. The vial was then placed in a 0 °C ice bath until all the reactants and catalyst were fully dissolved. 4-NBSA (freshly prepared stock solution, 0.5 M in THF, 10  $\mu$ L, 5 mol% for a racemic reaction or, 4  $\mu$ L, 2 mol% for an asymmetric reaction) was added to the solution via syringe. The reaction mixture was stirred at 0 °C for 4 h, and then quenched at the same temperature by addition of  $\text{NEt}_3$  ( $\sim$ 10  $\mu$ L). The reaction was filtered through a short silica plug, and the plug was washed with small amounts of toluene and DCM sequentially. The combined organic solutions were concentrated under vacuum to yield the crude products mixture, which was dissolved in  $\text{CDCl}_3$ , and analyzed with  $^1\text{H}$  NMR spectroscopy (the two adjacent benzylic protons  $\alpha$  and  $\beta$  to the indole ring and the methylene protons in the benzylsulfanyl group were integrated, if well resolved from the rest NMR resonances). The relative rate constant  $k_{\text{rel}}$  for 5-substituted indoles are with respect to the rate constant of *H*-indole ( $k_{\text{rel}} = 1$ ). The absolute rate constant  $k$  ( $k_{\text{rac}}$  and  $k_{\text{asym}}$ ) for 5-R-indoles are calculated with the equation:  $k = k_{\text{rel}} \times k_{H\text{-indole}}$ , assuming that the kinetic profiles of substituted indoles are the same as *H*-indole.

General procedure for in situ IR study:

Followed the procedure described in section 1.

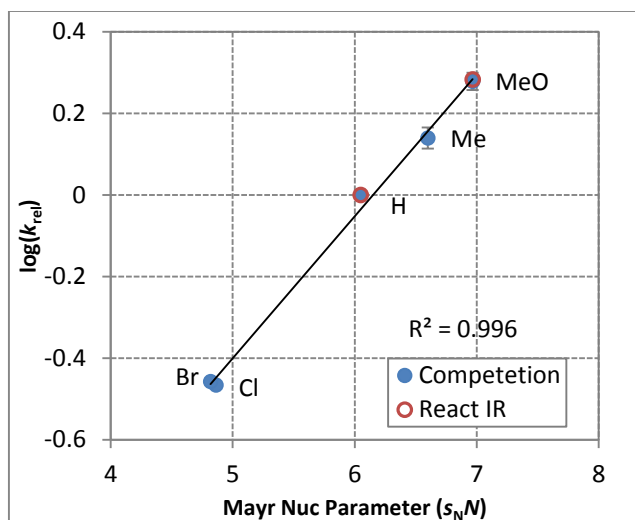
$N$  is the Mayr nucleophilicity parameter,  $s_N$  is the nucleophile-specific parameter, both obtained from the Mayr database of reactivity parameter.

For the racemic background reaction:

R	$N$	$s_N$	$s_N N$	$k_{\text{rel}}^a$				$\log k_{\text{rel}}$	$k_{\text{rel}}^b$ (RIR)
				I	II	III	average		
MeO	6.22	1.12	6.97	1.97	1.94	1.79	1.90	0.29	1.92
Me	6.00	1.10	6.60	1.44	1.32	-	1.38	0.15	-
H	5.55	1.09	6.05	1	-	-	1	0	1
F	-	-	-	0.505	0.532	0.505	0.514	-0.30	-
Cl	4.42	1.10	4.86	0.342	-	-	0.342	-0.47	-
Br	4.38	1.10	4.82	0.348	-	-	0.348	-0.46	-

<sup>a</sup> Obtained from competition experiments.

<sup>b</sup> Obtained from independent in situ IR study.

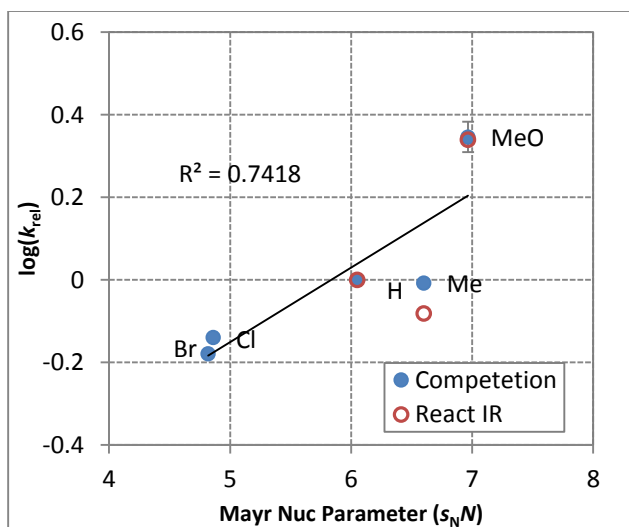


For thiourea **5**-catalyzed asymmetric reaction:

R	N	$s_N$	$s_N N$	$k_{rel}^a$				$\log k_{rel}$	$k_{rel}^b$ (RIR)
				I	II	III	average		
MeO	6.22	1.12	6.97	2.23	2.41	2.02	2.22	0.35	2.19
Me	6.00	1.10	6.60	0.98	0.99	-	0.98	0.003	0.83
H	5.55	1.09	6.05	1	-	-	1	0	1
F	-	-	-	1.01	1.04	0.94	1.00	0.008	1.16
Cl	4.42	1.10	4.86	0.73	-	-	0.73	-0.14	-
Br	4.38	1.10	4.82	0.66	-	-	0.66	-0.18	0.70

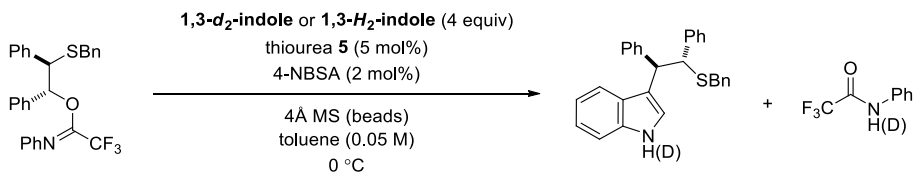
<sup>a</sup> Obtained from competition experiments.

<sup>b</sup> Obtained from independent in situ IR study.



## 5. Data for kinetic isotope effect study

General information:



The KIE study was performed with in situ IR spectroscopy. 1,3-*d*<sub>2</sub>-indole was synthesized according to the procedure below, and the deuterium incorporation ratio were determined by <sup>1</sup>H NMR to be 96% (position 3) and >99% (position 1). A modified substrate **3a** with *N*-phenyltrifluoroacetimidate was used to avoid rapid isotope scrambling between the acidic protons on substrate **3a** and the deuterium at 3-position of 1,3-*d*<sub>2</sub>-indole catalyzed by Brønsted acid. It has been demonstrated that the acetimidate substrate undergoes quantitative protonation and decomposition to form epi-sulfonium 4-nitrobenzene-sulfonate, and thereby the structure of the leaving group does not affect the reaction kinetic profile. Therefore, the KIE of the modified **3a** can represent that of **3a** under the same condition. Although the other proton sources (thiourea and 4-NBSA) were not precluded, a large excess of 1,3-*d*<sub>2</sub>-indole (4 equiv) and a relatively small amount of thiourea and acid (5 mol% and 2 mol%, respectively) were used to make sure the total isotopic concentration of exchangeable H was less than 3%.

Procedure of KIE study with in situ IR monitoring:

An oven-dried two-necked reaction vessel equipped with an 1/8" long stir bar was charged with indole (35.1 mg, 0.30 mmol) or 1,3-*d*<sub>2</sub>-indole (35.7 mg, 0.30 mmol) in a glove-box under dry nitrogen atmosphere (H<sub>2</sub>O < 0.1 ppm), and sealed with rubber septum. Thiourea **1a** (freshly prepared stock solution 0.015 M in toluene, 667 μL, 10.0 μmol), molecular sieves (4Å, beads, 40 mg, activated) and anhydrous toluene (433 μL) were transferred into the vessel quickly under air atmosphere and the vessel was purge with dry nitrogen several times before it was attached to an in situ infrared (IR) spectroscopy probe that had been dried with a heat gun. An ice bath was applied to cool the reaction mixture down to 0 °C with stirring for 5 min, and a background IR spectrum was collected (256 scans). Continuous data collection was started (4 spectra/min, 50 scans/spectrum). A freshly prepared stock solution of **3a'** (36.9 mg, 0.075 mmol) in toluene (0.4 mL) was added by syringe to the vessel. When the IR absorbance of the trichloroacetimidate C=N bond (height to baseline, 1713 cm<sup>-1</sup>) had become level. A freshly prepared stock solution of 4-NBSA (4 μL of a solution of 101.6 mg 4-NBSA in 1 mL THF, 2.0 μmol) was added to start the reaction. The reaction was monitored until the absorbance of **3a'** at 1670 cm<sup>-1</sup> had become level. Data was processed analogous to previously described in section 1.

## Kinetic isotope effect data

Rates of independent KIE reactions catalyzed by 4-NBSA and chiral thiourea **5**. Rates are provided in  $\text{M s}^{-1}$  ( $\times 10^{-5}$ ). Rate data become unreliable after 40% conversion due to peak overlap, and so only data from first 40% conversion are used here.

conversion of <b>3a'</b> (%)	[ <b>3a'</b> ] (M)	1,3- <i>H</i> <sub>2</sub> -indole		1,3- <i>d</i> <sub>2</sub> -indole (exp. I)		1,3- <i>d</i> <sub>2</sub> -indole (exp. II)	
		[ <b>3a'</b> ] <sup>a</sup>	[amide] <sup>b</sup>	[ <b>3a'</b> ]	[amide]	[ <b>3a'</b> ]	[amide]
15	0.043	3.66	3.84	4.30	5.00	3.60	4.34
30	0.035	2.51	2.50	3.05	3.59	2.43	2.82
40	0.030	1.39	1.30	1.76	2.15	1.33	1.42

<sup>a</sup> based on the N=C IR peak in the substrate **3a'**.

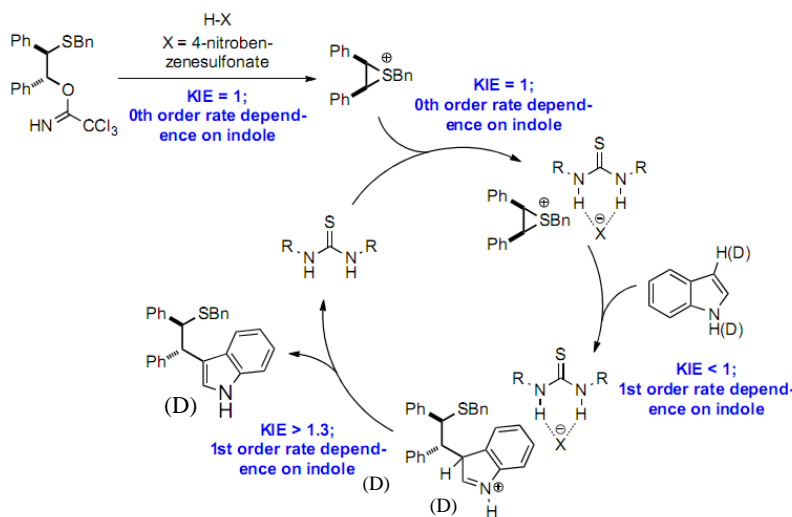
<sup>b</sup> based on the O=C IR peak in the by-product *N*-phenyltrifluoroacetamide.

conversion (%)	$r_{\text{H}}/r_{\text{D}}$			
	experiment I		experiment II	
	[ <b>3a'</b> ]	[amide]	[ <b>3a'</b> ]	[amide]
15	0.85	0.76	1.02	0.88
30	0.82	0.70	1.03	0.89
40	0.80	0.60	1.05	0.91

KIE ( $k_{\text{H}}/k_{\text{D}}$ ) =  $0.93 \pm 0.12$  (based on [**3a'**]) or, KIE ( $k_{\text{H}}/k_{\text{D}}$ ) =  $0.86 \pm 0.13$  (based on both [**3a'**] and [amide]). (**an inverse secondary kinetic isotope effect**)

The statistical value indicates an inverse secondary KIE. This is in consistence with indole addition being the rds ( $\text{sp}^2$  to  $\text{sp}^3$ ). However, since the error bar for this type of in situ IR analysis is usually about 10-15%, the saying that no primary KIE was observed would be a more rigorous conclusion.

## Discussion about the rate-limiting step of thiourea-catalyzed epi-sulfonium ion opening with indole



As shown in the scheme above, the 1st order rate dependence on indole (see section 1) has suggested that the rate limiting step for the reaction is either nucleophilic ring opening or re-aromatization. The  $\text{p}K_{\text{a}}$ -corrected Mayr

analysis (see section 2) supports the indole addition (ring opening) being the rds. A KIE study would be able to further verify this assumption if the absence of a primary KIE was observed at 3 position of indole.

If ring opening is the rds, besides the bond formation event in the indole addition to epi-sulfonium ion, another factor that can contribute to the KIE value is any interaction involving indole N-H(D) bond in the rate-limiting step. If indole N-H is broken during the rate-limiting step, a primary KIE ( $> 1.3$ ) should be observed; otherwise, a non-primary KIE should be observed ( $\sim 1.0$ ). In either case, if re-aromatization is rate-determining, meaning that the C-H(D) at position 3 is broken during this event, an overall primary KIE ( $> 1.3$ ) should be obtained. The absence of this observation excludes the possibility of re-aromatization being the rate-limiting step, and supports the indole nucleophilic addition being the rate-limiting step when taken together with other experimental results discussed in the previous paragraph.

Synthesis of *N*-phenyltrifluoroacetimidate:

To a solution of 2-(benzylthio)-1,2-diphenylethanol (300 mg, 0.94 mmol) and 2,2,2-trifluoro-*N*-phenylacetimidoyl chloride (216 mg, 169  $\mu$ L, 1.0 mmol) in DCM (5.0 mL) at 0 °C was added sodium hydride (60% suspension in mineral oil, 41.6 mg, 1.0 mmol). The mixture was stirred at room temperature for 2 h. Water and ethyl acetate were added to quench and dilute the reaction mixture. The aqueous layer was separated and extracted with EtOAc. The combined organic layers were washed with brine, dried over Na<sub>2</sub>SO<sub>4</sub>, concentrated and applied to flash column chromatography to obtain the product as a pale yellow gel ( $>90\%$  yield).

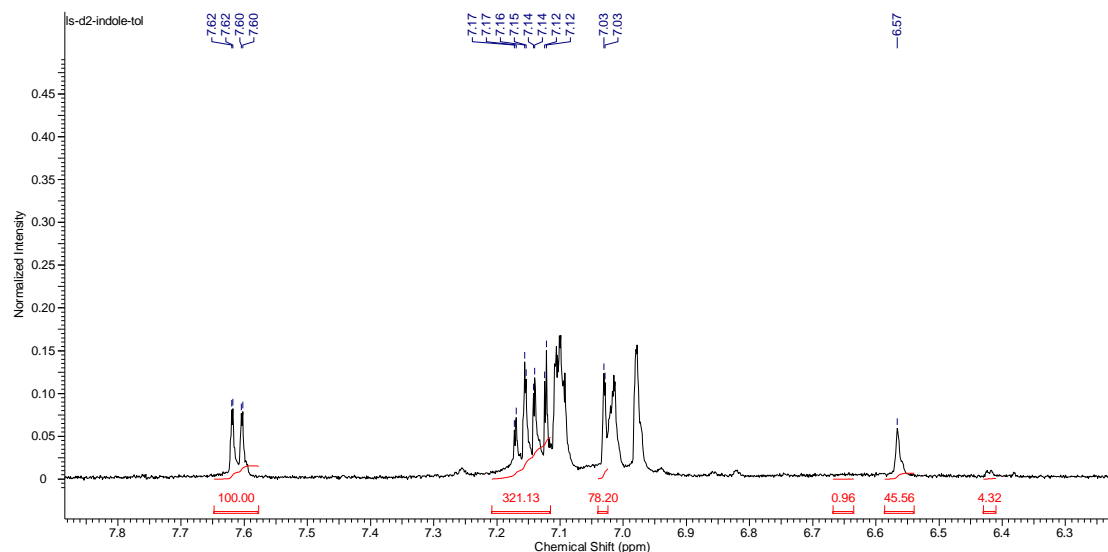
Characterization: IR (Film): 3031, 1707 (s), 1598, 1490, 1453, 1310, 1207 (s), 1137 (s), 1073, 1028, 968, 913, 695 (s) cm<sup>-1</sup>; <sup>1</sup>H NMR: (500 MHz, CDCl<sub>3</sub>)  $\delta$  7.44 - 7.20 (m, 13H), 7.20 - 6.97 (m, 5H), 6.61 (d,  $J=7.8$  Hz, 2H), 6.25 (br. s., 1H), 4.21 (d,  $J=7.8$  Hz, 1H), 3.76 (d,  $J=13.3$  Hz, 1H), 3.62 (d,  $J=13.3$  Hz, 1H); <sup>13</sup>C NMR: (125 MHz, CDCl<sub>3</sub>)  $\delta$  143.93, 137.82, 137.59, 136.97, 129.09, 129.00, 128.54, 128.41, 128.23, 128.11, 127.86, 127.55, 127.25, 127.05, 123.78, 119.33, 81.90, 54.17, 36.36; MS (ESI-APCI) exact mass calculated for [M-(CCl<sub>3</sub>C=NHO)] (C<sub>21</sub>H<sub>19</sub>S) requires  $m/z$  303.1, found  $m/z$  303.1.

Synthesis of 1,3-*d*<sub>2</sub>-indole:

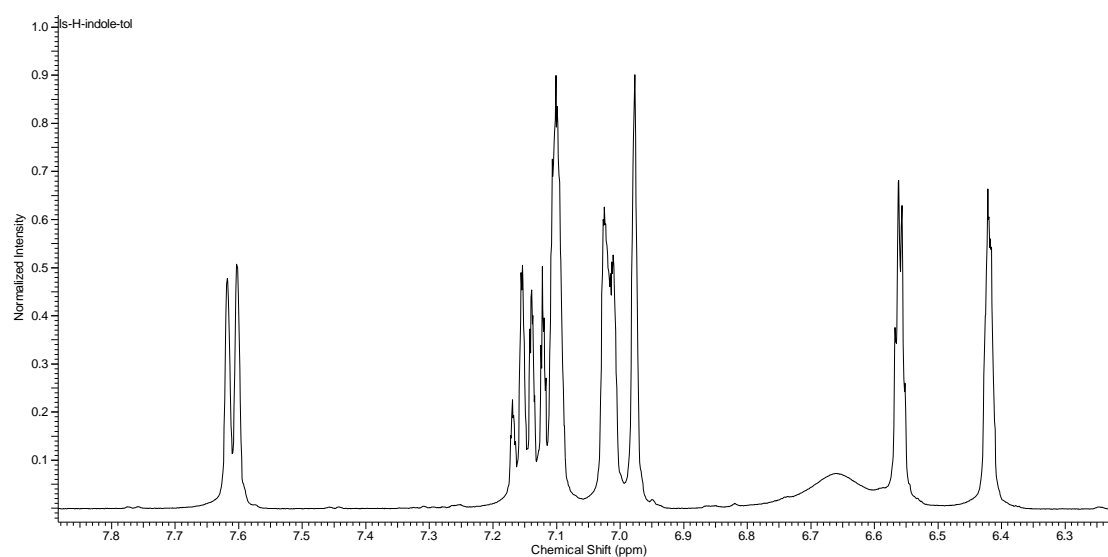
The mixture of indole (585 mg, 5 mmol) and *d*<sub>2</sub>-sulfuric acid (D<sub>2</sub>SO<sub>4</sub>, 0.001 M in D<sub>2</sub>O, 1 mL) was refluxed under nitrogen atmosphere for 48 h. The reaction was then cooled to room temperature, and extracted with anhydrous EtOAc (dried over 4Å MS overnight). The extract was washed with D<sub>2</sub>O twice, dried over Na<sub>2</sub>SO<sub>4</sub>, concentrated and applied to flash column chromatography to yield 3-*d*-indole as white crystals. (<sup>1</sup>H NMR showed partial incorporation of deuterium into the 2 position of indole under this relatively harsh condition.)

The obtained 3-*d*-indole was then dissolved in *d*<sub>4</sub>-methanol (CD<sub>3</sub>OD, 1 mL) and stirred under nitrogen atmosphere for 1 h. The solvent was then removed under vacuum, and the resulting solid was re-dissolved in *d*<sub>4</sub>-methanol (CD<sub>3</sub>OD, 1 mL) and stirred overnight under nitrogen atmosphere. The solvent was removed under vacuum to yield the desired 1,3-*d*<sub>2</sub>-indole as white/pale pink crystals. The isotope incorporation ratio of the product was determined by <sup>1</sup>H NMR (in *d*<sub>8</sub>-toluene) to be 96% (position 3), 54% (position 2) and  $>99\%$  (position 1).

### 1,3-*d*<sub>2</sub>-indole:



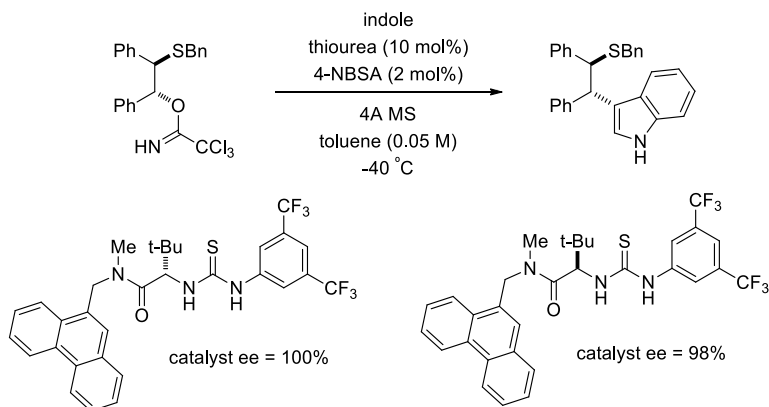
### indole:



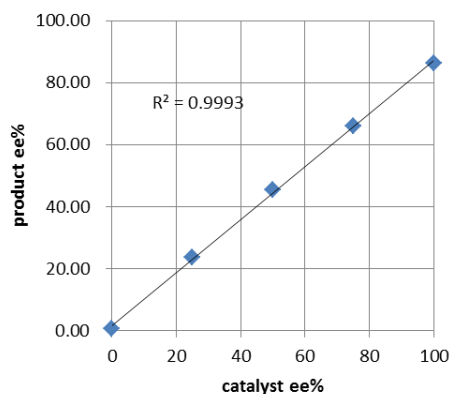
## 6. Data sets for non-linear effect study

### General information:

Non-linear effect study was conducted with a thiourea catalyst structurally analogues to **1d**, shown in the scheme below. This catalyst gives 85% ee under the model reaction condition (when **1d** provides 93% ee). The similar levels of stereo-induction and analogues structures led us to assume that the two catalysts induce selectivity in the same manner. The non-linear effect study was done at  $-40$  °C, a decreased temperature compared to the model condition in order to further exclude the effect of any background reaction. Otherwise, the procedure can refer to section 2.



cat ee% (R)	product ee%
0	0.67
25	23.63
50	45.40
75	66.14
100	86.18



## 7. Data kinetic analysis of reactions catalyzed by thiourea 1a-1e

Following the same procedure as described in section 3, reactions with thiourea **1a-1e** were analyzed with in situ IR spectroscopy. Data for thiourea **1d** are shown in section 1. Rates are provided in  $\text{M s}^{-1}$  ( $\times 10^{-5}$ ).

Reaction condition:  $[\mathbf{3a}]_i = 0.050 \text{ M}$ ,  $[4\text{-NBSA}]_T = 0.0010 \text{ M}$ ,  $[\text{thiourea}]_T = 0.0050 \text{ M}$ .

conversion of <b>3a</b> (%)	<b>[3a]</b> (M)	<b>1a</b> run I	<b>1a</b> run II	<b>1b</b> run I	<b>1b</b> run II	<b>1e</b> run I	<b>1e</b> run II
10	0.045	1.16	1.08	2.23	2.41	2.31	2.42
20	0.040	0.73	0.68	1.49	1.57	1.53	1.50
30	0.035	0.39	0.34	0.85	0.92	0.97	0.96
40	0.030	0.26	0.22	0.56	0.62	0.73	0.78
50	0.025	0.18	0.15	0.42	0.46	0.59	0.57
60	0.020	0.17		0.29	0.39	0.49	0.45

The following rate data are based on initial rates taken at 10% conversion of **3a**.  $1.40 \pm 1.4$

thiourea	<b>1a</b>	<b>1b</b>	<b>1e</b>	<b>1d<sup>b</sup></b>
$r_{\text{asym,observed}} (10^{-5} \text{ M s}^{-1})$	$1.12 \pm 0.06$	$2.32 \pm 0.10$	$2.36 \pm 0.06$	$6.08 \pm 0.36$
$r_{\text{rac}} (10^{-6} \text{ M s}^{-1})$	$1.40 \pm 1.4$			
$\ln(k_{\text{asym,major}})$	$2.79 \pm 0.07$	$3.67 \pm 0.05$	$3.71 \pm 0.03$	$4.72 \pm 0.09$
$\ln(k_{\text{asym,minor}})$	$1.16 \pm 0.07$	$1.54 \pm 0.05$	$1.34 \pm 0.03$	$1.91 \pm 0.09$
$\ln(\text{er})^a$	1.64	2.12	2.37	2.81

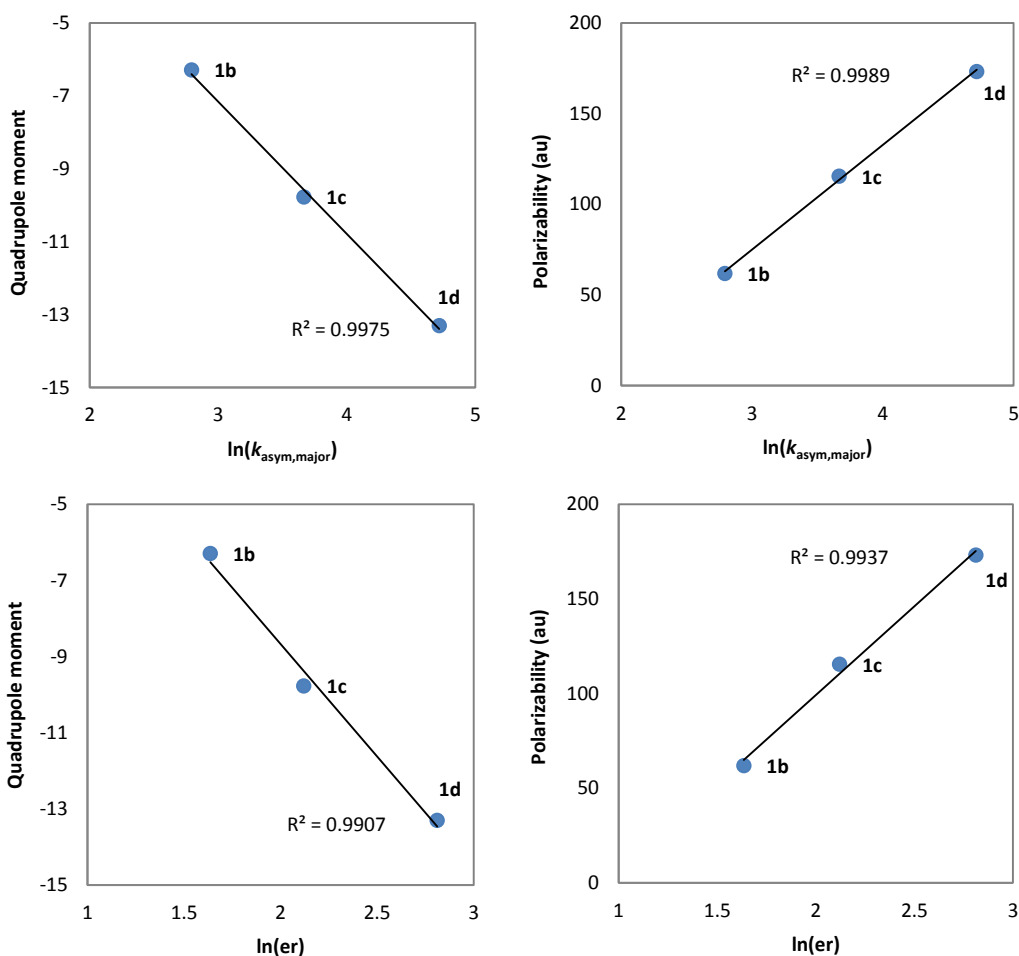
<sup>a</sup> Enantiomeric ratio data at  $0^\circ \text{C}$  were calculated based on the Eyring analysis in section 4. The direct experimental measurement of reaction ee at  $0^\circ \text{C}$  does not provide accurate data for the intrinsic enantioselectivity of the catalysts due to the competing racemic background reaction at this temperature. <sup>b</sup> Rate data for catalyst **1a** was calculated on the basis of over 6 reactions under the standard in situ IR condition, most of which are presented in section 1.

## 8. Correlations of arene properties with rate and enantioselectivity for catalysts **1b-1e**

The rate and enantioselectivity data were obtained in the same manner as in section 5. The ee's at 0 °C were calculated on the basis of the Eyring plots (section 4). The rates were measured by in situ IR spectroscopy. Quadrupole moments of different arenes were obtained from: Ng, K. M.; Ma, N. L.; Tsang, C. W. *Rapid Commun. Mass Spectrom.* **1998**, *12*, 1679–1684. Polarizabilities of different arenes were obtained from: Waite, J.; Papadopoulos, M. G.; Nicolaides, C. A. *J. Chem. Phys.* **1982**, *77*, 2536–2539, and the website of theoretical spectral database of polycyclic aromatic hydrocarbons (<http://astrochemistry.ca.astro.it/database/pahs.html>).

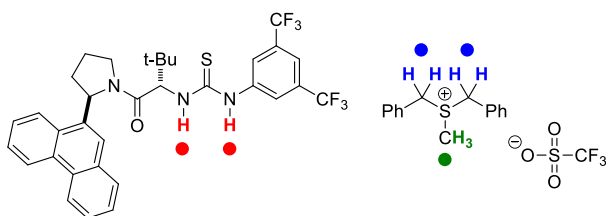
arene	polarizability	quadrupole moment	catalyst	$\ln(k_{\text{asym,major}})$	$\ln(\text{er})$
benzene	61.9	-6.29	<b>1b</b> (phenyl)	2.79	1.64
naphthalene	115.5	-9.77	<b>1c</b> (2-naphthyl)	3.67	2.12
phenanthrene	173.2	-13.30	<b>1d</b> (9-phenanthryl)	4.72	2.81
pyrene	205.7	-14.69	<b>1e</b> (4-pyrenyl)	4.54	2.55

Note: Pyrenyl catalyst **1e** can't fit into these correlations. An explanation has been provided in the main text. However, we can't fully understand this completely on this stage.



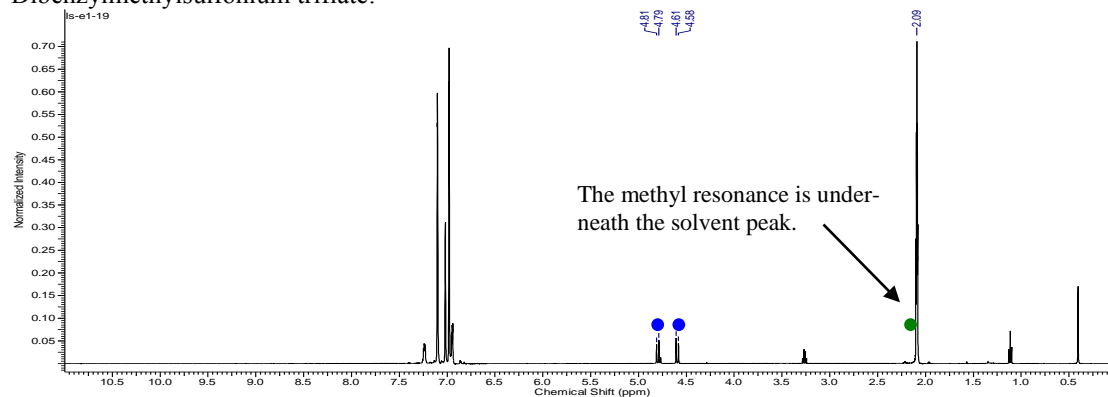
## 9. NMR binding study of thiourea **1** and dibenzylmethylsulfonium triflate **12**

General procedure for qualitative binding studies in  $d_8$ -toluene: An oven-dried vial was charged with thiourea **1** (5.0  $\mu\text{mol}$ ), **12** (4.0 mg, excess), and anhydrous  $d_8$ -toluene (0.5 mL). The suspension was placed in an ultrasound sonicator for 2-3 min. The mixture was filtered through a short plug with cotton to remove the insoluble white solid after sonication, and the cotton was washed with a small amount of  $d_8$ -toluene. The final concentration of the thiourea-sulfonium salt solution is ca. 0.0010 M. The composition of the complex is 1.05:1 (thiourea : sulfonium triflate) by  $^1\text{H}$  NMR analysis. The chemical shift of the diagnostic resonances are shown below (toluene  $-\text{CH}_3$   $\delta = 2.09$  as reference). For the synthesis of dibenzylsulfonium triflate salt, see: Miyatake, K. et. al. *J. Org. Chem.* **1998**, *63*, 7522–7524.

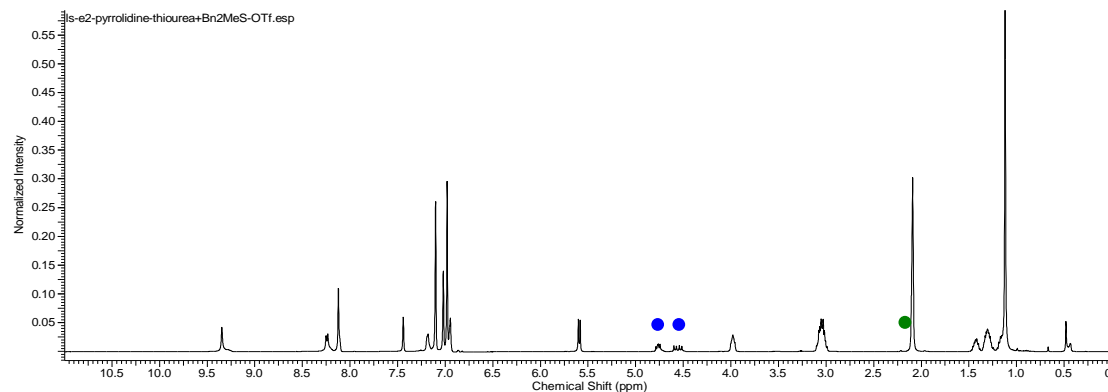


	thiourea N-H (ppm)	benzyl protons (ppm)	methyl protons (ppm)
thiourea <b>1d</b>	8.68, 7.25	-	-
<b>12</b>	-	4.80, 4.59	2.09
1:1 complex	9.92, 7.68	4.18, 4.03, 3.78	1.31

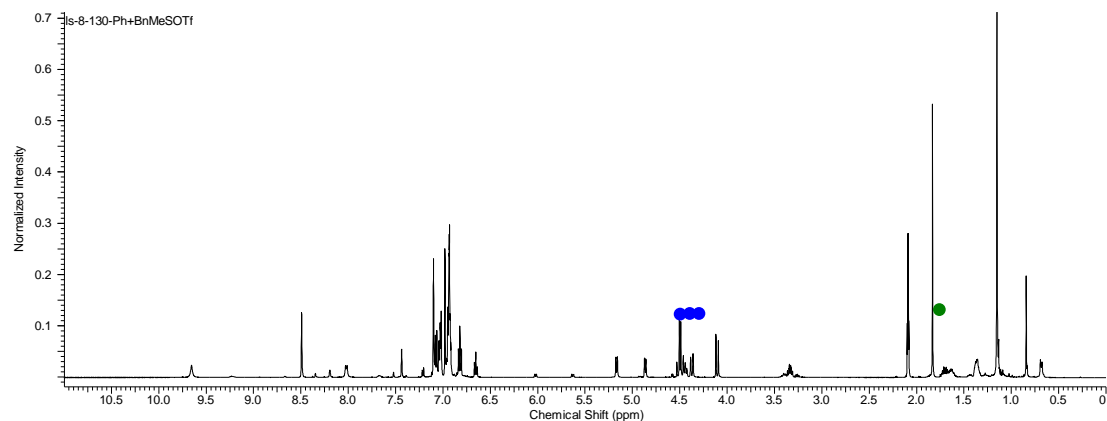
Dibenzylmethylsulfonium triflate:



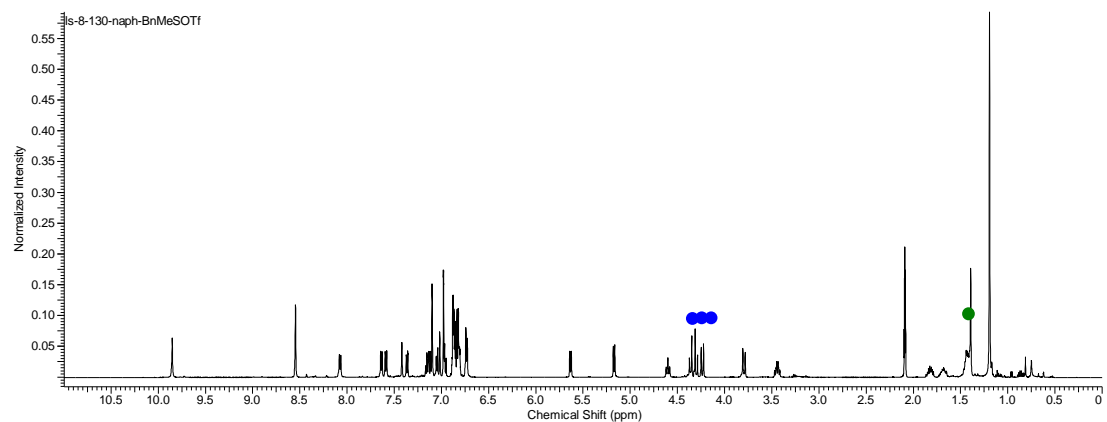
Thiourea **1a**-sulfonium triflate complex:



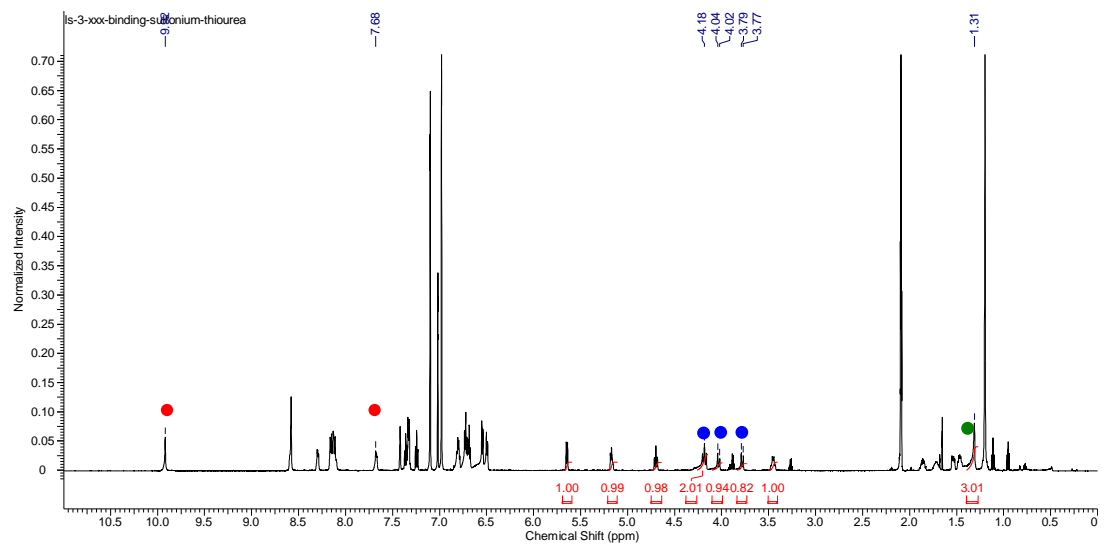
Thiourea **1b**-sulfonium triflate complex:



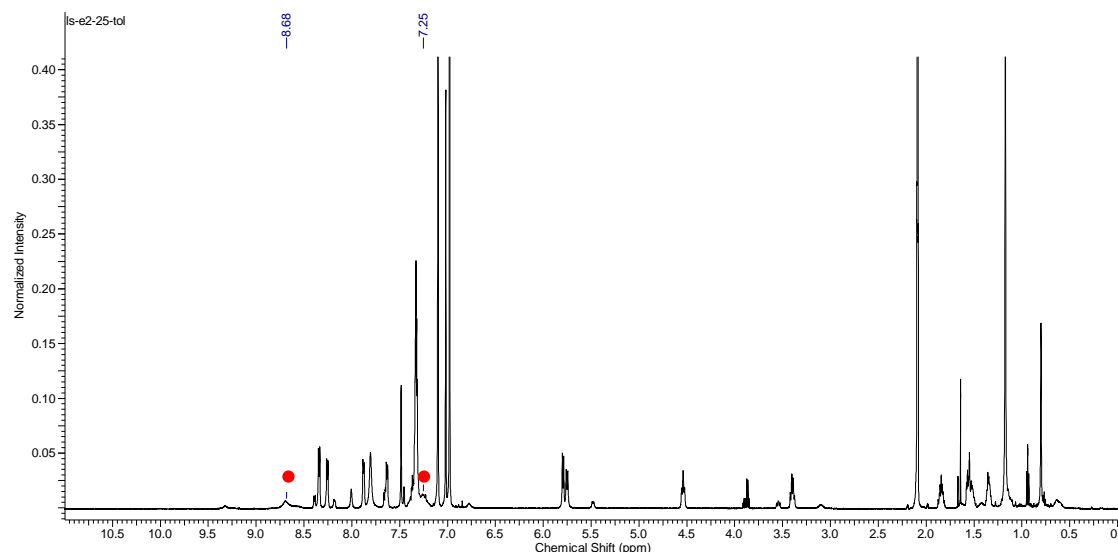
Thiourea **1c**-sulfonium triflate complex:



Thiourea **1d**-sulfonium triflate complex:



### Thiourea **1d**:



General procedure for quantitative binding studies in  $\text{CDCl}_3$ : An oven-dried vial was charged with thiourea **1** (0.050 mmol), **12** (18.9 mg, 0.050 mmol), and anhydrous  $\text{CDCl}_3$  (ca. 0.5 mL). The resultant solution was transferred to a 1.0 mL volumetric flask and diluted to 1.0 mL (final concentration: 0.050 mM), a  $^1\text{H}$  NMR spectrum of which was then recorded at 23 °C. The solution is further diluted to 0.025 mM, 0.010 mM, 0.0050 mM, 0.0020 mM, and 0.0010 mM, and each solution was subjected to  $^1\text{H}$  NMR analysis at the same temperature. The chemical shift of the  $-\text{CH}_3$  group on the sulfonium salt **12** was plotted against the total concentration of thiourea **1**, and the data fit was made on the basis of the following equations:

$$K_a = \frac{\alpha}{(1-\alpha)^2 [\text{conc.}]}$$

$$\alpha = \frac{\delta_{\text{obs}} - \delta_0}{\delta_{\text{max}} - \delta_0}$$

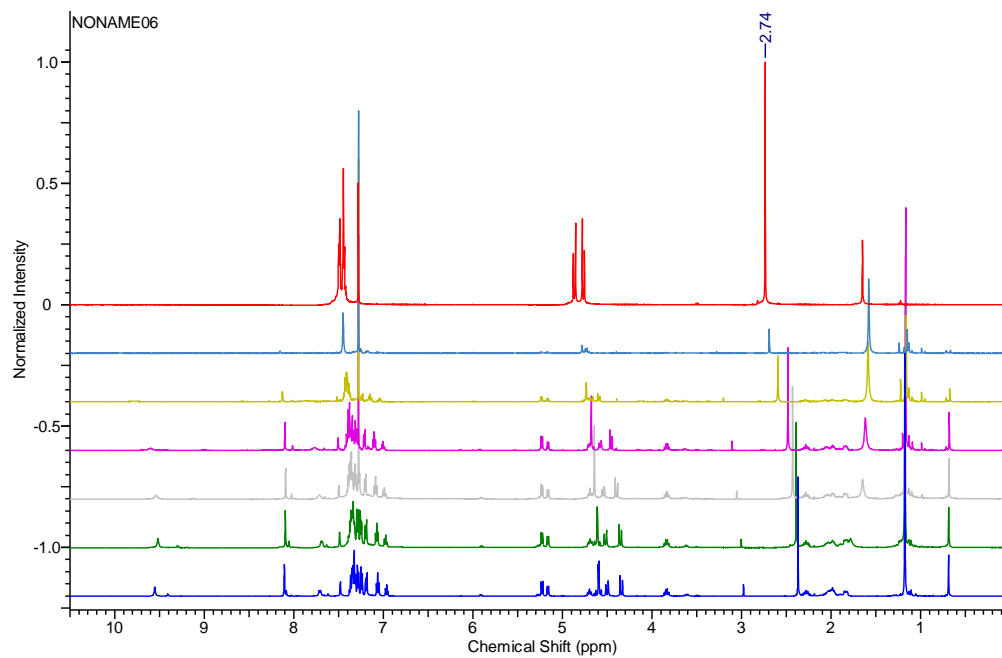
In which,  $K_a$  is the association constant,  $[\text{conc.}]$  is the total concentration of thiourea **1**,  $\delta_{\text{obs}}$  is the observed chemical shift of the methyl protons at  $[\text{conc.}]$  in ppm,  $\delta_{\text{max}}$  is the chemical shift of the methyl protons when **12** is complete bound to thiourea **1**, and  $\delta_0$  is the chemical shift the methyl protons in the absence of any thiourea ( $\delta_0 = 2.74$  ppm).

The parameters  $1/[\text{conc.}]$  and  $(1-\alpha)^2/\alpha$  were subjected to linear regression to yield the  $K_a$  value (slope) and  $R^2$ .

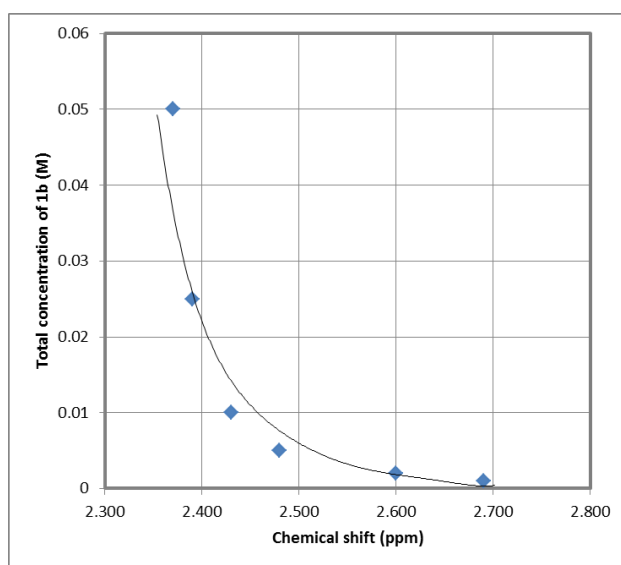
The data fit can also reply on the spreadsheet provided on the following website: <http://www.dur.ac.uk/j.m.sanderson/science/downloads.html>.

NMR spectra:

Phenyl thiourea **1b**:

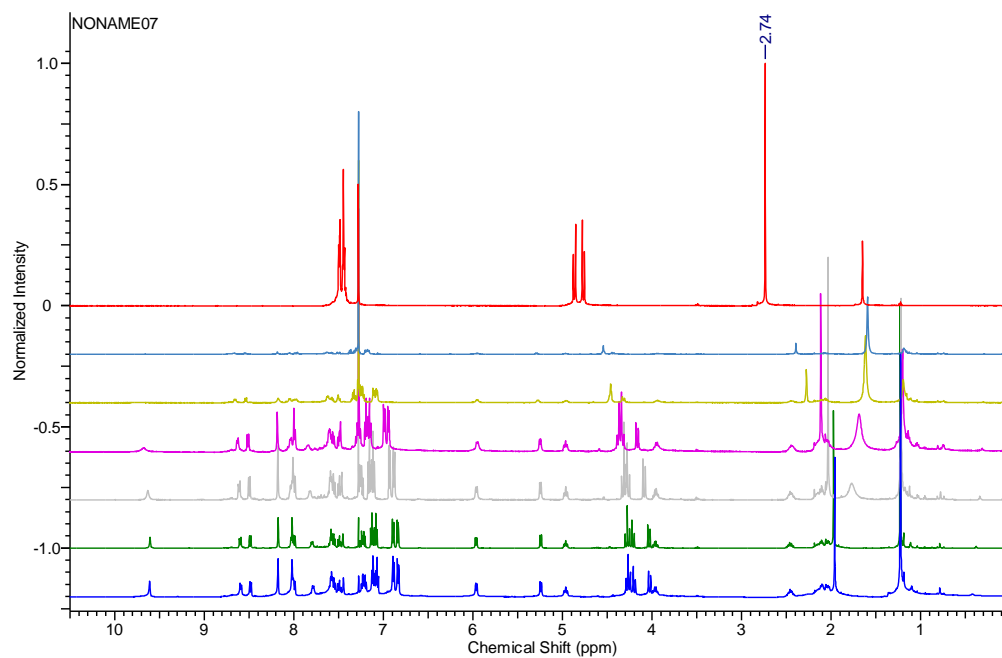


spectrum color	conc (M)	$\delta$ (ppm)
blue	0.050	2.370
green	0.025	2.390
gray	0.010	2.430
purple	0.005	2.480
yellow	0.002	2.600
iceblue	0.001	2.690

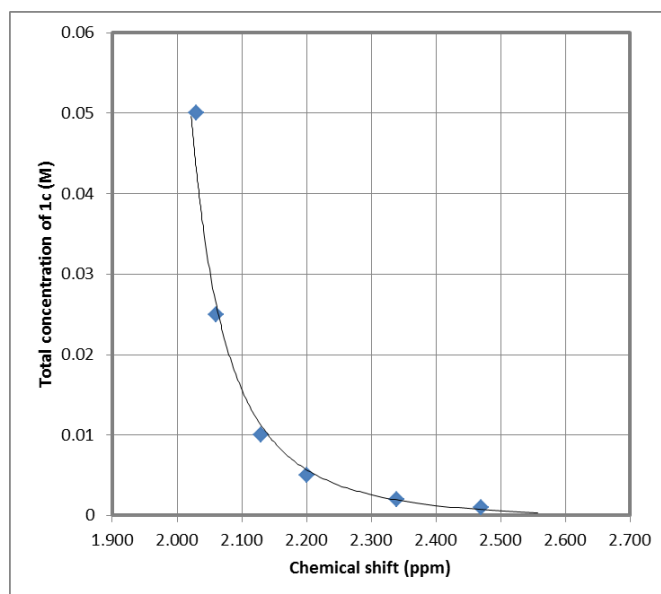


$$K_a = (1.16 \pm 0.16) \times 10^2, R_2 = 0.927$$

1-Naphthyl thiourea **1c**:

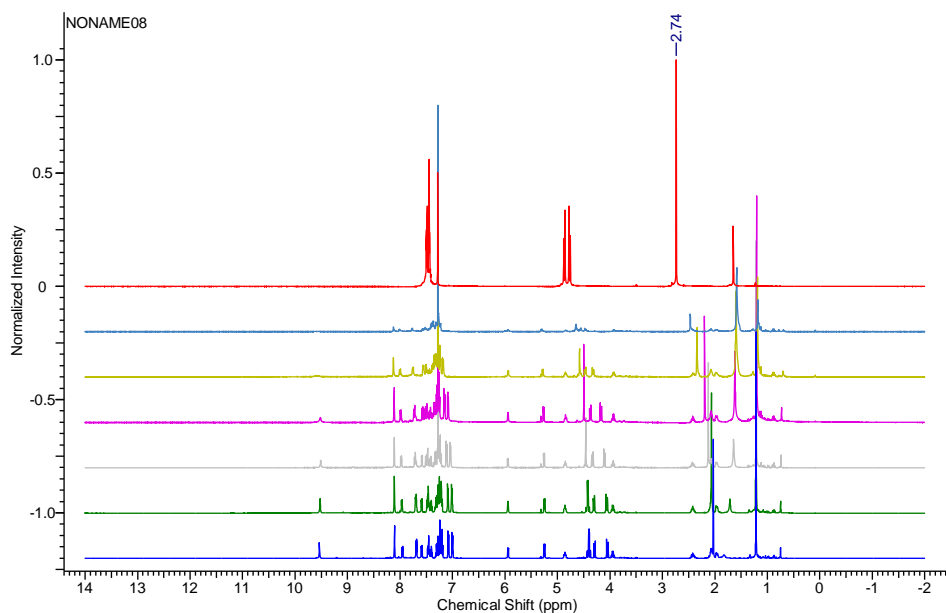


spectrum color	conc (M)	$\delta$ (ppm)
blue	0.05	2.030
green	0.025	2.060
gray	0.01	2.130
purple	0.005	2.200
yellow	0.002	2.340
iceblue	0.001	2.470

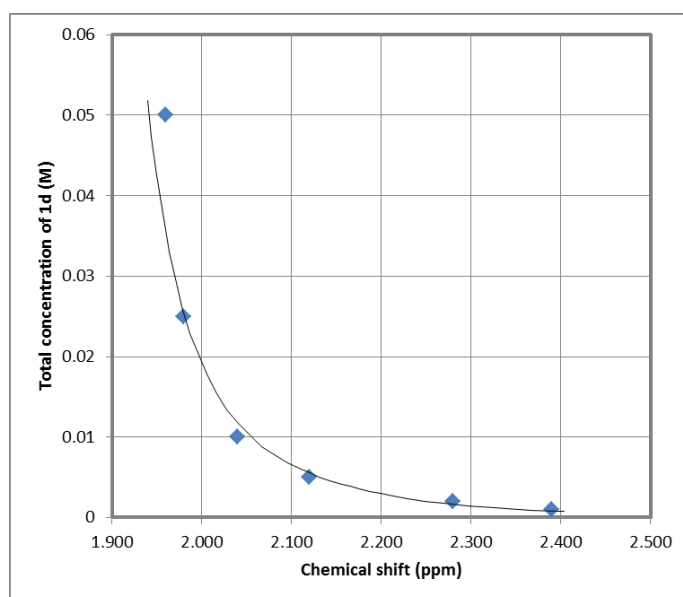


$$K_a = (7.02 \pm 0.37) \times 10^2, R_2 = 0.989$$

9-Phenanthryl thiourea **1d**:



spectrum color	conc (M)	$\delta$ (ppm)
blue	0.05	1.960
green	0.025	1.980
gray	0.01	2.040
purple	0.005	2.120
yellow	0.002	2.280
iceblue	0.001	2.390

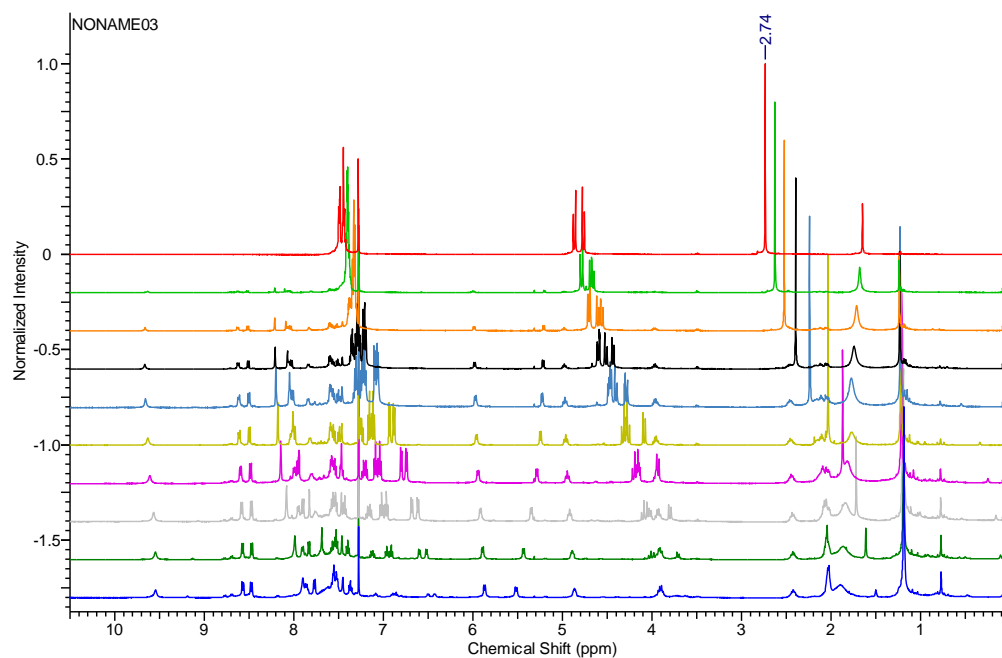
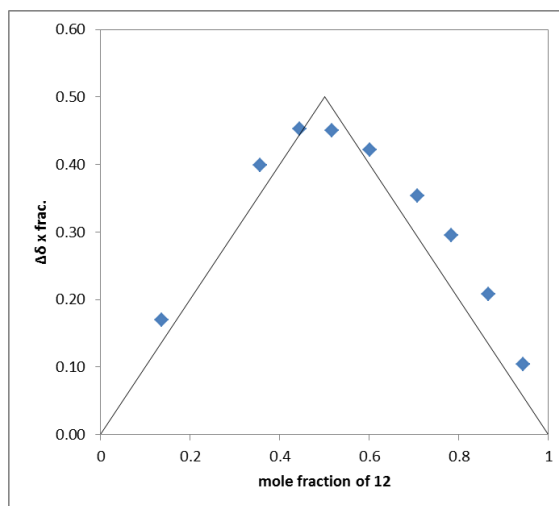


$$K_a = (1.00 \pm 0.03) \times 10^3, R_2 = 0.997$$

Job plot analysis:

The stoichiometry of the **1d•12** complex was determined using Job's method of continuous variation. A 2 mL solution containing 25.3 mg of **1d** (0.04 mmol, 0.02 M, solution A) in CDCl<sub>3</sub> and a 2 mL solution containing 15.1 mg of **12** (0.04 mmol, 0.02 M, solution B) in CDCl<sub>3</sub> were prepared in 2 mL volumetric flasks. A series of solutions were made in separate NMR tubes by combining certain volumes of solution A and solution B. For each sample, the mole fraction of substrate was determined analytically by integration of the substrate signals relative to the catalyst signals. The  $\Delta\delta$  for the methyl protons on **12** was determined at each mole fraction. The collected data was plotted as  $\Delta\delta \times$  substrate mole fraction vs. substrate mole fraction. The stoichiometry of the **1d•12** complex was determined using this method to be 1.08 : 1.

mole fraction of <b>12</b>	$\Delta\delta \times$ mole fraction
0.137	0.17
0.356	0.40
0.444	0.45
0.517	0.45
0.602	0.42
0.708	0.35
0.784	0.29
0.867	0.21
0.944	0.10



## 10. Structure-reactivity and structure-selectivity relationships of indoles and other $\pi$ -nucleophiles

Indoles pK<sub>a</sub>, inductive Hammett constant, calculated hydrogen bond energy involving indole N-H bond

R	$k_{\text{asym}}/k_{\text{rac}}^a$ (10 <sup>3</sup> )	pK <sub>a</sub>				$\sigma_I^e$	calc. H-bond energy (kcal/mol) <sup>f</sup>	
		calc. by ACD labs	exp. In H <sub>2</sub> O <sup>b</sup>	exp. In DMSO <sup>c</sup>	exp. In DMSO <sup>d</sup>		to benzene	to DMA <sup>g</sup>
H	8.7	17.00	16.97	20.82±0.01	20.95	0.00	2.65	8.17
Me	6.1	17.17		20.95±0.06		-0.04	2.61	8.02
MeO	9.8	16.70		20.71±0.04		0.27	2.66	8.18
F	16.5	16.16	16.30			0.52	2.88	8.56
Cl	18.4	16.09				0.47	2.97	8.92
Br	17.5	16.04	16.13			0.50	2.97	8.92

<sup>a</sup> For H-indole, the value was obtained from reaction progress study by in situ IR spectroscopy (conditions: 0.050 mmol **3a**, 0.10 mmol indole, 0.0050 mmol **1d**, 0.0010 mmol 4-NBSA, 50 mg 4Å MS in 2 mL toluene at 0 °C; see section 1 for procedure), and initial rates were taken at 10% conversion of **3a**. For the rest indole derivatives, the values were based on competition experiments (see section 2), and calculated using the following equation:

$$(k_{\text{asym}}/k_{\text{rac}})_{\text{NuH}} = (k_{\text{rel,asym,NuH}}/k_{\text{rel,rac,NuH}}) \times (k_{\text{asym,indole}}/k_{\text{rac,indole}}) = 8680 \times (r_{\text{rel,asym,NuH}}/r_{\text{rel,rac,NuH}})$$

<sup>b</sup> See: Yagil, G. *J. Phys. Chem.* **1967**, *71*, 1034-1044.

<sup>c</sup> Conducted using Bordwell method with 2-naphthylacetonitrile as indicator. For detailed procedure, see: Matthews, W. S.; Bares, J. E.; Bartmess, J. E.; Bordwell, F. G.; Cornforth, F. J.; Drucker, G. E.; Margolin, Z.; McCallum, R. J.; McCollum, G. J.; Vanier, N. R. *J. Am. Chem. Soc.* **1975**, *97*, 7006-7014.

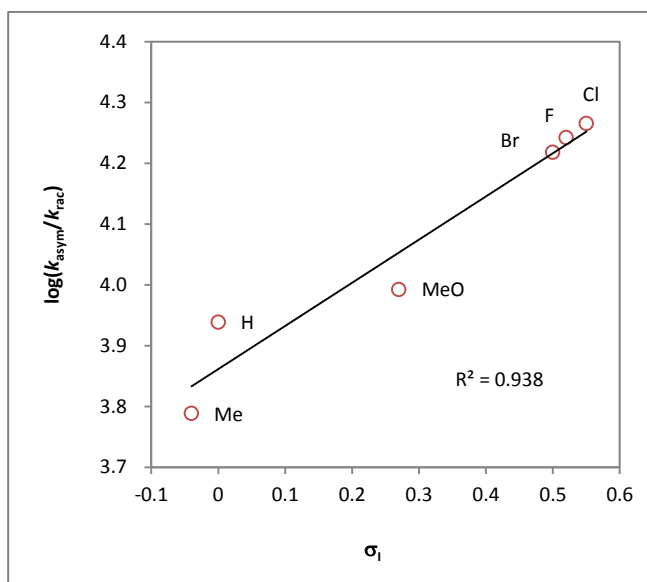
<sup>d</sup> See: Bordwell, F. G.; Drucker, G. E.; Fried, H. E. *J. Org. Chem.* **1981**, *46*, 632-635.

<sup>e</sup> The inductive Hammett constants are obtained from Hansch, C.; Leo, A. *Substituent Constants for Correlation Analysis in Chemistry and Biology*; Wiley-Interscience: NY, 1979.

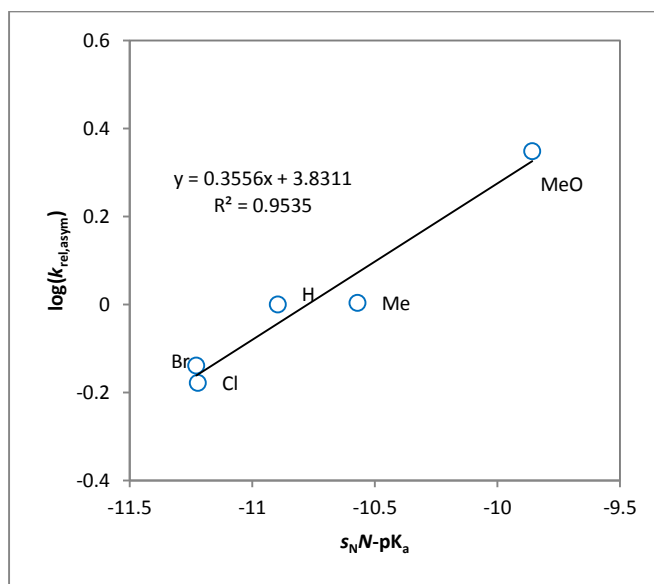
<sup>f</sup> Conducted using Gaussian 09, DFT B3LYP 6-31G(d).

<sup>g</sup> DMA = dimethylacetamide; amide oxygen as H-bond donor.

### Correlation between $\log(k_{\text{asym}}/k_{\text{rac}})$ and $\sigma_1$ of indole derivatives



### pK<sub>a</sub>-corrected Mayr analysis of the asymmetric reaction



### Structure-reactivity-selectivity study of $\pi$ -nucleophiles

General procedure:

For competition experiments: Following the procedure described in section 2, a second nucleophile was applied to a competition experiment with indole, and the relative rate with respect to indole was determined with  $^1\text{H}$  NMR spectroscopy. The relative rate of indole is set to 1.

For reaction kinetic study with in situ IR spectroscopy: Followed the procedure described in section 1. The reaction stoichiometry is shown below –

Azulene – 0.075 mmol **3a**, 0.15 mmol azulene, 7.5  $\mu\text{mol}$  **1d** or none, 7.5  $\mu\text{mol}$  4-NBSA (0.5 M in THF), 50 mg 4Å

MS, 1.5 mL toluene.

Pyrrole – 0.075 mmol **3a**, 0.15 mmol azulene, 7.5  $\mu\text{mol}$  **1d** or none, 3.75  $\mu\text{mol}$  4-NBSA (0.5 M in THF), 50 mg 4Å MS, 1.5 mL toluene.

*N*-methylindole – 0.10 mmol **3a**, 0.20 mmol azulene, 10.0  $\mu\text{mol}$  **1d** or none, 5.0  $\mu\text{mol}$  4-NBSA (0.5 M in THF), 50 mg 4Å MS, 1.5 mL toluene.

NuH	$r_{\text{rel,asym}}^{a,b}$	$r_{\text{rel,rac}}^{a,b}$	$(r_{\text{asym}}/r_{\text{rac}})_{\text{rel}}$ (compt.) <sup>b</sup>	$r_{\text{asym}}^c$ ( $10^{-6}$ M/s)	$r_{\text{rac}}^c$ ( $10^{-6}$ M/s)	$r_{\text{asym}}/r_{\text{rac}}$ (RIR) <sup>c</sup>
indole	1	1	1	1.40	60.8	43.4
benzotriazole	9.5	10.3	0.92	n/a <sup>d</sup>	n/a <sup>d</sup>	n/a <sup>d</sup>
azulene	0.038	0.26	0.15	4.10	13.2	3.2
pyrrole	0.21	2.03	0.11	1.17	3.69	3.2
<i>N</i> -methylindole	0.13	0.99	0.13	1.03	3.92	3.8

<sup>a</sup> Rate relative to reaction with indole under the same condition.

<sup>b</sup> Obtained from competition experiments with 1:1 nucleophile to indole.

<sup>c</sup> Obtained from reaction kinetic study with in situ IR, and initial rates taken at 10% conversion of **3a**.

<sup>d</sup> Preliminary results showed that the rate determining step of benzotriazole-involving reaction is not indole nucleophilic addition, but prior to this step. Therefore, the rate acceleration effect enabled by the thiourea-nucleophile interaction during the nucleophilic addition transition state cannot be probed by direct kinetic analysis.

## 11. Reaction kinetics with tetrafluoroboric acid (HBF<sub>4</sub>)

General procedure: see section 3.

Rates of episulfonium ring opening with indole catalyzed by HBF<sub>4</sub> in the presence and absence of **1d**. Rates are provided in M s<sup>-1</sup> ( $\times 10^{-5}$ ).

Reactions with different thiourea **1d** loadings:

Reaction condition: [**3a**]<sub>i</sub> = 0.050 M, [indole]<sub>i</sub> = 0.10 M, [HBF<sub>4</sub>]<sub>T</sub> = 0.00050 M

conversion of <b>3a</b> (%)	[ <b>3a</b> ] (M)	[NuH] (M)	[ <b>1d</b> ] <sub>T</sub> = 0 mM	[ <b>1d</b> ] <sub>T</sub> = 0.5 mM	[ <b>1d</b> ] <sub>T</sub> = 2.0 mM	[ <b>1d</b> ] <sub>T</sub> = 2.5 mM	[ <b>1d</b> ] <sub>T</sub> = 5.0 mM	[ <b>1d</b> ] <sub>T</sub> = 5.0 mM	[ <b>1d</b> ] <sub>T</sub> = 7.5 mM
20	0.040	0.090	5.93	8.43	1.29	1.26	1.57	1.65	1.34
30	0.035	0.085	4.22	6.28	9.93	9.92	1.15	1.29	1.05
40	0.030	0.080		2.06	5.71	5.70	7.32	8.69	6.26

The deduction of the binding constant  $K_{1d\cdot 10'}$  is relied on the following equations:

$$(1) r_{\text{cat,obs}} = r_{\text{uncat}} + r_{\text{cat}} = r_{\text{uncat,max}} \times [\mathbf{10}'] / [\mathbf{10}']_{\text{T}} + r_{\text{cat,max}} \times [\mathbf{1d}\cdot\mathbf{10}'] / [\mathbf{10}']_{\text{T}}$$

$$(2) K_{1d\cdot 10'} = [\mathbf{1d}\cdot\mathbf{10}'] / ([\mathbf{10}'] [\mathbf{1d}]); [\mathbf{10}']_{\text{T}} = [\mathbf{1d}\cdot\mathbf{10}'] + [\mathbf{10}']$$

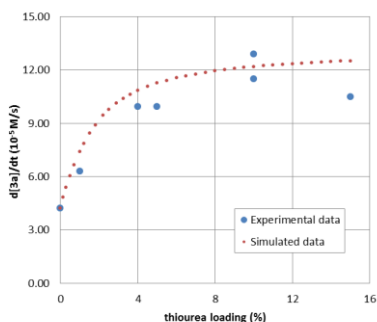
$$(3) [\mathbf{1d}]_{\text{T}} = [\mathbf{1d}\cdot\mathbf{10}'] + [\mathbf{1d}]$$

Here,  $r_{\text{rac,max}}$  is the rate of the reaction in the absence of **1d** ( $r_{\text{rac,max}} = 4.22 \times 10^{-5}$  M/s), and  $r_{\text{cat,max}}$  is the rate of the reaction under saturation kinetics regime. In these equations, **1d**•**10'** denotes the complex between **1d** and **10'** via anion-binding.

Procedure for stepwise approximation of  $K_a$ :

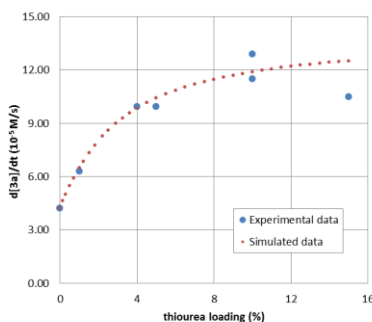
- (1) Assume  $r_{\text{cat,max}} = 13 \times 10^{-5} \text{ M/s}$ ;
- (2) Based on the experimental raw data  $r_{\text{cat,obs}}$  and  $[\mathbf{1d}]_T$ , calculate the association constant  $K_a$  according to the above equations for each data point (blue dots in the figure below, 7 data points in total with different loadings of  $\mathbf{1d}$ );
- (3) Obtain the average  $K_a$  value;
- (4) Simulate the rate of reaction ( $r_{\text{cat,obs}}$ ) for a series of hypothetical thiourea loadings (red dots in the figure below), again using the equations above;
- (5) Adjust the assumed  $r_{\text{cat,max}}$  value and repeat steps 2-4, until the simulated data are in the best agreement with the experimental data.
- (6) Use the average  $K_a$  value as the association constant and the standard deviation of the 7  $K_a$  values from different  $\mathbf{1d}$  loadings as the error bar.

In this case,  $r_{\text{cat,max}} = 14.0 \times 10^{-5} \text{ M/s}$  provides the best fit. For comparison, see the data below:



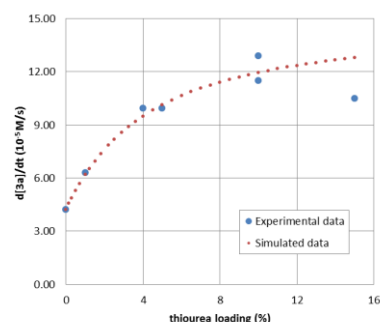
$$r_{\text{cat,max}} = 13.2 \times 10^{-5} \text{ M/s}$$

$$K_a = (1.7 \pm 2.1) \times 10^3 \text{ M}^{-1}$$



$$r_{\text{cat,max}} = 14.0 \times 10^{-5} \text{ M/s}$$

$$K_a = (7.9 \pm 4.6) \times 10^2 \text{ M}^{-1}$$



$$r_{\text{cat,max}} = 15.0 \times 10^{-5} \text{ M/s}$$

$$K_a = (5.5 \pm 2.1) \times 10^2 \text{ M}^{-1}$$

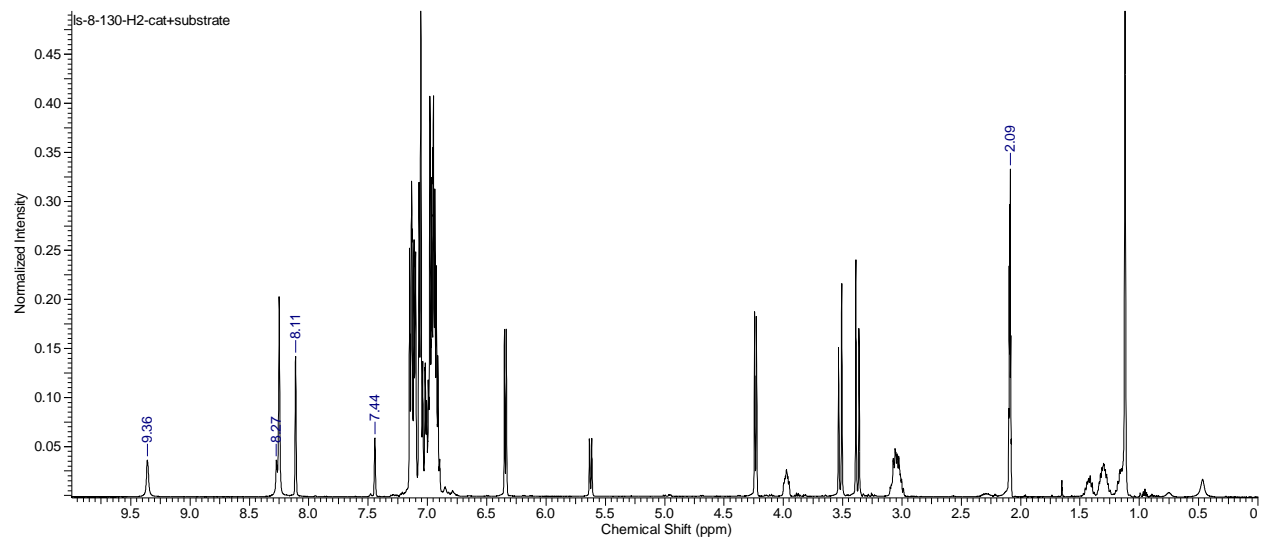
Control experiments with in the presence and the absence of thiourea  $\mathbf{1d}$ :

Reaction condition:  $[\mathbf{3a}]_i = 0.050 \text{ M}$ ,  $[\text{NuH}]_i = 0.10 \text{ M}$ ,  $[\text{HBF}_4]_T = 0.00050 \text{ M}$

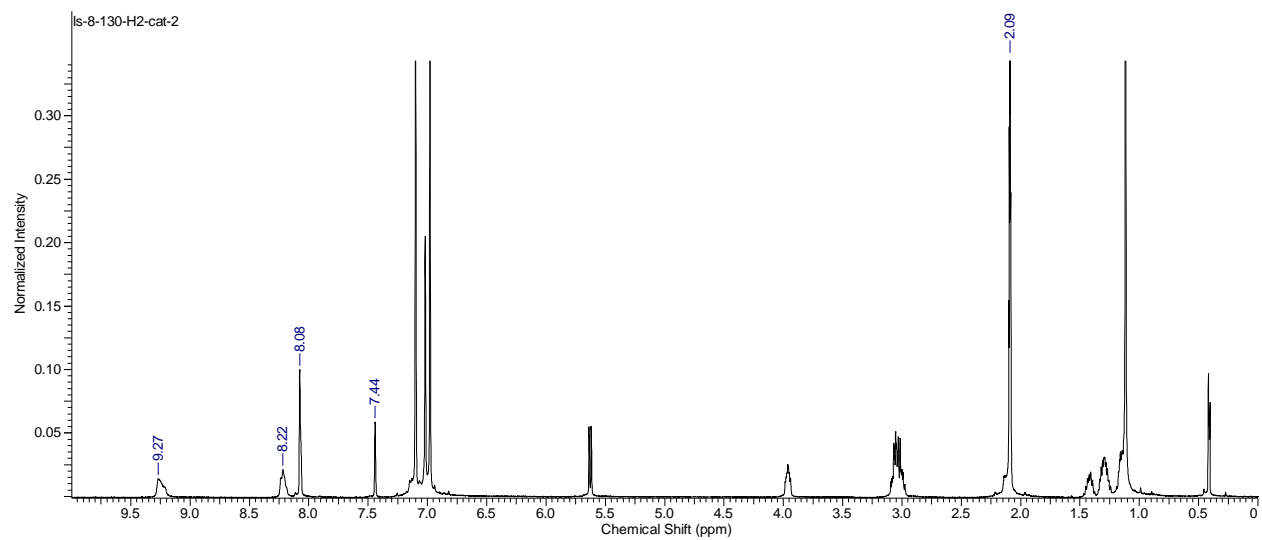
conversion of $\mathbf{3a}$ (%)	$[\mathbf{3a}]$ (M)	$[\text{NuH}]$ (M)	with indole		with <i>N</i> -Me indole	
			$[\mathbf{1d}]_T = 5.0$ mM	$[\mathbf{1d}]_T = 0$ mM	$[\mathbf{1d}]_T = 5.0$ mM	$[\mathbf{1d}]_T = 0$ mM
			10	0.045	0.095	3.30
20	0.040	0.090	2.32	0.36	0.85	2.00
30	0.035	0.085	1.50	0.14	0.75	1.42
40	0.030	0.080	0.96	0.080	0.76	1.06
50	0.025	0.075	0.71	0.065	0.71	0.72
60	0.020	0.070	0.47			0.56
70	0.015	0.065	0.37			

## 12. Thiourea 1a/1b – substrate 3a association

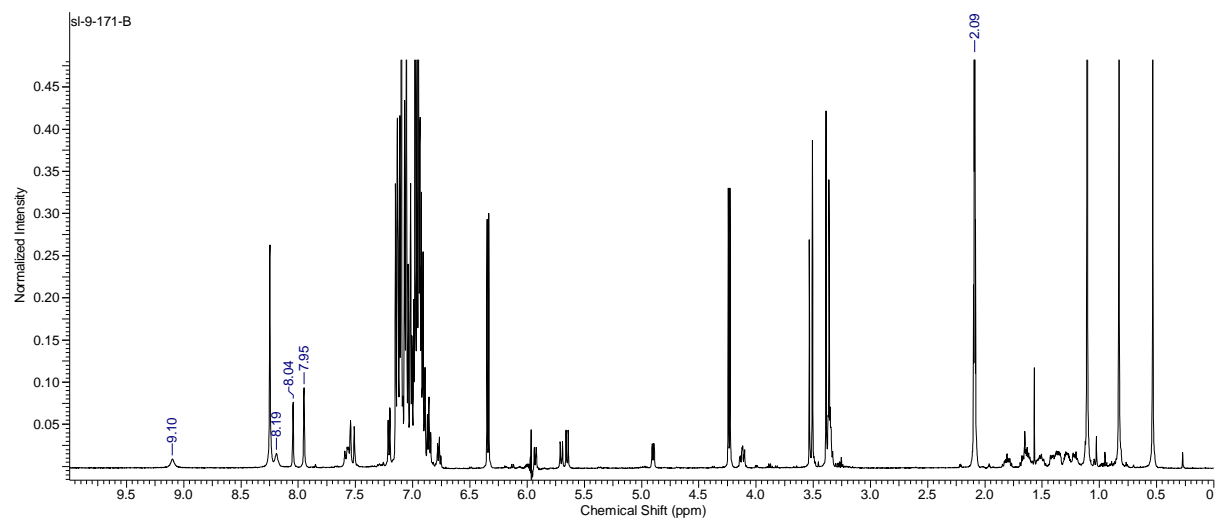
1a – 3a complex in  $d_6$ -toluene:



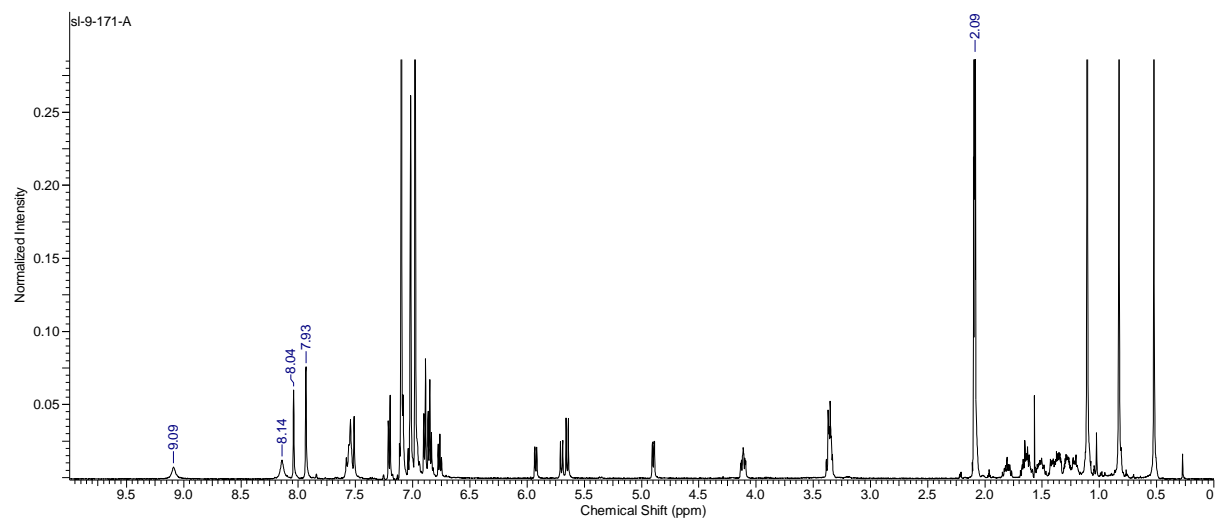
1a in  $d_6$ -toluene:



**1b – 3a complex in  $d_6$ -toluene:**

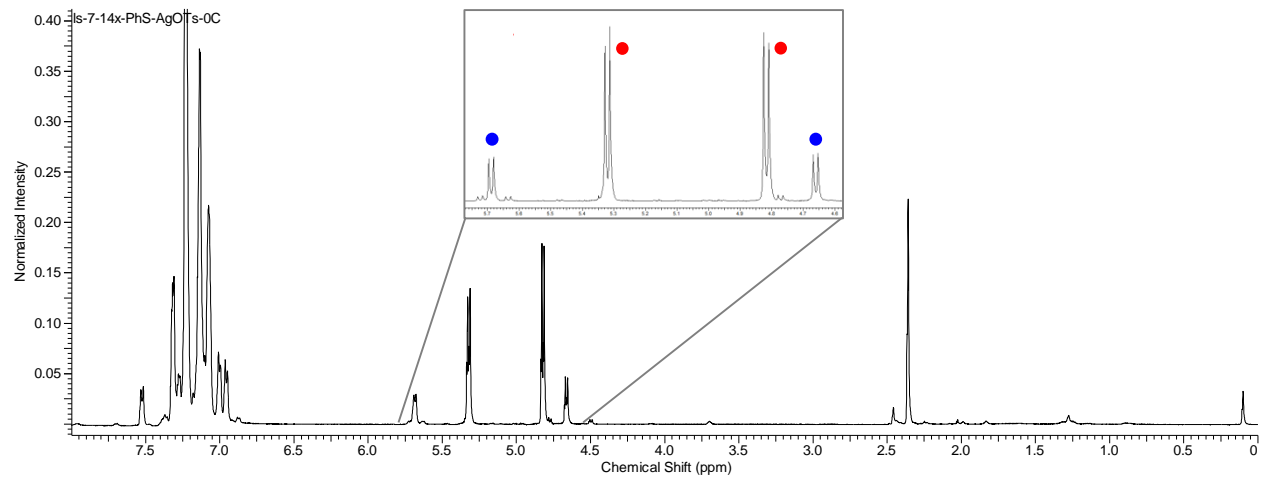


**1b in  $d_6$ -toluene:**



### 13. NMR spectrum of covalent adduct 7

Resonances of 7 are labeled with blue dots, and those of 6 are labeled with red. Spectrum taken in  $d_8$ -toluene at 0 °C.

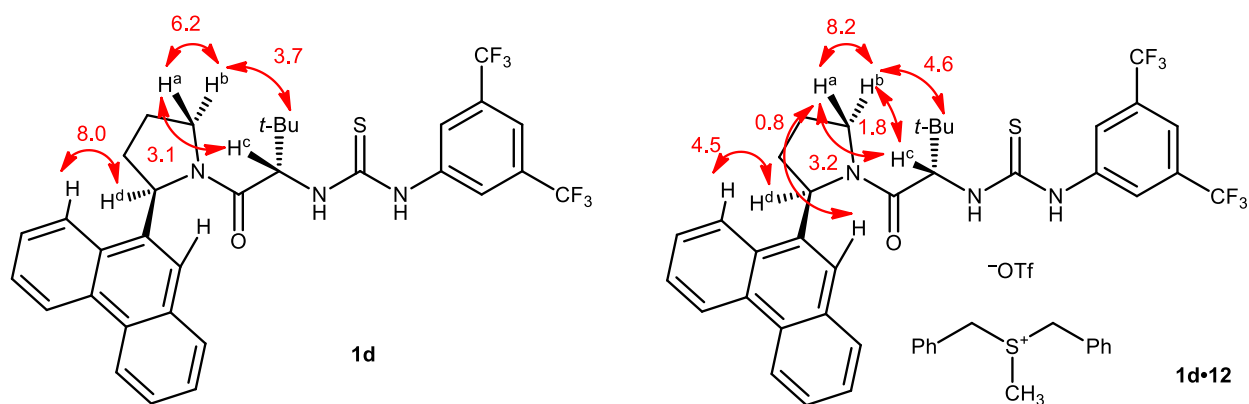


#### 14. Nuclear Overhauser effect studies on thiourea **1d** and complex **1d•12**

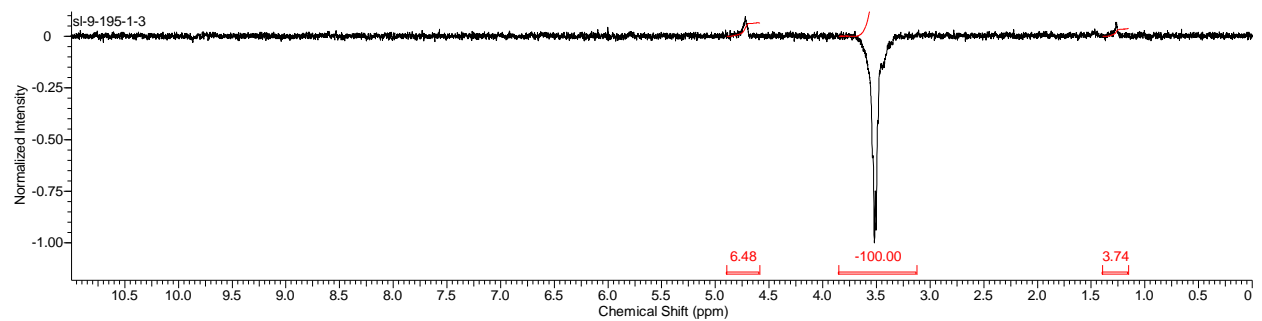
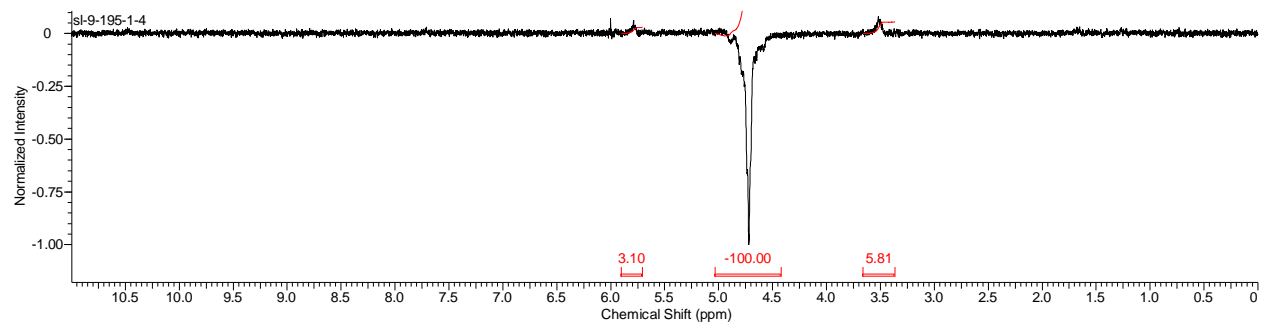
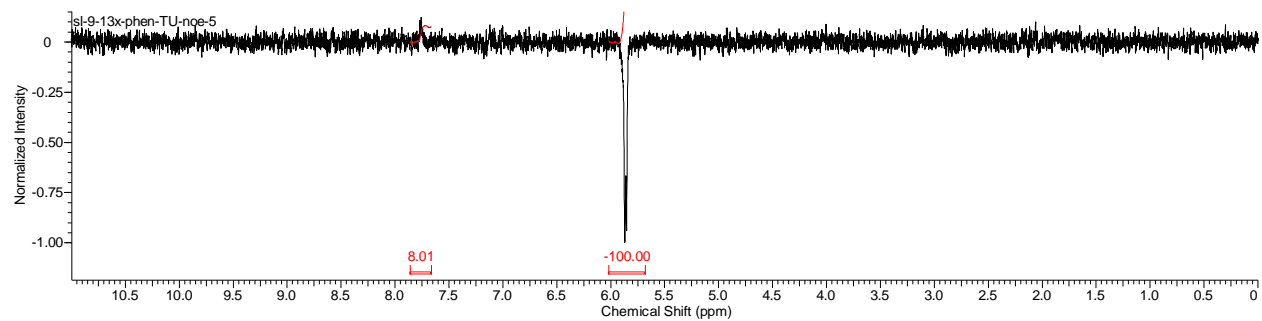
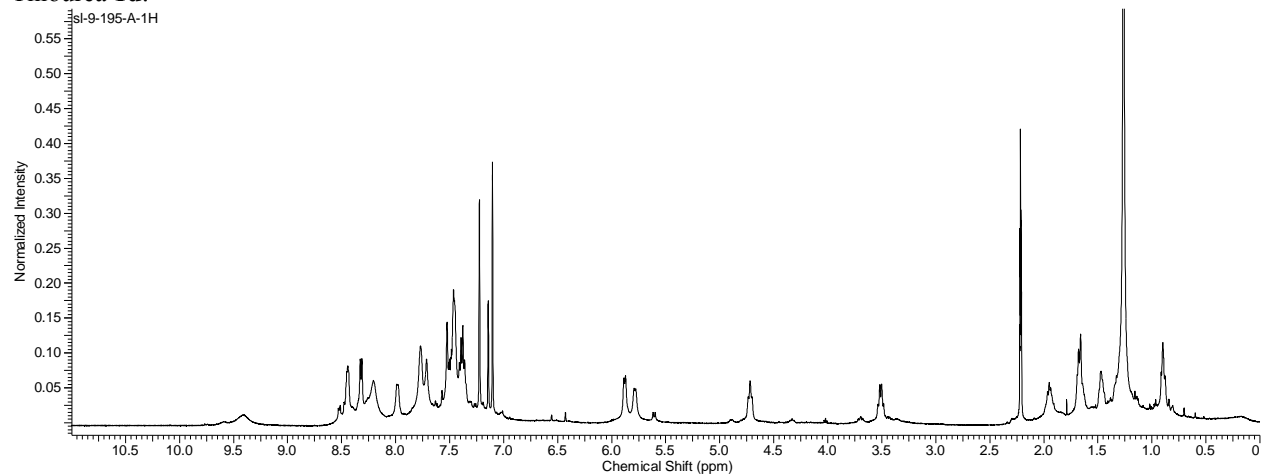
General information: The nOe studies were conducted on Inova 500 NMR spectrometer. Thiourea **1d** or complex **1d•12** was dissolved in  $d_8$ -toluene with a concentration of 0.040 M or 0.033 M, respectively. The spectra were recorded at 23.0 °C with 1.000 second relaxation delay, 90.0 ° pulse, 0.500 second mixing time, 2.048 second acquisition time, and 0.55 Hz line broadening.

nOe signals (strength of the nOe signal is indicated in the parenthesis in %)

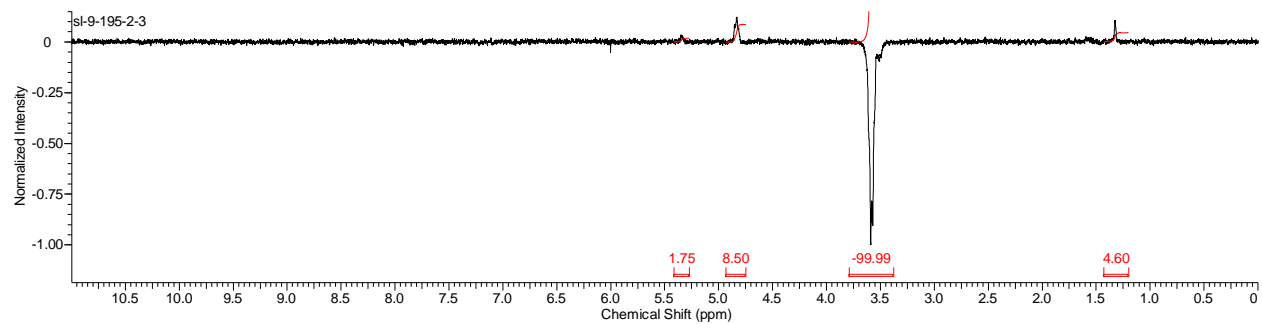
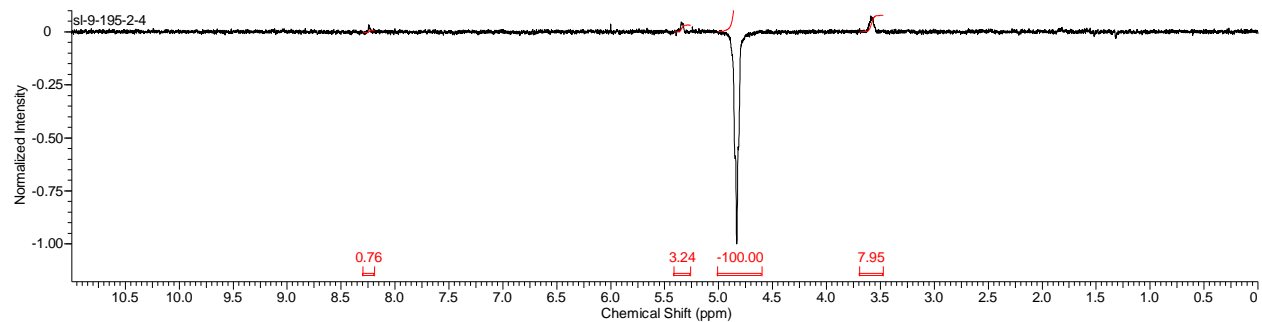
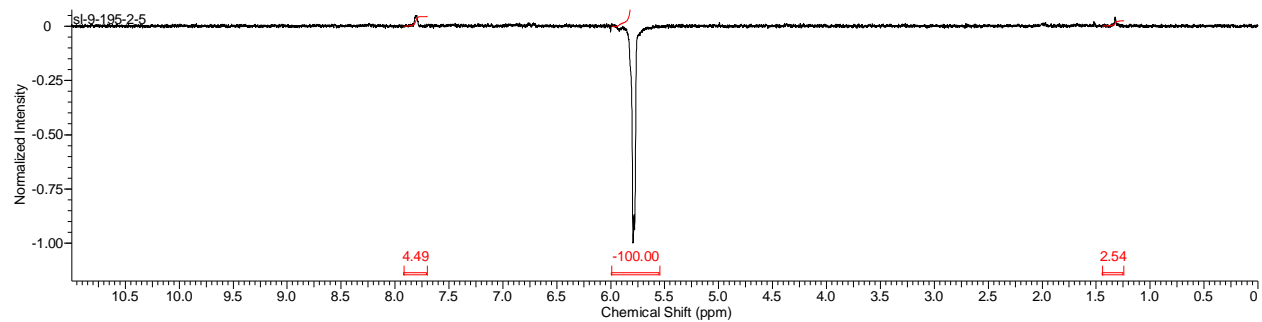
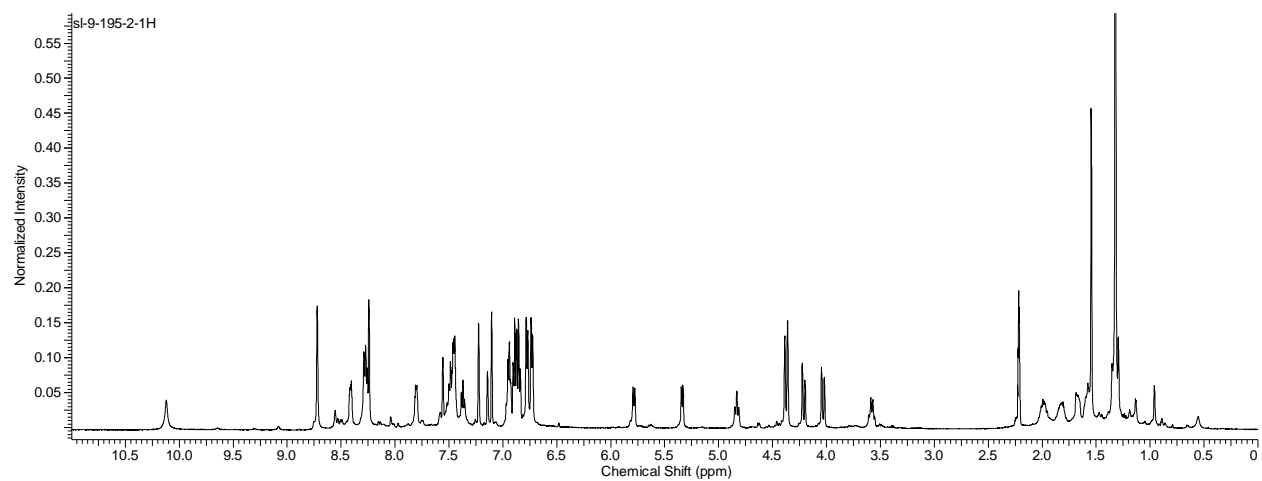
Chemical shift of the key protons: in **1d**, H<sup>a</sup> – 4.7 ppm, H<sup>b</sup> – 3.5 ppm, H<sup>c</sup> – 5.8 ppm, H<sup>d</sup> – 5.9 ppm; in **1d•12**, H<sup>a</sup> – 4.8 ppm, H<sup>b</sup> – 3.6 ppm, H<sup>c</sup> – 5.3 ppm, H<sup>d</sup> – 5.8 ppm.



Thiourea 1d:

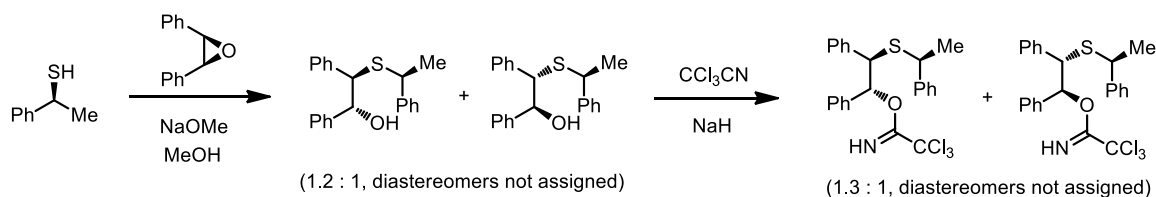


Complex 1d•12:



## 15. Catalyst-controlled diastereoselective episulfonium ion ring-opening

Synthesis of substrate:



(*S*)-1-phenylethylthiol was synthesized according to procedures outlined in Knoppe, S.; Kothalawala, N.; Jupally, V. R.; Dassb; A.; Bürgi, T. *Chem. Commun.* **2012**, *48*, 4630–4632.

The substrate **3q** was synthesized according to a two-step procedure reported in Lin, S.; Jacobsen, E. N. *Nat. Chem.* **2012**, *4*, 817–824.

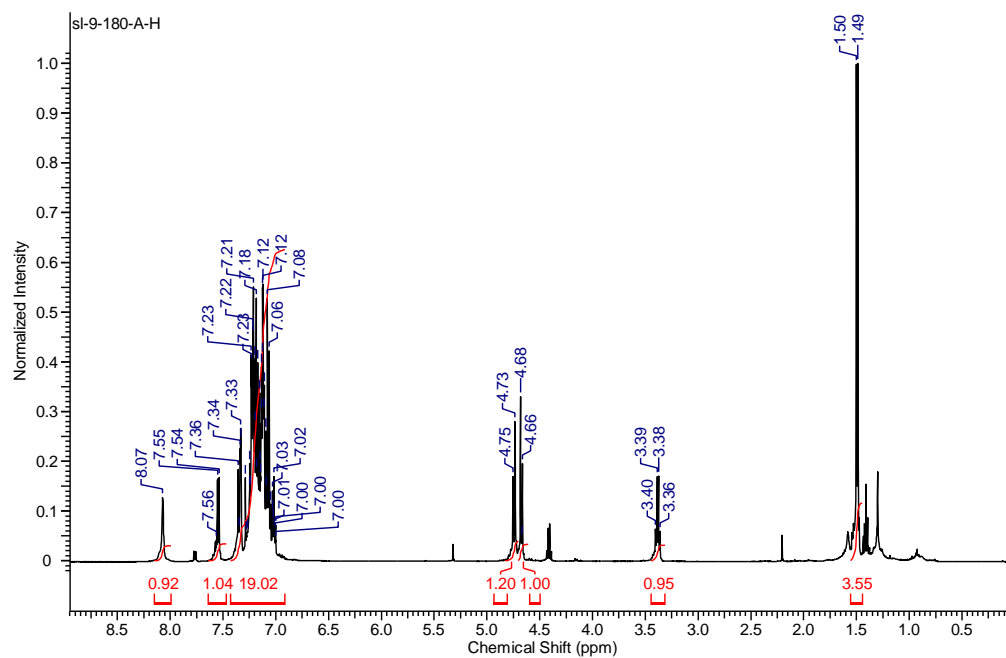
Characterization of **3q**: IR (Film): 3339, 3030, 1665 (s), 1583, 1492, 1453, 1289 (s), 1074 (s), 1028, 992, 824 (s)  $\text{cm}^{-1}$ ;  $^1\text{H}$  NMR: (500 MHz,  $\text{CDCl}_3$ )  $\delta$  = 1.45 (d,  $J$ =7.32 Hz, 3 H), 1.53 (d,  $J$ =6.84 Hz, 3 H), 3.62 (q,  $J$ =7.32 Hz, 1 H), 3.86 (d,  $J$ =6.35 Hz, 1 H), 3.96 (d,  $J$ =7.81 Hz, 1 H), 4.19 (q,  $J$ =7.16 Hz, 1 H), 6.01 (d,  $J$ =6.84 Hz, 1 H), 6.13 (d,  $J$ =8.30 Hz, 1 H), 6.76 - 7.32 (m, 15 H) 8.26 (s, 1 H), 8.37 (s, 1H);  $^{13}\text{C}$  NMR: (125 MHz,  $\text{CDCl}_3$ )  $\delta$  = 161.3, 161.3, 143.9, 143.8, 138.8, 137.4, 129.7, 128.7, 128.7, 128.6, 128.4, 128.3, 128.2, 128.2, 128.0, 127.9, 127.7, 127.7, 127.5, 127.4, 127.4, 127.3, 127.1, 84.5, 83.0, 55.3, 54.7, 45.3, 43.9, 23.3, 22.4; MS (ESI-APCI) exact mass calculated for  $[\text{M} - (\text{CCl}_3\text{C}=\text{NHO})]$  ( $\text{C}_{22}\text{H}_{21}\text{S}$ ) requires  $m/z$  317.1, found  $m/z$  317.0.

Characterization of products:

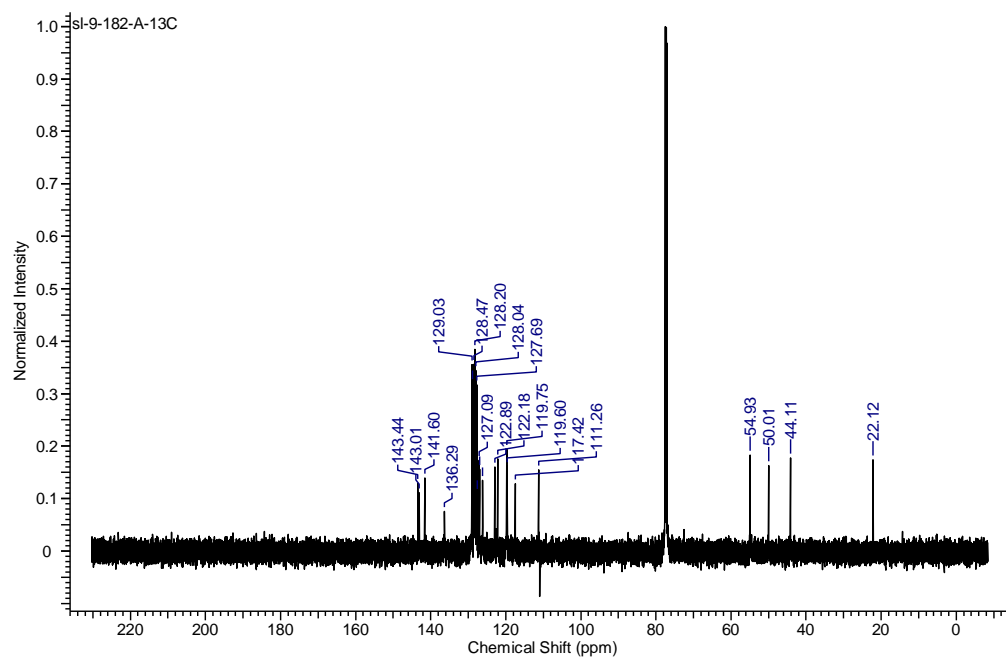
(*R,R,S*)-**4q**: IR (Film): 3420 (br, s), 3027, 2922 (s), 1718, 1601, 1491 (s), 1453 (s), 1098, 910 (s)  $\text{cm}^{-1}$ ;  $^1\text{H}$  NMR: (500 MHz,  $\text{CDCl}_3$ )  $\delta$  = 8.07 (br. s., 1 H), 7.64 - 7.47 (m, 1 H), 7.43 - 7.31 (m, 2 H), 7.27 - 7.05 (m, 16 H), 4.74 (d,  $J$  = 9.3 Hz, 1 H), 4.67 (d,  $J$  = 10.3 Hz, 1 H), 3.38 (q,  $J$  = 6.8 Hz, 1 H), 1.49 (d,  $J$  = 6.8 Hz, 4 H);  $^{13}\text{C}$  NMR: (125 MHz,  $\text{CDCl}_3$ )  $\delta$  = 143.4, 143.0, 141.6, 136.3, 129.0, 128.8, 128.5, 128.2, 128.0, 127.7, 127.6, 127.1, 126.9, 126.2, 122.9, 122.2, 119.7, 119.6, 117.4, 111.3, 54.9, 50.0, 44.1, 22.1; MS (ESI-APCI) exact mass calculated for  $[\text{M} - (\text{PhMeCHS})]$  ( $\text{C}_{22}\text{H}_{21}\text{S}$ ) requires  $m/z$  328.1, found  $m/z$  328.0;  $[\alpha]_{\text{D}}^{24} = -56.2$  ( $c$  = 0.011,  $\text{CDCl}_3$ ).

(*S,S,S*)-**4q**: IR (Film): 3422 (br, s), 3027, 2923 (s), 1719, 1600, 1490 (s), 1454 (s), 1098, 910 (s)  $\text{cm}^{-1}$ ;  $^1\text{H}$  NMR: (500 MHz,  $\text{CDCl}_3$ )  $\delta$  = 8.07 (br. s., 1 H), 7.64 - 7.47 (m, 1 H), 7.43 - 7.31 (m, 2 H), 7.27 - 7.05 (m, 16 H), 4.74 (d,  $J$  = 9.3 Hz, 1 H), 4.67 (d,  $J$  = 10.3 Hz, 1 H), 3.38 (q,  $J$  = 6.8 Hz, 1 H), 1.49 (d,  $J$  = 6.8 Hz, 4 H);  $^{13}\text{C}$  NMR: (125 MHz,  $\text{CDCl}_3$ )  $\delta$  = 144.8, 142.8, 141.7, 136.3, 129.5, 129.1, 128.6, 128.5, 128.0, 127.9, 127.9, 127.5, 127.2, 126.9, 126.1, 122.5, 122.1, 119.8, 119.6, 117.4, 111.2, 54.5, 49.9, 43.9, 23.1; MS (ESI-APCI) exact mass calculated for  $[\text{M} - (\text{PhMeCHS})]$  ( $\text{C}_{22}\text{H}_{21}\text{S}$ ) requires  $m/z$  328.1, found  $m/z$  328.0;  $[\alpha]_{\text{D}}^{24} = -148$  ( $c$  = 0.009,  $\text{CDCl}_3$ ).

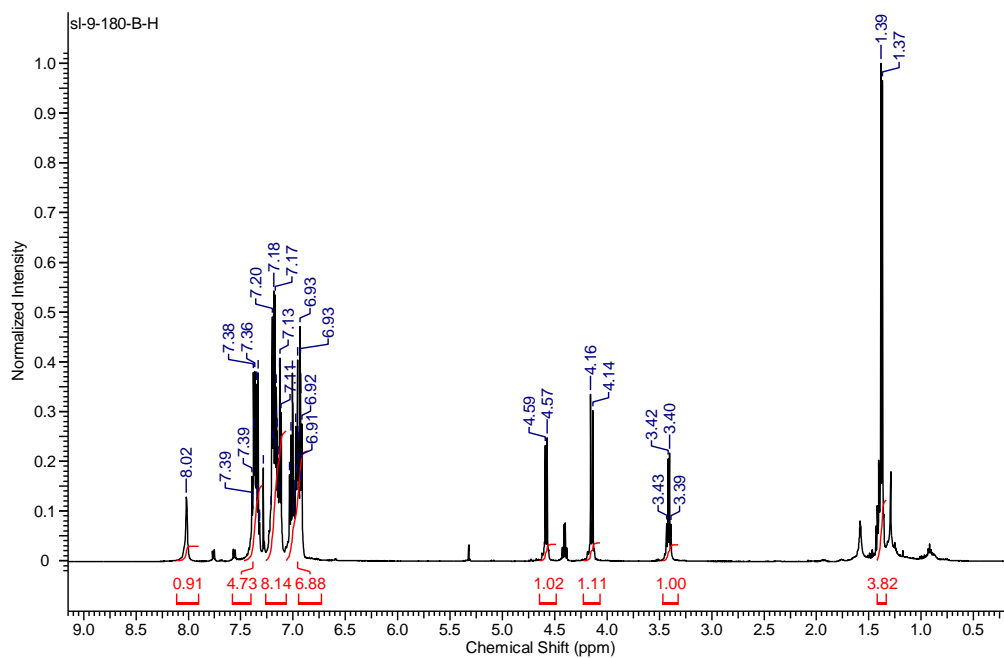
*(R,R,S)*-4q, <sup>1</sup>H NMR:



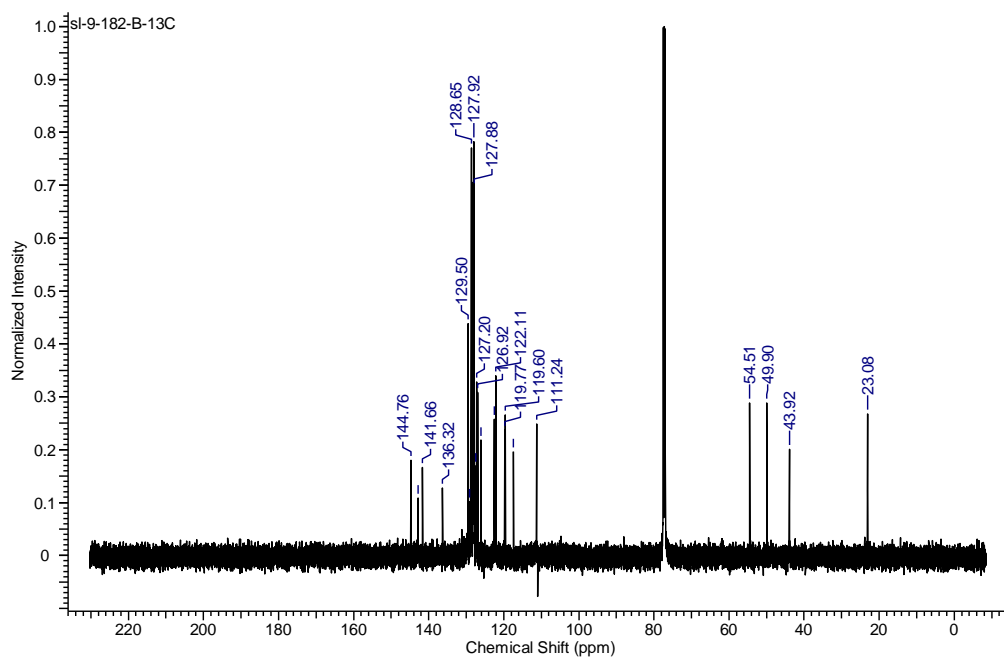
*(R,R,S)*-4q, <sup>13</sup>C NMR:



(*S,S,S*)-**4q**, <sup>1</sup>H NMR:

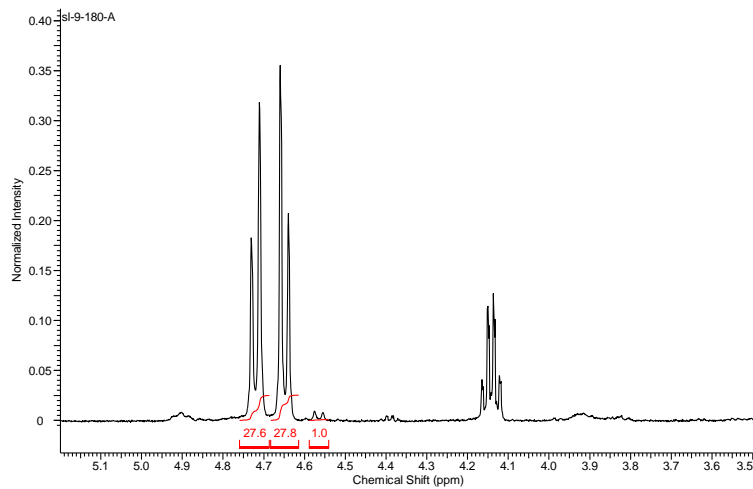


(*S,S,S*)-**4q**, <sup>13</sup>C NMR:

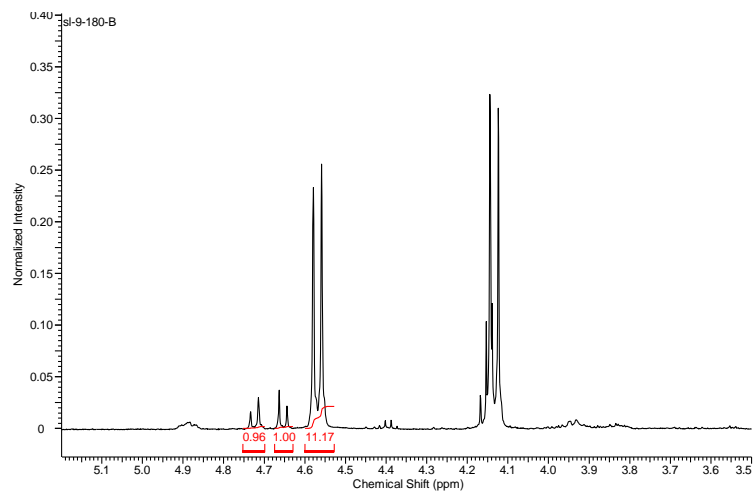


Determination of diastereoselectivity by crude  $^1\text{H}$  NMR:

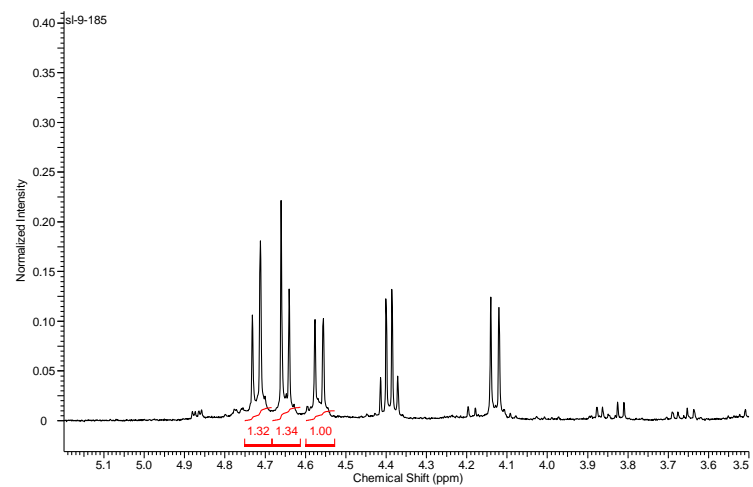
With (4*S*,7*R*)-**1d**:  $\text{dr} = [(27.62+27.79)/2] : 1.00 = 27.7 : 1$



With (4*R*,7*S*)-**1d**:  $\text{dr} = [(0.96+1.00)/2] : 11.19 = 1 : 11.4$



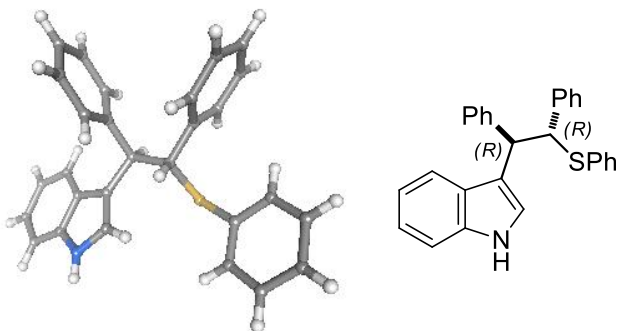
Without thiourea:  $\text{dr} = [(1.32+1.34)/2] : 1.00 = 1.3 : 1$



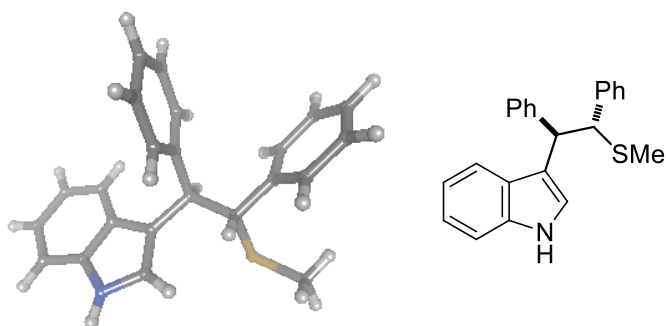
## 16. Crystallographic data of compounds 4b, 4c and 4h

The crystallographic data have been included in the \*.cif files as part of the supporting information. In this section are presented the crystal structures, absolute configuration assignments and conditions for growing the crystals.

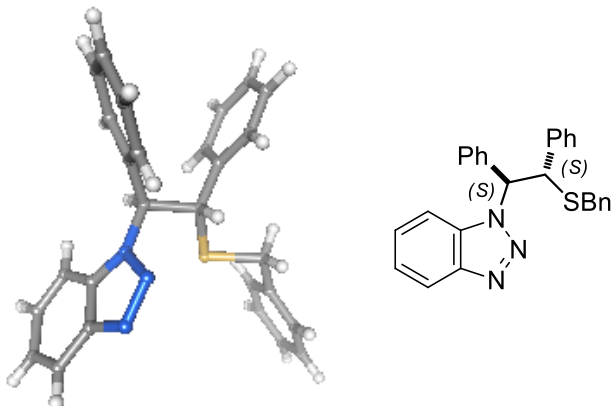
**4b:** (grew in hexanes/*i*-PrOH at room temperature, as a single enantiomer)



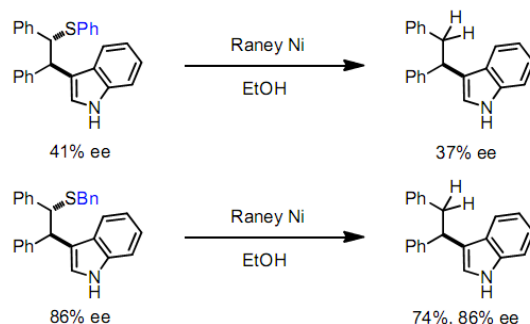
**4c:** (grew in hexanes/MeOH at room temperature, as a 1:1 mixture of enantiomers)



**4h:** (grew in hexanes/*i*-PrOH at room temperature, as a single enantiomer)



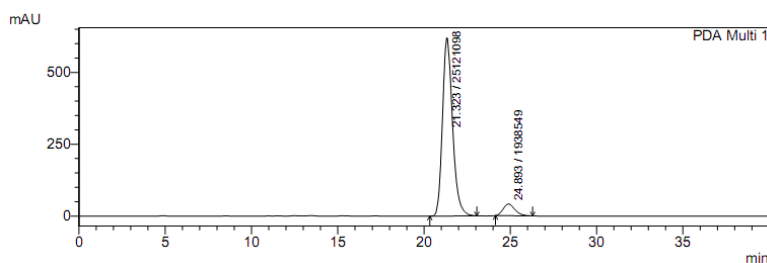
The absolute stereochemistry of product **4a** was determined by derivatization (reductive removal of the sulfanyl group –SPh) and comparison with product **4b**, as (*R*, *R*).



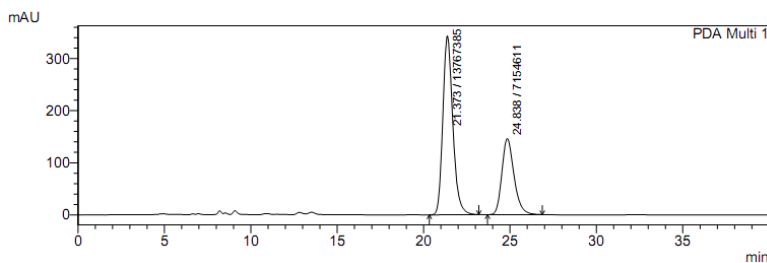
Procedure for Raney Ni promoted reduction of products **4a** and **4b**:

To a solution of the freshly prepared sulfide product (1 equiv) in ethanol (0.05 M) at room temperature was added Raney 2800 nickel (slurry in water, about the same volume as ethanol). The biphasic mixture was stirred vigorously until TLC showed complete consumption of the starting material. The mixture was then filtered through a celite plug, and diluted with water and DCM. The aqueous layer was separated and extracted with DCM. The combined organic layers were dried over Na<sub>2</sub>SO<sub>4</sub>, concentrated on vacuum, and applied to flash column chromatography. The product was obtained as a white solid, and <sup>1</sup>H NMR and mass spectroscopic data matched literature report perfectly. The enantiomeric excess was determined by chiral HPLC analysis (ChiralPak OD-H, 10% *i*-PrOH, 1 mL/min, 220 nm, *t*<sub>r</sub>(major) = 21 min, *t*<sub>r</sub>(minor) = 25 min).

Reduction product from **4a**:



Reduction product from **4b**:



## 17. NCIPLOT visualization of noncovalent interactions

The figures showing noncovalent interactions are generated using NCIPLOT 1.0 (for .xyz type input files) and NCIPLOT 3.0 (for .wfn type input files). The .xyz and .wfn files were generated using Gaussian 09, with structures optimized at the M05-2X level of density functional theory.

Input files:

<major_TS_xyz.nci>	<minor_TS_xyz.nci>
1 major_TS.xyz cutoffs 0.04 1 cube -8.5 -5.2 0.5 4.9 3.8 7.3	1 minor_TS.xyz cutoffs 0.04 1 cube -3.61 -4.78 0.83 9.42 3.5 6.73

<major_TS_wfn.nci>	<minor_TS_wfn.nci>
1 major_TS.xyz cutoffs 0.04 1 cube -4.37 -4.0 1.0 2.57 2.27 4.9	1 minor_TS.xyz cutoffs 0.04 1 cube -1.9 -2.75 0.88 8.2 2 3.8

Coordinates of Gaussian optimized transition structures:

major TS				minor TS			
S	4.13821200	2.33744200	-0.40722200	S	-4.25119000	-2.07713200	0.46960400
O	-0.54079700	2.22256500	-0.81305600	O	0.05334600	-2.38349400	-1.14668600
N	0.52718500	3.74085700	0.45122400	N	-0.85579700	-4.01759100	0.10806700
N	2.00382100	1.76073500	-1.92498400	N	-2.60958300	-1.55220700	-1.57985700
H	1.32744400	1.06640600	-2.25885100	H	-1.99700200	-0.88451600	-2.06247500
N	3.35946900	-0.00779600	-1.50465900	N	-3.65074500	0.27318900	-0.74575800
H	2.65468600	-0.54012600	-2.02707800	H	-3.23623300	0.72193500	-1.57069300
C	1.22621500	1.59865500	2.09723200	C	-0.59101100	-2.00523400	2.02816200
H	1.93205500	2.01918500	1.38936900	H	-1.51253100	-2.15219300	1.47630900
C	1.62535800	0.40199900	2.77663800	C	-0.50351700	-0.83812500	2.85501500
C	0.74678600	-0.21934000	3.68949000	C	0.67289300	-0.57771200	3.58915700
C	-0.54346000	0.40556900	3.94444700	C	1.74119300	-1.56629700	3.55383600
C	-0.89953800	1.59673400	3.25683800	C	1.63409100	-2.69062900	2.69193500
C	0.01910700	2.18132700	2.30084400	C	0.43493100	-2.88028500	1.89778600
C	-0.36498300	3.46749100	1.58293000	C	0.33008400	-4.08398200	0.97199300
H	-1.38396000	3.38249800	1.20719000	H	1.22018000	-4.12162500	0.34229900
C	-0.15792100	4.70953500	2.46773800	C	0.09905900	-5.39856800	1.74365500
H	-0.40572100	4.51694700	3.51063200	H	0.61722300	-5.41248800	2.70069100
H	-0.78193200	5.52901800	2.10125700	H	0.44651700	-6.24259700	1.14178000
C	1.32360600	5.02938000	2.25272200	C	-1.42218300	-5.44126900	1.88944300
H	1.58833000	6.04789400	2.53329900	H	-1.80371900	-6.43203900	2.13221600
H	1.93756700	4.34016600	2.83386800	H	-1.73963800	-4.74629600	2.66871700
C	1.53279000	4.77317800	0.75698600	C	-1.91630900	-4.95081600	0.52917600
H	1.32876500	5.67260600	0.17098900	H	-1.99020200	-5.77617600	-0.18339500
H	2.53735600	4.41449600	0.53579600	H	-2.87490400	-4.44057300	0.59995700
C	0.40039900	3.01374500	-0.67273200	C	-0.91188100	-3.11066200	-0.88818100
C	1.48562500	3.10853100	-1.74734100	C	-2.22685100	-2.95097600	-1.66223700
H	2.31646300	3.70895400	-1.38731400	H	-3.02079100	-3.50956200	-1.17461500
C	3.13097600	1.32117000	-1.31479900	C	-3.47222900	-1.07699000	-0.65267300
C	4.32500800	-0.84261300	-0.90655300	C	-4.29124400	1.19921500	0.09357000

C	5.62274100	-0.43395800	-0.58820600	C	-4.86887000	0.92054800	1.33780800
H	5.95801900	0.56648800	-0.79889200	H	-4.92461100	-0.08484200	1.71594800
C	6.47943800	-1.34733900	0.01141400	C	-5.38834500	1.97157100	2.08409800
C	6.11057200	-2.65517000	0.29266800	C	-5.37526100	3.28975900	1.65720900
H	6.79510900	-3.34614500	0.76224200	H	-5.78787400	4.08614800	2.25825900
C	4.82786800	-3.04021300	-0.07679800	C	-4.80666400	3.53215700	0.41236500
C	3.93340600	-2.16877200	-0.67450700	C	-4.27257100	2.52675100	-0.37255400
H	2.95164700	-2.50671000	-0.97837900	H	-3.83149500	2.75596700	-1.33411800
C	1.00266600	3.75952600	-3.06603300	C	-2.14568800	-3.47534500	-3.11900900
C	2.18698400	3.76776400	-4.03867100	C	-3.48800300	-3.17973600	-3.79687500
H	1.92366000	4.32957300	-4.93823000	H	-3.51940900	-3.65941400	-4.77821500
H	2.45664400	2.75285900	-4.33346000	H	-3.63149200	-2.10670900	-3.93338600
H	3.06576200	4.23336600	-3.58475200	H	-4.32222200	-3.55843200	-3.20025400
C	-0.18519200	3.04582300	-3.71746400	C	-1.01275200	-2.85896200	-3.94519500
H	-0.38531000	3.51014600	-4.68711500	H	-1.08803700	-3.22596900	-4.97268200
H	-1.08618900	3.13258700	-3.10913500	H	-0.03399800	-3.14140200	-3.55514500
H	0.01347100	1.98574600	-3.87965700	H	-1.06761800	-1.77017000	-3.96267100
C	0.60387900	5.20467500	-2.74454900	C	-1.94108800	-4.99375800	-3.05059900
H	0.25751700	5.70596000	-3.65104200	H	-1.87443600	-5.40477500	-4.06035300
H	1.45271300	5.76986500	-2.34948600	H	-2.77612800	-5.48255400	-2.54133500
H	-0.20956600	5.23942000	-2.01319000	H	-1.01509700	-5.24827600	-2.52616700
H	-1.64116400	1.00131700	-2.00512400	H	0.88241400	-0.93155200	-2.43890200
N	-2.63057900	0.76508500	-2.04595400	N	1.83824900	-0.61408400	-2.57887400
C	-3.10656900	-0.41870200	-2.49915300	C	2.16991000	0.65970100	-2.90274200
C	-3.67891800	1.55413000	-1.62275800	C	2.98486800	-1.34106900	-2.33558300
C	-4.48843800	-0.44044800	-2.38901100	C	3.54705000	0.80914400	-2.86385800
H	-2.42591500	-1.18043100	-2.85218500	H	1.40266000	1.39373300	-3.10602100
C	-4.87820900	0.83129900	-1.84994500	C	4.09237700	-0.47626000	-2.53339700
C	-3.67748900	2.82360100	-1.03826300	C	3.14356500	-2.67892600	-1.96256000
H	-5.13304400	-1.23105800	-2.73838500	H	4.08432200	1.70383600	-3.13586900
C	-6.10536800	1.40754300	-1.48523600	C	5.39205200	-0.97820200	-2.35519800
C	-4.90405300	3.36442300	-0.68499600	C	4.43827000	-3.14333100	-1.79462100
H	-2.74643300	3.34757300	-0.87430800	H	2.27739900	-3.30706400	-1.80915000
C	-6.10642200	2.66717800	-0.90713300	C	5.55206300	-2.30417800	-1.99013800
H	-7.03582700	0.88240100	-1.66762700	H	6.25476000	-0.34217700	-2.51872200
H	-4.93984900	4.34914400	-0.23633800	H	4.59873500	-4.17585600	-1.51103500
H	-7.04543100	3.12898900	-0.62938100	H	6.54809000	-2.70776400	-1.85885000
H	-5.70766800	0.51757800	1.08227900	O	-0.83455800	0.24557500	-2.88434400
C	-5.17876700	0.44748200	2.03425800	O	-2.68127700	1.86456000	-2.92651900
S	-4.23975200	-1.09814200	2.17282700	S	-1.33494800	1.53534900	-3.46547700
H	-4.49587000	1.28898500	2.13373700	O	-0.34186500	2.61893600	-3.38158700
H	-5.89914000	0.45712000	2.85083000	C	-1.58651500	1.20234700	-5.20015800
C	-3.18319000	-0.92789300	0.65063100	H	-1.96412100	2.10826300	-5.66876400
C	-4.25340000	-1.62549900	-0.08720100	H	-0.63049200	0.91659100	-5.63425400
H	-3.11038300	0.13353600	0.41098100	H	-2.30776000	0.39309500	-5.29532400
C	-1.84162000	-1.57491300	0.83730400	C	0.74503300	0.62582700	4.32050400
H	-5.18775600	-1.09405200	-0.17724700	C	-1.58419500	0.06528200	2.90082800
C	-4.24403400	-3.00890200	-0.52967600	H	-2.48137000	-0.17439200	2.34153100
C	-0.72001300	-0.94523600	0.30906200	C	-0.31384000	1.51022500	4.33851500
C	-1.70318600	-2.78786600	1.52068200	H	-0.23191200	2.43011300	4.90347900
C	-3.10597000	-3.58689000	-1.11700100	C	-1.49585100	1.22700800	3.63356800
C	-5.44182500	-3.73920900	-0.45714500	H	-2.32847500	1.91919800	3.65741100
C	0.53124200	-1.54354800	0.43248400	C	2.87547200	-1.46159200	4.38647100
H	-0.80698600	0.00959900	-0.18946300	H	2.95680600	-0.63216800	5.07478100
C	-0.45235700	-3.37499300	1.64492500	C	2.69077900	-3.62928200	2.66804000
H	-2.57066000	-3.28410800	1.94244200	C	3.78353100	-3.50763200	3.50002100

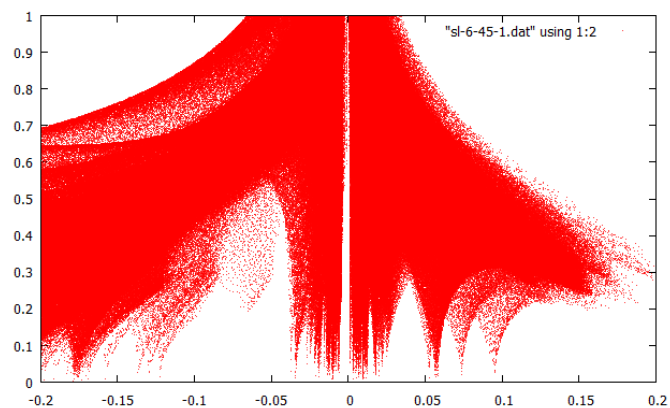
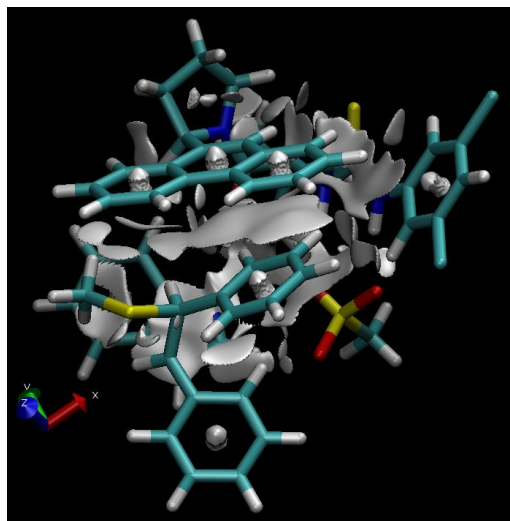
C	-3.17672700	-4.88377600	-1.60866000	H	4.56830500	-4.25316300	3.47631300
H	-2.19318800	-3.02125500	-1.24958800	C	3.87056400	-2.41701800	4.37829700
C	-5.49087400	-5.04522600	-0.91687000	H	2.63675900	-4.47538300	1.99663500
H	-6.31848600	-3.27957000	-0.01572900	H	1.64264500	0.87882200	4.86771300
C	0.66898400	-2.75749900	1.09141900	H	4.71665000	-2.32164200	5.04704300
H	1.39458800	-1.04473500	0.01544100	H	3.91521700	-1.25823300	0.44761000
H	-0.34983900	-4.31445500	2.17292200	C	4.58927900	-0.84427700	1.19746300
C	-4.35563500	-5.61621600	-1.49490100	S	4.08208400	0.82076900	1.70996300
H	-2.30493800	-5.30781800	-2.08828300	H	5.60547100	-0.82265200	0.80933200
H	-6.40828500	-5.61364800	-0.83913800	H	4.54096500	-1.46272600	2.09049900
H	1.64596100	-3.21223400	1.19314900	C	4.21335500	1.66246300	0.06165800
H	-4.39878200	-6.63036600	-1.87164800	C	2.82763100	1.31700300	-0.33664700
O	-0.00511500	-0.14195300	-2.82401300	H	4.92785200	1.08466000	-0.52237300
O	1.68042000	-1.93473500	-2.76492900	C	4.63533800	3.10257300	0.16396000
S	0.33559900	-1.53676900	-3.25397800	H	2.66469700	0.25234400	-0.45449000
O	-0.74364800	-2.50467800	-2.96858700	C	1.64261700	2.10921800	-0.26236800
C	0.47524300	-1.45968100	-5.03154100	C	5.39078600	3.64895600	-0.87275600
H	0.73574000	-2.45093800	-5.39520900	C	4.27460400	3.90706700	1.24638300
H	-0.48251200	-1.14147800	-5.43789700	C	1.60600300	3.50645700	-0.46755900
H	1.25482200	-0.74388400	-5.28365800	C	0.44075900	1.40720500	-0.02564900
C	1.17074700	-1.41325000	4.30762300	C	5.76571300	4.98889400	-0.84105000
C	2.88804000	-0.16441000	2.50412800	H	5.68495000	3.02362500	-1.70772700
H	3.54065400	0.33644100	1.79686400	C	4.65174200	5.24416400	1.27945200
C	2.40614000	-1.95941100	4.02707900	H	3.68342300	3.49596200	2.05612900
H	2.70445800	-2.88153700	4.51007700	C	0.39707300	4.17202400	-0.40972900
C	3.27589200	-1.33405300	3.11801400	H	2.50687300	4.04385200	-0.72145200
H	4.24154200	-1.77083900	2.89523100	C	-0.75367800	2.09543100	0.08417500
C	-1.45403700	-0.12605900	4.88039500	H	0.46236000	0.32842500	0.08504800
H	-1.20474000	-1.03244100	5.41312800	C	5.39400400	5.78920100	0.23443400
C	-2.14320200	2.20277800	3.54554800	H	6.34989800	5.40352100	-1.65232300
C	-3.00512200	1.66868400	4.48036400	H	4.36413900	5.86105600	2.12086800
H	-3.94275100	2.16559300	4.69856400	C	-0.77691400	3.47323300	-0.11869200
C	-2.65810500	0.48801800	5.15126400	H	0.35766500	5.23476700	-0.60582000
H	-2.42114600	3.11974000	3.04223200	H	-1.66646900	1.56023700	0.29789700
H	0.52500200	-1.92734200	5.00543900	H	5.68564500	6.83120700	0.26205100
H	-3.32846200	0.06115400	5.88666500	H	-1.72060900	4.00255700	-0.07438200
Cl	8.09795100	-0.83491600	0.41249100	Cl	-6.07984000	1.61047500	3.64592000
Cl	4.32265600	-4.67951600	0.24718800	Cl	-4.74760400	5.17588200	-0.17242900

Promolecular approximation (using \*.xyz files as input):

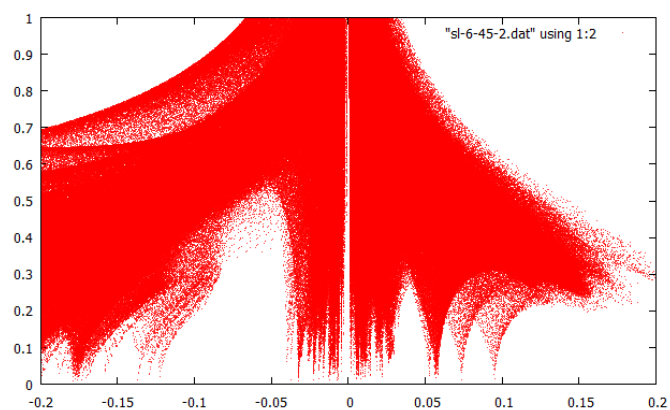
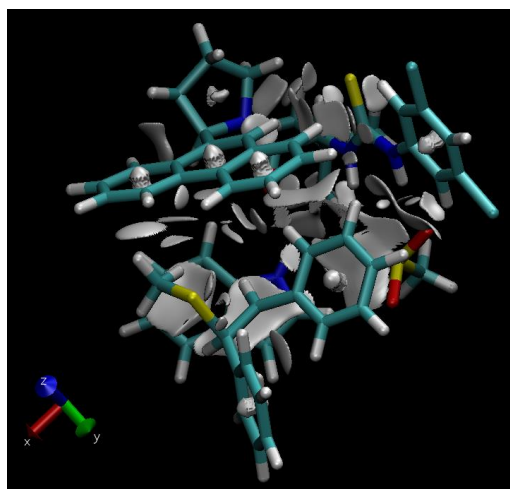
Full system

Noncovalent interactions, including cation- $\pi$ , hydrogen bonding,  $\pi$ - $\pi$ , hydrophobic and steric interactions are all shown in grey.

**13d•TS<sub>major</sub>**

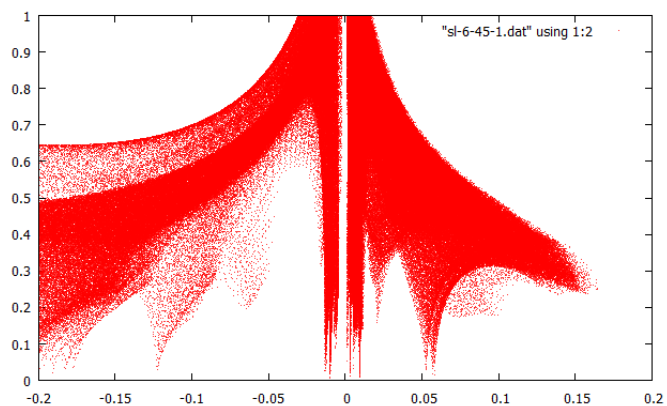
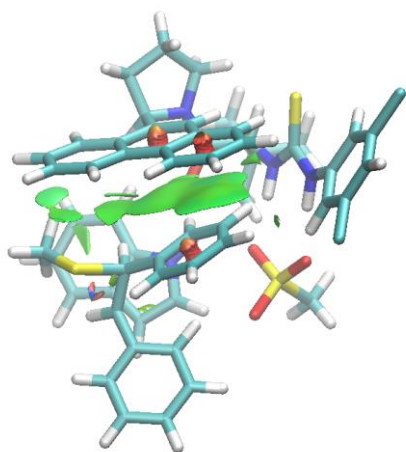


**13d•TS<sub>minor</sub>**

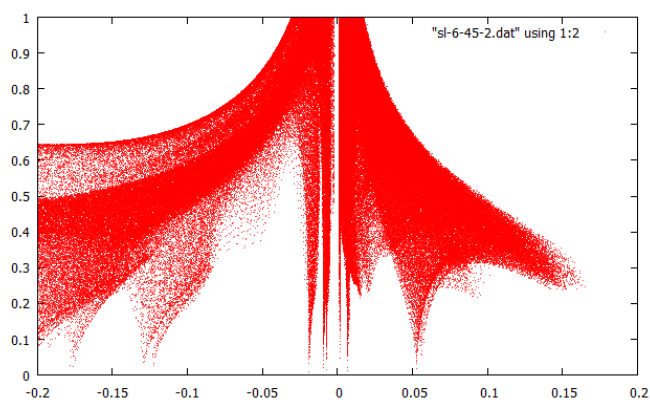
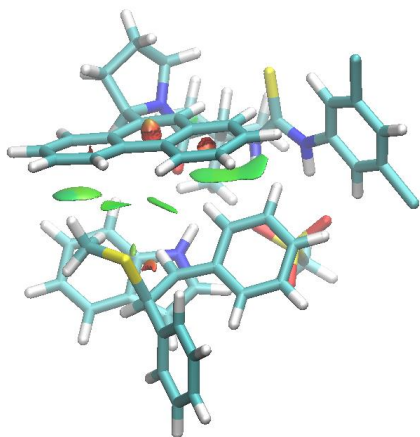


Truncated system showing only the cation- $\pi$  component

**13d•TS<sub>major</sub>**



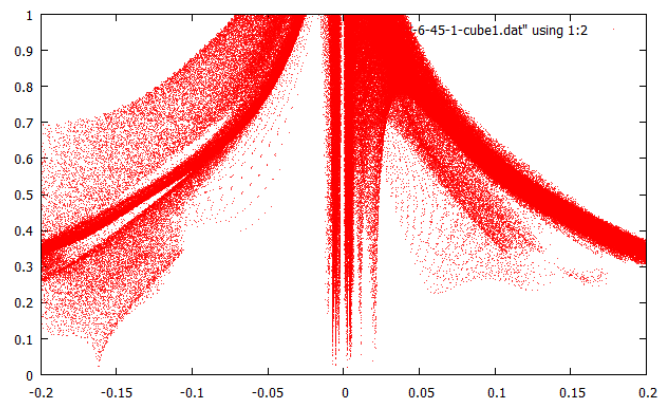
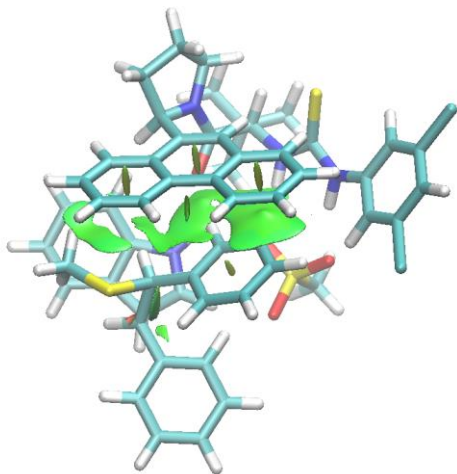
**13d•TS<sub>minor</sub>**



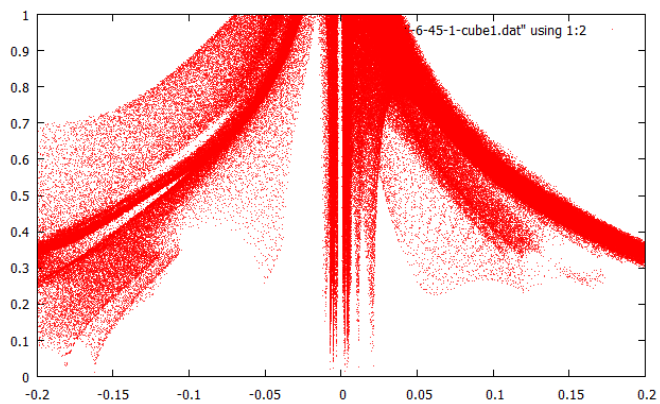
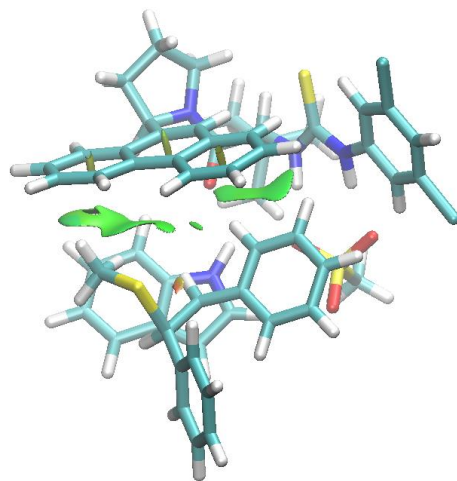
SCF calculation (using \*.wfn files as input)

Truncated system showing only the cation- $\pi$  component

**13d•TS<sub>major</sub>**



**13d•TS<sub>minor</sub>**



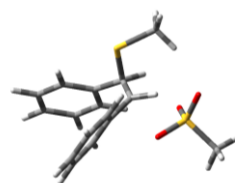
## 18. Computational data

Energy diagram of uncatalyzed reaction (M05-2X). Energy values are in a. u.

14

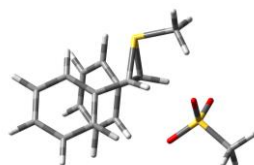


TS<sub>14-15</sub>

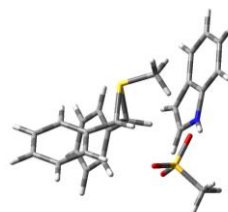


E = -1642.39244511			E + ZPE = -1642.075203			E = -1642.34047271			E + ZPE = -1642.025285		
G = -1642.125499			imaginary frequencies: 0			G = -1642.075366			imaginary frequencies: 1		
C	0.22069400	0.47458700	1.07223400	C	0.18549000	0.54186700	0.99930500				
H	1.18096600	0.98034700	1.19622400	H	1.19800300	0.92189400	1.11053400				
C	0.45981600	-0.77294700	0.18782700	C	0.14255500	-0.84879100	0.53772000				
H	1.06005600	-1.49135200	0.74468200	H	1.02351500	-1.44456100	0.73718500				
C	-0.75314500	1.45123500	0.45964000	C	-0.75820100	1.57442000	0.46606400				
C	-2.13262400	1.32038600	0.63123400	C	-2.11508900	1.60877200	0.78386200				
C	-0.25991600	2.48121300	-0.34262200	C	-0.22236300	2.50485200	-0.42764900				
C	-3.00476800	2.20963400	0.01388900	C	-2.93854100	2.56973400	0.20745900				
H	-2.52762700	0.51293300	1.23715900	H	-2.53656800	0.88760300	1.47437400				
C	-1.13489300	3.36775400	-0.96471000	C	-1.05387500	3.46056000	-1.00292800				
H	0.81025000	2.58166400	-0.48087300	H	0.83306500	2.45468900	-0.67262400				
C	-2.50816800	3.23504400	-0.78657500	C	-2.40936300	3.49545500	-0.68750400				
H	-4.07231200	2.09892700	0.15639100	H	-3.99133400	2.59437400	0.45790400				
H	-0.74092100	4.16505000	-1.58239400	H	-0.63867300	4.18020700	-1.69674500				
H	-3.18857400	3.92764500	-1.26611800	H	-3.05186900	4.24329800	-1.13492100				
C	-0.78825800	-1.43630700	-0.32846600	C	-0.99677200	-1.48288800	-0.14774100				
C	-1.42479900	-0.97538300	-1.48220500	C	-1.58123000	-0.88295500	-1.26683500				
C	-1.33705800	-2.50433700	0.37965000	C	-1.44399400	-2.73441200	0.28618200				
C	-2.59850000	-1.57842500	-1.91858200	C	-2.62101900	-1.52847900	-1.92592500				
H	-1.00295500	-0.14086200	-2.02666600	H	-1.18904700	0.05369900	-1.63472200				
C	-2.51926700	-3.09915300	-0.05216900	C	-2.49450700	-3.36525000	-0.36541700				
H	-0.84254700	-2.86203800	1.27403600	H	-0.97663200	-3.19755200	1.14674300				
C	-3.15043300	-2.63789900	-1.20271600	C	-3.08524100	-2.75969000	-1.47242200				
H	-3.08669000	-1.21486400	-2.81380400	H	-3.06489000	-1.06909200	-2.79922800				
H	-2.94010800	-3.92561500	0.50624600	H	-2.84634500	-4.32730300	-0.01668300				
H	-4.06714400	-3.10337500	-1.54248100	H	-3.90014300	-3.25315400	-1.98677100				
O	1.23703100	-0.37550900	-0.98928500	O	1.40825100	-0.43853200	-1.32209700				
S	2.80561300	-0.05849900	-0.75772800	O	3.07079100	-0.86952000	0.45200700				
O	3.29732100	-0.90034600	0.32587700	O	2.89917900	1.39177400	-0.55958600				
O	3.00096600	1.38148000	-0.68620900	S	-0.30298700	-0.29992000	2.58212800				
S	-0.28474100	-0.05414600	2.75109100	C	1.35699600	-0.50407100	3.30459000				
C	1.37592800	-0.37835700	3.41968600	H	2.07889600	-0.72664800	2.51634000				
H	1.94488300	-1.04603300	2.77359700	H	1.63200600	0.41773000	3.81272800				
H	1.92331300	0.55492400	3.54466100	S	2.75395900	-0.06526800	-0.76054600				
H	1.24313500	-0.84946400	4.39219600	H	1.30642800	-1.32382200	4.01787900				
C	3.40734800	-0.65041400	-2.31702900	C	3.93520700	-0.54069300	-2.00714500				
H	4.47624400	-0.44826900	-2.34125700	H	3.71395700	0.01687100	-2.91408800				
H	3.20791000	-1.71686400	-2.37786900	H	4.92825300	-0.29541800	-1.63743700				
H	2.89387000	-0.10522100	-3.10512300	H	3.83973900	-1.61016300	-2.17806300				

15



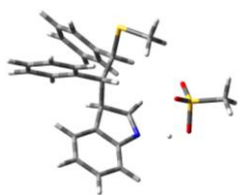
15•indole



E = -1642.34710061		E + ZPE = -1642.031989		E = -2006.15462774		E + ZPE = -2005.705488	
G = -1642.084221		imaginary frequencies: 0		G = -2005.767738		imaginary frequencies: 0	
C	-0.07148200	-0.89889400	0.55647400	H	2.19282100	1.56990200	0.93107800
H	-1.03580900	-1.36503600	0.33924000	N	2.65922500	0.66798700	1.00256600
C	-0.13082800	0.55352700	0.82958100	C	2.25936400	-0.36474300	1.81540100
H	-1.12869300	0.98828500	0.81268500	C	3.54353700	0.18489100	0.07262000
C	1.12242700	-1.48694600	-0.11819500	C	2.88752300	-1.52331500	1.44378700
C	2.11931600	-2.20931400	0.52826200	H	1.52657200	-0.18175500	2.58501300
C	1.17812200	-1.28406400	-1.50043600	C	3.71870000	-1.20068800	0.31900700
C	3.18463700	-2.72571800	-0.20561400	C	4.19963900	0.84974000	-0.96984300
H	2.06745700	-2.37697200	1.59755400	H	2.76725000	-2.48689800	1.91145400
C	2.24235300	-1.80491100	-2.22475500	C	4.58103400	-1.93007600	-0.51603700
H	0.38046900	-0.72850200	-1.98199200	C	5.03512700	0.09940800	-1.77954400
C	3.24751600	-2.52344100	-1.57948900	H	4.04961300	1.91038000	-1.13157700
H	3.96080000	-3.28718200	0.29844000	C	5.22358600	-1.27960500	-1.55435700
H	2.28730900	-1.64938200	-3.29488300	H	4.74065700	-2.98836400	-0.34771300
H	4.07612700	-2.92606500	-2.14798400	H	5.56074500	0.58082600	-2.59479000
C	0.97788400	1.47420900	0.46054900	H	5.89104600	-1.83387300	-2.20224200
C	2.24374900	1.46875400	1.04241800	H	2.09990400	0.04355300	-2.39285900
C	0.68999700	2.35098100	-0.58887300	C	1.13929900	0.55392100	-2.43364200
C	3.21979200	2.34612800	0.58243200	S	-0.14862000	-0.65835900	-2.01408300
H	2.47396300	0.79191200	1.85678400	H	1.11419100	1.37451900	-1.71227400
C	1.67429900	3.21867000	-1.04864300	H	0.92835200	0.91028900	-3.43978700
H	-0.29179600	2.31646500	-1.04727000	C	-1.37046000	0.37437500	-1.01526200
C	2.93665400	3.22124300	-0.46198200	C	-0.38888100	-0.37068300	-0.20063700
H	4.20010700	2.34514200	1.04108600	H	-1.14775400	1.42960200	-1.14098500
H	1.45170300	3.89464300	-1.86408900	C	-2.81308100	0.03457800	-1.11396600
H	3.69869900	3.90306300	-0.81735000	H	0.42744300	0.23625000	0.17834900
O	-1.89644600	0.41597700	-1.55641700	C	-0.78573100	-1.53549800	0.64382100
S	-3.02792600	0.03323000	-0.66946000	C	-3.70632500	1.09733500	-0.95858700
O	-3.16746400	0.95755300	0.49590200	C	-3.29451000	-1.26128700	-1.31728100
O	-2.98140100	-1.39198300	-0.24558300	C	-1.59382500	-1.25659100	1.74838000
S	0.03887600	-0.51007800	2.36509600	C	-0.33870100	-2.83270700	0.40852600
C	-1.70113700	-0.70332100	2.87116700	C	-5.07638800	0.85876400	-1.00743300
H	-1.81656800	-0.16949100	3.81187400	H	-3.31513800	2.08945200	-0.76809400
H	-2.35644200	-0.28608400	2.10191400	C	-4.66309600	-1.48816000	-1.37638300
H	-1.88986200	-1.76597100	3.00310300	H	-2.60987700	-2.09367000	-1.42751800
C	-4.51566200	0.22264900	-1.63289700	C	-1.96322900	-2.28859900	2.60343100
H	-4.58486300	1.26042800	-1.95044000	H	-1.89679600	-0.23381600	1.93665100
H	-4.44748900	-0.43954600	-2.49280200	C	-0.71928400	-3.86147300	1.26495300
H	-5.36363200	-0.04583400	-1.00727400	H	0.31688300	-3.03737800	-0.42937300
				C	-5.55556800	-0.42903800	-1.22171800
				H	-5.76642100	1.68267100	-0.87992600
				H	-5.03304500	-2.49193300	-1.54000900
				C	-1.53413300	-3.59104400	2.35991500
				H	-2.58764600	-2.07330600	3.46084400

	H	-0.37366800	-4.87021500	1.07890000
	H	-6.62180300	-0.61103300	-1.26656400
	H	-1.82879800	-4.39195600	3.02593900
	O	0.96683800	2.73090400	0.01790800
	O	-1.46439600	3.17033400	0.13666200
	S	-0.22846200	2.90578600	0.90867800
	O	-0.33735800	1.78812300	1.87972500
	C	0.08685500	4.38144000	1.85812400
	H	0.99606000	4.23368500	2.43650100
	H	0.20118200	5.21238900	1.16606300
	H	-0.76240700	4.54537500	2.51743000

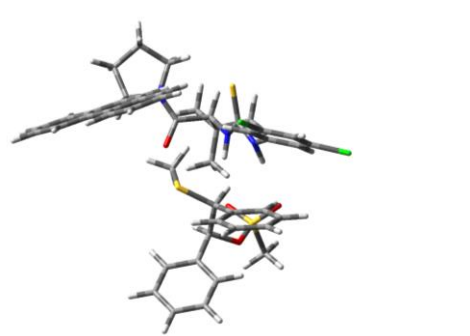
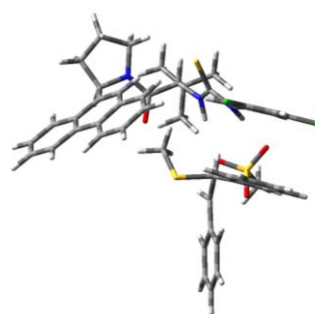
16

TS<sub>15-16</sub>

E = -2006.18786022	E + ZPE = -2005.738082		E = -2006.12507323	E + ZPE = -2005.676865			
G = -2005.738082	imaginary frequencies: 0		G = -2005.737433	imaginary frequencies: 1			
C	0.81605500	-1.42302600	0.26104600	H	-0.61200300	-2.21149200	-0.51568700
C	0.59415800	0.11950000	0.30838600	N	0.28832700	-1.87168100	-0.90963300
H	-0.23442500	0.28777100	1.00242100	C	0.37450300	-0.90234100	-1.85415500
S	1.07395700	-2.10921800	1.94196500	C	1.55426500	-2.28303000	-0.57087100
H	-0.10776500	-1.88287800	-0.09584800	C	1.70174200	-0.65772700	-2.16623700
C	1.79169500	0.89307000	0.81867800	H	-0.53533400	-0.46639500	-2.23402900
C	2.90026500	1.16310200	0.01027300	C	2.48154900	-1.54221100	-1.35372300
C	1.78456900	1.38427700	2.12466000	C	1.96815200	-3.21438700	0.38706600
C	3.97208600	1.90423900	0.49916400	H	2.05536700	0.02373400	-2.92423100
H	2.93533500	0.79511700	-1.00751500	C	3.85768400	-1.76876100	-1.17618700
C	2.85418900	2.12509900	2.61743100	C	3.33085900	-3.40289300	0.54763700
H	0.92825900	1.18435100	2.75783800	H	1.24392600	-3.76687100	0.97234500
C	3.95174400	2.38890500	1.80422900	C	4.26717400	-2.69182100	-0.22917000
H	4.82177900	2.10352800	-0.14193400	H	4.58503600	-1.23885400	-1.78073200
H	2.82638700	2.49850800	3.63320900	H	3.68466700	-4.12086500	1.27640300
H	4.78420700	2.96866000	2.18267300	H	5.32360400	-2.88128400	-0.08689500
C	1.94703400	-1.85271600	-0.64624800	H	4.04495300	0.45094200	0.41209200
C	1.67216500	-2.20584100	-1.96912200	C	3.94129000	0.74466500	1.45723800
C	3.27408500	-1.88571200	-0.20746700	S	2.47431200	1.78110800	1.71715400
C	2.69580900	-2.56154500	-2.84327200	H	3.86473800	-0.15453300	2.06665000
H	0.64514000	-2.21899600	-2.31698700	H	4.80777900	1.33012800	1.75916600
C	4.29748700	-2.24716500	-1.07675500	C	1.18527700	0.65222300	0.97786000
H	3.50690400	-1.61847500	0.81599700	C	1.39469900	1.35097400	-0.30382200
C	4.01352600	-2.58012000	-2.39851700	H	1.59040000	-0.36047300	0.97466400
H	2.46066500	-2.83349800	-3.86461700	C	-0.11677700	0.76582400	1.71742200
H	5.31914700	-2.26898900	-0.71901200	H	2.36102500	1.20957600	-0.76209900
H	4.81216700	-2.86090000	-3.07332500	C	0.50105200	2.29459300	-0.93082300
C	-0.63632100	-2.04537600	2.55291200	C	-0.86634300	-0.38494900	1.93733300
H	-1.29837500	-2.59302800	1.88395300	C	-0.58935700	2.00076100	2.17362900
H	-1.00412500	-1.02667400	2.66231500	C	-0.89323800	2.09930800	-0.92261600
H	0.88356800	0.53700600	-1.81923600	C	1.05752700	3.36818100	-1.65056400

C	0.11455300	0.70015200	-1.05901900	C	-2.10339300	-0.30480800	2.57104100
C	-0.32959300	2.14217000	-0.94564100	H	-0.51930400	-1.34444400	1.58206800
C	-1.18758800	0.06374100	-1.47104400	C	-1.81362200	2.07562600	2.82335900
C	-1.70649100	2.16826100	-1.19056600	H	-0.01696900	2.90694400	2.00643600
C	0.33068200	3.32132800	-0.62955900	C	-1.70554000	2.98411100	-1.61855300
H	-1.33878800	-0.99081400	-1.66054400	H	-1.33911600	1.22625000	-0.46232000
C	-2.45887300	3.32930800	-1.12815200	C	0.23354400	4.26766000	-2.30379900
C	-0.41328700	4.50177900	-0.56917700	H	2.13343900	3.49792300	-1.66529600
H	1.39305800	3.33348800	-0.42770700	C	-2.57621200	0.92425000	3.01245800
C	-1.78720600	4.50782200	-0.81103900	H	-2.70662300	-1.19552200	2.66661100
H	-3.52361000	3.31099700	-1.31910600	H	-2.17810400	3.03423100	3.16990100
H	0.08762800	5.42973600	-0.32528300	C	-1.15001300	4.07203500	-2.28722300
H	-2.33712300	5.43817500	-0.75162900	H	-2.77163200	2.80383600	-1.64209200
N	-2.18602200	0.87014500	-1.50566600	H	0.65933100	5.10774100	-2.83618300
H	-3.62053800	0.18698200	-1.25943700	H	-3.54448400	0.98787900	3.49126600
S	-3.80474700	-1.24846200	0.32177900	H	-1.79347900	4.76353700	-2.81665200
O	-2.87545900	-2.26747500	-0.17315200	O	-2.12811100	-2.63746500	0.14425500
O	-3.32713600	-0.35497600	1.37290300	O	-4.18128800	-1.30320000	0.58704900
O	-4.38443900	-0.41113200	-0.89406700	S	-3.16793200	-1.69781700	-0.40120300
H	-0.62750300	-2.52579100	3.53073000	O	-2.53099000	-0.56934500	-1.13907200
C	-5.30349300	-2.04031700	0.84112800	C	-4.02702500	-2.65392700	-1.64344200
H	-5.05012000	-2.67381400	1.68851300	H	-3.30849100	-2.97877900	-2.39290500
H	-6.01367000	-1.27056000	1.13168900	H	-4.48264700	-3.51169700	-1.15419200
H	-5.68063700	-2.63497300	0.01315200	H	-4.79013000	-2.02246600	-2.09308000

13d•14

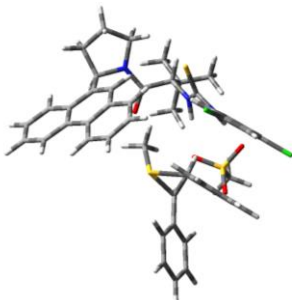
13d•TS<sub>14-15</sub>

E = -4400.32135130	E + ZPE = -4399.431709	E = -4400.29160766	E + ZPE = -4399.403501				
G = -4399.529653	imaginary frequencies: 0	G = -4399.499005	imaginary frequencies: 1				
S	1.33473400	-2.56639400	2.13371700	S	1.26270800	1.74105000	-2.76006800
O	2.74291900	-0.96777700	-1.72294500	O	2.70662600	1.36660000	1.30383000
N	4.32879100	-1.58621500	-0.24373700	N	4.25859500	1.65977000	-0.30051400
N	1.03114500	-2.81713500	-0.52725400	N	0.89369700	2.76008700	-0.31076100
H	0.56247700	-2.40205600	-1.32638000	H	0.36671100	2.69797900	0.55881500
N	-0.85544400	-2.31687300	0.60193000	N	-0.97622700	1.93888400	-1.26092000
H	-1.32875400	-2.63930600	-0.23354400	H	-1.45880900	2.50303300	-0.56169300
C	3.48935400	0.63003000	1.25298400	C	3.53003100	-0.94935800	-1.06363000
H	3.16784200	-0.37585400	1.50010300	H	3.18030600	-0.08303400	-1.61500200
C	2.86062800	1.71057000	1.95436100	C	2.91802800	-2.21195400	-1.35901400
C	3.18849700	3.04609800	1.63367600	C	3.27088800	-3.35976300	-0.61577300
C	4.19168800	3.28851800	0.60616200	C	4.30294700	-3.23703700	0.40443700
C	4.79654400	2.19101300	-0.06095100	C	4.88843000	-1.97019900	0.66430200
C	4.40636000	0.83718800	0.27741300	C	4.45390800	-0.80695400	-0.08282100
C	5.05509400	-0.33135400	-0.44540800	C	5.05453500	0.55269000	0.23388100

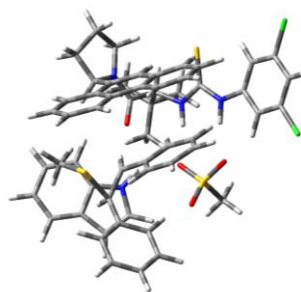
H	5.07894200	-0.12684500	-1.51502800	H	5.10963600	0.67274400	1.31521900
C	6.43949600	-0.66764800	0.13633800	C	6.41040200	0.76320600	-0.46427000
H	6.99059700	0.22408900	0.43178500	H	6.99364200	-0.15516000	-0.51985400
H	7.02537100	-1.21711500	-0.60522900	H	6.98851200	1.51677700	0.07715800
C	6.08784800	-1.57521700	1.31910400	C	5.99603100	1.29595200	-1.83911700
H	6.92883500	-2.17384600	1.66682200	H	6.80509900	1.79799500	-2.36806300
H	5.72757800	-0.96973800	2.15177100	H	5.63602500	0.47313000	-2.45853300
C	4.94898400	-2.44650100	0.77504100	C	4.83994300	2.24876700	-1.51517900
H	5.34357500	-3.35521200	0.31534200	H	5.21338600	3.25462600	-1.30952700
H	4.22499300	-2.71842800	1.54442300	H	4.09829400	2.29528900	-2.31298900
C	3.18636400	-1.79760600	-0.93146100	C	3.10179200	1.98601400	0.31844600
C	2.43804300	-3.11941800	-0.72351200	C	2.28246500	3.16733900	-0.21826000
H	2.78274600	-3.61993000	0.17910100	H	2.60105600	3.42845700	-1.22614600
C	0.48687900	-2.55826200	0.68645100	C	0.36874800	2.15144800	-1.39314500
C	-1.72559000	-1.95159700	1.65355200	C	-1.85026600	1.22405300	-2.09804500
C	-1.50818600	-0.79426000	2.40202400	C	-1.49158200	0.02573800	-2.72040800
H	-0.63588600	-0.17831900	2.23355900	H	-0.49204800	-0.36880300	-2.63276000
C	-2.45770800	-0.43262100	3.34514300	C	-2.45525200	-0.65369200	-3.44888500
C	-3.61735000	-1.17040700	3.55603900	C	-3.76484200	-0.20900000	-3.56670400
H	-4.35185100	-0.85744700	4.28345900	H	-4.50089900	-0.76666500	-4.12610800
C	-3.80693700	-2.30628600	2.78437600	C	-4.09246700	0.97025600	-2.91296700
C	-2.87594000	-2.71530100	1.83954700	C	-3.16261800	1.69683400	-2.18596800
H	-3.04599100	-3.60323000	1.24678300	H	-3.45226600	2.60030200	-1.66843700
C	2.62420800	-4.09437200	-1.91856800	C	2.42733900	4.43386100	0.66894900
C	1.96128100	-5.42655900	-1.55202300	C	1.55005200	5.53965200	0.07022500
H	2.08650600	-6.14208300	-2.36853500	H	1.71869200	6.47520200	0.60927600
H	0.89345400	-5.29501200	-1.37035300	H	0.49056400	5.28932000	0.14252400
H	2.41008200	-5.85394100	-0.65154800	H	1.78917200	5.70354300	-0.98383500
C	2.00548900	-3.55859200	-3.21510100	C	2.02166700	4.19613000	2.12850900
H	2.21709300	-4.26146800	-4.02519600	H	2.11491600	5.13985900	2.67319600
H	2.41072400	-2.58200200	-3.47640400	H	2.65893200	3.45182300	2.60380700
H	0.91991900	-3.46728400	-3.13693800	H	0.98864800	3.85642300	2.22172100
C	4.12185600	-4.32959500	-2.14173400	C	3.89058100	4.88867400	0.62917300
H	4.26214500	-5.03787300	-2.96140700	H	4.01480900	5.77884300	1.25005600
H	4.59065700	-4.75605500	-1.25154100	H	4.19529400	5.14565100	-0.38878000
H	4.64234300	-3.40535200	-2.40424000	H	4.56261000	4.11667900	1.01293300
H	0.57183600	0.52910700	-1.64374500	H	0.61417000	0.11136500	1.42080900
C	0.66249300	0.97269300	-0.65421700	C	0.71926100	-0.78800500	0.81835300
S	-0.73662100	2.05945100	-0.24523100	S	-0.67045100	-1.93482200	1.07571700
H	0.76707400	0.17947500	0.08582600	H	0.78934800	-0.52987900	-0.23726800
H	1.56259700	1.58331500	-0.63342600	H	1.62604100	-1.30836400	1.11848600
C	-2.10411100	0.93414100	-0.70735000	C	-2.06683600	-0.75609500	0.81592000
C	-2.25058100	0.91689500	-2.24205100	C	-2.08685400	-0.49797400	2.26580300
H	-1.79183500	-0.06659100	-0.39771500	H	-1.65203000	0.10470400	0.29157800
C	-3.38874900	1.28257600	0.00620400	C	-3.28382300	-1.30557200	0.10851500
H	-1.27226100	0.76399600	-2.69285400	H	-1.27451800	0.12126000	2.61453100
C	-2.91968100	2.11765400	-2.84964400	C	-2.81886200	-1.22794400	3.29780200
C	-4.27520900	0.26024900	0.34752900	C	-4.49097800	-0.60842500	0.22672200
C	-3.73128100	2.60433900	0.29851700	C	-3.22422700	-2.45052200	-0.68455600
C	-4.31024000	2.24257800	-2.86971700	C	-3.67384400	-2.30901300	3.04770500
C	-2.12825100	3.13914400	-3.37278100	C	-2.62387900	-0.79458400	4.61628100
C	-5.47990900	0.55172800	0.98151400	C	-5.62750000	-1.07388700	-0.42433000
H	-4.01798800	-0.76807100	0.12432000	H	-4.52919000	0.28818800	0.83202600
C	-4.93411300	2.89536500	0.93218700	C	-4.36722100	-2.91086100	-1.33512900
H	-3.05958000	3.40942500	0.02522600	H	-2.28746200	-2.97915800	-0.80683400
C	-4.89828500	3.37918900	-3.41216600	C	-4.31284900	-2.94098500	4.10645000

H	-4.92594500	1.45537800	-2.45471200	H	-3.82922500	-2.66389800	2.03966100
C	-2.71923900	4.28186800	-3.90382900	C	-3.27454900	-1.41963300	5.66833000
H	-1.04970700	3.04298000	-3.35192200	H	-1.96664500	0.04681000	4.80003600
C	-5.81100600	1.87021500	1.27716700	C	-5.57095200	-2.22819000	-1.20229400
H	-6.14940600	-0.25540500	1.25334200	H	-6.55612100	-0.52561800	-0.33224500
H	-5.18470300	3.92413800	1.15806300	H	-4.30686700	-3.79817500	-1.95246200
C	-4.10487200	4.40164400	-3.92687600	C	-4.11998200	-2.49724100	5.41230100
H	-5.97695400	3.46972400	-3.42499800	H	-4.96573200	-3.78111800	3.90988200
H	-2.09660500	5.07208400	-4.30313700	H	-3.12177600	-1.07450100	6.68230400
H	-6.74429900	2.09828300	1.77646500	H	-6.45876300	-2.58618300	-1.70825500
H	-4.56572000	5.28751800	-4.34524400	H	-4.62641400	-2.99270900	6.23093000
O	-0.96924300	-1.59500900	-2.69193800	O	-0.91915300	2.24812000	2.02329600
O	-2.97212000	-2.48475000	-1.49957200	O	-2.81175100	3.09467000	0.67531800
S	-2.42538200	-1.70554400	-2.60844800	S	-2.38008400	2.52249200	1.96714700
O	-3.08146800	-0.25041400	-2.62809400	O	-3.17412900	1.30443000	2.37741200
C	-3.08362700	-2.32957300	-4.12946200	C	-2.74034000	3.73723100	3.21531900
H	-4.16818700	-2.27428300	-4.07222400	H	-3.81023900	3.93063000	3.19982000
H	-2.69906600	-1.71664600	-4.94058900	H	-2.43230400	3.33948200	4.17929300
H	-2.75192900	-3.36163200	-4.22303800	H	-2.18223700	4.63883700	2.97231900
C	2.52096700	4.07737500	2.32761400	C	2.59592000	-4.56656400	-0.89693100
C	1.89497500	1.43571700	2.94494200	C	1.92598500	-2.29490900	-2.35901500
H	1.66379200	0.39941100	3.16807700	H	1.68393700	-1.39856600	-2.92017900
C	1.57935400	3.79161000	3.29294000	C	1.62160100	-4.62802700	-1.87057100
H	1.07859100	4.60184600	3.80749400	H	1.11634100	-5.56594700	-2.06310000
C	1.26141900	2.46083800	3.60973300	C	1.28180300	-3.48497800	-2.61351700
H	0.51869500	2.24334600	4.36528200	H	0.51863700	-3.53807100	-3.37850500
C	4.59035300	4.59324300	0.24930000	C	4.74867500	-4.34863300	1.14859500
H	4.14507300	5.44419200	0.74439200	H	4.32371200	-5.32460400	0.96244400
C	5.77413700	2.44900000	-1.04802500	C	5.89319900	-1.87472200	1.65299100
C	6.14426100	3.73464100	-1.37437800	C	6.30892800	-2.97845000	2.36387500
H	6.89599200	3.90551200	-2.13441400	H	7.08199100	-2.87924100	3.11508700
C	5.54468800	4.81839000	-0.71811500	C	5.72962000	-4.22888000	2.10815300
H	6.24864300	1.62326500	-1.56031600	H	6.35441100	-0.91803700	1.85627300
H	2.73705300	5.11314100	2.10706300	H	2.82998300	-5.46447500	-0.34278800
H	5.83079200	5.83204300	-0.96825100	H	6.05350000	-5.10191500	2.66022800
Cl	-5.26245300	-3.24238600	2.99809000	Cl	-5.73366100	1.54722900	-2.99834200
Cl	-2.22622700	1.02166200	4.27205800	Cl	-2.02240500	-2.16198400	-4.21450100

**13d•15**



**13d•15•indole**



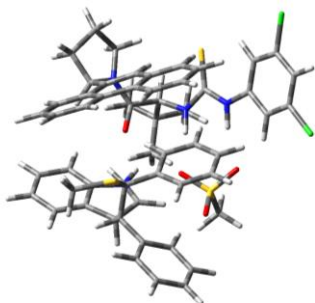
E = -4400.30529036	E + ZPE = -4399.416942	E = -4764.10277915	E + ZPE = -4763.079597
G = -4399.511565	imaginary frequencies:	G = -4763.183090	imaginary frequencies: 0
S	-1.40221100 -1.95095800 -2.59922000	S	3.61753400 2.92332000 0.02659200
O	-2.94389800 -1.01337600 1.34989600	O	-1.00847100 1.97399800 -0.30317900
N	-4.42170700 -1.35340200 -0.30756300	N	-0.18678600 3.41089600 1.22854300

N	-1.17094700	-2.69616700	-0.03939700	N	1.52932100	2.22890200	-1.49417900
H	-0.64513200	-2.59811500	0.83045700	H	0.98077400	1.53128400	-2.00789000
N	0.79113200	-2.22332600	-1.02482500	N	3.18611600	0.67892300	-1.43644500
H	1.17453800	-2.76124400	-0.23939500	H	2.53770500	0.15199000	-2.03138900
C	-3.34215700	1.08384700	-1.23232800	C	1.00625200	1.18230900	2.38854200
H	-3.11055800	0.15396100	-1.74081700	H	1.56841300	1.85988800	1.75555400
C	-2.49949100	2.21199800	-1.50698400	C	1.67740600	-0.00944500	2.81446800
C	-2.67605500	3.41770000	-0.79280500	C	0.99538900	-0.96196900	3.60125800
C	-3.78252700	3.51017400	0.15012500	C	-0.38240900	-0.68514800	3.98253100
C	-4.59744300	2.37266100	0.39097900	C	-0.99038700	0.53899400	3.59402900
C	-4.31919500	1.12583200	-0.29424700	C	-0.27024400	1.46729300	2.74699500
C	-5.12018500	-0.11825800	0.05737200	C	-0.93755000	2.76398800	2.30686600
H	-5.28134100	-0.13224800	1.13465800	H	-1.94773400	2.56062400	1.95152300
C	-6.43125400	-0.23074200	-0.74144400	C	-0.91306200	3.83309600	3.41394800
H	-6.86946300	0.74477100	-0.95009000	H	-1.05892400	3.40544300	4.40482800
H	-7.15356300	-0.82750200	-0.17850200	H	-1.69797100	4.57057400	3.22720000
C	-5.99531500	-0.97947600	-2.00519400	C	0.46852400	4.46591300	3.23507600
H	-6.82632500	-1.43388700	-2.54318200	H	0.55239200	5.44837200	3.69738600
H	-5.48003400	-0.29483600	-2.68102800	H	1.23141300	3.81643300	3.66621100
C	-5.00862800	-2.02480400	-1.47449300	C	0.64021900	4.53220700	1.71471000
H	-5.53084800	-2.93493100	-1.16792700	H	0.25610400	5.47257700	1.31474300
H	-4.23572900	-2.27722900	-2.20013900	H	1.68076900	4.40968900	1.41571100
C	-3.33495400	-1.70840300	0.41316200	C	-0.22860600	2.89133900	-0.01558000
C	-2.58537900	-2.99697500	0.05591100	C	0.79440700	3.39956200	-1.03882500
H	-2.89777600	-3.36411000	-0.92051800	H	1.52353700	4.02699700	-0.53612200
C	-0.56546300	-2.29109700	-1.17244000	C	2.75093400	1.89696900	-1.00875400
C	1.77766300	-1.68798700	-1.86398500	C	4.35543100	-0.05387600	-1.15646600
C	1.55212200	-0.64601800	-2.76771300	C	5.47709100	0.42045500	-0.46685400
H	0.56332000	-0.24805400	-2.91850800	H	5.52819000	1.43328700	-0.11099700
C	2.63173800	-0.13722000	-3.47318100	C	6.54038900	-0.44606900	-0.24344500
C	3.92848700	-0.60343200	-3.31646800	C	6.55614000	-1.76194500	-0.67738900
H	4.75304200	-0.18031200	-3.87027100	H	7.39539300	-2.41388700	-0.48601100
C	4.12004300	-1.62470300	-2.39452200	C	5.43909400	-2.19599900	-1.38054300
C	3.07718900	-2.17309700	-1.66620900	C	4.35416700	-1.37677600	-1.63390500
H	3.26094700	-2.95003600	-0.93541100	H	3.50891200	-1.75431600	-2.19336300
C	-2.83859200	-4.12873300	1.08796800	C	0.21202000	4.26293700	-2.18468300
C	-1.98118700	-5.33664600	0.68924700	C	1.38205600	4.67623100	-3.08443600
H	-2.24071200	-6.19257600	1.31715800	H	1.03566700	5.38883800	-3.83696300
H	-0.91677700	-5.12975900	0.81514300	H	1.80181900	3.81065800	-3.59844700
H	-2.15217500	-5.61347000	-0.35458800	H	2.18023000	5.14553200	-2.50333600
C	-2.50172200	-3.72036300	2.52749500	C	-0.85063700	3.55829400	-3.02759600
H	-2.61372800	-4.59653200	3.17268400	H	-1.13291400	4.21116900	-3.85818100
H	-3.16549700	-2.93510200	2.88642300	H	-1.75082100	3.35318100	-2.44847500
H	-1.47804400	-3.35387500	2.62603400	H	-0.48672500	2.61779100	-3.43962800
C	-4.31920600	-4.51758200	1.01183700	C	-0.40242000	5.51642900	-1.55036000
H	-4.53104000	-5.31086700	1.73212600	H	-0.83286800	6.15120200	-2.32779100
H	-4.57731800	-4.88926700	0.01631400	H	0.35195300	6.10130700	-1.01708800
H	-4.96812900	-3.66978900	1.24785900	H	-1.20433900	5.25846600	-0.85109200
H	-0.60166500	-0.15419100	1.58882200	H	-2.01273600	1.04246600	-2.18557000
C	-0.80886500	0.70929900	0.96292900	N	-3.00116100	0.82736500	-2.28320600
S	0.62210800	1.83417700	0.95258300	C	-3.47264700	-0.22294400	-3.02573500
H	-0.99280400	0.40722000	-0.06504800	C	-4.05819800	1.49089200	-1.71503600
H	-1.66223000	1.26870200	1.33754600	C	-4.84143700	-0.27688600	-2.94459300
C	2.01946000	0.65897100	0.68046700	H	-2.77404100	-0.88057700	-3.51889400
C	1.81983300	0.96670300	2.11149300	C	-5.24616900	0.80973800	-2.10154500
H	1.61566000	-0.30369100	0.37901800	C	-4.09168100	2.63463300	-0.90382200

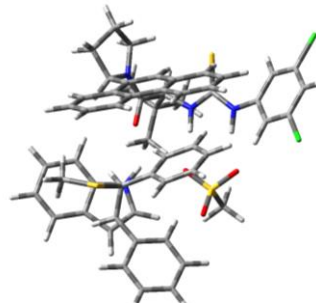
C	3.21947100	1.15753500	-0.05590000	H	-5.47785400	-1.00541600	-3.41947500
H	1.29659800	0.18870500	2.65525900	C	-6.48355000	1.27342600	-1.61907700
C	2.76199100	1.80159400	2.90335100	C	-5.32679200	3.06868600	-0.45570600
C	3.15468200	2.11710100	-1.06192300	H	-3.17642300	3.13962200	-0.62695600
C	4.44399000	0.58528400	0.29954600	C	-6.51348100	2.38936700	-0.80171100
C	3.14112000	3.09594100	2.54413900	H	-7.40111700	0.76890600	-1.89684900
C	3.31648700	1.20506900	4.03743400	H	-5.38491200	3.95083700	0.17002300
C	4.32175400	2.52257000	-1.70452600	H	-7.46227700	2.75986500	-0.43423100
H	2.19889800	2.53721100	-1.35553000	H	-5.23823000	0.37179600	0.86149200
C	5.60253600	0.98907000	-0.35273300	C	-4.39511900	0.42153600	1.54898300
H	4.46983800	-0.17409000	1.07373700	S	-3.59884800	-1.20804700	1.66788500
C	4.05940300	3.79085400	3.32120300	H	-3.67372300	1.15196800	1.19323700
H	2.72561300	3.56663700	1.66142400	H	-4.72447000	0.67170500	2.55429400
C	4.24136800	1.90287500	4.80690300	C	-2.21908100	-1.13712700	0.34741100
H	3.04872500	0.18505000	4.28116100	C	-3.50768000	-1.67341900	-0.12961300
C	5.54384600	1.96115500	-1.34951800	H	-2.01237400	-0.09561700	0.10984000
H	4.26893800	3.26501800	-2.49046200	C	-1.02546500	-1.96979200	0.61118800
H	6.54981200	0.53937500	-0.08582300	H	-4.11090600	-0.96715900	-0.69616500
C	4.61011500	3.19681400	4.45400500	C	-3.70874600	-3.11105300	-0.48556900
H	4.34590900	4.79587400	3.04011900	C	0.18703900	-1.48204900	0.12688900
H	4.67293100	1.43297000	5.68103600	C	-1.07914400	-3.21683000	1.24499800
H	6.44982800	2.27510300	-1.85240300	C	-2.87768400	-3.66887400	-1.45957800
H	5.32597300	3.74124800	5.05640700	C	-4.74262300	-3.86049400	0.07279400
O	0.55713800	-1.91590200	2.21742200	C	1.33864300	-2.25405600	0.24423300
O	2.05994600	-3.54572900	1.15252900	H	0.21933700	-0.51444000	-0.36021200
S	1.87097800	-2.63456000	2.31373000	C	0.07692700	-3.96879900	1.38010000
O	2.99367900	-1.70628500	2.56584200	H	-2.01691300	-3.60340300	1.62631500
C	1.73980900	-3.69282600	3.74095200	C	-3.09117600	-4.98320600	-1.86281700
H	2.67113900	-4.24557400	3.84007500	H	-2.07473400	-3.08721900	-1.89889100
H	1.56725800	-3.06922900	4.61532100	C	-4.94450300	-5.17562600	-0.33242800
H	0.90490800	-4.37237100	3.58377100	H	-5.38577100	-3.41965700	0.82586000
C	-1.76200700	4.46798300	-1.02565700	C	1.28519400	-3.49150300	0.87052800
C	-1.44394900	2.08918500	-2.43586800	H	2.27392700	-1.88226400	-0.14667000
H	-1.34116300	1.15395100	-2.97474600	H	0.03606500	-4.93158000	1.87322000
C	-0.72812800	4.32744700	-1.92862300	C	-4.11747500	-5.73755500	-1.30101700
H	-0.04109300	5.14914500	-2.08741400	H	-2.44476700	-5.41503300	-2.61563800
C	-0.56594400	3.13022000	-2.64715500	H	-5.74452500	-5.75758000	0.10695200
H	0.24058200	3.02453200	-3.36192000	H	2.18667200	-4.08260600	0.96834000
C	-4.07710100	4.70668000	0.83523600	H	-4.27256600	-6.76172100	-1.61582200
H	-3.47884600	5.58897000	0.65756000	O	-0.22954400	0.42952800	-2.93983600
C	-5.67339000	2.48713600	1.29886100	O	1.62852700	-1.16999700	-2.98964800
C	-5.93803200	3.66966900	1.95357600	S	0.24106000	-0.89934900	-3.44715900
H	-6.77072900	3.73265100	2.64223200	O	-0.72368000	-1.98399000	-3.19323800
C	-5.12950300	4.79038800	1.72036200	C	0.34270300	-0.72250000	-5.21875900
H	-6.31393200	1.63504600	1.47973200	H	0.68902700	-1.66615300	-5.63395200
H	-1.85626000	5.40161700	-0.48923700	H	-0.64801000	-0.47851200	-5.59663100
H	-5.33443400	5.72412600	2.22795200	H	1.04554600	0.07602000	-5.44518100
Cl	5.73452100	-2.22403000	-2.13432800	C	1.69776500	-2.11862800	3.99627100
Cl	2.35018500	1.18183400	-4.58434100	C	3.01652900	-0.22682400	2.43155100
				H	3.51057700	0.52210900	1.82236000
				C	3.01069600	-2.31507500	3.61977200
				H	3.52819600	-3.21150300	3.93799500
				C	3.67800400	-1.36785900	2.82583600
				H	4.70523200	-1.53149400	2.52413700
				C	-1.13867900	-1.59215500	4.75343300
				H	-0.70806400	-2.54358300	5.03092800

	C	-2.29445500	0.82744900	4.05715900
	C	-2.99792800	-0.06624100	4.83868600
	H	-3.98841400	0.18685800	5.19803700
	C	-2.41855500	-1.29852400	5.17384100
	H	-2.74778600	1.77838200	3.80905300
	H	1.21640500	-2.87023100	4.60600100
	H	-2.96698300	-2.01278200	5.77448300
	Cl	7.92526400	0.15546100	0.63371600
	Cl	5.40061800	-3.84297900	-1.95361100

**13d•16**



**13d•TS<sub>15-16</sub>**



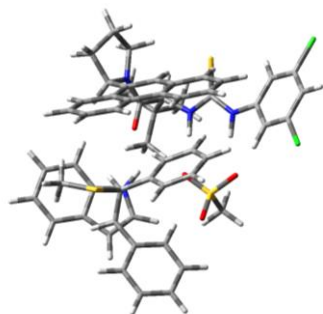
E = -4764.13974856		E + ZPE = -4763.113516		E = -4764.08845567		E + ZPE = -4763.065308	
G = -4763.212107		imaginary frequencies: 0		G = -4763.166284		imaginary frequencies: 1	
S	-4.73998100	1.41520600	-0.21764800	S	4.13821200	2.33744200	-0.40722200
O	-0.38923100	2.66885700	1.28738100	O	-0.54079700	2.22256500	-0.81305600
N	-1.60328900	3.91335600	-0.13314800	N	0.52718500	3.74085700	0.45122400
N	-2.83259500	1.28114800	1.65860800	N	2.00382100	1.76073500	-1.92498400
H	-2.03946400	0.77985900	2.06927200	H	1.32744400	1.06640600	-2.25885100
N	-3.47389100	-0.73253100	0.85162800	N	3.35946900	-0.00779600	-1.50465900
H	-2.85107000	-1.07129100	1.59086500	H	2.65468600	-0.54012600	-2.02707800
C	-1.14766900	1.86945900	-1.98201300	C	1.22621500	1.59865500	2.09723200
H	-2.12186100	1.99446100	-1.52153100	H	1.93205500	2.01918500	1.38936900
C	-0.92988300	0.65901500	-2.71669800	C	1.62535800	0.40199900	2.77663800
C	0.33052600	0.40306300	-3.29739600	C	0.74678600	-0.21934000	3.68949000
C	1.36013800	1.42711300	-3.19482000	C	-0.54346000	0.40556900	3.94444700
C	1.10953800	2.61208300	-2.45129300	C	-0.89953800	1.59673400	3.25683800
C	-0.17914600	2.80473000	-1.81762100	C	0.01910700	2.18132700	2.30084400
C	-0.44403800	4.07213100	-1.01857800	C	-0.36498300	3.46749100	1.58293000
H	0.42658700	4.30470000	-0.40922600	H	-1.38396000	3.38249800	1.20719000
C	-0.86463000	5.25382600	-1.90946500	C	-0.15792100	4.70953500	2.46773800
H	-0.34572800	5.24604700	-2.86711900	H	-0.40572100	4.51694700	3.51063200
H	-0.64793600	6.19533900	-1.39794800	H	-0.78193200	5.52901800	2.10125700
C	-2.37682300	5.05520500	-2.04101600	C	1.32360600	5.02938000	2.25272200
H	-2.90250800	5.95548600	-2.35596200	H	1.58833000	6.04789400	2.53329900
H	-2.58399200	4.26414700	-2.76287400	H	1.93756700	4.34016600	2.83386800
C	-2.80349300	4.60175300	-0.64109900	C	1.53279000	4.77317800	0.75698600
H	-3.03556600	5.45689900	-0.00140500	H	1.32876500	5.67260600	0.17098900
H	-3.65763200	3.92650000	-0.66909900	H	2.53735600	4.41449600	0.53579600
C	-1.49024700	3.12681400	0.94968200	C	0.40039900	3.01374500	-0.67273200
C	-2.75338200	2.73199500	1.71573400	C	1.48562500	3.10853100	-1.74734100
H	-3.63327000	3.10383900	1.19888100	H	2.31646300	3.70895400	-1.38731400
C	-3.64025200	0.61799700	0.79175700	C	3.13097600	1.32117000	-1.31479900
C	-3.98063400	-1.78522500	0.06780700	C	4.32500800	-0.84261300	-0.90655300

C	-4.85315700	-1.65642800	-1.01808800	C	5.62274100	-0.43395800	-0.58820600
H	-5.24513100	-0.69885000	-1.31029400	H	5.95801900	0.56648800	-0.79889200
C	-5.21572300	-2.79873100	-1.72180200	C	6.47943800	-1.34733900	0.01141400
C	-4.76614900	-4.06880900	-1.39764200	C	6.11057200	-2.65517000	0.29266800
H	-5.06482900	-4.93915500	-1.96266300	H	6.79510900	-3.34614500	0.76224200
C	-3.91415100	-4.16449900	-0.30403700	C	4.82786800	-3.04021300	-0.07679800
C	-3.51723400	-3.06174600	0.42992500	C	3.93340600	-2.16877200	-0.67450700
H	-2.84918100	-3.17855400	1.27323000	H	2.95164700	-2.50671000	-0.97837900
C	-2.81157100	3.29693100	3.15487700	C	1.00266600	3.75952600	-3.06603300
C	-4.13189500	2.83371000	3.77952500	C	2.18698400	3.76776400	-4.03867100
H	-4.25976400	3.29390400	4.76236500	H	1.92366000	4.32957300	-4.93823000
H	-4.14464200	1.74958600	3.90199500	H	2.45664400	2.75285900	-4.33346000
H	-4.98331000	3.11330000	3.15377800	H	3.06576200	4.23336600	-3.58475200
C	-1.64624600	2.85139600	4.04247400	C	-0.18519200	3.04582300	-3.71746400
H	-1.81198800	3.22411500	5.05705800	H	-0.38531000	3.51014600	-4.68711500
H	-0.69582100	3.24261600	3.67909100	H	-1.08618900	3.13258700	-3.10913500
H	-1.56344200	1.76505300	4.08172400	H	0.01347100	1.98574600	-3.87965700
C	-2.80929100	4.82652700	3.04818900	C	0.60387900	5.20467500	-2.74454900
H	-2.86670400	5.27043800	4.04450700	H	0.25751700	5.70596000	-3.65104200
H	-3.66692900	5.18326500	2.47085500	H	1.45271300	5.76986500	-2.34948600
H	-1.89386200	5.19159100	2.57262400	H	-0.20956600	5.23942000	-2.01319000
H	0.81490900	1.32780600	2.01667300	H	-1.64116400	1.00131700	-2.00512400
N	1.81937600	1.15757700	1.85395500	N	-2.63057900	0.76508500	-2.04595400
C	2.34079700	-0.02320000	1.90190600	C	-3.10656900	-0.41870200	-2.49915300
C	2.76870200	2.14313500	1.47937800	C	-3.67891800	1.55413000	-1.62275800
C	3.80827600	0.03378900	1.60069300	C	-4.48843800	-0.44044800	-2.38901100
H	1.73803500	-0.87417900	2.20256100	H	-2.42591500	-1.18043100	-2.85218500
C	3.99090100	1.50097300	1.29582000	C	-4.87820900	0.83129900	-1.84994500
C	2.59241100	3.50831400	1.33835000	C	-3.67748900	2.82360100	-1.03826300
H	4.31061200	-0.21723700	2.54661200	H	-5.13304400	-1.23105800	-2.73838500
C	5.09939600	2.24078300	0.91433100	C	-6.10536800	1.40754300	-1.48523600
C	3.71662400	4.24015000	0.96128100	C	-4.90405300	3.36442300	-0.68499600
H	1.62552400	3.95788900	1.50734900	H	-2.74643300	3.34757300	-0.87430800
C	4.94721300	3.61725900	0.74352400	C	-6.10642200	2.66717800	-0.90713300
H	6.06218500	1.76948300	0.75961200	H	-7.03582700	0.88240100	-1.66762700
H	3.63284500	5.31167400	0.83292500	H	-4.93984900	4.34914400	-0.23633800
H	5.79983900	4.21391500	0.44664100	H	-7.04543100	3.12898900	-0.62938100
H	6.56361300	-0.25685900	-1.52746800	H	-5.70766800	0.51757800	1.08227900
C	5.77014500	-0.08877900	-2.25648400	C	-5.17876700	0.44748200	2.03425800
S	4.51939600	-1.40644300	-2.23639800	S	-4.23975200	-1.09814200	2.17282700
H	5.29964700	0.88032200	-2.08426000	H	-4.49587000	1.28898500	2.13373700
H	6.21365500	-0.08898700	-3.25178400	H	-5.89914000	0.45712000	2.85083000
C	3.54095800	-0.88519600	-0.77755700	C	-3.18319000	-0.92789300	0.65063100
C	4.38844800	-0.92933600	0.52877400	C	-4.25340000	-1.62549900	-0.08720100
H	3.25812700	0.15858600	-0.95753600	H	-3.11038300	0.13353600	0.41098100
C	2.28610300	-1.72260100	-0.70880400	C	-1.84162000	-1.57491300	0.83730400
H	5.35674500	-0.48294800	0.28959800	H	-5.18775600	-1.09405200	-0.17724700
C	4.67778200	-2.31692500	1.06271500	C	-4.24403400	-3.00890200	-0.52967600
C	1.04868200	-1.10539800	-0.50673200	C	-0.72001300	-0.94523600	0.30906200
C	2.33825400	-3.11688200	-0.81165000	C	-1.70318600	-2.78786600	1.52068200
C	3.80683600	-3.00152900	1.91554300	C	-3.10597000	-3.58689000	-1.11700100
C	5.86317000	-2.94420600	0.67213100	C	-5.44182500	-3.73920900	-0.45714500
C	-0.10635600	-1.86646000	-0.35083700	C	0.53124200	-1.54354800	0.43248400
H	0.97922700	-0.02313700	-0.48679500	H	-0.80698600	0.00959900	-0.18946300
C	1.17945400	-3.87276200	-0.68376400	C	-0.45235700	-3.37499300	1.64492500
H	3.28809200	-3.61074000	-0.97595700	H	-2.57066000	-3.28410800	1.94244200

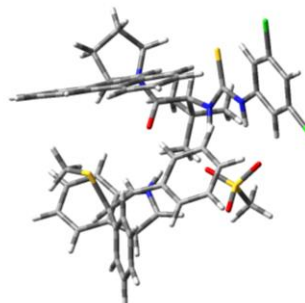
C	4.12140800	-4.28128300	2.36294600	C	-3.17672700	-4.88377600	-1.60866000
H	2.85924700	-2.57986900	2.22398500	H	-2.19318800	-3.02125500	-1.24958800
C	6.17352300	-4.22720500	1.11099600	C	-5.49087400	-5.04522600	-0.91687000
H	6.54468300	-2.42460600	0.00834800	H	-6.31848600	-3.27957000	-0.01572900
C	-0.04188900	-3.25223100	-0.43730900	C	0.66898400	-2.75749900	1.09141900
H	-1.05210600	-1.37129500	-0.17801900	H	1.39458800	-1.04473500	0.01544100
H	1.23286600	-4.95131200	-0.76110400	H	-0.34983900	-4.31445500	2.17292200
C	5.30149700	-4.89918500	1.96175800	C	-4.35563500	-5.61621600	-1.49490100
H	3.42869900	-4.79441200	3.01736700	H	-2.30493800	-5.30781800	-2.08828300
H	7.09537400	-4.69656400	0.79151600	H	-6.40828500	-5.61364800	-0.83913800
H	-0.93893000	-3.84606500	-0.32188400	H	1.64596100	-3.21223400	1.19314900
H	5.53954700	-5.89677400	2.30851300	H	-4.39878200	-6.63036600	-1.87164800
O	-0.48625900	-0.00085700	2.82114800	O	-0.00511500	-0.14195300	-2.82401300
O	-1.82045200	-2.06492500	2.83119400	O	1.68042000	-1.93473500	-2.76492900
S	-0.60857400	-1.39608200	3.36117100	S	0.33559900	-1.53676900	-3.25397800
O	0.65014300	-2.15761700	3.22214700	O	-0.74364800	-2.50467800	-2.96858700
C	-0.88739400	-1.21301300	5.11278800	C	0.47524300	-1.45968100	-5.03154100
H	-0.98273200	-2.20715700	5.54346200	H	0.73574000	-2.45093800	-5.39520900
H	-0.03702900	-0.68908300	5.54345300	H	-0.48251200	-1.14147800	-5.43789700
H	-1.80381100	-0.64499000	5.25864900	H	1.25482200	-0.74388400	-5.28365800
C	0.53525600	-0.84804900	-3.91595800	C	1.17074700	-1.41325000	4.30762300
C	-1.96040600	-0.29895000	-2.80246600	C	2.88804000	-0.16441000	2.50412800
H	-2.91903700	-0.07052200	-2.35029900	H	3.54065400	0.33644100	1.79686400
C	-0.47626500	-1.78385300	-3.97033600	C	2.40614000	-1.95941100	4.02707900
H	-0.28821700	-2.74513000	-4.43101900	H	2.70445800	-2.88153700	4.51007700
C	-1.73991100	-1.50823600	-3.42073300	C	3.27589200	-1.33405300	3.11801400
H	-2.52897600	-2.24920300	-3.46222200	H	4.24154200	-1.77083900	2.89523100
C	2.61143400	1.28537700	-3.83014400	C	-1.45403700	-0.12605900	4.88039500
H	2.81716000	0.40144800	-4.41516400	H	-1.20474000	-1.03244100	5.41312800
C	2.12714300	3.58806400	-2.36092000	C	-2.14320200	2.20277800	3.54554800
C	3.34399800	3.41855500	-2.98408600	C	-3.00512200	1.66868400	4.48036400
H	4.10475400	4.18498800	-2.90376100	H	-3.94275100	2.16559300	4.69856400
C	3.58304300	2.25948200	-3.73564900	C	-2.65810500	0.48801800	5.15126400
H	1.94851500	4.49820500	-1.80496300	H	-2.42114600	3.11974000	3.04223200
H	1.50357700	-1.10450200	-4.32214200	H	0.52500200	-1.92734200	5.00543900
H	4.52700100	2.12891400	-4.25004700	H	-3.32846200	0.06115400	5.88666500
Cl	-6.28053200	-2.61891200	-3.09373400	Cl	8.09795100	-0.83491600	0.41249100
Cl	-3.30375200	-5.73625400	0.14640000	Cl	4.32265600	-4.67951600	0.24718800

Enantioselectivity-determining transition state (M05-2X). Energy values are in a. u.

**13d•TS<sub>major</sub>**



**13d•TS<sub>minor</sub>**

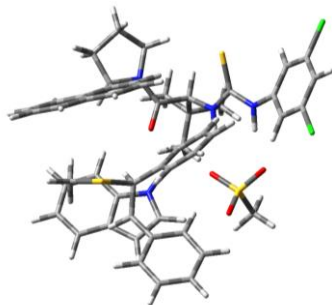


E = -4764.08845567		E + ZPE = -4763.065308		E = -4764.08362480		E + ZPE = -4763.061392	
G = -4763.166284		imaginary frequencies: 1		G = -4763.165540		imaginary frequencies: 1	
S	4.13821200	2.33744200	-0.40722200	S	-4.25119000	-2.07713200	0.46960400
O	-0.54079700	2.22256500	-0.81305600	O	0.05334600	-2.38349400	-1.14668600
N	0.52718500	3.74085700	0.45122400	N	-0.85579700	-4.01759100	0.10806700
N	2.00382100	1.76073500	-1.92498400	N	-2.60958300	-1.55220700	-1.57985700
H	1.32744400	1.06640600	-2.25885100	H	-1.99700200	-0.88451600	-2.06247500
N	3.35946900	-0.00779600	-1.50465900	N	-3.65074500	0.27318900	-0.74575800
H	2.65468600	-0.54012600	-2.02707800	H	-3.23623300	0.72193500	-1.57069300
C	1.22621500	1.59865500	2.09723200	C	-0.59101100	-2.00523400	2.02816200
H	1.93205500	2.01918500	1.38936900	H	-1.51253100	-2.15219300	1.47630900
C	1.62535800	0.40199900	2.77663800	C	-0.50351700	-0.83812500	2.85501500
C	0.74678600	-0.21934000	3.68949000	C	0.67289300	-0.57771200	3.58915700
C	-0.54346000	0.40556900	3.94444700	C	1.74119300	-1.56629700	3.55383600
C	-0.89953800	1.59673400	3.25683800	C	1.63409100	-2.69062900	2.69193500
C	0.01910700	2.18132700	2.30084400	C	0.43493100	-2.88028500	1.89778600
C	-0.36498300	3.46749100	1.58293000	C	0.33008400	-4.08398200	0.97199300
H	-1.38396000	3.38249800	1.20719000	H	1.22018000	-4.12162500	0.34229900
C	-0.15792100	4.70953500	2.46773800	C	0.09905900	-5.39856800	1.74365500
H	-0.40572100	4.51694700	3.51063200	H	0.61722300	-5.41248800	2.70069100
H	-0.78193200	5.52901800	2.10125700	H	0.44651700	-6.24259700	1.14178000
C	1.32360600	5.02938000	2.25272200	C	-1.42218300	-5.44126900	1.88944300
H	1.58833000	6.04789400	2.53329900	H	-1.80371900	-6.43203900	2.13221600
H	1.93756700	4.34016600	2.83386800	H	-1.73963800	-4.74629600	2.66871700
C	1.53279000	4.77317800	0.75698600	C	-1.91630900	-4.95081600	0.52917600
H	1.32876500	5.67260600	0.17098900	H	-1.99020200	-5.77617600	-0.18339500
H	2.53735600	4.41449600	0.53579600	H	-2.87490400	-4.44057300	0.59995700
C	0.40039900	3.01374500	-0.67273200	C	-0.91188100	-3.11066200	-0.88818100
C	1.48562500	3.10853100	-1.74734100	C	-2.22685100	-2.95097600	-1.66223700
H	2.31646300	3.70895400	-1.38731400	H	-3.02079100	-3.50956200	-1.17461500
C	3.13097600	1.32117000	-1.31479900	C	-3.47222900	-1.07699000	-0.65267300
C	4.32500800	-0.84261300	-0.90655300	C	-4.29124400	1.19921500	0.09357000
C	5.62274100	-0.43395800	-0.58820600	C	-4.86887000	0.92054800	1.33780800
H	5.95801900	0.56648800	-0.79889200	H	-4.92461100	-0.08484200	1.71594800
C	6.47943800	-1.34733900	0.01141400	C	-5.38834500	1.97157100	2.08409800
C	6.11057200	-2.65517000	0.29266800	C	-5.37526100	3.28975900	1.65720900
H	6.79510900	-3.34614500	0.76224200	H	-5.78787400	4.08614800	2.25825900
C	4.82786800	-3.04021300	-0.07679800	C	-4.80666400	3.53215700	0.41236500
C	3.93340600	-2.16877200	-0.67450700	C	-4.27257100	2.52675100	-0.37255400
H	2.95164700	-2.50671000	-0.97837900	H	-3.83149500	2.75596700	-1.33411800

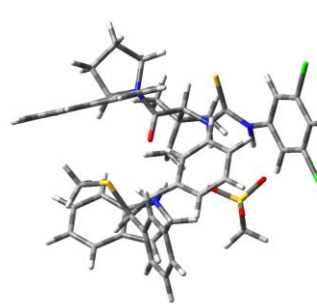
C	1.00266600	3.75952600	-3.06603300	C	-2.14568800	-3.47534500	-3.11900900
C	2.18698400	3.76776400	-4.03867100	C	-3.48800300	-3.17973600	-3.79687500
H	1.92366000	4.32957300	-4.93823000	H	-3.51940900	-3.65941400	-4.77821500
H	2.45664400	2.75285900	-4.33346000	H	-3.63149200	-2.10670900	-3.93338600
H	3.06576200	4.23336600	-3.58475200	H	-4.32222200	-3.55843200	-3.20025400
C	-0.18519200	3.04582300	-3.71746400	C	-1.01275200	-2.85896200	-3.94519500
H	-0.38531000	3.51014600	-4.68711500	H	-1.08803700	-3.22596900	-4.97268200
H	-1.08618900	3.13258700	-3.10913500	H	-0.03399800	-3.14140200	-3.55514500
H	0.01347100	1.98574600	-3.87965700	H	-1.06761800	-1.77017000	-3.96267100
C	0.60387900	5.20467500	-2.74454900	C	-1.94108800	-4.99375800	-3.05059900
H	0.25751700	5.70596000	-3.65104200	H	-1.87443600	-5.40477500	-4.06035300
H	1.45271300	5.76986500	-2.34948600	H	-2.77612800	-5.48255400	-2.54133500
H	-0.20956600	5.23942000	-2.01319000	H	-1.01509700	-5.24827600	-2.52616700
H	-1.64116400	1.00131700	-2.00512400	H	0.88241400	-0.93155200	-2.43890200
N	-2.63057900	0.76508500	-2.04595400	N	1.83824900	-0.61408400	-2.57887400
C	-3.10656900	-0.41870200	-2.49915300	C	2.16991000	0.65970100	-2.90274200
C	-3.67891800	1.55413000	-1.62275800	C	2.98486800	-1.34106900	-2.33558300
C	-4.48843800	-0.44044800	-2.38901100	C	3.54705000	0.80914400	-2.86385800
H	-2.42591500	-1.18043100	-2.85218500	H	1.40266000	1.39373300	-3.10602100
C	-4.87820900	0.83129900	-1.84994500	C	4.09237700	-0.47626000	-2.53339700
C	-3.67748900	2.82360100	-1.03826300	C	3.14356500	-2.67892600	-1.96256000
H	-5.13304400	-1.23105800	-2.73838500	H	4.08432200	1.70383600	-3.13586900
C	-6.10536800	1.40754300	-1.48523600	C	5.39205200	-0.97820200	-2.35519800
C	-4.90405300	3.36442300	-0.68499600	C	4.43827000	-3.14333100	-1.79462100
H	-2.74643300	3.34757300	-0.87430800	H	2.27739900	-3.30706400	-1.80915000
C	-6.10642200	2.66717800	-0.90713300	C	5.55206300	-2.30417800	-1.99013800
H	-7.03582700	0.88240100	-1.66762700	H	6.25476000	-0.34217700	-2.51872200
H	-4.93984900	4.34914400	-0.23633800	H	4.59873500	-4.17585600	-1.51103500
H	-7.04543100	3.12898900	-0.62938100	H	6.54809000	-2.70776400	-1.85885000
H	-5.70766800	0.51757800	1.08227900	O	-0.83455800	0.24557500	-2.88434400
C	-5.17876700	0.44748200	2.03425800	O	-2.68127700	1.86456000	-2.92651900
S	-4.23975200	-1.09814200	2.17282700	S	-1.33494800	1.53534900	-3.46547700
H	-4.49587000	1.28898500	2.13373700	O	-0.34186500	2.61893600	-3.38158700
H	-5.89914000	0.45712000	2.85083000	C	-1.58651500	1.20234700	-5.20015800
C	-3.18319000	-0.92789300	0.65063100	H	-1.96412100	2.10826300	-5.66876400
C	-4.25340000	-1.62549900	-0.08720100	H	-0.63049200	0.91659100	-5.63425400
H	-3.11038300	0.13353600	0.41098100	H	-2.30776000	0.39309500	-5.29532400
C	-1.84162000	-1.57491300	0.83730400	C	0.74503300	0.62582700	4.32050400
H	-5.18775600	-1.09405200	-0.17724700	C	-1.58419500	0.06528200	2.90082800
C	-4.24403400	-3.00890200	-0.52967600	H	-2.48137000	-0.17439200	2.34153100
C	-0.72001300	-0.94523600	0.30906200	C	-0.31384000	1.51022500	4.33851500
C	-1.70318600	-2.78786600	1.52068200	H	-0.23191200	2.43011300	4.90347900
C	-3.10597000	-3.58689000	-1.11700100	C	-1.49585100	1.22700800	3.63356800
C	-5.44182500	-3.73920900	-0.45714500	H	-2.32847500	1.91919800	3.65741100
C	0.53124200	-1.54354800	0.43248400	C	2.87547200	-1.46159200	4.38647100
H	-0.80698600	0.00959900	-0.18946300	H	2.95680600	-0.63216800	5.07478100
C	-0.45235700	-3.37499300	1.64492500	C	2.69077900	-3.62928200	2.66804000
H	-2.57066000	-3.28410800	1.94244200	C	3.78353100	-3.50763200	3.50002100
C	-3.17672700	-4.88377600	-1.60866000	H	4.56830500	-4.25316300	3.47631300
H	-2.19318800	-3.02125500	-1.24958800	C	3.87056400	-2.41701800	4.37829700
C	-5.49087400	-5.04522600	-0.91687000	H	2.63675900	-4.47538300	1.99663500
H	-6.31848600	-3.27957000	-0.01572900	H	1.64264500	0.87882200	4.86771300
C	0.66898400	-2.75749900	1.09141900	H	4.71665000	-2.32164200	5.04704300
H	1.39458800	-1.04473500	0.01544100	H	3.91521700	-1.25823300	0.44761000
H	-0.34983900	-4.31445500	2.17292200	C	4.58927900	-0.84427700	1.19746300
C	-4.35563500	-5.61621600	-1.49490100	S	4.08208400	0.82076900	1.70996300

H	-2.30493800	-5.30781800	-2.08828300	H	5.60547100	-0.82265200	0.80933200
H	-6.40828500	-5.61364800	-0.83913800	H	4.54096500	-1.46272600	2.09049900
H	1.64596100	-3.21223400	1.19314900	C	4.21335500	1.66246300	0.06165800
H	-4.39878200	-6.63036600	-1.87164800	C	2.82763100	1.31700300	-0.33664700
O	-0.00511500	-0.14195300	-2.82401300	H	4.92785200	1.08466000	-0.52237300
O	1.68042000	-1.93473500	-2.76492900	C	4.63533800	3.10257300	0.16396000
S	0.33559900	-1.53676900	-3.25397800	H	2.66469700	0.25234400	-0.45449000
O	-0.74364800	-2.50467800	-2.96858700	C	1.64261700	2.10921800	-0.26236800
C	0.47524300	-1.45968100	-5.03154100	C	5.39078600	3.64895600	-0.87275600
H	0.73574000	-2.45093800	-5.39520900	C	4.27460400	3.90706700	1.24638300
H	-0.48251200	-1.14147800	-5.43789700	C	1.60600300	3.50645700	-0.46755900
H	1.25482200	-0.74388400	-5.28365800	C	0.44075900	1.40720500	-0.02564900
C	1.17074700	-1.41325000	4.30762300	C	5.76571300	4.98889400	-0.84105000
C	2.88804000	-0.16441000	2.50412800	H	5.68495000	3.02362500	-1.70772700
H	3.54065400	0.33644100	1.79686400	C	4.65174200	5.24416400	1.27945200
C	2.40614000	-1.95941100	4.02707900	H	3.68342300	3.49596200	2.05612900
H	2.70445800	-2.88153700	4.51007700	C	0.39707300	4.17202400	-0.40972900
C	3.27589200	-1.33405300	3.11801400	H	2.50687300	4.04385200	-0.72145200
H	4.24154200	-1.77083900	2.89523100	C	-0.75367800	2.09543100	0.08417500
C	-1.45403700	-0.12605900	4.88039500	H	0.46236000	0.32842500	0.08504800
H	-1.20474000	-1.03244100	5.41312800	C	5.39400400	5.78920100	0.23443400
C	-2.14320200	2.20277800	3.54554800	H	6.34989800	5.40352100	-1.65232300
C	-3.00512200	1.66868400	4.48036400	H	4.36413900	5.86105600	2.12086800
H	-3.94275100	2.16559300	4.69856400	C	-0.77691400	3.47323300	-0.11869200
C	-2.65810500	0.48801800	5.15126400	H	0.35766500	5.23476700	-0.60582000
H	-2.42114600	3.11974000	3.04223200	H	-1.66646900	1.56023700	0.29789700
H	0.52500200	-1.92734200	5.00543900	H	5.68564500	6.83120700	0.26205100
H	-3.32846200	0.06115400	5.88666500	H	-1.72060900	4.00255700	-0.07438200
Cl	8.09795100	-0.83491600	0.41249100	Cl	-6.07984000	1.61047500	3.64592000
Cl	4.32265600	-4.67951600	0.24718800	Cl	-4.74760400	5.17588200	-0.17242900

13c•TS<sub>major</sub>



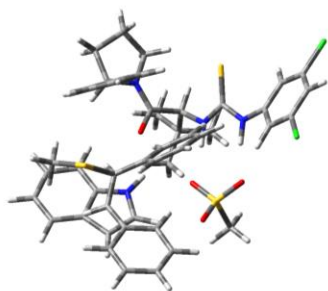
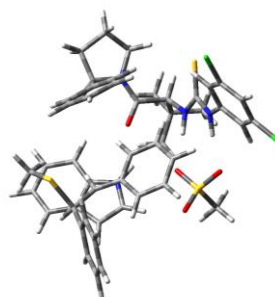
13c•TS<sub>minor</sub>



E = -4610.44769819	E + ZPE = -4609.473068	E = -4610.44383754	E + ZPE = -4609.469174				
G = -4609.573038	imaginary frequencies: 1	G = -4609.570325	imaginary frequencies: 1				
S	3.52898400	-2.73827700	-0.33079900	S	2.58611400	-2.58040100	-1.76800700
O	-0.69549300	-1.84594400	1.21403600	O	-0.60845800	-2.18120900	0.91037600
N	-0.18923600	-3.83354900	0.29174700	N	-0.72019400	-3.92150200	-0.51227000
N	2.12207200	-1.57967900	1.63495200	N	2.19805200	-2.42848400	0.87079400
H	1.73156300	-0.71974500	2.03003800	H	2.12108200	-1.82027900	1.69156600
N	3.74165000	-0.27078700	0.74373100	N	3.68206500	-0.92445900	0.08465400
H	3.34767400	0.45845900	1.34824300	H	3.80091100	-0.71757600	1.08476500
C	-0.36043800	-2.26660900	-2.07336600	C	-1.18408000	-1.88783400	-2.42265500
H	0.58445700	-2.41686500	-1.56240300	H	-0.18553200	-2.22474700	-2.16713500
C	-0.40116600	-1.40014300	-3.19278500	C	-1.33309900	-0.85286400	-3.37779100

C	-1.57430400	-1.18641200	-3.86062800	C	-2.57774800	-0.41466500	-3.73473800
C	-2.76481800	-1.83486700	-3.44004300	C	-3.73319900	-0.98509600	-3.13945200
C	-2.73490900	-2.68985700	-2.30140400	C	-3.58814300	-2.00343200	-2.15404600
C	-1.49135400	-2.89973000	-1.62177400	C	-2.27329100	-2.46161200	-1.81624600
C	-1.45510400	-3.86464800	-0.44831800	C	-2.11570200	-3.62996700	-0.85475600
H	-2.26089000	-3.61239300	0.24139200	H	-2.65455600	-3.41491700	0.06899700
C	-1.52678200	-5.33336700	-0.91254200	C	-2.55401500	-4.95453400	-1.50982300
H	-2.14440200	-5.45218700	-1.80127300	H	-3.42350200	-4.83508900	-2.15343500
H	-1.93868800	-5.95243000	-0.11081800	H	-2.78650900	-5.68608300	-0.73109700
C	-0.05642400	-5.68236800	-1.14743000	C	-1.29659300	-5.37294600	-2.27433800
H	0.13118800	-6.75435800	-1.18960300	H	-1.29543300	-6.42485800	-2.55673800
H	0.28748500	-5.23201600	-2.08026900	H	-1.19862100	-4.77171300	-3.17951400
C	0.64672800	-5.02036300	0.03708000	C	-0.16683100	-5.04063800	-1.29609700
H	0.63929700	-5.67720700	0.91036400	H	0.04153400	-5.89073200	-0.64525900
H	1.66905000	-4.72375100	-0.19040300	H	0.75206800	-4.73334700	-1.79509600
C	0.09009100	-2.79613400	1.10136100	C	-0.07145600	-3.17038900	0.39945300
C	1.40278000	-2.81217100	1.88698400	C	1.34101200	-3.59341100	0.82559200
H	2.04139500	-3.61383500	1.52466900	H	1.76581000	-4.26627100	0.08232700
C	3.12335000	-1.48310800	0.72928400	C	2.83931800	-1.94693500	-0.21479500
C	4.72399000	0.22783700	-0.13590900	C	4.35728900	-0.00545500	-0.73381100
C	5.79387800	-0.53854900	-0.60350200	C	4.77238500	-0.26106100	-2.04357500
H	5.90256000	-1.57126900	-0.31869500	H	4.59164200	-1.21624800	-2.50546000
C	6.71963500	0.06047100	-1.44542200	C	5.43156900	0.74567000	-2.73905600
C	6.63572900	1.39190000	-1.82972000	C	5.71268600	1.98647700	-2.18620700
H	7.36810000	1.83433600	-2.48863600	H	6.23010100	2.75085900	-2.74712300
C	5.57774100	2.13238500	-1.32045200	C	5.30436400	2.19900800	-0.87308000
C	4.62346300	1.58124100	-0.48021900	C	4.63419400	1.23688700	-0.13888800
H	3.82232700	2.18575800	-0.07607300	H	4.29870000	1.44595700	0.86900300
C	1.17877500	-3.06368800	3.40372300	C	1.34346000	-4.34867000	2.18813100
C	2.55180100	-3.04305800	4.08553100	C	2.80317300	-4.57562400	2.60148200
H	2.44831400	-3.34279800	5.13136200	H	2.83601400	-5.23498200	3.47243200
H	2.99106800	-2.04520700	4.05625300	H	3.29605800	-3.63834300	2.86292300
H	3.24432900	-3.73319700	3.59614400	H	3.37145900	-5.04459300	1.79368400
C	0.26513200	-2.03358100	4.07625000	C	0.61103900	-3.59941000	3.30698600
H	0.24512900	-2.23284900	5.15135900	H	0.71912100	-4.16882400	4.23439000
H	-0.75652500	-2.09781200	3.70037100	H	-0.45447100	-3.50363800	3.09167900
H	0.61695400	-1.01201500	3.92610600	H	1.01980200	-2.60266900	3.47157400
C	0.56333000	-4.45840200	3.56915100	C	0.67072700	-5.71245100	1.99298300
H	0.39046600	-4.66085900	4.62844400	H	0.65376900	-6.24936600	2.94396700
H	1.23148600	-5.23341200	3.18415400	H	1.21908400	-6.32508300	1.27240300
H	-0.39838100	-4.53803200	3.05399600	H	-0.36325500	-5.60674500	1.65276900
H	-1.18588300	-0.07767400	2.14059000	H	-0.35896000	-0.63282500	2.33749800
N	-2.05214900	0.44923400	2.21725100	N	-1.00783400	0.10851500	2.58417300
C	-2.11625600	1.79601600	2.35366300	C	-0.65182700	1.40574600	2.72402900
C	-3.32855100	-0.06938000	2.15188700	C	-2.36433200	-0.02631800	2.78372500
C	-3.44138100	2.19941200	2.38973500	C	-1.77758700	2.17157000	2.99138100
H	-1.21302000	2.38742300	2.39617700	H	0.38219700	1.70457600	2.61308100
C	-4.23786400	1.01069400	2.28475600	C	-2.88419300	1.26061300	3.07905500
C	-3.76135000	-1.38426700	1.96316900	C	-3.17387300	-1.16420700	2.72868900
H	-3.78491700	3.20861200	2.55171300	H	-1.77219100	3.22558400	3.21809200
C	-5.61768300	0.75574600	2.23117500	C	-4.25645600	1.39530200	3.34552800
C	-5.12847900	-1.60432200	1.90875500	C	-4.52318700	-0.99750700	2.99672000
H	-3.04044800	-2.18222500	1.86078300	H	-2.74761800	-2.12625000	2.47985700
C	-6.04890700	-0.54788300	2.04390500	C	-5.05911600	0.26715500	3.30728600
H	-6.33150800	1.56293400	2.34713600	H	-4.67648800	2.36294400	3.59594700
H	-5.49794600	-2.61170300	1.76353800	H	-5.17992000	-1.85778700	2.97082500

H	-7.10966400	-0.76133300	2.00661900	H	-6.11651500	0.35489200	3.52263600
H	-5.33507200	0.69832200	-0.48507000	O	1.70153700	-0.53303400	2.98700200
C	-4.98201600	0.35897800	-1.46040700	O	4.12064000	-0.16040000	2.76288200
S	-3.77210600	1.50833800	-2.16747000	S	2.83668200	0.40945100	3.25207700
H	-4.53005200	-0.62697700	-1.36191600	O	2.55911300	1.77965800	2.77724700
H	-5.81856900	0.30951900	-2.15436900	C	2.99103900	0.48864200	5.02536100
C	-2.53113700	1.48794900	-0.78138800	H	3.81518000	1.15782600	5.26138300
C	-3.26326300	2.62171300	-0.18318500	H	2.05739600	0.87012600	5.43300900
H	-2.65792800	0.55071200	-0.23760400	H	3.19210400	-0.51433300	5.39410700
C	-1.13201800	1.66860400	-1.29932100	C	-5.03311700	-0.56236600	-3.51964600
H	-4.26898000	2.41127800	0.14420100	H	-5.12379800	0.20496400	-4.28008500
C	-2.84936000	4.01153300	-0.16761100	C	-4.76765400	-2.53291300	-1.56266300
C	-0.10612400	0.90823800	-0.74686700	C	-6.01379700	-2.10659800	-1.95206000
C	-0.85292400	2.56099900	-2.33964100	H	-6.89661300	-2.53120400	-1.49126100
C	-1.51858100	4.37893700	0.09402700	C	-6.15238200	-1.11611100	-2.95108800
C	-3.83510200	5.00400800	-0.30479200	H	-4.68787000	-3.28865400	-0.79237700
C	1.19578200	1.05430000	-1.22152400	H	-7.13889400	-0.79318900	-3.25837200
H	-0.31351500	0.19033000	0.03537000	H	-4.12782500	0.28180900	0.39909600
C	0.44552700	2.70213700	-2.80924000	C	-4.76652800	0.93018300	-0.19983900
H	-1.64548200	3.15846100	-2.77714800	S	-3.79659000	2.12997300	-1.15638900
C	-1.18974300	5.72315600	0.20524100	H	-5.47552400	1.44842700	0.44220700
H	-0.75818100	3.63226100	0.27644900	H	-5.29755600	0.32444400	-0.93125200
C	-3.48947200	6.34300200	-0.23146500	C	-3.00409700	3.04361100	0.24760000
H	-4.86194300	4.71104200	-0.49072300	C	-1.85436300	2.11072700	0.32687800
C	1.47598600	1.95008000	-2.24619800	H	-3.65441400	2.91201100	1.11109500
H	1.98691000	0.45521000	-0.79385300	C	-2.76923500	4.50318700	-0.03806400
H	0.65457700	3.39865300	-3.61095600	H	-2.12681200	1.11482600	0.65407500
C	-2.16465000	6.70132900	0.02636100	C	-0.56828300	2.21455500	-0.28792300
H	-0.17028900	5.99301400	0.44567500	C	-2.68775600	5.38211100	1.04226300
H	-4.24548700	7.10632600	-0.35982700	C	-2.59714800	4.99394800	-1.33296000
H	2.49153700	2.06075400	-2.60528700	C	0.11400300	3.42629200	-0.53235700
H	-1.89850000	7.74793700	0.10471600	C	0.02408900	0.99042100	-0.67141900
O	0.81850700	0.84512900	2.49439400	C	-2.41386600	6.73048200	0.83565500
O	2.89141400	2.10158500	2.04551400	H	-2.83654200	5.00835000	2.04824300
S	1.51426400	2.16923100	2.59477400	C	-2.32730600	6.34225200	-1.53968300
O	0.69268800	3.28247400	2.07575600	H	-2.65721000	4.32450900	-2.18219700
C	1.70560000	2.46578200	4.34390700	C	1.33253800	3.40264700	-1.18629200
H	2.20880500	3.42099900	4.47420800	H	-0.29011600	4.36260200	-0.17869500
H	0.71658400	2.48798300	4.79710600	C	1.21878600	0.98494500	-1.36981800
H	2.30165500	1.65938000	4.76552800	H	-0.47763800	0.05610000	-0.44342400
C	-3.98361500	-1.65115800	-4.14233600	C	-2.22935000	7.21198700	-0.45690400
H	-3.98271900	-1.00262900	-5.01103800	H	-2.34905300	7.40197100	1.68193800
C	-3.94994900	-3.31392000	-1.90315300	H	-2.19161700	6.71239000	-2.54755600
C	-5.11418800	-3.12131500	-2.60612000	C	1.86925100	2.19083800	-1.62956100
H	-6.02358500	-3.61437200	-2.28651000	H	1.87345000	4.32459400	-1.35205600
C	-5.13296300	-2.28541800	-3.74524000	H	1.64683300	0.04821100	-1.70496600
H	-3.96286000	-3.96088200	-1.03600600	H	-2.01669900	8.26046600	-0.62040600
H	-6.05362400	-2.14777100	-4.29833100	H	2.81082700	2.18342700	-2.16413500
Cl	8.05795400	-0.89089200	-2.03649100	Cl	5.94250600	0.42825300	-4.37750500
Cl	5.43749600	3.81306700	-1.77219500	Cl	5.60710800	3.75738800	-0.15294400
H	-1.61496900	-0.52196200	-4.71545600	H	-0.44719100	-0.42099300	-3.82542100
H	0.50626400	-0.89840800	-3.50190700	H	-2.70408400	0.36716400	-4.47426300

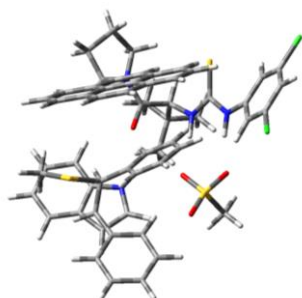
13b•TS<sub>major</sub>13b•TS<sub>minor</sub>

E = -4456.81118821		E + ZPE = -4455.885402		E = -4456.80858652		E + ZPE = -4455.881626	
G = -4455.984297		imaginary frequencies: 1		G = -4455.979388		imaginary frequencies: 1	
S	-3.96796900	2.07308900	-0.39874400	S	4.45474300	-1.40616500	-0.72665000
O	0.49309100	2.30660700	0.61736500	O	0.21490900	-2.47388600	0.45756500
N	-0.53828500	3.97663500	-0.47480100	N	1.38465200	-3.85400700	-0.87065600
N	-2.11307600	1.53691000	1.46332000	N	2.67563700	-1.44211400	1.28607000
H	-1.47242200	0.85118600	1.87317700	H	1.93148900	-0.94381300	1.78553300
N	-3.42404500	-0.22547800	0.90942600	N	3.38246600	0.61987100	0.70001400
H	-2.78886900	-0.76193000	1.51032300	H	2.85936600	0.92466700	1.52978700
C	-0.42295200	2.05823400	-2.62707700	C	0.93860200	-1.70926000	-2.76057300
H	-1.36127000	2.20430500	-2.10216400	H	1.94089100	-1.84989900	-2.36979400
C	-0.30352400	1.01609300	-3.54485800	C	0.63843000	-0.55800100	-3.48578200
C	0.89958700	0.79028300	-4.20357400	C	-0.65080500	-0.34228100	-3.96295800
C	1.99014000	1.61839300	-3.94402500	C	-1.64349900	-1.28533300	-3.70885700
C	1.87327600	2.65622000	-3.02470200	C	-1.34575600	-2.43387200	-2.98162700
C	0.66535700	2.88717500	-2.36203600	C	-0.05181400	-2.65938200	-2.50820100
C	0.57331400	4.07885100	-1.42553600	C	0.24446600	-3.96138200	-1.78632700
H	1.51251900	4.15935400	-0.87758700	H	-0.64582700	-4.25102700	-1.22757800
C	0.24997000	5.38395200	-2.17575200	C	0.69324600	-5.07889000	-2.74605600
H	0.69616900	5.39852400	-3.16923700	H	0.20635900	-4.99682100	-3.71688600
H	0.62927700	6.23647900	-1.60631300	H	0.44787100	-6.05111800	-2.31118200
C	-1.27913700	5.39969200	-2.18823700	C	2.21149700	-4.89840500	-2.80368900
H	-1.69952200	6.38201300	-2.39965500	H	2.73578700	-5.77977900	-3.17057900
H	-1.65471000	4.69394600	-2.93135400	H	2.46453700	-4.05358100	-3.44648700
C	-1.63599900	4.90989000	-0.78390900	C	2.57593100	-4.57258500	-1.35339900
H	-1.63596700	5.73757100	-0.06964800	H	2.72544600	-5.48589000	-0.77146300
H	-2.59447800	4.39523100	-0.75153100	H	3.45940600	-3.94026700	-1.27861000
C	-0.49014700	3.04938800	0.49818800	C	1.27443300	-3.06311700	0.21228500
C	-1.67317800	2.91879600	1.45680100	C	2.48630700	-2.87084100	1.12658400
H	-2.51394200	3.50452500	1.09432700	H	3.38582300	-3.25334700	0.65121700
C	-3.14265600	1.09039100	0.70550500	C	3.45833100	-0.71692500	0.45441800
C	-4.35527900	-1.04325500	0.23895600	C	3.88553500	1.70004000	-0.04094200
C	-5.62599400	-0.60598700	-0.14139700	C	4.04112100	1.68262300	-1.43068400
H	-5.94406600	0.40472900	0.05033200	H	3.85912600	0.78366800	-1.99615400
C	-6.47359100	-1.50217200	-0.77624300	C	4.44572900	2.84467500	-2.07054200
C	-6.11846900	-2.81889200	-1.03611800	C	4.69582700	4.03032000	-1.39297000
H	-6.79422100	-3.49616700	-1.53712400	H	5.01285200	4.92207200	-1.91305300
C	-4.86103000	-3.22883300	-0.61354300	C	4.51710000	4.01880700	-0.01482400
C	-3.97613300	-2.37377500	0.02348500	C	4.11913700	2.88310200	0.67240500
H	-3.01440000	-2.72703300	0.37111000	H	3.95673100	2.91136400	1.74062800
C	-1.34210400	3.44533600	2.87962500	C	2.33833100	-3.61408500	2.47927400
C	-2.58901300	3.24862200	3.74878200	C	3.57078200	-3.28632300	3.32932400
H	-2.43766300	3.71952200	4.72316700	H	3.56135900	-3.88961600	4.24046900
H	-2.79400500	2.18900900	3.90636800	H	3.58111800	-2.23303300	3.61250700

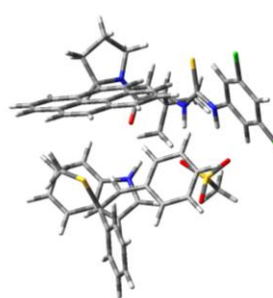
H	-3.46928900	3.69819700	3.28180100	H	4.49364400	-3.49964800	2.78356400
C	-0.14874800	2.74720200	3.53998900	C	1.07195700	-3.23917800	3.25596800
H	-0.05098800	3.11616700	4.56484400	H	1.09121000	-3.74806000	4.22374200
H	0.78164100	2.95959000	3.01217300	H	0.17040000	-3.54999100	2.72602800
H	-0.27561100	1.66443700	3.57784500	H	1.00448600	-2.16529600	3.43477700
C	-1.04246500	4.94505300	2.76694100	C	2.31745400	-5.11873100	2.18490500
H	-0.81440200	5.35124100	3.75492200	H	2.22137200	-5.67720700	3.11861200
H	-1.90250100	5.49076700	2.36898000	H	3.24159800	-5.43740700	1.69476100
H	-0.17985900	5.13438900	2.12146700	H	1.47210700	-5.38995600	1.54578000
H	1.53397900	0.88184800	1.66071200	H	-0.95863000	-1.38423600	1.74595000
N	2.51111100	0.60014100	1.69775700	N	-1.96417600	-1.25571900	1.83459100
C	2.93792600	-0.62748600	2.08161400	C	-2.54493900	-0.12487300	2.30205900
C	3.59534100	1.37373300	1.34105900	C	-2.93939200	-2.13186000	1.40526000
C	4.31916600	-0.69149500	1.99376300	C	-3.92104600	-0.22114200	2.18121800
H	2.22851200	-1.38876200	2.37237200	H	-1.93881200	0.69604600	2.65976000
C	4.76369500	0.59472700	1.53912100	C	-4.19917900	-1.51812500	1.63343400
C	3.64801300	2.67494300	0.83597600	C	-2.82757800	-3.40324500	0.83638900
H	4.92817000	-1.52868400	2.29568000	H	-4.63115400	0.50484700	2.54319000
C	6.01597000	1.14642600	1.22301600	C	-5.37074000	-2.21000200	1.28830400
C	4.89701600	3.19086500	0.52810100	C	-4.00215100	-4.05866800	0.50071900
H	2.73526000	3.23478600	0.69641900	H	-1.85305400	-3.84140500	0.67690700
C	6.07030300	2.43740100	0.72119700	C	-5.26185100	-3.47120000	0.72614200
H	6.92465700	0.57804100	1.38466300	H	-6.34418800	-1.77046500	1.47431900
H	4.97384100	4.19859700	0.13949700	H	-3.95107200	-5.04918600	0.06620200
H	7.02931100	2.87946900	0.48202200	H	-6.15707200	-4.02066200	0.46348400
H	5.58262700	0.51002000	-1.39464600	O	0.56006200	-0.02455700	2.61449500
C	5.07657700	0.50415300	-2.36182200	O	1.99555900	1.97483700	2.74077200
S	4.11827000	-1.01629900	-2.61152900	S	0.72830000	1.34588000	3.20026000
H	4.40586400	1.36003300	-2.41885300	O	-0.47290200	2.18435700	3.03808800
H	5.81793700	0.55087300	-3.15798300	C	0.93573400	1.08455700	4.95343900
C	3.02530200	-0.91450400	-1.10372700	H	1.07694500	2.05324300	5.42731500
C	4.06755200	-1.69687100	-0.41337100	H	0.04077700	0.59812200	5.33554300
H	2.98487900	0.13083300	-0.79605700	H	1.80884600	0.45340000	5.10577100
C	1.66523700	-1.49216900	-1.36836200	H	-4.23922200	-1.69868000	-1.60543900
H	5.00683500	-1.19119200	-0.25423300	C	-5.03935700	-1.16871600	-2.12152900
C	4.02162200	-3.10957100	-0.08103500	S	-4.66048300	0.59374800	-2.35079100
C	0.55003500	-0.84501100	-0.84634400	H	-5.97321200	-1.29193200	-1.57709300
C	1.50122000	-2.64061000	-2.15029800	H	-5.14967000	-1.58326400	-3.12311300
C	2.86111000	-3.70594600	0.43844700	C	-4.60135100	1.14112400	-0.58075200
C	5.20632600	-3.85728700	-0.18752400	C	-3.20579700	0.72240600	-0.28098600
C	-0.72274300	-1.35834600	-1.08646000	H	-5.29524300	0.49991300	-0.03838600
H	0.65841200	0.06863900	-0.27727500	C	-4.98327900	2.59143200	-0.42989300
C	0.23102200	-3.14376300	-2.39123300	H	-3.07163200	-0.35311500	-0.31448300
H	2.36386900	-3.15109100	-2.56484700	C	-2.00330400	1.46596300	-0.27006200
C	2.89640500	-5.03720500	0.83236000	C	-5.58601200	3.00229600	0.75825100
H	1.95861400	-3.13254400	0.60067700	C	-4.71887500	3.53457000	-1.42444300
C	5.21997500	-5.19477300	0.17159900	C	-1.89840100	2.84673800	0.03701200
H	6.10066500	-3.38406800	-0.57598200	C	-0.82666600	0.72007100	-0.53498000
C	-0.88595300	-2.50492700	-1.85319800	C	-5.90437100	4.34170700	0.96047700
H	-1.58456100	-0.84658900	-0.68075700	H	-5.80177600	2.27351500	1.53002500
H	0.11080000	-4.03432300	-2.99464100	C	-5.04047400	4.87211000	-1.22405800
C	4.06230300	-5.78371600	0.68420800	H	-4.24509700	3.23204400	-2.35072000
H	2.00766200	-5.47616600	1.26511500	C	-0.65796200	3.44632800	0.05144500
H	6.12715800	-5.77523200	0.06738600	H	-2.77326200	3.41231100	0.31720600
H	-1.87811400	-2.89902900	-2.03512300	C	0.40381800	1.34685500	-0.55503800
H	4.07795300	-6.82425100	0.98345600	H	-0.89496300	-0.34194700	-0.74324600

O	-0.14639800	-0.37650300	2.40236900	C	-5.62925000	5.27942100	-0.02973600
O	-1.84340200	-2.15798200	2.25237800	H	-6.36767400	4.64952200	1.88880000
S	-0.49120900	-1.79415300	2.74536800	H	-4.82831600	5.59594400	-2.00017500
O	0.57844700	-2.74684600	2.38145300	C	0.48957200	2.70465600	-0.25287800
C	-0.60287000	-1.83368600	4.52617200	H	-0.56515100	4.48641400	0.33083000
H	-0.86032100	-2.84626700	4.82801800	H	1.29311100	0.77514300	-0.77676700
H	0.36204700	-1.54452100	4.93744400	H	-5.87630400	6.32151900	0.12594400
H	-1.37622800	-1.13462500	4.83734100	H	1.45949600	3.18498900	-0.22728800
Cl	-8.05992300	-0.95769400	-1.25615000	Cl	4.62121700	2.82021300	-3.80674500
Cl	-4.37133400	-4.87739000	-0.91548400	Cl	4.80281600	5.48863400	0.87821400
H	0.99220800	-0.02862600	-4.90537000	H	1.41507800	0.17533700	-3.66815300
H	-1.15167500	0.36880800	-3.72676200	H	-0.88361200	0.55584800	-4.52036800
H	2.92788100	1.45581600	-4.46248900	H	-2.64828400	-1.12216500	-4.07740500
H	2.72175000	3.30351200	-2.82134500	H	-2.12153400	-3.16540500	-2.77696900

13e•TS<sub>major</sub>



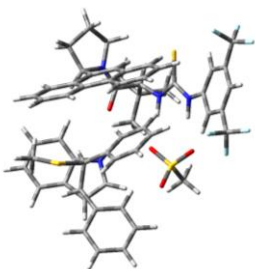
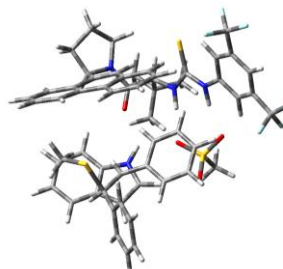
13e•TS<sub>minor</sub>



E = -4840.32342183		E + ZPE = -4839.288399		E = -4840.31824362		E + ZPE = -4839.282191	
G = -4839.391946		imaginary frequencies: 1		G = -4839.386173		imaginary frequencies: 1	
S	4.19294900	2.35627500	-0.06599600	S	-4.22188100	-2.15436700	0.65684200
O	-0.46630800	2.39993400	-0.48906100	O	-0.10864800	-2.32737100	-1.38424600
N	0.61201900	3.68790100	1.00234600	N	-0.86425200	-4.03093300	-0.12133300
N	2.06239200	2.09628100	-1.67645000	N	-2.81558100	-1.53480100	-1.53703400
H	1.38243000	1.48605600	-2.14118600	H	-2.26555600	-0.83876300	-2.05374100
N	3.38647800	0.25885100	-1.56854800	N	-3.80045700	0.23975900	-0.54293600
H	2.67209800	-0.16767300	-2.16974600	H	-3.48725800	0.72228600	-1.39345800
C	1.27806100	1.28528700	2.26158100	C	-0.37751800	-2.12036200	1.87250900
H	1.99977800	1.82108200	1.65500300	H	-1.34823900	-2.21955900	1.39974200
C	1.64386400	-0.03209100	2.69884000	C	-0.20429500	-1.03952100	2.80114500
C	0.71556800	-0.78278100	3.45744100	C	1.03995500	-0.89093500	3.45825100
C	-0.54237800	-0.20775800	3.80116500	C	2.08775600	-1.82271000	3.19972500
C	-0.87668000	1.10851800	3.37007600	C	1.90349600	-2.86923800	2.25071200
C	0.07629300	1.84182900	2.55713300	C	0.61990800	-2.99149200	1.57994600
C	-0.28098600	3.24108100	2.07744800	C	0.41273200	-4.13195000	0.59522700
H	-1.30459500	3.24173200	1.70390700	H	1.22562100	-4.11976000	-0.13242900
C	-0.04597100	4.30698200	3.16199300	C	0.28098100	-5.49356000	1.30606000
H	-0.29034100	3.93924100	4.15761700	H	0.90981300	-5.56015700	2.19182700
H	-0.65832600	5.18751400	2.95012900	H	0.55739300	-6.29488200	0.61556300
C	1.43936700	4.63684600	2.99129300	C	-1.21231100	-5.56101700	1.62725500
H	1.72264900	5.58758300	3.44079900	H	-1.55905900	-6.56794900	1.85521000
H	2.04640600	3.84859200	3.43870900	H	-1.43769000	-4.91490400	2.47743000
C	1.63439600	4.63943200	1.47159100	C	-1.86487400	-4.99861100	0.36521100
H	1.43884500	5.62848600	1.05006800	H	-2.01752500	-5.78292200	-0.38016800
H	2.63233200	4.31188800	1.18228700	H	-2.81089600	-4.50276600	0.57476100
C	0.48220100	3.14888800	-0.22350300	C	-1.03328500	-3.08256100	-1.06437300

C	1.57044400	3.40300700	-1.26902400	C	-2.41801100	-2.92146700	-1.70164600
H	2.41497000	3.91097000	-0.81181600	H	-3.15089800	-3.51316100	-1.16025900
C	3.17630600	1.53637600	-1.14774700	C	-3.58382300	-1.10738700	-0.50901900
C	4.33503300	-0.68055800	-1.11682800	C	-4.34835300	1.12538700	0.39802500
C	5.64327900	-0.35386400	-0.75065000	C	-4.69334700	0.80831000	1.71728300
H	6.00059700	0.65968800	-0.80846500	H	-4.63276700	-0.20134200	2.08341900
C	6.48156800	-1.36764800	-0.30635400	C	-5.13453700	1.82451700	2.55598400
C	6.08304200	-2.69484600	-0.22663500	C	-5.26315900	3.14401300	2.15218500
H	6.75363100	-3.46475100	0.12534500	H	-5.60969800	3.91362800	2.82544600
C	4.79099900	-2.99048900	-0.64188000	C	-4.92072000	3.42519900	0.83498500
C	3.91427700	-2.01730800	-1.09075700	C	-4.47270200	2.45509800	-0.04319500
H	2.92404900	-2.28151400	-1.43675000	H	-4.19790200	2.71682500	-1.05655000
C	1.10529600	4.28147700	-2.45498800	C	-2.46348000	-3.39488300	-3.17777900
C	2.28217200	4.40661300	-3.42851100	C	-3.86583500	-3.09731200	-3.71962000
H	2.03482900	5.11928600	-4.21913000	H	-3.97921000	-3.53802700	-4.71313900
H	2.50960900	3.44491400	-3.89044000	H	-4.03595900	-2.02229100	-3.79721500
H	3.18181600	4.75722700	-2.91573500	H	-4.63722600	-3.51455600	-3.06675900
C	-0.11422200	3.72863500	-3.19839300	C	-1.41827000	-2.72916000	-4.07866900
H	-0.30845200	4.35593800	-4.07288700	H	-1.58924800	-3.04965900	-5.11028000
H	-1.00483800	3.74229100	-2.56865300	H	-0.40492300	-3.01853100	-3.79644200
H	0.04421600	2.70507700	-3.54059000	H	-1.48114500	-1.64124300	-4.04012400
C	0.76419800	5.66714000	-1.89400500	C	-2.23200700	-4.91072600	-3.18502200
H	0.43195200	6.32418900	-2.70078600	H	-2.24857100	-5.28343700	-4.21151600
H	1.63604900	6.12737900	-1.42082100	H	-3.01170500	-5.43241200	-2.62332700
H	-0.04329400	5.61172200	-1.15718000	H	-1.25973100	-5.16702100	-2.75357700
H	-1.56995800	1.42639500	-1.89444600	H	0.58100300	-0.81329600	-2.65068600
N	-2.56428700	1.22768100	-1.98223300	N	1.51340600	-0.46294100	-2.85675100
C	-3.06518700	0.16473600	-2.65317500	C	1.78454000	0.82647900	-3.16903400
C	-3.59617700	1.94857800	-1.41868900	C	2.69491900	-1.16411900	-2.72724700
C	-4.44822700	0.15649500	-2.55224600	C	3.15686200	1.01384100	-3.23584700
H	-2.39981800	-0.53203400	-3.14312700	H	0.98553000	1.54467100	-3.28848200
C	-4.81058600	1.31241800	-1.78193700	C	3.76064100	-0.26503100	-2.98965700
C	-3.56852700	3.08455500	-0.60481200	C	2.91558200	-2.50474300	-2.39996700
H	-5.10900400	-0.53471100	-3.05058100	H	3.64534900	1.92830400	-3.53185800
C	-6.02632200	1.83930400	-1.31763900	C	5.08235500	-0.73613300	-2.92735900
C	-4.78437900	3.57974300	-0.15982900	C	4.23061500	-2.93779100	-2.34366200
H	-2.62603800	3.54295300	-0.34103900	H	2.07948900	-3.15803300	-2.19521100
C	-6.00131000	2.96737700	-0.51279800	C	5.30365400	-2.06487100	-2.60663900
H	-6.96771400	1.38135500	-1.59865600	H	5.91357800	-0.07399700	-3.14178200
H	-4.79953000	4.46264200	0.46666200	H	4.43894100	-3.97111800	-2.09622500
H	-6.93111700	3.39190700	-0.15562400	H	6.31685000	-2.44387400	-2.56260900
H	-5.71382100	0.44874600	1.04911600	O	-1.19928700	0.35002600	-2.92447300
C	-5.21788800	0.15246000	1.97519900	O	-3.07459700	1.92590500	-2.73585100
S	-4.31733700	-1.41108000	1.78552000	S	-1.77343400	1.65175800	-3.40178900
H	-4.51816500	0.92890100	2.27919800	O	-0.79739000	2.75285000	-3.35424800
H	-5.96359100	-0.00077900	2.75361500	C	-2.16910400	1.38823400	-5.12184500
C	-3.22581900	-0.93740400	0.35290000	H	-2.61097500	2.30202700	-5.51256900
C	-4.29106000	-1.45127200	-0.52998800	H	-1.24890800	1.15151700	-5.65201600
H	-3.14518400	0.14984000	0.34299600	H	-2.87429700	0.56237800	-5.19096100
C	-1.89015600	-1.61744200	0.42141400	C	1.22778700	0.17042100	4.37954600
H	-5.21253100	-0.89057000	-0.52779000	C	-1.23674800	-0.13567500	3.06763200
C	-4.30276200	-2.71982500	-1.23874200	H	-2.19074400	-0.26552800	2.56985600
C	-0.75638900	-0.89679000	0.05996700	C	0.17683700	1.06483500	4.61098400
C	-1.76792400	-2.94901900	0.83233100	H	0.32229800	1.87753500	5.31291000
C	-3.16355300	-3.20911800	-1.89910900	C	-1.04307900	0.91212500	3.96114100
C	-5.52238500	-3.40893300	-1.34574900	H	-1.85219800	1.60543200	4.15427000

C	0.48929700	-1.51833900	0.06630200	C	3.31408300	-1.70501200	3.90760800
H	-0.82921000	0.14720800	-0.21262800	C	2.96644500	-3.75501500	2.02598900
C	-0.52224500	-3.55925300	0.84426700	C	4.15490000	-3.65020400	2.74332800
H	-2.64344100	-3.51634700	1.12888000	H	4.95061500	-4.36192300	2.56274100
C	-3.25464500	-4.37880800	-2.64195600	C	4.32963100	-2.64139100	3.68172700
H	-2.23112900	-2.66160400	-1.89184400	H	2.86726100	-4.54735200	1.29620100
C	-5.59387000	-4.59385100	-2.05984100	H	5.25667700	-2.56260100	4.23752000
H	-6.40001700	-3.01683600	-0.84494200	H	3.91892600	-1.09770100	-0.02234100
C	0.60969900	-2.84821000	0.44801000	C	4.63866000	-0.66976800	0.67579500
H	1.36151700	-0.94803800	-0.22067200	S	4.11699000	0.96748500	1.26119800
H	-0.43235400	-4.58968900	1.16339300	H	5.61673800	-0.60539800	0.20332900
C	-4.45726700	-5.07743700	-2.71034300	H	4.68938200	-1.30514700	1.55707100
H	-2.37939800	-4.72773600	-3.17322800	C	4.06330200	1.83238400	-0.37739800
H	-6.52942100	-5.13380600	-2.12233400	C	2.66336100	1.43423000	-0.66666200
H	1.58069200	-3.32598900	0.45882600	H	4.74812300	1.29669100	-1.03318000
H	-4.51680000	-5.99379900	-3.28402200	C	4.42223800	3.29176000	-0.29483300
O	0.04419900	0.42420300	-2.95266600	H	2.53623100	0.36534700	-0.79140900
O	1.68280900	-1.40562700	-3.12374800	C	1.45651500	2.16665000	-0.45077700
S	0.36050900	-0.90152500	-3.57489600	C	4.97374200	3.90470800	-1.41985900
O	-0.74901200	-1.87015300	-3.45862500	C	4.18903500	4.05128900	0.85230600
C	0.54451700	-0.57046900	-5.31924000	C	1.33716100	3.56816000	-0.57974500
H	0.78680400	-1.50594400	-5.81814600	C	0.31587600	1.39771900	-0.13180900
H	-0.39472200	-0.16850800	-5.69309700	C	5.26570500	5.26522100	-1.40973400
H	1.34850300	0.15070200	-5.44960600	H	5.17260300	3.31576900	-2.30751600
C	1.04362600	-2.09974600	3.86702800	C	4.48530000	5.40957000	0.86404100
C	2.87901400	-0.59464000	2.36113200	H	3.76004000	3.58907700	1.73313600
H	3.58299800	-0.01075000	1.77783000	C	0.11304800	4.17125500	-0.36528600
C	2.28374700	-2.63625900	3.50427600	H	2.18260000	4.16172700	-0.89254900
H	2.53061800	-3.64613700	3.81089600	C	-0.88950100	2.02120000	0.13240500
C	3.19123100	-1.89065300	2.75912000	H	0.39335800	0.31690400	-0.07986400
H	4.14518000	-2.32025500	2.47929600	C	5.01867000	6.02081300	-0.26775500
C	-1.45901600	-0.95759300	4.58461900	H	5.68944500	5.73081300	-2.29001200
C	-2.11031900	1.64467800	3.76261200	H	4.29671400	5.99049000	1.75752300
C	-2.99137500	0.91189800	4.55514300	C	-0.99364600	3.40427800	0.00547200
H	-3.92899000	1.35922400	4.86346400	H	0.00816000	5.23908700	-0.50052800
C	-2.67779600	-0.37955000	4.95533200	H	-1.75126700	1.43179200	0.40718300
H	-2.38367600	2.64974700	3.46865600	H	5.24580000	7.07899900	-0.25723800
H	-3.36863200	-0.94856200	5.56662300	H	-1.94994400	3.88395600	0.17228600
Cl	8.11359000	-0.96195300	0.15424700	Cl	-5.52768500	1.41911000	4.20659800
Cl	4.24853800	-4.64798800	-0.56937100	Cl	-5.03624700	5.07444300	0.27591400
C	-1.10609900	-2.29421100	4.98384800	C	3.48132000	-0.61920900	4.83820700
C	0.08414300	-2.84015900	4.63906300	C	2.49192200	0.27960000	5.05562000
H	-1.82144900	-2.85599900	5.57294400	H	4.42550300	-0.53898500	5.36386700
H	0.33846200	-3.84819800	4.94522200	H	2.63155700	1.09312000	5.75770200

1d•TS<sub>major</sub>1d•TS<sub>minor</sub>

E = -4518.98464444				E + ZPE = -4517.931828				E = -4518.98083825				E + ZPE = -4517.927940				
G = -4518.040549				imaginary frequencies: 1				G = -4518.038035				imaginary frequencies: 1				
S	-3.39879900	-2.98652000	-0.92826500	S	-3.17908700	-3.24566700	0.02572400	S	1.14420100	-2.31255100	-1.22895000	S	0.64733800	-4.17069500	-0.05680200	
O	1.23953600	-2.23023900	-0.96778500	O	1.14420100	-2.31255100	-1.22895000	N	0.64733800	-4.17069500	-0.05680200	N	-1.59277400	-2.26001000	-1.89445600	
N	0.32335300	-3.97811000	0.10417900	N	0.64733800	-4.17069500	-0.05680200	N	-1.59277400	-2.26001000	-1.89445600	H	-1.16032300	-1.44380600	-2.34162800	
N	-1.26345200	-2.02136100	-2.22602100	N	-1.59277400	-2.26001000	-1.89445600	H	-1.16032300	-1.44380600	-2.34162800	N	-3.16248100	-0.80867200	-1.16167100	
H	-0.65969400	-1.22271600	-2.44936400	H	-1.16032300	-1.44380600	-2.34162800	N	-3.16248100	-0.80867200	-1.16167100	H	-2.82008300	-0.24429100	-1.94864900	
N	-2.85708600	-0.47242900	-1.78836200	N	-3.16248100	-0.80867200	-1.16167100	H	-2.82008300	-0.24429100	-1.94864900	C	0.22452700	-2.23785400	1.92247800	
H	-2.22257800	0.14394300	-2.30869900	H	-2.82008300	-0.24429100	-1.94864900	C	0.22452700	-2.23785400	1.92247800	H	-0.58218100	-2.60179900	1.29623200	
C	-0.79553300	-2.13783700	1.87263700	C	0.22452700	-2.23785400	1.92247800	H	-0.58218100	-2.60179900	1.29623200	C	0.93130100	-0.62270300	3.64451400	
H	-1.38936800	-2.61023100	1.09778400	H	-0.58218100	-2.60179900	1.29623200	C	0.93130100	-0.62270300	3.64451400	C	2.24050100	-1.25997300	3.63871800	
C	-1.41828200	-1.08185400	2.61433100	C	0.93130100	-0.62270300	3.64451400	C	2.24050100	-1.25997300	3.63871800	C	2.50664400	-2.31739200	2.72821700	
C	-0.69066100	-0.39077600	3.60611400	C	2.24050100	-1.25997300	3.63871800	C	2.50664400	-2.31739200	2.72821700	C	1.45943600	-2.78990100	1.84244400	
C	0.67427000	-0.81420700	3.88493600	C	2.50664400	-2.31739200	2.72821700	C	1.45943600	-2.78990100	1.84244400	C	1.75018300	-3.93599700	0.88385500	
C	1.24944300	-1.88051300	3.14253300	C	1.45943600	-2.78990100	1.84244400	C	1.75018300	-3.93599700	0.88385500	H	2.65011500	-3.70062300	0.31390400	
C	0.48251300	-2.53011700	2.09920700	C	1.75018300	-3.93599700	0.88385500	H	2.65011500	-3.70062300	0.31390400	C	1.84978300	-5.29172900	1.61172800	
C	1.09829000	-3.67893400	1.31293300	H	2.65011500	-3.70062300	0.31390400	C	1.84978300	-5.29172900	1.61172800	H	2.29730600	-5.20028000	2.59949900	
H	2.11268400	-3.41544800	1.01751300	C	1.84978300	-5.29172900	1.61172800	H	2.29730600	-5.20028000	2.59949900	H	2.44935100	-5.98465600	1.01530300	
C	1.02972100	-5.01103500	2.07977600	H	2.29730600	-5.20028000	2.59949900	H	2.44935100	-5.98465600	1.01530300	C	0.39354800	-5.75527500	1.66027200	
H	1.19180600	-4.87953600	3.14880400	H	2.44935100	-5.98465600	1.01530300	C	0.39354800	-5.75527500	1.66027200	H	0.28735600	-6.82091300	1.85862200	
H	1.78607400	-5.69682800	1.68903400	C	0.39354800	-5.75527500	1.66027200	H	0.28735600	-6.82091300	1.85862200	H	-0.14528800	-5.20347400	2.43231300	
C	-0.37507400	-5.51884600	1.74392500	H	0.28735600	-6.82091300	1.85862200	H	-0.14528800	-5.20347400	2.43231300	C	-0.14081200	-5.37033600	0.28142200	
H	-0.49826400	-6.58676200	1.91849400	H	-0.14528800	-5.20347400	2.43231300	C	-0.14081200	-5.37033600	0.28142200	H	0.05201100	-6.16047000	-0.44834400	
H	-1.11343700	-4.98424100	2.34283100	C	0.05201100	-6.16047000	-0.44834400	H	0.05201100	-6.16047000	-0.44834400	H	-1.20453400	-5.14027600	0.30029000	
C	-0.54660400	-5.15622200	0.26439800	H	-1.20453400	-5.14027600	0.30029000	H	-1.20453400	-5.14027600	0.30029000	C	0.41009300	-3.29065100	-1.04960100	
H	-0.19709400	-5.96317900	-0.38376700	C	0.41009300	-3.29065100	-1.04960100	C	0.41009300	-3.29065100	-1.04960100	C	-0.82858500	-3.49448700	-1.93025100	
H	-1.57920900	-4.91327000	0.01578100	C	-0.82858500	-3.49448700	-1.93025100	H	-0.82858500	-3.49448700	-1.93025100	H	-1.47113800	-4.26000400	-1.50448800	
C	0.41147600	-3.14959400	-0.95145600	H	-1.47113800	-4.26000400	-1.50448800	C	-1.47113800	-4.26000400	-1.50448800	C	-2.62129500	-2.05639900	-1.04131000	
C	-0.58388800	-3.30270100	-2.10487200	C	-2.62129500	-2.05639900	-1.04131000	C	-2.62129500	-2.05639900	-1.04131000	C	-4.10233100	-0.11636500	-0.38445100	
H	-1.34821000	-4.02996600	-1.84504500	C	-4.10233100	-0.11636500	-0.38445100	C	-4.10233100	-0.11636500	-0.38445100	C	-4.64014600	-0.53964100	0.83566500	
C	-2.47478400	-1.77680300	-1.67038700	C	-4.64014600	-0.53964100	0.83566500	H	-4.64014600	-0.53964100	0.83566500	H	-4.40348400	-1.51307600	1.23073300	
C	-3.88321700	0.24728500	-1.15003600	H	-4.40348400	-1.51307600	1.23073300	H	-4.40348400	-1.51307600	1.23073300	C	-5.50772300	0.29740800	1.53274300	
C	-5.03929500	-0.30291700	-0.58970500	C	-5.50772300	0.29740800	1.53274300	C	-5.50772300	0.29740800	1.53274300	H	-5.87450800	1.54726000	1.06054100	
C	-5.23056200	-1.36004600	-0.65400900	H	-5.87450800	1.54726000	1.06054100	H	-5.87450800	1.54726000	1.06054100	H	-6.55668700	2.17742700	1.61165400	
C	-5.94591100	0.52894700	0.06316900	C	-6.55668700	2.17742700	1.61165400	C	-6.55668700	2.17742700	1.61165400	C	-5.34137900	1.95281200	-0.15843300	
C	-5.76714100	1.90053500	0.14403700	C	-5.34137900	1.95281200	-0.15843300	C	-5.34137900	1.95281200	-0.15843300	C	-4.47406000	1.14686200	-0.87743900	
H	-6.48941600	2.52994900	0.64392300	C	-4.47406000	1.14686200	-0.87743900	H	-4.47406000	1.14686200	-0.87743900	H	-4.06821800	1.48979000	-1.82106100	
C	-4.63656300	2.44075700	-0.45964900	H	-4.06821800	1.48979000	-1.82106100	C	-4.06821800	1.48979000	-1.82106100	C	-0.48314500	-3.95484700	-3.37041900	
C	-3.70230400	1.63974800	-1.09622700	C	-0.48314500	-3.95484700	-3.37041900	C	-0.48314500	-3.95484700	-3.37041900	C	-1.79224000	-4.02780400	-4.16388000	
H	-2.83203200	2.08309500	-1.56438300	C	-1.79224000	-4.02780400	-4.16388000	H	-1.79224000	-4.02780400	-4.16388000	H	-1.60614800	-4.47898500	-5.14150600	
C	0.06140900	-3.78400500	-3.42680300	H	-1.60614800	-4.47898500	-5.14150600	H	-1.60614800	-4.47898500	-5.14150600	H	-2.21320700	-3.03308200	-4.31811900	
C	-1.04664300	-3.85246900	-4.48314000	H	-2.21320700	-3.03308200	-4.31811900									
H	-0.65903900	-4.30830300	-5.39750200													
H	-1.41683100	-2.85520100	-4.72513500													

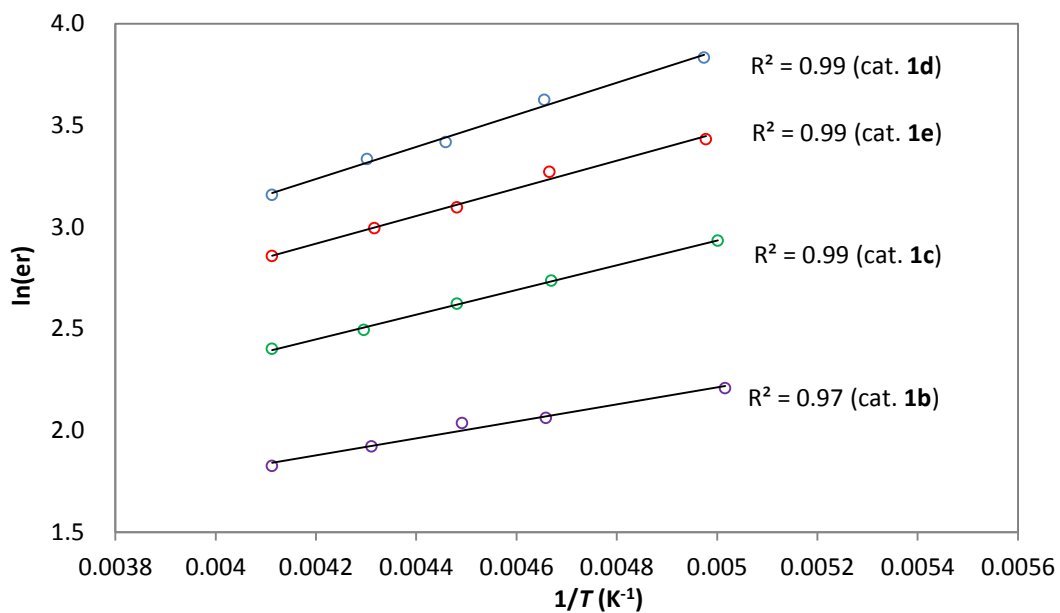
H	-1.89134800	-4.44974700	-4.12988400	H	-2.53701200	-4.63305100	-3.64013400
C	1.19166700	-2.88333600	-3.93284600	C	0.50353700	-3.03930700	-4.10131400
H	1.51240900	-3.24063100	-4.91534700	H	0.62650400	-3.40312700	-5.12530300
H	2.05374700	-2.90899100	-3.26519100	H	1.48293100	-3.04189100	-3.62060400
H	0.87268600	-1.84520500	-4.03079500	H	0.14929500	-2.00897000	-4.14254200
C	0.61525800	-5.19248500	-3.18144700	C	0.12267900	-5.36031100	-3.27226700
H	1.08185600	-5.57260700	-4.09290000	H	0.38630000	-5.72049600	-4.26906800
H	-0.17972800	-5.88647500	-2.89462200	H	-0.58785500	-6.06705900	-2.83508700
H	1.37609400	-5.18894900	-2.39460400	H	1.03376100	-5.36102100	-2.66658500
H	2.24253400	-0.76779100	-1.93869200	H	1.63464300	-0.68280800	-2.46655800
N	3.18374400	-0.38445800	-1.87871500	N	2.47428200	-0.11163900	-2.51670400
C	3.50835400	0.87988500	-2.23938000	C	2.46842700	1.21510300	-2.78613000
C	4.30179400	-1.02824800	-1.39446800	C	3.75403500	-0.51104800	-2.18996100
C	4.85670800	1.10183500	-2.00678100	C	3.74534000	1.73137000	-2.62398300
H	2.75026300	1.55033900	-2.61826800	H	1.54819400	1.72048500	-3.04399300
C	5.39023900	-0.12274100	-1.48198600	C	4.59550900	0.62805700	-2.27664100
C	4.44626500	-2.31385300	-0.86518100	C	4.24166100	-1.77057200	-1.83090800
H	5.39839600	1.99798200	-2.26422100	H	4.03738500	2.74665600	-2.83986200
C	6.65669500	-0.52815200	-1.03051900	C	5.96560700	0.48775100	-2.00231900
C	5.70694000	-2.68270000	-0.42237600	C	5.59773700	-1.87594800	-1.56576900
H	3.59564500	-2.97885200	-0.81212300	H	3.57032400	-2.61477900	-1.76230300
C	6.80234800	-1.80230400	-0.50585500	C	6.45280500	-0.76051600	-1.65304700
H	7.50774800	0.13886100	-1.10653400	H	6.63270100	1.33876600	-2.07998500
H	5.85598000	-3.67372000	-0.01256500	H	6.01116900	-2.83792200	-1.29024100
H	7.77439000	-2.13265300	-0.16212900	H	7.50844000	-0.88579600	-1.44821600
H	5.98828000	0.25816200	1.53246200	O	-0.30133700	-0.02161800	-3.11147100
C	5.35932500	0.16660100	2.41936800	O	-2.50137400	1.06500800	-3.19952300
S	4.14618600	1.51044100	2.53144100	S	-1.08894500	1.12941000	-3.66275600
H	4.83560600	-0.78715400	2.39643800	O	-0.42147600	2.42565000	-3.45963000
H	5.97997100	0.22626400	3.31216700	C	-1.15645100	0.85392400	-5.42399000
C	3.25137400	1.23299200	0.92225700	H	-1.73972100	1.65579700	-5.87085200
C	4.23158100	2.14247100	0.29950400	H	-0.13922800	0.85995500	-5.80989300
H	3.39138200	0.18941700	0.63876000	H	-1.62931000	-0.10939700	-5.60347500
C	1.80486000	1.62118800	1.02499900	C	0.60443300	0.48449600	4.45476300
H	5.24889900	1.78591100	0.26920800	C	-1.37232600	-0.60165600	2.82374200
C	4.01570100	3.52049200	-0.10182400	H	-2.12807800	-1.04520000	2.18505200
C	0.85060900	0.82023900	0.40598100	C	-0.66728100	1.01896200	4.44804400
C	1.40717000	2.76644200	1.72402100	H	-0.89251200	1.86883500	5.07985400
C	2.83726400	3.92559900	-0.75096800	C	-1.67262700	0.46779900	3.63596900
C	5.06724300	4.43596700	0.07440300	H	-2.67573300	0.87252500	3.65093000
C	-0.49369100	1.18125500	0.45926400	C	3.25260200	-0.88312900	4.54674800
H	1.13839900	-0.08778500	-0.10556800	H	3.06015400	-0.09955700	5.26573900
C	0.06575300	3.11500800	1.77864500	C	3.78593500	-2.91893800	2.74274500
H	2.14348100	3.39617100	2.21194200	C	4.75118700	-2.54126800	3.65176800
C	2.72084100	5.23410600	-1.20072800	H	5.71522700	-3.03390100	3.65465700
H	2.04325700	3.22334200	-0.96501000	C	4.47750800	-1.51717600	4.57066000
C	4.92600700	5.74879900	-0.34401000	H	4.01261500	-3.70767300	2.03836000
H	5.97873600	4.11074600	0.56253500	H	1.35317900	0.93648900	5.09036200
C	-0.88922000	2.32608200	1.13785400	H	5.22476700	-1.22097900	5.29600600
H	-1.22777400	0.55131600	-0.02415400	C	-5.99512300	-0.16209500	2.87385600
H	-0.23834500	4.00266100	2.31842400	C	-5.64269000	3.32643300	-0.67623900
C	3.75063800	6.14623000	-0.98430700	F	-6.28462600	-1.47107700	2.88306700
H	1.82357900	5.52546900	-1.72983600	F	-5.05707200	0.03402000	3.82646800
H	5.72796000	6.45785900	-0.18652900	F	-7.09325000	0.50493200	3.26525200
H	-1.93409600	2.60009800	1.18313700	F	-6.82306100	3.78257000	-0.22571800
H	3.64701700	7.16740600	-1.32877600	F	-4.70404600	4.21360200	-0.27205000

O	0.54493600	0.15390100	-2.83166100	F	-5.66736100	3.37002100	-2.01428600
O	-1.41173100	1.61450500	-3.12518200	H	4.48569400	-0.24538900	0.66422300
S	0.05146600	1.47467400	-3.33877100	C	4.94559000	0.31965800	1.47536500
O	0.86627000	2.61103500	-2.86375000	S	3.93137300	1.74022600	1.96563900
C	0.26909600	1.41193400	-5.10894300	H	5.93746700	0.65279400	1.17665800
H	-0.08879100	2.34925900	-5.52869600	H	5.01353300	-0.32027300	2.35189700
H	1.32777700	1.27653100	-5.32077600	C	3.93050700	2.63801200	0.34433500
H	-0.30841600	0.57501400	-5.49592300	C	2.73757100	1.92679900	-0.18138400
C	-1.33386100	0.66793000	4.28010700	H	4.82405400	2.31240200	-0.18586200
C	-2.75397500	-0.72718200	2.33374100	C	3.90360000	4.13558500	0.49096200
H	-3.28860100	-1.28379100	1.57244500	H	2.89535200	0.86381000	-0.31919200
C	-2.63882700	1.00763900	3.98988100	C	1.37118600	2.34240100	-0.17768000
H	-3.10840000	1.82522900	4.52236700	C	4.47755600	4.91224800	-0.51511000
C	-3.36295200	0.30339400	3.01287400	C	3.29484300	4.76459000	1.57792200
H	-4.39244800	0.55971900	2.79764900	C	0.94451800	3.68021100	-0.33112300
C	1.44450200	-0.21274200	4.90078700	C	0.41027800	1.31388100	-0.05936100
H	1.02797400	0.60181300	5.47542700	C	4.42424300	6.30134800	-0.45056800
C	2.56007400	-2.30222000	3.46092100	H	4.96417300	4.42783700	-1.35345500
C	3.28071100	-1.70804800	4.47582200	C	3.24574100	6.15223800	1.64483700
H	4.27456800	-2.06632300	4.71590800	H	2.84179200	4.17318600	2.36456900
C	2.71846700	-0.64706700	5.19886300	C	-0.40645700	3.96869700	-0.33662000
H	3.00505700	-3.12409800	2.91515300	H	1.66465300	4.46805700	-0.49149400
H	-0.80808300	1.23582600	5.03476200	C	-0.93626500	1.62528600	-0.01587100
H	3.27693100	-0.17364700	5.99669800	H	0.73517300	0.28121300	0.01365200
C	-7.10384400	-0.09944800	0.77658000	C	3.80481000	6.92344700	0.62903500
C	-4.38942800	3.91442300	-0.34561100	H	4.86926300	6.89407300	-1.23926000
F	-7.54847100	-1.20080200	0.15447500	H	2.76785400	6.63077500	2.48970200
F	-6.75410400	-0.46889700	2.02751800	C	-1.34504900	2.94909600	-0.16392300
F	-8.13913000	0.74935800	0.89739600	H	-0.73893200	4.98628100	-0.48946600
F	-5.53849400	4.61262600	-0.36682900	H	-1.66582100	0.83900300	0.10762000
F	-3.77980000	4.21877700	0.82298500	H	3.76263300	8.00369200	0.68193500
F	-3.60739500	4.37833500	-1.32729900	H	-2.40042900	3.18933700	-0.16643900

### 19. Data sets for Eyring analysis

Procedure: An oven-dried vial was charged with **1a** (0.025 mmol, 1.0 equiv), thiourea catalyst (0.0025 mmol, 0.10 equiv), indole (0.05 mmol, 2.0 equiv) and 4Å molecular sieves (15 mg, powder, activated). The flask was cooled to -78 °C, and toluene was added with stirring. The vial was placed in a -30 °C cryocool until all the reactants and catalyst were fully dissolved, and was brought to the desired temperature (-30 to -75 °C). 4-NBSA (0.5 M in THF, 0.00125 mmol, 0.05 equiv) was added directly into the solution via a 10 µL syringe. The reaction mixture was stirred at that temperature until TLC showed full conversion of the starting material, and then quenched at the same temperature by addition of NEt<sub>3</sub> (~10 µL). The reaction was directly applied to flash column chromatography with a pipette containing 1¼ inches of silica gel using hexanes/EtOAc (20:1 to 10:1) as eluent. The enantiomeric excess was determined by chiral HPLC analysis (ChiralPak AD-H, 10% *i*-PrOH, 1 ml/min, *t*<sub>1</sub> = 24 min, *t*<sub>2</sub> = 33 min). The differential activation parameters were calculated using the following relationship:

$$\ln(\text{er}) = -\Delta\Delta H^\ddagger/RT + \Delta\Delta S^\ddagger/RT \text{ (where } R = 1.986 \text{ cal/mol}\cdot\text{K)}$$



catalyst	ee (%)					$\Delta\Delta H^\ddagger$ (kcal/mol)	$\Delta\Delta S^\ddagger$ (eu)	calc. ee (%) at 0 °C
	(temperature (°C))							
<b>1d</b>	91.8	93.1	93.6	94.8	95.8	$-1.56 \pm 0.08$	$-0.14 \pm 0.35$	88.7
	(-30.0)	(-40.7)	(-48.9)	(-58.4)	(-72.1)			
<b>1e</b>	89.1	90.5	91.4	92.7	93.7	$-1.35 \pm 0.07$	$0.13 \pm 0.32$	85.6
	(-30.0)	(-41.5)	(-50.0)	(-58.8)	(-72.3)			
<b>1c</b>	83.4	84.7	86.5	87.8	89.9	$-1.11 \pm 0.03$	$0.64 \pm 0.12$	82.9
	(-30.0)	(-40.4)	(-50.0)	(-59.0)	(-73.2)			
<b>1b</b>	72.2	74.5	76.9	77.4	80.2	$-0.83 \pm 0.07$	$0.26 \pm 0.32$	67.4
	(-30.0)	(-41.2)	(-50.5)	(-58.5)	(-73.8)			
<b>1a</b>	11.7	11.0	n.d.	9.7	n.d.	$0.14 \pm 0.41$	$1.03 \pm 1.81$	13.2
	(-30.3)	(-41.7)		(-59.6)				

# Chapter Five

## Mechanistic Analysis of Chromium-Catalyzed Intermolecular Carbonyl-Ene Reaction

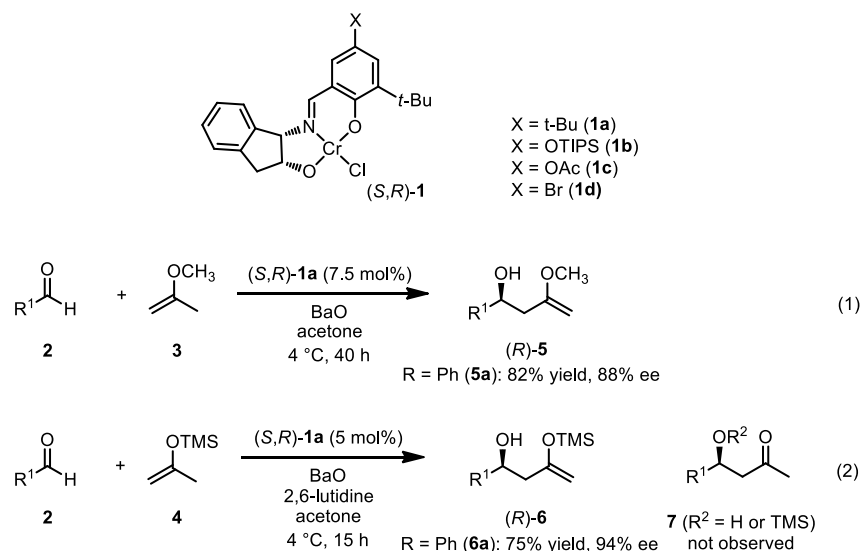
### 5.1 Background – Recapitulation of the Chromium-Catalyzed Carbonyl-Ene Reaction

The chromium-catalyzed carbonyl-ene reaction was developed in the Jacobsen group about a decade ago (Scheme 5-1).<sup>1</sup> In this reaction, a Lewis acidic chromium (III) center supported by a tridentate Schiff base ligand is employed as the catalyst (**1**), promoting the pericyclic ene reaction between a variety of alkyl/arylaldehydes (**2**) and electron-rich olefins: methoxypropene (**3**) or trimethylsilyl enol ether (**4**). The products,  $\beta$ -hydroxy methyl enol ethers (**5**) or  $\beta$ -hydroxy silyl enol ethers (**6**) are generally obtained with high yields and in excellent enantioselectivity. In the cases with **4** as the nucleophile, the ene products **6** are generated exclusively. This observation is in clear contrast to the traditional Lewis-acid catalysis of

---

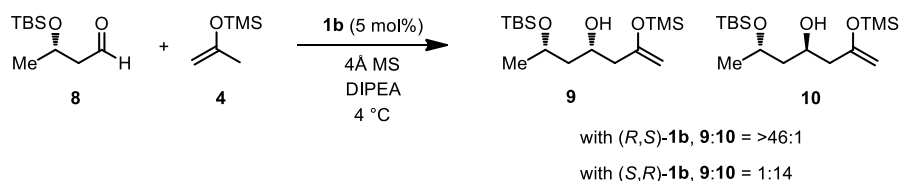
<sup>1</sup> (a) Ruck, R. T.; Jacobsen, E. N. *J. Am. Chem. Soc.* **2002**, *124*, 2882–2883; (b) Ruck, R. T.; Jacobsen, E. N. *Angew. Chem. Int. Ed.* **2003**, *42*, 4771–4774.

reactions involving the same classes of electrophiles and nucleophiles, which is usually dominated by the Mukaiyama aldol pathway and produces  $\beta$ -hydroxyketone derivatives (**7**).<sup>2</sup>



**Scheme 5-1.** Enantioselective carbonyl-ene reactions catalyzed by Schiff base Cr(III) complexes (**1**).

The substrate scope of the aldehyde was also extended to enantioenriched  $\beta$ -hydroxybutyraldehyde **8**, which undergoes the reaction with remarkable levels of catalyst control, selectively furnishing diastereomeric products (**9/10**) with each enantiomer of catalyst.

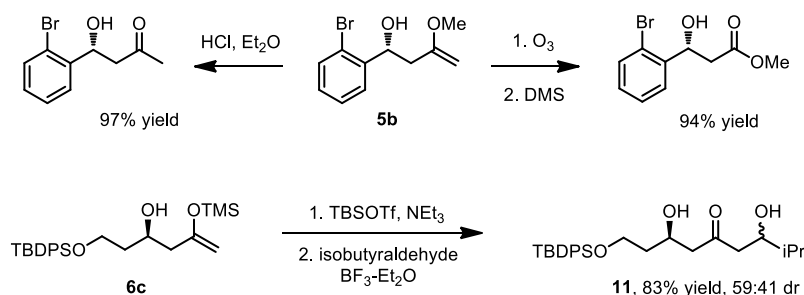


**Scheme 5-2.** Catalyst-controlled diastereoselective carbonyl-ene reactions.

The products of the asymmetric carbonyl-ene reaction with 2-methoxypropene (**5b**) can be derivatized to form the corresponding ketones and esters, and the products derived from silyl

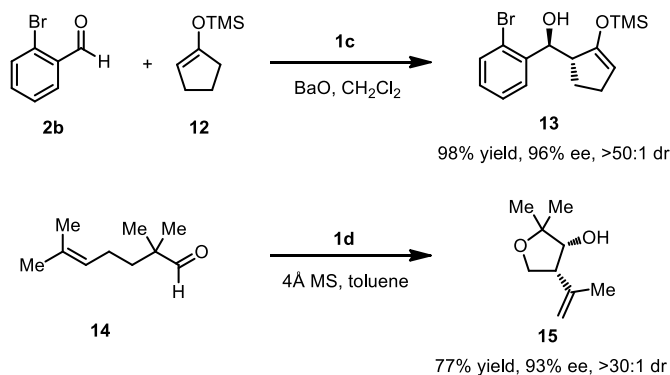
<sup>2</sup> For a review on Lewis acid catalyzed Mukaiyama aldol reaction, see: (a) Mukaiyama, T.; Kobayashi, S. *Org. React.* **1994**, *46*, 1; for two reports prior to the initial publication of Ruck and Jacobsen (ref. 1b) that describes the formation of carbonyl-ene product in company with aldol product with aluminum catalysis, see: (b) Shoda, H.; Nakamura, T.; Tanino, K.; Kuwajima, I. *Tetrahedron Lett.* **1993**, *34*, 6281–6284; (c) Mikami, K.; Matsukawa, S. *J. Am. Chem. Soc.* **1993**, *115*, 7039–7040.

enol ethers (**6c**) can participate in an aldol reaction with another aldehyde electrophile to access polyoxygenated product **11** (Scheme 5-3).



**Scheme 5-3.** Product derivatization.

This methodology was further applied in the construction of cyclic hydrocarbon frameworks by employing cyclic trimethylsilyl enol ethers (e.g. **12**) as the nucleophile or by performing the transformation in an intramolecular setting (**14**) (Scheme 5-4).<sup>3</sup> Multiple stereogenic centers are set in these reactions with both excellent diastereoselectivity and high enantioselectivity. Notably, in the intramolecular carbonyl-ene reaction, typically unreactive nucleophiles such as 1,1-disubstituted alkene are readily engaged in the cyclization, indicating that chromium complexes **1** are very potent Lewis acid catalysts.



**Scheme 5-4.** Construction of cyclic products by Cr-catalyzed carbonyl-ene reaction.

In this reaction, the Cr complex is postulated to perform as a Lewis acid catalyst that activates the aldehyde through single-point binding. The indispensable role of a desiccant, such

<sup>3</sup> Grachan, M. L.; Tudge, M. T.; Jacobsen, E. N. *Angew. Chem. Int. Ed.* **2008**, *47*, 1469–1472.

as BaO and molecular sieves (MS) is likely to strip a molecule of water from the Cr center and free a coordination site for substrate binding. The unprecedented reactivity of these catalysts in activating poorly electrophilic aldehydes towards nucleophilic addition is quite intriguing and provides a promising new strategy for Lewis acid catalysis.

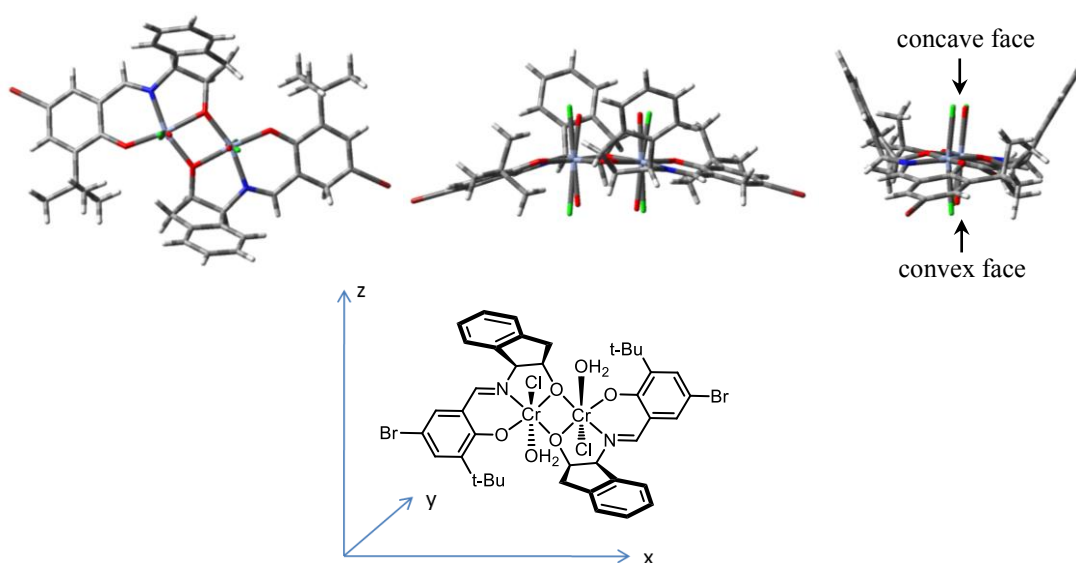


**Figure 5-1.** Crystal structure of catalyst **1d** viewed along the y axis (top left), the z axis (top middle) and the x axis (top right).

The way by which these catalysts induce high enantioselectivity has also triggered considerable curiosity. A crystal structure was obtained for catalyst **1d**, indicating that it is a dimeric complex with  $C_2$  symmetry (Figure 5-1). The catalyst bears two faces on which the aldehyde substrate could approach, the face surrounded by the amino indanol residues (denoted as the concave face) and the one on the opposite side of the chromium core structures (denoted as the convex face).<sup>4</sup> Each side could accommodate the substrate assembly in the carbonyl-ene transition state and energetically differentiate the two diastereomeric pathways. Intuitively, the relatively “flat” convex face would be incapable of distinguishing the two competing pathways effectively, making it unlikely to be the hosting site for the reactants. In contrast, the concave

<sup>4</sup> The “convex face” also shows a slight curvature wrapping the active site. The nomenclature is only for clarity in future discussions.

side presents a binding domain that is more stereochemically defined, suggesting that this face of the complex catalyzes the reaction. However, the convex side of the catalyst appears to be the more accessible between the two from a steric point of view. Therefore, in order for the reaction to occur on the concave side, attractive interactions between the catalyst and the substrates must be present, serving to stabilize the reaction pathway efficiently over the presumably poorly selective convex pathway.

In the previous chapter, we discussed the prominent role of cation- $\pi$  interactions can play in the stabilization of polarized reaction transition states. The presence of aromatic groups in the catalyst cavity on the concave face led us to advance the hypothesis that such interaction might also be involved in the stabilization of the carbonyl-ene transition structure, as partial positive charges would emerge on the nucleophile as it approaches the aldehyde. This attractive interaction, in addition to the Lewis-acid activation, leading to enhanced reactivity, making the concave pathway outcompeting the convex pathway.

Furthermore, such a cation- $\pi$  interaction might also provide a basis for enantioinduction, as the aromatic group of the  $C_2$  symmetric catalyst pocket would only interact with one of the two enantiomeric substrate assemblies in the transition state.

Although these proposals are purely based on intuition, this mode of cooperative catalysis, in which charge distribution in a polarized transition state is stabilized by both acidic and basic functionalities on the catalyst, has been demonstrated in reactions promoted by small organic molecules,<sup>5</sup> and is novel and highly interesting to the field of Lewis acid catalysis.<sup>6</sup> Understanding the way these catalysts induce high enantioselectivity would serve as mechanistic

---

<sup>5</sup> (a) Brown, A. R.; Uyeda, C.; Brotherton, C. A. *J. Am. Chem. Soc.* **2013**, *135*, 6747–6749. (b) Uyeda, C.; Jacobsen, E. N. *J. Am. Chem. Soc.* **2011**, *133*, 5062–5075.

<sup>6</sup> Shao, Z.; Zhang, H. *Chem. Soc. Rev.* **2009**, *38*, 2745–2755.

basis for further development of asymmetric reactions with this class of catalysts. Therefore, computational analyses were conducted with the goal of elucidating the role of the ligand in the reaction mechanism.

## 5.2 Kinetic Analysis and Non-Linear Effect Studies<sup>7</sup>

Kinetic studies of the Cr-catalyzed carbonyl-ene reaction were conducted with substrate **5b** and **12** in the presence of catalyst **1c** under synthetic relevant conditions (see Scheme 5-4) by NMR analysis of the periodically removed aliquots from the reaction mixture. A linear plot was obtained between the observed reaction rate constant and the concentration of catalyst **1c**, revealing that the ground state and the transition state of the reaction bear the same number of catalyst molecules.

The dimeric structure in the solid phase may or may not be retained in the reaction medium. In order to further discern the stoichiometry of the catalyst in the rate-limiting transition structure, non-linear effect (NLE) studies were carried out.<sup>8</sup> The reactions conducted with scalemic mixtures of catalyst **1c** displayed a strictly linear dependence of product ee on catalyst ee, showing that diastereomeric interactions between different catalyst molecules do not exist during the reaction. In contrast, the reactions promoted by the catalysts synthesized from scalemic mixtures of the Schiff base ligand exhibits a prominent positive NLE (Figure 5-2). One possible explanation for these observations is that the catalyst exists as two forms: heterodimeric [(*R,S*)-(*S,R*)] and homodimeric structures [(*R,S*)-(*R,S*) and ((*S,R*)-(*S,R*))] in the solution phase, and the different reactivity of the two species caused the pronounced NLE. To test this hypothesis, the reaction rate NLE was also measured with catalysts prepared from ligands with different ee's. Results were in excellent agreement with theoretical prediction, which was

---

<sup>7</sup> Work presented in this section was conducted by a former graduate student, Rebecca T. Ruck. See: Ruck, R. T. Ph. D. Dissertation, Harvard University, 2003.

<sup>8</sup> For a review on non-linear effect studies, see: Girard, C.; Kagan, H. B. *Angew. Chem. Int. Ed.* **1998**, *37*, 2922–2959.

obtained through fitting the enantioselectivity NLE values in a mathematical model advanced for situations involving a dimeric catalyst.<sup>9</sup>

Taken together, the experimental data provided compelling evidence that catalyst **1c** exists as a thermodynamically stable dimeric structure in solution, and is also served as the active species in the catalytic carbonyl-ene reaction.

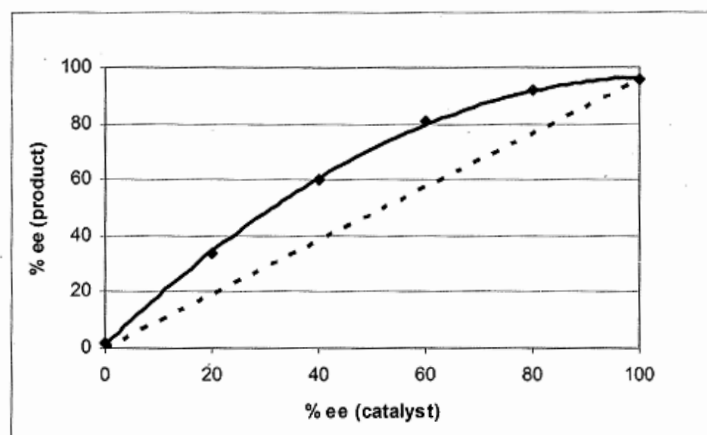


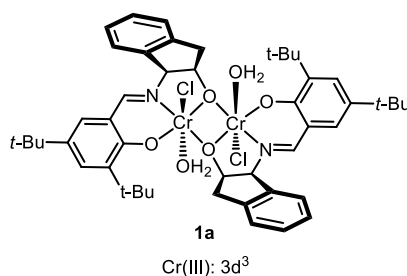
**Figure 5-2.** Non-linear effect displayed in reactions using catalyst **1c** prepared from scalemic mixtures of the Schiff base ligand. The figure is reproduced from ref. 7. A more proper title for the x axis is “% ee (ligand)”.

<sup>9</sup> Blackmond, D. G. *J. Am. Chem. Soc.* **1997**, *119*, 12934–12939.

## 5.3 Computational Analyses of the Intermolecular Carbonyl-Ene Reaction

### 5.3.1 Determination of the Catalyst Spin State

As discussed in the previous section, the Cr catalysts of the carbonyl-ene reaction exist as dimeric structures in both the ground state and the transition state of reaction. Each of the two chromium atoms is in +3 oxidation state, and possesses three valence electrons. Therefore, the complex can adopt a number of different spin states depending on the electronic structure of the valence shell of the chromium atoms (Figure 5-3).



possible spin states:

- A.  $S = 1$  ( $S_1 = 1/2$ ,  $S_2 = 1/2$ )
- B.  $S = 2$  ( $S_1 = 1/2$ ,  $S_2 = 3/2$ )
- C.  $S = 3$  ( $S_1 = 3/2$ ,  $S_2 = 3/2$ )
- C'.  $S = 0$  ( $S_1 = 3/2$ ,  $S_2 = -3/2$ )

**Figure 5-3.** Spin state analysis of catalyst **1a**.

According to classical crystal field theory, the d orbitals of the octahedral Cr centers are degenerate as three low energy  $t_{2g}$  and two high energy  $e_g$  orbitals. In principle, spin state **C** bearing six unpaired electrons, three on each Cr atom should be the energetically most favorable structure. DFT computations were carried out to probe this hypothesis using the B3LYP level of theory in combination with the 6-31G(d) basis set for the light atoms (C, H, O, etc.) and electron core potentials (ECPs) with a double- $\xi$ -basis set (LanL2DZ) applied to the metal centers.<sup>10</sup>

<sup>10</sup> The level of theory and ECP approximation have been validated in a few other systems for use of structure and energy prediction of Cr and other first row transition metals. See: (a) Strassner, T.; Houk, K. N. *Org. Lett.* **1999**, *1*, 419–421; (b) Merlic, C. A.; Miller, M. M.; Hietbrink, B. N.; Houk, K. N. *J. Am. Chem. Soc.* **2001**, *123*, 4904–4918; (c) Yang, Q.; Tong, X.; Zhang, W. *J. Mol. Struct.: Theochem.* **2010**, *957*, 84–89; for a review, see: (d) Niu, S.; Hall, M. B. *Chem. Rev.* **2000**, *100*, 353–405.

Results indicate that the septet ( $S = 3$ , **C**) spin state indeed displays the lowest energy compared to the triplet ( $S = 3$ , **A**) and the quintet ( $S = 3$ , **B**), with a difference of more than 23 kcal/mol (Figure 5-4). The structures predicted for the three spin states bear striking resemblance, implying the stability of the dimeric scaffold against redistribution of the valence electrons.<sup>11</sup>

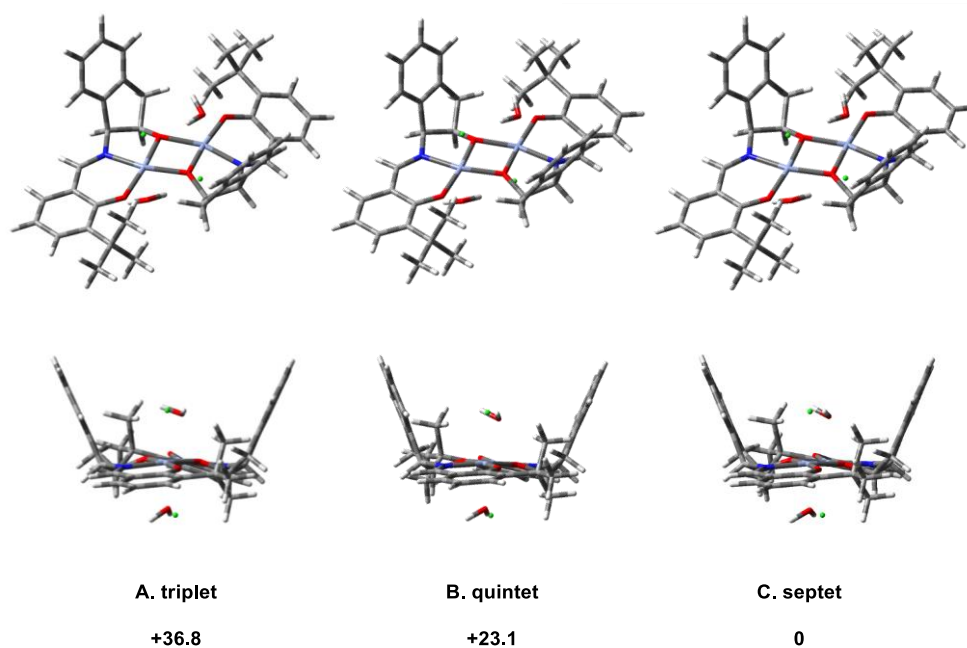


**Figure 5-4.** Energies of the triplet, quintet and septet spin states. Top structures show the top view, and the bottom ones show the side view. Numbers are the predicted energy in kcal/mol relative to the lowest energy spin state.

The septet spin state can also exist as an apparent singlet state, with the two chromium cores antiferromagnetically coupled (Scenario **C'** in Figure 5-3). Computations show that the energy of this structure is very similar to that of the septet ( $\Delta E = 0.27$ , Figure 5-5), indicating that the antiferromagnetic coupling between the two chromium atoms is minimal, and these two spin states may co-exist in the reaction. This is supported by experimental spin density measurement by the Evans method using NMR spectroscopy.<sup>12</sup> The overall magnetic

<sup>11</sup> In comparison, the structure of manganese-salen complexes varies significant in different spin states. See ref. 10a.

<sup>12</sup> Garland, C. W.; Nibler, J. W.; Shoemaker, D. P. *Experiments in Physical Chemistry*, 8<sup>th</sup> Ed.; McGraw-Hill; New York: 2003, p. 371–379.

susceptibility of catalyst **1a** was determined as  $S = 2.3$  in acetone at room temperature. Since the possibility of the quintet state has been ruled out by calculation, this value indicates the presence of a mixture of  $S = 0$  and  $S = 3$  spin states in solution.

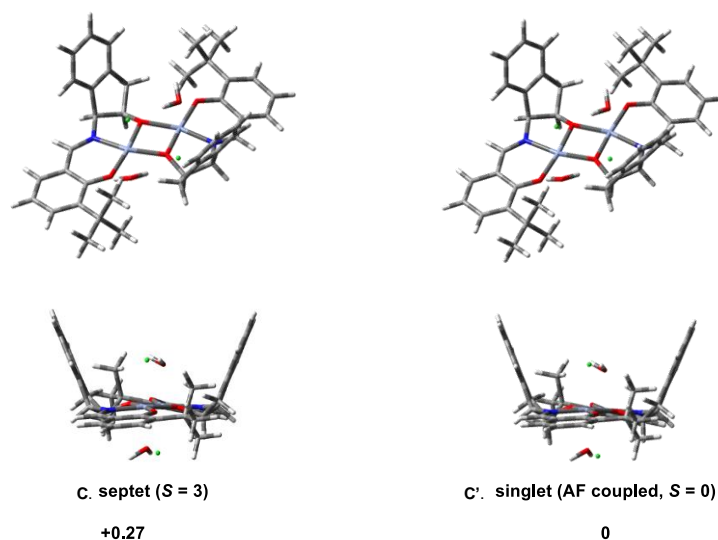


**Figure 5-5.** Energies of the antiferromagnetically coupled singlet and septet spin states. Top structures show the top view, and the bottom one show the side view. Numbers are the predicted energy in kcal/mol relative to the lowest energy structure.

The role of the catalyst is likely that of a traditional Lewis acid,<sup>13</sup> with the aldehyde substrate replacing a water molecule during the reaction. This means that the coordination sphere of the Cr atoms will not be perturbed significantly, and that the spin state should remain the same throughout the course of the reaction. Due to the nearly perfect structure-overlay between the singlet (**C**) and the septet catalyst (**C'**) frameworks as well as their similar energy, we conducted all the calculations in the latter sections using the septet spin state. The two catalyst spin states were compared in predicting the enantioselectivity of the reaction involving substrate **1a** and **4**, with results showing essentially no discrepancy between the two (see Section 5.3.3).

<sup>13</sup> This hypothesis is supported by evaluation of aldehyde **2a** bound to catalyst **1a** by DFT calculation, which shows no significant spin density distribution on the substrate. A simple experiment with a radical clock, cyclopropanecarboxaldehyde, as the electrophile in the reaction would validate this hypothesis.

### 5.3.2 Asynchronicity of the Rearrangement

The uncatalyzed carbonyl-ene reaction is known to favor a concerted pathway, with the C–C bond formation and the H atom transfer occurring simultaneously. This is corroborated by DFT calculations shown in Figure 5-6. Acetaldehyde was used as a simplified model in this analysis to reduce the size of the system, together with 2-methoxypropene **3**. A 2-D scan of the forming C–C bond ( $d_1$ ) and the cleaving C–H bond ( $d_2$ ) reveals a highly synchronous process with the lowest energy pathway almost perfectly aligning with the diagonal of the energy surface (arrow in yellow).

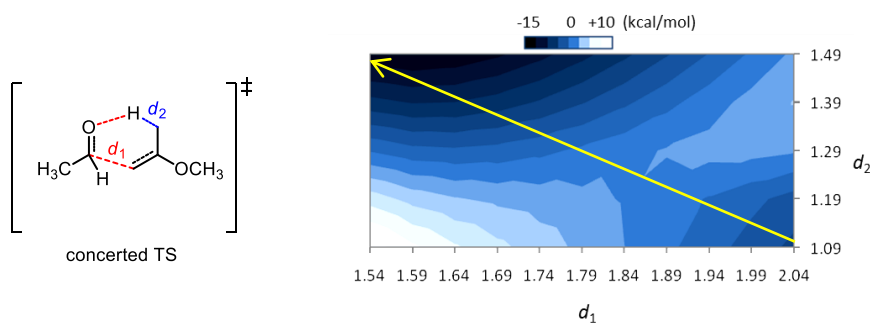


**Figure 5-6.** Concertedness of the uncatalyzed carbonyl-ene reaction. Calculated performed at B3LYP/6-31G(d) level of theory.

In contrast, when catalyst **1** is introduced to the system, the ene reaction becomes highly asynchronous, with the C–C bond formation leading the C–H bond cleavage (Figure 5-7). A stationary point corresponding to a ground state intermediate (**B**) was identified, with a partially formed C–C bond ( $d_1 = 1.75 \text{ \AA}$ ) and an energy only 0.01 kcal/mol lower than its preceding transition state (**A**).<sup>14</sup> This “pre-ene” ground state then undergoes a concerted pathway (**C**) with an activation energy of 3.3 kcal/mol, leading to the formation of the ene product.

<sup>14</sup> An analogous intermediate has been located by DFT computation in an I<sub>2</sub>-catalyzed Mukaiyama aldol reaction, with a C–C forming bond distance of 1.68 Å. See: Wang, L.; Wong, M. W. *Tetrahedron Lett.* **2008**, *49*, 3916–3920.

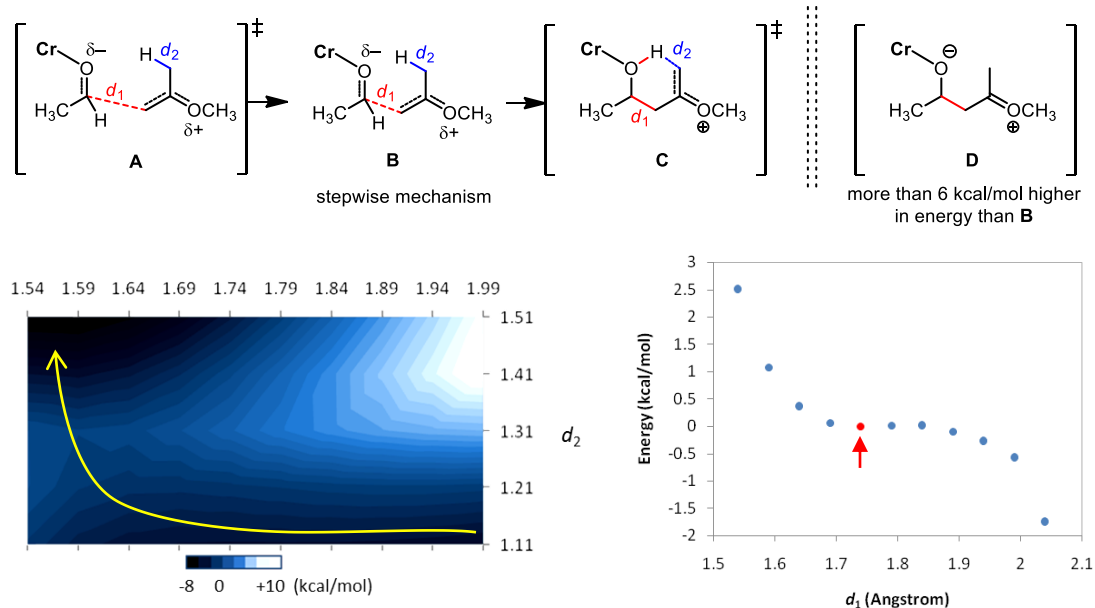


**Figure 5-7.** Asynchronicity of the Cr-catalyzed carbonyl-ene reaction. Left: 2-D scanning of  $d_1$  and  $d_2$ ; right: 1-D scanning of only  $d_1$ , with the ground state stationary point labeled with an arrow. Calculated performed at B3LYP/6-31G(d) level of theory.

The reaction involving benzaldehyde **2a** as the electrophile was also modeled with the same methods. The stepwise nature of the reaction pathway becomes more pronounced than with acetaldehyde, with the “pre-ene” ground state bearing a shorter  $d_1$  (1.68 Å) and a lower relative energy to transition state prior to it (1.7 kcal/mol). Nevertheless, the C–C bond is not fully formed in intermediate **B**, which distinguishes the carbonyl-ene reaction catalyzed by Cr complex **1** from other Lewis acid-catalyzed systems that are proposed to proceed through the formation of a discrete carbocation/oxocarbenium ion intermediate (**D**) with fully constructed C–C bond prior to H-atom transfer.<sup>15</sup>

It is also revealed by computational analysis that the corresponding reaction involving silyl enol ether (**4**) has a very similar mechanistic profile, with the formation of the “pre-ene” intermediate of type **B** followed by a concerted pericyclic rearrangement. The absence of a

<sup>15</sup> (a) Singleton, D. A.; Hang, C. *J. Org. Chem.* **2000**, *65*, 895–899; (b) Wong, C. T.; Wong, M. W. *J. Org. Chem.* **2007**, *72*, 1425–1430; (c) Lee, J. M.; Helquist, P.; Wiest, O. *J. Am. Chem. Soc.* **2012**, *134*, 14973–14981; (d) Morao, I.; McNamara, J. P.; Hillier, I. H. *J. Am. Chem. Soc.* **2003**, *125*, 628–629;

cationic intermediate of type **D** precludes the Mukaiyama aldol pathway from happening, in accord with the experimental observation that the ene product was detected from the reaction mixture as the only product.<sup>16</sup>

To summarize, the Cr-catalyzed carbonyl-ene reaction proceeds through a two-step mechanism. In the first step the nucleophile approaches the catalyst-bound aldehyde, forming a “pre-ene” complex with a partially formed C–C bond. This is followed by a rate-limiting, pericyclic reaction with the completion of the C–C bond formation and the H-atom transfer occurring concurrently and furnishing the product. The second step is also enantio-determining.

---

<sup>16</sup> The Mukaiyama aldol reaction can also occur through a concerted C–C bond formation/silyl transfer process. However, this reaction pathway cannot be located in the presence of catalyst **1a**, presumably due to unfavorable pre-organization of the corresponding transition state in the sterically confined environment around Cr center.

### 5.3.3 Origin of Enantioselectivity

To elucidate the origin of enantioselectivity of the Cr-catalyzed carbonyl-ene reaction, the enantio-determining transition states were modeled using DFT methods. As discussed previously, the B3LYP functional has been validated for the computational analyses of first row transition metals. However, it cannot accurately predict the effect of dispersion forces, which is an important component of the cation- $\pi$  interaction. In order to assess our initial hypothesis that the  $\pi$ -electrons inside the concave reactive site serve to stabilize partial positive charge built up in the transition state, we also examined this system with the M06 level of theory, a theory specifically parametrized for the prediction of the structure and energy of metal complexes as well as the scale of dispersion interactions.<sup>17</sup>

The lowest energy conformations of the major and the minor diastereomeric transition states were located and validated by their vibrational frequencies. When the substrate assembly was adapted into the concave face of the catalyst, both B3LYP and M06 predicted the correct sense of enantioinduction, although in different magnitudes (Table 5-1, entries 1-2). The pathways with substrate coordinating to the convex face of the catalyst were also evaluated. Interestingly, based on computation with the B3LYP functional, the reaction is expected to occur on the less sterically encumbered convex face, favored by 0.5 kcal/mol (entry 1). However, the pro-(*R*) transition state was calculated to have a lower energy with catalyst (*S,R*)-**1a**, opposing the experimental observation.

The relative reactivity of the two faces of the Cr catalyst in the carbonyl-ene reaction is inversed when the M06 level of theory was applied, showing that the lowest energy pathways for the generation of both the (*R*) and the (*S*) products occur inside the concave cavity (Table 5-1, entry 2). As discussed earlier, this is likely a result of M06 being able to estimate the dispersion

---

<sup>17</sup> Zhao, Y.; Truhlar, D. G. *Theor. Chem. Account* **2008**, *120*, 215–241.

component of the attractive interactions provided by the aromatic groups in the concave face, which B3LYP fails to do. When the catalyst in an antiferromagnetically coupled singlet state was examined in this context, the same product configuration and very similar differential energies of activation were produced, showing again that the coupling between the two Cr centers is minimal and does not affect the computational predictions (entries 3 & 4 vs. entries 1 & 2).

Since acetone is used as the solvent and BaO is added to the reaction as a desiccant, we also considered the situation where acetone serves as the ancillary ligand replacing water (entries 5-6). In addition, solvent effects were examined using polarizable continuum model (PCM) method (entries 7-8). Under both circumstances, the predicted product configuration matched the experimental findings, with the magnitude of the differential activation energy slightly reduced.

**Table 5-1.** Predicted energy differences between various reaction pathways.

entry	method	relative energy to concave, pro-( <i>S</i> ) transition state			
		concave, pro-( <i>S</i> ) (kcal/mol)	concave, pro-( <i>R</i> ) (kcal/mol)	convex, pro-( <i>S</i> ) (kcal/mol)	convex, pro-( <i>R</i> ) (kcal/mol)
1	B3LYP	0	+1.0	+1.5 <sup>‡</sup>	-0.5 <sup>^</sup>
2	M06	0	+3.3	+5.9	+3.7
3 <sup>a</sup>	B3LYP	0	+1.0 <sup>^</sup>	n.d.	n.d.
4 <sup>a</sup>	M06	0	+3.0	n.d.	n.d.
5 <sup>b</sup>	B3LYP	0	+1.0	n.d.	n.d.
6 <sup>b</sup>	M06	0	+2.6	n.d.	n.d.
7 <sup>c</sup>	B3LYP	0	+1.2	n.d.	n.d.
8 <sup>c</sup>	M06	0	+2.0 <sup>*</sup>	n.d.	n.d.

<sup>a</sup> Cr atoms in antiferromagnetically coupled singlet state. <sup>b</sup> with acetone as the ancillary ligand replacing H<sub>2</sub>O. <sup>c</sup> with acetone as the solvent using polarizable continuum model. The number labeled with \*, <sup>‡</sup> or <sup>^</sup> represent the calculated relative energy of a partially optimized structures with the cleaving C–H bond (*d*<sub>2</sub>) fixed at a distance identical to the fully optimized structure in entry 1, pro-(*R*) (for <sup>^</sup>), pro-(*S*) (for <sup>‡</sup>) or entry 2, pro-(*R*) (for <sup>\*</sup>); full optimization has not converge on meaningful transition state structures. n.d. = not determined. Uncorrected electronic energy values are shown.

By scrutinizing the two diastereomeric transition structures, one can identify a few protons bearing a partial positive charge in close proximity to the aromatic ring of the aminoindanol portion of the ligand (Figure 5-8). In the minor pathway, the formyl proton on the aldehyde resides within 2.65 Å of the  $\pi$ -face of the cavity, while in the major transition state, one of the  $\alpha$ -protons on the nucleophile lies above the aromatic group with a distance of 2.55 Å (M06) or 2.82 Å (B3LYP). As revealed by the electrostatic potential map of the substrate assembly in the transition state, the  $\alpha$ -proton bears substantially more positive character than the formyl proton, making it a better  $\pi$ -acceptor. Taken together, we propose that the difference in the strength of the cation– $\pi$  interaction in the two diastereomeric transition states lies at the origin of the enantioselectivity. A number of asymmetric metal-catalyzed reactions have been suggested to rely on noncovalent interactions provided by the ligand for efficient catalysis, primarily through directing effect via substrate binding.<sup>18</sup> However, a mechanism in which the cation– $\pi$  interaction in addition to the Lewis acid-base association cooperatively stabilizes the charge buildup in the transition state has not been reported previously.<sup>19</sup>

Uncovering of the novel cooperative noncovalent mechanism has spurred us to develop new catalysts that are computationally predicted to improve the reactivity and selectivity of the reaction. Based on the analyses in Chapter 4 and in other literature precedent on cation– $\pi$

---

<sup>18</sup> For a review on functional group directed metal catalysis, see: (a) Hoveyda, A. H.; Evans, D. A.; Fu, G. C. *Chem. Rev.* **1993**, *93*, 1307–1370; For examples on intramolecular cooperative catalysis by a combination of Lewis acid and Lewis base, see: (b) Takamura, M.; Kunabashi, Kanai, M.; Shibasaki, M. *J. Am. Chem. Soc.* **1999**, *121*, 2641; (c) Takamura, M.; Funabashi, K.; Kanai, M.; Shibasaki, M. *J. Am. Chem. Soc.* **2001**, *123*, 6801; (d) Shibasaki, M.; Yoshikawa, N.; *Chem. Rev.* **2002**, *102*, 2187; for a reaction exhibiting cooperativity between Lewis acid and enamine catalysis, see: (e) Daka, P.; Xu, Z.; Alexa, A.; Wang, H. *Chem. Commun.* **2011**, *47*, 224–226.

<sup>19</sup> For a system in which a cation– $\pi$  interaction was invoked between the ligand and the metal center, see: (a) Ishihara, K.; Fushimi, M.; Akakura, M. *Acc. Chem. Res.* **2007**, *40*, 1049–1055; For a system proposing a C–H– $\pi$  interaction that helps to organize the transition state of reaction, see: (b) Yamakawa, M.; Yamada, I.; Ryoji Noyori, R. *Angew. Chem. Int. Ed.* **2001**, *40*, 2818–2821.

interactions,<sup>20</sup> we reasoned that both increasing the electron density and expanding the size of the aromatic group on the ligand might lead to a stronger ligand–substrate association in the transition state by means of enhancing the cation– $\pi$  attraction. Proposed catalyst frameworks were evaluated with computation methods (Table 5-2). It was anticipated by both B3LYP and M06 that introduction of naphthalene instead of benzene to the ligand scaffold would lead to an improvement in the reaction enantioselectivity (entry 2 vs. entry 1). In the transition structures, both the forming C–C bond and the forming C–H bond display shorter distances compared to the corresponding structures with catalyst **1a**, indicating a later transition state on the reaction coordinate. Based on Hammond postulate, this is consistent with an increased stabilizing effect of the naphthalene group in the exothermic reaction.

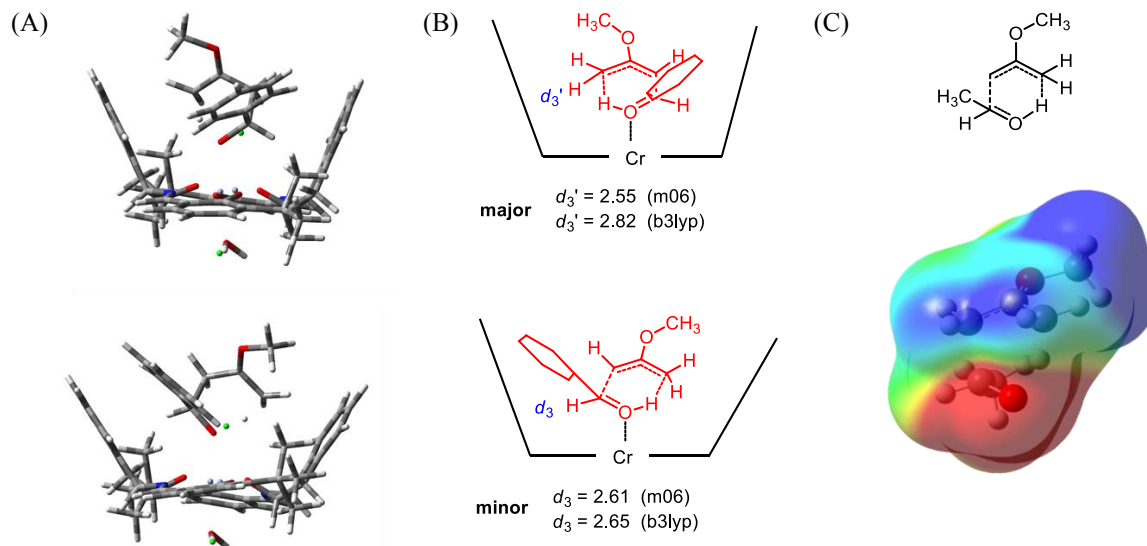


**Figure 5-8.** DFT-predicted lowest energy transition states leading to the enantiomeric products. (A) Structures optimized at M06/6-31G(d); the top one is the major pro-(*S*) transition state, and the bottom one is the minor pro-(*R*) transition state. (B) The same structures in part A with chemdraw representation;  $d_3$  is the distance between the formal proton and the  $\pi$ -face of the aminoindanol group, and  $d_{3'}$  is the distance between an  $\alpha$ -proton of methoxypropene and the  $\pi$ -face of the aminoindanol group. (C) Structure of the substrate assembly in the transition state and its electron potential map (B3LYP/6-31G(d)), with blue representing positive potentials and red representing negative potentials.

<sup>20</sup> Ma, J.; Dougherty, D. A. *Chem. Rev.* **1997**, *97*, 1303–1324.

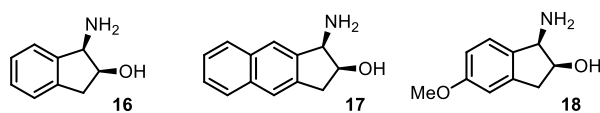
For the anisole derivative, the B3LYP functional predicted increased differential energy of activation with respect to parent catalyst **1a**, while M06 shows essentially no effect by introducing the methoxy group.

The synthesis of these new catalysts as well as evaluation of their activity in the carbonyl-ene reaction is currently underway.

**Table 5-2.** Effect of the structure of the aminoindanol on the predicted enantioselectivity of reaction.

structure of aminoindanol	experimental ee	predicted $\Delta\Delta E^\ddagger$ with M06 (kcal/mol)	predicted $\Delta\Delta E^\ddagger$ with B3LYP (kcal/mol)
<b>16</b>	88%	3.25	1.00
<b>17</b>	n.d.	4.23	1.63
<b>18</b>	n.d.	3.20*	1.69

The number with an asterisk (\*) represents the energy of the partially optimized structure with the cleaving C–H bond restricted at a distance same to that in entry 1.



### 5.3.4 Effect of the *ortho*-Substituents on Arylaldehyde Substrate

In the substrate scope study of the carbonyl-ene reaction between aldehydes (**2**) and 2-methoxypropene (**3**), an intriguing beneficial effect of the *ortho*-substituent of the arylaldehyde on the enantioselectivity of the reaction was observed (Table 5-3, entry 1 & 2 vs. entry 3, entry 5 vs. entry 6). However, when both of the *ortho*-positions are substituted, a decreased ee was observed instead (entry 4). We were curious to see if this general trend can be reproduced with DFT methods to both validate the computational model proposed in the previous discussions and to gain insights into this substitution effect. Indeed, such observations were also produced with the transition state models we obtained in Section 5.3.3 with both M06 and B3LYP functionals.

**Table 5-3.** Effect of the *ortho*-substituent of arylaldehyde on the enantioselectivity of reaction.

entry	substituent	experimental ee%	predicted $\Delta\Delta E^\ddagger$ with M06 (kcal/mol)	predicted $\Delta\Delta E^\ddagger$ with B3LYP (kcal/mol)
1	H <sup>a</sup>	88	3.25	1.00
2	4-CH <sub>3</sub> <sup>a</sup>	89	n.d.	n.d.
3	2-CH <sub>3</sub> <sup>a</sup>	94	3.35	2.03
4	2,6-di-Cl <sup>b</sup>	86	1.76	n.d.
5	3-Br <sup>b</sup>	86	n.d.	n.d.
6	2-Br <sup>b</sup>	96	4.26	3.45

<sup>a</sup> reaction run in ethyl acetate. <sup>b</sup> reaction run in acetone. In acetone the ee of the same reaction is usually 1-4% higher than in ethyl acetate.

An explanation for these *ortho*-substitution effects can be advanced by comparing the structures of the diastereomeric transition states of reactions involving different aldehydes (Figure 5-9). The catalyst framework in the minor transition state with 2-bromobenzaldehyde (**2b**) displays a significant distortion from the free catalyst, with an increase in the dihedral angle (D) between the two “aromatic walls” of more than 12°. This perturbation to the catalyst structure may lead to increased energy of the transition state. In contrast, the corresponding major transition state for **2b** as well as both the major and the minor transition states of the

benzaldehyde (**2b**)-involving reaction have only a marginal structural deviation from the free catalyst ( $\Delta D \leq 5^\circ$ ). This difference is likely caused by the steric interaction between the *ortho*-bromine atom and the proximal aminoindanol motif, resulting in a catalyst structure change in the corresponding minor transition state to alleviate the repulsion.<sup>21</sup>

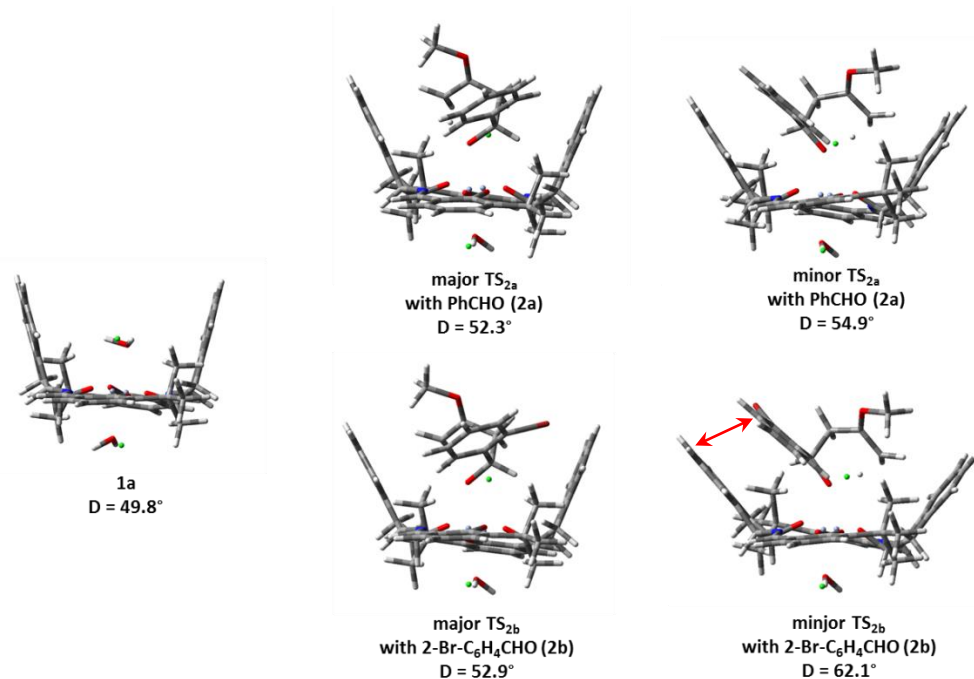


**Figure 5-9.** Structural comparison between catalyst **1a** and the diastereomeric transition states with PhCHO (**2a**) and 2-Br-C<sub>6</sub>H<sub>4</sub>CHO (**2b**), with dihedral angle between the two aromatic groups on aminoindanol groups shown as D. The proposed steric repulsion between the *ortho*-bromine atom and the ligand is represented as a red arrow.

<sup>21</sup> One can argue that enantio-induction in the reaction with benzaldehyde may arise from the discrepancy in the dihedral angle D (52.3° for major vs. 54.9° for minor). However, results from a semi-quantitative analysis are in disagreement with this argument. If the steric distortion is the only source of enantio-differentiation, one can define the relative energy of both major TS<sub>2a</sub> and major TS<sub>2b</sub> as zero, because they have very similar D values. Therefore, the relative energy of minor TS<sub>2a</sub> is 3.25 and that of minor TS<sub>2b</sub> is 4.26, both in kcal/mol. From major TS<sub>2a</sub> to minor TS<sub>2a</sub>, a 2.6° distortion of catalyst structure causes a 3.25 kcal/mol energy rise, while from minor TS<sub>2a</sub> to minor TS<sub>2b</sub>, a more sizable 7.2° distortion angle leads only to a 1.01 kcal/mol energy rise. The inconsistency between the magnitude of catalyst structure change and that of the energy change indicates that such rationale for stereo-induction mechanism is ungrounded.

## 5.4 Outlook

To summarize, on the basis of experimental kinetic analyses conducted previously by Ruck et. al., we evaluated the carbonyl-ene reaction catalyzed by dimeric chromium complex **1a** with DFT computational modeling. A detailed mechanistic picture emerged in which Lewis acid coordination with the aldehyde electrophile operates synergistically with  $\pi$ -stabilization of the cationic character developing on the nucleophile in the energetically favored reaction transition state.

From a synthetic point of view, the elucidation of the critical role of the cation- $\pi$  stabilizing element in the enantioinduction mechanism led to the identification of a catalyst framework expected to be more enantioselective. If this computational result could be validated by experimental studies, the new catalyst not only would provide an improvement to the enantioselectivity of the reaction, but might also extend the substrate scope to more challenging alkylaldehydes.

From a mechanistic point of view, the novel cooperativity observed between a metal center and its supporting ligand in the synergistic stabilization of a polarized transition state is fundamentally interesting. It provides a new view on how enantioinduction in a metal-catalyzed transformation can be achieved, and might emerge as a new principle for reaction development.

## Experimental Section

### Table of Content

1. Energy surface of the carbonyl-ene reaction by 2-D scan 281
2. Computational data for the enantio-determining transition states 282

#### 1. Energy surface of the carbonyl-ene reaction by 2-D scan

Reaction between acetaldehyde and 2-methoxypropene under uncatalyzed conditions. Energy unit is a.u. Only the decimal fractions are shown. Top row shows the distance of the cleaving C–H bond, and the most left-hand side column shows the distance of the forming C–C bond. Method: B3LYP/6-31G(d).

	<b>1.11</b>	<b>1.21</b>	<b>1.31</b>	<b>1.41</b>	<b>1.51</b>
<b>1.54</b>	-0.95813	-0.95588	-0.95591	-0.96195	-0.96868
<b>1.59</b>	-0.9604	-0.95783	-0.95685	-0.96233	-0.96893
<b>1.64</b>	-0.96155	-0.9586	-0.95639	-0.9612	-0.96722
<b>1.69</b>	-0.96201	-0.95865	-0.955	-0.95906	-0.9646
<b>1.74</b>	-0.96211	-0.95834	-0.95309	-0.95617	-0.96117
<b>1.79</b>	-0.96209	-0.95791	-0.95107	-0.95283	-0.95729
<b>1.84</b>	-0.9621	-0.95753	-0.94933	-0.94926	-0.95311
<b>1.89</b>	-0.96226	-0.95731	-0.94803	-0.94565	-0.94875
<b>1.94</b>	-0.96256	-0.95734	-0.94726	-0.94216	-0.94451
<b>1.99</b>	-0.96304	-0.9576	-0.94693	-0.93895	-0.94032
<b>2.04</b>	-0.96491	-0.95821	-0.94534		

Reaction between acetaldehyde and 2-methoxypropene under **1a**-catalyzed conditions. Energy unit is a.u. Only the decimal fractions are shown. Top row shows the distance of the cleaving C–H bond, and the most left-hand side column shows the distance of the forming C–C bond. B3LYP/6-31G(d).

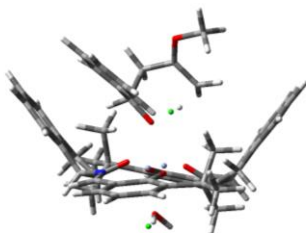
	<b>1.09</b>	<b>1.19</b>	<b>1.29</b>	<b>1.39</b>	<b>1.49</b>
<b>1.54</b>	-0.2051884	-0.2143104	-0.2252552	-0.2359892	-0.245263
<b>1.59</b>	-0.2093983	-0.2171122	-0.2270565	-0.2372132	-0.246082
<b>1.64</b>	-0.2125933	-0.2187384	-0.2274642	-0.2369622	-0.2453852
<b>1.69</b>	-0.2151958	-0.2196964	-0.2269234	-0.2356667	-0.2435981
<b>1.74</b>	-0.2175075	-0.2204082	-0.2257976	-0.2336678	-0.2410578
<b>1.79</b>	-0.2197298	-0.2211883	-0.2243899	-0.2312396	-0.2380301
<b>1.84</b>	-0.2219825	-0.2222234	-0.2229591	-0.2285998	-0.2347247
<b>1.89</b>	-0.2243168	-0.223581	-0.2217384	-0.2259206	-0.2313034
<b>1.94</b>	-0.2267411	-0.2252456	-0.2209663	-0.2233354	-0.227889
<b>1.99</b>	-0.2292325	-0.2271534	-0.220905	-0.2209513	-0.2245725
<b>2.04</b>	-0.2317619	-0.2292298	-0.2216374	-0.2188623	-0.2214234

## 2. Computational data for the enantio-determining transition states

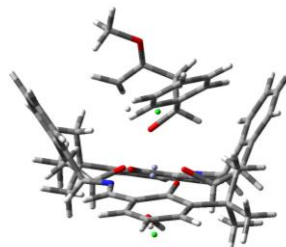
Reaction between benzaldehyde **1a**, 2-methoxypropene **3** and catalyst **1a**. Energy unit is a.u..

With B3LYP/6-31G(d):

TS<sub>pro-(R)</sub>



TS<sub>pro-(S)</sub>



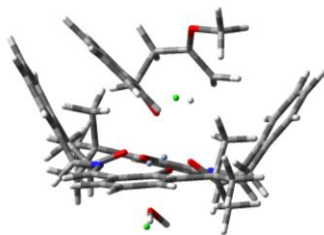
E = -3707.70979432		E + ZPE = -3706.714498		E = -3707.71142668		E + ZPE = -3706.716378	
G = -3706.811709		imaginary frequencies: 1		G = -3706.813547		imaginary frequencies: 1	
Cr	2.12243400	-0.39309800	-0.45759800	Cr	2.09368600	-0.54563000	-0.42563100
Cr	-0.92119100	0.03870600	-0.99389100	Cr	-0.90627500	0.11389600	-1.00789600
O	0.41546800	-1.45029700	-0.54575600	O	0.28781800	-1.43056800	-0.41614500
O	3.88500900	0.40685300	-0.51214400	O	3.91929900	0.07417600	-0.55419200
O	0.74385400	1.09264600	-0.68162100	O	0.85818400	1.03939300	-0.78693000
O	-2.63941600	-0.80197100	-1.31294600	O	-2.68557800	-0.59728800	-1.26073900
N	2.93270200	-2.22498600	-0.53964700	N	2.71710600	-2.44436900	-0.32536500
N	-1.62169600	1.83786500	-1.52378400	N	-1.45756200	1.91403300	-1.68020300
C	0.56960500	-2.75228200	-1.08622300	C	0.30773800	-2.79741800	-0.79496600
C	1.94556400	-3.30745600	-0.60539800	C	1.62434700	-3.41873000	-0.23629600
C	1.60133100	-3.99403700	0.71006600	C	1.22351000	-3.85018300	1.16935400
C	2.44094200	-4.38464300	1.74923000	C	2.02737500	-4.14612100	2.26516300
C	1.89746600	-5.09173800	2.82632400	C	1.42041800	-4.57976300	3.44816800
C	0.53484500	-5.40624200	2.85120200	C	0.03068800	-4.71493400	3.52315300
C	-0.30582200	-5.00277500	1.80824100	C	-0.77316500	-4.41273000	2.41847400
C	0.23214100	-4.28537200	0.74024600	C	-0.16944900	-3.97606700	1.24045500
C	-0.45927900	-3.73886400	-0.48864400	C	-0.80377000	-3.59362500	-0.07859600
C	4.20484200	-2.48609200	-0.55952700	C	3.95683900	-2.83049200	-0.33066200
C	5.28224100	-1.54605800	-0.48852800	C	5.12137000	-1.99821000	-0.38354400
C	5.07662900	-0.12068800	-0.44417100	C	5.05580000	-0.56186200	-0.47494600
C	6.23581800	0.73355800	-0.35219600	C	6.29369000	0.17856200	-0.50339700
C	7.48786500	0.13146200	-0.33260900	C	7.48250500	-0.53904700	-0.45767800
C	7.68862600	-1.26242600	-0.39508800	C	7.54606100	-1.94524100	-0.38305600
C	6.59256000	-2.08650700	-0.47154700	C	6.37393600	-2.66049700	-0.34586100
C	6.08040700	2.26470000	-0.26949700	C	6.28727800	1.71866000	-0.57067500
C	5.26334700	2.63631900	0.99314200	C	5.56612900	2.28977800	0.67576100
C	5.38409600	2.79480600	-1.54764200	C	5.58728600	2.19008900	-1.86956600
C	7.44068500	2.98423300	-0.16269000	C	7.71267000	2.30871300	-0.58385200
C	0.83209500	2.29143600	-1.43703100	C	1.01675700	2.20030100	-1.58456000
C	-0.60473900	2.90284400	-1.57529800	C	-0.37715800	2.90381600	-1.70932500
C	-0.66662900	3.94249400	-0.46407100	C	-0.37000100	3.91083200	-0.56787200
C	-1.77055500	4.64547800	0.01661500	C	-1.43517000	4.62449500	-0.02252700
C	-1.57812600	5.61601900	1.00471200	C	-1.17707900	5.56816000	0.97782000
C	-0.29690000	5.87306600	1.50441800	C	0.13315500	5.79045600	1.41795000
C	0.80804000	5.16766300	1.01833700	C	1.19846300	5.06761600	0.86965900
C	0.61890000	4.20478300	0.02697400	C	0.94120200	4.12394700	-0.12483400
C	1.65255500	3.36278400	-0.68170000	C	1.91332600	3.24492200	-0.87831900

C	-2.79222200	2.02782200	-2.04860800	C	-2.60320200	2.16450000	-2.22988500
C	-3.85713400	1.07636200	-2.18915500	C	-3.72096300	1.27441100	-2.36048900
C	-3.73430400	-0.31317300	-1.83238200	C	-3.70398400	-0.09475700	-1.91395300
C	-4.86486000	-1.17921400	-2.06155100	C	-4.85050700	-0.91899800	-2.20792600
C	-6.02223100	-0.61797100	-2.58991200	C	-5.93669200	-0.32422500	-2.84095100
C	-6.14492200	0.74292000	-2.92835900	C	-5.96965800	1.02599600	-3.23625800
C	-5.06501600	1.57189600	-2.73667200	C	-4.86158300	1.80648800	-3.00938100
C	-4.77802000	-2.68750800	-1.75159700	C	-4.86352100	-2.42173300	-1.85875600
C	-4.48911500	-2.91093500	-0.24665500	C	-4.74482600	-2.61636800	-0.32954400
C	-3.66534800	-3.32950400	-2.61750000	C	-3.69698400	-3.13107800	-2.59056100
C	-6.09231400	-3.42839700	-2.07392900	C	-6.16752300	-3.11652100	-2.30368700
H	0.50620500	-2.71094700	-2.18063800	H	0.23894600	-2.88096200	-1.88691100
H	2.30340900	-4.06682000	-1.32026800	H	1.89438100	-4.30870300	-0.82859600
H	3.49746300	-4.13066000	1.74138200	H	3.10560300	-4.01892700	2.22023700
H	2.53843000	-5.39638800	3.64914800	H	2.03341000	-4.80409800	4.31686900
H	0.12573200	-5.96401000	3.68988600	H	-0.42900100	-5.05155800	4.44889300
H	-1.36640100	-5.24423600	1.83271600	H	-1.85430700	-4.51548500	2.48099600
H	-1.40482800	-3.23169600	-0.27959300	H	-1.71674900	-2.99989600	0.01184900
H	-0.67710500	-4.53876000	-1.21108300	H	-1.06226900	-4.48674900	-0.66653900
H	4.50157900	-3.53774300	-0.64193400	H	4.14832600	-3.90881100	-0.29456800
H	8.36965000	0.75851300	-0.26499200	H	8.42187800	0.00173000	-0.47839000
H	6.71236300	-3.16744500	-0.51261200	H	6.38846400	-3.74673500	-0.28071600
H	5.81122300	2.35283700	1.89996100	H	6.12247500	2.03960400	1.58720000
H	4.29735200	2.12989600	1.01498300	H	4.55711000	1.88800100	0.77902800
H	5.09792200	3.72115900	1.02706600	H	5.50890900	3.38425100	0.60786700
H	4.40769600	2.33190600	-1.69417300	H	4.56486400	1.81619500	-1.93253100
H	5.99953600	2.58900500	-2.43241100	H	6.13725000	1.83758900	-2.75108800
H	5.25124300	3.88233000	-1.47934700	H	5.56460500	3.28693800	-1.90708100
H	7.99652700	2.68900500	0.73502500	H	8.27752800	2.04972800	0.31937600
H	7.27036200	4.06518600	-0.10131000	H	7.64621900	3.40185400	-0.62566500
H	8.07590400	2.80224400	-1.03778900	H	8.28922400	1.98191200	-1.45745900
H	1.25450800	2.07485500	-2.42377800	H	1.40335900	1.92411600	-2.57208900
H	-0.68684100	3.40612600	-2.55006100	H	-0.42295600	3.44541500	-2.66690200
H	-2.77178200	4.43990400	-0.35192300	H	-2.45371000	4.45504500	-0.36342700
H	-2.43112100	6.16871900	1.38904400	H	-1.99685800	6.13947500	1.40620500
H	-0.15933300	6.62696200	2.27530200	H	0.32511600	6.53204100	2.18939300
H	1.80289800	5.36869400	1.40832200	H	2.21399900	5.23853400	1.21865700
H	2.37253300	2.89006000	-0.00856600	H	2.64859600	2.75200600	-0.23682900
H	2.22786700	3.97248300	-1.39246300	H	2.47325300	3.83006000	-1.62181300
H	-3.00410500	3.02135300	-2.45750100	H	-2.74148300	3.15464200	-2.67836700
H	-6.88222700	-1.25464900	-2.76445600	H	-6.81074000	-0.92706800	-3.05837200
H	-4.40473300	-3.98490500	-0.03423400	H	-4.71738200	-3.68675700	-0.08584400
H	-5.30890800	-2.51293400	0.36508700	H	-5.60511000	-2.17421100	0.18615700
H	-3.56367000	-2.41948400	0.05707600	H	-3.84463000	-2.14252500	0.06053700
H	-3.55819300	-4.39322400	-2.36661500	H	-3.66840400	-4.19241900	-2.31048000
H	-2.70514900	-2.83311100	-2.47105500	H	-2.73476900	-2.67647600	-2.35232000
H	-3.92328600	-3.25960500	-3.68093600	H	-3.83574900	-3.07384300	-3.67678700
H	-5.97146400	-4.49211600	-1.83856000	H	-6.11257500	-4.17966800	-2.04219500
H	-6.35717000	-3.35642700	-3.13502600	H	-6.32192700	-3.05335500	-3.38717600
H	-6.93637100	-3.05500600	-1.48162000	H	-7.05117000	-2.70247800	-1.80358000
Cl	2.23966200	-0.32961400	1.89049000	Cl	2.25499100	-0.31167700	1.91152000
Cl	-0.49976000	-0.32561100	-3.40856400	Cl	-0.52214700	-0.47662700	-3.38513600
O	2.29094600	-0.29706100	-2.54239800	O	2.25483700	-0.66439400	-2.50652100
H	1.39010300	-0.36137300	-2.98484600	H	1.34745500	-0.65517700	-2.94088900
H	2.86131500	-0.98269900	-2.92342600	H	2.72095900	-1.45676800	-2.81604800
H	-5.12370800	2.62586200	-3.00092800	H	-4.84127400	2.84610500	-3.33065100

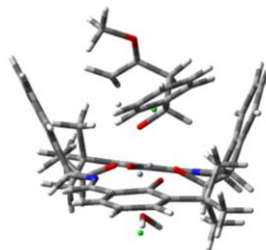
C	-0.96965300	-1.52929500	2.83001500	H	8.50902600	-2.44538900	-0.35091100
C	-1.32411700	-0.41756300	3.61332200	H	-6.84862200	1.42863600	-3.73019700
C	-0.82763300	0.89739100	3.17704000	C	-0.15272100	2.09736000	2.60906300
C	-1.56744000	1.23479300	1.78080400	C	-0.94477000	1.33904100	3.48412200
H	0.08642000	-1.56434200	2.54687600	C	-1.08886000	-0.09726000	3.18761600
H	-1.42051600	-2.49793200	3.02424400	C	-1.94471600	-0.19869100	1.82259300
H	0.24048300	0.84277800	2.95358000	H	0.80238200	1.63094300	2.34942300
H	-1.04584100	1.68361100	3.90049500	H	-0.13648000	3.18040400	2.68244200
O	-1.47062000	0.15043000	0.91533400	H	-0.11299500	-0.54127700	2.97685500
H	-1.31743800	-0.93649300	1.72996100	H	-1.60897000	-0.63629400	3.98028400
O	-2.28276900	-0.37797200	4.52149800	O	-1.39467600	0.63533400	0.85365300
C	-2.96656300	-1.58758300	4.88949100	H	-0.74588400	1.60582500	1.55964300
H	-3.57281900	-1.94727700	4.05334900	O	-1.81209400	1.81615800	4.36057400
H	-3.61015300	-1.31212600	5.72446300	C	-1.88371700	3.23476400	4.58157300
H	-2.25149800	-2.35587900	5.19746400	H	-2.23587400	3.74076900	3.67853900
H	-0.99220900	2.08044300	1.39154300	H	-2.60214300	3.36449900	5.39051700
H	8.69527400	-1.66839100	-0.37685700	H	-0.90543900	3.62725600	4.87413700
H	-7.07447200	1.12004200	-3.34340300	H	-1.82452700	-1.24729400	1.53041300
C	-3.01369000	1.65225200	2.04080000	C	-3.41388200	0.10080700	2.10455200
C	-4.08221100	0.85800400	1.61259800	C	-4.01704300	1.27667800	1.64824100
C	-3.29207900	2.84136700	2.73027100	C	-4.17933800	-0.80180300	2.85509600
C	-5.40148200	1.23790000	1.87573900	C	-5.35607800	1.54804000	1.94114700
H	-3.87050100	-0.04506000	1.05181100	H	-3.43284500	1.96422600	1.04599600
C	-4.60756900	3.22158400	2.99451300	C	-5.51639900	-0.53476400	3.14778900
H	-2.47483600	3.48226300	3.05313700	H	-3.72764800	-1.72758000	3.20757500
C	-5.66953000	2.41787700	2.56992700	C	-6.11007100	0.64553200	2.69225100
H	-6.21905700	0.61273500	1.52541300	H	-5.81325000	2.46312700	1.57243900
H	-4.80452300	4.14783100	3.52881500	H	-6.09623000	-1.24941300	3.72636300
H	-6.69530200	2.71501000	2.77245800	H	-7.15297000	0.85457200	2.91554500

With M05-2X/6-31G(d):

TS<sub>pro-(R)</sub>



TS<sub>pro-(S)</sub>



E = -3705.81321361	E + ZPE = -3704.820568	E = -3705.81839915	E + ZPE = -3704.824045				
G = -3704.912459	imaginary frequencies: 1	G = -3704.913087	imaginary frequencies: 1				
Cr	2.11665800	-0.43287600	-0.44876800	Cr	2.08406800	-0.60183700	-0.48707200
Cr	-0.83262600	0.07306400	-1.07220000	Cr	-0.84411600	0.11854200	-1.07842000
O	0.41134800	-1.45627800	-0.60963200	O	0.27991000	-1.44575200	-0.50851600
O	3.85747600	0.36706800	-0.44050200	O	3.90086500	-0.01486100	-0.62499900
O	0.82073000	1.08267600	-0.67183600	O	0.92934500	0.99581700	-0.85484000
O	-2.55518100	-0.73275000	-1.37628400	O	-2.64266100	-0.53504400	-1.24479100
N	2.90145400	-2.25713900	-0.55785400	N	2.64182100	-2.50539300	-0.31202000
N	-1.49093100	1.88878900	-1.53581000	N	-1.36094700	1.94551800	-1.66192200
C	0.56744400	-2.71811400	-1.20439500	C	0.27486600	-2.79742200	-0.88154000
C	1.89520500	-3.30601100	-0.66882600	C	1.51542800	-3.42855100	-0.20694600

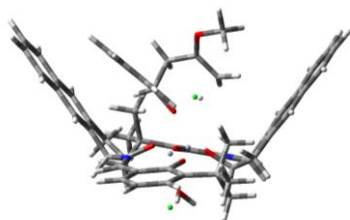
C	1.46463700	-3.94623900	0.63037600	C	0.99955200	-3.68057600	1.19583800
C	2.22463900	-4.27779100	1.74072800	C	1.70059500	-3.83048100	2.38136600
C	1.60524900	-4.93966100	2.79953600	C	0.98464900	-4.03054400	3.56142700
C	0.25129800	-5.26633600	2.73374800	C	-0.40784500	-4.08286200	3.54572400
C	-0.51115600	-4.90883800	1.62213800	C	-1.10920100	-3.93649300	2.34828800
C	0.09908700	-4.22922100	0.57616400	C	-0.39662200	-3.73603900	1.17393200
C	-0.50484500	-3.68537700	-0.68783900	C	-0.90421500	-3.51200700	-0.22207300
C	4.16661000	-2.52616000	-0.51824300	C	3.86956000	-2.90710300	-0.24184300
C	5.23822200	-1.58970600	-0.39418900	C	5.04326700	-2.09407100	-0.29212100
C	5.03181400	-0.16985900	-0.35068500	C	5.00558500	-0.66879700	-0.45775400
C	6.18150700	0.68369800	-0.23718100	C	6.24775100	0.05300400	-0.46436000
C	7.42963500	0.09108800	-0.17950700	C	7.42060200	-0.66982300	-0.34374100
C	7.63447300	-1.29965100	-0.22888700	C	7.46134100	-2.06901300	-0.20619000
C	6.54579500	-2.12304100	-0.33681000	C	6.28213100	-2.76429300	-0.17661800
C	6.00041700	2.20066000	-0.17667400	C	6.23787900	1.57791200	-0.57825500
C	5.17617800	2.57305100	1.06535600	C	5.48608400	2.17133300	0.62367800
C	5.32427500	2.70324900	-1.46239700	C	5.58965800	2.01357600	-1.90174100
C	7.33728600	2.93404500	-0.06474200	C	7.64890500	2.16675600	-0.56124500
C	0.95836300	2.27464300	-1.40254300	C	1.11020200	2.14994800	-1.62789100
C	-0.45248300	2.92157500	-1.52369900	C	-0.25470700	2.89363300	-1.66757400
C	-0.51114300	3.85029100	-0.33326100	C	-0.18677600	3.78490600	-0.44967900
C	-1.61503500	4.48098300	0.22313600	C	-1.21889200	4.44590400	0.20136300
C	-1.42621400	5.31607200	1.32314100	C	-0.90910900	5.28722400	1.26970600
C	-0.15369700	5.49783400	1.86215900	C	0.41556200	5.44881500	1.67747000
C	0.95202400	4.86140300	1.29968300	C	1.44636900	4.76772700	1.02941200
C	0.76849700	4.04449500	0.19184200	C	1.13936100	3.93395700	-0.03884600
C	1.78905200	3.28312700	-0.60063000	C	2.05576900	3.11990500	-0.90701400
C	-2.66007900	2.11862000	-2.03307100	C	-2.52303200	2.25237100	-2.13108300
C	-3.75158600	1.19769700	-2.14345600	C	-3.67290700	1.40408100	-2.20950300
C	-3.65611800	-0.18834200	-1.78843500	C	-3.67159900	0.02770600	-1.80230200
C	-4.83967500	-0.99632800	-1.87091700	C	-4.86291000	-0.74425000	-2.01995500
C	-6.01235700	-0.40042900	-2.30467000	C	-5.97571100	-0.09760300	-2.52924300
C	-6.10192300	0.95183200	-2.67301100	C	-5.99440700	1.26298400	-2.87682300
C	-4.97672900	1.73194400	-2.59342100	C	-4.84380400	1.99264200	-2.73405900
C	-4.77465100	-2.47658700	-1.49069600	C	-4.88043700	-2.24190700	-1.70770100
C	-4.34475900	-2.62817400	-0.02116300	C	-4.66641700	-2.46962500	-0.20623000
C	-3.79457400	-3.20685900	-2.42208600	C	-3.79959600	-2.95721200	-2.53308000
C	-6.13118900	-3.16669400	-1.62991300	C	-6.21697200	-2.89174400	-2.07038900
H	0.55692800	-2.63210000	-2.30485900	H	0.27870200	-2.90145100	-1.98123800
H	2.26769300	-4.08961900	-1.35631900	H	1.78281600	-4.38500100	-0.69541800
H	3.27706900	-3.99893000	1.80064200	H	2.78782300	-3.75188100	2.40585300
H	2.18233300	-5.20097000	3.68496700	H	1.51830500	-4.13322200	4.50479300
H	-0.21696600	-5.79279200	3.56453900	H	-0.95181800	-4.23329400	4.47749300
H	-1.57686300	-5.14169300	1.58011200	H	-2.20049500	-3.96632800	2.33116900
H	-1.45032500	-3.14537300	-0.52987800	H	-1.81624700	-2.90368100	-0.28664200
H	-0.70477000	-4.47917000	-1.42552700	H	-1.11495300	-4.46510800	-0.73519500
H	4.46345000	-3.58444800	-0.59756300	H	4.04299500	-3.98998800	-0.13429600
H	8.31024800	0.72487300	-0.09422700	H	8.37063900	-0.13940100	-0.35061700
H	6.66869500	-3.20665900	-0.37642500	H	6.27857300	-3.84910100	-0.05861800
H	5.73994400	2.33736100	1.97927100	H	6.04140600	1.97726100	1.55247600
H	4.22583200	2.03091700	1.11321100	H	4.48546100	1.74041000	0.73958900
H	4.96695600	3.65440100	1.06829700	H	5.39174200	3.26291300	0.50892600
H	4.35361000	2.22597300	-1.63632900	H	4.56737800	1.63543500	-2.00779000
H	5.96601300	2.50068400	-2.33236900	H	6.17947200	1.64530900	-2.75388300
H	5.17394200	3.79220900	-1.40455500	H	5.56636200	3.11241000	-1.96245200
H	7.88789100	2.65827200	0.84595200	H	8.18767000	1.93006200	0.36723900

H	7.15159700	4.01600500	-0.02017300	H	7.58102300	3.26113500	-0.63046200
H	7.98588300	2.74719400	-0.93262000	H	8.25344400	1.82062600	-1.41191700
H	1.39413000	2.06952800	-2.39415400	H	1.46101300	1.88931100	-2.64072400
H	-0.51866200	3.49779400	-2.46409700	H	-0.31716100	3.51530600	-2.57995500
H	-2.62028500	4.30483500	-0.16369200	H	-2.25530500	4.31065200	-0.11275700
H	-2.28489600	5.80950500	1.77760400	H	-1.70486700	5.82496900	1.78476700
H	-0.02258000	6.14138400	2.73096400	H	0.64704700	6.11013400	2.51172000
H	1.94659600	4.99581400	1.72545300	H	2.47902900	4.88223000	1.35976500
H	2.53049100	2.75745800	0.01651100	H	2.81939400	2.55838400	-0.35058200
H	2.34676600	3.95369200	-1.27392800	H	2.58768700	3.75885000	-1.63034100
H	-2.85982000	3.13216000	-2.41469200	H	-2.65807500	3.26962100	-2.53282400
H	-6.91646300	-1.00317900	-2.37098600	H	-6.89027400	-0.66537200	-2.68552000
H	-4.26315700	-3.69505200	0.24095800	H	-4.63869100	-3.54847300	0.01520800
H	-5.09893600	-2.17471200	0.64267100	H	-5.48843500	-2.02191000	0.37197500
H	-3.37906600	-2.14455200	0.17184700	H	-3.73526700	-2.01310700	0.14403000
H	-3.70410600	-4.26327600	-2.12422600	H	-3.78207200	-4.02826600	-2.27771000
H	-2.79847200	-2.74990900	-2.41050800	H	-2.80097800	-2.54002900	-2.36538500
H	-4.16616600	-3.17988900	-3.45619300	H	-4.02080200	-2.87003400	-3.60639700
H	-6.03192400	-4.22309000	-1.34430100	H	-6.16791400	-3.96504400	-1.84003400
H	-6.50266500	-3.14147100	-2.66391500	H	-6.44728800	-2.79494900	-3.14086800
H	-6.89393300	-2.71814000	-0.97712000	H	-7.05431100	-2.47173100	-1.49497200
Cl	2.18189700	-0.47199000	1.86838200	Cl	2.28902500	-0.31080500	1.80651600
Cl	-0.44026200	-0.26212500	-3.42728400	Cl	-0.56468400	-0.43927200	-3.40463300
O	2.37402700	-0.28908300	-2.52382800	O	2.25836100	-0.76391100	-2.56227700
H	1.50188600	-0.34415300	-3.00300600	H	1.36104700	-0.71748900	-2.99469400
H	2.94989300	-0.98443200	-2.87302600	H	2.67372700	-1.59233300	-2.84240900
H	-5.01475700	2.78784700	-2.86581200	H	-4.81210000	3.04352200	-3.02690600
C	-1.13885800	-1.72128700	2.58031300	H	8.41722400	-2.57987600	-0.11546000
C	-1.53816000	-0.64596700	3.38836400	H	-6.90064500	1.71270700	-3.27643100
C	-0.88749400	0.64074200	3.15659800	C	-0.08369600	2.00331400	2.62111900
C	-1.44492900	1.15098500	1.73893200	C	-0.90792300	1.20316500	3.41789100
H	-0.05372300	-1.79598600	2.42866200	C	-1.01024600	-0.21903100	3.08253700
H	-1.66577500	-2.67349700	2.62833200	C	-1.82328100	-0.25599600	1.70793800
H	0.19433900	0.51724500	3.03526600	H	0.89084800	1.55556000	2.38567000
H	-1.13022200	1.38039500	3.92481800	H	-0.08972500	3.08601000	2.73572400
O	-1.36388500	0.14522900	0.81168700	H	-0.02486300	-0.65906500	2.87656500
H	-1.33134900	-1.04587900	1.51970300	H	-1.54915200	-0.79190100	3.84342100
O	-2.64179900	-0.58945900	4.09872300	O	-1.23123600	0.58039400	0.79228600
C	-3.51668900	-1.71436400	4.11405800	H	-0.61377800	1.55752400	1.54074000
H	-3.93169900	-1.87748300	3.11082100	O	-1.84676500	1.64357600	4.22815800
H	-4.31742400	-1.45810400	4.80926700	C	-2.04335100	3.04950800	4.34706200
H	-2.99127900	-2.61304300	4.45786600	H	-2.36582300	3.46048900	3.38176200
H	-0.75817500	1.97896800	1.48315900	H	-2.82964900	3.17842100	5.09250000
H	8.64245200	-1.70503600	-0.17937500	H	-1.12360500	3.54839000	4.67622200
H	-7.04806500	1.36398300	-3.01637500	H	-1.72087700	-1.31099100	1.39682700
C	-2.86071900	1.66731700	1.90096400	C	-3.28662900	0.07332100	1.92456800
C	-3.92494500	1.00101900	1.29993900	C	-3.86438900	1.16855200	1.28586900
C	-3.12199300	2.81140200	2.65611900	C	-4.08752900	-0.73683000	2.73077800
C	-5.22692100	1.47925900	1.42451200	C	-5.22477300	1.43140100	1.42255400
H	-3.71109200	0.11560600	0.70581400	H	-3.23686700	1.78947900	0.64650600
C	-4.41957200	3.29148800	2.78670800	C	-5.44158000	-0.46600900	2.88637400
H	-2.29373300	3.34851700	3.12296300	H	-3.64986900	-1.60863800	3.22318700
C	-5.47784000	2.62855800	2.16655500	C	-6.01725500	0.61679300	2.22409900
H	-6.03891200	0.95436400	0.91961700	H	-5.66857300	2.26813400	0.88307600
H	-4.60771100	4.19225500	3.37060200	H	-6.05533000	-1.11135000	3.51363800
H	-6.49283700	3.01180400	2.26164000	H	-7.08215800	0.81860000	2.32968800

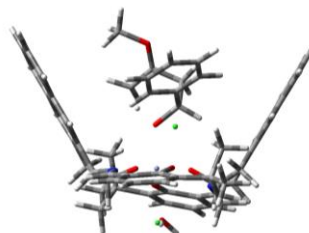
Reaction between benzaldehyde **1a**, 2-methoxypropene **3** and catalyst bearing aminoindanol **17**. Energy unit is a.u..

With B3LYP/6-31G(d):

TS<sub>pro-(R)</sub>



TS<sub>pro-(S)</sub>



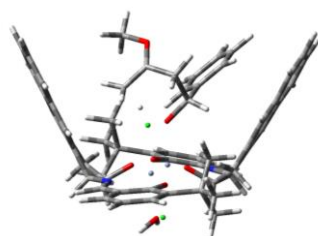
E = -4014.99201269			E + ZPE = -4013.903022			E = -4014.99456559			E + ZPE = -4013.906014		
G = -4014.006754			imaginary frequencies: 1			G = -4014.009987			imaginary frequencies: 1		
Cr	2.13094400	0.39827300	-0.82838000	Cr	2.15689900	-0.19337800	-0.89218900				
Cr	-0.89609500	-0.21080800	-1.31261100	Cr	-0.92597800	0.06347300	-1.35788500				
O	0.88897000	-1.17640000	-1.00573800	O	0.50167900	-1.34207600	-0.96879000				
O	3.51190100	1.75647300	-0.82812200	O	3.86960800	0.70007700	-0.97162900				
O	0.31498800	1.32680500	-0.92334000	O	0.68998800	1.21583500	-1.05205000				
O	-2.23557800	-1.56031400	-1.69925100	O	-2.59411200	-0.86123700	-1.67274400				
N	3.52133900	-1.02829600	-1.05796700	N	3.06053300	-1.97708300	-1.01696700				
N	-2.19480500	1.27095800	-1.67455700	N	-1.75261400	1.83227300	-1.80778500				
C	1.47372800	-2.28058700	-1.67721000	C	0.72486700	-2.62681700	-1.52785100				
C	2.96230400	-2.37242000	-1.22529500	C	2.12641900	-3.10577200	-1.04418300				
C	2.89362200	-3.24309300	0.02245500	C	1.81765800	-3.75054700	0.30141400				
C	3.79895500	-3.38298600	1.04314800	C	2.65495000	-4.02086200	1.35246200				
C	3.55460100	-4.32857400	2.07896300	C	2.14672500	-4.67929300	2.50787000				
C	2.36586600	-5.13321300	2.02950800	C	0.76122200	-5.05521800	2.54993800				
C	1.44391200	-4.94674400	0.96016700	C	-0.07782300	-4.74786000	1.44060200				
C	1.69835900	-4.01236300	-0.01493800	C	0.44132900	-4.10592900	0.34255000				
C	0.86315700	-3.62195700	-1.21450400	C	-0.24134200	-3.67419700	-0.93650300				
C	4.80578400	-0.83652100	-1.07872800	C	4.34348300	-2.17129000	-1.06784800				
C	5.49600500	0.40801700	-0.92768300	C	5.37037000	-1.17423900	-1.01702200				
C	4.81355500	1.66935300	-0.79154500	C	5.08926800	0.23676000	-0.94386000				
C	5.60975500	2.86376100	-0.64550200	C	6.20118300	1.15228600	-0.86546900				
C	6.99260900	2.72949900	-0.65707600	C	7.48463000	0.62075000	-0.89198000				
C	7.65927300	1.49606500	-0.80331100	C	7.75929000	-0.75862900	-0.98587800				
C	6.91229200	0.35145200	-0.93769500	C	6.70824100	-1.64115000	-1.04505100				
C	4.93854400	4.24004600	-0.47206800	C	5.96190900	2.67010200	-0.74320500				
C	4.07449900	4.23467700	0.81370100	C	5.16117300	2.96536500	0.55002800				
C	4.07175900	4.56525900	-1.71421600	C	5.20060400	3.18963900	-1.98815800				
C	5.96890400	5.37887200	-0.32774500	C	7.28162100	3.46409300	-0.65497200				
C	-0.04378100	2.52930800	-1.58800000	C	0.65381000	2.46090000	-1.72861200				
C	-1.60637300	2.61994000	-1.63904400	C	-0.82746100	2.96472700	-1.73487100				
C	-1.96566800	3.48055300	-0.43417800	C	-0.92112200	3.80949200	-0.47214800				
C	-3.19654300	3.70359900	0.13535000	C	-2.03849100	4.24757100	0.19450200				
C	-3.32015700	4.61369300	1.22281200	C	-1.89787500	5.07528100	1.34417900				
C	-2.14811800	5.28301900	1.71379900	C	-0.58022300	5.44551900	1.78287100				
C	-0.89151400	5.02654600	1.09773100	C	0.55368700	4.97114300	1.06305400				
C	-0.80516800	4.14931200	0.04286400	C	0.38480700	4.16640500	-0.03823900				
C	0.40276300	3.76783500	-0.77941600	C	1.42491400	3.54713600	-0.94419200				
C	-3.38086400	1.09049400	-2.16719800	C	-2.93879100	1.97470500	-2.30825900				
C	-4.06094100	-0.15388300	-2.38299300	C	-3.92217700	0.95313900	-2.52494300				

C	-3.45311800	-1.43958000	-2.15807500	C	-3.69558800	-0.44174200	-2.24462600
C	-4.22794000	-2.62042500	-2.45168400	C	-4.72394200	-1.38341500	-2.61538200
C	-5.52952700	-2.45094900	-2.91078800	C	-5.90495600	-0.88119100	-3.15166700
C	-6.12585300	-1.19323200	-3.12098400	C	-6.14264400	0.48661900	-3.38231300
C	-5.38780300	-0.06146900	-2.86790600	C	-5.14820400	1.38697300	-3.08528100
C	-3.61756900	-4.02674300	-2.28541800	C	-4.51568500	-2.90386700	-2.45375800
C	-3.19790600	-4.26090000	-0.81333700	C	-4.30542300	-3.26236900	-0.96495400
C	-2.39637700	-4.17235100	-3.22736700	C	-3.29575700	-3.34873400	-3.29777100
C	-4.61393500	-5.14593900	-2.65272300	C	-5.73016200	-3.71815700	-2.94785700
H	1.38515900	-2.14754300	-2.76241900	H	0.65877000	-2.57648200	-2.62199300
H	3.54275900	-2.90544100	-1.99654300	H	2.51206400	-3.87251300	-1.73633700
H	4.69533100	-2.76959700	1.09356500	H	3.69865800	-3.71608200	1.33876400
H	0.53551000	-5.54630800	0.93580500	H	-1.12938200	-5.02625900	1.48137100
H	-0.20159100	-3.51014300	-0.99575300	H	-1.24095800	-3.25581200	-0.79819100
H	0.95014900	-4.36788900	-2.01783000	H	-0.34214500	-4.51976500	-1.63300700
H	5.44354300	-1.71366700	-1.23532000	H	4.69277100	-3.20594000	-1.15876100
H	7.60576900	3.61679100	-0.54760600	H	8.33201500	1.29454200	-0.83588500
H	7.39567400	-0.61729600	-1.04873400	H	6.88612100	-2.71298900	-1.10721700
H	4.70942800	4.11299400	1.69963000	H	5.75130800	2.69689200	1.43462900
H	3.34780800	3.42093500	0.80998200	H	4.22878500	2.40014500	0.58761500
H	3.54063600	5.18899700	0.91243800	H	4.93205800	4.03746400	0.61283500
H	3.31344800	3.80085400	-1.88640500	H	4.24875900	2.67428200	-2.12104600
H	4.69972200	4.63582800	-2.61124500	H	5.80158300	3.04153900	-2.89407500
H	3.57185800	5.53324700	-1.58009300	H	5.00768800	4.26563600	-1.88807400
H	6.61269900	5.24648900	0.54966400	H	7.87953400	3.17985600	0.21891900
H	5.43711000	6.32896100	-0.20257800	H	7.05148100	4.53153700	-0.56070400
H	6.60756600	5.47513100	-1.21391000	H	7.90022600	3.34057600	-1.55182400
H	0.37317800	2.53081400	-2.60052200	H	1.02978700	2.34362700	-2.75117100
H	-1.90055200	3.14896200	-2.55778300	H	-0.98417700	3.60936600	-2.61372400
H	-4.08689000	3.18785900	-0.21625400	H	-3.03751100	3.96456600	-0.13060200
H	-0.00611900	5.53522800	1.47347200	H	1.54873500	5.24350700	1.40869900
H	1.28573200	3.53573200	-0.17906700	H	2.27042300	3.11029900	-0.40711000
H	0.67975000	4.58417100	-1.46116800	H	1.83210700	4.29619300	-1.63849700
H	-3.93600500	1.98171000	-2.47819100	H	-3.23050200	2.97908300	-2.63496200
H	-6.12673200	-3.32827700	-3.13215300	H	-6.69242500	-1.57439300	-3.42313600
H	-2.74153400	-5.25367800	-0.70495300	H	-4.13461100	-4.34173500	-0.85712500
H	-4.07416100	-4.22258800	-0.15346100	H	-5.18959200	-2.99900600	-0.37330000
H	-2.48334900	-3.50755200	-0.47908600	H	-3.45442600	-2.72702200	-0.54538200
H	-1.91819000	-5.14970200	-3.07872300	H	-3.11292200	-4.42228300	-3.15747700
H	-1.65846500	-3.38785500	-3.05398800	H	-2.39467500	-2.79923100	-3.02414700
H	-2.71516300	-4.11087100	-4.27470100	H	-3.48413600	-3.17628500	-4.36413700
H	-4.12524400	-6.11833500	-2.52159800	H	-5.51818500	-4.78616300	-2.82169000
H	-4.94044000	-5.08281700	-3.69709500	H	-5.93834100	-3.54913300	-4.01080500
H	-5.50421500	-5.13694000	-2.01230700	H	-6.64000900	-3.49630200	-2.37746800
Cl	2.29226800	0.31901900	1.51487200	Cl	2.34555900	-0.18691200	1.45275200
Cl	-0.45631600	-0.20195400	-3.75194100	Cl	-0.52775700	-0.19402900	-3.78884500
O	2.18886600	0.70263200	-2.89908800	O	2.27209300	-0.04151000	-2.97455500
H	1.35151800	0.36687400	-3.34343000	H	1.36279000	-0.12927500	-3.39554200
H	2.94923100	0.29247600	-3.33961100	H	2.85381300	-0.69905500	-3.38693800
H	-5.81484600	0.92571400	-3.03265300	H	-5.28520600	2.44870900	-3.28128200
C	-0.24906600	-2.02694300	2.34742600	H	8.78672300	-1.10870100	-1.00322600
C	-0.94318300	-1.18864800	3.23621700	H	-7.08682200	0.81225700	-3.80792200
C	-0.95568700	0.25160100	2.93065400	C	-0.39133200	1.70175800	2.47253900
C	-1.80817200	0.43430400	1.57158000	C	-1.03243700	0.73102500	3.25583600
H	0.74089200	-1.66051900	2.06160200	C	-0.95409200	-0.66716200	2.79292000
H	-0.32349200	-3.10575800	2.44481300	C	-1.80615400	-0.75054400	1.42623300

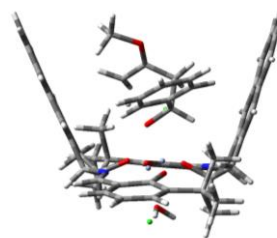
H	0.05585300	0.59931700	2.70800800	H	0.61824900	1.42948600	2.15130300
H	-1.41452000	0.83999100	3.72600900	H	-0.54526200	2.75614800	2.67793300
O	-1.36525600	-0.46325300	0.60502000	H	0.07619300	-0.92270300	2.53398000
H	-0.81898300	-1.49515800	1.30788000	H	-1.36540100	-1.36896300	3.51936600
O	-1.82158500	-1.57386600	4.14452700	O	-1.41731700	0.27029900	0.56173400
C	-2.02242400	-2.97582100	4.39109400	H	-0.92440600	1.24206600	1.37332000
H	-2.50081000	-3.44415100	3.52625400	O	-1.93848300	0.95938500	4.18974800
H	-2.68504900	-3.02436100	5.25472700	C	-2.21625700	2.31306500	4.59251400
H	-1.07146900	-3.46881600	4.61237200	H	-2.68714200	2.86546900	3.77520300
H	-1.57634900	1.45982600	1.26817100	H	-2.90439000	2.22624100	5.43291700
H	8.74427700	1.46097000	-0.80553800	H	-1.29710900	2.81767200	4.90319100
H	-7.14571100	-1.12769400	-3.48716800	H	-1.52087800	-1.72339800	1.01147100
C	-3.30049900	0.29761700	1.86552800	C	-3.29916000	-0.73077900	1.74002900
C	-4.04023200	-0.78103300	1.37056100	C	-4.09891900	0.36501400	1.40271100
C	-3.95163400	1.25621000	2.65508300	C	-3.88944200	-1.81820400	2.39842500
C	-5.40114100	-0.90466200	1.66503600	C	-5.45921600	0.37706700	1.72209300
H	-3.54622200	-1.50578300	0.73397800	H	-3.64865600	1.19653400	0.87120600
C	-5.30922100	1.13455700	2.95035500	C	-5.24670100	-1.80963300	2.71819800
H	-3.39839400	2.11229300	3.03372300	H	-3.28360000	-2.68506700	2.65660400
C	-6.03988700	0.04952400	2.45768500	C	-6.03788400	-0.70764100	2.38211600
H	-5.96234900	-1.74426400	1.26243200	H	-6.06958500	1.23324900	1.44518000
H	-5.79619500	1.89087200	3.56076200	H	-5.68801900	-2.66418100	3.22487000
H	-7.09872000	-0.04524300	2.68463300	H	-7.09678100	-0.69965400	2.62684000
C	-4.57176500	4.87932900	1.84297000	C	-3.02185400	5.54407300	2.07864600
H	-5.45571600	4.36667100	1.47127300	H	-4.01810900	5.26858400	1.73938800
C	-2.28358500	6.18689400	2.80302000	C	-0.45135100	6.26576600	2.93721000
C	-3.51140500	6.42360600	3.37969700	C	-1.56131600	6.70195800	3.62703100
H	-3.59789100	7.11894700	4.21033900	H	-1.44402000	7.33037500	4.50576500
C	-4.66774200	5.76332400	2.89472500	C	-2.86031100	6.33793700	3.19357300
H	-5.63190300	5.95828200	3.35664300	H	-3.72959200	6.69189100	3.74128900
H	-1.39469400	6.69200100	3.17387800	H	0.54625300	6.54552900	3.26780500
C	2.14130700	-6.08303300	3.06292600	C	2.97115900	-4.97547200	3.62642000
C	4.45687500	-4.50531000	3.16231100	H	4.01777400	-4.68174200	3.59393400
H	5.35236300	-3.88942400	3.19994300	C	0.26878400	-5.71730900	3.70686200
C	3.03928500	-6.23246200	4.09689500	C	1.09665000	-5.99443600	4.77243800
H	2.85382200	-6.96526400	4.87780500	H	0.70398400	-6.50274900	5.64910800
C	4.20826800	-5.43414700	4.14843400	C	2.46154400	-5.61827900	4.73284800
H	4.90858200	-5.55766500	4.97001300	H	3.10533900	-5.83801200	5.58023000
H	1.24373600	-6.69652200	3.02122000	H	-0.78007400	-6.00440900	3.73638500

With M05-2X/6-31G(d):

TS<sub>pro-(R)</sub>



TS<sub>pro-(S)</sub>



E = -4012.86058203	E + ZPE = -4011.772791	E = -4012.86731526	E + ZPE = -4011.780288
G = -4011.870093	imaginary frequencies: 1	G = -4011.876472	imaginary frequencies: 1
Cr	-2.19686100 -0.06837800 -0.88867300	Cr	2.16164300 -0.50601900 -0.87637700

Cr	0.80999900	-0.00334500	-1.46550100	Cr	-0.79823800	0.09886100	-1.47061900
O	-0.72324200	1.27103200	-1.10184000	O	0.40193000	-1.44422100	-0.99312700
O	-3.76201900	-1.18088400	-0.83658700	O	3.94634600	0.18632300	-0.94409100
O	-0.61705600	-1.30117700	-1.02526300	O	0.92642400	1.04851200	-1.14724600
O	2.33838600	1.11137800	-1.81728000	O	-2.55516600	-0.63202000	-1.73746300
N	-3.32140400	1.56328100	-1.07006500	N	2.82227300	-2.38413900	-0.83068200
N	1.82339000	-1.67629900	-1.81820500	N	-1.39623400	1.93511300	-1.93875800
C	-1.13204300	2.42658200	-1.78777400	C	0.48971600	-2.75541700	-1.48287600
C	-2.54132400	2.77856300	-1.25787000	C	1.74477000	-3.36709300	-0.81970000
C	-2.22759500	3.55910800	-0.00239300	C	1.20916900	-3.74076500	0.54715800
C	-2.98827800	3.75859200	1.11433500	C	1.87098700	-3.89661700	1.73086000
C	-2.48493600	4.56788000	2.16648400	C	1.13917300	-4.21651000	2.90444600
C	-1.19970000	5.17719600	2.02940200	C	-0.27887000	-4.37498900	2.82898000
C	-0.43418900	4.93171000	0.85941900	C	-0.93250100	-4.19856600	1.58044900
C	-0.92989300	4.11908900	-0.12336600	C	-0.20034700	-3.88959500	0.46638200
C	-0.27418700	3.63037500	-1.38410800	C	-0.66038600	-3.59826500	-0.93344100
C	-4.61221000	1.59402500	-0.98259200	C	4.06799800	-2.72524200	-0.76106800
C	-5.48186800	0.48335500	-0.76544500	C	5.19606500	-1.84913400	-0.74106300
C	-5.01025900	-0.86920500	-0.68288100	C	5.08405100	-0.42010500	-0.82329100
C	-5.97164500	-1.91364400	-0.46325500	C	6.28870200	0.36160300	-0.79518800
C	-7.30516200	-1.56034700	-0.36199300	C	7.49723600	-0.30535700	-0.70475900
C	-7.77020700	-0.23669700	-0.45821600	C	7.60936900	-1.70536300	-0.63400200
C	-6.86165200	0.76814000	-0.65703100	C	6.46713900	-2.46001000	-0.65063400
C	-5.50494300	-3.36345200	-0.33323300	C	6.20401700	1.88750000	-0.83883200
C	-4.57092300	-3.48993400	0.88007800	C	5.43799800	2.38768000	0.39606600
C	-4.80400200	-3.81407400	-1.62407400	C	5.52092900	2.35000200	-2.13550200
C	-6.67143100	-4.32625400	-0.10515700	C	7.58570100	2.54160800	-0.80776200
C	-0.49753400	-2.54331300	-1.66799700	C	1.05844500	2.25944800	-1.83812900
C	1.01722800	-2.89632300	-1.73827100	C	-0.34170000	2.93434800	-1.84630600
C	1.24908500	-3.68905300	-0.47230100	C	-0.34590300	3.71802100	-0.55567700
C	2.43570800	-4.02986800	0.11683900	C	-1.41206600	4.22344500	0.13542700
C	2.43037500	-4.73615100	1.34662700	C	-1.18863400	4.96305400	1.32491200
C	1.18162600	-5.04775000	1.96701800	C	0.15172700	5.15834200	1.78372800
C	-0.02897500	-4.70722000	1.30981900	C	1.23233000	4.61217600	1.04141800
C	0.00775000	-4.05916100	0.10433600	C	0.98594800	3.90477000	-0.10495300
C	-1.11954300	-3.62881400	-0.78542100	C	1.94413500	3.22670600	-1.04266000
C	3.02917700	-1.69673200	-2.27977200	C	-2.56519900	2.21900800	-2.40542900
C	3.91972600	-0.58480100	-2.42582400	C	-3.66534700	1.32103900	-2.57986000
C	3.53700700	0.77405000	-2.17420100	C	-3.59555700	-0.08234100	-2.28789900
C	4.53394000	1.79918900	-2.30699500	C	-4.73038500	-0.89848300	-2.61504900
C	5.81598800	1.42361800	-2.67045300	C	-5.86371800	-0.27529500	-3.10794700
C	6.18944500	0.09454000	-2.92788800	C	-5.95349100	1.10704600	-3.33856000
C	5.24194900	-0.88970800	-2.81180300	C	-4.85298500	1.88548400	-3.09365000
C	4.15705600	3.26169000	-2.06109700	C	-4.66392500	-2.41600900	-2.43714400
C	3.65749800	3.45296200	-0.61919800	C	-4.47448400	-2.76390400	-0.95541500
C	3.08325800	3.69242500	-3.07287500	C	-3.51696200	-2.98352000	-3.28803000
C	5.34872600	4.20238700	-2.24318900	C	-5.94632200	-3.10884700	-2.89927300
H	-1.11958700	2.25779100	-2.87845600	H	0.53565200	-2.76562400	-2.58654300
H	-3.06159500	3.43875700	-1.97814600	H	2.06898400	-4.27425000	-1.36447100
H	-3.96134900	3.27765800	1.23498200	H	2.94636000	-3.72571300	1.81119000
H	0.56525600	5.36619700	0.77727400	H	-2.02048900	-4.29560300	1.52673100
H	0.77187400	3.32229500	-1.24562700	H	-1.61201300	-3.05439800	-0.99707200
H	-0.28563500	4.39528300	-2.17734900	H	-0.77345700	-4.52245800	-1.52419300
H	-5.10498800	2.57313700	-1.09486000	H	4.29803500	-3.80212000	-0.72256000
H	-8.04620000	-2.34016600	-0.19865200	H	8.41782400	0.27468500	-0.68390900
H	-7.18700200	1.80722300	-0.73005500	H	6.51905600	-3.54838400	-0.59132700

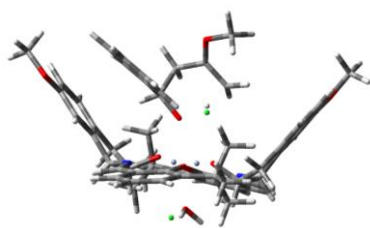
H	-5.13269300	-3.32048000	1.80966700	H	6.01099600	2.17443700	1.30976400
H	-3.75289400	-2.76212700	0.85083800	H	4.45886600	1.90600900	0.49821400
H	-4.14220400	-4.50367600	0.92506700	H	5.29242200	3.47796800	0.33594700
H	-3.94952600	-3.17730900	-1.87773400	H	4.51720200	1.92636100	-2.25035200
H	-5.50986800	-3.78976400	-2.46723100	H	6.11963400	2.05094400	-3.00833400
H	-4.44996700	-4.85044800	-1.51465200	H	5.44291000	3.44795700	-2.14549700
H	-7.22603000	-4.09762700	0.81600700	H	8.14239500	2.29543700	0.10763800
H	-6.27911900	-5.34776000	-0.00535200	H	7.46678400	3.63351800	-0.83452900
H	-7.37965100	-4.32731600	-0.94621900	H	8.19905300	2.25639800	-1.67468000
H	-0.95022500	-2.50557000	-2.67203900	H	1.43332100	2.08642300	-2.86115500
H	1.21860500	-3.51665400	-2.62960400	H	-0.41790200	3.62751000	-2.70435900
H	3.39466300	-3.72823900	-0.31134100	H	-2.43849000	4.05659700	-0.20010500
H	-0.98091200	-4.96025400	1.78067500	H	2.25089200	4.74419300	1.41154200
H	-1.98788000	-3.22409700	-0.24937800	H	2.74808700	2.67635500	-0.53479300
H	-1.47416600	-4.47377900	-1.39764900	H	2.42309400	3.95668700	-1.71530500
H	3.43761100	-2.66988000	-2.59447800	H	-2.74690400	3.25709500	-2.72727600
H	6.58116900	2.19076400	-2.77402900	H	-6.73533800	-0.88166300	-3.34598700
H	3.35513900	4.50026200	-0.46163500	H	-4.39080800	-3.85498900	-0.82797900
H	4.46400600	3.22494800	0.09599400	H	-5.33609100	-2.41561100	-0.36663800
H	2.80443600	2.80242400	-0.39072100	H	-3.57985400	-2.28961300	-0.53800500
H	2.75958700	4.72466200	-2.86600100	H	-3.43156500	-4.06959300	-3.12705100
H	2.20529400	3.03688900	-3.04875700	H	-2.55480600	-2.51563000	-3.05285200
H	3.49488400	3.66719800	-4.09172200	H	-3.71674800	-2.81609000	-4.35608000
H	5.02361800	5.23616100	-2.06088400	H	-5.83133200	-4.19467700	-2.77582600
H	5.75465500	4.16233000	-3.26354600	H	-6.15941700	-2.92003200	-3.96106300
H	6.16302700	3.98376500	-1.53722900	H	-6.82189800	-2.80357600	-2.30854700
Cl	-2.29691600	0.05143900	1.42120800	Cl	2.31786100	-0.37006400	1.43469600
Cl	0.38396300	0.09840700	-3.83848200	Cl	-0.44039400	-0.26751000	-3.82617900
O	-2.39486900	-0.37639500	-2.94899200	O	2.37868300	-0.51330200	-2.95291000
H	-1.54975000	-0.17777700	-3.43751700	H	1.48915500	-0.48003400	-3.40231000
H	-3.10421100	0.15082100	-3.34328000	H	2.84081000	-1.30021000	-3.27632600
H	5.49950800	-1.93221800	-3.00572000	H	-4.87370900	2.95736500	-3.29802900
C	0.60307000	1.99700300	2.08943000	H	8.58938300	-2.17139400	-0.56138400
C	1.18615000	1.08886900	2.98246200	H	-6.87215600	1.53778300	-3.73055900
C	0.89268300	-0.32926600	2.78270000	C	-0.21886700	1.72071400	2.38458700
C	1.62974800	-0.73548500	1.42068500	C	-1.00009400	0.80862700	3.09894000
H	-0.45428400	1.79404200	1.87045500	C	-0.99802200	-0.58440700	2.64458700
H	0.87534700	3.05066200	2.11622800	C	-1.78164800	-0.57208700	1.25396300
H	-0.17882400	-0.48509000	2.61205800	H	0.78144900	1.35202300	2.12343100
H	1.26851200	-0.95483500	3.59762500	H	-0.28506900	2.78433000	2.60301300
O	1.31721700	0.15946000	0.42703200	H	0.02219700	-0.92779800	2.42967800
H	1.00792000	1.33575100	1.06950300	H	-1.50500000	-1.25495100	3.34538300
O	2.19486900	1.34075400	3.78546600	O	-1.25427600	0.39096300	0.42146300
C	2.73789900	2.65747500	3.82439100	H	-0.72067500	1.33705900	1.25721000
H	3.22129800	2.88580500	2.86588500	O	-1.96921400	1.12077000	3.93029100
H	3.48186200	2.64824900	4.62228000	C	-2.24333100	2.49932000	4.17536500
H	1.95765600	3.39727200	4.04142400	H	-2.58211600	2.98373600	3.25005100
H	1.20786500	-1.73094600	1.20040500	H	-3.03951100	2.51585400	4.92112400
H	-8.83318900	-0.02412300	-0.37047800	H	-1.35472300	3.01805800	4.55598600
H	7.21114000	-0.14062900	-3.21715400	H	-1.58825300	-1.58282700	0.85229800
C	3.12516800	-0.82789100	1.65515900	C	-3.26559700	-0.38562400	1.49128900
C	3.98876400	0.07635100	1.03988600	C	-3.91680600	0.76505700	1.05477900
C	3.65943100	-1.79650600	2.50643400	C	-4.00094000	-1.36726400	2.15775200
C	5.36309900	0.00688100	1.25262000	C	-5.28547900	0.92315900	1.25637300
H	3.56895000	0.82318500	0.36935300	H	-3.33604600	1.52517900	0.53118400
C	5.03054600	-1.86701500	2.72415400	C	-5.36397000	-1.20642600	2.37510100

H	2.99925700	-2.51884500	2.99299800	H	-3.49929500	-2.27927400	2.49340400
C	5.88902200	-0.96584200	2.09639500	C	-6.01264800	-0.06072000	1.91827600
H	6.01948700	0.70888800	0.73681500	H	-5.78545800	1.81660200	0.88312100
H	5.42916300	-2.63667400	3.38522700	H	-5.92615900	-1.98360000	2.89123100
H	6.96362600	-1.02803100	2.26243900	H	-7.08340400	0.06068600	2.07511000
C	3.63210400	-5.09839700	2.00245400	C	-2.25852800	5.49223800	2.08783900
H	4.57930500	-4.85204900	1.52084000	H	-3.27711300	5.34505000	1.72475400
C	1.19254300	-5.68720500	3.23164400	C	-2.02443800	6.17415200	3.25696200
C	2.37412500	-6.01106400	3.84958400	C	0.35737700	5.86321700	2.99525600
H	2.36423800	-6.49903500	4.82288500	C	-0.70127600	6.35891300	3.71627900
C	3.60832900	-5.71964500	3.22586400	H	-0.52291700	6.89924600	4.64453100
H	4.54013100	-5.98790100	3.72153400	H	-2.85705300	6.57772000	3.83093100
H	0.23763400	-5.91507800	3.70631600	H	1.37995700	6.00365100	3.34675700
C	-0.70712900	5.97590200	3.08997300	C	1.77636900	-4.36671200	4.15909800
C	-1.44617800	6.17003000	4.23060400	C	2.85773700	-4.23723300	4.21083900
H	-1.05511700	6.78982600	5.03599000	C	-0.99489500	-4.67993100	4.01162700
C	-2.71655100	5.56898700	4.36506000	C	-0.34611700	-4.82380600	5.21336000
H	-3.29429100	5.72704000	5.27411200	H	-0.91126700	-5.06111900	6.11334800
C	-3.22039300	4.78664100	3.35600000	C	1.05441900	-4.66476300	5.28812300
H	-4.19850700	4.31529300	3.45621900	H	1.55945100	-4.77755700	6.24602500
H	0.27482700	6.43877400	2.97873300	H	-2.07745100	-4.80044600	3.94681900

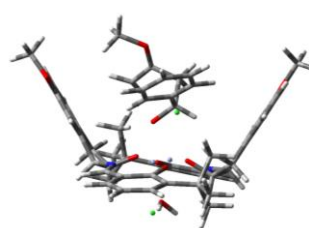
Reaction between benzaldehyde **1a**, 2-methoxypropene **3** and catalyst bearing aminoindanol **18**. Energy unit is a.u..

With B3LYP/6-31G(d):

TS<sub>pro-(R)</sub>



TS<sub>pro-(S)</sub>



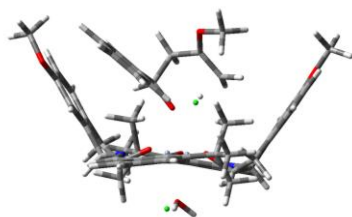
E = -3936.74947060	E + ZPE = -3935.689076	E = -3936.75217912	E + ZPE = -3935.691483				
G = -3935.793825	imaginary frequencies: 1	G = -3935.794877	imaginary frequencies: 1				
Cr	2.14660800	0.16247900	-0.66862200	Cr	2.13736700	-0.20740700	-0.74464400
Cr	-0.92281400	-0.10992700	-1.16365900	Cr	-0.94331500	0.06496100	-1.19682900
O	0.74173600	-1.26471800	-0.83561500	O	0.47643400	-1.34386500	-0.80098100
O	3.66280900	1.36795500	-0.66997700	O	3.85574900	0.67522800	-0.83778800
O	0.44499700	1.28392700	-0.76456100	O	0.68026100	1.21025700	-0.91626700
O	-2.39728700	-1.30508600	-1.55500200	O	-2.61926600	-0.85393400	-1.48712900
N	3.37326900	-1.40453200	-0.90354100	N	3.02832300	-1.99796500	-0.85370800
N	-2.05026500	1.50638500	-1.52486700	N	-1.76632800	1.83547000	-1.64442900
C	1.19260900	-2.44353000	-1.48337500	C	0.68267100	-2.64071900	-1.33881800
C	2.67611000	-2.68527000	-1.06377600	C	2.08878800	-3.12366800	-0.87003800
C	2.55131300	-3.55422900	0.18018000	C	1.79199000	-3.77138300	0.47672300
C	3.50000800	-3.81875700	1.15436100	C	2.66489000	-4.07328700	1.50780100
C	3.18949900	-4.73460700	2.17321900	C	2.16791500	-4.73152300	2.64522500
C	1.94056700	-5.37182200	2.19153800	C	0.81161200	-5.07638900	2.72460200
C	0.99350400	-5.08468800	1.19886200	C	-0.05479900	-4.76076600	1.66865000
C	1.29114700	-4.16989500	0.19479700	C	0.43098500	-4.10606700	0.54309200
C	0.44862500	-3.69852900	-0.96967500	C	-0.28566700	-3.66877300	-0.71517700
C	4.67022700	-1.34817200	-0.94745200	C	4.31002300	-2.20043300	-0.90200300

C	5.49058100	-0.18219000	-0.82033200	C	5.34363000	-1.20964700	-0.86498200
C	4.94810400	1.14486600	-0.67721300	C	5.07234900	0.20396900	-0.80971000
C	5.86958800	2.25061700	-0.57283300	C	6.19109500	1.11259600	-0.74884900
C	7.22967100	1.97145200	-0.62153100	C	7.47074800	0.57174800	-0.77189500
C	7.75886800	0.67302600	-0.76742100	C	7.73548100	-0.81062400	-0.84632400
C	6.89225100	-0.38771500	-0.86678700	C	6.67794200	-1.68634800	-0.88984600
C	5.35198600	3.69267700	-0.40539900	C	5.96320100	2.63375700	-0.64858000
C	4.53945500	3.80168600	0.90881300	C	5.17108900	2.95432600	0.64383600
C	4.47909000	4.08626200	-1.62320600	C	5.19922700	3.13958000	-1.89745900
C	6.50057400	4.71891400	-0.31967100	C	7.28907200	3.41951200	-0.57918800
C	0.22251000	2.53201900	-1.40279700	C	0.64507000	2.44865000	-1.60654300
C	-1.32250600	2.78579700	-1.47590400	C	-0.83264400	2.96290500	-1.59732100
C	-1.60370900	3.67527000	-0.27156200	C	-0.89365900	3.83215700	-0.34894900
C	-2.83130900	4.03625600	0.26778300	C	-2.01064400	4.30112600	0.32676100
C	-2.86356400	4.94441100	1.33868500	C	-1.82963200	5.15958500	1.42379200
C	-1.66988000	5.47019500	1.85360200	C	-0.53895700	5.54514400	1.81297200
C	-0.44182800	5.09401800	1.29553600	C	0.57671600	5.05456100	1.11941800
C	-0.40386900	4.20060300	0.23012000	C	0.40430600	4.19191400	0.04285900
C	0.78390700	3.69676500	-0.55398600	C	1.43743800	3.53844700	-0.84702700
C	-3.24522800	1.45506000	-2.02619400	C	-2.96015000	1.98212300	-2.12492500
C	-4.05323900	0.29115600	-2.25154000	C	-3.95141100	0.96430600	-2.32415500
C	-3.59052500	-1.05285100	-2.02331400	C	-3.72629400	-0.43105100	-2.04516800
C	-4.48577500	-2.14318300	-2.32445800	C	-4.76292300	-1.36948400	-2.40087400
C	-5.75744500	-1.83447600	-2.79470500	C	-5.94921400	-0.86370700	-2.92193300
C	-6.21234500	-0.51946200	-3.00779700	C	-6.18512800	0.50478600	-3.15037500
C	-5.35878400	0.52603900	-2.74612400	C	-5.18357300	1.40196500	-2.86755800
C	-4.03253100	-3.60738300	-2.15089400	C	-4.55865400	-2.89016400	-2.23667800
C	-3.66288500	-3.88327300	-0.67257200	C	-4.33986100	-3.24370700	-0.74792700
C	-2.81879000	-3.88601200	-3.07198300	C	-3.34586700	-3.34318100	-3.08653000
C	-5.13829500	-4.61228300	-2.53476800	C	-5.77952500	-3.70128000	-2.72008400
H	1.09268200	-2.32974700	-2.57017200	H	0.60073200	-2.60806100	-2.43273900
H	3.18547000	-3.26702600	-1.84959200	H	2.46642900	-3.89087200	-1.56594700
H	4.46885200	-3.32953100	1.17469800	H	3.71351700	-3.79337300	1.48697200
H	1.69545500	-6.08636700	2.96925300	H	0.41979400	-5.58376100	3.59882500
H	0.02682100	-5.58338300	1.22468700	H	-1.10560200	-5.03249000	1.74206000
H	-0.58325300	-3.45302500	-0.70481900	H	-1.27077600	-3.22574800	-0.54952900
H	0.40301300	-4.45689300	-1.76488300	H	-0.42856600	-4.51171000	-1.40771800
H	5.20950800	-2.28779000	-1.11071300	H	4.65293100	-3.23816400	-0.98022500
H	7.93553000	2.79064000	-0.54468900	H	8.32305700	1.24025300	-0.72860700
H	7.26761400	-1.40317100	-0.97762900	H	6.84793600	-2.76021300	-0.93649900
H	5.18923100	3.62611400	1.77475600	H	5.76376800	2.69486300	1.52944000
H	3.72874200	3.07252100	0.94562400	H	4.23493300	2.39638800	0.69373200
H	4.11570500	4.80980400	1.00640100	H	4.94965200	4.02882700	0.69143500
H	3.63500300	3.40735300	-1.74696100	H	4.24216900	2.63053300	-2.01587100
H	5.07521700	4.06687400	-2.54426400	H	5.79355800	2.97110000	-2.80422800
H	4.09504100	5.10663500	-1.49574300	H	5.01620800	4.21877200	-1.81411100
H	7.15681000	4.53446000	0.53888300	H	7.88914300	3.14490700	0.29632800
H	6.07643000	5.72211600	-0.19745300	H	7.06729500	4.49009300	-0.50097500
H	7.11482200	4.73165500	-1.22803700	H	7.90252400	3.27715300	-1.47682600
H	0.65638500	2.51309400	-2.40821300	H	1.00459200	2.31552400	-2.63313700
H	-1.54927600	3.34471500	-2.39584600	H	-1.00030900	3.59621200	-2.48231000
H	-3.77114800	3.63231300	-0.09511300	H	-3.02164800	4.02314300	0.04335900
H	-1.68396000	6.16775500	2.68338900	H	-0.38929100	6.21484400	2.65242900
H	0.47772300	5.50750300	1.70267100	H	1.57355200	5.34771300	1.43971200
H	1.60809100	3.34501200	0.07243100	H	2.27166300	3.09346000	-0.29840000
H	1.18703200	4.48314800	-1.20744600	H	1.86450000	4.26040400	-1.55797100

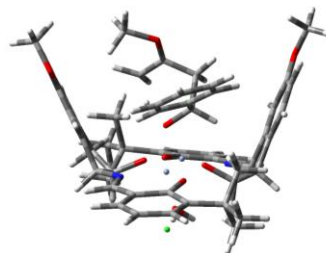
H	-3.70051700	2.40107100	-2.33741700	H	-3.25280000	2.98708200	-2.44896000
H	-6.44345200	-2.64267900	-3.02187600	H	-6.74275900	-1.55439500	-3.18209600
H	-3.32067700	-4.92009200	-0.55616700	H	-4.17246500	-4.32327700	-0.63674100
H	-4.53858800	-3.74595400	-0.02521500	H	-5.21889200	-2.97404500	-0.15141500
H	-2.87316500	-3.21332600	-0.32969500	H	-3.48353700	-2.71046300	-0.33661600
H	-2.45842000	-4.91234300	-2.92153000	H	-3.16822400	-4.41742400	-2.94484400
H	-2.00036900	-3.19167500	-2.87823200	H	-2.44042600	-2.79822000	-2.81849600
H	-3.10814700	-3.78277000	-4.12458000	H	-3.53911900	-3.17191600	-4.15224800
H	-4.76043800	-5.63207700	-2.39737000	H	-5.57001900	-4.76980600	-2.59397500
H	-5.43967200	-4.51426200	-3.58399900	H	-5.99532400	-3.53283100	-3.78163300
H	-6.03212100	-4.50624800	-1.90822500	H	-6.68428100	-3.47574400	-2.14305100
Cl	2.29795600	0.07367700	1.67703900	Cl	2.32799800	-0.17639200	1.60107300
Cl	-0.47965900	-0.15549000	-3.60075000	Cl	-0.56553100	-0.21147400	-3.62521900
O	2.24307400	0.45126000	-2.74033900	O	2.24525100	-0.08415400	-2.83042300
H	1.37061400	0.21835100	-3.18311200	H	1.33175400	-0.16348500	-3.24311100
H	2.94201600	-0.06426800	-3.17193700	H	2.80984300	-0.76228300	-3.23324000
H	-5.67654100	1.55357600	-2.91114900	H	-5.31967300	2.46406700	-3.06206900
C	-0.48200200	-1.96542400	2.49596200	H	8.76035500	-1.16828100	-0.86112700
C	-1.09081900	-1.05973400	3.37915600	H	-7.13392300	0.83353100	-3.56320300
C	-0.95377500	0.37308200	3.07010300	C	-0.39012500	1.78301300	2.57296500
C	-1.77874500	0.63557300	1.70729100	C	-1.03925400	0.84807900	3.38862800
H	0.53875600	-1.69906400	2.20576500	C	-0.95526100	-0.56766500	2.98524900
H	-0.66421500	-3.03145100	2.59451400	C	-1.80119300	-0.70333900	1.61694500
H	0.08907500	0.61356800	2.85048400	H	0.61690200	1.49314600	2.26005600
H	-1.35300900	1.00855900	3.86143200	H	-0.54292700	2.84677100	2.72501900
O	-1.43421800	-0.31422700	0.75016000	H	0.07638100	-0.83250600	2.74196000
H	-0.99278500	-1.38209700	1.45609800	H	-1.37320800	-1.24059500	3.73487500
O	-2.01290900	-1.34969200	4.28162600	O	-1.42259100	0.29737500	0.72555700
C	-2.36678800	-2.72143700	4.51977500	H	-0.92463300	1.28033600	1.49762900
H	-2.87674100	-3.13598200	3.64551700	O	-1.96756400	1.11448400	4.29356800
H	-3.04581000	-2.70091000	5.37178600	C	-2.26836700	2.48266600	4.61521800
H	-1.47802300	-3.31401700	4.75579000	H	-2.71933000	2.98764100	3.75619900
H	-1.43508100	1.62606300	1.39371900	H	-2.98162900	2.43404200	5.43780300
H	8.83371400	0.52377500	-0.79803200	H	-1.36242900	3.01008900	4.92889100
H	-7.21613100	-0.34346600	-3.38196600	H	-1.50002900	-1.68322700	1.23117800
C	-3.27783200	0.66554300	1.99399300	C	-3.29451000	-0.69387400	1.92788900
C	-4.12745500	-0.33893400	1.51954600	C	-4.10472000	0.38955700	1.57580100
C	-3.82680100	1.71152300	2.74906000	C	-3.87394800	-1.77758500	2.60173700
C	-5.49584900	-0.30436600	1.80227800	C	-5.46473200	0.39344900	1.89629700
H	-3.71329000	-1.13017000	0.90522800	H	-3.66395700	1.21815800	1.03196200
C	-5.19205800	1.74955400	3.02975700	C	-5.23098300	-1.77721800	2.92279800
H	-3.18406200	2.51135800	3.10924800	H	-3.25956700	-2.63527700	2.87058000
C	-6.03286100	0.73706100	2.55958600	C	-6.03254200	-0.68730000	2.57222900
H	-6.14270400	-1.08809700	1.41577500	H	-6.08260600	1.24030900	1.60798900
H	-5.60045200	2.57605700	3.60531900	H	-5.66410100	-2.62898300	3.44118800
H	-7.09812900	0.76737400	2.77367700	H	-7.09130500	-0.68574700	2.81778000
O	-4.10960600	5.24754900	1.81570800	O	-2.97911900	5.55461400	2.05848800
O	4.17592500	-4.93929600	3.09645900	O	3.09021400	-4.99048900	3.62013700
C	-4.21650100	6.21022000	2.85003100	C	-2.87972000	6.53448600	3.07835400
H	-5.28456200	6.32192100	3.04685500	H	-3.90333000	6.74444800	3.39460400
H	-3.71307200	5.87925900	3.76876400	H	-2.30408600	6.17005000	3.94072800
H	-3.80094800	7.18009800	2.54504800	H	-2.41695300	7.45819500	2.70683800
C	3.92492000	-5.83729200	4.16235300	C	2.65276400	-5.62259900	4.80959400
H	4.82991600	-5.83923300	4.77288700	H	3.53729000	-5.71600300	5.44271600
H	3.07545900	-5.50921000	4.77693300	H	1.89575600	-5.02241900	5.33244200
H	3.73199900	-6.85598300	3.79875700	H	2.24315200	-6.62272000	4.61158000

With M05-2X/6-31G(d):

TS<sub>pro-(R)</sub>



TS<sub>pro-(S)</sub>



E = -3934.73573028			E + ZPE = -3933.676713			E = -3934.74079847			E + ZPE = -3933.680256		
G = -3933.774583			imaginary frequencies: 1			G = -3933.775372			imaginary frequencies: 1		
Cr	2.13785400	0.01015400	-0.79153300	Cr	2.14070400	-0.39954400	-0.75467800				
Cr	-0.87217700	-0.03595100	-1.26313400	Cr	-0.84552500	0.10879500	-1.29256200				
O	0.65618200	-1.31986000	-0.94357700	O	0.41339200	-1.39403700	-0.85332100				
O	3.70744600	1.11538300	-0.77930500	O	3.89960200	0.35484700	-0.84239500				
O	0.57338200	1.26147000	-0.92066700	O	0.84660700	1.11710800	-0.98562600				
O	-2.42901600	-1.14403100	-1.49737500	O	-2.58215100	-0.67869400	-1.52447600				
N	3.24882800	-1.62669400	-0.97817500	N	2.86721200	-2.25270800	-0.73901500				
N	-1.90303600	1.63192100	-1.59198300	N	-1.52117500	1.92922100	-1.71645700				
C	1.02871600	-2.50037500	-1.60534700	C	0.53673300	-2.69943200	-1.35240300				
C	2.46278700	-2.84439000	-1.13386200	C	1.82485900	-3.27280700	-0.71990800				
C	2.21128700	-3.62843100	0.13263500	C	1.32581200	-3.69568500	0.64725900				
C	3.06616000	-3.86596300	1.18866900	C	2.03337600	-3.88303500	1.81517900				
C	2.62987000	-4.68830000	2.23463300	C	1.33945200	-4.28581800	2.96420300				
C	1.35624500	-5.26254500	2.19540700	C	-0.04205800	-4.48872500	2.92135700				
C	0.50393300	-4.99700100	1.12077200	C	-0.73998000	-4.29169300	1.72557800				
C	0.92120600	-4.16688100	0.09396200	C	-0.05880600	-3.89802300	0.58749000				
C	0.18049200	-3.68383600	-1.12107000	C	-0.57396300	-3.58549100	-0.78863900				
C	4.54061200	-1.66373500	-0.90584500	C	4.12469100	-2.55161900	-0.68523700				
C	5.41893800	-0.55665900	-0.70776500	C	5.22276300	-1.63764400	-0.67320700				
C	4.95527700	0.79878100	-0.63122300	C	5.05903600	-0.21281200	-0.74249300				
C	5.92405700	1.83869100	-0.42392500	C	6.23564700	0.61037800	-0.72402600				
C	7.25649900	1.47866500	-0.33115200	C	7.46804200	-0.01361200	-0.65304900				
C	7.71351600	0.15214700	-0.42382700	C	7.63080000	-1.40906100	-0.59352500				
C	6.79762700	-0.84880000	-0.60866000	C	6.51562100	-2.20358600	-0.60204400				
C	5.46663700	3.29125300	-0.29420300	C	6.09800400	2.13280800	-0.75401000				
C	4.54369800	3.42525400	0.92651800	C	5.33376800	2.59669300	0.49579700				
C	4.75612300	3.74203500	-1.57945700	C	5.38139400	2.58272600	-2.03672600				
C	6.64032500	4.24806300	-0.07807300	C	7.45811200	2.83155900	-0.73676400				
C	0.42485100	2.49528800	-1.57282800	C	0.92059300	2.33810500	-1.67039100				
C	-1.09085400	2.84995500	-1.57277700	C	-0.50128100	2.96457000	-1.63399900				
C	-1.25273700	3.69016100	-0.32770400	C	-0.48865200	3.74137000	-0.33828400				
C	-2.42362500	4.07636700	0.29689100	C	-1.56095000	4.20744500	0.39770600				
C	-2.34352000	4.89468500	1.42931900	C	-1.30804900	4.95900000	1.55133100				
C	-1.09918300	5.28070800	1.93362100	C	0.00430100	5.24209200	1.93742600				
C	0.07182600	4.88293100	1.28409500	C	1.07449800	4.74609100	1.18593900				
C	-0.00154800	4.10009600	0.14397700	C	0.83215500	3.98722200	0.05323500				
C	1.09563000	3.59903000	-0.74698500	C	1.79661400	3.33017700	-0.89366400				
C	-3.11314300	1.64551500	-2.04280200	C	-2.71007400	2.17655000	-2.15274200				
C	-4.00310000	0.53126000	-2.17396500	C	-3.77982600	1.24106100	-2.31926700				
C	-3.62249700	-0.81995000	-1.88621500	C	-3.65331500	-0.16211000	-2.04649200				
C	-4.61589200	-1.84894500	-2.00502000	C	-4.76372000	-1.01624000	-2.36041700				

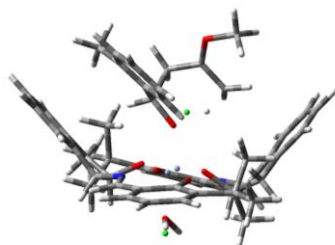
C	-5.89404100	-1.48467800	-2.39437800	C	-5.92799300	-0.42903900	-2.82524000
C	-6.26591900	-0.16246000	-2.68569500	C	-6.07233900	0.95173300	-3.03755400
C	-5.32129400	0.82635200	-2.57899800	C	-4.99688000	1.76749500	-2.80299000
C	-4.23958100	-3.30360700	-1.71751100	C	-4.63843900	-2.53295900	-2.20239900
C	-3.75432100	-3.45222800	-0.26557300	C	-4.40602500	-2.89604200	-0.73031100
C	-3.15614700	-3.75834900	-2.70797700	C	-3.48840900	-3.04781100	-3.08181200
C	-5.42828200	-4.25068300	-1.88474300	C	-5.90456600	-3.26546400	-2.64904500
H	0.96447100	-2.36944800	-2.70014100	H	0.56256300	-2.69916100	-2.45690300
H	2.95724500	-3.50240900	-1.87375700	H	2.17246900	-4.16001200	-1.28291500
H	4.05381200	-3.41057100	1.26035200	H	3.10142000	-3.68210900	1.89524400
H	1.01698500	-5.90881100	3.00142300	H	-0.58728700	-4.79331000	3.81135500
H	-0.49821600	-5.42992100	1.10637900	H	-1.82100400	-4.44238400	1.69565400
H	-0.84554800	-3.34847800	-0.91164900	H	-1.53805100	-3.06004700	-0.81027800
H	0.11251600	-4.45751800	-1.90322700	H	-0.68787200	-4.49408400	-1.40339700
H	5.02658400	-2.64652100	-1.01444700	H	4.39142100	-3.62023500	-0.65573600
H	8.00287200	2.25527400	-0.17671500	H	8.36780500	0.59882300	-0.63908100
H	7.11610600	-1.89036300	-0.67580500	H	6.60634100	-3.28980100	-0.55006500
H	5.11060900	3.24717800	1.85140000	H	5.92673000	2.39499000	1.39931400
H	3.71692900	2.70698200	0.90159600	H	4.37297700	2.08130100	0.60701400
H	4.12698800	4.44370600	0.97670400	H	5.15056300	3.68190800	0.44746200
H	3.89266300	3.11188500	-1.81902000	H	4.38734300	2.13293800	-2.13720900
H	5.45216100	3.70662500	-2.43035600	H	5.97366200	2.30391200	-2.92063500
H	4.41281000	4.78222800	-1.47137200	H	5.27375800	3.67822300	-2.03973100
H	7.20016700	4.01928600	0.83991800	H	8.03459200	2.59674400	0.16934800
H	6.25475000	5.27224100	0.02107700	H	7.30457300	3.91942200	-0.75379200
H	7.34268300	4.24220000	-0.92408000	H	8.06861100	2.57192100	-1.61372900
H	0.82132100	2.44098800	-2.59975900	H	1.26976500	2.18315200	-2.70530000
H	-1.33454200	3.45012100	-2.46770400	H	-0.62552100	3.66517100	-2.48042800
H	-3.40890400	3.74528400	-0.03385900	H	-2.59707000	4.00136500	0.12658600
H	-1.03071000	5.89680000	2.82710500	H	0.20738100	5.82883600	2.83026000
H	1.03915800	5.19325300	1.67988500	H	2.09658700	4.94567400	1.50855900
H	1.95862400	3.18431800	-0.20914200	H	2.61419500	2.79440000	-0.39125600
H	1.47345400	4.40136800	-1.40111200	H	2.25820600	4.06126500	-1.57712100
H	-3.52390000	2.61437600	-2.36708900	H	-2.93762800	3.21272400	-2.45074300
H	-6.65624400	-2.25572700	-2.49068400	H	-6.78210100	-1.06286300	-3.05436700
H	-3.46656900	-4.49717900	-0.06732700	H	-4.30629500	-3.98766400	-0.61945300
H	-4.56707200	-3.18744500	0.43019800	H	-5.25431000	-2.56430400	-0.11319300
H	-2.89471500	-2.80513500	-0.05364200	H	-3.50481000	-2.41966900	-0.33004600
H	-2.82166300	-4.77890400	-2.46364800	H	-3.36389700	-4.13274000	-2.94020000
H	-2.28538400	-3.09299200	-2.70289400	H	-2.53899900	-2.55169700	-2.85273300
H	-3.56316000	-3.77298300	-3.72886200	H	-3.71109900	-2.86955500	-4.14357100
H	-5.10447000	-5.27844700	-1.66913200	H	-5.74935900	-4.34796600	-2.54155100
H	-5.82261300	-4.24055700	-2.91034800	H	-6.14399000	-3.07095400	-3.70418600
H	-6.25085100	-4.01171200	-1.19516900	H	-6.77903800	-2.99830800	-2.03850300
Cl	2.23889100	-0.09733500	1.51317600	Cl	2.33075000	-0.30593700	1.55671500
Cl	-0.55832900	-0.19032100	-3.64158300	Cl	-0.52249100	-0.21893200	-3.65301700
O	2.27709100	0.26310400	-2.86792800	O	2.32339700	-0.37069600	-2.83567600
H	1.39784500	0.08816900	-3.30168300	H	1.42595300	-0.36951000	-3.26944800
H	2.92481200	-0.33434700	-3.26829400	H	2.81047700	-1.13601700	-3.17404700
H	-5.57838900	1.86429400	-2.79612200	H	-5.06119400	2.84041400	-2.99225700
C	-0.70850700	-2.05893400	2.24324500	H	8.62728100	-1.84094800	-0.53555300
C	-1.24680200	-1.15417200	3.15809500	H	-7.01327400	1.35307500	-3.40735400
C	-0.83885500	0.24777100	3.03901500	C	-0.21985800	1.70888100	2.51428900
C	-1.47981900	0.76037000	1.66752700	C	-0.99115900	0.81852700	3.25537600
H	0.36210800	-1.93862000	2.03255700	C	-0.98974200	-0.58838100	2.83725300
H	-1.07834200	-3.08234700	2.19536500	C	-1.77863500	-0.60784500	1.45084100

H	0.24711300	0.33115500	2.92382500	H	0.77452200	1.33620100	2.23744900
H	-1.21008900	0.86305500	3.86394000	H	-0.28984800	2.78146000	2.68360000
O	-1.22113700	-0.15358000	0.67188800	H	0.02723000	-0.94601400	2.62783600
H	-1.02598000	-1.30386600	1.27000100	H	-1.50026800	-1.23763600	3.55506000
O	-2.31917000	-1.35264300	3.89737000	O	-1.27344000	0.36538200	0.61505800
C	-2.96445400	-2.61996100	3.85494900	H	-0.73211000	1.28035600	1.41843400
H	-3.39559300	-2.79066800	2.86010700	O	-1.97150300	1.14912200	4.07269700
H	-3.76066800	-2.57311200	4.59957700	C	-2.23892000	2.53097300	4.28992300
H	-2.26180800	-3.42458500	4.10344300	H	-2.56571300	3.01144800	3.35695700
H	-0.94992500	1.70918700	1.46506200	H	-3.04196500	2.56620700	5.02822900
H	8.77589800	-0.06604400	-0.34264800	H	-1.34721800	3.04071000	4.67811300
H	-7.28426300	0.06473900	-2.99268800	H	-1.56086500	-1.61365000	1.04935200
C	-2.96194700	1.00793600	1.85689700	C	-3.26607000	-0.45698300	1.69103000
C	-3.90085900	0.17379400	1.25518800	C	-3.94748700	0.68504000	1.27837000
C	-3.40907000	2.06989400	2.64268900	C	-3.97418500	-1.46678300	2.34370400
C	-5.26385300	0.41175100	1.40719600	C	-5.31926800	0.80373100	1.48673000
H	-3.54745300	-0.65250000	0.64219200	H	-3.39072100	1.47323700	0.77081800
C	-4.76867700	2.30973200	2.80127200	C	-5.34029900	-1.34619100	2.56757900
H	-2.67856700	2.73489400	3.11043700	H	-3.44833800	-2.37101100	2.66121300
C	-5.70213600	1.48344200	2.17826000	C	-6.01959500	-0.21057300	2.13130400
H	-5.97897900	-0.23796800	0.90137100	H	-5.84245200	1.69256500	1.13552600
H	-5.09949100	3.16062900	3.39577500	H	-5.88022300	-2.14672900	3.07180300
H	-6.76739900	1.68010100	2.29104800	H	-7.09269700	-0.11913900	2.29226600
O	-3.53450900	5.24581600	1.98235900	O	-2.41278800	5.34703100	2.24957700
O	3.52049800	-4.87146600	3.24165700	C	-2.21945500	6.13507100	3.39569000
C	-3.51314600	5.98165800	3.17627600	H	-3.21449700	6.36625200	3.78518600
H	-4.55719200	6.13833200	3.46200800	H	-1.64627700	5.59728700	4.16930300
H	-2.99775400	5.43388200	3.98229800	H	-1.69632700	7.07418500	3.16073200
H	-3.02811800	6.96156900	3.04711500	O	2.10060400	-4.44932100	4.07638100
C	3.11949200	-5.64079700	4.34446500	C	1.45934600	-4.85309000	5.25691700
H	3.96130400	-5.64367300	5.04174100	H	2.23898800	-4.94408000	6.01791200
H	2.24013200	-5.20503800	4.84361700	H	0.71615700	-4.11249600	5.59118200
H	2.88799800	-6.67854000	4.05755200	H	0.96034300	-5.82729300	5.13525500

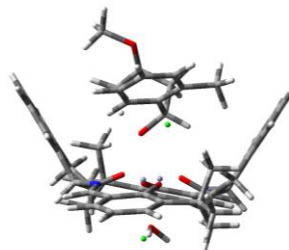
Reaction between *o*-methylbenzaldehyde, 2-methoxypropene **3** and catalyst **1a**. Energy unit is a.u..

With B3LYP/6-31G(d):

TS<sub>pro-(R)</sub>



TS<sub>pro-(S)</sub>



E = -3747.02199253	E + ZPE = -3745.998311	E = -3747.02523517	E + ZPE = -3746.002347
G = -3746.096099	imaginary frequencies: 1	G = -3746.100893	imaginary frequencies: 1
Cr	2.16276900 -0.42760300 -0.46881900	Cr	2.14915600 -0.53273900 -0.43568400
Cr	-0.88316400 -0.05912000 -1.03887600	Cr	-0.83984300 0.14383100 -1.05785500
O	0.48319700 -1.52149300 -0.54723600	O	0.34425800 -1.41804500 -0.47120400
O	3.90776500 0.41149800 -0.52122400	O	3.97694200 0.09378500 -0.51398600

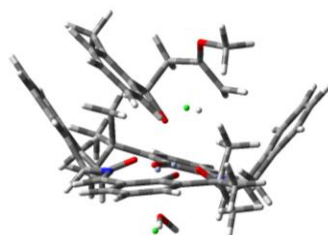
O	0.76042200	1.03381900	-0.73319700	O	0.92773500	1.05981300	-0.79067900
O	-2.57681800	-0.95029100	-1.36147000	O	-2.61443900	-0.55719900	-1.36465800
N	3.01705200	-2.24118100	-0.51117600	N	2.77602200	-2.43208400	-0.37118800
N	-1.60605600	1.70076600	-1.65198400	N	-1.36571200	1.95375400	-1.72748400
C	0.67175200	-2.82448600	-1.07429900	C	0.37184500	-2.77533500	-0.88188700
C	2.05475500	-3.34570000	-0.57569700	C	1.68445400	-3.41023800	-0.32748600
C	1.71298800	-4.02787600	0.74291400	C	1.27122900	-3.89181500	1.05751000
C	2.54987000	-4.38928500	1.79484100	C	2.06605400	-4.22457600	2.14945500
C	2.01141200	-5.09930800	2.87263700	C	1.45086500	-4.71117200	3.30717300
C	0.65637400	-5.44570700	2.88579100	C	0.06193400	-4.86359500	3.36009800
C	-0.18206400	-5.07086300	1.83035000	C	-0.73251200	-4.52254900	2.26008300
C	0.35045000	-4.35026700	0.76165900	C	-0.12120800	-4.02918000	1.10857100
C	-0.34035600	-3.82957500	-0.47880200	C	-0.74566400	-3.59406500	-0.19904500
C	4.29482400	-2.47314300	-0.50030400	C	4.01628600	-2.81607800	-0.36837600
C	5.34838900	-1.50683400	-0.41990800	C	5.18000900	-1.98096600	-0.38143000
C	5.10877100	-0.08613700	-0.40795900	C	5.11317600	-0.54280100	-0.43728100
C	6.24466100	0.79671700	-0.29862300	C	6.35064200	0.19923100	-0.43232900
C	7.50936900	0.22506700	-0.23364700	C	7.53978300	-0.51780700	-0.38696400
C	7.74403300	-1.16452600	-0.26610900	C	7.60444600	-1.92526600	-0.34477500
C	6.66984500	-2.01560500	-0.35787300	C	6.43291100	-2.64246000	-0.34218400
C	6.05073700	2.32487900	-0.24635100	C	6.34325300	1.74035400	-0.46708300
C	5.18477300	2.69704600	0.98311800	C	5.60591300	2.28489000	0.78170300
C	5.38336300	2.81711000	-1.55458300	C	5.65922500	2.23744000	-1.76502700
C	7.38936500	3.07862300	-0.10812400	C	7.76785800	2.33218000	-0.45033500
C	0.84485900	2.19646400	-1.54426600	C	1.10635200	2.23010300	-1.56960400
C	-0.59842300	2.76927100	-1.77345700	C	-0.28232300	2.93988100	-1.71423200
C	-0.70615500	3.91949200	-0.78191700	C	-0.29769900	3.92789000	-0.55623600
C	-1.82539500	4.68200100	-0.44487100	C	-1.37287000	4.63388300	-0.02060000
C	-1.66622500	5.78560800	0.39737600	C	-1.13410100	5.56019600	1.00076100
C	-0.40341600	6.11353100	0.90354500	C	0.16726500	5.77407900	1.47024500
C	0.71365100	5.34168700	0.57316000	C	1.24279100	5.05930800	0.93106900
C	0.55879800	4.24638000	-0.27842600	C	1.00464600	4.13220000	-0.08358000
C	1.62279600	3.32618100	-0.82677100	C	1.99031900	3.26376200	-0.83171500
C	-2.77980200	1.85103500	-2.18220100	C	-2.49483900	2.21458200	-2.30493800
C	-3.83504900	0.88287300	-2.27279400	C	-3.61084200	1.32912100	-2.47711200
C	-3.68694100	-0.49286800	-1.87505800	C	-3.61134400	-0.04373100	-2.04254000
C	-4.80826300	-1.38142000	-2.06215000	C	-4.75176600	-0.86059900	-2.37664100
C	-5.98141100	-0.85265500	-2.58906600	C	-5.81719600	-0.25738700	-3.03649500
C	-6.12835200	0.49536000	-2.96738100	C	-5.83369300	1.09596200	-3.42116400
C	-5.05705600	1.34411300	-2.81873900	C	-4.73001600	1.87043700	-3.15450100
C	-4.69460300	-2.87859700	-1.71071900	C	-4.77827100	-2.36584800	-2.04098100
C	-4.38157900	-3.05494000	-0.20435100	C	-4.69623900	-2.57279000	-0.51099100
C	-3.58449600	-3.52856400	-2.57385900	C	-3.59610200	-3.07256800	-2.74997600
C	-6.00204300	-3.64721400	-1.99292400	C	-6.07346500	-3.05264700	-2.52193100
H	0.61754000	-2.79398700	-2.16938400	H	0.31446000	-2.83294000	-1.97614300
H	2.43549800	-4.10400100	-1.27981200	H	1.96365900	-4.27944100	-0.94588400
H	3.60021200	-4.11084700	1.79619500	H	3.14351900	-4.08673800	2.12081300
H	2.65051700	-5.38176000	3.70480500	H	2.05656600	-4.96524800	4.17281000
H	0.25148000	-6.00620500	3.72475300	H	-0.40476000	-5.24399000	4.26514700
H	-1.23697100	-5.33684800	1.84549900	H	-1.81272200	-4.64051100	2.30661400
H	-1.29973000	-3.34317700	-0.28418900	H	-1.65632400	-2.99923700	-0.09021400
H	-0.53165200	-4.64038300	-1.19656800	H	-1.00670800	-4.46258100	-0.82159500
H	4.61752700	-3.51872800	-0.55934500	H	4.20941000	-3.89468900	-0.35945700
H	8.37389400	0.87412500	-0.15200300	H	8.47853500	0.02445900	-0.38230400
H	6.81577700	-3.09396000	-0.37597400	H	6.44808500	-3.72998000	-0.30387600
H	5.70804000	2.43794100	1.91149900	H	6.15169100	2.01726200	1.69459700

H	4.22919400	2.17083200	0.98074900	H	4.59662600	1.87910500	0.86425100
H	4.99617100	3.77859700	0.99558700	H	5.54701200	3.38039700	0.73548300
H	4.42418600	2.32682300	-1.72437100	H	4.63915700	1.86149300	-1.85038400
H	6.03200000	2.61362500	-2.41588200	H	6.22265100	1.90583100	-2.64616200
H	5.22069100	3.90178200	-1.50844900	H	5.63329800	3.33478400	-1.77942000
H	7.92310400	2.81012200	0.81116300	H	8.32151800	2.05553300	0.45459700
H	7.19147100	4.15587700	-0.06887000	H	7.70039600	3.42587300	-0.47096800
H	8.05635000	2.89916900	-0.95978300	H	8.35591200	2.02372600	-1.32293100
H	1.30578800	1.93914200	-2.50318600	H	1.51303500	1.96578900	-2.55227600
H	-0.65801400	3.17361400	-2.79453700	H	-0.30383000	3.49852900	-2.66293900
H	-2.81171100	4.42942200	-0.82437400	H	-2.38431400	4.47158900	-0.38519500
H	-2.52976100	6.38981000	0.66224600	H	-1.96189800	6.12526100	1.42196900
H	-0.29128100	6.97313300	1.55927900	H	0.34454500	6.50338000	2.25682700
H	1.69398600	5.59758700	0.96799500	H	2.25154400	5.22404100	1.30216600
H	2.27665800	2.90713600	-0.05668000	H	2.71398000	2.76163800	-0.18430700
H	2.26714400	3.85933200	-1.53890200	H	2.56347700	3.85953700	-1.55646600
H	-3.00351800	2.81971200	-2.64077600	H	-2.61801500	3.21036400	-2.74539900
H	-6.83489900	-1.50618800	-2.73065000	H	-6.68649500	-0.85541400	-3.28449000
H	-4.27749100	-4.12112400	0.03703000	H	-4.67575500	-3.64486900	-0.27455800
H	-5.19919900	-2.65219200	0.40722000	H	-5.56829500	-2.13256400	-0.01326100
H	-3.45993100	-2.54098600	0.07260000	H	-3.80370000	-2.10221700	-0.09911300
H	-3.46021100	-4.58409900	-2.29754300	H	-3.57735600	-4.13661400	-2.47926000
H	-2.62945500	-3.01590400	-2.45202400	H	-2.63883800	-2.62258400	-2.48419900
H	-3.85635400	-3.48925900	-3.63541500	H	-3.70806700	-3.00492100	-3.83867700
H	-5.86261000	-4.70209600	-1.72971000	H	-6.02904200	-4.11792200	-2.26710100
H	-6.28311100	-3.60907000	-3.05163700	H	-6.20131500	-2.98109600	-3.60831000
H	-6.84293600	-3.26893700	-1.39918800	H	-6.96730000	-2.63816200	-2.04058800
Cl	2.27170400	-0.34620900	1.88337200	Cl	2.26654100	-0.35831500	1.91214300
Cl	-0.42099800	-0.48895500	-3.45040800	Cl	-0.40552200	-0.41796100	-3.44357300
O	2.35183200	-0.36948100	-2.55162400	O	2.35094600	-0.60968200	-2.51327700
H	1.45821100	-0.47006000	-3.00449900	H	1.45095900	-0.59508600	-2.96457200
H	2.94751000	-1.04649600	-2.90855000	H	2.82481400	-1.39562400	-2.82740600
H	-5.13409000	2.38822000	-3.11553700	H	-4.69703800	2.91282100	-3.46559100
C	-0.94406900	-1.63598500	2.79323900	H	8.56759000	-2.42496900	-0.31092300
C	-1.29703900	-0.49566900	3.56082100	H	-6.69626900	1.50626900	-3.93717400
C	-0.78966100	0.80043100	3.11173800	C	-0.09051700	2.07260200	2.62389700
C	-1.54887200	1.16519800	1.71470200	C	-0.92659500	1.30058500	3.45940800
H	0.12349700	-1.68542300	2.55615600	C	-1.11015900	-0.11462200	3.11078500
H	-1.39761500	-2.59626900	3.02094600	C	-1.96858300	-0.15054200	1.73361500
H	0.27071700	0.72481900	2.85955900	H	0.86911500	1.59272100	2.40280500
H	-0.97487700	1.58643800	3.84117000	H	-0.04994300	3.15089000	2.74521000
O	-1.46492700	0.10190900	0.83737300	H	-0.14751200	-0.57768900	2.88011600
H	-1.29796500	-1.10982700	1.69688600	H	-1.64079300	-0.66353800	3.88803100
O	-2.24174500	-0.44471400	4.47521500	O	-1.35760100	0.65235000	0.78365800
C	-2.94051200	-1.64298400	4.86310400	H	-0.65027000	1.65801700	1.54808100
H	-3.55021500	-2.00624400	4.03180200	O	-1.77660000	1.77094500	4.35021100
H	-3.58004300	-1.34451900	5.69293600	C	-1.81181700	3.18312200	4.62760800
H	-2.23366500	-2.41270400	5.18450100	H	-2.14718100	3.73123000	3.74350500
H	-0.96173700	2.01380800	1.34543300	H	-2.53095800	3.29773700	5.43794000
H	8.75891100	-1.54624600	-0.21295000	H	-0.82517500	3.53625400	4.94017400
H	-7.06921800	0.84675000	-3.37952900	H	-1.90251000	-1.20306800	1.43833200
C	-2.99622900	1.58566500	1.99699400	C	-3.42127100	0.24647700	2.00379900
C	-4.03260900	0.75647900	1.54826000	C	-3.86092500	1.51307300	1.59901700
C	-3.31795500	2.77498700	2.68997000	C	-4.32372400	-0.61656400	2.66481600
C	-5.37145800	1.07375600	1.77649000	C	-5.16409100	1.94447400	1.84568900
H	-3.76876200	-0.13206900	0.98735400	H	-3.16531900	2.15093100	1.06456700

C	-4.66997600	3.08186800	2.90115600	C	-5.63273900	-0.17025800	2.89458800
C	-5.69405600	2.24554400	2.45914300	C	-6.05762100	1.09749700	2.49931400
H	-6.15370300	0.41702800	1.40450400	H	-5.48186500	2.93064600	1.51611600
H	-4.91910300	4.00324000	3.42410400	H	-6.33237800	-0.83884300	3.39176500
H	-6.73206100	2.51512900	2.63709800	H	-7.07998200	1.41305800	2.69066400
C	-2.27620900	3.73084600	3.23303600	C	-3.93986800	-2.00307400	3.13727600
H	-1.96626700	3.45603800	4.25104700	H	-3.33656000	-2.54395000	2.40092600
H	-1.37547200	3.77911500	2.61578500	H	-3.36008400	-1.97873700	4.06954700
H	-2.68314000	4.74529900	3.29125100	H	-4.83511100	-2.60163300	3.33327500

With M05-2X/6-31G(d)

TS<sub>pro-(R)</sub>



TS<sub>pro-(S)</sub>



E = -3745.09609824		E + ZPE = -3744.073251		E = -3745.10143078		E + ZPE = -3744.078210	
G = -3744.164861		imaginary frequencies: 1		G = -3744.167735		imaginary frequencies: 1	
Cr	2.12177900	-0.50128100	-0.58041400	Cr	2.15549500	-0.58372700	-0.47720400
Cr	-0.84895400	-0.08012200	-1.10449000	Cr	-0.75564000	0.14387300	-1.13261500
O	0.43352900	-1.56926500	-0.61342300	O	0.35464500	-1.44070600	-0.58118700
O	3.85096700	0.32502600	-0.65983100	O	3.96943000	0.02700400	-0.54222900
O	0.80073100	0.98505900	-0.86004800	O	1.00801700	1.01938500	-0.82877300
O	-2.57824400	-0.92348800	-1.25070700	O	-2.54628300	-0.49809600	-1.36830300
N	2.93927800	-2.31398500	-0.59341400	N	2.72942700	-2.48378300	-0.36568300
N	-1.56808800	1.67522200	-1.68340200	N	-1.25558600	1.99145700	-1.67675800
C	0.59895100	-2.85500500	-1.15092000	C	0.37875500	-2.77613900	-1.00676500
C	1.95500800	-3.38814300	-0.63007700	C	1.60882700	-3.41532700	-0.32163300
C	1.57907100	-3.97241700	0.71219300	C	1.05960600	-3.72198400	1.05541000
C	2.37745600	-4.22524300	1.81643400	C	1.72830600	-3.88354900	2.25754400
C	1.80530200	-4.84564200	2.92579300	C	0.98576400	-4.17118700	3.40253400
C	0.45937400	-5.20978700	2.91576700	C	-0.39904500	-4.30958100	3.33217200
C	-0.34261900	-4.92959100	1.81005200	C	-1.06576900	-4.14599000	2.11730000
C	0.22002400	-4.28988700	0.71326200	C	-0.33063200	-3.83373300	0.98237200
C	-0.43306800	-3.82140600	-0.55653200	C	-0.80666000	-3.53978100	-0.41216400
C	4.20737900	-2.55635900	-0.50673700	C	3.95811600	-2.87946100	-0.28565500
C	5.25505200	-1.59375700	-0.38058600	C	5.12550600	-2.05648600	-0.28812900
C	5.02108900	-0.17846800	-0.41608200	C	5.07845000	-0.62644800	-0.40259600
C	6.13647700	0.70131900	-0.20867300	C	6.31721900	0.10159300	-0.38608800
C	7.38768100	0.13648600	-0.03453000	C	7.49389300	-0.61756600	-0.28136300
C	7.62440600	-1.24941600	-0.04044000	C	7.54270800	-2.01978000	-0.18422900
C	6.56279500	-2.09860500	-0.20696600	C	6.36770100	-2.72255100	-0.18533000
C	5.91830300	2.21406400	-0.16555500	C	6.30027500	1.62856200	-0.46369500
C	4.94331700	2.55859700	0.97121800	C	5.54651200	2.19111500	0.75175600
C	5.39099000	2.71159600	-1.51919200	C	5.65009600	2.08893800	-1.77788900
C	7.21474300	2.97586200	0.11306300	C	7.70819700	2.22427100	-0.43440800
C	0.87802000	2.11536900	-1.69132900	C	1.21247600	2.19723400	-1.55834900
C	-0.55124300	2.71806200	-1.80753700	C	-0.15132100	2.94194000	-1.62447100
C	-0.58117600	3.77444200	-0.72989700	C	-0.12410300	3.80780500	-0.38559300

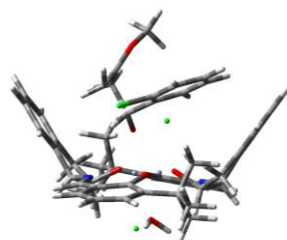
C	-1.67460100	4.46366200	-0.22148900	C	-1.17347600	4.46903200	0.23804100
C	-1.44887800	5.50710700	0.67269700	C	-0.89873100	5.27664200	1.34139600
C	-0.15083300	5.83313900	1.06636500	C	0.40913500	5.40924100	1.80955700
C	0.93912000	5.11205800	0.58336200	C	1.45822300	4.73671700	1.18301800
C	0.71783400	4.08167200	-0.32366100	C	1.18586200	3.93583100	0.08059900
C	1.71995600	3.21161200	-1.02412300	C	2.13142300	3.14459300	-0.77633400
C	-2.75214500	1.84357500	-2.16992600	C	-2.39910100	2.30818400	-2.18449900
C	-3.82755800	0.89831900	-2.18079600	C	-3.54730600	1.46497200	-2.31599900
C	-3.69544100	-0.44682200	-1.70521400	C	-3.56227100	0.08286300	-1.93047200
C	-4.85971400	-1.28561000	-1.70997000	C	-4.75460100	-0.67817500	-2.17692800
C	-6.04898900	-0.75867700	-2.18629400	C	-5.85432600	-0.01738100	-2.69656800
C	-6.17367800	0.55288000	-2.67098000	C	-5.85685700	1.34745100	-3.02709500
C	-5.06664500	1.36337800	-2.66664400	C	-4.70430100	2.06770600	-2.85406000
C	-4.75645700	-2.72780800	-1.21286100	C	-4.78508500	-2.17884700	-1.88017200
C	-4.30617800	-2.74964600	0.25715800	C	-4.58276000	-2.42454000	-0.37937800
C	-3.77492200	-3.50643500	-2.10261500	C	-3.70287200	-2.89304300	-2.70505400
C	-6.09860700	-3.45741400	-1.27396900	C	-6.12407000	-2.81448300	-2.25815500
H	0.54968100	-2.82539700	-2.25305200	H	0.41591400	-2.83786700	-2.10930200
H	2.32501100	-4.19593500	-1.29033100	H	1.89609300	-4.35452200	-0.83224600
H	3.42356400	-3.91758400	1.83260900	H	2.80786700	-3.74502600	2.32239400
H	2.41294200	-5.04596300	3.80656800	H	1.49219200	-4.28248400	4.35985100
H	0.02848700	-5.70378100	3.78574100	H	-0.96633400	-4.54123600	4.23296800
H	-1.40303700	-5.18902900	1.81151400	H	-2.14936900	-4.25972300	2.05548400
H	-1.38808000	-3.29962300	-0.39700800	H	-1.72195200	-2.93337200	-0.45786900
H	-0.63277600	-4.65416600	-1.25011200	H	-1.00047900	-4.46221300	-0.98425300
H	4.52553300	-3.61130500	-0.52188700	H	4.13753200	-3.96439100	-0.21530300
H	8.24341400	0.79046300	0.12066500	H	8.44064700	-0.08145800	-0.26961100
H	6.70738900	-3.18022500	-0.19736300	H	6.36997700	-3.81067700	-0.10364000
H	5.40233700	2.33533800	1.94494700	H	6.10575300	1.98198700	1.67490300
H	4.00950700	1.98936200	0.90989700	H	4.54959600	1.74989600	0.86016100
H	4.70449600	3.63383900	0.95045200	H	5.44258000	3.28405400	0.66056300
H	4.46298700	2.21017700	-1.80937800	H	4.63156800	1.70364500	-1.89490700
H	6.13805100	2.53347100	-2.30652800	H	6.24483400	1.74538700	-2.63692000
H	5.20393100	3.79540400	-1.47418700	H	5.61748700	3.18857400	-1.81391200
H	7.65895500	2.69592900	1.07875900	H	8.24838000	1.97126600	0.48892600
H	6.99593600	4.05182600	0.15224400	H	7.63445800	3.31948100	-0.48094600
H	7.96708100	2.82258200	-0.67396700	H	8.31438100	1.89897300	-1.29211900
H	1.27334400	1.83645500	-2.68123800	H	1.59932600	1.96818200	-2.56572700
H	-0.66655900	3.19953800	-2.79575900	H	-0.18518300	3.58279000	-2.52496800
H	-2.69420500	4.18999200	-0.49991300	H	-2.19743600	4.36381100	-0.12463800
H	-2.29650200	6.05567400	1.08301700	H	-1.70893500	5.81163000	1.83628000
H	0.00910600	6.64510600	1.77490800	H	0.61319400	6.04418600	2.67101600
H	1.95250800	5.35290100	0.90598900	H	2.47849200	4.83227000	1.55540900
H	2.45634100	2.75369900	-0.34860800	H	2.87550000	2.56824300	-0.20919200
H	2.28657800	3.78419800	-1.77542500	H	2.68768300	3.80445900	-1.46162800
H	-2.97662800	2.81768700	-2.63188800	H	-2.51896600	3.33288000	-2.57168600
H	-6.93813100	-1.38676400	-2.19604300	H	-6.77079500	-0.57563600	-2.87508400
H	-4.21937400	-3.78869000	0.61331600	H	-4.58007000	-3.50594400	-0.16714700
H	-5.05292300	-2.23667400	0.88513300	H	-5.39713400	-1.96134000	0.19844200
H	-3.34049700	-2.24927300	0.39270500	H	-3.64224800	-1.99149400	-0.02255900
H	-3.61051900	-4.51652300	-1.69539400	H	-3.68986900	-3.96589300	-2.45683800
H	-2.80671800	-2.99999000	-2.19044300	H	-2.70323200	-2.48011200	-2.53063500
H	-4.19142400	-3.61488600	-3.11399900	H	-3.91983300	-2.79827900	-3.77856100
H	-5.96986400	-4.48455000	-0.90488000	H	-6.08597800	-3.89054200	-2.03879000
H	-6.48521700	-3.52498000	-2.30035000	H	-6.34592400	-2.70488600	-3.32913900
H	-6.86242900	-2.97386500	-0.64783200	H	-6.96177800	-2.39233800	-1.68480700

Cl	2.23619300	-0.41047800	1.73027300	Cl	2.28622200	-0.39412900	1.83456100
Cl	-0.55767400	-0.58109400	-3.44725700	Cl	-0.40834600	-0.34126100	-3.46700000
O	2.30220500	-0.48726200	-2.66743000	O	2.39036700	-0.68146600	-2.55064100
H	1.41569600	-0.59685700	-3.10833900	H	1.50514900	-0.62166300	-3.00621600
H	2.88705700	-1.18738000	-2.99068100	H	2.80918200	-1.50578400	-2.83793500
H	-5.13028500	2.38999800	-3.03075400	H	-4.66169100	3.12285800	-3.12972900
C	-1.10267200	-1.75091500	2.58733900	H	8.50113100	-2.52747900	-0.10309500
C	-1.46103800	-0.64397300	3.37176700	H	-6.75302300	1.80896800	-3.43581200
C	-0.73763300	0.60030500	3.14035800	C	-0.09107500	1.91456900	2.63887900
C	-1.24558900	1.14201200	1.71004800	C	-0.96661800	1.12103500	3.38619200
H	-0.02259300	-1.88051800	2.44315100	C	-1.10641700	-0.28957300	3.01433700
H	-1.67876800	-2.67406100	2.64177800	C	-1.87335800	-0.27043400	1.61278500
H	0.33611200	0.41463200	3.03152700	H	0.88319500	1.44890300	2.43706600
H	-0.94443500	1.34969500	3.90756900	H	-0.07808600	2.99559500	2.77063000
O	-1.24245000	0.11394900	0.80405700	H	-0.13402200	-0.76421900	2.82466700
H	-1.26961500	-1.07796600	1.52745900	H	-1.68140700	-0.85319900	3.75393700
O	-2.57723600	-0.51938200	4.05203400	O	-1.17304900	0.53092300	0.74172300
C	-3.51003900	-1.59772600	4.06459800	H	-0.57537600	1.49050800	1.53063300
H	-3.89623000	-1.76993400	3.05152500	O	-1.91460800	1.56890100	4.18152400
H	-4.32110100	-1.27933800	4.72110900	C	-2.05257400	2.97561800	4.36164600
H	-3.04572000	-2.51112500	4.45471000	H	-2.33395300	3.44764200	3.41175000
H	-0.48144000	1.89407800	1.43567300	H	-2.84938800	3.10480700	5.09574700
H	8.63283200	-1.63220800	0.09884800	H	-1.11884100	3.41486400	4.73359700
H	-7.13091400	0.91167700	-3.04232900	H	-1.81763000	-1.32594800	1.28735500
C	-2.61704500	1.78162300	1.85580500	C	-3.31935400	0.17929200	1.76224800
C	-3.70571000	1.14962000	1.25568500	C	-3.69913600	1.38273100	1.16629500
C	-2.82335500	2.97960000	2.56342300	C	-4.28402000	-0.57289600	2.45396600
C	-4.98344100	1.69442100	1.30183000	C	-5.00668700	1.84827500	1.23071600
H	-3.52295800	0.22272700	0.71593200	H	-2.94117800	1.93428100	0.61285200
C	-4.11141700	3.52078100	2.59295900	C	-5.59377400	-0.09072100	2.51433800
C	-5.18629900	2.89761200	1.96791800	C	-5.96384500	1.10527400	1.91111600
H	-5.80389700	1.18332700	0.79712700	H	-5.27821000	2.77546500	0.72606300
H	-4.26689200	4.46239100	3.12330900	H	-6.34391800	-0.68607000	3.03777500
H	-6.17564100	3.35170300	2.00544900	H	-6.99694400	1.44574700	1.96242000
C	-1.72843000	3.69082300	3.30758200	C	-3.97424200	-1.88517300	3.11529900
H	-1.60479400	3.28751000	4.32445900	H	-3.19476700	-2.44779900	2.58612400
H	-0.75341800	3.62775000	2.80765600	H	-3.62942000	-1.75459100	4.15246400
H	-1.96385200	4.75661900	3.42036300	H	-4.87015800	-2.51825800	3.15435100

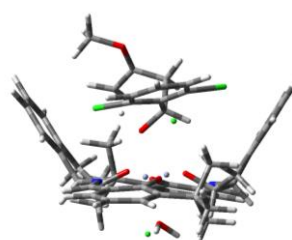
Reaction between 2,6-dichlorobenzaldehyde, 2-methoxypropene **3** and catalyst **1a**. Energy unit is a.u..

With m06-2X/6-31G(d):

TS<sub>pro-(R)</sub>



TS<sub>pro-(S)</sub>



E = -4624.94512657	E + ZPE = -4623.968065	E = -4624.94424690	E + ZPE = -4623.969646
G = -4624.063359	imaginary frequencies: 1	G = -4624.062455	imaginary frequencies: 1

Cr	2.12161100	-0.53452700	-0.73854600	Cr	2.24017300	-0.58625700	-0.45825300
Cr	-0.75017100	0.53337500	-1.06128600	Cr	-0.64741000	0.19641700	-1.12031500
O	0.25999600	-1.20450900	-0.82896400	O	0.43102400	-1.42562500	-0.57455400
O	3.92609400	0.11487000	-0.65086100	O	4.05163800	0.04167700	-0.46754200
O	1.09077900	1.21050900	-0.72836900	O	1.11306300	1.04861200	-0.74375900
O	-2.59867700	0.05792100	-1.32713700	O	-2.42957800	-0.44184300	-1.39178600
N	2.58969300	-2.40823400	-1.04040100	N	2.83407100	-2.47909400	-0.50198100
N	-1.13656900	2.46454300	-1.34037400	N	-1.09566000	2.05861400	-1.66099300
C	0.17539700	-2.39913500	-1.56535100	C	0.44736700	-2.73539600	-1.08339100
C	1.41936200	-3.26395200	-1.20985200	C	1.72554000	-3.42342700	-0.54218400
C	0.95466000	-4.01893900	0.01407400	C	1.27514900	-3.95210300	0.79741200
C	1.69935300	-4.64576800	1.00102600	C	2.03916200	-4.32340500	1.89225600
C	1.02916100	-5.36034400	1.99263600	C	1.39515400	-4.87332800	2.99814700
C	-0.36207400	-5.45358900	1.97832200	C	0.01361600	-5.05947500	2.98844700
C	-1.10445200	-4.80545600	0.99360600	C	-0.74767000	-4.67211500	1.88701900
C	-0.43977700	-4.06962600	0.02229000	C	-0.11215100	-4.09186500	0.79691500
C	-1.01244400	-3.24506700	-1.09348100	C	-0.69602300	-3.56570600	-0.48569700
C	3.81231000	-2.82683700	-1.06252300	C	4.06588600	-2.87141300	-0.48545200
C	4.99392400	-2.03779100	-0.87265300	C	5.22846200	-2.04365200	-0.42619200
C	5.00144700	-0.61142600	-0.65862200	C	5.16925400	-0.61032300	-0.40879900
C	6.27100700	0.03516100	-0.46459300	C	6.40368900	0.12252900	-0.35085300
C	7.41866700	-0.73434700	-0.51433900	C	7.58665600	-0.59402900	-0.32640500
C	7.41413300	-2.12170500	-0.73879800	C	7.64617700	-1.99863900	-0.35374800
C	6.21266800	-2.75426700	-0.91199100	C	6.47565600	-2.70738000	-0.40228800
C	6.32223000	1.54059200	-0.20039300	C	6.37723200	1.65065900	-0.31328600
C	5.56173000	1.86079400	1.09640300	C	5.62772900	2.12181900	0.94299500
C	5.73406200	2.30571900	-1.39598100	C	5.71858900	2.19647800	-1.59004300
C	7.75342000	2.04644800	-0.01367300	C	7.78173700	2.25194000	-0.24905300
C	1.35323600	2.45673700	-1.30569300	C	1.37329300	2.20716900	-1.48986800
C	0.04829900	3.30872500	-1.24380800	C	0.03326300	2.98885800	-1.63765100
C	0.18568900	4.06053900	0.05737500	C	0.06211200	3.94707500	-0.46732800
C	-0.78483000	4.75391900	0.76811400	C	-0.96418800	4.73133200	0.04422400
C	-0.41399400	5.43878300	1.92623000	C	-0.69937400	5.57724600	1.11963900
C	0.91415100	5.42893700	2.35373800	C	0.58539600	5.64673500	1.66166400
C	1.88483800	4.73033600	1.63546800	C	1.61921900	4.87904000	1.12775400
C	1.51371300	4.04173600	0.48591400	C	1.35143700	4.02967700	0.06003600
C	2.36358300	3.23617900	-0.45054300	C	2.29454000	3.13993100	-0.69278300
C	-2.26724000	2.92904700	-1.75625900	C	-2.24853800	2.39660400	-2.12727400
C	-3.46948300	2.18779700	-1.99352700	C	-3.39851600	1.55690800	-2.29753500
C	-3.55688200	0.76246200	-1.84713700	C	-3.41191000	0.15363900	-2.00123500
C	-4.75555700	0.10711000	-2.28957000	C	-4.55984000	-0.61214500	-2.39429200
C	-5.81533500	0.89776100	-2.69923500	C	-5.64950000	0.06648200	-2.91557100
C	-5.76183700	2.30048000	-2.75811400	C	-5.67319300	1.45472900	-3.11910500
C	-4.58658200	2.92775300	-2.43678000	C	-4.54373900	2.17927400	-2.83604500
C	-4.82539200	-1.42102600	-2.33598100	C	-4.55473700	-2.13706900	-2.26300400
C	-4.72404500	-2.01126800	-0.92494700	C	-4.50775000	-2.54185100	-0.78643700
C	-3.69467600	-1.95549900	-3.22848500	C	-3.35346300	-2.72413200	-3.02024600
C	-6.14158700	-1.91690600	-2.93745200	C	-5.81232100	-2.76766200	-2.86256300
H	0.11798000	-2.18104300	-2.64693200	H	0.41851200	-2.71745000	-2.18732900
H	1.62102700	-3.98451300	-2.02596600	H	2.00207300	-4.27238600	-1.19710600
H	2.78677000	-4.56408600	1.02212300	H	3.11801400	-4.16514900	1.90130100
H	1.59638800	-5.85097300	2.78211300	H	1.97446500	-5.15966600	3.87439200
H	-0.87202900	-6.02445300	2.75406100	H	-0.47652000	-5.50570000	3.85271000
H	-2.19494800	-4.85136800	0.99420700	H	-1.82744100	-4.81981100	1.87936700
H	-1.83837300	-2.58916000	-0.77948300	H	-1.59158700	-2.94181300	-0.34828100
H	-1.39488000	-3.87325600	-1.91451900	H	-0.98024800	-4.38188000	-1.17012700

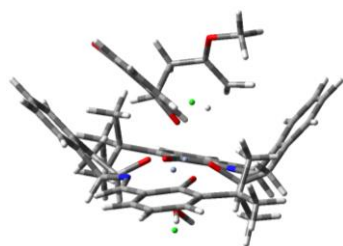
H	3.98182600	-3.89886200	-1.25215800	H	4.25357900	-3.95605100	-0.53489200
H	8.38440500	-0.25327800	-0.37261900	H	8.52987300	-0.05337300	-0.28354500
H	6.17427300	-3.83191800	-1.07933900	H	6.48571000	-3.79833300	-0.41978000
H	6.08964400	1.42898000	1.95881800	H	6.19900000	1.85982800	1.84503500
H	4.54398600	1.45504000	1.09351700	H	4.63697200	1.66254500	1.03192900
H	5.51126600	2.95155000	1.24406200	H	5.51067000	3.21702500	0.92531200
H	4.70218000	2.00760500	-1.60910600	H	4.70112000	1.81514500	-1.72762700
H	6.33666500	2.12027800	-2.29709100	H	6.31124600	1.91473300	-2.47262500
H	5.75428200	3.38839900	-1.19677800	H	5.68109200	3.29606000	-1.55080100
H	8.25545700	1.56792100	0.83923300	H	8.32836100	1.93480200	0.65041600
H	7.72963100	3.12703900	0.18432300	H	7.70146500	3.34720700	-0.21448000
H	8.36883700	1.89098000	-0.91130200	H	8.38509700	1.99432900	-1.13141100
H	1.69837400	2.34140400	-2.34703600	H	1.79295800	1.94878700	-2.47588000
H	0.04027500	4.02864700	-2.08279300	H	0.03750600	3.55847900	-2.58452300
H	-1.82430000	4.75770400	0.43341200	H	-1.96638700	4.68764600	-0.38322000
H	-1.16305200	5.98848500	2.49452900	H	-1.49697300	6.19561900	1.53045100
H	1.19446700	5.97279900	3.25483900	H	0.78362600	6.31414400	2.49961600
H	2.92118100	4.71587200	1.97446500	H	2.62478800	4.93598400	1.54546500
H	3.03617500	2.53257800	0.05800400	H	2.95982400	2.54821500	-0.04770000
H	2.99261600	3.89050100	-1.07514700	H	2.93845100	3.72960700	-1.36460900
H	-2.32212000	4.00392400	-1.99358200	H	-2.37546300	3.43391800	-2.47665100
H	-6.74039800	0.41907400	-3.01378400	H	-6.53503000	-0.49844400	-3.20016500
H	-4.70351900	-3.11184400	-0.97239500	H	-4.44751400	-3.63729600	-0.68747600
H	-5.59677800	-1.71592500	-0.32307100	H	-5.41370900	-2.20013200	-0.26350900
H	-3.82284700	-1.66773100	-0.40522500	H	-3.64457200	-2.10291900	-0.27730900
H	-3.74948300	-3.05390800	-3.28228900	H	-3.36255600	-3.82186700	-2.93572000
H	-2.70428300	-1.66995100	-2.85851900	H	-2.39862800	-2.34903600	-2.63657400
H	-3.79403200	-1.56012300	-4.24961400	H	-3.40743200	-2.46561000	-4.08761500
H	-6.12921200	-3.01515700	-2.96996100	H	-5.74645700	-3.86016900	-2.76693600
H	-6.28735800	-1.55746500	-3.96605300	H	-5.92214000	-2.53501900	-3.93130100
H	-7.01377400	-1.61766600	-2.33833500	H	-6.72674200	-2.44911100	-2.34173700
Cl	2.28918900	-0.82238500	1.57192400	Cl	2.30729900	-0.55734200	1.86226000
Cl	-0.50441400	0.39765100	-3.49132300	Cl	-0.27398500	-0.24933300	-3.46324100
O	2.30436100	-0.23753600	-2.80103300	O	2.50574200	-0.58071800	-2.53291100
H	1.40721600	-0.02634600	-3.18788000	H	1.62825500	-0.53008000	-3.00406800
H	2.62841000	-1.02504300	-3.26206700	H	2.95557200	-1.38025800	-2.84242100
H	-4.49270100	4.01170100	-2.52343100	H	-4.50889600	3.25214400	-3.03275200
C	0.50769800	1.66535600	2.98488600	H	8.60877100	-2.50441300	-0.33225400
C	-0.84214800	1.47619100	3.47308100	H	-6.55910800	1.93263600	-3.53150800
C	-1.96035200	1.94514900	2.68100400	C	0.10587900	2.04648200	2.50420900
C	-2.20163000	0.92702800	1.42594500	C	-0.81313300	1.36393200	3.30639200
H	0.66590800	2.70845200	2.68068000	C	-1.00362900	-0.06787500	3.05717400
H	1.31501700	1.30599300	3.62345900	C	-1.72324400	-0.21000300	1.64011400
H	-1.70415100	2.90006200	2.21134800	H	1.04478000	1.51001100	2.31370400
H	-2.88514900	2.01316900	3.26311800	H	0.18074100	3.13231400	2.55056400
O	-1.04056000	0.64938200	0.82641100	H	-0.03097100	-0.56358400	2.93937700
H	0.51322000	1.09769200	2.01393000	H	-1.60278200	-0.55365300	3.83318500
O	-1.15088000	0.80237700	4.53419400	O	-1.14217600	0.62730200	0.73093700
C	-0.13240400	0.14217800	5.30720800	H	-0.45081800	1.58967600	1.44384100
H	0.40391400	-0.57018300	4.67266900	O	-1.73148200	1.91863300	4.06610500
H	-0.67058900	-0.38075800	6.09808700	C	-1.69788400	3.32971400	4.27709400
H	0.55048400	0.88225000	5.73624100	H	-1.94519200	3.85892000	3.34860600
H	-2.87963500	1.53529300	0.80131200	H	-2.45484400	3.53064900	5.03704800
H	8.35008900	-2.67494400	-0.76710000	H	-0.70896700	3.64156800	4.63406500
H	-6.62881600	2.86702200	-3.09058600	H	-1.52958000	-1.26148800	1.36615600
C	-3.01568600	-0.25968600	1.93608300	C	-3.23633800	-0.04062000	1.77961600

C	-2.46256700	-1.47319300	2.37542800	C	-3.96217800	1.11304800	1.45341600
C	-4.41467800	-0.18011700	1.99686400	C	-4.02136500	-1.10964900	2.23684400
C	-3.25199800	-2.53119300	2.82219900	C	-5.35223900	1.16454500	1.47252200
C	-5.22290800	-1.21593300	2.44583200	C	-5.40788700	-1.08139000	2.30125800
C	-4.63229000	-2.40219000	2.85696300	C	-6.07894300	0.05906200	1.88746700
H	-2.76206300	-3.44653900	3.14863300	H	-5.85022600	2.08665000	1.18210900
H	-6.30256900	-1.08626200	2.45536100	H	-5.94288500	-1.95960300	2.65494100
H	-5.25040500	-3.22702700	3.20564100	H	-7.16588100	0.09491200	1.90765200
Cl	-0.74046000	-1.72850000	2.39737300	Cl	-3.16546700	2.63041300	1.08686700
Cl	-5.25085400	1.27692800	1.47132000	Cl	-3.25247300	-2.59700800	2.76138000

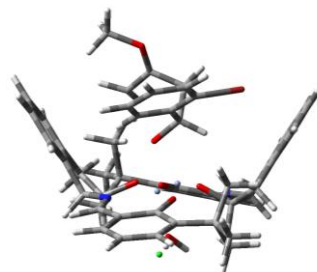
Reaction between *o*-bromobenzaldehyde, 2-methoxypropene **3** and catalyst **1a**. Energy unit is a.u..

With B3LYP/6-31G(d):

TS<sub>pro-(R)</sub>



TS<sub>pro-(S)</sub>



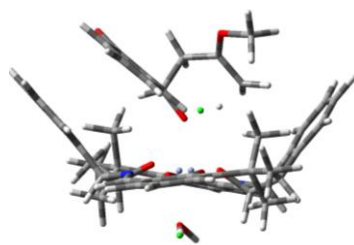
E = -6278.50856396			E + ZPE = -6277.523358			E = -6278.51405900			E + ZPE = -6277.528866		
G = -6277.623231			imaginary frequencies: 1			G = -6277.627129			imaginary frequencies: 1		
Cr	2.33821100	-0.49862200	-0.45540400	Cr	2.33368900	-0.48063900	-0.53613500	Cr	-0.56248300	0.50016900	-1.18091900
Cr	-0.69504100	-0.45572900	-1.17553200	Cr	0.48432300	-1.21399300	-0.81745900	Cr	4.19687900	0.02335100	-0.41081000
O	0.73544500	-1.71608700	-0.41340400	O	4.19687900	0.02335100	-0.41081000	O	1.23068200	1.23421700	-0.66678500
O	4.02334200	0.44095700	-0.58389300	O	1.23068200	1.23421700	-0.66678500	O	-2.36567300	0.00219700	-1.66733600
O	0.85128600	0.78861700	-1.01833700	O	-2.36567300	0.00219700	-1.66733600	O	2.84294100	-2.39836200	-0.78318000
O	-2.31917400	-1.50138200	-1.37584800	O	2.84294100	-2.39836200	-0.78318000	O	-0.93488100	2.43538700	-1.54552200
N	3.31312600	-2.22615800	-0.16936500	O	-0.93488100	2.43538700	-1.54552200	C	0.45260400	-2.48355500	-1.45260700
N	-1.52039500	1.12183400	-2.08697800	C	0.45260400	-2.48355500	-1.45260700	C	1.69638800	-3.29418300	-0.97115500
C	1.04364400	-3.06450100	-0.73238300	C	1.69638800	-3.29418300	-0.97115500	C	1.18738400	-3.99854000	0.27945300
C	2.43625900	-3.40060100	-0.11409000	C	1.18738400	-3.99854000	0.27945300	C	1.90685900	-4.59212200	1.31187400
C	2.08597900	-3.92911300	1.27081500	C	1.90685900	-4.59212200	1.31187400	C	1.20676400	-5.23592300	2.33665500
C	2.89935200	-4.08695100	2.38971200	C	1.20676400	-5.23592300	2.33665500	C	-0.19077600	-5.28243100	2.31857600
C	2.36631900	-4.69223200	3.53201400	C	-0.19077600	-5.28243100	2.31857600	C	-0.90871500	-4.68213700	1.27911300
C	1.04109600	-5.13921200	3.54317600	C	-0.90871500	-4.68213700	1.27911300	C	-0.21174200	-4.03610500	0.25950900
C	0.22600200	-4.97049800	2.41888000	C	-0.21174200	-4.03610500	0.25950900	C	-0.74548900	-3.32735300	-0.96557200
C	0.75146600	-4.35275800	1.28422900	C	-0.74548900	-3.32735300	-0.96557200	C	4.05642000	-2.85999500	-0.79252100
C	0.08006500	-4.05317800	-0.03716100	C	4.05642000	-2.85999500	-0.79252100	C	5.26598400	-2.11920600	-0.59184100
C	4.60067300	-2.35673600	-0.05700800	C	5.26598400	-2.11920600	-0.59184100	C	5.28655300	-0.69420100	-0.38220600
C	5.57977700	-1.31319900	-0.07616100	C	5.28655300	-0.69420100	-0.38220600	C	6.56027000	-0.05401800	-0.16170000
C	5.24517200	0.06650400	-0.31794400	C	6.56027000	-0.05401800	-0.16170000	C	7.70086100	-0.84712400	-0.18954300
C	6.30820800	1.04140500	-0.29779000	C	7.70086100	-0.84712400	-0.18954300	C	7.68162100	-2.23849800	-0.41428900
C	7.60074700	0.58808500	-0.06417800	C	7.68162100	-2.23849800	-0.41428900	C	6.47304500	-2.86155300	-0.61001900
C	7.93003800	-0.76536200	0.15266400	C	6.47304500	-2.86155300	-0.61001900	C	6.64145700	1.46154100	0.10633400
C	6.92495200	-1.70140600	0.14442900	C	6.64145700	1.46154100	0.10633400	C	5.83734800	1.80544700	1.38527000
C	6.00932800	2.53694000	-0.52050200	C	5.83734800	1.80544700	1.38527000	C	6.09151800	2.24518200	-1.11131800
C	5.03924200	3.04181200	0.57680500	C	6.09151800	2.24518200	-1.11131800				
C	5.39993600	2.74777100	-1.92867500								

C	7.28194000	3.40539500	-0.43974200	C	8.09087100	1.93696500	0.33622300
C	0.88556400	1.80011800	-2.01541000	C	1.53440200	2.50115200	-1.22347800
C	-0.58332600	2.22717200	-2.35990400	C	0.20628000	3.32525100	-1.31492100
C	-0.79506300	3.50872100	-1.56808500	C	0.18447700	4.10866900	-0.01021900
C	-1.97215800	4.23256100	-1.37550900	C	-0.87309800	4.79853100	0.57871700
C	-1.91059800	5.46347000	-0.71820600	C	-0.63841300	5.52701500	1.75018800
C	-0.68627700	5.95838300	-0.25652100	C	0.64203600	5.56174000	2.31520200
C	0.48947700	5.22835900	-0.44471200	C	1.69955900	4.86392300	1.72128500
C	0.43154000	4.00188100	-1.10810200	C	1.46518600	4.13398600	0.55572500
C	1.56887600	3.08516900	-1.49058100	C	2.43620400	3.32499300	-0.27387900
C	-2.67846600	1.09582700	-2.66888000	C	-2.00572900	2.86938700	-2.13078500
C	-3.65881100	0.04753800	-2.63181400	C	-3.16202200	2.10919700	-2.50934000
C	-3.43150800	-1.22810400	-2.00564400	C	-3.27879600	0.68749400	-2.31087300
C	-4.47332100	-2.22279900	-2.08472900	C	-4.44166600	0.02095400	-2.84305400
C	-5.65603900	-1.88048400	-2.73182600	C	-5.41960000	0.80165900	-3.45056800
C	-5.88251900	-0.62748500	-3.33143300	C	-5.32572300	2.19762200	-3.60218600
C	-4.88307200	0.31605200	-3.28931100	C	-4.19626100	2.83534100	-3.14820200
C	-4.26524700	-3.63422200	-1.49741300	C	-4.58601100	-1.51342400	-2.77265400
C	-4.00635100	-3.55393000	0.02708700	C	-4.61890200	-1.98431300	-1.30090700
C	-3.07208000	-4.31617600	-2.21244700	C	-3.40634500	-2.17633800	-3.52662600
C	-5.49753800	-4.54058300	-1.69831900	C	-5.88723700	-2.01129600	-3.43640400
H	1.04313200	-3.19803800	-1.82087500	H	0.44907700	-2.35159200	-2.54197000
H	2.90268500	-4.21410200	-0.69429600	H	1.95959900	-4.04646300	-1.73306700
H	3.92655900	-3.73246500	2.39136200	H	2.99192000	-4.53955500	1.34313000
H	2.98650400	-4.81495800	4.41572500	H	1.75301800	-5.69464300	3.15641100
H	0.64105200	-5.61732700	4.43377800	H	-0.72378100	-5.78238300	3.12324900
H	-0.80576700	-5.31565100	2.43192400	H	-1.99538300	-4.70779700	1.27373300
H	-0.91850800	-3.61971200	0.05960200	H	-1.61943600	-2.69888600	-0.77790200
H	-0.02461900	-4.96396700	-0.64434600	H	-1.03506700	-4.04865900	-1.74390200
H	4.99532000	-3.37154300	0.06484000	H	4.18502600	-3.93280000	-0.97454600
H	8.41215700	1.30656800	-0.04406400	H	8.66686700	-0.38195000	-0.02867900
H	7.14413300	-2.75355600	0.31578800	H	6.42308000	-3.93600700	-0.77549100
H	5.51837800	2.99279800	1.56205800	H	6.29563900	1.33378700	2.26293900
H	4.12720800	2.44488300	0.61944300	H	4.80519700	1.45781800	1.32029400
H	4.77019300	4.08914400	0.38681600	H	5.83906400	2.89119300	1.54917100
H	4.48775700	2.16496600	-2.06007400	H	5.06095400	1.96693200	-1.33429100
H	6.11518500	2.44867200	-2.70515000	H	6.70154400	2.04806500	-2.00170400
H	5.16516200	3.80904700	-2.08134300	H	6.13033700	3.32415000	-0.91255400
H	7.76818100	3.33678800	0.54046200	H	8.55432000	1.44888400	1.20162500
H	7.00918900	4.45525000	-0.59687000	H	8.08750400	3.01546000	0.53148100
H	8.01658000	3.13946100	-1.20926600	H	8.72795400	1.76513400	-0.53956000
H	1.38596800	1.41344600	-2.90864900	H	1.98511300	2.37409300	-2.21409900
H	-0.64015500	2.45529600	-3.43435300	H	0.27591000	4.03100000	-2.15721200
H	-2.92893200	3.85277000	-1.72463600	H	-1.86756300	4.77590700	0.13938900
H	-2.82018200	6.03553700	-0.55846700	H	-1.45124600	6.07888100	2.21573100
H	-0.65109900	6.91610400	0.25622400	H	0.81720000	6.13832200	3.22006300
H	1.43957200	5.61454400	-0.08333800	H	2.69111800	4.88909500	2.16682300
H	2.23969800	2.84795200	-0.66043700	H	3.07620300	2.66481500	0.31762100
H	2.18423000	3.53863800	-2.27974000	H	3.09836500	3.98415100	-0.85304600
H	-2.94852600	1.95721200	-3.28831600	H	-2.03647100	3.93033700	-2.40352000
H	-6.45105300	-2.61473800	-2.79598100	H	-6.30485200	0.31710800	-3.84556000
H	-3.83384500	-4.55924400	0.43337400	H	-4.69330600	-3.07822200	-1.25497300
H	-4.87743300	-3.13104100	0.54419700	H	-5.48759400	-1.56617400	-0.77871800
H	-3.13797100	-2.93249300	0.24980200	H	-3.72298600	-1.67309600	-0.76488000
H	-2.87959400	-5.30265200	-1.77017200	H	-3.47534500	-3.26904400	-3.44365600
H	-2.16503900	-3.71446000	-2.14236400	H	-2.44264700	-1.85341200	-3.13129000

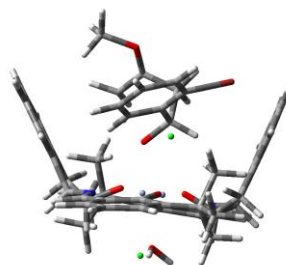
H	-3.29943500	-4.46313900	-3.27492600	H	-3.43722000	-1.91685600	-4.59156900
H	-5.29118200	-5.52750500	-1.26824200	H	-5.92663600	-3.10453000	-3.36777600
H	-5.73258300	-4.68896400	-2.75845700	H	-5.93827000	-1.74778800	-4.49928000
H	-6.39071700	-4.14540700	-1.19948100	H	-6.78336300	-1.62081800	-2.93942100
Cl	2.31546100	-0.01863600	1.84455000	Cl	2.30223500	-0.71773600	1.80554100
Cl	-0.12183300	-1.23389800	-3.45856200	Cl	-0.03791800	0.31735800	-3.59041500
O	2.61282300	-0.77709700	-2.51425400	O	2.65507000	-0.20047000	-2.58516900
H	1.74697100	-1.00633500	-2.96985000	H	1.78472300	-0.05940000	-3.06834200
H	3.25876300	-1.46550700	-2.73638300	H	3.11122000	-0.94218900	-3.01273400
H	-5.02069100	1.28804000	-3.75873500	H	-4.07571900	3.90904500	-3.27907200
C	-0.78684400	-1.46589400	2.78291700	H	8.61012400	-2.80087200	-0.42399100
C	-1.30317600	-0.32230500	3.41355000	H	-6.12389800	2.74833700	-4.09036600
C	-0.91737800	0.98575100	2.85997400	C	0.06133200	1.73209200	2.78184300
C	-1.59150900	1.10377400	1.39812600	C	-0.87614200	0.93222400	3.45047700
H	0.28134600	-1.41230700	2.55293200	C	-1.14025200	-0.40828800	2.89718900
H	-1.14313400	-2.45294300	3.06194300	C	-1.87516200	-0.18976200	1.47984700
H	0.16190900	1.02015300	2.69386600	H	0.98538600	1.21232800	2.51003500
H	-1.24666400	1.81454300	3.48425400	H	0.17638200	2.77893600	3.04509900
O	-1.33640800	-0.05378800	0.67222400	H	-0.19917200	-0.91734600	2.67223700
H	-1.12858000	-1.02884400	1.61188800	H	-1.77027600	-1.01462400	3.54711800
O	-2.31583500	-0.29128200	4.26191100	O	-1.15098400	0.71789800	0.71516200
C	-2.88580400	-1.52296600	4.73554400	H	-0.47661700	1.48312000	1.62303600
H	-3.40290500	-2.03603900	3.91975200	O	-1.76055500	1.34990100	4.34053800
H	-3.60000200	-1.23304100	5.50571800	C	-1.68938700	2.70215000	4.82397800
H	-2.11101900	-2.16860400	5.15882300	H	-1.90144500	3.40632200	4.01482600
H	-1.08713500	1.96230800	0.94286800	H	-2.45493900	2.77269700	5.59622400
H	8.96227800	-1.05259600	0.32724000	H	-0.70140600	2.90515500	5.24724200
H	-6.82557100	-0.42341900	-3.82896200	H	-1.85320700	-1.18280200	1.02136400
C	-3.09540900	1.37849600	1.52285400	C	-3.32360900	0.25738800	1.68710300
C	-4.00707600	0.38583400	1.13478600	C	-3.68683600	1.58392300	1.41404500
C	-3.63731900	2.57526600	2.01539200	C	-4.33612200	-0.59005300	2.15604600
C	-5.38563800	0.56889700	1.23456300	C	-4.98746200	2.04572400	1.60960700
H	-3.60332600	-0.53113000	0.72335300	H	-2.92190800	2.24266600	1.01797000
C	-5.01385500	2.77727900	2.12163700	C	-5.64412800	-0.14965200	2.35555500
C	-5.89368700	1.76879900	1.73081100	C	-5.97135900	1.17802900	2.08355300
H	-6.05700200	-0.22107500	0.90961200	H	-5.23406300	3.07893000	1.38040100
H	-5.38682700	3.72043700	2.50607000	H	-6.39508200	-0.84452000	2.71516100
H	-6.96537900	1.92924000	1.81040000	H	-6.99048200	1.52269000	2.23472600
Br	-2.51821200	4.03394000	2.57824700	Br	-3.98602300	-2.44326400	2.54185700

With M05-2X/6-31G(d):

TS<sub>pro-(R)</sub>



TS<sub>pro-(S)</sub>



E = -6276.46374368	E + ZPE = -6275.478096	E = -6276.47110056	E + ZPE = -6275.486771
G = -6275.569802	imaginary frequencies: 1	G = -6275.579249	imaginary frequencies: 1

Cr	2.25809200	-0.61579300	-0.49642700	Cr	2.33866600	-0.50152400	-0.65028100
Cr	-0.70551200	-0.46802000	-1.21471100	Cr	-0.49097300	0.54037400	-1.24625800
O	0.64253100	-1.79030500	-0.48229300	O	0.49876600	-1.18807500	-0.99644200
O	3.93342900	0.30606800	-0.60997400	O	4.19132100	-0.02574200	-0.51742900
O	0.85494000	0.73362200	-1.00962200	O	1.29865500	1.21387700	-0.69516600
O	-2.36164400	-1.44573400	-1.34299400	O	-2.30755700	0.09314700	-1.67157200
N	3.18355600	-2.35983800	-0.24986300	N	2.79697000	-2.41924400	-0.90243600
N	-1.49859500	1.14967000	-2.04558600	N	-0.84842300	2.49427700	-1.41663700
C	0.91818500	-3.11565800	-0.85589600	C	0.46529700	-2.41429700	-1.67926900
C	2.27154300	-3.49596300	-0.20726000	C	1.62248800	-3.26118400	-1.09930100
C	1.85368600	-3.96324700	1.16808200	C	0.99592900	-3.80420400	0.16729000
C	2.60048000	-4.05771500	2.33209100	C	1.60032600	-4.24655700	1.33191000
C	1.99997600	-4.59584000	3.46923800	C	0.79007100	-4.68248200	2.38022800
C	0.67857400	-5.03922400	3.42834000	C	-0.59740800	-4.67942100	2.25054100
C	-0.07163100	-4.92397000	2.25872700	C	-1.19929100	-4.23449800	1.07322400
C	0.51703600	-4.36495500	1.13210600	C	-0.39439900	-3.78659600	0.03697300
C	-0.08737600	-4.07800800	-0.21306200	C	-0.78748500	-3.19995400	-1.28910800
C	4.45909100	-2.50567100	-0.08998700	C	3.98768000	-2.91599100	-0.80794900
C	5.44451100	-1.47256800	-0.07879000	C	5.19667600	-2.19978200	-0.54898100
C	5.13299600	-0.09425800	-0.32807900	C	5.24098700	-0.77406000	-0.39014000
C	6.20341400	0.86302200	-0.30092200	C	6.50773100	-0.15716400	-0.11213100
C	7.48166200	0.40103900	-0.04261700	C	7.62551300	-0.96877100	-0.03935800
C	7.78982400	-0.95066400	0.19237400	C	7.58696800	-2.36359000	-0.21456300
C	6.77681000	-1.87119500	0.17040100	C	6.38140000	-2.96436200	-0.46213600
C	5.90861100	2.34413900	-0.54130700	C	6.58366100	1.35256200	0.11645400
C	4.95794900	2.86304900	0.54792300	C	5.73667600	1.72117300	1.34464800
C	5.30318500	2.54420400	-1.93879100	C	6.10522900	2.10835600	-1.13304400
C	7.17501000	3.19926600	-0.47761500	C	8.01118100	1.82232900	0.39799700
C	0.92067000	1.73908800	-1.99045100	C	1.61896100	2.48544700	-1.18684100
C	-0.52888000	2.21802300	-2.29375900	C	0.31581300	3.33240200	-1.15422200
C	-0.69224200	3.44562400	-1.43304500	C	0.34853600	3.94882800	0.22540300
C	-1.85371000	4.15472100	-1.15138400	C	-0.67941200	4.55835600	0.93130500
C	-1.75241200	5.35531500	-0.45588800	C	-0.39879200	5.12148100	2.17646400
C	-0.50674000	5.82495300	-0.03886200	C	0.89222900	5.06068200	2.70218700
C	0.64991000	5.09481500	-0.29538200	C	1.91932800	4.43966300	1.99131400
C	0.55263000	3.89835100	-0.99806700	C	1.64204100	3.88548800	0.74754100
C	1.64943200	2.97647100	-1.44607400	C	2.56714500	3.19364100	-0.21199100
C	-2.66740000	1.17691300	-2.59218900	C	-1.94817800	2.98958800	-1.87619300
C	-3.68755100	0.17469500	-2.50827000	C	-3.14368500	2.27614800	-2.20703800
C	-3.49138900	-1.09439500	-1.87221500	C	-3.25934900	0.84778600	-2.12852800
C	-4.60244400	-2.00131400	-1.80151400	C	-4.48213500	0.23979700	-2.57287000
C	-5.80706500	-1.60826400	-2.36090500	C	-5.51919800	1.07056100	-2.96053700
C	-5.99462100	-0.37162500	-2.99940500	C	-5.42615600	2.47217600	-2.98563100
C	-4.93824700	0.50082500	-3.07140100	C	-4.23877600	3.05809600	-2.63361800
C	-4.42088800	-3.36469700	-1.13343100	C	-4.60853000	-1.28422600	-2.62616100
C	-4.00983600	-3.18124600	0.33823200	C	-4.51099600	-1.87447700	-1.21417400
C	-3.36559100	-4.17441900	-1.90316500	C	-3.51399900	-1.86238700	-3.53702800
C	-5.70997600	-4.18613400	-1.13358100	C	-5.95116100	-1.73039100	-3.20755900
H	0.93922900	-3.21544700	-1.95482100	H	0.55136800	-2.25873100	-2.76988300
H	2.72800400	-4.34330100	-0.75441300	H	1.87951500	-4.08985900	-1.78672500
H	3.62829700	-3.69552600	2.37020000	H	2.68348800	-4.21151700	1.45132500
H	2.56650000	-4.66815200	4.39603200	H	1.24568100	-5.01473800	3.31156500
H	0.22688900	-5.46743700	4.32231300	H	-1.21875700	-5.01362000	3.08110100
H	-1.11413500	-5.24741200	2.23084900	H	-2.28487600	-4.20987200	0.97397500
H	-1.08144700	-3.60950100	-0.16221900	H	-1.66932500	-2.54574100	-1.25270600
H	-0.19439000	-4.99193700	-0.81961600	H	-0.99805300	-3.98218800	-2.03741700

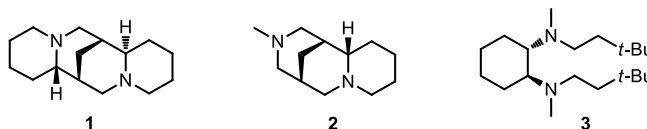
H	4.84155500	-3.53035000	0.04307500	H	4.09452200	-4.00477000	-0.93935100
H	8.30370500	1.11298700	-0.01583900	H	8.59384300	-0.51641300	0.16588800
H	6.97991900	-2.92802400	0.35153800	H	6.31428200	-4.04573700	-0.59207200
H	5.45723800	2.85012300	1.52715100	H	6.18731100	1.30216000	2.25567300
H	4.05043400	2.25594700	0.63011200	H	4.71399200	1.33437200	1.27366000
H	4.66859400	3.90331200	0.33045600	H	5.69607800	2.81597100	1.46157700
H	4.37410600	1.97945400	-2.07012700	H	5.08102800	1.84120200	-1.41357400
H	6.01439700	2.22004400	-2.71266300	H	6.76165100	1.88431600	-1.98662900
H	5.09122400	3.61148300	-2.10474700	H	6.15018800	3.19351200	-0.95371800
H	7.66372600	3.14266600	0.50535300	H	8.43184400	1.35700300	1.30069700
H	6.90847700	4.25092800	-0.65114800	H	8.00526900	2.90865400	0.56247500
H	7.90762500	2.91424700	-1.24651800	H	8.68838200	1.62120400	-0.44451000
H	1.40168600	1.34824500	-2.90063900	H	2.03220100	2.41431300	-2.20691400
H	-0.59993300	2.50336400	-3.35886200	H	0.36575600	4.12835400	-1.91985200
H	-2.82981400	3.77639200	-1.46158800	H	-1.69071900	4.60149000	0.52263200
H	-2.65294100	5.91953200	-0.21520000	H	-1.19022100	5.61796000	2.73740200
H	-0.44366700	6.76157500	0.51361600	H	1.09966500	5.50430500	3.67537300
H	1.61985600	5.45393200	0.04936500	H	2.92564300	4.38197400	2.40703200
H	2.33310100	2.67498100	-0.63917000	H	3.23449700	2.46128300	0.26309000
H	2.26684200	3.44551900	-2.22813300	H	3.20516600	3.92045600	-0.73996500
H	-2.92586700	2.05967200	-3.19769200	H	-1.98500800	4.07740900	-2.04813700
H	-6.65807800	-2.28508200	-2.31704400	H	-6.45855900	0.62536800	-3.28179000
H	-3.85062100	-4.16251900	0.81424300	H	-4.55925400	-2.97416100	-1.25302900
H	-4.81311500	-2.66319000	0.88781700	H	-5.34622000	-1.51986800	-0.59142200
H	-3.08951700	-2.59200100	0.43463700	H	-3.57945900	-1.58422400	-0.71668000
H	-3.16332100	-5.12560300	-1.38595100	H	-3.58823600	-2.96062100	-3.56000200
H	-2.42347300	-3.62468300	-2.01211600	H	-2.50796500	-1.58581800	-3.20434300
H	-3.73636600	-4.41145700	-2.91034100	H	-3.63943400	-1.49394500	-4.56519100
H	-5.52485300	-5.15192400	-0.64324700	H	-5.97748600	-2.82802700	-3.24808400
H	-6.06202700	-4.39934400	-2.15252600	H	-6.10155400	-1.35908800	-4.23125700
H	-6.52151300	-3.68576400	-0.58555200	H	-6.80252900	-1.40658200	-2.59172200
Cl	2.26883900	-0.24316900	1.78970200	Cl	2.34915000	-0.78122400	1.65552600
Cl	-0.24865000	-1.21762700	-3.46317200	Cl	-0.05797100	0.52225700	-3.61141500
O	2.54885500	-0.84575600	-2.56036300	O	2.67120400	-0.17403500	-2.68712300
H	1.69739600	-1.06368000	-3.02845100	H	1.81418900	0.01510400	-3.15959200
H	3.19118300	-1.53831800	-2.77119600	H	3.08743200	-0.92968600	-3.12635100
H	-5.05313400	1.47113600	-3.55722900	H	-4.11885700	4.14208000	-2.67726200
C	-0.95381400	-1.70338200	2.62274700	H	8.50185200	-2.94763300	-0.14597500
C	-1.46840900	-0.56356400	3.25511800	H	-6.27573400	3.07065900	-3.30682800
C	-0.87260200	0.72185700	2.90473900	C	0.11230200	1.50159700	2.80262100
C	-1.34827600	1.04318600	1.40473000	C	-0.85738600	0.66187600	3.35686600
H	0.13952500	-1.71696900	2.52305400	C	-1.06967200	-0.64929900	2.73802700
H	-1.41729400	-2.67905700	2.76383600	C	-1.76051900	-0.34407600	1.33315200
H	0.21913800	0.64457800	2.86446100	H	1.05768200	1.00113200	2.55098400
H	-1.19397400	1.52937000	3.56806900	H	0.19916000	2.53827100	3.12498900
O	-1.26582200	-0.08222500	0.62714800	H	-0.12028500	-1.15065400	2.50228400
H	-1.16047700	-1.17135200	1.48404900	H	-1.71781200	-1.29250100	3.33869100
O	-2.62476600	-0.48492500	3.87301600	O	-0.99972500	0.57628800	0.65351200
C	-3.42165000	-1.65895300	4.01023200	H	-0.35534900	1.31805900	1.62184600
H	-3.74958900	-2.00557300	3.02178800	O	-1.82171900	1.03794900	4.16985000
H	-4.28633000	-1.36295400	4.60611600	C	-1.86824600	2.39496200	4.60077200
H	-2.86360100	-2.45124000	4.52286800	H	-2.04857700	3.05330600	3.74161100
H	-0.63501900	1.81535400	1.06379900	H	-2.70227100	2.45547600	5.30170100
H	8.81674600	-1.24911300	0.39026400	H	-0.93359400	2.68057200	5.09843900
H	-6.96113100	-0.11978400	-3.42996500	H	-1.74341100	-1.32667800	0.82578900
C	-2.76123600	1.60118800	1.41236100	C	-3.19720600	0.13774900	1.49457700

C	-3.7976000	0.8266180	0.8865420	C	-3.5118370	1.4446960	1.1115390
C	-3.0960470	2.8690220	1.8917680	C	-4.2528510	-0.6422690	1.9713400
C	-5.0994140	1.3032500	0.8009880	C	-4.8062800	1.9432580	1.1776130
H	-3.5447760	-0.1647740	0.5143170	H	-2.7034930	2.0597980	0.7201520
C	-4.3923300	3.3667990	1.8110330	C	-5.5546240	-0.1595160	2.0562670
C	-5.3979480	2.5837160	1.2552070	C	-5.8362460	1.1388130	1.6513880
H	-5.8715600	0.6721730	0.3613350	H	-5.0104540	2.9575060	0.8370040
H	-4.6030830	4.3670710	2.1842360	H	-6.3420010	-0.8140440	2.4243150
H	-6.4104310	2.9775410	1.1843480	H	-6.8574800	1.5118410	1.7017290
Br	-1.7859180	3.9980220	2.6861380	Br	-4.0039690	-2.4599600	2.4896550



## A1.2 A New *trans*-1,2-Cyclohexanediamine-Based Ligand for Asymmetric Deprotonation

Naturally occurring sparteine exist primarily as the (7*S*,7*aR*,14*S*,14*aS*) enantiomeric form ((-)-sparteine) (Scheme A1-3). Although (+)-sparteine is also a natural product, the abundance of it is very limited. In addition, the chemical community has been experiencing a devastating shortage of (-)-sparteine recently.<sup>3</sup>



**Scheme A1-3.** Structure of (-)-sparteine (**1**) and its surrogates (**2** & **3**).

Research has been directed at seeking for a surrogate that could replace sparteine in the asymmetric deprotonation of *N*-Boc-pyrrolidine. Campos and O'Brien have made significant contributions in this field, having identified several potent chiral diamine ligands, including a synthetic "(+)-sparteine surrogate" (**2**)<sup>4</sup>, and a *trans*-1,2-cyclohexanediamine derivative (**3**)<sup>5</sup>. The successful incorporation of **3** in highly enantioselective deprotonation of *N*-Boc pyrrolidine is especially attractive, because the ligand can be easily prepared from bulk industrial byproducts, 1,2-cyclohexanediamine (mixture of stereoisomers) in three steps. While **3** has been used in directed allylation and carboxylation of *N*-Boc-pyrrolidine, it has not been established in the context of Negishi coupling for the synthesis of arylpyrrolidines. Since studies have shown that the enantioenriched 2-lithio-*N*-Boc-pyrrolidine is configurationally stable at low temperature, we

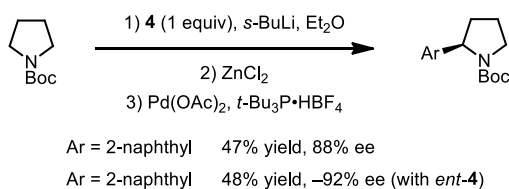
<sup>3</sup> [http://pipeline.corante.com/archives/2010/06/16/sparteine\\_and\\_other\\_fine\\_chemical\\_shortages.php](http://pipeline.corante.com/archives/2010/06/16/sparteine_and_other_fine_chemical_shortages.php).

<sup>4</sup> Stead, D.; Carbone, G.; O'Brien, P.; Campos, K. R.; Coldham, I.; Sanderson, A. *J. Am. Chem. Soc.* **2010**, *132*, 7260–7261.

<sup>5</sup> Stead, D.; O'Brien, P.; Sanderson, A. *Org. Lett.* **2008**, *10*, 1409–1412.

hypothesized that transmetallation with  $\text{ZnCl}_2$  followed by Pd-catalyzed cross coupling with arylbromide can be achieved via this intermediate with retained stereochemical information.<sup>6</sup>

Indeed, this method provided the desired *N*-Boc-2-arylpiperidine in good yield and excellent enantioselectivity on two substrates we examined (Scheme A1-4). Taken together with the easy access to both enantiomeric forms of the ligand, we anticipate this approach to be practical in the synthesis of a variety of arylpiperidine-derived thiourea catalysts.



**Scheme A1-4.** Synthesis of *N*-Boc-arylpiperidine assisted by ligand **4**.

### A1.3 Proposed Total Synthesis of Sparteine and “Sparteine Surrogate” Using Hydrolytic Kinetic Resolution of Terminal Epoxide and Stereoselective Aza-Sakurai Cyclization

Complementary to the development of sparteine surrogate ligands, the efficient enantioselective syntheses of sparteine can also serve to solve the problem caused by the shortage of both enantiomers of sparteine. Perhaps more importantly, a modular synthesis of sparteine would allow access to structurally modified analogs, which is potentially highly desirable due to the versatility of sparteine in asymmetric synthesis.<sup>7</sup> The first asymmetric total synthesis of sparteine was accomplished by Aubé et. al. in 15 steps.<sup>8</sup> We propose a more concise approach, using methods developed in the Jacobsen group including a Co-catalyzed hydrolytic kinetic resolution of terminal epoxide and a thiourea-catalyzed aza-Sakurai cyclization (Scheme A1-5). The route starts with an  $\text{S}_{\text{N}}2$  reaction of a commercially available epichlorohydrin **4** with

<sup>6</sup> Barker, G.; McGrath, J. L.; Klapars, A.; Stead, D.; Zhou, G.; Campos, K. R.; O’Brien, P. *J. Org. Chem.* **2011**, *76*, 5936–5953.

<sup>7</sup> Chuzel, O.; Riant, O. in *Topics in Organometallic Chemistry*, Volume 15, 2005, pp 59–92.

<sup>8</sup> Smith, B. T.; Wendt, J. A.; Aubé, J. *Org. Lett.* **2002**, *4*, 2577–2579.

alkynyl Grignard reagent **5**. The intermediate **6** is hydrolytic resolved by the action of a Co(salen) complex to form diol **7**, setting up the first stereogenic center. Mitsunobo reaction selectively at the primary position, reduction with NaBH<sub>4</sub>, and *cis*-selective hydrogenation of the alkyne leads to the aza-Sakurai precursor. Thiourea **10** would then catalyze the aza-Sakurai cyclization, ideally in a diastereoselective fashion, to yield **11**.<sup>9</sup> A few functional group manipulation operations would furnish structure **14**, which would undergo intramolecular condensation upon workup to generate tricycle **15**. Acylation of **15** by acryloyl chloride at enamine nitrogen would give intermediate **16**. Upon irradiation, **16** would undergo a cascade reaction comprising an aza-Claisen rearrangement and *N*-acyliminium ion (**18**) formation, and reductive quenching of the reaction mixture would provide tetracycle **19** in one operation.<sup>10</sup> Lithium aluminum hydride would then reduce both of the lactam carbonyl group and complete the synthesis of sparteine, in overall 11 steps.

The synthesis of “(+)-sparteine surrogate” (**2**) can be realized from intermediate **12** through the following steps (Scheme A1-6): (a) DIBAL reduction of the nitrile group to a primary amine; (b) protection of the resultant primary amine with Boc<sub>2</sub>O; (c) ozonolysis of the double bond to form an aldehyde; (d) reductive amidation of the resultant aldehyde with the Boc-protected amine; (e) LAH reduction of both the secondary Boc-amine and the amide on the right-hand portion to furnish the final product **2**.

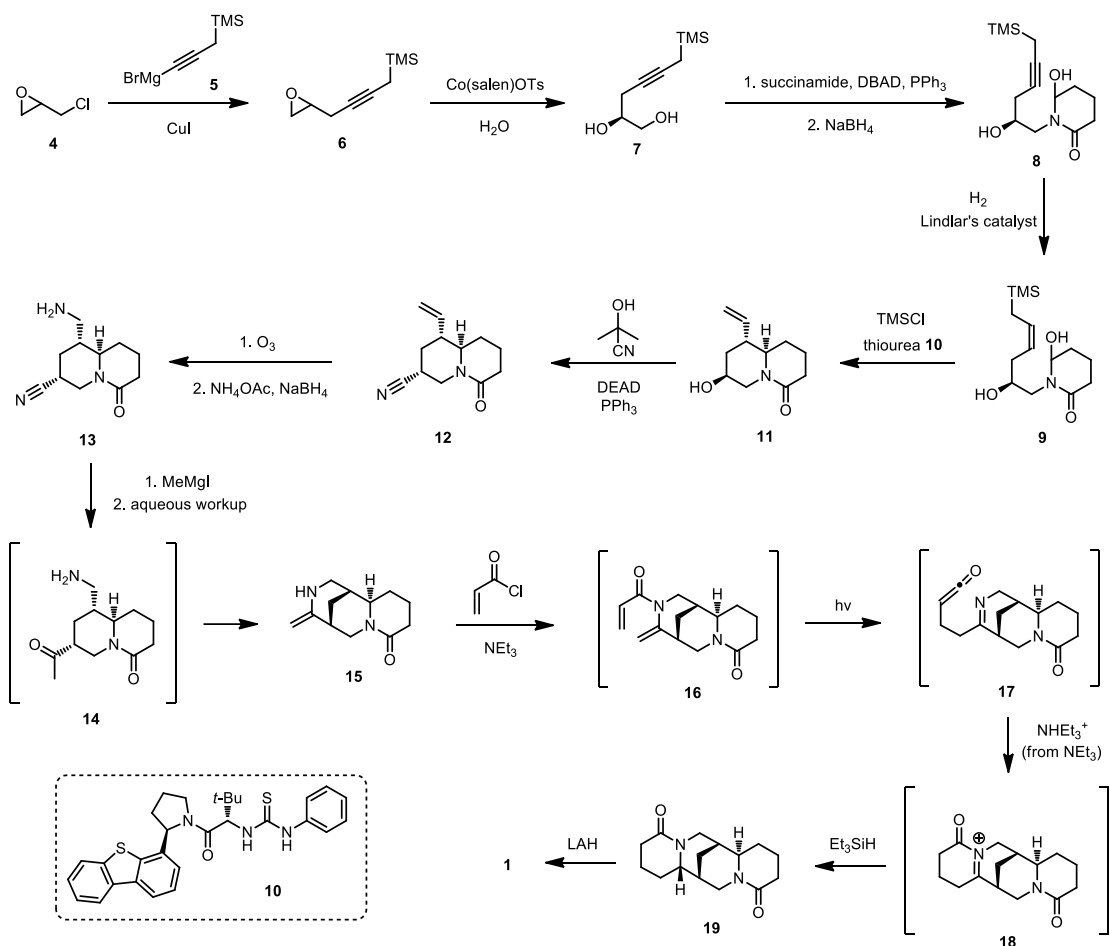
Although this proposed synthetic strategy would still not be practical for bulk production of sparteine, it does provide a modular approach to accessing analogs of this natural product. All the functional group manipulation steps are simple and well established. If successfully realized,

---

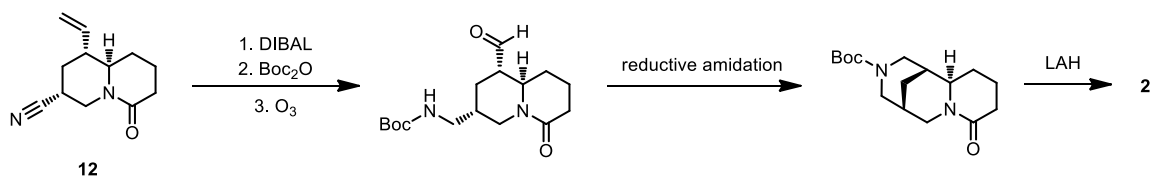
<sup>9</sup> Park, Y.; Schindler, C. S. Jacobsen, E. N. *Manuscript in preparation*.

<sup>10</sup> Bois, F.; Gardette, D.; Gramain, J. C. *Tetrahedron Lett.* **2000**, *41*, 8769–8772.

this strategy would showcase the power of asymmetric catalysis in accelerating construction of structural and stereochemical complexity in organic synthesis.



**Scheme A1-5.** Proposed total synthesis of sparteine.



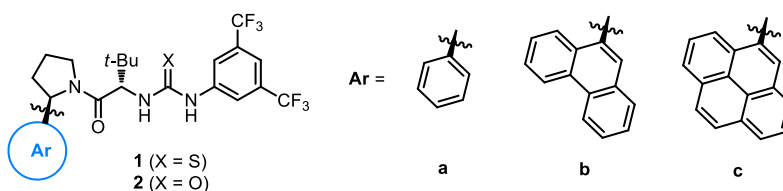
**Scheme A1-6.** Proposed total synthesis of (+)-sparteine surrogate.

# Appendix II

## Crystal Structure of Arylpyrrolidine-Derived Thiourea and Squaramide Binding to Tetramethylammonium Chloride

### A2.1 Arylpyrrolidine-Derived Thiourea Binding to Tetramethylammonium Chloride

Single crystals of tetramethylammonium chloride bound to thioureas **1a-c** and urea **2a** have been obtained through vapor diffusion method. Specifically, the catalyst and  $\text{NBu}_4^+\text{Cl}^-$  (in excess) were dissolved in  $\text{CDCl}_3$  with sonication, and the solution was transferred to a small glass vial after removal of insoluble precipitates. A 1:1 complex was formed based on  $^1\text{H}$  NMR analysis. This vial was covered on the top with aluminum foil to control the speed of vapor diffusion, and placed in a sealed flask containing hexanes. This system was allowed to stand at room temperature for a few days before observation of single crystal precipitation.



**Scheme A2-1.** Structures of thiourea **1** and urea **2**.

In the crystal structure, these complexes all exist in 2:1 (catalyst: $\text{NBu}_4^+\text{Cl}^-$ ) stoichiometry, with the chloride anion surrounded by four hydrogen bonds provided from the thiourea/urea molecules. In addition, the tetramethylammonium ion is also wrapped by the two aromatic groups on the catalyst, and the short distance between the two units (ca. 4 Å) indicates the presence of an attractive cation– $\pi$  interaction in the association event in the solid phase. The key distances related to these interactions are presented in Table A2-1.

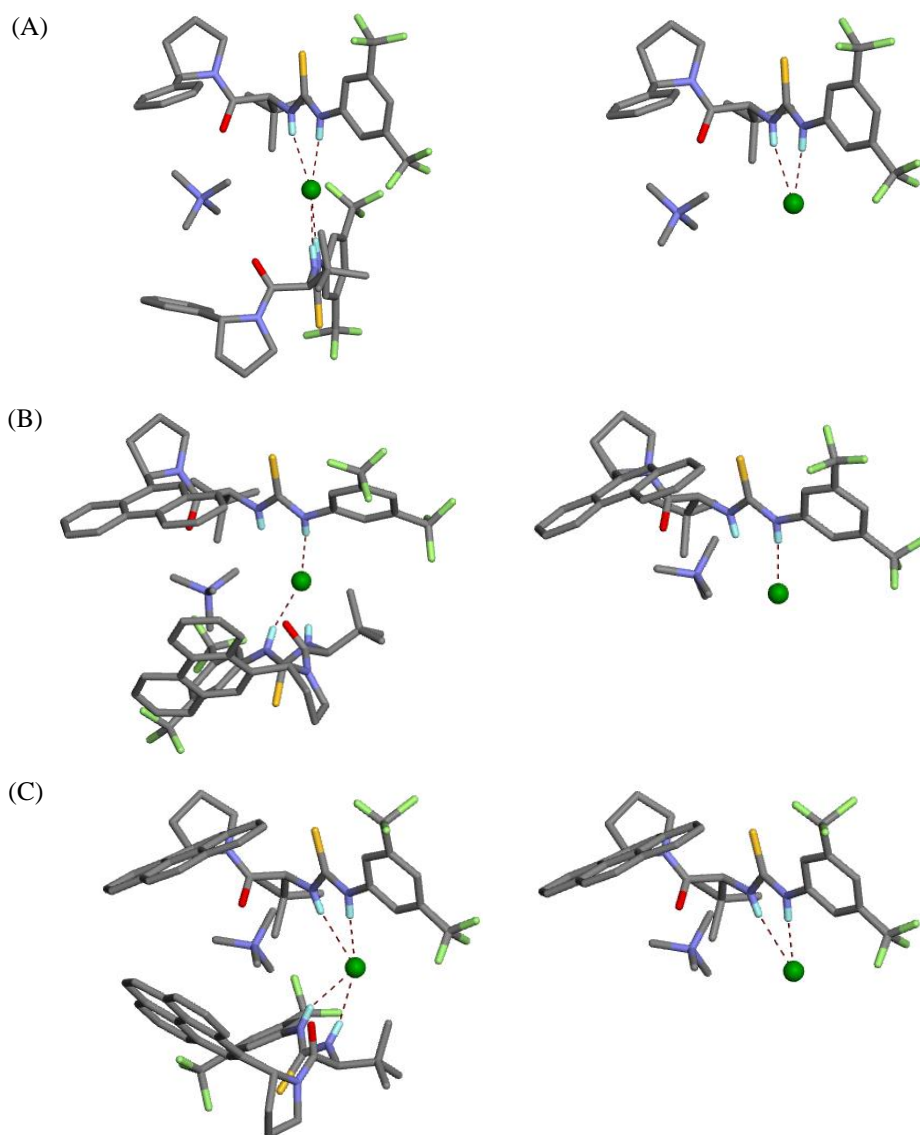


**Figure A2-1.** Crystal structures of tetramethylammonium chloride bound to (A) **1a**, (B) **1b**, (C) **1c**. In the depictions on the right, the bottom thiourea molecule is omitted for clarity. All hydrogen atoms are omitted for clarity except the thiourea N–H's.

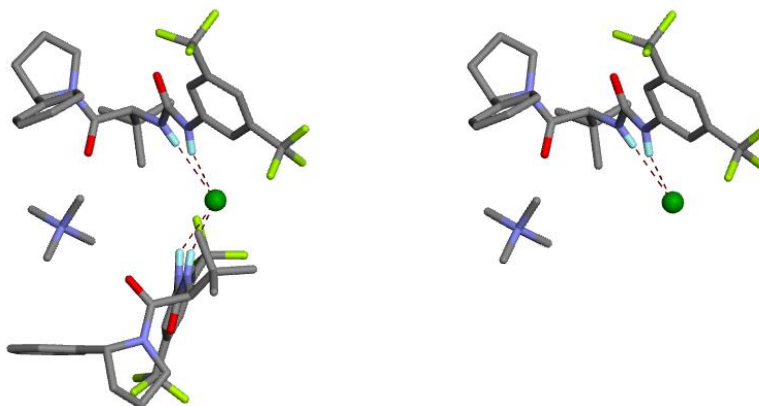


**Figure A2-2.** Crystal structures of tetramethylammonium chloride bound to **2a**. In the depiction on the right, the bottom thiourea molecule is omitted for clarity. All hydrogen atoms are omitted for clarity except the thiourea N–H’s.

**Table A2-1.** Distance of noncovalent interactions in the crystal structure.<sup>a</sup>

catalyst	H-bonds	N– $\pi$ distance <sup>b</sup>
<b>1a</b>	2.55, 2.32	4.44
<b>1b</b>	2.70, 2.46	4.24
<b>1c</b>	2.60, 2.28	4.09
<b>2a</b>	2.68, 2.33	4.23

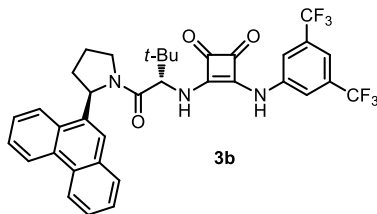
<sup>a</sup> Only distances between the tetrabutylammonium chloride and the top catalyst (but not the bottom one) in Figures A2-1 and A2-2 are presented. Numbers represent the distances in Å.

<sup>b</sup> N– $\pi$  distance refers to the distance between the nitrogen atom in the cation and the  $\pi$ -face of the aromatic group on the catalyst.

The data reveal that as the aromatic group on the catalyst increases in size (**1a** to **1c**), the distance between the tetramethylammonium ion and the  $\pi$ -face of the aromatic group decreases. Both this observed trend and the magnitude of the N– $\pi$  distance are consistent with an attractive cation– $\pi$  interaction existing in the catalyst-ion pair complex.

## A2.2 Arylpyrrolidine-Derived Squaramide Binding to Tetramethylammonium Chloride

A single crystal of tetramethylammonium chloride bound to squaramide **3b** have also been obtained through vapor diffusion method described in the previous section (Scheme A2-2).



**Scheme A2-2.** Structures of squaramide **3b**.

In the crystal structure, this complex also exhibit a 2:1 (catalyst:NBu<sub>4</sub><sup>+</sup>Cl<sup>-</sup>) association stoichiometry, with the chloride anion bound to the squaramide motif through H-bonding and NBu<sub>4</sub><sup>+</sup> surrounded by the phenanthryl groups (Figure A2-3). The key distances related to these interactions are shown in Table A2-2.

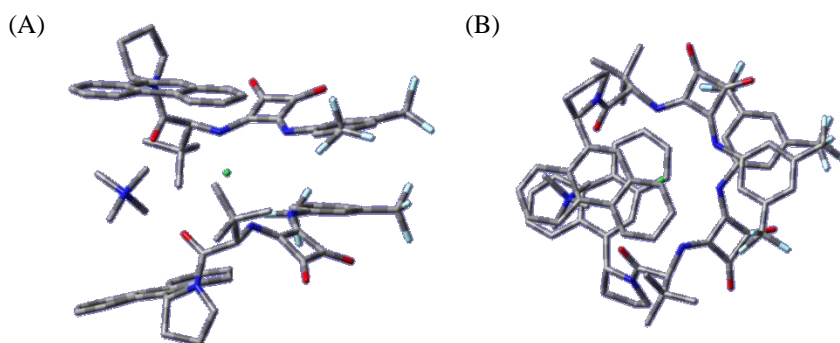


**Figure A2-3.** Crystal structures of tetramethylammonium chloride bound to **3b**. All hydrogen atoms are omitted for clarity. (A) side view; (B) top view.

**Table A2-2.** Distance of noncovalent interactions in the crystal structure.<sup>a</sup>

catalyst	H-bonds	N- $\pi$ distance <sup>b</sup>
<b>1b</b>	2.70, 2.46	4.24
<b>3b</b>	2.31, 2.28	4.33

<sup>a</sup> Only distances between the tetrabutylammonium chloride and the top catalyst (but not the bottom one) in Figures A2-1 and A2-3 are presented. Numbers represent the distances in Å.

<sup>b</sup> N- $\pi$  distance refers to the distance between the nitrogen atom in the cation and the  $\pi$ -face of the aromatic group on the catalyst.

Compared to the thiourea counterpart **1b**, **3b** has substantially shorter H-bond distances, consistent with squaramide being a better H-bond donor than thiourea. The N- $\pi$  distance is slightly longer, but still falls in the range of an attractive cation- $\pi$  interaction. The most striking difference between the crystal structures of **1b** and **3b** is that **3b** exist as a C<sub>2</sub>-symmetric complex,

while **1b** does not. The  $C_2$  rotation axis of the complex involving **3b** almost aligns with the straight line containing Cl and N atoms of the tetramethylammonium chloride. The “bite angle” of the two squaramide motifs to the chloride anion is considerably larger than that in the thiourea complex. The cationic host is sandwiched between the two phenanthryl groups, with one side of it almost completely exposed to the exterior. Although these findings are based on the solid state structures, they might have implication on the difference in the catalytic mechanism between thiourea and squaramide.